2019

Doctoral Thesis - *Doktorego Tesia*

Transdisciplinar Methodologies on Medieval and post-Medieval Pottery Analysis: An Archaeometric Approach to Basque and Riojan Productions

Erdi Aro eta Erdi Aro osteko buztingintzaren ikerketari buruzko metodologia transdiziplinarrak: Euskal eta Errioxar ekoizpenen azterketa arkeometrikoa

Estefania Calparsoro Forcada
Supervisor - *Zuzendaria*: Javier García Iñañez

Doctoral Programme in Scientific Cross-Disciplinary Approaches to Heritage and Landscape (SCAHL)
Diziplinarteko Estrategia Zientifikoak Ondarean eta Paisaian Doktorego Programa (DEZOP)

eman ta zabal zazu
Universidad del País Vasco
Euskal Herriko Unibertsitatea
FACULTY OF ARTS
UNIVERSITY OF THE BASQUE COUNTRY

Contents

List of Figures

List of Tables

List of Acronyms

AAS Atomic Absorption Spectrometry
Absortzio Atomikoaren Espektrometria

alr additive log ratio
Zatiki Logaritmiko Gehigarria

CRM Certificate Reference Material
Erreferentziazko Material Zertifikatua

clr centered log ratio
Erdiratutako Zatiki Logaritmikoa

CE Current Era (Equivalent to AD)
Oraingo Aroa

ED-XRF Energy-Dispersive X-Ray Fluorescence
Energia Sakabanatzailezko X izpien Fluoreszentzia

EFT Equivalent Firing Temperature
Erreketa Tenperatura Baliokidea

ERC European Research Council
Europako Ikerketa Kontseilua

GUM Guide to the Expression of Uncertainty in Measurement
Neurketen Ziurgabetasuna Adierazteko Gida

HCA Hierarchical Cluster Analysis
Multzokatze Hierarkikoaren Analisia

HFSE High Field Strength Elements
Eremu Altuko Indar Elementuak

ICP-AES Inductively Coupled Plasma Atomic Emission Spectrometry
Induktiboki Akoplatutako Plasmaren Emisio Atomikoaren Espektrometria

ICP-MS Inductively Coupled Plasma Mass Spectrometry
Induktiboki akoplatutako plasmaren masa espektrometria

IUPAC International Union of Pure and Applied Chemistry
Kimika Puru eta Aplikatuko Nazioarteko Batasuna

NAA Neutron Activation Analysis
Neutroien aktibazio bidezko analisia

MIC Micaceous
Mikatsu

MINECO Ministerio Español de Economía y Competitividad *Ekonomia eta Lehiakortasunaren Ministerioa*

MURR Missouri University Research Reactor
Misuri Unibertsitateko Ikerketa Erreaktorea

CVM Compositional Variation Matrix
Konposizioa-Aldakortasun Matrizea

LDGP Laboratorio de Documentació Geométrica del Patrimonio
Ondarearen Dokomentazio Geometrikoaren Laborategia

LDPE Low Density Polyethylene
Dentsitate baxuko Polietilenoa

LOD Limit of Detection
Detekzio Muga

LOI Loss on Ignition
Erreketa Bidezko Galera

LOQ Limit of Quantification
Kuantifikazio Muga

LG Lead Glazed
Berunezko Beiratua

LR La Rioja
Errioxa

PCA Principal Component Analysis
Osagai Nagusien Analisia

PCRU Paste Compositional Reference Unit
Pasta Konposiziozko Erreferentzia-unitatea

RG Reference Group
Erreferentziazko Multzoa

SD Standard Deviation
Desbideratze Estandarra

SNR Signal to Noise Ratio
Seinale-Zarata Proportzioa

SEM-EDS Scanning Electron Microscopy-Energy Dispersive X-Ray Spectroscopy
Ekorketa bidezko Mikroskopio Elektronikoa - Energia Sakabanatzailezko X Izpien Espektroskopia

SU Stratigaphic Unit
Unitate Estratigrafikoa

TBC The Basque Country
Euskal Herria

TLG Tin Lead Glazed
Eztainu-Berunezko Beiratudunak

vt Total Variation
Aldakortasun Totala

XRD X-Ray Diffraction
X Izpien Bidezko Difrakzioa

Esker onak

Hemen aurkezten den lanak ez luke argirik ikusiko, hau aurrera eramateko prozesuan parte hartu duten pertsona eta erakundeengatik izan ez balitz. Lehenik eta behin, nire zuzendariari eman behar dizkiot eskerrak, urte guzti hauetan nirekin pazientzia handiz ideia bakoitza eztabaidatzeko prest egon delako, baita aukera eman didalako bere ikerketa-motibazioen gainetik, nire askatasunean jardun ahal izateko. Ikerketa hau CERANOR proiektuaren barne dago (HAR-2013-46853) eta haren jarraipena izan duen proiektuan ere, alegia, CERANOR-2 (HAR2017-84219-P). Biak dira Ekonomia eta Lehiakortasunaren Ministerioak finantziatutako proiektuak, hala nola, AEI/FEDER, EU eta lehenengoaren baitan asignatu zidaten, hain zuzen, ikerketa hau burutzeko izan dudan kontratua (BES-2014-068940).

Baliabide ekonomikoez gain, hainbat eragileek berebiziko garrantzia izan dute ikerketa honen bilakaeran. Esaterako, Eusko Jaurlaritzaren bidez, erregistro arkeologikoak gordeak dituen hamaika materialetara iristeko aukera izan dut. Bide batez, *Bizkaiko Arkeologia Museoko* Sonia Anibarrosi eskerrak eman nahi dizkiot, Urduñako zeramikak eskuragarri egiteagatik. Hortaz gain, Blanka Gómez de Segurari eskertzen diot, *Euskal Buztingintza Museoko* materialak gure esku jartzeagatik. Era berean, Errioxa aldean, *Consejería de Cultura de La Rioja* eta *ArqueoRiojako*, Teresa Angulo eta Fernando Porresi, Logroñoko zeramikak helarazteagatik eta haien inguruko ekarpenengatik. Azkenik, Javier Cenicerosi, *Museo Histórico Arqueológico Najerillensetik*, bertan gordeta dauden aurkikuntzak gurekin elkarbanatzeagatik.

Zeramika guzti horiek aztertu ahal izateko oraindik guztiz osaturik ez dagoen arkeometriako laborategi baten beharraren aurrean, atzerrian burutu ditudan ikerketa-egonaldiak oso aberasgarriak suertatu zaizkit, horregatik, eskerrak eman nahi nizkioke Michael Glascocki *The Archaeometry Laboratoryn* hiru hilabetez bere ezagutzak elkarbanatzeagatik. Era berean, Berlineko Carlos Morales-Merinori eta Frau Reicheri *Rathgen Forschunglsborera* gonbidatzeagatik. Garrantzia berdinarekin, departamentu desberdinen arteko benetako kolaborazioa ahalbidetu dutenei, hala nola, Gorka Aranari egindako ICP-MS analisi guztiengatik, Maite Magureguiri ED-XRFrekin prestatutako laguntzagatik, besteren artean. Gainera, UPV/EHU-ko SGIker-X Izpien Zerbitzu Orokorrak, LASPEAk ete Geokronologia eta Geokimika Isotopikoko

Ikerkuntza Zerbitzu Orokorrak eskainitako laguntza eta baliabide teknikoak ere eskertzekoak dira. Ezin ahaztu, Juanjo Larreak eskainitako laguntza desinteresatua Nafarroako historia buruz.

Era inpertsonalean eskertu nahiko nuke, software irekia garatzera dedikatzen diren anonimo guztiei eta hura lizentzia irekiarekin konpartitzera animatzen direnak zeinen lanari esker tesi honen atal asko aberastu edota posible izan dira (adibidez R-n sortutako pakete guztiak, LaTeX-eko txantiloiak, hainbat *script*, etab.).

Era pertsonalago batean, aipamen berezia egin nahiko nieke GPACeko ikerketa taldekideei egunero hor egoteagatik. Bestalde, urrutiago daudenak, baina nolabait proiektu hau gauzatzeko era batera edo bestera lagundu dutenak, Jaume Buxeda i Garrigósen kasua bezala, zeini esker bereziak eman nahi dizkiot, R eta LaTeX erakusteagatik.

Azkenik, nire familia, lagun eta bikoteari eskerrak, diren bezalakoak izateagatik eta lan hau egitera animatu nautelako, nahiz eta zertara dedikatzen ari naizen ondo ez jakin! Gainera, amaierako idazketa-prozesuan eta berrikuspenean lagundu didaten guztiei esker bereziak ematen dizkiet.

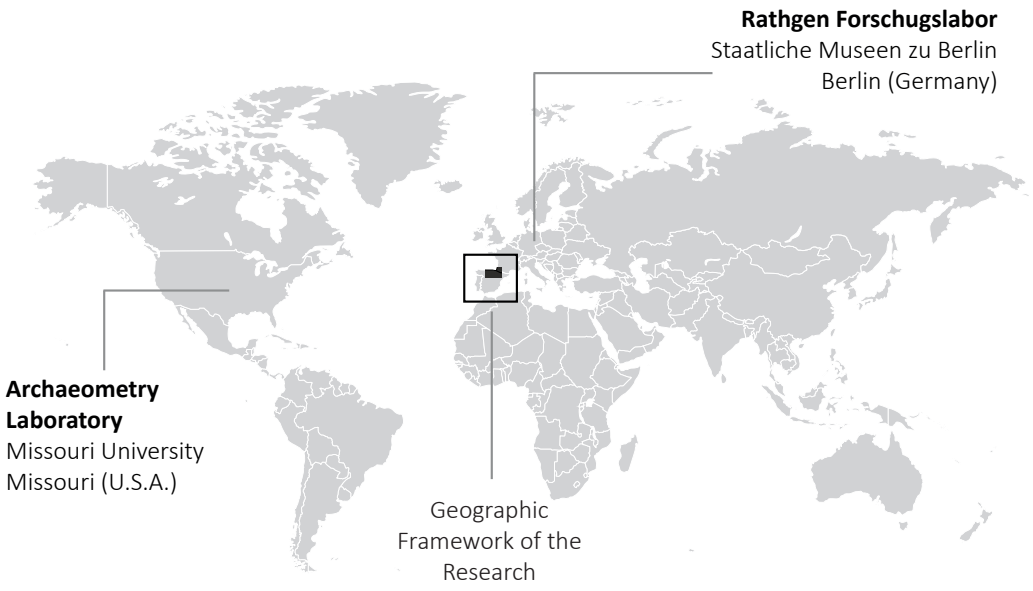

Figure 1: Ikerketa-egonaldiak egin diren tokiak ikerketa esparru geografikoa zehaztuz.

Part I

Background - *Aurrekariak*

We live on an island surrounded by a sea of ignorance. As our island of knowledge grows, so does the shore of our ignorance.
- John Archibald Wheeler -

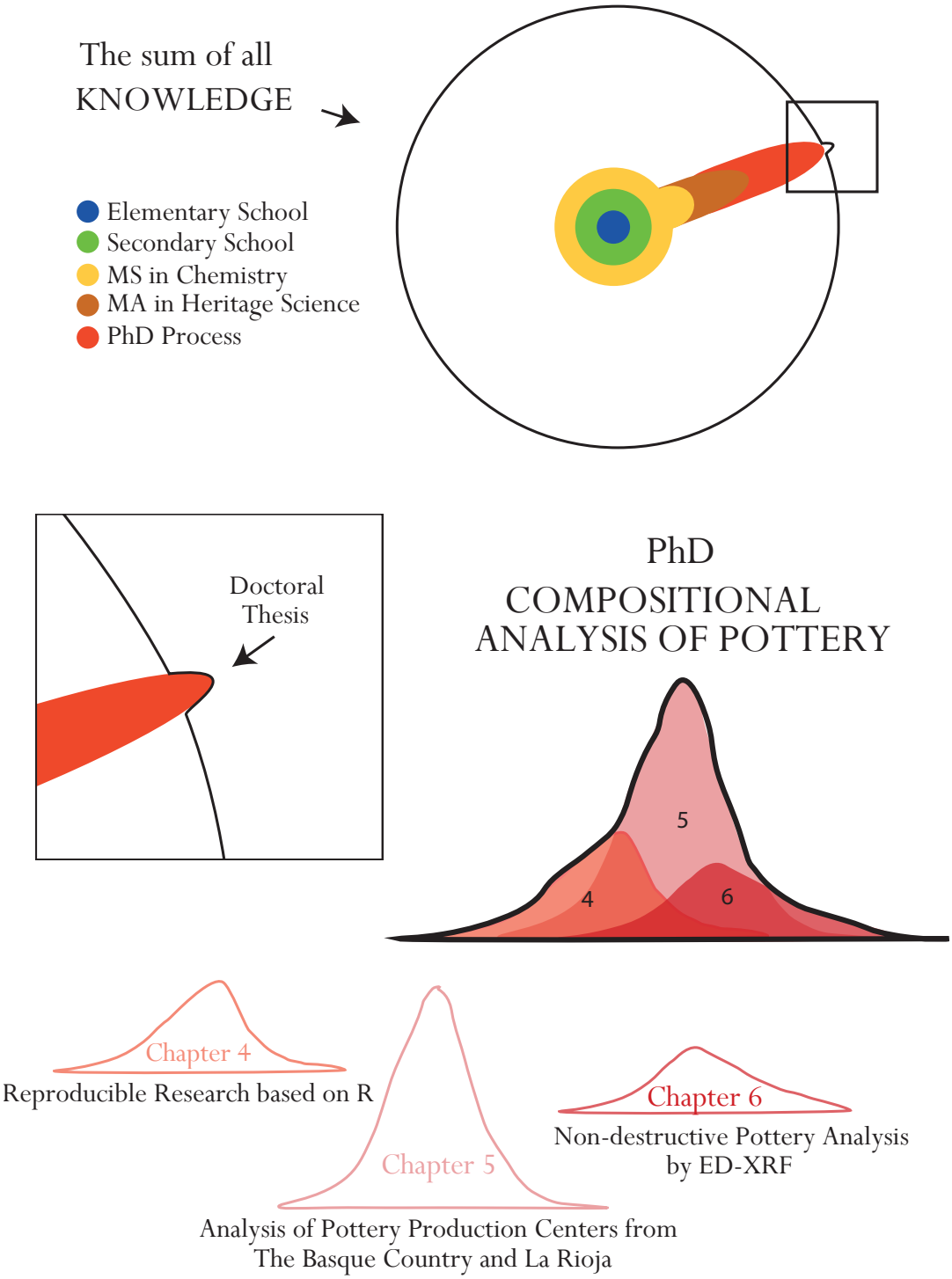

Figure 0.2: Illustration based on the Illustrated guide to a PhD of Matt Might.

Chapter 1

Sarrera

Hemen aurkezten den doktorego-tesia Euskal Herriko Unibertsitatearen (UPV/EHU) Arkeologia, Geografia eta Historiaurrea Sailean eta unibertsitate beraren Kimika Analitikoko Sailarekin lankidetza estuan egindako hainbat urteko ikerketaren emaitza da. Askotan, ahoa betetzen zaigu proiektuen diziplinartekotasunaz hitz egiterakoan. Hala ere, horren atzean, maiz, bildu baino ez dira egiten diziplinak, benetako elkarrekintzarik edo elkarrizketarik gabe; hori bai, ikerketa-proposamenetarako ondo baino hobeto geratzen da. Aitzitik, aipatutako sailean Kimikako Lizentziarekin ikerketa-proiektu bat gauzatzeak, nahitaez, diziplinartekoa bihurtzen du lan hau, mugak gaindituz eta bi eremuen ezagutza elkarrekin trukatuz. Askotan, ez da erraza arkeologoen eta kimikarien artean lan egitea, arazo zientifikoei aurre egiteko modua eta haien ikuspegiak oso desberdinak baitira. Aitzitik, arkeologia-departamentu batean murgiltzeko abenturak ikerketaren esparrua aberastea ekarri du, eta hori hurrengo orrialdeetan islatzea espero dugu.

Duela gutxi proposatu den ereduari jarraikiz; doktorego-tesi honek, batetik, diziplina arkeometrikoaren aurrerapenera zuzendutako ikerketa eta, bestetik, iraganari buruzko ezagutza lortzeko errutina arkeometrikoen aplikazioa biltzen ditu (Buxeda i Garrigós eta Madrid i Fernandez, 2017). Ikuspegi diziplinarteko integratua, atzeraelikadurako prozesu etengabean eta iteratiboan gauzatu da. Ildo horretan, errutina arkeometrikoen aplikazioak zeramikaren konposizioa aztertzeko R-n oinarritutako tresna konputazional berregingarriak eraikitzen lagundu du (4. kapitulua). Era berean, Euskal Herriko eta Errioxako zeramika ekoizteko zentroei buruzko ezagutza lortzeko erabili ziren errutina arkeometriko horiek (5. kapitulua) Erdi Aroko eta Erdi Aro osteko zeramika arkeologikoen sailkapen ez-suntsigarria garatzeko oinarri gisa hartu dira (6. kapitulua).

1.1 *Zeramikaren azterketa: zertarako?*

Definizio akademiko ohikoenaren arabera, arkeologiak giza elkarteak aztertzen ditu, haiek atzean uzten dituzten aztarna materialen bidez (González-Ruibal and Ayán Vila, 2018). Analizatzen diren material guztien artean, zeramikak berebiziko garrantzia du (Pérez-Arantegui, 2008), erakusten duen dualtasuna dela eta; alegia, dimentsio kulturala eta dimentsio naturala (Buxeda i Garrigós, 2008; Glascock, 2016; Roux, 2019; Fowler et al., 2019). Zeramikaren azterketaren motibazio nagusiak dimentsio kulturalarekin du zerikusia; hau da, aldaketa sozial, ekonomiko eta politikoen adierazle kronologiko eta kultural gisa duen eraginarekin (adib., Blomster et al. 2005). Ildo horretan, zeramika estu lotuta dago hura ekoiztu eta kontsumitu den testuinguruarekin (Fowler et al., 2019). Izan ere, zeramikek lehengaien eraldaketa bat jasaten dute artefaktu bilakatzeko. Prozesu horretan zenbait propietate fisiko bilatzen dira azken objektuari nahi diren gaitasunak (adib., moldagarritasuna) eta diseinu formala emateko, nahi den funtzioa bete dezan. Aldi berean, buztingileak teknika bat edo beste hautatzea haren trebetasun teknikoek, ohiturek eta bizi den gizartearen testuinguru kulturalak baldintzatuko dute. Aipatu beharra dago teknologiaren eta teknikaren arteko desberdintasunak ezagutza zientifikoaren aplikazioarekin zerikusia duela. Teknologia, dagokion jarduerari ezagutza zientifikoa aplikatzen zaionean esaten da, eta, aldiz, teknikarekin, zientzia aurreko buztingilearen ogibideaz ari gara; hau da, ezagutza zientifikorik aplikatzen ez zen garaiaz.

Beraz, zeramika aztertzeko metodologia egokiei jarraikiz, iraganeko gizarteei buruzko hipotesi solidoak formula daitezke (Roux, 2019; Fowler et al., 2019), eta garrantzi berezia hartzen dute beste dokumentazio-iturri erabilgarririk ez dagoenean. Hala ere, hori guztia zeramikaren dimentsio naturalari esker bakarrik da bideragarria, haren egoera materialari lotuta baitago eta honako ezaugarri hauek baititu:

- Nonahikotasuna (ubikuitatea): zeramikaren hedapen kronologikoari eta banaketa geografikoari erreparatuz, ezagutzen den material zabalduena da. Erregistro arkeologikoko objektu bakanetako bat da indusketa arkeologikoetan zein gainazaleko prospekzioetan agertzen dena (Escribano, 2014).

- Ugaritasuna: lehengai nagusia (buztina) gizateriarentzat eskuragarri egon da betidanik. Horrenbestez, iraganaren testuinguru arkeologikoan, gehien agertzen den kultura materialeko elementua da.

- Iraunkortasuna: erregistro arkeologikoan kontserbatzeko baldintza ezin hobeak ditu. Zumeak, egurrak, oihalek eta beste material organiko batzuek bizi-ziklo askoz laburragoak dituzte. Era berean, beirak edo metalezko objektuek birziklapen-prozesuak jasaten dituzte. Beraz, zeramiken kasuan ez bezala, horiek kultura jakin batekin izan dezaketen lotura ezagutzea larriki edo erabat oztopatzen da.

Arkeologian egiten diren galdera askori ezin zaie erantzun aztarna materialen behaketa zuzenaz lortutako informazioaren bidez. Galdera horietako batzuei aztarna horiek duten alderdi naturalaren bidez erantzun behar zaie; izan ere, aztarnak objektu materialak dira (Neustupny, 1971; Buxeda i Garrigós et al.; Buxeda i Garrigós et al., 1995; Buxeda i Garrigós and Madrid i Fernández, 2017). Zeramika arkeologikoak material konposatuak dira eta bi azpitaldetan sailkatzen dira: sinpleak eta konplexuak. Alde batetik, zeramika sinpleek ez dute estaldurarik, baizik eta, gehienez, kanpotik aplikatutako apaindurak, edonola ere, substantzia berririk gehitu gabe. Bestalde, zeramika konplexuek estaldurak, beiratuak edota engobeak dituzte. Bi kasuetan, gorputz zeramikoa osagai plastikoek eta ez-plastikoek (sendogarriak) osatzen dute. Osagai horien nahasketak ezaugarri bereziak sortzen ditu; besteak beste, testura, kolorea, egoera koloidala, plastikotasuna, lehortzea, eta partikulen tamaina. Gainera, baliteke ezpurutasunak egotea buztinetan edo erantsitako sendogarrietan. Gehigarri horien artean, hauek erabiltzen dira maiz, besteak beste: kuartzoak, feldespatoak, mikak, karbonatoak, burdin oxidoak eta materia organikoa (landaredia, material bituminosoak, etab.) (Shepard, 1956).

Aipatutako osagaiak biltzen dituen nahasketa bat lortutakoan, erre egiten da. Erreketa-prozesuak hiru etapa nagusi ditu (Rice, 1996; Shepard, 1956). Lehenengo etapa (i) *deshidratazioa* da eta plastikotasunaren galera dakar. Bigarren etapa (ii) *oxidazioa* da, eta etapa horretan CO_2-a askatzen da eta konposatu kimikoek erreakzionatu egiten dute, konposatu berriak sortuz eta kolore-aldaketak eraginez. Giroan oxigeno nahikorik ez badago (zenbait kasutan nahita eragiten da), kolore grisaxkak lortzen dira, burdin osagaien erredukzioa dela eta; kasu horietan, erredukziozko erreketaz ari gara. Hala ere, eskuarki, erreketa ingurune oxidatzailean gauzatzen da. Hirugarren etapa (iii) *bitrifikazioa* da, eta etapa horretan osagaiak matrize amorfo bat bilakatzen dira. Tenperaturaren arabera, zeramikazko egiturak hainbat sinterizazio-maila lor ditzake; horrela, partikulak maila desberdinetan itsasten dira beren artean (Shepard, 1956). Aldaketa horiek SEM irudien bidez ebalua daitezke, zeramikazko egiturak duen mikroegitura behatuta.

Sendogarriak zeramikari eransten zaizkion materialak dira (harea, landare-zuntzak, hondarra, maskorra, harri birrindua, zeramika hautsia). Erreketa-aldian gehiegizko uzkurdura saihesteko gehitzen dira, besteak beste; horrela, piezen pitzadura ekiditen da. Sendogarri moten artean, hareak, harriak eta material organikoak daude (maskorrak, erretako azalak, etab.). Sendogarri arruntenek feldespatoak, zeramika pusketak, kuartzoa, beira bolkanikoa, karbonatoak eta mika hartzen dituzte barne. Feldespatoak egonkorrenen artean daude, eta karbonatoak, berriz, ezegonkorrenen artean. Txamota[1] ere erabiltzen da zeramika-piezei trinkotasuna emateko. Txamota zeramika zati txikiz osatuta dago, eta, aldez aurretik erre denez, ez da askorik uzkurtzen. Adibide gisa, Mexiko Berriko eta Arizonako Pueblo indiar komunitateko

[1]Ingelesez, *grog*; frantsesez, *chamotte*; eta gaztelaniaz, *chamota*.

buztingileen lana dugu; izan ere, pieza hautsiak erabiliz ekoizten dute zeramika berria, iraganarekiko etenik gabeko loturari eutsiz (Grugel, 2005).

Zeramika konplexuetan, estaldurak aplikatzen dira (pinturak edota beiratuak barne). Estaldura horiek hiru modutara aplikatu ohi dira. Batetik, aldi berean aplika daitezke lehen erreketan (adib., pigmentu mateak). Bestetik, aldez aurretik erretako gorputz zeramikoari aplikatu ahal zaizkio. Behin bakarrik erretako piezari *bizkotxoa* esaten diogu, eta, normalean, eztainu-berunezko beiratuak dituzten zeramikak ekoizteko erabiltzen da. Azkenik, hirugarren erreketa bat ezar daiteke beiratutako piezaren gainean, isla metalikoak lortzeko erabili izan dena luze (Conesa, 2011).

Estalkietarako erabiltzen diren konposatuek baldintza jakin batzuk bete behar dituzte aplikagarriak izateko; esaterako, egonkortasun termiko nahikoa eta hedapen-koefiziente zehatz batzuk izatea. Izan ere, faktore horiek estaldura-gainazalarekin izango duten itsaspenean eragingo dute (Molera et al., 1997). Beruna luze erabili izan da beiratuetan, bi arrazoi nagusirengatik: alde batetik, urgarri gisa erabil daitekeelako; eta, bestetik, buztinarenaren antzeko hedapen-koefizientea duelako. Aitzitik, koefiziente horiek desberdinak direnean, baliteke beiratuak pitzatzea edo haustea (Tite et al., 1998). Gainera, egonkortasun termikoa ez duten pigmentuak ere erabiltzen dira, baina haiek erreketaren ondoren bakarrik ezar daitezke; beraz, beiratze-prozesurik jasaten ez dutenez, itxura guztiz desberdina dute. Pigmentu horien adibide ditugu malakita, azurita edota limonita, zeinak berdea, urdina eta horia lortzeko erabiltzen diren, hurrenez hurren (Shepard, 1956).

Beiratutako zeramikek duten konplexutasuna dela eta, aparteko ikerketa-lerro bat eskatzen dute (Tite et al., 2008). Horrenbestez, hemen zenbait pista baino ez dira emango testuinguruan kokatzeko. Lehenik eta behin, funtzioari dagokionez, apaintzeko edota piezak iragazgaizteko aplikatzen dira estaldurak. Horrenbestez, asko erabiltzen dira baxeran, hala nola likidoak gordetzeko ontzietan. Tradizionalki, beiratu mota ugari badaude ere, Iberiar penintsulan, harea, beruna eta metal oxidoak nahasiz lortutakoak dira ohikoenak. Gainera, eztainu-berunezkoak erabili dira apaindurarik gabeko pieza zuriak lortzeko edota zuriaren gainean apaindura monokromoak edo polikromoak ezartzeko. Beruna urgarri gisa erabiltzen da, eta metal oxidoetan oinarritzen diren pigmentuak beiratuaren gainetik edo azpitik aplika daitezke, lehen aipatu bezala bi edo hiru urratseko teknologiak erabiliz (Molera et al., 1997).

Beiratu zuri opakua lortzeko gehien erabiltzen den osagaia kasiterita da (SnO_2). Izan ere, arestian aipatutako propietate egokiak ditu eta, gainera, errefrakzio-indize egokia du beiratu zuri-zuriak egin ahal izateko (Vendrell et al., 2000; Molera et al., 1999). Adibide adierazgarrienetako bat maiolika zeramika famatua da. Tipologia horrek eztainu-berunezko beiratu bat du eta kanpo-azalera osoan aplikatzen zaio kolore argiko pastak dituzten gorputz zeramikoen gainean (Iñañez et al., 2008; Guirao et al., 2014). Pigmentuak aplikatzeko, ohikoa da frita bat prestatzea; hau da, aldez aurretik erretako kuartzoaren, berunaren eta beste osagai batzuen nahasketa, zeina bat-batean

hozten den beira lortzeko (adib., kobalto beira). Horretaz gain, engobeak ere erabil daitezke; hau da, beiratuaren eta gorputz zeramikoaren artean aplikatzen diren buztin-nahasketa baten geruza meheak. Batzuetan, beiraturik gabe ere erabiltzen dira horiek; alegia, besterik gabe engobea egitura zeramikoaren gainazalean aplikatuta.

Faktore horiek guztiak kontuan hartuz (buztinezko nahasketak, erreketak, beiratuen aplikazioa, etab.), agerikoa da buztingileak gaur egun kimika deitzen dugun arlo horri buruzko ezagutza minimo bat menperatu behar zuela. Orain arte, buztingileen artisautzaren arteari buruz ezagutzen den lehen laburpena 1556. urtean Zipriano Piccolpassok argitaratutakoa da, *Le Tre Libri dell'Arte del Vasaio* (Buztingintzaren artearen hiru liburuak), eta, bertan, lehengaiak eta fabrikazio-prozesuak deskribatzen dira. Laburpen horretan, maiolika zeramikari buruz ezagutzen den lehen dokumentazio idatzia jasotzen da. Hala ere, orain dela gutxi Montelupon aurkitu zen *Codice Calabranci* (XV. mendearen bigarren erdialdekoa), *Furnace Secrets* liburuan argitaratutakoa, mendebaldeko buztingintzari buruz orain arte ezagutzen den lehen gidaliburu gisa har daiteke; beraz, lehenengo tokia kendu die aurreko aurkikuntzei (Chiarantini et al., 2015).

Zeramiken beiratuaren teknologia kultura islamikoaren bidez ezarri zen Iberiar penintsulan, oraindik ere aztergai den prozesu konplexu baten bidez (Salinas and Pradell, 2018). Gainera, Erdi Aroan eta Aro Modernoan (Calparsoro et al., 2019c), teknologia-transferentzia horrek garapen diakroniko motelago bat izan zuen iparraldean, penintsulako beste gune batzuekin alderatuz gero; esaterako, Valentziarekin (adib., Manises eta Paterna) (Coll Conesa, 2009; Mesquida García, 2002; Pérez-Arantegui et al., 2008), Talavera de la Reinarekin edo Sevillarekin (Fernández de Marcos, 2018).

Aipatu beharra dago al-Andaluseko hastapenetan beiratze-teknika berezi bat hedatu zela Iberiar penintsulan zehar, idorraren bidezko dekorazioa deiturikoa (gaztelaniaz, *cuerda seca*), bereziki azulejuetarako erabiltzen zena (Chapoulie et al., 2005). Teknika horretan, uretan disolbagarriak diren beiratu-nahasketak substantzia koipetsu baten lerro finen bidez bereizten dira gainazalean, beren eremuetatik atera ez daitezen. Pigmentu ilunak erabiltzen dira; adibidez, manganeso karbonatoa koipearekin nahasten da koloreztatutako eremu bakoitzaren inguruan lerro iluna sortzeko (Campbell, 2006).

Aldez aurretik azaldutako zeramikaren bidimentsionaltasunari dagokionez (naturala eta kulturala), hiru ikerketa-eremu nagusi jorra daitezke zeramikaren azterlan arkeometrikoetan (Buxeda i Garrigós and Madrid i Fernández, 2017):

(a) Ekoizpen-prozesuari buruzko ikerketa, zeramika nola egiten zen ulertzeko.

(b) Ekoizpen-teknikei eta eraldaketa teknologikoei buruzko ikerketa.

(c) Erreketaren ondoren zeramikak duen errendimenduaren ezaugarriei buruzko ikerketa.

Gainera, hiru galdera horiek zeramikaren bizi-zikloaren bi ikuspegietatik landu daitezke: ekoizpenetik eta kontsumotik. Ekoizpena (a) eta eraldaketa teknologikoak (b) egokiago ebaluatzen dira ekoizpenaren ikuspegitik; aldiz, errendimenduaren ezaugarriak (c) kontsumoaren ikuspegitik landu beharko lirateke (Buxeda i Garrigós eta Madrid i Fernandez, 2017). Ildo horretan, kontsumoan oinarritutako ikuspegiek giza ezagutzaren bilakaera eta mundu materialarekin duen harremana ikertzea ahalbidetzen dute (Criado-Boado et al., 2019).

Ekoizpenean oinarritutako ikuspegiak ez dira gomendagarriak erretako zeramikak (c) duen errendimendu errealaren ezaugarriak aztertzeko, pieza akastunez beteta dagoelako. Aitzitik, oso egokia da lehenengo bi ikerketa motei ekiteko; alegia, ekoizpena (a) eta zeramikaren teknologia (b) (Buxeda i Garrigós and Madrid i Fernández, 2017). Doktorego-tesi honetan egindako analisi arkeometrikoek, hain zuzen ere, ikerketa-helburu horiei jarraitzen diete. Hori dela eta, ekoizpen-guneetan zentratu da ikerketa.

Hasieran planteatutako ezaugarriez gain (nonahitasuna, ugaritasuna eta iraunkortasuna), Erdi Aroko eta Erdi Aro osteko buztingintza-ohiturek ez dituzte soilik produktuen hondakinak utzi (adib., platerak, ontziak, etab.). Izan ere, beste jarduera batzuk ez bezala, ekoizpen horiek garatzeko erabiltzen ziren egiturek (adib., zeramika ekoizteko labeak), maiz, gaur egunera arte iraun dute (Conesa, 2011). Eraikitako ondare hori iraganaren zeramika-ekoizpenaren zantzu denez, posible da zeramika ekoizteko guneak geografikoki kokatzea. Aitzitik, aurreko denboraldietan, Historiaurrerainokoetan, zailagoa da horrelako egiturak topatzea. Kasu horietan, adierazgarriagoa izaten da patroi geologikoekin alderatzea. Doktorego-tesi honetan Erdi Aroko eta Erdi Aro osteko zeramikak jorratzen dira, garai horietako zeramikaren jarduera tradizionala barne hartuz. Beraz, aurrerantzean hemen egingo ditugun aipamenak bi aldi horiei aplikatuko zaizkio hertsiki, kontrakoa adierazten ez bada behintzat.

Iraganeko ekoizpen-jarduerak utzitako zantzuetara itzuliz, hainbat erreminta erabili izan dira buztingintzan (Conesa, 2011). Alde batetik, lehen aipatu dugun bezala, zeramika-labeak proba zuzenena dira. Gainera, aurretik dagoen tailer batean zeramika ekoizteko beste tresna batzuk ere aurki daitezke: tornuak, zeramikazko errotarriak, frita ehotzeko sistemak, labeko matoiak edota treberak (beiratze-teknologia sartu ondoren erabiltzen hasi zirenak). Azken horiek labe barruan piezak bereizteko asmoz erabiltzen ziren. Zeramika-ekoizpenaren beste zantzu bat pieza akastunak dira. Halakoak ez ziren salmentarako erabiltzen; beraz, baliteke ekoizpen-guneetatik oso gertu egotea (ikus 3.3. atala). Gainera, buztingileen hondakindegiak identifikatzeak balio handiko materiala ematen du ekoizpenaren karakterizazio arkeometrikorako. Horrela, helburua ekoizpen-zentroak karakterizatzeko aztarna kimiko bat ematea denean, material horiek interes handikoak dira, zeramika-ekoizpenaren zuzeneko ebidentzia adierazten baitute. Gainera, buztingileek erabiltzen dituzten tresnetako batzuk (adib., treberak edo labeko hodiak) kontsumorako erabiltzen diren buztin berdinekin fabrikatzen ziren oro har.

Hori dela eta, haien analisia oso baliagarria da ekoizpen-guneen karakterizaziorako (Buxeda i Garrigós eta Madrid i Fernandez, 2017).

Horrenbestez, zeramika-ekoizpenaren ebidentziarik zuzenetarikoa labe baten identifikazioa izango litzateke. Horrelako jarduerak identifikatzeko bestelako iturriak ez-materialak dira (adib., toponimia.). Gure inguruko herri askotan, oraindik ere, iraganeko buztingintzaren jardueraren lekuko diren toponimiak ditugu (adib., Ollerias izeneko kaleak). Ildo horretan, idatzitako dokumentazioa beste ikerketa-abiapuntu oso emankorra da, aztertzen ari garen kronologiari dagokionez. Adibidez, Ibabe etnografoak Euskal Herriko buztingintza herrikoiari buruzko ikerketa sakon bat burutu zuen eta, horrela, panorama zabal bat eskaini zuen (Ibabe, 1995a). Haren lana oso interesgarria izan da hemen aurkezten den doktorego-tesiaren garapenerako.

Lan honek zubiak eraiki nahi dituenez hainbat diziplinaren artean, prozesu arkeologikoari buruzko testuinguru labur bat aurkezten da hurrengo lerroetan. Indusketa arkeologikoen printzipioei dagokienez, estratua jatorrizko edo testuinguruaren oinarrizko unitate gisa defini daiteke; hau da, formakuntza-prozesuetako unitate txikiena. Unitate estratigrafikoei (ingelesetik SU) aldi kronologikoa eman dakieke, froga nahikoak ematen badira (adib., txanponak, zeramika edo bestelako tresna adierazgarri batzuk). Gainera, SU-tan agertzen diren zeramika zatikiak mihiztatze[2] zeramikoa deritzona osatzen dute (Buxeda i Garrigós eta Madrid i Fernandez, 2017). Gainera, mihiztatze horiei dagokienez, kuantifikatzeko hainbat estrategia daude, eta oso garrantzitsuak dira aztarnategi arkeologiko bakoitzaren materialtasuna islatzeko orduan. Esate baterako, kuantifikazioa eremuan egiten bada, banakoen proportzioek hainbat kronologiari buruzko pistak eman ditzakete testuinguru jakin batzuetan. Izan ere, garai batzuk zeramika proportzio jakin batzuekin ezaugarritu dira aurreko lan batzuetan (Solaun, 2005). Hala ere, kuantifikazio-estrategien analisia tesi honen irismenetik kanpo dago. Gai horren inguruko eztabaida sakonago baterako, ikus (Buxeda i Garrigós and Madrid i Fernández, 2017; Shennan, 1988; Escribano, 2017a).

Doktorego-tesi honetan aztertutako materialak nagusiki museoen bildumetatik atera ziren; hau da, ez ziren zuzenean indusketa arkeologikoetatik atera. Salbuespen gisa, Logroñoko zeramikak indusketa aurrera eraman zuen enpresak berak jaso, dokumentatu eta sailkatu zituen azterketa arkeometrikoaren aurretik. Lan honetarako, tipologia-aniztasunaren eta estatistika-esanahiaren arteko oreka bilatu nahi izan zen banakoen kopurua zehazteko unean (xehetasun gehiagorako, ikus 3.3. atala). Gainera, aipatu behar da desberdintasun nabarmena dagoela estratifikazio arkeologikoaren eta post-estratifikazio arkeologikoaren artean. Lehenbizikoa zeramikaren multzoan oinarritzen da, eta bigarrena, berriz, laginketa bateko banakoetan. Beraz, ez bada banakoen gehieneko kopurua (MxNI) arkeometrikoki karakterizatu, ohartarazi behar da

[2]Ingelesez, *assemblage*

populazioaren post-estratifikazioa laginketa-frakzioaren emaitzetan oinarritutako inferentzia bat besterik ez dela (Buxeda i Garrigós eta Madrid i Fernandez, 2017).

Eredu Arkeometrikoa

Aldez aurretik azaldutako arrazoi guztien arabera, ez da harritzekoa zeramikaren konposizio-analisia zientzia arkeologikoko gai landuenetako bat izatea (Glascock, 2016; Hunt, 2016). Lan honetan jarraitutako eredu arkeometrikoa Buxeda i Garrigósek eta beste egile batzuek proposatu zuten (Buxeda i Garrigós et al., 1995; Buxeda i Garrigós, 2008; Buxeda i Garrigós et al., 2008), eta duela gutxi berrikusi da (Buxeda i Garrigós eta Madrid i Fernandez, 2017). Ikuspegi horren arabera, azterketa arkeometrikoa ez datza soilik objektuen analisi kimikoan, baizik eta eredu batera hurbiltzean, era interaktiboan eta jarraituan, haien rola ulertzeko.

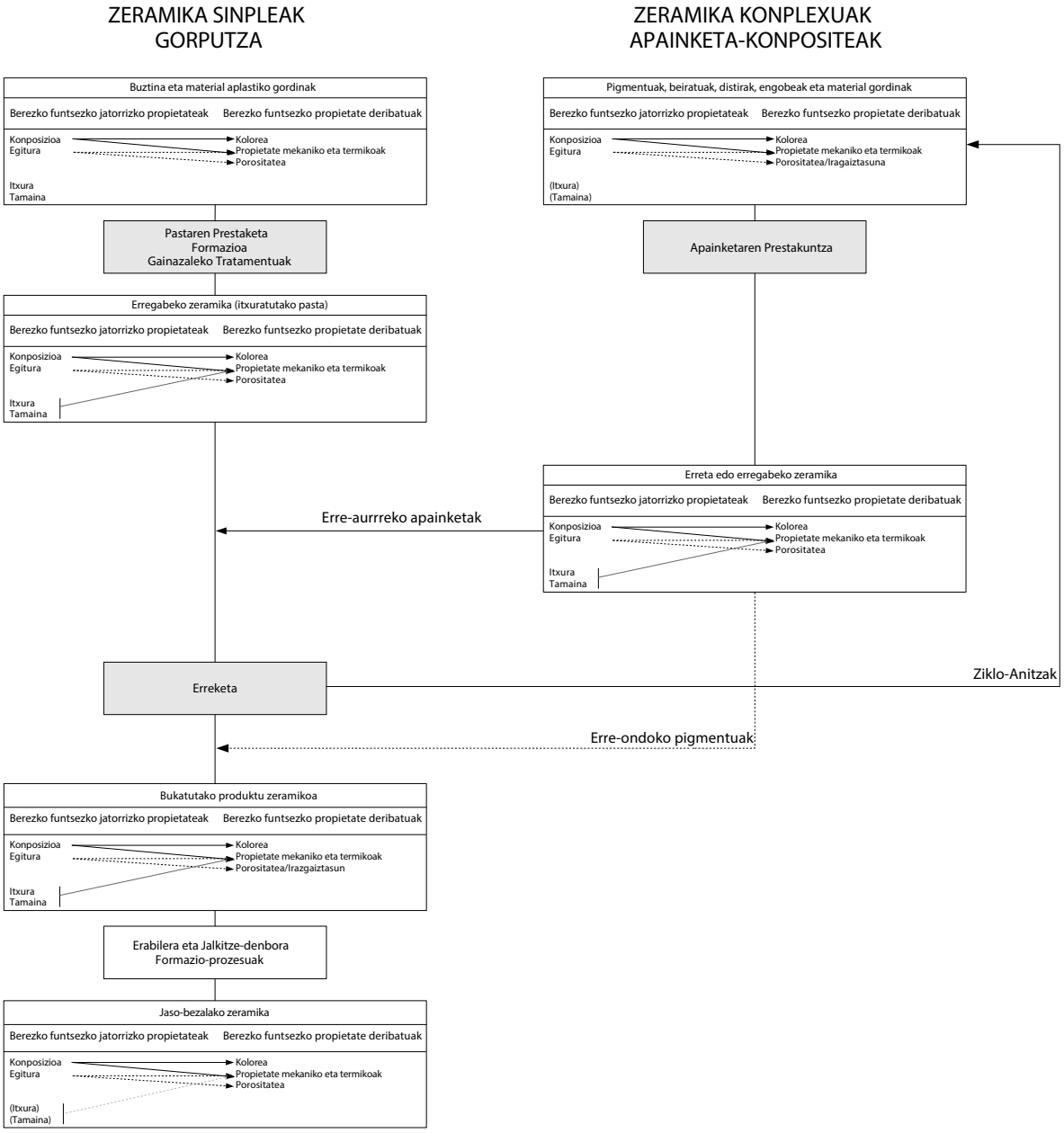

Figure 1.1: Zeramika ekoizpenetik arkeologia-erregistrora bitarteko fluxu-diagrama (Buxeda i Garrigós eta Madrid i Fernandez, 2017).

Buxedak eta beste egile batzuek proposatutako fluxu-diagrama (ikus 1.1. irudia) zeramiken *chaine operatoire*-an oinarritzen da (Roux, 2019). Katea zeramika aurkitzen denetik hasten da; hau da, gune arkeologikoan jasotzen denetik hura ekoizteko erabilitako lehengaiak erauzi ziren arte. Seguruenik, lehengaia erauzi zen gunea ekoizpen-gunetik oso gertu zegoen, edo ekoizpen-gunean bertan. Kontuan hartu behar da zeramikak material sintetikoak direla, erreketa jasan eta eraldatutako lehengaiak baitira. Era berean, zeramika-pasta buztinaren manipulazioaren emaitza da, sendogarriak gehitu, beste buztin batzuekin nahasi edo ekintza horiek konbinatzearen ondoriozkoak. Beraz, naturan ez direnez zuzenean horrela aurkitzen, ez dago zuzenean bateragarria den fase geologikorik.

Gainera, ezinezkoa da giza manipulazioaren eragina zuzentzea lehengaiei dagokienez, normalean ezezaguna baita zeramikariak pasta prestatzeko jarraitu zuen prozesua (Buxeda i Garrigós, 2008; Buxeda i Garrigós and Madrid i Fernández, 2017). Lehengaiekin zuzenean lan ez egiteak ez dakar inolako arazorik kimikaren aldetik jatorria ezartzeko; izan ere, buztinaren jatorrizko tokia ekoizpenaren berdina izan ohi zen, garraioak eragiten zituen kostuak kontuan hartuta. Beraz, pasten jatorriari buruzko azterketek ez dute inolako arazorik eragin behar, baldin eta haien prestaketa egonkorra izan zela onartzen bada; izan ere, errezeta zuzen baten aldaketak akats ugari eragin ditzake (Buxeda i Garrigós, 2008; Buxeda i Garrigós and Madrid i Fernández, 2017). Ondorioz, zeramikaren jatorria haren ezaugarri kimikoaren bidez zehaztea denean helburua, funtsezkoa da ekoizpen-zentroa zehaztea; hau da, zeramikariak pasta egin zuen lantegia identifikatzea.

Errutinaren araberako konposizio-analisia eredu kimiko desberdinak identifikatzean datza; hau da, multzo zeramiko esanguratsuak identifikatzean, oinarrizko konposizio-balioei hainbat aldagaiko estatistika-estrategiak aplikatuta (Hein and Kilikoglou, 2015; Glascock, 2016; Buxeda i Garrigós and Madrid i Fernández, 2017). Multzo zeramiko esanguratsuak oinarri kimikoko sailkapen baten unitate txikienak dira. PCRU esaten zaie ingelesez, eta pastaren konposizioko erreferentzia-unitate gisa definitzen dira[3] (Bishop et al., 1982, 290 or.).

Ikuskatutako ikaskuntzan (ingelesez, *supervised learning*), zeramika-mihiztatzea iturri jakin bati (adib., tailer bat) eslei dakioke, proba arkeologiko sendoak egonez gero (adib., labeko tresnak, labe-egiturak edo buztingintzako akatsak). Gero, PCRUak datu-baseekin erka daitezke, lehendik dauden erreferentzia-taldeekin (ingelesez, RG) bat ote datozen aztertzeko, eta, horren arabera, jatorri exogenoa (ekoizpen-zentrotik ezberdina dena) ezar daiteke. Hala ere, ekoizpenetan froga arkeologiko nahikoak dauden kasuetan, PCRUa tokiko jatorrikotzat jo daiteke, eta RG berria osatzen da, tokiko ekoizpenari esleitzen zaiona. Litekeena da, baita ere, zeramika ezin esleitu ahal izatea ez tokiko jatorriari, ez jatorri exogeno bati. Doktorego-tesi honetan, zehaztugabeak (ingelesez, *undetermined*) izena eman diegu talde horiei.

[3]Euskaraz, PKEU; ingelesez, PCRU; eta gaztelaniaz, URCP. Hala ere, lan hau elebiduna denez, ingelesezko bertsioak erabiliko dira.

Buxeda i Garrigósen eta Madrid i Fernandezen (2017) diagramaren arabera (ikus 1.1. irudia), pastaren nahasketa egin ondoren, hura ehundura bihurtuko da prozesu tekniko baten ondorioz (adib., forma ematea, erreketa, etab.). Horrela lortutako pastaren produktuari ehundura deritzogu eta gorputz zeramikoaren ezaugarri naturalak (jatorrizko konposizio mineralogiko eta petrografikoak) eta artifizialak konbinatzen ditu. Pastatik ehundurarako eraldaketak; aldaketa kimikoak (Hein and Kilikoglou, 2015), mineralogikoak (Maggetti, 1981) eta mikroegituzkoak (Maniatis and Tite, 1981; Buxeda i Garrigós, 1995) eragiten ditu. Horregatik, konposizio multzoak identifikatu ondoren, multzo kimiko horiek osatzen dituzten ehunduren ezaugarriak aztertzen dira, mikroegituraren eta analisi mineralogikoen bidez. Ustekabeko ekoizpen-prozesuaz gain, hainbat eraldaketa eta kutsatze gerta daitezke pasta prestatzeko prozesuaren une desberdinetan; besteak beste, pastaren prestaketa teknikoaren fasean, modelatuan, erreketan, etab.; objektu zeramiko horien erabilpen-aldia eta jalkitzearen ondorengoko aldian. Kutsadura- eta eraldaketa prozesu horiek zeramikazko mihiztatzean duten eragina 5.1. atalean aztertzen da.

Egia esan, eredua azaldutakoa baino askoz konplexuagoa da, eta kontuan izan behar dira, batetik, arkeologiarekin zerikusia duten zenbait faktore, eta, bestetik, zeramikariek Antzinaroan garatzen zuten jarduera. Lehenik eta behin, gogoan izan behar da aitzinari buruz benetan ezagutzen duguna partziala dela, tailer bateko hondakin materialen berreskurapena bezala (hau da, azpiegituraren hondarrak eta produktuak). Bigarrenik, kontuan izan behar da lantegi berak erreferentzia multzo (RG) bat baino gehiago aurkez dezakeela; izan ere, baliteke buztingileak pasta bat baino gehiago prestatu izatea askotariko zeramika-tipologiak egiteko. Gainera, pasta berak hainbat ehundura sor ditzake, zeramikariak prozesu tekniko bat edo beste (modelatua, erreketa, etab.) erabiltzen baitu lortu nahi duen produktuaren arabera (Buxeda i Garrigós eta Madrid i Fernandez, 2017).

Hirugarrenik, baliteke ingurune berean dauden lantegiek lehengai berberak erabiltzea eta pasta modu berean prestatzea. Kasu horietan, tailer horietan ekoiztutako zeramikek antzeko konposizio kimikoak izango dituzte; beraz, lantegiak ezin izango dira RG ezberdinen bidez identifikatu. Eremu hau ziurgabetasun edo bereizmen gabeko espazioaren gune gisa ezagutzen da (Buxeda i Garrigós eta Madrid i Fernandez, 2017), (Picon, 1973, 105 or.)-tik egokitua). Gune horietan ezingo dira analitikoki bereizi buztingile desberdinek erabiltzen dituzten lehengaiak, haien ezaugarriak oso berdintsuak direlako; izan ere, eremu geologiko oso berdintsuak izaten dira (Buxeda i Garrigós eta Madrid i Fernandez, 2017).

Edozein materialen jatorria analisi kimikoaren bidez zehazteko, jatorriaren postulatua hartzen da oinarri gisa, eta, horren arabera, jatorri bereko lehengaien arteko aldakortasunak jatorri desberdineko lehengaien artekoa baino txikiagoa izan behar du, eta jatorrien arteko desberdintasunak identifikatzeko modukoak izan behar dira. Bestela esanda, jatorri bera duten materialak antzekoagoak izango dira leku desberdinetatik datozenak baino. Ondoren, ikuspegi horrek hainbat gehikuntza izan

ditu, eta gaur egun Pollardek (Pollard et al., 2008) ezarritako bost baldintzetan oinarritzen da: bereizgarria, singularra, aurreikus daitekeena, neurgarria eta egonkorra izatea.

Zeramiken jatorria zehazteko, bi maila aztertu ohi dira: ikuspegi kimika eta ikuspegi petrografikoa (Buxeda i Garrigós eta Madrid i Fernandez, 2017). Hala ere, metodo petrografikoen emaitzak egokiagoak izaten dira zeramiken pasta trauskila denean, tamaina handiko inklusio ez-plastikoak dituenean. Kasu horietan, inklusioetan harrizko zatiak hautematen badira eta haien tamaina nahikoa bada, haien jatorri geologikoa zehazteko aukera ematen dute (Buxeda i Garrigós, 2008). Aitzitik, pasta dekantatuagoak dituzten zeramiketan, doktorego-tesi honetan aztertzen direnen modukoetan, oso nekeza edo ezinezkoa izan daiteke metodo petrografikoak erabiltzea jatorria zehazteko (Buxeda i Garrigós, 2008).

Doktorego-tesi honetan landutako errutina arkeometrikoaren arazoak aurretik planteatutako ikerketei lotuta daude: ekoizte-prozesuak (a), konposizio multzo esanguratsuak identifikatzea inplikatzen dutenak; eta haien jatorria eta teknologia (b). Zeramikaren analisia askoz ere zabalagoa izan daiteke ebaluatuko diren ezaugarrien arabera. Esate baterako, propietate fisikoen artean, propietate mekanikoek (hala nola gogortasuna eta erresistentzia) eta termikoek berebiziko garrantzia dute, gizakiek objektu horiei ematen dieten erabilerarekin eta erabilgarritasunarekin zuzenean loturik baitaude (esaterako, sukaldeko tresna erregogorrak, eraikuntzarako balio handiko materialak, etab.) Buxeda i Garrigós (2008).

Gainera, aipatzekoa da ikerketa honetan beste material zeramiko batzuk kanpo geratu direla; esaterako, zeramikaren eraikuntzarekin zerikusia dutenak (adib., azulejuak), edota haietan aurkitzen diren hondakin organikoak, zeinek iraganean giza portaerari buruzko informazio baliotsua eman dezaketen Blanco-Zubiaguirre et al. (2016, 2018).

Laburbilduz, atal honetan zeramikaren analisiak duen garrantzia jorratu da, dimentsio kulturala eta naturala biltzen dituelako. Gainera, zeramikaren azterketaren bidez iraganari buruzko informazioa lortzeko zer ikuspegi mota erabil daitezkeen azaldu da. Zeramikaren ekoizpena (a), teknologia (b) edo errendimendua (c) ekoizpenaren edo kontsumoaren ikuspegitik azter daitezke. Ildo horretan, doktorego-tesi honetan burutu den ikerketa zeramikaren ekoizpenean eta teknologian oinarritu da Erdi Aroko eta Erdi Aro osteko ekoizpen-guneak aztertuta. Ildo horretan, bost ikerketa-kasu hautatu dira (5. kapitulua). Helburu horretarako jarraitu den eredu arkeometrikoa multzo zeramiko esanguratsuak definitzean datza, eta haien jatorria zehaztean, hurrengo atalean azalduko den moduan.

1.2 *Ikerketa arkeometrikoaren gaur egungo erronkak*

Arkeometriako ikerketa-ikuspegiak

Duela gutxi proposatu den moduan Buxeda i Garrigós eta Madrid i Fernandezek proposatu zuten moduan (2017), arkeometriak garapen bat izan du gaur egun bi ikerketa bideetara zabaltzea heldu dela (ikus 1.2. irudia). Alde batetik, (a) arkeometriaren *ikerketa-arazoak* jorratu daitezke, eta horiek, diziplinaren aurrerapenera bideratuta daude (adib. metodo berrien garapena). Bestetik, (b), arkeometriako *errutina arazoak* landu daitezke, eta, azken horiek gizarte-sistemei buruzko ezagutzan sakontzeko erabiltzen dira (adib. ezarritako errutinen aplikazioa datu eta hipotesi berriak lortzeko).

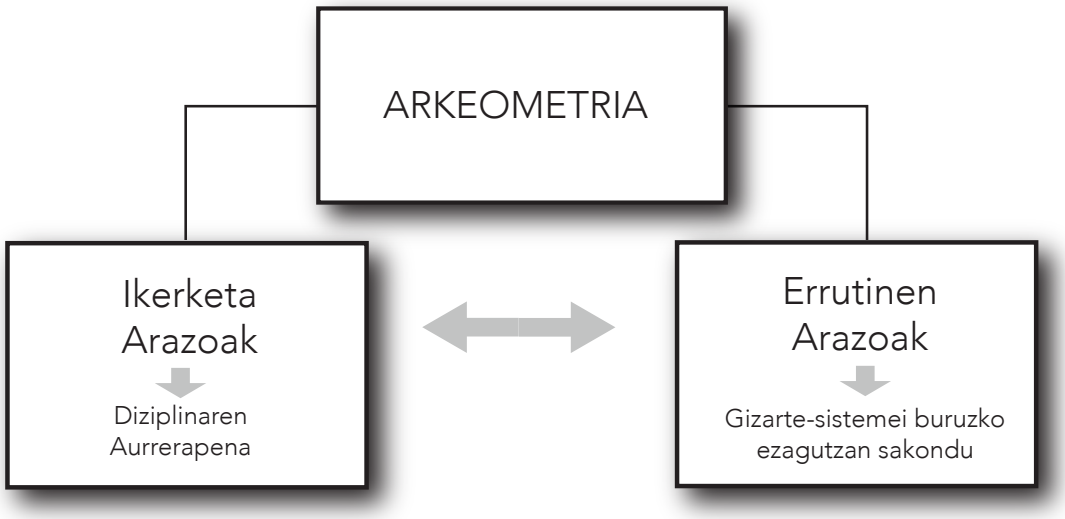

Figure 1.2: Arkeometriaren ikerketa-ikuspegiak, beste lan batetik moldatua (Buxeda i Garrigós eta Madrid i Fernandez, 2017).

Doktorego-tesi honen irismenak bi ikerketa-lerroak biltzen ditu. Alde batetik, 4. eta 6. kapituluak (a) ikerketa-arazoen erronkak lantzera bideratuta daude, batetik, R-n oinarritutako ikerketa berregingarria burutzeko metodologia bat garatuz, eta bestetik, ED-XRFan oinarritutako metodo ez-suntsitzaileak aztertuz. Aldi berean, 5. kapituluan, ezarritako errutina arkeometrikoak aplikatzen dira Euskal Herriko eta Errioxako ekoizpen zeramikoak hobeto ulertzeko. Beraz, (b) errutina-arazoen lerroari lotuta dago hirugarren hau. Gainera, aurreko atalean planteatutako eredu teorikoaren barruan kokatzen da. Eredu teoriko horrek iraganeko buztingintza hobeto ezagutzea du helburu, eta, horretarako, konposizio-talde esanguratsuen identifikazioan oinarritzen da.

Bi ikerketa-lerroek lotura sinergiko handiak dituztela oinarritzat hartuz, errutina arkeometrikoen aplikazioak berebiziko garrantzia izan du ikerketa arkeometrikoei buruzko erronkei aurre egiteko, diziplinaren aurrerapenera bideratuta baitaude. Alde batetik, R-n oinarritutako ikuspegi berritzailea eraiki da, errutina arkeometrikoak aplikatuz behatu diren eskakizunen arabera, ondo ezarritako teknika analitikoak aplikatu ondoren (ICP-MS eta NAA) eta dagokion azterketa kimiometrikoekin batera. Horrela, tresna horiek iteratiboki garatu dira, eta haien aplikazioa eta garapena atzeraelikadurako prozesu etengabea izan da. Bestalde, aldez aurretik metodologia suntsitzailearen bidez lortutako zeramikaren sailkapena (ICP-MS) hartu da oinarri gisa, ED-XRFn oinarritutako bahetze ez-suntsitzailearen metodologia garatzeko.

Arkeometriaren ikuspegi zabala

Doktorego-tesi honetan aukeratutako ikerketa-horizonteak kokatzeko, arkeometriaren egungo erronkak kontuan hartuko dituen testuinguru zabalagoa eman behar da. Halaber, saihestezina dirudi ikerketa-lerroaren eta haren bilakaerari buruzko testuinguru labur batek.

Eszeptizismoa barne (González-Ruibal, 2014), zientzien aplikazioa ezinbestekoa izan da arkeologiaren arloan lehen mailako paradigma-aldaketak eragiteko. Kristiansenek hiru iraultza teoriko identifikatu zituen arkeologiaren arloan; hirurek metodo zientifikoekin zerikusia izan dute Kristiansen (2014). Lehenengoa arkeologia diziplina zientifiko gisa ezartzearekin batera etorri zen, XIX. mendearen erdialdean. Kasu honetan geologiaren eta biologiaren metodoak bereganatu zituen arkeologiak, eta zientzia bihurtu zuen jauzia eman zuen. Bigarren iraultza erradiokarbonoaren datazioak eragin zuen XX. mendearen erdialdera, eta, aldi berean, diziplinaren horizontea izugarri handitu zuen, galdera berriak planteatuz eta interpretazio berriak proposatuz. Halaber, hirugarren "iraultza zientifikoa" gaur egungo arkeologia ari da jasaten. Azken horrek Big Data, eredu kuantitatibo berriak eta DNA eta analisi isotopikoen erabilera orokorra eragiten duten ikerketa-lerro berritzaileek bultzatutako paradigma teoriko berria sortu nahi du.

Zientzia esperimentaletatik hartutako teknika analitikoak aplikatzean datza Arkeometria, kultura materiala haren dimentsio naturaletik aztertzeko aukera ematen baitute. Tresna analitikoekin aztertu aurretik, artefaktuak prestatu egin behar dira, eta zeharkako informazioa emango dute aztertu ditugun objektuen berezko konposizioaren arabera; kasu honetan, aukeratukotako objektuak zeramikak dira (Boulanger et al., 2013a; Buxeda i Garrigós, 1999, 2008; Buxeda i Garrigós and Madrid i Fernández, 2017).

Arkeometriaren edo zientzia arkeologikoaren sorrera, diziplina gisa, arkeologiaren bigarren iraultzarekin bat dator; izan ere, metodo zientifikoak bereganatu zituenean kristalizatu zen (Kristiansen, 2014). Google-k indexatutako liburuetan bilaketa batek

argi islatzen du fenomeno hori (ikusi 1.3. irudia). Gainera, terminologiaren bilakaera ikus daiteke kontzeptu bera adierazteko. Grafikoak 2008. urtera arte indexatutako liburuen emaitzak baino ezin ditu erakutsi. Hala ere, "Archaeological Science"-k 52 milioi emaitza ematen ditu, eta "Archaeometry"-k, berriz, 720.000 emaitza. Beraz, joera horrek gorantz jarraitu duela baiezta daiteke. Hala ere, zientzia arkeologikoaren terminologia zabalagoa da, eta horrek ere eragina du emaitza horietan.

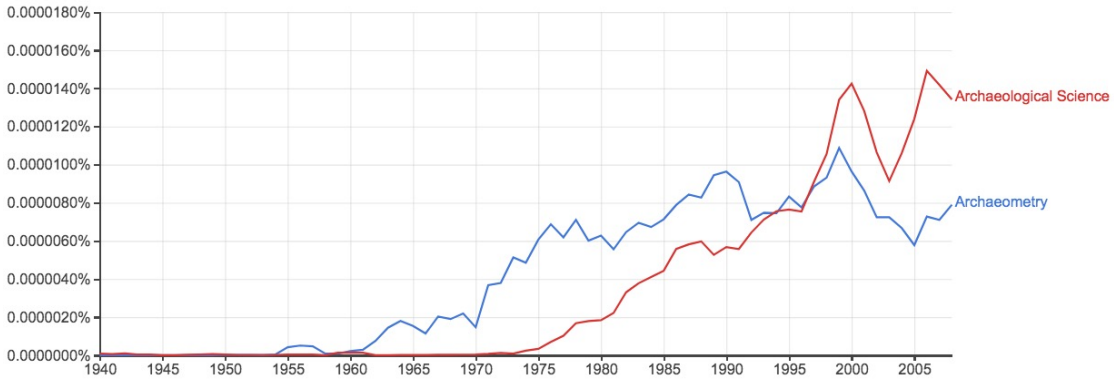

Figure 1.3: "Archaeometry" eta "Archaeological Science" terminoen bilakaera Google-k indexatutako liburuak kontutan hartuta 2008ra arte. y-ardatzean, bakoitaren erabileraren ehunekoa azaltzen da Ingelesez idatzitako liburuei dagokionez. Grafikoa berregiteko hurrengo url-ra joan: `http://goo.gl/3Fq6VH`

Zeramikaren ikerketa arkeometrikoari dagokionez, hastapenetan nabarmenak izan ziren analisi petrografikoak. Eredu gisa Sheparden lana daukagu, (Shepard, 1948); gero, analisi kimiko aurreratuagoekin berraztertuko zen (Neff and Bishop, 1988; Neff, 2003). Era berean, *Ceramics for the Archaeologist* liburuak arkeologoentzako erreferentzia gisa funtzionatu zuen, zeramikaren analisiaren printzipioak eta estrategiak argi eta garbi ezarriz (Shepard, 1956). Gainera, *Pottery Analysis: a source-book* liburuan, ekoizpen-teknologiak eta zeramikaren analisiak sakonago estaltzen zituen erreferentzia-gida osatu bat eskaini zuen Prudence Ricek (1987). Azkenekoz argitaratu zenetik goitik behera berridatzi da, eta duela gutxi argitaratu da bertsio berritua (Rice, 2015).

Geroago jorratzen den bezala, aipatu beharra dago arkeometriaren zutabe nagusi bat zeramiken analisi kimikoek osatzen dutela, bai pasten (gorputz zeramikoen) analisiari dagokionez, bai beiratu edota estaldurei dagokienez. Gainera, beste propietate fisiko batzuk aztertzea (besteak beste, sendotasuna, erresistentzia termikoa eta gogortasuna) oso garrantzitsua da zeramikei buruzko ulermen handiagoa lortzeko (Tite et al., 2001).

Izan ere, propietate horiek eragin zuzena dute produktuak izango duen erabilgarritasunean (adib., material erregogorrak edota eraikuntzarako gogortasun handiko materialak). Ildo horretan, berebiziko garrantzia du beiratuen azterketak. Izan

ere, haien aplikazioa estuki loturik dago garapen teknologikoekin (Tite et al., 1998; Pérez-Arantegui et al., 2001b,a)). Orobat, bestelako lan asko argitaratu dira zeramiken beste alderdi batzuei buruz, hala nola mineralek baldintza desberdinen pean dituzten eraldaketak (adib., (Maritan et al., 2006; Maggetti, 1981)), edota zeramikek jasaten dituzten kutsadurak eta eraldaketak, oinarri sendo bat eskainiz ohiko errutina arkeometrikoetan lortzen diren emaitzen interpretaziorako (adib., Buxeda i Garrigós (1999); Boulanger et al. (2013a)).

Arkeologian metodo zientifikoen inplementazioak eta, bereziki, zeramika-analisiek gorakada handia izan dute azken hamarkadetan. Gainera, gero eta ohikoagoa den diziplinartekotasunak ezaugarritzen ditu lan horiek. Horrela islatzen dute azken urteetan argitaratutako lan zientifikoek. Gaiaren inguruko interesa handitu egin da azken urteetan; argitalpen ugari egin dira, eta aldizkari espezializatuak sortu gaiari buruz, hala nola *Archaeometry*, *Journal of Archaeological Science*, *Journal of Archaeological Science:Reports* eta *Heritage Science*.

Ildo horretan, diziplinarteko hainbat ikuspegi aurkezten dituzten lanak argitaratu dira (Pollard, 2007; Hunt, 2016). Azterlan horietan, materialen zientziei buruzko ikuspegiak ezartzen dira, baina baita arkeologia, antropologia eta geologiako ikuspegiak ere. Gainera, zientzia fisikoek zeramikaren ekoizpenaren, distribuzioaren eta kontsumoaren analisiari egin dioten ekarpena ebaluatu da. Horrek guztiak garbi uzten du bi arloak erabat integratu direla azken urteotan (Tite, 1999).

Are gehiago, arkeologo teorikoaren eta arkeologo zientifikoaren arteko erabateko fusio osoa planteatua izan da (Martinón-Torres and Killick, 2015). Era berean, badirudi joera berriak azaleratzen ari direla, ikuspegi arkeometrikoen potentzialari buruzko berrikuspen kritikoekin, gizarte-ereduak adierazteko (Roux, 2019), hala nola zeramiken konposizio-aldakortasunak gizartearekin dituen loturak sakonago aztertzen dituzten lanak (Buxeda i Garrigós and Madrid i Fernández, 2017; Fowler et al., 2019).

Espainiako egoerari dagokionez, duela gutxi zeramikaren analisi arkeometrikoaren heltze-mailaren berrikuspen bat argitaratu da, Erdi Aroan zentratua (Grassi and Quirós, 2018). Zeramikari buruzko argitalpenak nabarmen ugaritu ziren laurogeita hamarreko hamarkadan, ikuspegi arkeometrikoekin. Horren erakusgarri da eremu honetan argitaratu diren lan zientifikoen bolumen handia; besteak beste, tesi ugari, hain zuzen ere, Kataluniako esparruan bultzada berezia izan dutenak.

Horren adibide dira Buxeda i Garrigósen Cluniako *Terra Sigilatari* buruzkoak, besteak beste (Buxeda i Garrigós, 1994; Buxeda i Garrigós, 1995, 1999; Buxeda i Garrigós et al., 2003; Buxeda i Garrigós, 2008), Molerarenak (Molera et al., 1997, 1999, 2001) edo Vendrellenak (Vendrell et al., 2000), bi egile horiek beiratuen analisian egin dituzten ekarpen nabarmenak barne. Horren haritik doaz Iñañezek maiolikari buruz egindako lanak (Iñañez et al., 2010, 2013). Azken horiek berebiziko garrantzia izan dute Iberiar penintsulako maiolika zeramikaren bilakaera ulertzeko, eta, zerrenda luzeagoa

bada ere, Kataluniako azken lanak aipatuko ditugu; esaterako, Puig Puig (2016) eta Fernandezek (Fernández de Marcos, 2018) berriki argitaratutako doktorego-tesiak. Bi lanotan, hurbilketa arkeometrikoak erabiltzen dira zeramiken jatorrizko analisiak egiteko; Euskal Herriari buruzkoak lehenengo kasuan, eta Sevillako ekoizpenei buruzkoak, berriz, bigarren kasuan.

Errioxako eta Euskal Herriko arkeometriaren egoerari buruzko literatura espezifikoa kapitulu honetako azken atalean jorratuko da. Oraingoz, arkeometriaren literaturari buruzko ikuspegi orokor bat eman nahi izan da, teknika arkeometrikoen egungo egoeraren ikuspegi zehatza lortzea ezinezkoa dela onartuz. Arkeometriako joera internazionalak biltzen dituen sintesi on baterako, ikus Montero Ruiz et al. (2008). Bertan, arkeologiako azterlanetan arkeometriak duen rola jorratzen da, horretarako bibliometriako analisi sakon bat eginez. Gainera, egileak bi puntu nagusi identifikatzen ditu, arkeometriaren garapen egoki baterako, ondoren beste egile batek ere berrikusi eta gogorarazten dituenak Grassi and Quirós (2018). Lehenik eta behin, maila guztietan trebakuntza-beharra nabarmentzen da. Batetik, espezialistek datuak eskuratzeaz eta haien interpretazioa balioztatzeaz arduratu behar lukete. Bestetik, historialariek eta arkeologoek oinarrizko trebakuntza sistematiko bat jaso behar lukete, espezialisten emaitzen jasotzaile nagusiak baitira, eta, aldi berean, adituak gidatu behar baitituzte ikerketa-ildoak lantzen eta ikerketa-arazoak konpontzen. Horrez gain, erakundeen aldetik, beharrezkoa litzateke arkeometriaren aintzatespen handiago bat izatea, bai unibertsitatean, bai ikerketa-zentro publikoetan. Izan ere, oro har, haien bidez ezagutzen ditugu gizarte-zientziak eta zientzietako langileen kurrikulumen konfigurazioak. Halaber, inbestitzearekin lortzen da aintzatespena, bai itzal handiko adituengan, bai laborategi eta hornikuntza zientifikoan. Horrela, behingoz, Arkeometria arkeologiaren ezagutza-esparru gisa agertzen da Montero Ruiz et al. (2008).

Teknika analitikoen bilakaera

Aurreko lerroetan, joera arkeometrikoak eta literatura berrikusi dira. Hurrengo lerroek zeramikaren konposizio-analisiak eta egungo estrategiak jorratzea dute helburu. Bigarren iraultza arkeologikoari dagokionez, 50eko hamarkada energia nuklearraren agerpenaren lekuko izan zen (Kristiansen, 2014; Perlman and Asaron, 1969). Arkeologia-interpretazioek bide berriak hartu zituzten, eta analisi-metodo zientifiko berriak asimilatu, kimika (aztarna-analisiak), biologia (polenaren analisiak), geologia (asentamendu-ereduak), etab. barne hartuta.

Orduz geroztik, analisi zeramikoak teknika analitiko suntsitzaileak erabiltzearen mende egon dira (Pollard, 2007; Glascock, 2016; Arantegui, 2018). Besteak beste, teknika nagusi hauek erabili dira: neutroien aktibazioaren analisia (NAA), absortzio atomikoaren espektrometria (AAS), induktiboki akoplatutako plasmaren emisio atomikoaren espektrometria (ICP-AES), eta induktiboki akoplatutako plasmaren

masa-espektrometria (ICP-MS) (Pollard, 2007; Hunt, 2016). Denetan berriena ICP-MS da, nahiz eta teknika horrek lagina osorik edo partzialki suntsitzea eskatzen duen (analisi zeramikorako 250 mg inguru erabiltzen dira). Gainera, laginaren manipulazio- eta erauzketa-teknikek eragina izan dezakete azken emaitzetan (Boulanger et al., 2013a), eta oraindik ere erronka dira laginaren aurretratamenduan zehar gertatzen diren kutsadura-arazoak (adib., digestio azidoa edo fusio alkalinoa) eta konposatu berriak gehitzeak (adib., $LiBO_4$ fusio alkalinorako) eragin ditzakeen interferentziak. Hala ere, saiakerak egin dira antzeko matrizeetan eragin horiek ahalik eta gehien murriztu daitezen (Madinabeitia et al., 2008).

Bestalde, gorakada handia jasaten ari diren bestelako hurbilketa analitiko suntsitzaileak analisi isotopikoan oinarritzen dira (adib., Habicht-Mauche et al. (2002)), edo laser bidezko ablazioan (Neff, 2012; Resano et al., 2005; Giussani et al., 2009). Gainera, Raman espektroskopian oinarritutako lanak, eta bereziki, haiek zeramiken azterketan duten aplikagarritasuna ere jorratu dira (Colomban and Treppoz, 2001; Colomban, 2003; Colomban et al., 2004; Colomban, 2008). Bestalde, beste teknika espektroskopiko batzuk LED argi-iturri desberdinetan oinarrituta daude (adib., (Mounier et al., 2016)).

Hala ere, gaur egun ICP-MS da teknika egokienetarikoa, jatorri-analisia egiteko, aldi bereko kuantifikazioa ematen baitu, detekzio-muga egokiekin. Gainera, NAArekin alderatuz, askoz ere merkeagoa eta eskuragarriagoa da ICP-MS analisiak burutzeko behar den azpiegitura (Arantegui, 2018). Doktorego-tesi honetan egindako konposizio-analisi gehienak teknika honen bidez egin ziren.

Aitzitik, hamarkadetan zehar Neutron Activation Analysis (NAA) zeramikei aplikatu ondoren (Glascock Michael D and Neff, 2007), mundu osoko eskualde eta kronologietako milaka zeramika-zatikiren konposizio-datuak biltzen dituen datu-base bat eraiki da (ikus 1.4. irudia). Ildo horretan, XIV.-XVIII. mendeetako Iberiar penintsulako maiolika zeramika garrantzitsuenak karakterizatu ziren teknika horren bidez (Iñañez et al., 2008). Datu horiek doktorego-tesi honetan erabili dira hain zuzen, aztertu diren zeramiken jatorriekin erkatzeko. Horren ondorioz, Errioxako eskualdean agertutako zeramika exogenoak identifikatu dira.

Figure 1.4: MURRen dauden karpetak aztertutako zeramika erregistroekin, mundu osoko jatorriak bilduz. CC BY NC SA E. Calparsoro

Azterketa ez-Suntsitzailearen Bidean

Hurrengo lerroek XRF tekniketan oinarritutako konposizio analisien bilakaera jorratzen da. Horren helburua, 6. kapituluan aurkeztutako emaitzak eta eztabaida testuinguruan kokatzeko beharrezkoak diren aurrekariak eskaintzea da. Arestian aipatu diren teknika analitikoez gain (ICP-MS, NAA, etab.), zeramikaren analisiari dagokionez, gaur egungo hurbilketa kuantitatibo ugari, X izpien fluoreszentzian (XRF) oinarritzen dira (Hunt, 2016; Hunt and Speakman, 2015; Millhauser et al., 2011; Speakman and Steven Shackley, 2013; Kuhn and Sempowski, 2001). Izan ere, lagin-prestaketaren kostu txikiak eskatzen dituzte, eta elementu anitzen aldibereko determinazioa eskaini dezakete, 10 baino altuagoko zenbaki atomikoa duten elementuetan, hau da Na-tik gora abiatuz (Pollard, 2007; Speakman and Steven Shackley, 2013).

Gaur egun, zeramikari analisiari dagokionez, XRFaren hiru konfigurazio nagusi erabiltzen dira: guztizko islapena (TXRF), uhin-luzeraren bidezko sakabanaketa (WD-XRF) eta energia sakabanatzea (ED-XRF). Kasu guztietan, X izpi eta lagin-azaleraren arteko elkarrekintzatik sortutako erantzuna erregistratzen da. Hori lortzeko geometria edota ezaugarri desberdinak dituzte konfigurazio bakoitzak. Hori dela eta, ebazpen eta gaitasun desberdinak eskaintzen dituzte. Gainerakoekin alderatuz, TXRFren abantaila nagusia matrize-efektuen murrizketa da. Dena den, oraindik ere lagin-prestaketa eskatzen du. Oro har, partikula solidoen suspentsioa beharrezkoa izaten da likido eramaile batean (Fernández-Ruiz and García-Heras, 2007; García-Heras et al., 2001; García-Florentino et al., 2018). Zeramiken azterketari

dagokionez, teknika honen aplikazioaren hainbat lan argitaratu dira azken hamarkadetan (García-Heras et al., 2001; Cariati et al., 2003; Vanhoof et al., 2018).

WD-XRF sistemek 5 eV eta 20 eV arteko lan-ebazpenak eman ditzakete, beren konfigurazioaren arabera, eta ED-XRF sistemek 150 eV edo gehiagoko ebazpenak ematen dituzte, erabilitako detektagailu-motaren arabera. WD-XRFren bereizmen handienak abantailak ematen ditu espektro-gainezarpenak murriztean, eta, beraz, lagin konplexuak zehaztasun handiagoz karakterizatu daitezke. Gainera, zarata era nabarmenean murrizteko aukera dute, sentsibilitatea eta detekzio-mugak hobetuz. Hala ere, WD-XRF sistema baten osagai optiko osagarriak (adib., difrakzio-kristalak eta kolimadoreak) sistemaren eraginkortasuna jaitsiarazten dute. Hori konpentsatzeko, normalean, potentzia handiko X izpien iturriak erabiltzen dira, kostuan eta erabiltzeko erraztasunean eraginez. Horrenbestez tresna garezti samarrak izaten dira WD-XRFan oinarritutakoak. Gainera, konfigurazio horrekin espektroaren lortzeko puntu bakoitzeko egiten da (denbora asko kontsumituz), edo, bestela, aldi bereko detektagailuen kopuru oso mugatua du (hori aukera oso garestia izanik). ED-XRF-arekin, aldiz, espektro osoa aldi berean hartzen da, eta, beraz, taula periodikoko elementuak gehienak segundo gutxitan detekta daitezke.

Oro har, ED-XRF eta WD-XRF hedatuagoak daude zeramika arkeologikoen analisian. Masa lagin txikiak behar baitira (gutxi gorabehera 300 mg-tik gramo batzuetara). Horiek, bolatxo homogeneoetan (ingelesez *pellets*) konpaktatuta, edo perletan, elementu gehiengoen determinazio zehatzak eman ditzakete (Na, Mg, Al, Si, K, Ca eta Fe), hala nola, elementu gutxiengoena (Ti, P, S eta Mn), eta aztarnena (V, Ni, Cu, Zn, Br, Rb, Sr, Ba eta Pb) (De Vleeschouwer et al., 2011; Speakman et al., 2011). Askotan, "benchtop" edo finkatuta dagoen ED-XRFa nahiago izaten da, nahiz eta WD-XRFek detekzio-muga (LOD) hobeagoak eskaintzen dituen. Izan ere, lehenengoarekin konfigurazio batzuk erabiltzean, ez da laginaren prestaketarik behar (adib., birrintzea). Nolanahi ere, prestaketa minimo bat gomendagarria da, horrela azaleraren kutsadura saihesteko.

Ekoizpen-propioko WD-XRF espektrometroetan albo-ebazpen baxuetako (mikroi-mailan) neurketak lortzera iritsi daiteke, betiere optika polikapilarrak erabili. Hala ere, askotan ekipo komertzialak ez dira gai X izpi-sortaren diametroa mikroetaraino murriztezko, eta eskala milimetrikoan bakarrik neurtu dezakete. Gaur egun, aldiz, ED-XRF espektrometro komertzial eta konbentzionalek 25 μm-ko neurketak egitea ahalbidetzen dute (Ohmori et al., 2012).

Gainera, pXRF (XRF eramangarria) erabiltzen duten lanak ere gora egiten ari dira (Palumbo et al., 2015; Sheppard et al., 2011). Hala ere, tresnetan ezarritako kalibrazioek maiz ez dira aldakorrak, eta gailu batzuen softwareak ez dute ematen datu-tratamendurako aukerarik, eta, beraz, kutxa beltz moduan funtzionatzen dute. Kasu horietan aukera bakarra espektroak atera eta kanpoko software batean tratatzea da. Beraz, askotan ez dute behar bezala islatzen zeramika-matrizeen errealitatea.

pXRF gailuen azken bertsioek elementu arinen detekzio mugak hobetu dituzte, eta, kasu batzuetan, hutsean edo He atmosferan neurketak ere ahalbidetzen dituzte, horrela, elementu horien LODak oraindik eta gehiago hobetuz. Literaturan, analisi zientifikorako pXRF aplikagarritasuna luzez eztabaidatua izan da (Hunt and Speakman, 2015; Speakman and Steven Shackley, 2013; Speakman et al., 2011; Forster et al., 2011).

Doktorego-tesi honetan, hurbilketa ez-suntsitzaile bat garatu da, automatikoki aldakorra den kolimazio bikoitzeko sistema batekin ekipatutako ED-XRF gailu finko bat erabiliz, 1 mm-ko eta 25 μm-ko albo-ebazpenak eskaintzen dituenak (ikus 6. kapitulua). Proposatutako bahetze-metodologia honen helburua, ohiko metodo analitikoekiko hainbat abantaila eskaintzen dituen alternatiba sendo eta fidagarria aurkeztea da.

Ikerketa-berregingarritasuna, kode irekia eta R

Hurrengo lerroetan, kode irekia eta ikerketa-berregingarritasunak zeramiken konposizio-azterketan duten papera jorratuko da. Kontzeptu horiek hertsiki lotuta daude eta erronka zailak planteatzen dituzte; ez bakarrik arkeologian, baizik eta ezagutzaren kudeaketari buruzko beste arlo askotan ere. Kristiansenek (2014) proposatu zuen hirugarren iraultzara itzuliz; hau da, Big Data eta kuantifikazio-ereduena[4], bai kode irekia, bai ikerketa-berregingarritasunak ere funtsezko zeregina dute arkeologiaren egungo paradigma aldaketan.

Digitalizazioak ezagutza zientifikoaren kudeaketa zeharo eraldatu du. Lehendabiziko aldiz, ikerketen atzeko prozedurak partekatzea ahalbidetu baitu (adib., analisi estatistiko bat egiteko erabilitako kodea). Horrek ekarpen nabarmena eragin dio ikerketa zientifikoari, haren fidagarritasuna eta eraginkortasuna hobetuz. Izan ere, digitalizazioari esker ikerkuntzako prozedurak kontsultatu, ebaluatu eta berrinterpretatu daitezke (Stodden and Miguez, 2014; Goodman et al., 2016; Munafò et al., 2017). Halaber, konputazio-zientziak gero eta hedatuago daude ikerketa-eremu guztietan, baita Arkeologian ere. Horrela, egungo egoeran, arlo gehiagoetara zabaldu daiteke ikerketa konputazionalaren berregingarritasun-espektroa (ikus 1.5. irudia). Nahiz eta erabateko berregingarritasuna egoera egokiena izan, sarritan prozesu metodologikoak ez dira elkarbanatzen, zientziaren eta arkeologiaren aurrerapena oztopatuz. Joera horren arrazoi nagusia, metodo berregingarrien inguruko praktika ez-egokiak lirateke (Munafò et al., 2017).

Ikerketa-berregingarritasunaren terminologia eta esparru kontzeptuala oraindik ez dira estandarizatu hainbat ezagutza-eremuetan. Egoera horri aurre egiteko, duela gutxi

[4]Hirugarren iraultza arkeologikoa lotura du DNA eta analisi isotopikoekin baita ere. Hala ere, gai horiek ez daude doktorego-tesi honen ikerketa esparruan, beraz, ez dira jorratuko.

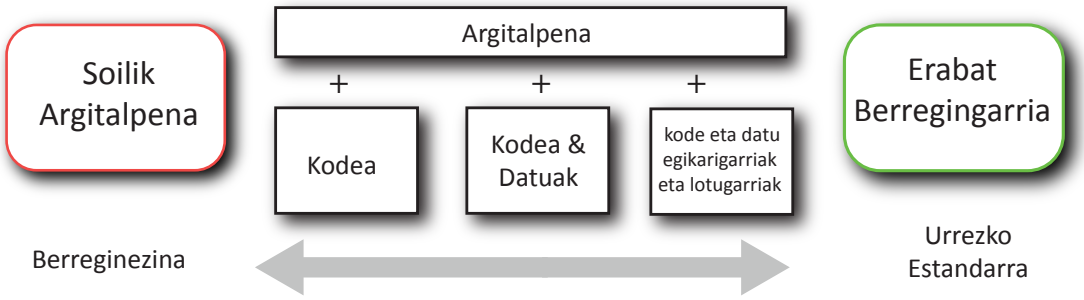

Figure 1.5: Ikerketa konputazionalaren berregingarritasun-espektroa. Beste lan batetik moldatuta (Peng, 2011).

berregingarritasunari buruzko terminologiaren berrikuspen bat argitaratu zen (Goodman et al., 2016). Bertan jorratzen diren definizioen artean, lan honen testuingururako esanguratsuenak aukeratu ditugu.

Ildo horretan, gaur egun eskura dugun softwarea erabiliz, gure ikerketaren emaitzak sarbide irekiaren bidez (*open access*) partekatzeko aukera dugu. Bestalde, metodo irekien bidez (*open method*), datuak manipulatzeko eta bistaratzeko erabiltzen diren errutinak ere partekatu daitezke. Hori gutxi balitz, zuzenean datuak gordinik ere argitaratu daitezke, datu irekiak edo *open data* deritzegu haiei (Marwick, 2017; Marwick et al., 2017). Egoera berri honek ikerketa berregingarri eta gardena sortzeko aukera ematen du, kolaboraziozko filosofia sustatuz.

Beste era batera esanda, *metodo irekia* prozedura bat zehatz-mehatz errepikatua izan dadin xehetasun nahikoak ematean direnean sortzen da, horrela, metodoaren erabateko berregingarritasuna bermatuz. Ildo horretan, doktorego-tesi honetan metodo ireki bat aurkezten da zeramika arkeologikoaren konposizio-analisia egiteko lan-fluxua proposatzen duena (ikus 4. kapitulua). Haren iturri-kodea biltegi batean biltzen da (ikus 4. kapitulua). Biltegi hori online eskuragarri dago GitHub plataformaren bidez[5]. Era horretan, arkeometriako zientzialarien komunitatea horrelako tresnekin lan egitera bultzatzea da helburua. Metodoa maila hasiberriko erabiltzaileentzat zuzendurik legoke, zeinak bestelako ezagutzarik gabe prozesuak berregiteko gai izan beharko lirateke. Baina, era berean, adituek ere erabili dezakete, script-ak aldatzeko aukera baitago. Horrenbestez, ikerketaren beharretara hobeto egokitzeko aukera ematen da.

Metodologia berregingarrien bidez, proposatutako metodoak *A manifesto for reproducible research* ikerlanean jasotako giltzarria jasotzen ditu (Munafò et al., 2017). Besteak beste, metodo irekien garapena eta partekatzea. Halaber, uztartzen ditu beste azterlan batzuetan ikerketa berregingarrirako egokitzat jotzen diren elementuak (Sandve et al., 2013; Stodden and Miguez, 2014). Gainera, gero eta argitalpen gehiago

[5] `https://github.com/esteful/arch_flow`

dira horrelako praktika berregingarriak bultzatzen dituztenak. Esaterako, aldizkari ugarik, estatistiketarako erabili den R kodea bidaltzeko aukera ematen dute (adib., *Journal of Statistical Software*). Testuinguru horretan, *Knitr* edo *Sweave* tresnak oso baliagarriak dira. Izan ere, LaTeX dokumentuetan R kodea ulergai egiten dute. Hori dela eta, kodearen exekuzio-emaitzak zuzenean renderizatzen dira amaierako argitalpenean eta horrek, gardentasun handia ematen dio prozesuari. Ildo horretan, datuen eskuragarritasunak ere funtsezko zeregina du, praktika guztiz berregingarriak izan daitezen. Zeramiken konposizio-analisietan, gainera, datu berriak datu baseetan daudenekin konparatzen dira behin eta berriro. Horrenbestez, erabiltzeko prest dauden datuen eskuragarritasuna nahitaezkoa bihurtzen da (Boulanger, 2017).

Antza denez, esparru akademikoan, oraindik ez dira ondo ulertzen arestian aipatutako kontzeptuak (sarbide irekia, metodo irekia, etab.). Aitzitik, egungo ikerketak finantzatzen dituzten erakundeek kontzeptu horiek jasotzen dituzte beren gidalerroetan; esaterako, H2020, non sarbide irekiaren bidez argitaratzea nahitaezkoa den. Berrikusketa labur bat egitearren, kode irekia edo *open source* delakoa, iturburu-kodea mota bat da zeina, ikuskatzeko, berrerabiltzeko edota banatzeko aukera ematen duen. Hura doan edo kostupean (adib., R, Linux edo LaTeX softwareak) eman daiteke(Marwick, 2017). Horrenbestez, ez da kostu ekonomikoarekin lotutako kontu bat, iturri-kodearen gardentasunari buruzkoa baizik. Beraz, software irekia ez du zertan doakoa izan beharrik, eta alderantziz, software pribatiboa doakoa izan daiteke, maiz gertatzen den bezala. Hortaz, kodea ikuskatzeko ematen den aukeran datza desberdintasun nagusia. Ikuskatzeko aukera ematen bada ere, horrek ez du esan nahi software hori nahi erara erabiltzea dagoenik. Hainbat lizentzia mota daude erabilera hori zehazteko, atribuzio desberdinak dituztenak. Lizentzia horiek eskaintzen dituzten irekiera-mailaren arabera desberdintzen dira, hau da, informazioa partekatzeko ematen duten aukeren arabera. Honako hauek dira ezagunenak: Creative Commons (ccw, 2019); bereziki softwarerako diseinatutako MIT lizentziak (MIT, 2019); eta, azkenik, General Public License litzentziak, GPL edo GNU-GPL laburduren bidez ezagutzen direnak (GPL, 2019). Doktorego-tesi honetan garatutako koderako GPL lizentzia aukeratu da, 3.0 atribuzioarekin (ikus 4. kapitulua). Lizentzia horrekin lana erabiltzeko, aztertzeko, partekatzeko edota aldatzeko aukera ematen da. Gainera, eratorritako lanek lizentzia berdina erabiltzera behartuta daude. Aipatu beharra dago kodearen garapena beste egile batzuen kodean oinarritu dela. Hala nola, atal nabarmen batean abiapuntutzat erabili da Buxeda i Garrigósek idatzitako kodea. Kasu honetan, egileak ez du soilik zeramika arkeologikoen analisirako kodea garatu, baizik eta ekarpen teoriko nabarmenak egin dizkio konposizio-datuen estatistika-analisiari (Buxeda i Garrigós, 2008; Buxeda i Garrigós and Kilikoglou, 2003; Martín-Fernández et al., 2015). Hala nola, beste egile batzuen software zatiak ere erabili izan dira, betiere, dagozkien erreferentziekin.

Aipatutako lizentziek eskaintzen dituzten elkarlanerako aukeren ondorioz, Arkeologiari era espezifikoan ezartzen zaizkion tresna asko sortu dira azken urteotan. Izan ere, software pribatiboarekin alderatuz, software askeak rol garrantzitsua jokatzen

du kode-garapen kolaboratiboaren esparruan. R programazio-lengoaia horren erakusle on bat da. Arkeologiari dagokionez, 2017an *R is for Archaeology* saioa ospatu zuten *Society of American Archaeologyk* arlo horretan azpimarratuz R programazio-lengoaiaren duen potentziala (Ris, 2017). Horren ondorioz, Arkeologian aplikazioa duten R software-paketeen zerrenda zabala garatu zen. Bestalde, horrelako jarduerekin erlazionatutako ekimenak, esaterako Open Science Interest Group (OSIG) delakoak, komunitate baten beharrari erantzuten dio, arkeologoei parte hartzen eta praktika zientifiko irekien onurak lortzen laguntzeko (Marwick et al., 2017).

Gaur egun, geroz eta lan gehiagotan partekatzen da erabilitako kodigoa (adib., (Carlson, 2012; Alberti, 2013; Baxter, 2015)). Azpimarragarria da, esate baterako, Baxterrek argitaratutako lana *Notes on Quantitative Archaeology using R* izenburuarekin. Lan honek, izugarri erraztu du R-ren erabilera arlo arkeologiko batzuetan, eta hemen aurkezten den lanaren inspirazio ere izan da. Era berean, konposizio-datuei erreparatuz, R kodearen xehetasun nahikoa ematen du, metodoak berregin ahal izateko. Ildo horretan, berriki argitaratu den argitalpen batek hainbat protokolo estatistiko aurkeztu ditu, Kataluniako ardo erromatarren anforen ekoizpenen datu kimikoak eta petrografikoak integratuz (Angourakis et al., 2018). Alde batetik, lan honetan, R *script*-ak material gehigarri bezala aurkezten dira; bestetik, bi pakete garatu dira R-n instalatzeko zuzenean eskuragarri daudenak. Gainera, kode irekiko tresnen izaerak hobetu egiten du *ad hoc* baliabideen diseinua, pertsonalizazio maila altuarekin. Seguruenik, konposizio-datuen analisi aurreraturako R lengoaian idatzitako pakete garrantzitsuenetako bat "Compositions" izenekoa da (Boogaart et al., 2010). Pakete honetan sartzen diren funtzioak konposizio-datuen berariazko beharretara egokituta daude, zenbait hurbilketa estatistiko barne. Horietako batzuk egungo lanean erabiltzen dira (adib., datuen alr eta clr eraldaketak).

Doktorego-tesi honetan, ekarpen metodologiko bat egin da kode irekiko R programazio-lengoaian oinarrituta, 4. kapituluan jorratzen dena. Horren ondorioz, GitHub[6] webgunean biltegi bat sortu da, berregite osoa burutzeko behar den kode guztia eskainiz. Proposatutako metodologiaren errendimendua zeramika erromaniko-britainiar datu-multzo ezagun baten adibidearekin frogatzen da (Tubb et al., 1980). Emaitza gisa, metodo ireki bat eskaintzen da zeramiken analisi arkeometrikorako diseinaturik. Horren bidez, sustatu egiten dira kode irekiko tresnetan oinarritutako ikerketa-ekimenak. Gainera, doktorego-tesi honetan aurkeztutako analisi kimiometrikoak egiteko, metodo horretan erabilitako prozedurak erabili dira, beraz atal horretan erabilitako prozedurak era zabalago batean jorratzen dira.

[6]GitHub elkarlaneko softwarearen garapenerako proiektuetarako mundu-mailako plataforma handiena da.

1.3 *Errioxako eta Euskal Herriko buztingintza ekoizpena*

Atal honetan, Euskal Herriko eta Errioxako orain arteko azterlan arkeometrikoen egoera aztertzen da. Helburua 5. kapituluan aurkezten diren kasu-azterketen testuingurua aurkeztea da. Aipatutako kapituluan Logroño, Nájera, Orduña, Durango eta Elosuko buztingintza-lantegien ezaugarritze arkeometrikoa lantzen da. Haren bidez, hobeto ulertu nahi dira Erdi Aroan eta Erdi Aro osteko giza dinamikak eta sare komertzial eta teknologikoak hobeto. Ikerketa tokiko zeramiken azterketa arkeometrikoan oinarritzen da, bai jatorri-analisien ikuspuntutik, bai teknologiari erreparatuz ere.

Iberiar penintsula buztingintza tradizionala —artisautza gisa— desagertzeko denbora gehien behar izan duen gunea da, Mendebaldeko Europari erreparatuz. Azken hamarkadetan esku hartu da haren zainketaren kontzientzia handiagoz eta, ondorioz, zeramikazko objektu herrikoien bilduma bat sortu da estatu mailan, material eta datuak biltzeko programa zientifiko batzuen laguntzaz. Hala nola, estatuko geografia osoan barreiatutako buztingintza-museoen sorrera ere. Eskualde batzuk aktiboagoak eta kontzienteagoak izan dira. Esate baterako, Katalunia jarduera gehienak burutu dituen eskualdea izan da, hari jarraiki, Euskal Herria eta ondoren Valentzia, Aragoi, Gaztela Mantxa, Errioxa, Galizia, Asturias, Gaztela eta Leon eta Extremadura (Pleguezuelo, 2016). Tamalez, estatuko testuingururik zatituenetako bat da Iberiar penintsulako buztingileen ezagutza historiko nahiz arkeologikoa, ekoizpen zeramikoari dagokionez. Penintsulako iparraldean, Erdi Aro eta Aro Modernoko euskal zeramika-erregistroa oso gutxi ikertu da, gainerako eskualdeekin alderatuz gero. Gaur egungo erregistroen arabera, hobeto ezagutzen dira Bartzelona, Valentzia, Aragoi edo Sevillako lantegietan ekoiztutako artefaktuak, iparraldeko guneenak baino. Are gehiago, zenbait kasuetan, kanpoan hobeto ezagutzen dituzte, hemen ekoiztutako zeramikak. Beraz, agerikoa da ikerketa sakon bat falta dela iparraldeko ekoizpena ondo ulertua izan dadin. Hutsune hori gainditzeko, zeramika horien ekoizpenean parte hartzen duten faktore teknologikoen azterketa zehatza egitea garrantzi handikoa da.

Bereziki, Iberiar penintsulako iparraldean eta erdialdean Erdi Aroko zeramikazko ekoizpenen arkeologia-ikerketen tradizio urri bat sumatzen da penintsulako gainerakoekin alderatuz. Penintsulako zeramika beiratuen kasuan, Gaztela eta Aragoiko koroetan hamabi ekoizpen-zentro identifikatu dira, XV eta XVIII. mendeen artean, baina datu arkeologikoak nahiko urriak dira oraindik (Iñañez et al., 2008). Aipatutako garaiari dagokionez, nabarmentzekoa da ARQUB eta haren kolaboratzaileak abiarazitako ikerketa. Bertan, diziplina anitzeko ikerketa-proiektu desberdinen esparruan, Gaztela eta Aragoiko Koroen ekoizpen-zentro gehienak aztertzeko ikuspegi arkeologiko eta fisiko-kimikoak garatu baitituzte. Lan horiek jatorrizko azterlan sorta zabala eskaintzen dute, zeramikazko gorputzen, pigmentuen eta beiratuen ezaugarri teknologikoak ebaluatuz. Ikerketa-lerro horren adibide ona da Iñañezen (2007) erreferentziazko dokotrego-tesia, Erdi Arotik eta Errenazimendurainoko ekoizpen nagusiak jorratzen dituena. Lan honetan zeramika maiolikoaren lehen ezaugarritze

arkeometriko sistematikoa garatu zen, eta, dokumentazio historikoaren arabera, haren ekoizpena, XVI. mendetik Talavera de la Reina eta Puente del Arzobispo (Toledo) herrietan hedatu zen. Maiolikak kalitate handikoak eta finak ziren, beiratu zuri batez bereiziak. Beiratu hori eztainua eta berunezko nahaste batean datza, eta hainbat oxido metaliko izan ditzake, besteak beste urdin, laranja, manganeso more-beltza eta esmeralda berde koloreak lortzeko. Lan horretan ezarritako RGren zerrendak, maiolika ekoizpen-gune nagusiak hartzen ditu barne: Bartzelona (BCN-B1B2, BCN-B3, BCN-B3, BCN-B3), Lleida, Manises, Muel, Sevilla, Talavera, Teruel, Villafranca de Penedes eta Villafeliche, besteak beste. Horiek oso interesgarriak izan dira doktorego-tesi honetan aztertutako zeramiken jatorri-analisia burutzeko. Horrela, aztertutako zenbait zeramikak Teruel, Muel edo Talavera de La Reina bezalako ekoizpen guneei esleitu zaizkie ebidentzia arkeometriko sendoei esker (ikus 5.2. eta 5.3. atalak).

Orain dela gutxi ARQUBn garatu zen doktorego-tesia ildo honetatik jarraitzen du Talavera de la Reina eta Sevillako lantegietan zentratutako ikerketarekin jarraituz Fernández de Marcos (2018). Antza denez, XVI. mendean, Talavera penintsulako barne-merkataritzaz arduratuko litzake, eta Sevillako lantegiek, berriz, atzerriko zeramika kontsumoa hornituko lukete. Bada, aipatutako lanean, ekoizpen haien ezaugarritze kimikoa burutzen da. Talaverako ekoizpenei dagokienez, aditu askok gogora ekartzen dute bertako zeramikak lantegi askotan imitatu zirela, iparraldea barne (Conesa, 2011). Hala eta guztiz ere, aztarnategietan Talavera-moduko piezak agertzen direnean, maiz Talaverako lantegiei esleitzen zaizkie, ezaugarri estilistiko edo tipologikoetan oinarrituz. Hori dela eta, iparraldeko aztarnategietan aurkitutako pasten ezaugarri kimikoak berebiziko garrantzia du zeramiken identifikazio eta banaketaren berrinterpretazioan.

Oraindik ere oso zatikatuta dago Euskal Herrian ekoiztutako zeramikei buruzko ezagutza. Nahiz eta azken urteotan aurrerapausoak eman diren. Esaterako, Iñañez ikerlariaren zuzendaritzapean, CERANOR (HAR-2013-46853) eta CERANOR-2 (HAR-2017-84219-P) proiektuei[7] esker berriki egin diren ekarpenak. Oro har, ikerketa eskasia handia dago eremu arkeometrikoari dagokionez, Arkeologiaren kasuan, eta bereziki Artearen Historian gertatzen den ez bezala. Ondorioz, erreferentziako multzo gutxi edo bat ere ez dago analisi kimikoetan oinarritutako jatorri-azterketetan erabil daitezkeenak. Lehen hurbilketa arkeometrikoen arabera, euskal zeramikaren errealitatea XVI. eta XVIII. mendeetan espero zena baino konplexuagoa da (Puig and Escribano, 2011; Puig, 2016). Ikus daitekeenez, egoera horrek nabarmen islatzen du joera bat Euskal Herriko aztarnategi arkeologikoen egungo azterlanetan, baina baita Europako eta Ipar Amerikako merkataritza atlantikoan eta euskal baleontzien kokalekuetan ere.

Horrelako azterlanik ez egoteak garrantzi handiko ezagutza-hutsune bat dakar, ezagutza arkeologiko eta historikoaren garapen egoki baterako. Gauza bera gertatzen

[7]Penintsulako ekoizpen-zeramikoen Arkeologiari eta Arkeometriari buruzko proiektuak (XVI. mendetik XVIII. mendera), MINECO/AEI/FEDER erakundeetatik laguntza jasotzen duena.

da Zamoran; bertan, CERANOR proiektuen ekarpenez gain (Sanchez-Garmendia et al., 2018), Pereruelako zeramika garaikideari buruzko azterlan etnoarkeometrikoak baino ez dira ezagutzen (Buxeda i Garrigós et al., 2003; Peacock, 1982).

Errioxako Buztingintzari Buruzko Ikerlanak

Logroñon eta Najeran kokatutako aztarnategiei dagozkie doktorego-tesi honetan aztertutako Errioxako testuinguruak. Bi hiriak Ebro ibaiaren inguruan daude eta 28 km-k banatzen dituzte. Kronologikoki, aztertutako materialak XVI. mendeari dagozkie Najerako kasuan eta, aldiz, XIII-XVIII mende tarteari Logroñoko kasuan. Aldi kronologiko dilatatu honen aurrean, ez du zentzu handirik testuinguru historiko-arkeologiko zabal bat ematea. Hala ere, aztertutako bost ikerketa-kasuen hasieran, testuinguru labur bat ematen da beharrezkotzat jo diren aipamenak eginez. Hori esanda, hurrengo lerroek errioxar eskualdeko buztingintzari buruzko literatura garrantzitsuena estaltzea dute helburu.

Nahiz eta aurreko kronologiei dagokien, aipatzekoa da erromatarren garaian *Tritium Magallum* delakoa, Hispaniako *terra sigillataren* ekoizpen zentro nagusia izan zela. Erromatar hiribildu hori gaur egungo Errioxako Tricio herriari dagokio eta Najeratik 2.6 km-tara kokatzen da. Gainera, azken ikerketek jasotzen duten moduan, *terra sigillataren* ekoizpena ez zen soilik hiribildu horretara eta bere lurraldean kokatutako lantegietara mugatu. Aitzitik, Kalahorra, Varea (egungo Logroño eskualdea), Libia (egungo Herramélluri) eta zenbait hiribilduek beren beharrak asetzeko lantegi propioak omen zituzten. Fenomeno hori behe-inperio garaian sustatuko zen batik bat, Alhama haranean kokatutako Kontrebezia Leukade eta Balsas-eko ekoizpen-zeramikoekin batera (Luezas Pascual, 2014).

Dokumentazio historikotik abiatuta, Errioxako ikuspegi orokor bat eskaini zuen Martínez Glerak (1994), Erdi Aro osteko buztingintza-jarduerei dagokionez. Informazio gehiena Ensenadaren Katastrotik[8] atera zuen. Antza denez, Harok menderatu zuen buztingintza-ekoizpena, eta, pixkanaka, Navarretek ordezkatu zuen. Ildo horri jarraiki, mendeetan zehar zeramika lantegien arteko langile-trukeak ere dokumentatu zituen Glerak. Ez da harritzekoa jarduera handiena Haron jazo izana, non hainbat tokitako ikastunak egon ziren (Martínez Glera, 1994). Hala ere, orain arte ez da aurkitu ekoizpen-zeramikoarekin lotutako egiturarik Haron, nahiz Navarreten.

[8] 1749an Gaztelako Koroan egin zen ikerketa estatistiko eta eskala handiko errolda. Fernando VI.-a Espainiako erregeak, eta bere ministroak agindu zuten. 15.000 leku baino gehiago ebaluatu ziren, baina euskal probintziak, Nafarroa edo Aragoiko Koroa ez ziren kontuan hartu. Biztanleria, lurralde-ezaugarriak, eraikinak, abereak, bulegoak, mota guztietako diru-sarrerak eta lanbideak, eta baita toki bakoitzaren informazio geografikoa ere jaso ziren.

Aitzitik, Logroñon aurkitutako eltzegileen hondakinek[9] agerian utzi zuten Erdi Aroan buztingintza gune desberdinduak egon zitezkeela (Martínez González, 2013). Alde batetik, *Hospital Viejo* kalean; besteak beste, hiru labe, hainbat trebera eta funtzio berdinarekin erabilitako teilak aurkitu ziren (Angulo and Porres, 2015). Bestetik, 2018ko udan beste lantegi bat aurkitu zen *Ollerías* kalean, tokiko buztingintza jarduerari lotutako toponimiarekin bat etorriz eta XVI. mendeari dagokiona (Gil Zubillaga and Luezas Pascual, 2018). Hortaz gain, Nájerako alkazarrean milaka pieza agertu ziren XVI. mendeari esleitzen zaizkionak. Horietatik, eztainu-berunez beiratutako lagin sorta bat arkeologikoki aztertua izan da (Ceniceros Herreros, 2012), eta horietako pieza batzuk arkeometrikoki aztertu dira doktorego-tesi honetan (ikusi 5.3. atala). Oro har, Erdi Aro osteko garaiari dagokionez, Errioxako Arkeologian material zeramiko gutxi ezagutzen da. Besteak beste, dokumentatutakoa zenbait erreskate-indusketetan lortutakoa da. Ildo horretan, pieza horien xehetasunik gabeko deskribapenak edo, gehienez, jatorri arkeologikoko piezak biltzen dituzten katalogoak existitzen dira (Martínez Glera and Álvarez González, 2012; Alvárez Clavijo, 2012). Ebaluazio horiek tipologia eta funtzioa izan dute ardatz. Bestalde aipatutako Logroñoko *Hospital Viejoko* aurkikuntzak, doktorego-tesi baten oinarri ere izan dira (Martínez González, 2013).

Euskal Herriko Buztingitzari Buzuko Ikerlanak

Euskal Herrian industriaurreko tokiko hainbat lantegi ezagutzen ditugu; besteak beste, toponimiari, dokumentazio idatziari, etnografiari edota zenbait ebidentzia arkeologikori esker. Nabarmentzekoa da, Ibabe etnografoak burutu duen lana Euskal Herriko zazpi probintzietako buztingintza dokumentatuz (Ibabe, 1995a,b). Hala nola, buztingintzako lanabesak, labeak edo akatsak dituzten zeramikak oinarritzat hartu izan dira lantegi horiek identifikatzeko (Escribano, 2009). Ildo horretan, duela gutxi, tokiko zenbait lantegi identifikatu ziren. Horretarako hainbat prospekzioetan eta kontsumo zentro desberdinetatik lortutako aztarnak ebaluatuz. Ondorioz, XIV-XVII mendeen artean Buradon Gatzaga, Ollerieta edota Egileta, tokiko ekoizpenaren zatirik handiena menderatuko luketela iradoki da (Escribano, 2014). Gipuzkoan, aldiz, ez dago ekoizpen ebidentziarik XIX. mendera arte. Dirudienez, ez zen erakargarria buztingintzaren lana Gipuzkoako gizartearentzat (Ibabe, 1995a).

Euskal zeramikari buruzko azterlanen artean lehenengoetarikoa Leandro Silvan kimikariarena litzateke (Silvan, 1982). Ondoren, Olaetxea eta Lopez de Herediaren doktorego-tesiak analisi arkeometrikoetan oinarritzen dira, Euskal zeramikaren ekoizpenaren historiaurreko garaiei ekiteko (Olaetxea, 2000; López de Heredia, 2014). Geroago, Solaunek (2005) tresna taxonomiko eta hermeneutikoak garatu zituen Erdi Aroko Euskal zeramikaren erregistroan oinarriturik (VIII-XIII mendeak). Azkenik, Escribanoren doktorego-tesiak (2014) aurreko lanari jarraitutasuna eman zion, XIV.

[9] Gaztelaniaz *testar* eta ingelesez, *potter's dump* bezala itzultzen da.

mendetik XVII. mendera Euskal zeramika-erregistroaren genealogia aztertuz eta Arabako lurraldeari erreparatuz. Hala ere, nahiz eta erreferentziazkoak izan diren aipatutako azkenengo bi lan horiek, ez dira ikuspegi arkeometriko batean oinarritzen. Aitzitik, Erdi Aro eta Aro Modernoari dagokienez, Euskal Herriari buruz egin diren azterlan arkeometrikoen artean, aipatzekoa da Puigen (2016) doktorego-tesia, non euskal zeramikaren lehenengo ezaugarritze arkeometriko sistematikoa burutzen den (Puig, 2016). Hala eta guztiz ere, lan horren ikuspegia kontsumo guneetara soilik mugatzen da. Ondorioz, definitutako PCRUren benetako jatorria oraindik zalantzazkoa da.

Chapter 2

Objectives

As addressed at the introduction (pag. 22), the goals of this work were established within the framework presented in *Designing Rigorous Research* by Buxeda i Garrigós and Madrid i Fernández (2017). Along these lines, this Doctoral Thesis integrates both, the application of well-established archaeometric routines and the development of innovative approaches aimed to solve archaeometric research problems. Both approaches have contributed in a synergistic way during the course of the present investigation (see Figure 2.1). On the one hand, a methodological contribution was conducted, which responds to archaeometric research problems such as the research reproducibility and non-destructiveness of compositional analysis of pottery (objectives 1 and 3). On the other hand, to achieve these goals, an archaeometric characterization of pottery production centers from The Basque Country and La Rioja was carried out (objective 2). Thus, within this transdisciplinary work the specific goals set are the following:

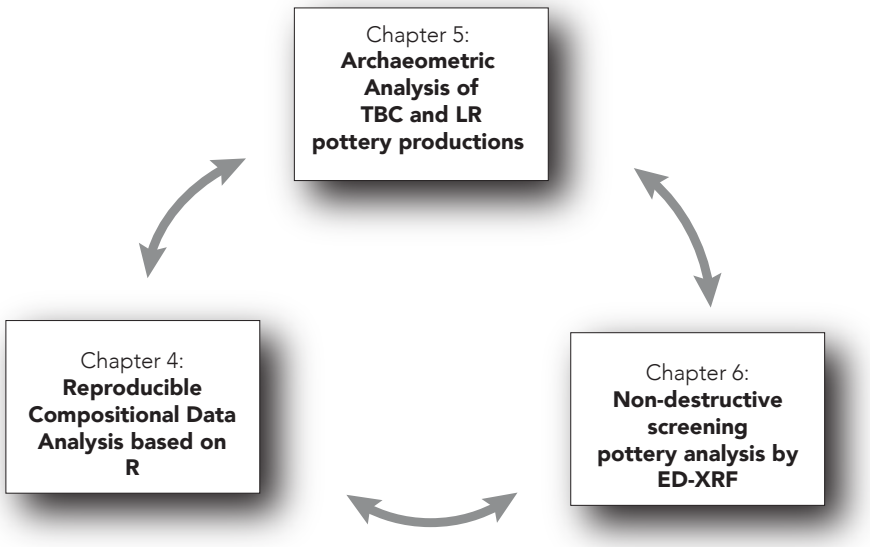

Figure 2.1: The goals addressed in each chapter present synergistic links. TBC: The Basque Country and LR: La Rioja.

1. Develop a reproducible research workflow based on open source software R. The aim of this research inquiry was to set up a basis for the collaborative development of open source tools for the research. Moreover, it intends to engage the scientific community to use such tools, especially those archaeometrists conducting compositional analysis. The results of this goal are presented in the Chapter 4 and in the repository published on the GitHub (`https://github.com/esteful/arch_flow`).

2. The archaeometric characterization of an array of pottery production centers from the northern Iberian Peninsula of medieval and post-medieval period. The results are presented in the Chapter 5 and include the five case studies. The aim of this research was to develop relevant background of knowledge to facilitate the reconstruction and interpretation of the processes involved in the manufacture, use, and post-depositional environment of the ceramics.

3. The exploration of non-destructive strategies for the pottery analysis by ED-XRF. This research inquiry is focused in the development of a non-destructive screening classification methodology for archaeological ceramics and the revision of the specific challenges these kinds of materials present in such analysis. The results are presented in Chapter 6. Moreover a specific publication deals with the content of this chapter (Calparsoro et al., 2019b)

Chapter 3

Materials and Methods

3.1 Ceramic Sample

In this Doctoral Thesis a sample of 347 Ic-s were subjected to archaeometric analysis. In addition, a sub-sample of 47 Ic-s were employed for the development of a non destructive screening methodology based on ED-XRF presented in the Chapter 6. With regard to Chapter 4, a dataset of Romano-British pottery (Tubb et al., 1980) was recycled to illustrate the open methodology presented. On the one hand, the nuances of the Romano-British pottery are out from the purview of this Doctoral Thesis. On the other hand, the 347 Ic-s constitute the main body of the present work. Therefore, in the following lines detailed description of these is presented.

The ceramics were obtained from five different archaeological sites located in the Northern Iberian Peninsula (see Figure 3.1). These sites are located in Logroño and Nájera in the Autonomous Community of La Rioja (LR), and in Orduña, Durango and Elosu in The Basque Country (TBC). Regarding the Basque, the first two correspond to the province of Biscay and the latter to Araba. The archaeological interventions of Logroño and Orduña respond to urgent excavations in plots where construction works had to be performed. These interventions were framed following the laws of 7/2004 of Cultural, Historic and Artistic Heritage of La Rioja and 7/1990 of Basque Cultural Heritage. Moreover, in the cases of Durango and Elosu, prospection works were intentionally carried out in order to obtain a ceramic record to widen the ethnographic knowledge about these production sites (Ibabe, 1995a). The lower archaeological evidence, as well as the availability of materials, resulted in a lower sub-sample selected from the last two sites (see Figure 3.2).

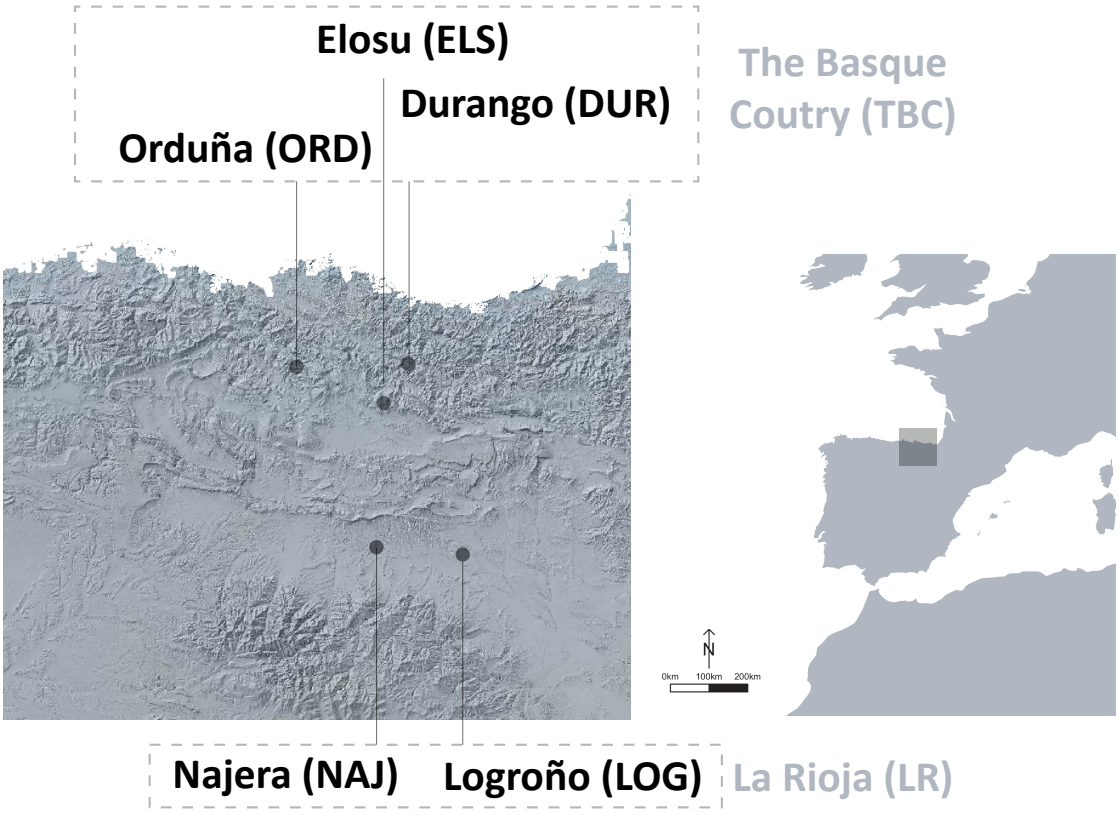

Figure 3.1: Map showing the procedence of the ceramics evaluated and their location.

For the selection of sites, priority was given to those that could be more directly linked to the ceramic production. Beyond the historical and ethnographic and/or toponymy that refers to each site, in the case of Logroño, Orduña and Elosu the crushing evidence was provided by the ceramic kilns in each site. In the former cases these were unearthed, whereas in Elosu the kiln remains erected, being one of the the fewest existing preindustrial kiln that can be visited in the Basque Country (along with the one of Eskoriatza). Regarding Durango, the lack of ceramic workshops identified was partially compensated by the large proportion of kiln-related materials (e.g. trivets or kiln-tubes) found in the site. Finally, for the case of Nájera, exclusively the large assemblage of tableware showing similar typologies could be taken as as basis to assign the subsequent local origin. Note that the findings of Nájera constituted the largest unearthed pottery assemblage corresponding to the post-Medieval period (Ceniceros Herreros, 2004).

The materials from all sites, except Nájera include kiln utensils such as trivets and kiln-tubes, both of them widely used to separate the pieces inside the ceramic kiln during the firing. Moreover, defective ceramics were also regarded, since they normally appear

very close to the pottery workshop where they have been manufactured. In the case of Elosu the oral tradition refers to a 20% of defective pieces in each firing (in which up to 8000 pieces could be fired each time) (Ibabe, 1995a). Thus, approximately 1600 defective ceramics (also called reuses) would be obtained every firing (which in the busiest periods was carried out every two months). In consequence, a high amount of reuses could be expected in the respective pottery workshops, and consider them as production evidence. However, these could also be sold for a lower price or exchanged by other goods in a lesser extent. Thus, a minor fraction of them would have had a radius of distribution, although this was probably very limited.

The Figure 3.2 shows the main typologies of evaluated ceramics, grouped by the sites from where they were obtained. As can be appreciated, overall, the tin lead glazed fraction is the highest, followed by the uncoated and the lead glazed one. In the case of Elosu, some ceramics with lead glazes and slips were also evaluated. The uncoated ceramics were mostly obtained in the earliest contexts of Logroño. The kiln utensils are also regarded within this category.

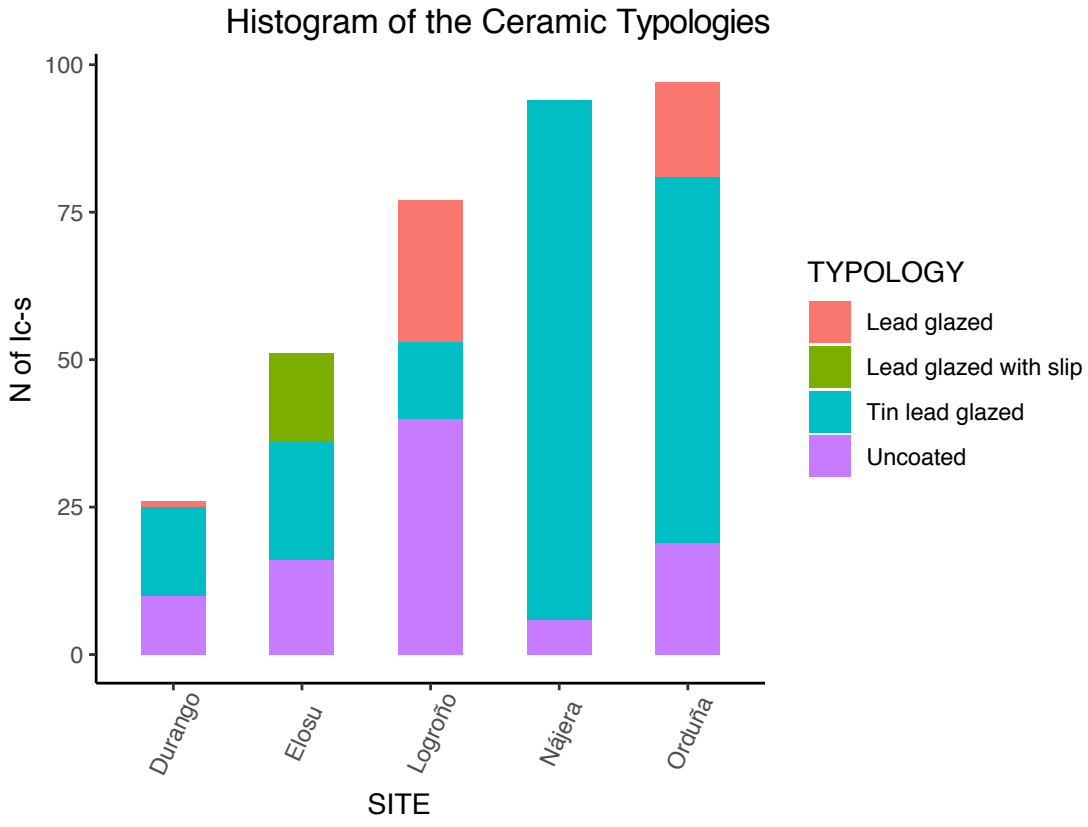

Figure 3.2: Histogram of the typologies of all the analyzed Ic-s grouped by site.

Regarding the forms, the ceramic assemblage includes a wide repertoire that can be grouped into four families, according to their utility: Tableware, Household , Religious and Production (see Figure 3.3). Most of the ceramics correspond to the first two groups, whereas only one home stoup represents the religious utility. The Production group includes all the sherds related to the ceramic manufacture. The detailed list is included in the Appendix B. Furthermore, the archaeological profiles of Orduña, Durango and Elosu, which were taken as a basis to identify the forms and construct the present classification can be consulted in the Appendix D. In the case of Logroño and Nájera, this previous step was performed elsewhere: see Angulo and Porres (2015) for the former, and Ceniceros Herreros (2012) for the latter. Note that some forms could not be determined. Hence, they were referred as undetermined. Each utility group includes the following forms:

- Household: Basin, canister, cooking pot, jug, lid, mortar, plant pot and vessel
- Production: Kiln utensil, Roof tile and paste
- Religious: Home stoup (a small bowl to contain the holy water)
- Tableware: Bowl, cup, jar, mug, pitcher, plate, porringer and sauce-boat
- Undefined: Undefined forms

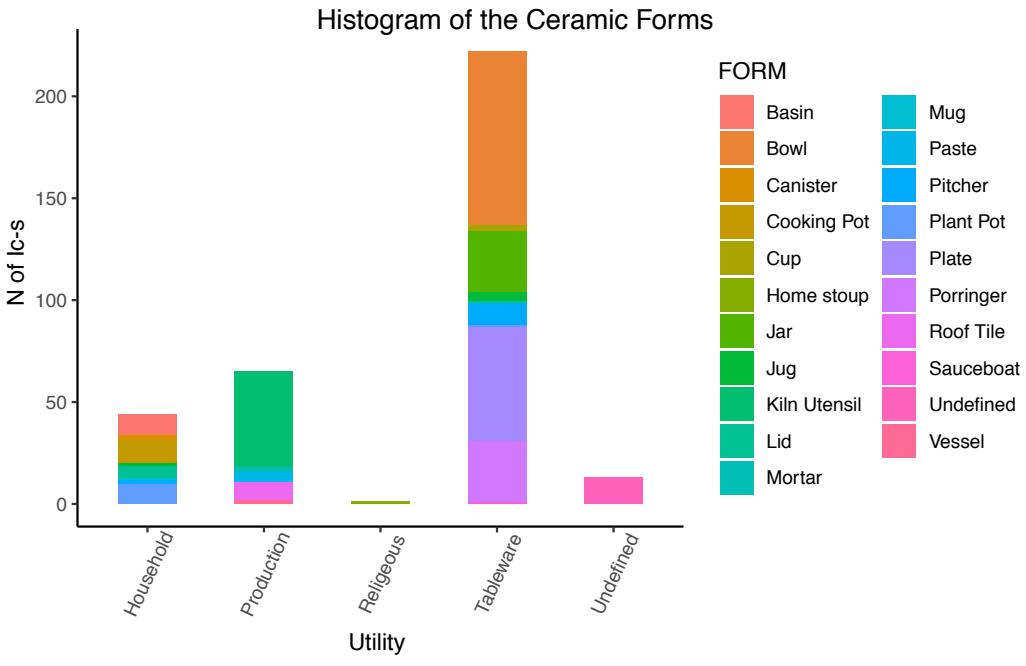

Figure 3.3: Histogram of the forms of all the analyzed Ic-s grouped by utility.

The chronological frame of the studied ceramics is very wide, dating back from the 13^{th}-15^{th} in the oldest site (Logroño) and extending to the period of 1900-1960 in the latest site (Durango). It is understandable that the detailed analysis of the varied historical events in such a a dilated chronological period deserves attention that goes beyond the objectives and possibilities of this work. However, a brief historical context of each archaeological site according to its location is included at the beginning of each case study. Nonetheless, the necessary need to contextualize certain aspects directly related to the archaeological sites, leads to compose a unbalanced story, focused on a handful of very specific topics, while other events barely relevant to the site will remain ignored. A more detailed description of each ceramic sample is given in their respective sections. However, a summary is provided along the following lines (see Appendix B for more details).

3.2 Archaeological Sites

Logroño (LOG)

The sample from Logroño consist on 76 unglazed, lead and tin-lead-glazed sherds. The ceramics were recovered from the archaeological excavations performed in 2009 in the Hospital Viejo street in the Riojan city of Logroño (Angulo and Porres, 2015). Three ceramic kilns and a local dump, along with numerous ceramic sherds were discovered. The operational period of the kilns was settled during the 13^{th}-15^{th} centuries. Most of the studied ceramics from this site date back to these chronologies. In addition, 5 sherds dating back to posterior chronologies (16^{th}-18^{th} centuries) were also selected in order to evaluate possible links between the different periods. The set consists of tableware (dishes, plates, pitchers, bowls...) as well as several construction (roof tiles) and kiln tools, both of them used most probably as kiln utensils. The samples were kindly provided by ArqueoRioja archaeological company, which performed an extensive work documenting the materials recovered in the mentioned excavation (Angulo and Porres, 2015). Furthermore, additional publications address the study of the archaeological site of Hospital Viejo and its ceramic production based on the findings of the first archaeological intervention (Martínez González, 2013). A summary of the 35 forms identified was published elsewhere (Martínez González, 2015). However, the materials under study in this Doctoral Thesis correspond to the second intervention that was carried out in the mentioned site.

Nájera (NAJ)

The ceramic assemble from Nájera consist on 94 tin-lead-glazed earthenware pottery ascribed to the 16^{th} century. It was recovered in the archaeological excavations performed

in the Alcázar of Nájera (La Rioja) during 2002, in order to protect the remains of the Alcázar (Ceniceros Herreros, 2004). The set consists of tableware (plates, porringers, pitchers, bowls) and household (pots). Some of the glazes also include blue, green, yellow, black and luster decorations. The ceramics are glazed completely in the interior and either completely, partially or unglazed in the exterior (Ceniceros Herreros, 2004). Other tin-lead glazed forms include sauce boats, salt shakers, etc. Moreover, unglazed cooking pots and lids were also analyzed.

Orduña (ORD)

The ceramics from Orduña were obtained in the interventions of the Zaharra 2-4 and Tras Santiago streets. The interventions were carried out between 2001 and 2002 and numerous ceramic fragments and the relicts of a ceramic kiln, which can be dated back to late 17^{th} and early 18^{th} century, were discovered (Cajigas Panera et al., 2004). For the archaeometric study a set of 97 ceramics from the 17^{th} to 19^{th} centuries, including different typologies such as bowls, basins, vessels, jars and kiln utensils, were selected. All of the specimens were provided by the Archaeological Museum of Biscay and for the selection, priority was given to pieces such as kiln furniture, when available, and others, such tableware based on their abundance and different representative typologies, since they can be linked to the local production.

Durango (DUR)

For the archaeometric study a sample of 26 ceramics ascribed from 17^{th} to 19^{th} chronologies, including different typologies such as bowls, basins, vessels, jars and kiln utensils, were selected (see Appendix B for more details). All of the specimens were provided by the Euskal Buztingintza Museoa/Museo de Alfarería Vasca of Ollerías (Elosu) and for the selection, priority was given to pieces such as kiln furniture, when available, and others, such tableware based on their abundance and different representative typologies, since they are can be linked to the local production. The materials were recovered by the ethnographer Enrike Ibabe in different archaeological prospections carried out in Gerediaga neighborhood of Abadiño, very close to Durango (Ibabe, 1995a).

Elosu (ELS)

For the archaeometric study a sample of 51 ceramics ascribed from 17^{th} to 19^{th} centuries, including different typologies such as bowls, basins, vessels, jars and kiln utensils, were selected (see Appendix B for more details). All of the specimens were provided by the

Euskal Buztingintza Museoa/Museo de Alfarería Vasca of Ollerías (Elosu) and for the selection, priority was given to pieces such as kiln furniture, when available, and others, such tableware based on their abundance and different representative typologies, since they are can be linked to the local production. The materials were recovered nearby the kiln of Ollerías by Blanka Gómez de Segura (the current director mentioned museum).

Geological contexts

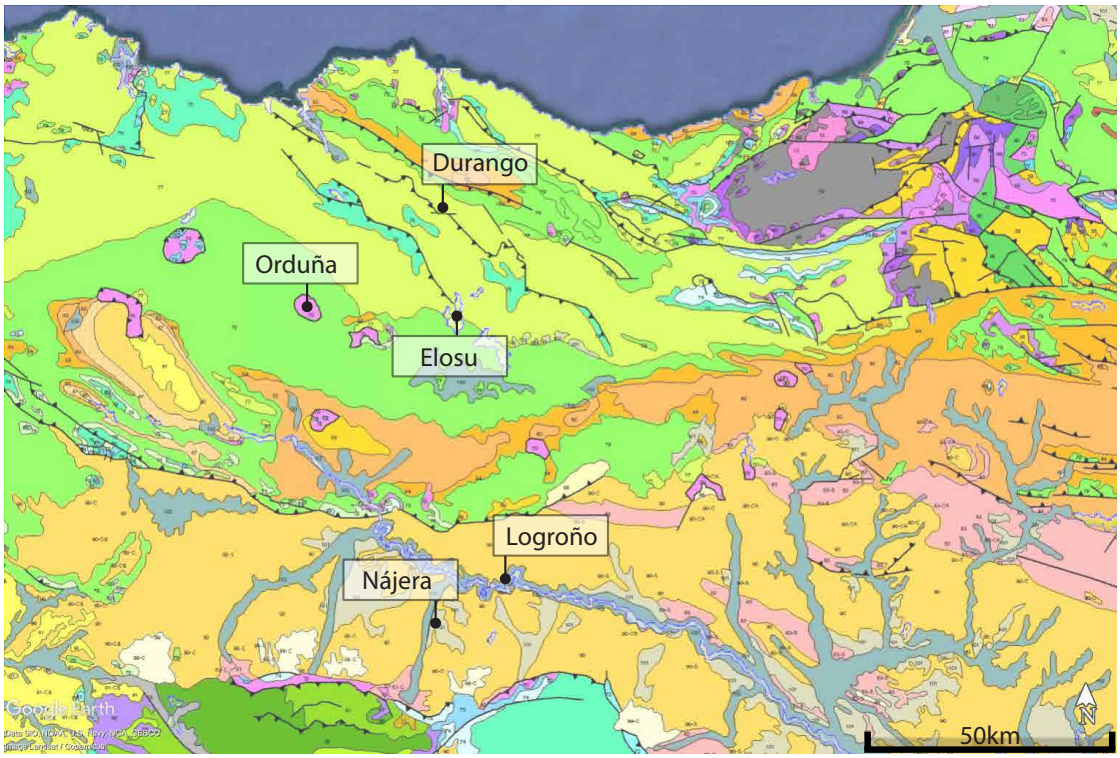

Figure 3.4: Geological Map (EVE-IGME, 1994), including locations of the five sites studied in this Doctoral Thesis. The legend can be consulted in the Figure A.1 of Appendix A.

All the production centers studied in this Doctoral Thesis are located in two regions (The Basque Country and La Rioja) that present different main geological characteristics. Whereas the sites located in the Basque Country correspond to geological strata from the the Mesozoic Era, Logroño and Nájera are in the middle Ebro valley, which is characterized by geological strata from the Cenozoic Era.

Concerning Orduña, from the geological point of view it is based on secondary crust of the Keuper (Upper Cretaceous) with alternating marls, marl-limestones and limestones, as well as bioclastic nodular calcarenites (calcarenites with lacazines). Ceramic pastes

ascribed to this site show low content of calcite inclusions and matrices characterized by autigenic quartz and pyroxenes (Solaun, 2005).

With regard to Elosu, the clays were extracted from the soils that nowadays are covered by a water dam (Urrunaga) (Ibabe, 1995a), which is formed by strata from the Cretaceous System. As suggested in the literature, the sediments present in this site must come from a river's flood basin -purged possibly by a natural decanting process-, perhaps from the Zadorra river, with large layers of Quaternary sediments deposited on the Cretaceous substratum that acquire greater extension in the Vitoria area, arriving to Miranda de Ebro (Solaun, 2005).

Concerning the production center of Durango, a clay-extraction site is depicted in the area known as Gerediaga (see Figure 5.57) (Ibabe, 1995a). Geologically, this site corresponds to the Upper Cretaceous crust and can be characterized by alternate detritus and abundant impure limestones and calcarenites.

In the case of the Logroño and Nájera, the geological strata characterizing these places correspond to the Cenozoic era. Although, no extraction site have been found in the literature, according to a study on the Oligocene-Miocene alluvial and fluvial fans of the northern Ebro Basin, high-quartz sandstones and sand deposits produced by the degradation of intrusive rocks could be expected to be present in the ceramic matrices from these sites (Yuste et al., 2004).

3.3 Experimental

This section is the one where the transdisciplinarity of this doctoral work becomes most evident. As has been anticipated, tools from Analytical Chemistry and Archaeology applied. Moreover, there is a heavy contribution of resources and know-how adopted from Computational Sciences, with specific applicability in research reproducibility. In an effort of building a bridge among these three fields, and in order to avoid misunderstandings, a detailed explanation of each process and technique is described in the following lines.

Sampling strategy

For the material selection, priority was given to the ceramic production centers. Thus, the sampling strategy was focused to the possible extent on kiln-related materials, in order to maximize the probability that materials belonged to the respective workshops within the different producing nuclei. In that sense, priority was given to pieces such as potters' dumps (with special focus on trivets), when available, and others such tableware based on their abundance. The pieces with potters failures such as those with forms that were not on purpose, over-fired, or those with drops of glaze from other pieces are also frequently indicative from the local production.

All the ceramics employed for the current Doctoral Thesis were carefully selected according to their representativeness regarding the corresponding sets. Since these are a subsample of a wider collection (in some cases, previously classified by the corresponding archaeologist) the considerations on the quantifying methods in Archaeology (Escribano, 2017b) were not regarded, since the percentages of each technotype were not meaningful because they are a deliberate subset. Thus their relative abundance is not regarded but their typological representativeness.

In this work, when a individual, Ic, sherd, potsherd or specimen is referred, a ceramic piece is being nominated, each of it called by an analytical ID (ANID). Therefore, each ANID may be constituted from one to a several fragments, and all corresponding to only one form, ceramic paste, typology and decoration. This point is highlighted, because in more than one occasion the archaeologist have simplified the classification by gathering together similar pieces according to their decoration. In those cases, we have only considered one of the fragments, understanding that the pastes can differ.

The nomenclature of each ceramic individual follows the same pattern. The pattern consist on three digits sequence after three letters corresponding to the site of procedence, that is, the site where they were unearthed: LOG for Logroño, NAJ for Nájera, ORD for Orduña, DUR for Durango and ELS for Elosu. In contrast, the compositional groups

bear the name of the provenance, that is the site were they would have been manufactured (e.g TER for Teruel, TAL for Talavera and so on).

Unlike other research projects involving analytical chemistry, where each sample can be reduced to a statistical observation and is frequently replaceable (e.g. water samples from the sea or soil and stone fragments), in this work every sample is unique, and loaded of history, being accompanied by heterogeneous information that will not be balanced among all the studied samples. Therefore, a database to enable the gathering of all available documentation and each archaeological record has been designed and created.

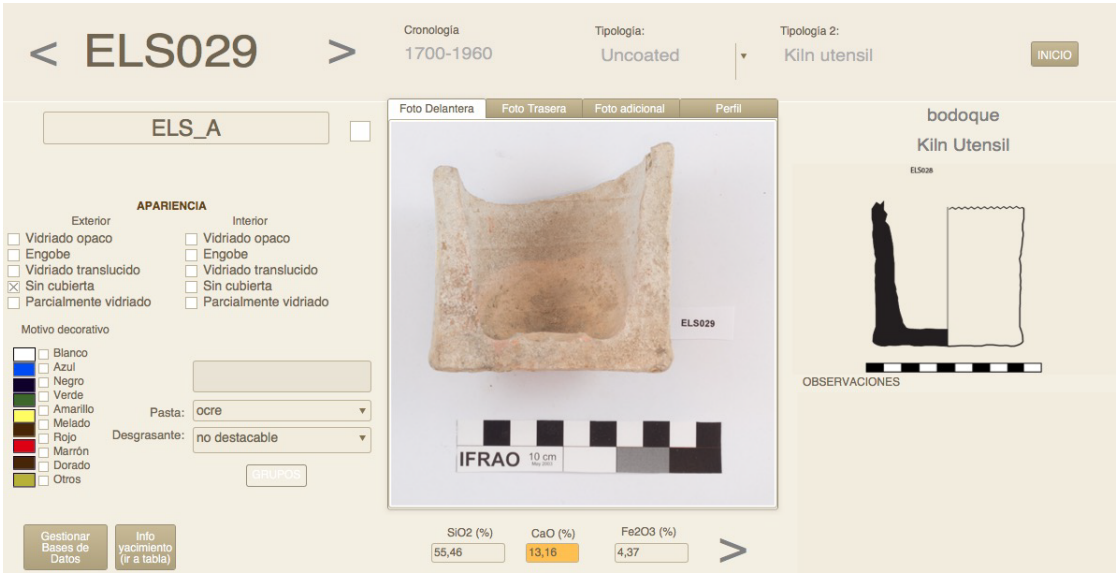

Figure 3.5: Screen-shoot showing a FileMaker example.

A database was created using the software FileMaker (see Figure 3.5) . The database, includes all the archaeological records obtained for each of the ceramic pieces, listed by their ANID: chronology, typology, stratigraphic unit, form, coating, paste type, picture, archaeological drawing of the profile, details of the provider (e.g. Museums) and any relevant information (deterioration state, cleaning treatments, etc).

Graphical documentation

For the graphical documentation, special attention was paid to achieve the most reliable reproduction in terms of the colors of the ceramic pieces. For this, a specific process was followed in obtaining photographs that includes the use of a color checker (in our case Color Checker Passport by XRite®). It was obtained a front and a back photo of each piece and with an artificial lighting system placed on each side at an angle of 45°s. The

lighting conditions were kept constant as much as possible and the white balance was applied using the standard card from Color Checker Passport. Likewise, an specific color profile was created for each lightning condition in order to guarantee the generation of a reproducible visual record with high chromatic fidelity. The raw files of each picture were edited with Lightroom CC from Adobe.

Archaeological Profile Drawing

The usual step when documenting of archaeological ceramics consist on a profile drawing that is performed with a tool called *countour* or *profile gauge*. The tool is similar to a comb with movable tines and by pressing on the piece, they adapt to the shape of the piece. The profile that is fixed in the former is then transferred to a paper (see Figure 3.6). The profile of the pieces is very useful to elucidate the form of the ceramic piece. From one small fragment, if the key parts are retained, the original form can be extrapolated. In this work the profiles of the Basque ceramics were obtained (Durango, Elosu and Orduña), while for the Riojan samples, in most of the cases, the formal analysis was previously performed by the archaeologist. The archaeological profiles can be consulted in the Appendix D.

Figure 3.6: Example of a profile gauge.Tenbergen

For the classification of the ceramic typologies in this work, the taxonomic criteria gathered in the *Tesauros del Patrimonio Cultural de Espanã*, particularly designed for ceramics, was followed. It is available on the oficial website[1]. With regard to the

[1]http://tesauros.mecd.es/tesauros/ceramica

nomenclature used, the dictionary of *Zeramika hiztegia* was employed. The terminology gathered in this book in English, Basque, Spanish and French is also available on the website of Euskalterm[2].

Sample powdering

Prior to NAA, ICP-MS and XRD analysis, the clayey pastes (≈ 10-15 g) were powdered for 2-4 min at 300 rpm using a Planetary Pulverissete 6 milling machine (Fritsch) equipped with a wolfram carbide cell. Prior to milling, glazes and outer surfaces were mechanically removed by means of a wolfram carbide abrading tool in order to prevent the contribution of the potential contamination from glaze and soil into the sample.

Neutron activation analysis (NAA)

NAA is an analytical technique, which can provide the composition of the analyzed ceramic sample in orders of μg/kg or ng/kg. Furthermore, a minimum amount of sample is needed (150-200 mg) and trace elements can be analyzed which makes the techniques very suitable for provenance analysis. The resources of neutrons necessary for the irradiation can be obtained through three sources: a nuclear reactor, a radioactive material (e.g. uranium) or a large particle accelerator (e.g. synchrotron). The higher is the flux of neutrons, the better is the response of the sample and so, the sensitivity of the technique. Since the nuclear reactor is the one that provides a higher flux of neutrons, most of the analyses are carried out by means of this option (Pollard, 2007).

When irradiating a sample, the atoms are excited and a nuclear rearrangement takes place on the atoms nuclei (see the NAA schematic process figure 3.7). As a result, a radioactive nucleus is generated and this will need certain time to return to a stable situation. In this process, which is called decay, some energy is released and this is what is registered. The pioneers of the application of NAA for the study of archaeological ceramics summarized three main possible nuclear reactions involved in the NAA, and from which the most frequent is "n, γ" type (Perlman and Asaron, 1969). In this reaction type, a neutron is captured by the target nucleus, and after a neutron strikes with the target, the excited nucleus, called product nucleus, emits spontaneously a characteristic prompt γ radiation (which is normally lost in the reactor) to obtain a more stable configuration and gives way to a radioactive daughter. The latter, after a certain time, will release more γ radiation (called delayed or decay γ rays). The rate of the decay is much lower than the prompt radiation yield and

[2]http://www.euskadi.eus/euskalterm/

depends on the unique half-life of the radioactive nucleus. This time range from fractions of seconds to several years (see the figure 3.7).

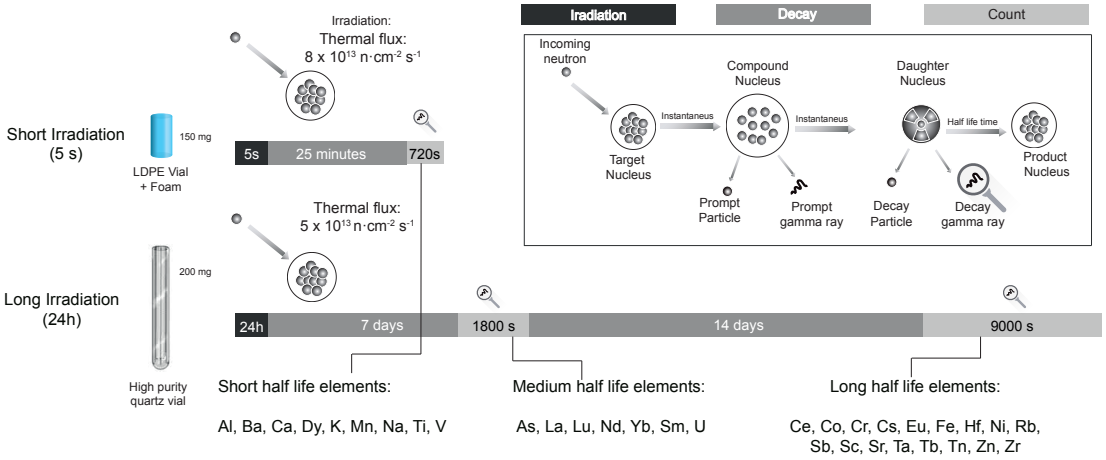

Figure 3.7: Schematic diagram of the nuclear processes involved in NAA. Thermal neutrons strike the target nucleus in the reactor producing a compound nucleus which decays instantaneously, emitting a prompt γ-ray and (usually) producing a radioactive daughter.

The NAA data presented in this doctoral work was obtained in the installations of Missouri University Research Reactor (MURR). The Archaeometry Laboratory of MURR, under the direction of M. Glascock has a long tradition on archaeometric materials, and has been analyzing ceramics for the last decades, building up one of the world largest databases of ceramic composition. Their long experience in this research field has evolved an lead to the development of the specific protocol for archaeological ceramic, the MURR protocol, which is the applied to conduct the analysis of the ceramics of this research, and is described below. The history and more details about the protocol can be found here (Glascock Michael D and Neff, 2007)

Milled samples were transferred to glass vials. Then, the powder was dried for at least 24 hours and afterwards was weighed in two bundles. In Low Density Polyethylene (LDPE) vials 150 mg of each sample were placed in order to apply NAA for short-life elements (e.g. Ca). Simultaneously, 200 mg were placed into glass vials for larger half-life elements (see Figure 3.7).

At Missouri University Research Reactor (MURR), NAA of pottery consisted of two irradiations and a total of three γ-ray counts. Short irradiations involved a pair of samples being transported through a pneumatic tube system into the reactor core for a 5 s neutron irradiation using a thermal flux of $8{\cdot}10^{13} n/cm^{-2}s^{-1}$. After 25 minutes of decay, the samples were counted for 720 s using a high-resolution germanium detector. This

count yielded data for nine short-life elements: Al, Ba, Ca, Dy, K, Mn, Na, Ti and V. For the long irradiation, bundles of 50 or 100 of the encapsulated quartz vials were irradiated for 24 h at a flux of 5 x $10^{13} n/cm^{-2}s^{-1}$. Following the long irradiation, samples decay for seven days, and then were counted for 2000 s (known as "middle count") on a high-resolution germanium detector coupled to an automatic sample changer. This middle count yielded determination of seven medium half-life elements: As, La, Lu, Nd, Sm, U and Yb. After additional two-week decay, a second count for 9000 s was carried out on each sample. This final measurement allowed the quantification of 17 long-life elements: Ce, Co, Cr, Cs, Eu, Fe, Hf, Ni, Rb, Sb, Sc, Sr, Ta, Tb, Th, Zn and Zr (Glascock, 1992). With the samples batch, SRM-1633a (coal fly) was prepared as standard (see the details in table A.2 in the Appendix), as well as quality control samples of SRM-278 (obsidian rock) and Ohio Red Clay (for analytical conditions, see (Glascock Michael D and Neff, 2007)).

Inductively Coupled Plasma Mass Spectrometry (ICP-MS)

Inductively Coupled Plasma Mass Spectrometry (ICP-MS) is an elemental and isotopic analytical technique capable of quantifying simultaneously most of the elements of the periodic table in a linear dynamic range of 8 orders of magnitude and down to ng/g. The ICP-MS analyses carried out in this work were conducted at the laboratory of the Analytical Chemistry Department of the Science and Technology Faculty (University of the Basque Country UPV/EHU) and the SGIker-Geochronology and Isotope Geochemistry facilities of the same university were used to perform the sample preparation. Previously, powdered samples were calcined to 1000°C in order to acquire the Loss on Ignition (LOI) values and to remove the organic matter present in the samples. The samples and the Certificate Reference Material (CRM) from the Geological Survey of Japan used for the calibration (andesite JA-2, granodiorite JG-1a, granite JG-2, and basalt JB-3) were fused using a Fluxy automatic gas fluxer (Corporation Scientifique Claisse, Canada). These CRMs are based on igneous rocks and the followed quantifying method was previously optimized for similar matrices (see elsewhere (Madinabeitia et al., 2008)). It involved the melting of approximately 250 mg of sample into a Pt-Au crucible together with 500 mg of a flux at more than 1100°C for several minutes. The flux agent was $LiBO_2$ (anhydrous, for analysis grade pure) of Corporation Scientifique Claisse, with solution of 50% LiBr (Merck Suprapur) in deionized water used as anti-adherent. The mixture was fused using Program #9 of Claisse with steps F4 and F5 extended to last 100 s and 200 s, respectively (approximately 9 minutes in total). The melted pearls were poured into a polypropylene beaker with a solution of HNO_3 with several drops of HF to ensure the stability of the High Field Strength Elements (HFSE). They were then diluted in several steps at 1:200 using Milli-Q water (1%HNO_3) and the resulting solutions were analyzed by ICP-MS. The commercial reagents (Merck Pro Analysis HF 50.2% and HNO_3 69.8%) were purified in a clean room by sub-boiling quartz-distillation (HNO_3)

and Teflon bottle-distillation (HF). Ultra-pure water (resistivity $\geq$ 18.2 $M\Omega$) was obtained by a MilliQ water purification system (Millipore) and polishing by reverse osmosis (Nanopure Barnstead). The internal standards (Sc, Y, In, Be, Bi) and ICP-MS calibration standards' solutions were prepared from 1000 $\mu g/mL$ stock solutions of Alfa Aesar (Specpure ©, Plasma standard solution, Germany) inside a class 100 clean room. All solutions were prepared using Milli-Q quality water. PL 20-200 μL and PL 500-5000 μL micro-pipettes (Eppendorf, Hamburg, Germany) with calibration standards and the dilutions of the samples were prepared gravimetrically using analytical balance model Mettler-Toledo XS205 (Colombus, OH, USA) with an uncertainty of $\pm$ 0.00001 g.

The elemental analysis of the extracts was performed by ICP-MS (NexION 300, Perkin Elmer) in a class 100 clean room. The argon used was supplied by Praxair (99.995 %, Madrid, Spain).^{27}Al, ^{28}Si, ^{31}P, ^{44}Ca, ^{85}Rb, ^{88}Sr, ^{90}Zr, ^{93}Nb, ^{115}In, ^{120}Sn, ^{133}Cs, ^{137}Ba, ^{139}La, ^{140}Ce, ^{141}Pr, ^{142}Nd, ^{147}Sm, ^{153}Eu, ^{158}Gd, ^{159}Tb, ^{164}Dy, ^{165}Ho, ^{166}Er, ^{169}Tm, ^{174}Yb, ^{175}Lu, ^{180}Hf, ^{181}Ta, ^{208}Pb, ^{232}Th and ^{238}U isotopes were determined in standard mode and ^{23}Na, ^{24}Mg, ^{39}K, ^{47}Ti, ^{51}V, ^{52}Cr, ^{55}Mn, ^{56}Fe, ^{59}Co, ^{60}Ni, ^{65}Cu and ^{66}Zn isotopes were determined in Kinetic Energy Discrimination (KED) mode with He in order to eliminate possible polyatomic interferences. The equipment includes a Oneneb pneumatic concentric nebulizer (Agilent), cyclonic spray chamber and standard nickel cones.

The plasma conditions such as argon flow of nebulizer, the torch position and the instrument lenses voltages were optimized before each measurement session aspirating a standard solution of 1 ng$\cdot mL^{-1}$ of Mg, Rh, In, Ba, Pb and U. The gas nebulizer flow was optimized obtaining a compromise between sensitivity and low oxides level (less than 2.5% for the CeO/Ce ratio). The working conditions for the sample introduction and data acquisition are shown in Table A.1 of the Appendix. Finally, the data were acquired and analyzed for the elemental quantitative analysis using the Nexion 1.5 software (Perkin Elmer SCIEXTM, Ontario, Canada).

The accuracy and reproducibility of the method were checked by repetitive analysis (n = 3) of the JA-2, JB-3, JG-1a and JG-2 certified reference materials from the Geological Survey of Japan. Finally, 3 blanks were prepared and analyzed (at the beginning, middle and final of each batch) as well, for the procedural quantification limit calculations following the International Union of Pure and Applied Chemistry (IUPAC) rules and according to the formula 3.1:

$$LOQ = \frac{(\overline{Y}_{blk} + 10SD_{blk}) - b}{m} \tag{3.1}$$

where $\overline{Y}_{blk}$ is the mean signal of three blank analyses and SD_{blk} is the standard deviation of them, m is the slope and b the intercept obtained from the calibration curve of each specific element.

During the process of sample preparation and measurement, each step can be a source of variability affecting the final results, thus each measurand (i.e. quantity intended to be measured) should be expressed with the corresponding uncertainty, which according to the International vocabulary of basic and general terms in metrology (VIM) is a "parameter associated with the result of a measurement, that characterizes the dispersion of the values that could reasonably be attributed to the measurand". Only in this way the result will be comparable to other results in the literature. From the different approaches available to express the uncertainty, in this work, the Guide to the Expression of Uncertainty in Measurement (GUM) was followed (Possolo, 2015). The GUM does not use random and/or systematic effects, but the so-called **expanded uncertainty (U_c)**. The expanded uncertainties are expressed in the Table A.3 of the Appendix A and they were calculated according to the following procedure.

First, calibration curves were obtained for each element and in each batch of specimens. Then, the residuals (S_y) and the sample corrected sum of squares (S_{xx}) were extracted according to equations 3.2 and 3.3 respectively, where y_i is the intensity, c_i the expected concentration of each CRM, $\overline{c}$ the mean of all expected concentrations, b the intercept, m the slope and n the number CRMs.

$$S_y = \sqrt{\frac{\Sigma(y_i - (mc_i + b))^2}{n - 2}} \tag{3.2}$$

$$S_{xx} = \Sigma(c_i - \overline{c})^2 \tag{3.3}$$

Given these expressions, the **uncertainty from the calibration** $U(c_c)$ and corresponding to each measurement was calculated according to the equation 3.4, where p is the number of replicate analysis and c_c is the concentration of the sample for a given element.

$$U(c_c) = \frac{S_y}{m}\sqrt{\frac{1}{n} + \frac{1}{p} + \frac{(c_c - \overline{c})^2}{S_{xx}}} \tag{3.4}$$

When there is no correlation between magnitudes, expanded uncertainty (U_c) can be calculated following the equation 3.5, where U(xi) is the standard uncertainty of each magnitude.

$$U_c = \sqrt{\Sigma(\frac{\partial df}{\partial x_i})^2 (U(x_i))^2} \tag{3.5}$$

In the present work. in all cases, the contribution of the calibration uncertainty was over 99%. Therefore, contributions of the remaining components were depreciable. In consequence, the expanded uncertainty could be equated with the calibration uncertainty. Moreover, regarding that the data showed a normal distribution, the obtained values were multiplied by the coverage factor (k=2), defining in this way a confidence interval of 95%. The obtained expanded uncertainties are listed in the Table A.3 of Appendix A.

Drift Correction

In order to correct the drift[3] of the instrument an external correction was applied. In our case, a random sample was used as DCS (drift correction standard), in order to resemble as much as possible, the matrix of the samples. The DCS was analyzed repeatedly every n samples (n = 6). According to the equation 3.6, the first one is called $[DCS]_a$, the second $[DCS]_b$, and so on. Then, regression fit is calculated for each analyte using the response in counts of the DCS and the corresponding factor applied to the results, as discussed in the referential work (Madinabeitia et al., 2008). The concentration of the sample ($[C]_0$) is corrected according to the following equation.

$$[C] = \frac{[C]_0 [DCS]_a}{[DCS]_a + \frac{[DCS]_b - [DCS]_a}{n}} \tag{3.6}$$

All the chemical data are subjected to variabilities of different sources which are addressed in the Chapter 5. In addition, the chemometric strategies and the R code employed to compute them, which has been the basis of the development of an "open method" for the statistical analysis of pottery compositional data are discussed in the Chapter 4.

[3] "The drift, often is a complex function of mass that is especially a problem of geological samples with their inherently composite matrix, as material is deposited on the cones and ion lens system."(Madinabeitia et al., 2008).

ED-XRF

The compositions of the pastes were also evaluated by Energy-Dispersive X-Ray Fluorescence (ED-XRF) in order to explore non-destructive strategies (addressed in the Chapter 6). The ED-XRF analyses were performed directly on the section of the sample cut by a precision cutter and placed directly in the instrument chamber. For the compositional characterization of the ceramic pastes and clayey reference materials the M4 Tornado (Bruker Nano GmbH, Berlin, Germany) energy dispersive X-Ray Fluorescence spectrometer was used. The set-up of this instrument includes two Rh tubes mounted with two collimation systems that allow to measure at two lateral resolutions (1 mm with the mechanical collimator and $0.25\mu m$ with the poly-capillar system). In order to perform a representative analysis of the samples and considering that their heterogeneity at microscopic scale will be higher than $0.25\mu m$ for this study measurements were conducted at 1 mm.

The X-ray tube implemented in this part of the set-up is a micro-focus side window Rh tube powered by a low-power HV generator and cooled by air. The X-ray tube can work at a maximum voltage of 50 kV and at a maximum current of 700 μA. The detection of the fluorescence radiation was performed by an XFlash®silicon drift detector with $30mm^2$ sensitive areas and energy resolution of 145eV for Mn-K_α. In order to improve the detection of the lightest elements (Z<11), filters were not used and measurements were acquired under vacuum (20 mbar). To achieve the vacuum, a diaphragm pump MV 10 N VARIO-B was used. For the focusing of the area under study, two video-microscopes were used, one of them to explore the sample under a low magnification (1 cm^2 area), and the other one to perform the final focusing (1 mm^2) area. The spectral data acquisition and treatment was performed using the software based on a modification of Esprit software from Brüker. For further details on the measurement conditions (e.g. times, collimator selection and number of analyses) see the Chapter 6). The Hyper Maps presented in this work were obtained using the polycapillary optics (down to $25\mu m$ of lateral resolution). Prior to obtaining the Hyper Maps, an elemental assignation and deconvolution of the spectral information was conducted. The elemental maps were obtained according to the intensity of the K_α line of each element detected in the present work. For those elements included in the CRM SRM679, the LODs were calculated according to the measurements carried out as pressed pellets following this formula:

$$LOD = 3C\sqrt{\frac{Background}{Net\ Intensity}} \tag{3.7}$$

where C is the real concentration and the background intensity was obtained from the spectra. In this formula, the net intensity was obtained subtracting the background (counts) from the element peak intensity (counts). The LODs of those elements not included in the certification were approximated according to the theoretical values provided by Bruker.

Additionally, μ-XRF analyses were performed in some glazes by an ArtTax (Röntec, currently Bruker) spectrometer. The spectrometer is equipped with an X-ray tube with Mo anode working at a maximum voltage of 50 KV and limit intensity of μ700 A and integrates a XFlash detector (5 mm^2) and beryllium window of 8 mm^2. The analyses were performed at 50KV and 100 μA. The X-rays are collimated by a Ta collimator allowing to analyze a spot size down to 0.1 mm. Prior to each measurement, the equipment was calibrated with a bronze standard reference, using the lines of Cu and Sn. The acquisition times were between 800 s and 1000 s. The recorded data were then processed with the MQuant software, in which fundamental parameters are used to calculate the concentrations.

X Ray diffraction (XRD)

XRD is a technique based on the diffraction caused in the X-rays applied and the interaction of the matter. The different lattice spacing in crystalline structures diffract uniquely the X-rays, revealing the structures present in the individual. X-Ray Diffraction (XRD) is used to determine the crystal phases of the ceramic body. These provide information about the minerals occurring in the clay (e.g. calcite, quartz, feldspars). Since these minerals occur only at certain temperatures, the Equivalent Firing Temperature (EFT), tha is the maximum firing temperature reached in the ceramic kiln can be estimated. The variations in the mineralogical phases and their subsequent EFT determine the fabric type. Thus, within the same compositional group, different fabrics can be found.

For the measurements a small amount of milled sherd is irradiated (in our case less than 1 g) by a collimated beam of monochromatic X-rays of a certain wavelength. These rays will be diffracted at different angles, depending on the crystal structures. The wavelength of the incident radiation must alike magnitude to the distance between the scattering points, the most common choice, and the one used for this work is the copper tube, which allow to identify the most relevant inter-planar distances (d) present in the mineral phases from the clayey matrices. The incident rays are reflected similarly to the light reflection and the X-ray penetrate into the surface of the crystal. Then are diffracted from the atomic layers in the crystal lattice generating constructive and destructive interference from successive layers. For each incident wavelength (λ), the difference in the distance traveled θ angle from the successive atom layers separated by d spacing is related by Bragg's law (Equation 3.8).

$$n\lambda = 2dsin\theta \tag{3.8}$$

The XRD analyses performed in this doctoral work were carried out by SGIKER general services at the University of the Basque Country (UPV/EHU). Every Ic subjected to chemical analysis was also analyzed by XRD (n = 347) in order to obtain

information about the spatial disposition of the elements quantified by ICP-MS. The XRD analysis were performed with a PANalytical Xpert PRO powder diffractometer equipped with a copper tube ($\lambda CuK_{avg} = 1.5418$, $\lambda CuK_{\alpha 1} = 1.54060$, $\lambda CuK\alpha 2 = 1.54439$) and Ni filter for removing the K_β wavelength, vertical goniometer (Bragg–Brentano geometry), programmable divergence aperture, automatic sample changer, secondary graphite monochromator, and PixCel detector.

The operating conditions for the Cu tube were 40 KV and 40 mA, and the angular range 2 θ was scanned between 5 °and 70°. The treatment of the diffractogram data and the identification of the mineral phases present was carried out with the X'pert HighScore (PANalytical) software package in combination with the Powder Diffraction File (PDF-2) database (International Center for Diffraction Data – ICDD, Pennsylvania, USA).

Scanning Electron Microscopy-Electron Dispersive Spectroscopy (SEM-EDS)

For the evaluation of the glazes by SEM-EDS analysis were conducted in the SGIKER general services from the University of the Basque Country and a great part of them was conducted in Rathgen Forschungslabor (Berlin, Germany). Prior to the analyses, cross sections of the sherds ($\approx$ 1 cm long) were prepared in epoxy resin molds and polished metalographically (down to below 1 μm).

Evaluation of the glazes was performed by means of an EVO 40 (Carl Zeiss) scanning electron microscopy (SEM) equipment and the elemental composition of the coatings determined by an electron dispersive spectrometry (EDS) analysis of areas corresponding to each color, using an X-Max (Oxford Instruments) equipment. Data were collected at voltage of 20 KV and a current of 50 mA for the acquisition of images and 200 mA for the acquisition of spectra. The working distance ranged between 8.5 and 18.5 mm. The EDS spectra were acquired and treated using the INCA software (Oxford Instruments). For the micro-structural characterization of the pastes, fresh fractures were cut perpendicularly to z axis of each piece in order to better asses the clayey inner structure, the Ic-s were previously coated by a conductive layer (20 nm of Au) and the detector was switched to secondary electrons (SE) mode. For a better comparison of the micro-structure, the SEM images showing different vitrification levels were all acquired at x20K magnification.

In the analyses conducted at Rathgen Forschungslabor EDS Quanta 200 from Fei environmental scanning electron microscopy (ESEM) was employed, which allows to work without the need of a conductive coating, in combination with the integrated energy dispersive XFlash 4010 X-ray analyzer from Bruker. The elemental composition of glazes was determined by EDS on areas of 50 μm^2 corresponding to each color. Data

were collected at voltage of 15-20 KV and a current of 50 μA for the acquisition of images, and 100 μA for the analyses, at 11.5 mm working distance (WD) and low-vacuum. The instrument was calibrated with Cu at the beginning of each working day. The detector was switched to secondary electrons (SE) for image acquisition and back scattered electrons (BSE) for analyses. The EDS spectra acquired were treated using Esprit V.1.9 software from Bruker Nano GmbH (Berlin, Germany).

Raman microscopy

Raman is a non-invasive spectroscopic technique in which a laser is used to beam the specimen, and the response is recorded on a sensor in the visible range. It is widely used to used to characterize pigments. The Raman analyses were performed with a Horiba XploRa (Jobin Yvon, Horiba Group, New Jersey USA) Raman microscope that is equipped with lasers of wavelengths 532 nm, 638 nm and 785 nm. The maximum spatial resolution is 1 μm. Integration times varied between 2s and 10 s with 10 accumulations. The calibration of the spectrum has a precision of 2 cm^{-1} numbers and it was performed at the beginning of the use of the device each working day, by the Raman band of 520 cm^{-1} of a crystalline silicon chip. The data obtained were interpreted by comparing the spectra with the pure reference compounds acquired from the Raman e-VISNICH database containing Raman spectra of natural, industrial and cultural heritage objects. Open databases such as RUUFF were also used for other Raman bands identification, in addition to comparing with the spectra of the literature. The interpretation was carried out using the OMNIC program.

UV-Vis Reflectance Spectroscopy

For the UV-Vis Reflectance spectroscopy carried out at Rathgen Forschungslabor, the Ic-s were irradiated with light from a 75W Xenon arc lamp. The focused light travels through a sequence of filters blocking IR and UV radiation and is guided by an optic fiber to the beam probe. The diffuse reflected light is then directed to the diode array spectrometer (Control development PDA 512). The spectra were recorded over the range of 400-740 nm. Measurements were taken against a Spectralon 99% diffuse reflectance standard.

Statistical Model

The values of the elemental concentrations of the ceramics studied are essentially compositional data and therefore require a specific treatment according to their nature (Aitchison, 1982). Considering the inescapable paradigms of any compositional data

analyst, the statistical model followed in this work is based on the observations of Aitchison and Buxeda and coauthors on compositional data (Aitchison, 1982; Buxeda i Garrigós and Kilikoglou, 2003).

The raw compositional data consist of vectors whose components are part of some whole (Aitchison, 1982). The sum of each component is equal to a constant $k(k \in R_+)$ (e.g 1 in proportions or 100 in percentages). These kinds of data are constrained, they are not absolute values since they have a dependency from one each other (Buxeda i Garrigós and Kilikoglou, 2003). Removing one or more components would influence the values of the other components. Therefore, it is not possible to consider the compositional data as independent from the number of components. Their sample space is called simplex and is defined in equation 3.9, where the S^D is the simplex in the D dimension.

$$S^D = \{(x_1, x_2 \ldots, x_D) > 0; \sum_{i=1}^{D} x_i = k\} \tag{3.9}$$

The values of the elemental compositions correspond to a special case of the dimensional D + 1 projective space, of the projective points in the origin, which are projected in the simplex S^d. In the way that the projective points are represented by homogeneous coordinates that have a constant sum k $(k \in R_+)$.

Since the compositional data is in the simplex space and not Euclidean space, the application of standard statistic methods as the multivariate analysis, can lead to spurious results. This problem was first posed by Karl Pearson (Pearson, 1897) and after a increasing worrying from the scientist community in the 60s Aitchson was among the firsts to address the problem, proposing some treatment for the data (Aitchison, 1982).

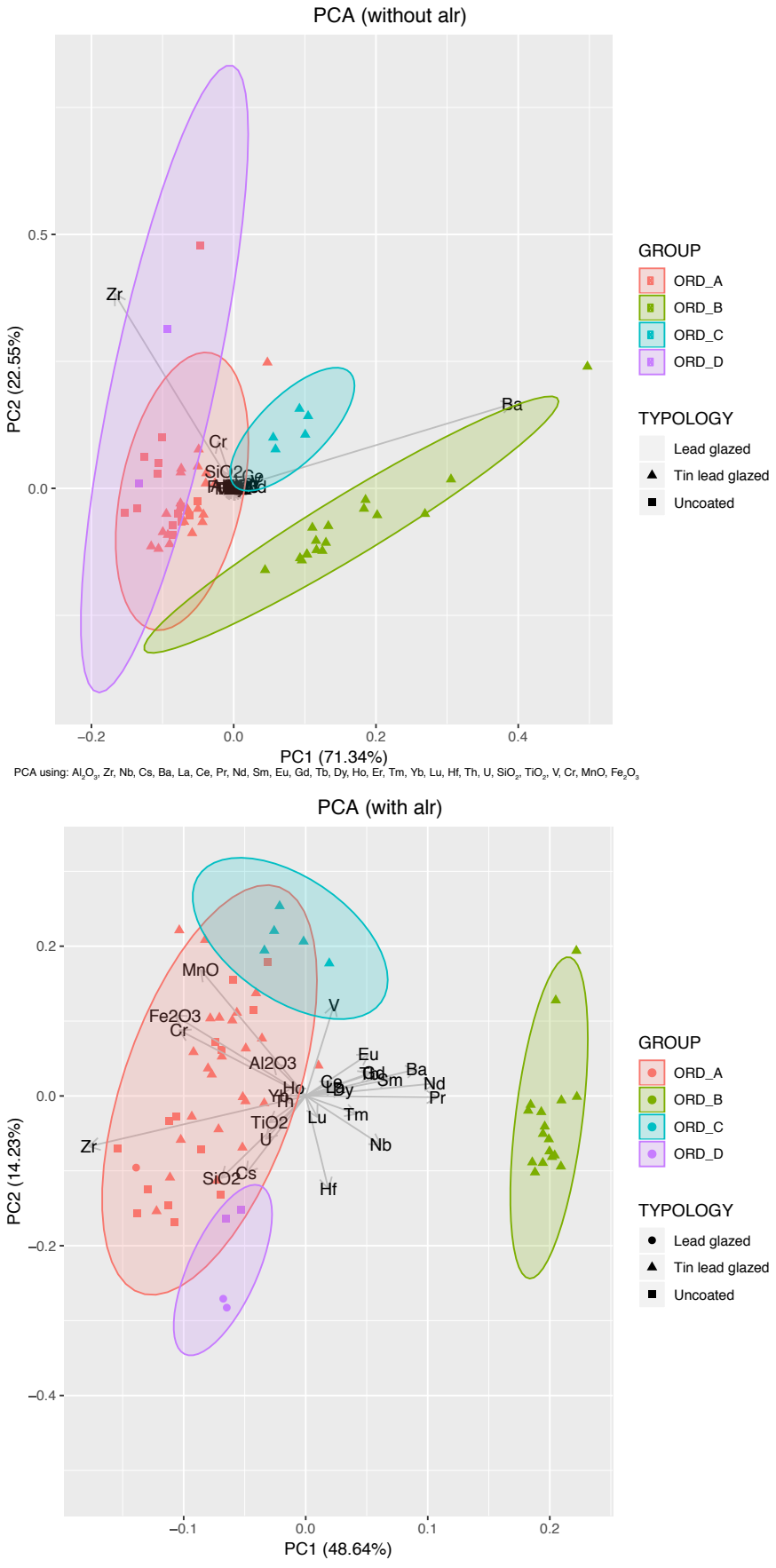

Figure 3.8: Comparison of PCA with and without alr transformation using Er as divisor applied on the same dataset.

Moreover, it has been suggested that geochemical data show neither a normal nor log-normal data distribution (Zhang et al., 2005). However, most of archaeological researchers use a logarithm transform because it acts as a "quasi-standardization" (Neff, 2000; Sayre, E.V., Harbottle, G., Bieber, A.M., Brooks, 1976; Martín-Fernández et al., 2015) that compensates for the differences in absolute magnitude between the major elements, such as Al, K, and Fe present at percent levels, and the trace elements, such as the rare earth elements (REEs) present at parts per million and below. Thus, the transformation places the elements onto more or less the same scale (Martín-Fernández et al., 2015). Moreover, Aitchison remarks the importance of using log-ratio analysis and its associated distance measures since these would satisfy certain invariance conditions required for a proper compositional data analysis, especially in multidimensional scaling and Hierarchical Cluster Analysis (HCA) (Aitchison et al., 2000).

Therefore, the data in the present work were transformed prior to the statistical analyses by using centered log ratio (clr) transformation and additive log ratio transformations (alr). On the one hand, clr consists on dividing all elements by the geometric mean according to the equation 3.10, where S^D is the simplex in the of D dimensions and g(x) is the geometric mean of all D+1 components of x (Aitchison, 1982; Boogaart et al., 2010).

$$x \in S^D \rightarrow Z = ln(\frac{x}{g(x)}) \in R^D \tag{3.10}$$

On the other hand, in alr transformation the component used as divisor is the one that introduces the lowest chemical variability to the entire set of specimens, according to the equation 3.11, where S^D is the simplex in the of D dimensions and $x_D = [x_1, \ldots, x_D]$. The influence of using alr or not in PCA can be observed in Figure 3.8. When applying the transformation, the role of minor and trace elements can be better assessed.

$$x \in S^D \rightarrow y = ln(\frac{x_D}{x_{D+1}}) \in R^D \tag{3.11}$$

Computational Tools

For the compositional data processing, R (Core Team, 2013) and RStudio were used. A specific methodology was developed for the chemometric analyses and the fully reproducible code can be accessed via public repository on GitHub (a website for the collaborative development of coding projects)[4] and shared under GPL license. The presentation and discussion about this methodology is presented in the Chapter 4.

[4] `https://github.com/esteful/arch_flow`

Part II

Results and Discussion
Emaitzak eta Eztabaida

Overview of the Results

This doctoral thesis is articulated in three milestones. The first one (see Chapter 4) deals with the development of an **Open Methodology for Compositional Data Analysis of Archaeological Pottery using R**. The output of this work is mainly supported by a repository[5] containing all the necessary code for its complete reproduction in R environment. Nonetheless, in this chapter, the theoretical basis of such work is addressed. In this way, the underlying procedures employed during the posterior chapters of the current doctoral thesis are presented and illustrated by means of a Romano-British Pottery dataset.[6]

The second milestone (see Chapter 5), covers the **Archaeometric Characterization** of the five selected pottery production centers. To obtain these results, measurements by means of ICP-MS and NAA were carried out. In this chapter, the compositional groups established within each ceramic assemblage of the archaeological sites from The Basque Country and La Rioja are discussed. For the discussion of each compositional group, the micro-structural properties and technological features are covered, based on XRD and SEM analyses of the clayey bodies and the glazes. To conclude each case study, the data obtained through these analytical techniques are framed in a broader context and the historical implications are discussed, updating the documentation and historical references known to date on each production center.

In the third milestone (Chapter 6), the previous archaeometric characterizations are used for the development of a **Non-destructive Screening Methodology based on ED-XRF for the classification of Medieval and post-Medieval Archaeological Ceramics**.

[5]The repository is provided as a supplementary material and can also be accessed online at `https://github.com/esteful/arch_flow`

[6]This dataset does not comprise the ceramic assemblage under study in this doctoral thesis. However, this well-known dataset from Tubb et al. (1980) was selected since it provides clearer results, when the purpose is to illustrate the developed computational tools.

The content of Chapter 4 is mainly supported by the mentioned repository on GitHub, whereas the Chapter 6 is based on the publication(Calparsoro et al., 2019b). In addition, the case studies are based on already published works, such as in the case of Nájera (Calparsoro et al., 2019d) and Orduña (Calparsoro et al., 2019a; Rodríguez Miranda et al., 2017); or they are in process of publication (Logroño, Durango and Elosu). Furthermore, the results presented in this doctoral thesis have been presented in several scientific communications (Calparsoro Forcada et al., 2016; Calparsoro et al., 2017b, 2019c, 2018, 2017a)

Somehow, R changed my opinion about humankind by observing how many people are really willing to participate in collective activities, looking for something that transcends their own interests. In this area, many activities are carried out without individual recognition.

Ross Ihaka, co-founder of R.

Chapter 4

Development of an Open Methodology for Compositional Data Analysis of Archaeological Pottery based in R

Abstract

This chapter presents a methodological approach devised for the archaeometric analysis of pottery. The comprehensive strategy is based on the open source R programming language and a repository is provided, which includes all the necessary code for a complete reproduction. It combines powerful data visualization tools (e.g. interactive heat maps, ternary diagrams, etc.) with robust statistical treatments of multivariate analysis (e.g. hierarchical clustering analysis or principal components analysis). In addition, it is designed to integrate both archaeological and chemical data, facilitating the processes of pattern extraction and identification of outliers, as well as the assessment of group membership probabilities used in archaeometric analysis routines. However, it can also be extended to other types of investigations involving geochemical data. The performance of the proposed methodology was tested with an example of a well-known dataset of Roman-British ceramics. As a result, an open archaeometric methodology was generated that encourages researchers to adopt reproducible research initiatives based on open source tools.

Compositional Analysis of Ceramics

The specific nature of compositional data and its implications for the statistical analysis have been widely discussed in literature(Aitchison, 1982; Bishop and Neff, 1989; Buxeda i Garrigós, 2008; Boogaart et al., 2010). For computing purposes, compositional data fundamentally involves an array of chemical elements which act as variables (columns). These are normally given for a set of ceramics pieces, named by their analytical ID (ANID) and presented in rows. These values are obtained after the chemical elemental analysis of ceramic pastes by means of different analytical techniques, most frequently, neutron activation analysis (NAA), inductively coupled plasma - mass spectrometry (ICP-MS) or X ray fluorescence spectroscopy (XRF) (Glascock, 2016; Hunt, 2016; Glascock, 2017). Before the arrival of these techniques, atomic absorption spectrophotometry dominated the field (Hunt, 2016) and such was the choice of Tubb et al. (Tubb et al., 1980) whose data have been used reiteratively in literature (Boulanger, 2017; Tubb et al., 1980), as exemplary and is the choice to illustrate the current work.

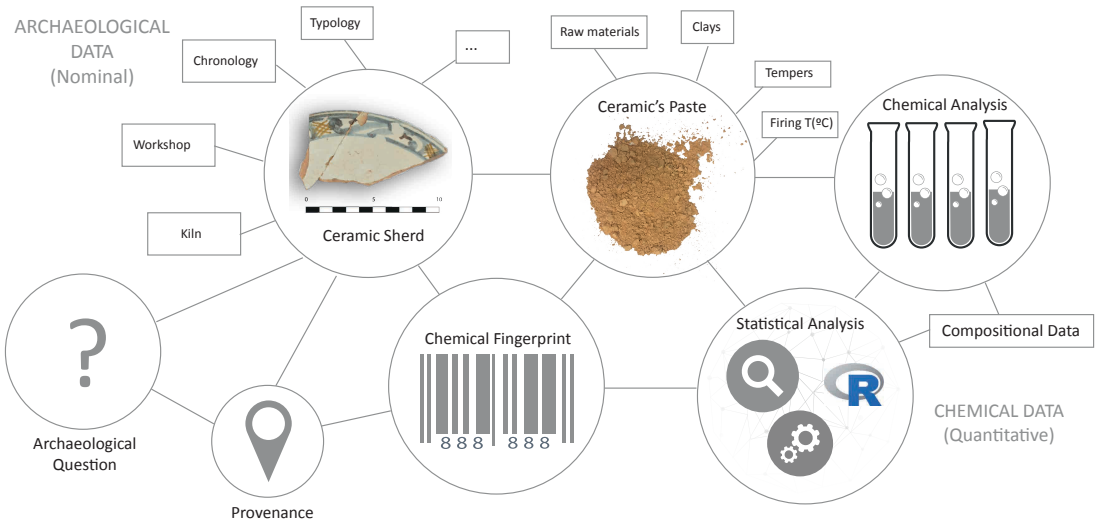

Figure 4.1: Main steps and factors involved in the archaeometric analysis of pottery

In terms of data dimensions, the number of chemical elements used is usually in order of tens and varies according to the employed analytical technique. The number of elements to be analyzed is determined by the suitability and technical limitations of each technique for each element, as well as the standards that have been used for its calibration. Orientatively, XRF, NAA and ICP-MS, can provide values from circa 40 elements to almost all of them, increasing respectively. Meanwhile, the number of individuals is determined by the size of the specific research project. Exploratory analysis of unknown sherds range typically from the order of tens to hundreds, whereas, the comparison with already existing data may lead to thousands of individuals to be included in the

dataset. This is the case of provenance studies which often imply the comparison of ceramics with already existing datasets, and application of tests to assess membership probabilities (e.g. test based on Mahalanobis distance test, such as T^2 Hotelling). In R, like in any architecture of spreadsheets , usually the rows correspond to ceramic individuals (identified by their ANIDs or analytical IDs) and the columns correspond to chemical elements. Then, the newly obtained compositional data is evaluated by means of multivariate statistical techniques and compositional groups are established according to different chemical patterns (Buxeda i Garrigós, 2008; Buxeda i Garrigós et al., 2003). Nevertheless, the complexity of statistical procedures has hindered the proper application of these procedures.

In contrast, initiatives carried out thanks to the proliferation of new sharing tools, have promoted the application of those in a more accessible manner and thus, have reduced the mentioned bridge. A good example is found in the referential book Quantifying Archaeology (Shennan, 1988) for which a complementary material written as R routines is attached (Carlson, 2012). More specifically, Quantitative Methods in Archaeology using R (Baxter, 2015) gathers the R code behind the processes discussed in the book. The aim of the current work is to present a novel workflow in R environment, designed to ease the process of compositional data analysis in a manner that is easy to reproduce, but also intends to engage the community in working with such tools. This section is not intended to be a tutorial, but rather a more extensive explanation, revisiting the theoretical aspects underlying the procedures applied to the proposed workflow by using a well-known dataset. The explanations on the code are commented with the code in the corresponding repository.

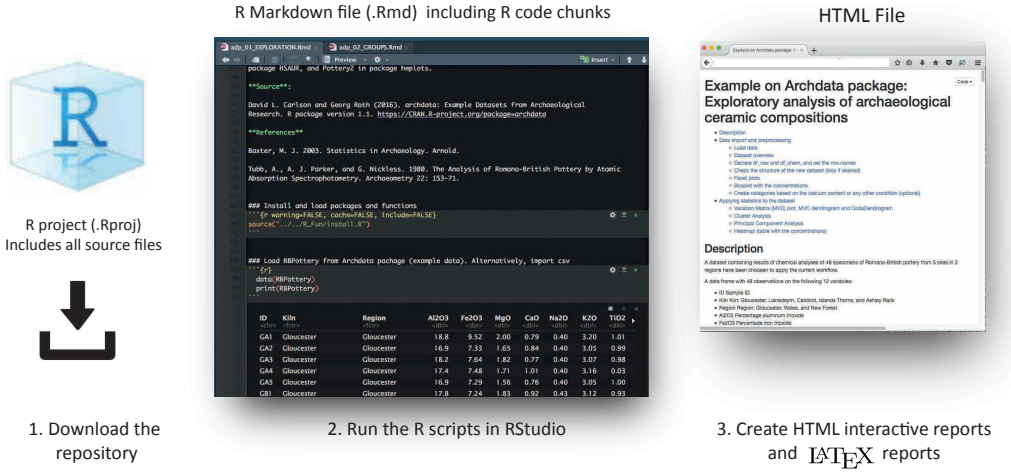

Figure 4.2: RStudio interface and the elements involved in the proposed workflow.

The dataset used to illustrate the proposed workflow corresponds to compositional data of of a Romano-British pottery set of pottery analyzed by atomic absorption spectrophotometry (Tubb et al., 1980). This dataset has been employed multiple times in literature in order to illustrate different statistical procedures carried out with R software (e.g. Baxter (2015)). This dataset, which includes many other datasets of the archaeological field ready-to-use with R, is available through the R package "ArchData"(Carlson and Roth, 2016).

Open Method based in R

The routines were designed with the purpose of being executed from the Rmarkdown file (rmd)-a file including code chunks- in RStudio program[1] The advantage of working with RStudio is that allows working within projects, which eases the control of the working space. In this way, the data and the output generated (i.e. charts, plots, tables...) during a project can be saved together, and most importantly, these can be accessed anytime along with the scripts used for the computational processes, which is often the main drawback hindering the reproducibility of a research project.

In order to put into practice the proposed workflow, the repository on GitHub (Calparsoro, 2019) can be downloaded or cloned. All the files required to follow the workflow are included in the repository, as well as the functions that have been specifically written for the current project. Their installation is easily performed by running the "install.R" file in the first chunk (more explanations are given in the rmd file). For this work, an example of the workflow applied to data from Tubb et al. (Carlson and Roth, 2016; Tubb et al., 1980) is included in the folder called "01-ArchData-Package". This folder, contains three folders, corresponding to each step proposed for the workflow, which are:

- 01. EXPLORATION: Perform the initial exploration of the dataset, including visualizations and statistical approach (includes rmd file)
- 02. GROUPS: Establish the compositional groups (includes one rmd file)
- 03. OUTPUT: Generate output Figures and tables (includes one tex file)

The R code to follow the workflow is included in chunks (pieces of code) in a rmd, along with the corresponding explanations in markdown language, a lightweight markup language with plain text formatting syntax. These files contain all the instructions, for importing the data and applying to it the statistics (e.g. PCA, HCA...). As a result, an HTML can be rendered (see Figure 4.2). In our case, the rendering to an HTML, also known as knitting (i.e. convert rmd file in HTML), results of most interest since it allows

[1] A rmd stands for R Markdown and is a type of file where R language is combined with Markdown language (a lightweight markup language with plain text formatting syntax).

an interactive exploration of the dataset. These scripts can not only be rerun with the example data in order to reproduce the method but, most interestingly, they can also be applied on new data added by the user in order to replicate it (Marwick, 2017). The user will find a straightforward starting point for the exploratory analysis of compositional data which can be customized deepening on the field to the desired extent, as the level of expertise allows. In this way, an attempt is made to engage the community in working with such a tool.

The most relevant procedures behind the steps involved in each of the three sections of the workflow are explained in the following lines. The advantage of this workflow is that the data are inserted once and different output are created according to it and automatically. The chunks can be executed separately, which allow the early detection of errors and the easy customizing of the code.

The first section of the workflow (01. EXPLORATION) includes two different groups of procedure types, data importing and preprocessing and applying statistics to the dataset. In the first group of functions, the goal is to explore the data, visualize the categorical data, etc. and in the second, to look for the variabilities of the data in order to identify potential compositional groupings and identify the elements responsible for the variabilities among the Ic-s, as well as the outlying observations. The specific aim of each code line accompanies the corresponding script and the main index is presented in the following lines.

01. EXPLORATION

1. Data import and preprocessing
    a) Load data
    b) Dataset overview
    c) Declare df_raw and df_chem
    d) Check the structure of the dataset
    e) Pie Chart in facet plots
    f) Box and whiskers plot with the concentrations
    g) Create categories based on a condition (optional)
2. Applying Statistics to the dataset
    a) Compositional Variation Matrix (CVM)
    b) CVM plot, dendrogram and CodaDendrogram
    c) Scatter Matrix Diagram
    d) Cluster Analysis

e) Principal Component Analysis

f) Heatmap (table with the concentrations)

g) Ternary Diagram

h) Outlier detection

i) Assessment of the group membership probability

Data import and preprocessing

As mentioned before, in order to illustrate the workflow, a popular dataset was employed. In this case, to obtain the data, a R package was installed and then *RBPottery* dataset was loaded to the global environment. Nevertheless, the most typical way of importing the data is by reading a "csv" file. The popular dataset from Tubb et al. (1980) adapted to be used easily in R by the creation of ArchData package (Carlson and Roth, 2016) contains values of chemical analyses obtained by atomic emission spectrophotometry corresponding to 48 specimens of Romano-British pottery. The data-frame contains information on the following 11 variables: Kiln, Region, Al_2O_3, Fe_2O_3, MgO, CaO, Na_2O, K_2O, TiO_2, MnO and BaO.

First of all, some checkups must be carried out in order to ensure that all the data are read correctly to ensure a proper computation. Note that, especially when using R for the first times, the data preprocessing step is the most tedious and crucial part of the work, whereas once all the data are correct (e.g. the right class and use of commas) the application of statistics and visualizing steps are the most straightforward part, allowing to focus on the exploration of the results. The checkups in order to avoid data misreading include, negative terminating data, missing values and the assignation of the right class to each data type. In R the numbers must be (numerical or integers class type) while the categories (e.g. region, kiln, ...) that are qualitative should be read as factors (possibly ordered) so that they can be properly handled by several functions. The user must be familiar with the different data classes handled in R.

Once the data have been correctly loaded to the system, several visualizing tools have been chosen in order to explore the nature of the data, most of the visualizations have been performed using ggplot2 package, which offers highly customizable options. The method is cross-platform, suitable for Linux, MacOS and Windows. However, there are some differences for Windows systems, that should be taken into account. For the specific details see "readme" file on the GitHub repository (Calparsoro, 2019).

The pie charts by facets show at one glance (see Figure 4.3) that the pieces under study correspond to 5 sites where ceramic kilns where found (Gloucester, Llanedeyrn, Caldicot, Islands Thorns, and Ashley Railsin) and 3 regions (Gloucester, Wales, and New Forest). Furthermore, the contribution of every kiln is evident through the pie charts.

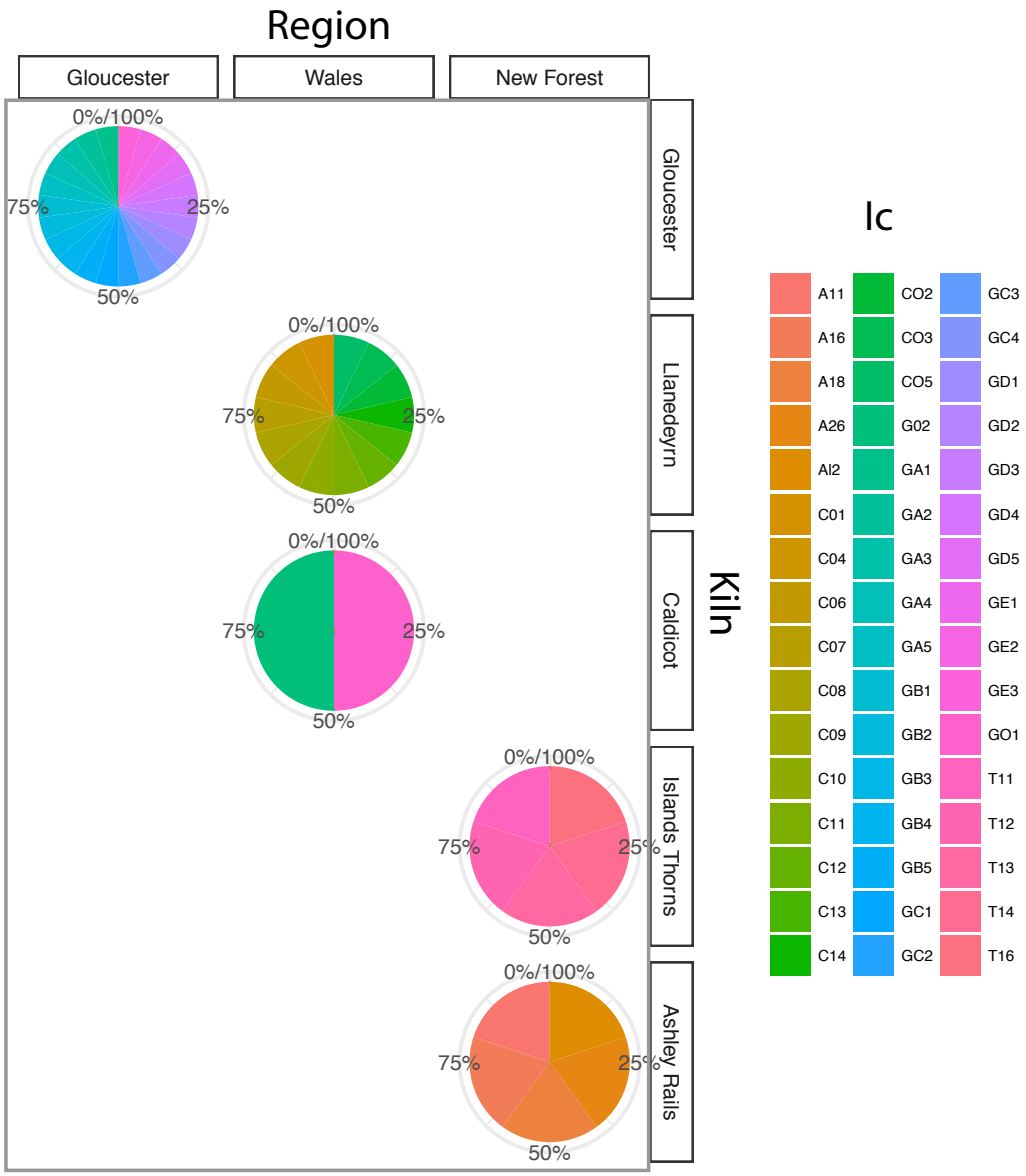

Figure 4.3: Pie charts displayed in facets obtained with *ggplot2* package of R showing the distribution of Ic among the regions and the kilns.

In order to work efficiently combining both chemical and categorical data, in the workflow two dataset are created, starting from the source data: df_chem and df_raw, the first one contains only chemical data (either numeric or integers) and the second contains also the categorical data (factors, regardless they are strings or numeric). Using two data-frames, we overcome the problem of, some functions where only numerical

values are accepted. Thus, by saving these data-frames to the global environment all the chunks could be run together, since their are ready to call df_chem and df_raw.

The loop created for the box and whisker plots allows assessing the distribution of every chemical element among every individual in the dataset simultaneously and pointing out the categories indicated before. In this step, preliminary patterns associated with different groups can be identified. The spacing between the different parts of the box indicate the degree of dispersion (spread) and skewness in the data. Five summary statistics are visualized (the median, two hinges and two whiskers), and all outliers values individually. The upper whisker extends from the hinge to the largest value no further than 1.5 * IQR from the hinge (where IQR is the inter-quartile range or distance between the first and third quartiles). The lower whisker extends from the hinge to the smallest value at most 1.5 * IQR of the hinge. Data beyond the end of the whiskers are called "outlier" points and are plotted individually. This method of outliers identification is called the Tukey method. The box plot function from ggplot2 allows identifying univariate outliers and removing them easily from the data-frame.

From the study of data of Romano-British pottery, it can be observed the different distribution of elements and identify several outlying values. As an example, the plot corresponding to Al_2O_3 is shown (see Figure 4.4). From the box and whiskers plots it is clear that pottery fired in the kilns from Gloucester and New Forests is richer in Al_2O_3, while those from Wales contain lower concentrations. Meanwhile, two outliers are detected in the kiln of Island Thomas. Note that the distribution of Caldicot is very compact due to the number of specimens, which are only two. All the box plots are included in the supplementary material. The typographic error detected by the creator of the package (Carlson and Roth, 2016) is evident in the plot of TiO_2, where a Ic contains a value very close to 0.

Moreover the graphs such as the scatter matrix (see Figure 4.5) shows the distribution of all elements by facing a selection of elements. This kin of visualization is very useful to assess the role of specific elements for discriminating different groups.

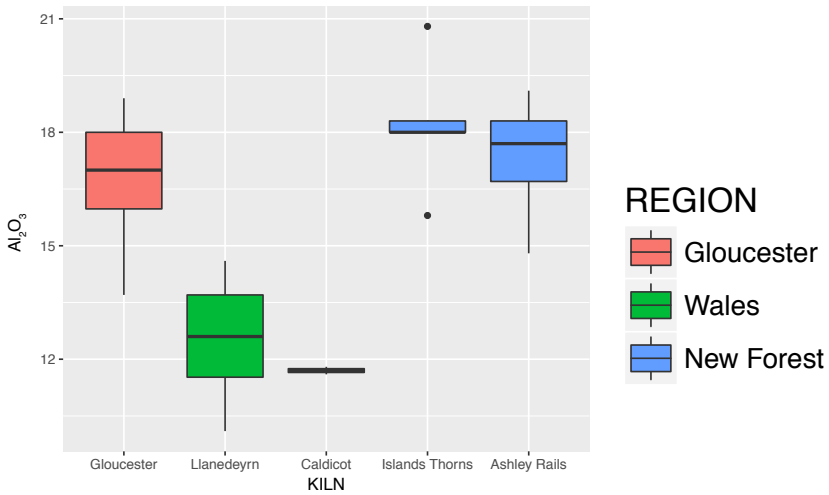

Figure 4.4: Box and Whiskers plot of Al_2O_3 concentrations for 48 Ic-s and displayed by kilns. The colors represent the region. X-axis (Gloucester, Llanedeyrn, Caldicot, Islands Thorns, and Ashley Railsin). Plot generated using *ggplot2* package.

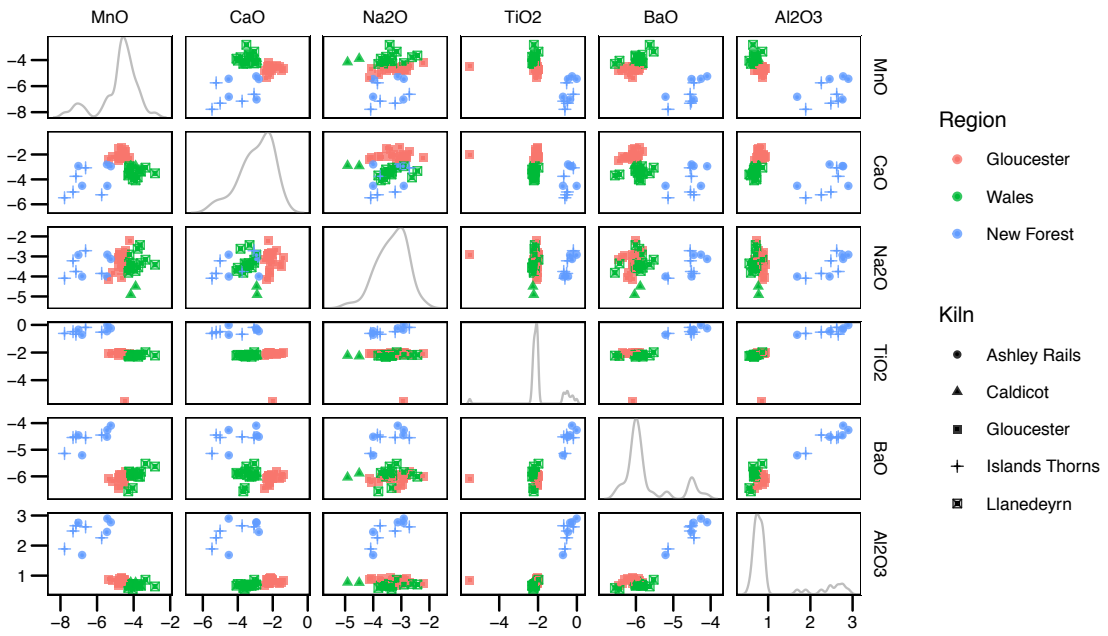

Figure 4.5: Scatter plot matrix of 48 Ic-s using alr transformation on the following elements: Al_2O_3, MgO, CaO, TiO_2 Na_2O, MnO and BaO. Fe_2O_3 used as divisor. On the diagonal, density estimation plots by kernels are shown for each of the transformed values.

In order to accomplish the preliminary data exploration, some code is provided to create new categories based on a chosen condition. As an example, the calcium content is proposed, adding new categories according to CaO concentration. In the case of Romano-British pottery, all the ceramics are very low in calcium content.

Applying statistics to the dataset

The statistical approaches used for the archaeological materials are constantly being rethought and, at this point, there is no ideal procedure. Most suitable method depends on the nature of the data each time (Glascock, 2016). The approach followed in the current workflow is based on Aitchison's approach and Buxeda's observations on compositional data (Buxeda i Garrigós, 1999; Aitchison, 1982; Buxeda i Garrigós and Kilikoglou, 2003). The strategies chosen for data exploration are based on the following ideas.

Matrix of Compositional Variation (CVM) and the graphical representations

The initial stages of the statistical analysis of archaeometric compositional data usually involve the examination of the degree of variability (Glascock, 2016). Thus, following the proposed workflow, after evaluating the individual variability of each element for each Ic in the box plots, the connection of variances among different elements in the dataset is analyzed. For this analysis, the matrix of compositional variability (CVM) is very handful (Buxeda i Garrigós and Kilikoglou, 2003). The graphical representation of the CVM, whose code derived from the version of Buxeda i Garrigós, is shown in Figure 4.6 and the corresponding table is generated for the evaluation and included with LaTeXsyntax in the final report (generated in the third step of the workflow). The CVM graph displays the individual contribution of the variability from each element to the whole dataset, from the highest to the lowest. In other words, this plot is the representation of the compositional evenness of the different elements on the dataset. Moreover, other values are displayed such as: vt = Total variability, H_2 = information entropy, H_2% = percentage of information entropy over the maximum possible, n = number of specimens. From the chart, it can be observed that MnO is the component adding more variability to the dataset, while Fe_2O_3 is the one varying less. The value of total variation describes the extent of variability of the set of ceramics; according to this measure, the polygenic or monogenic nature of the compositional data is hypothesized (Buxeda i Garrigós and Kilikoglou, 2003). In the case of Romano-British pottery, the total variation of the whole dataset is very high (4.2). This high value, suggests a polygenic nature of the set, anticipating that there are different compositional groups within this dataset. Actually, this is the case since we already know that there are three chemical highly distinguishable groups.

On the other hand, the dendrogram using the values of the CVM is created (see Figure 4.6). This type of plot allows identifying the relationships among different elements. From this plot, it is clear that CaO and MnO vary in a similar way that at the same time has no correlation with other elements variabilities.

In addition, another type of representation is automatically created from the same data. Regarding the special geometry of the simplex, the search for meaningful coordinates has suggested balances between two groups of parts —based on a sequential binary partition of a D-part composition —and a representation in the form of a CoDa-Dendrogram, which is a graphical representation of a sequential binary partition, together with additional statistical summaries of balances presented (Pawlowsky-Glahn and Egozcue, 2011).

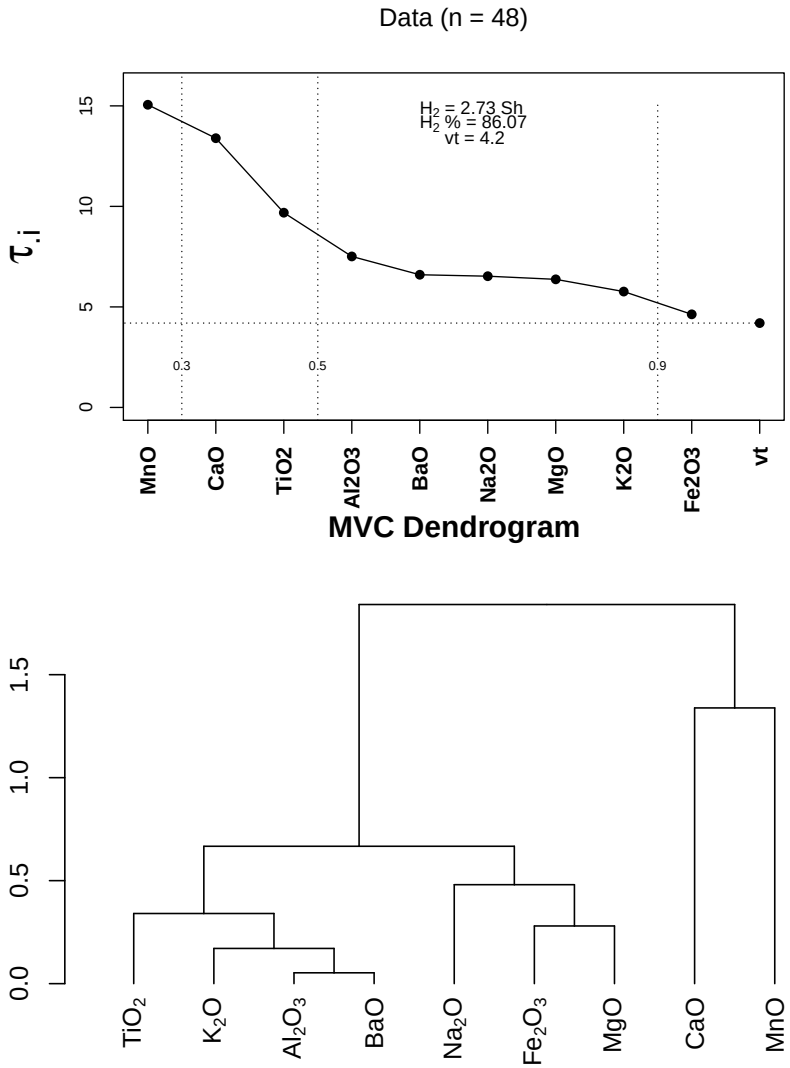

Figure 4.6: Graphical representation of the evenness of the compositional variability of 48 Ic-s. vt = Total variability, H_2 = information entropy, H_2%= percentage of information entropy over the maximum possible, n = number of specimens (above). Dendrogram of the compositional variability of 48 Ic-s (below).

Data transformation

As addressed in the methodology (Section 3.3), it has been suggested that geochemical data show neither a normal nor log-normal data distribution (Zhang et al., 2005). However, most of archaeological researchers use a logarithm transformation because it acts as a "quasi-standardization" (Neff, 2000; Sayre, E.V., Harbottle, G., Bieber, A.M., Brooks, 1976; Martín-Fernández et al., 2015) that compensates for the differences in

absolute magnitude between the major elements, such as Al, K, and Fe present at percent levels, and the trace elements, such as the rare earth elements (REEs) present at parts per million and below. Thus, the transformation places the elements onto more or less the same scale (Glascock, 2016). Moreover, Aitchison remarks the importance of using log-ratio analysis and its associated distance measures since these would satisfy certain invariance conditions required for a proper compositional data analysis, especially in multidimensional scaling and hierarchical cluster analysis (Aitchison et al., 2000).

The raw compositional data consist of vectors whose components are part of some whole (Aitchison, 1982). The sum of each component is equal to a constant (100 in percentages). These kinds of data are constrained, they are not absolute values since they have a dependency from one each other (Buxeda i Garrigós and Kilikoglou, 2003). Removing one or more analytes would influence the values of the other analytes. Therefore, it is not possible to consider the compositional data as independent from the number of components. Their sample space is called simplex. Since the compositional data is in the simplex space and not Euclidean, the application of standard statistic methods as the multivariate analysis can lead to spurious results (Aitchison, 1982). Therefore, according to Aitchison (Aitchison, 1982), the only real information in compositional data is given by the ratios between components.

In the workflow, the divisor used for the ratios will depend on the statistical analysis to be performed. On the one hand, for the hierarchical cluster analysis (HCA), a centered log ratio (clr) transformation is applied, which consists on dividing all the elements by the geometric mean (Boogaart et al., 2010). While on the other hand, for the principal component analysis (PCA), the component used as divisor is the one that introduces the lowest chemical variability to the entire set of specimens. This is called the additive log ratio transformation (alr). Both transformations are very easy to apply thanks to the functions included in the package Compositions (Boogaart et al., 2010). These choices are optional and the mentioned packages included other type of data transformation (e.g ilr) which could be applied depending on the nature and requirements of the dataset.

HCA and PCA

After data transformation, hierarchical clustering analysis (HCA) is performed. Similarity of individuals and the subsequent compositional groups they form are assessed by representing graphically the squared Euclidean distance using the centroid agglomerative algorithm on clr-transformed data (Figure 4.7). Whereas this plot is connected with the minimum spanning tree published by Tubb et al. (1980), in HCA from all the initial individuals that are in their base, a hierarchical process of agglomeration is established. This is the union in each stage of an individual with another or with another group, or from one group with another, until a single group

formed by all the individuals analyzed is obtained. In this way, the farther away from the base the union occurs, the less similar are the individuals that come together in its chemical composition. For the computation of such a plot, first a hierarchical clustering has been performed by *hclust* function and then it has been plotted with Dendextend package, which as ggplot2 offers a variety of customizable tools but is specifically to plot dendrograms. One of the clear advantages of the workflow is that allows coloring the labels of the individuals, thus correlations between categorical data and chemical similarities can be observed. In the case of Romano-British pottery, three main groups are clearly differentiated according to the region, whereas using the 12 available variables, the distinction among the 5 kilns was not that clear (see Figure 4.7).

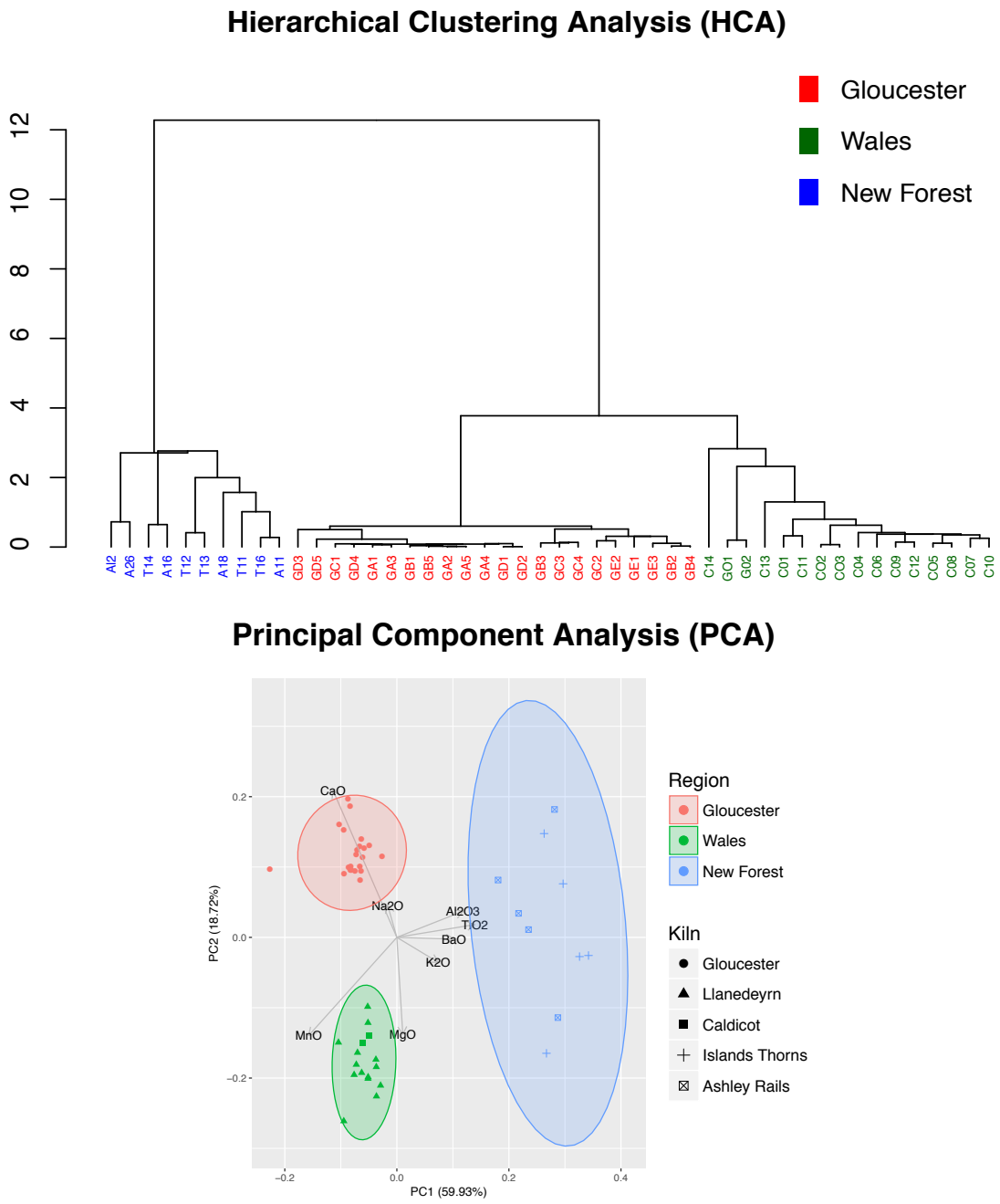

Figure 4.7: HCA of 48 Ic-s using the centroid agglomerative algorithm of the clr transformed values of:Al_2O_3, Fe_2O_3, MgO, CaO,TiO_2 Na_2O, MnO and BaO (above).PCA of 48 Ic-s using 7 variables, where the Fe_2O_3 has been used as divisor for the alr transformation (below).

Whereas the HCA provides information about the possible groupings between sherds according to their similarities, PCA provides similar information, but also points out which elements are the responsible for such similarities or dissimilarities. According to the PCA plot performed for the RBpottery dataset (see Figure 4.7), the ceramics from the kilns of Gloucester are notably richer in CaO and slightly in Na_2O, while welsh ceramics contain higher concentrations in MnO and MgO, in contrast the group of New Forest is richer in Al_2O_3, TiO_2, K_2O, and BaO. It is also notorious how GA4 individual contains an outlying value of TiO_2 as is far away from the other specimens from Gloucester.

Heatmap

In addition, a heatmap has been chosen for the exploration of specific chemical values (see Figure 4.8). This tool is enhanced when using the HTML version of the report since it is interactive and allows zooming. Summarizing the chemical dataset, in this table a color is assigned to each analyte for each specimen according to individual values, for higher values (warm colors) or lower (cold colors) to the average concentration for that analyte in the set of studied Ic-s , the intensity of the color indicates the dispersion of those values being the highest intensities farther from the average, which allows to quickly identify outlier values. Each color has been assigned according to the ratio of the specific concentration to the mean one for each element. From the example plot it is very easy to observe that the MnO value out-lies for C13 Ic and TiO_2 for CA4, which was previously warned by the author of ArchData package, pointing it as a typographic error.

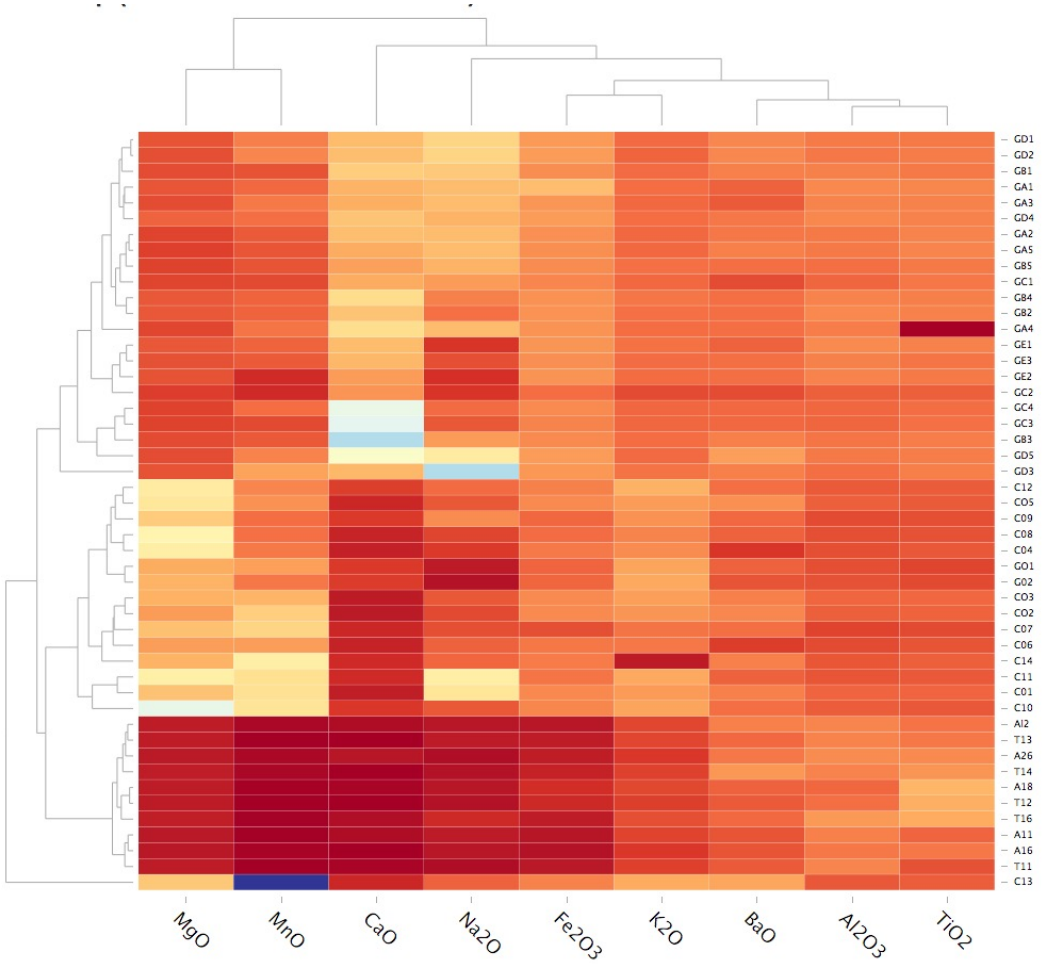

Figure 4.8: Heatmap showing the differences in the chemical compositions of the ceramics studied according to the color gradient for visualization (colder color indicates greater difference and warmer color minor difference.

Ternary plot

In the workflow three different ternary diagrams are included (see Figure 4.9): (i) the CaO-Al_2O_3-SiO_2 system, (ii) Fe_2O_3 + MgO + CaO-Al_2O_3-SiO_2 system (also known as the ceramic triangle) and (iii) the CaO-MgO-SiO_2 system. In several cases, SiO_2 is not determined, precluding the realization of these types of plots. In the present dataset, SiO_2 was not determined. This is not usually the case in ICP-MS or XRF analyses. In contrast in techniques such as NAA, the use of quartz vials obliges to exclude this Si element from the measurements (Glascock, 1992). The method provides the possibility to estimate SiO_2 concentrations as the difference between a given constant (chosen by the user) and the sum of the determined elements. In Tubb's dataset (Tubb et al., 1980),

since almost all major and minor elements were initially determined on calcined pastes (making negligible the effect of the loss on ignition), it was found reasonable to estimate SiO_2 concentrations using a constant of 98%.

Regarding the natural dimension of ceramics introduced in the Chapter 1, the role of phase diagrams (including ternary plots), on assessing firing temperature, conditions and source of raw materials was studied in deep by Heinmann (1989). From the statistical perspective, the ternary diagram offer the possibility to be adjusted depending on the dataset. For more details on the right adjustment for the ternary plots using R see Baxter (2015). In addition, the use of re-sampling methods (bootstrapping) has been proposed in order to overcome the problem that these diagrams do not take account on the sampling size hindering the statistical comparison between different sets (Steele and Weaver, 2002).

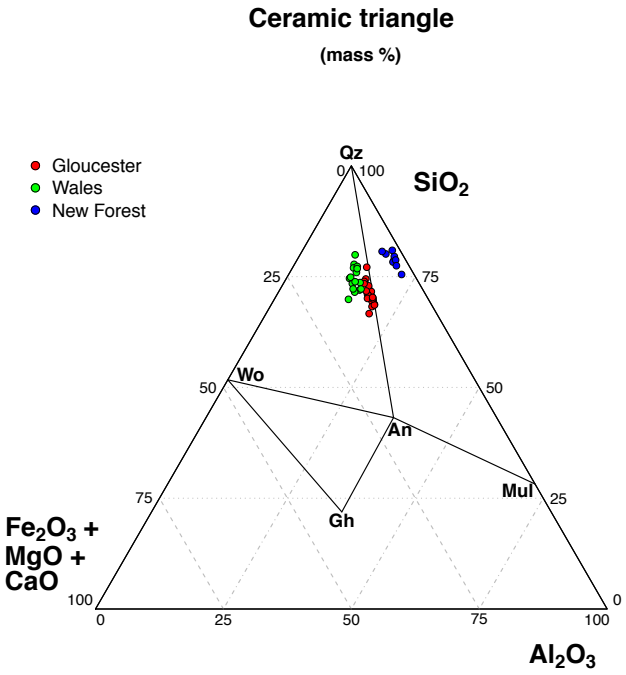

Figure 4.9: Diagram showing the Fe_2O_3+MgO+CaO-Al_2O_3-SiO_2 ternary system. SiO_2 values have been estimated. An:Anorthite, Gh:Gehlenite, Mul:mullite, Qz:quartz and Wo: Wollastonite (abbreviations after (Whitney and Evans, 2010)).

Outliers

In the last step of the exploratory analysis a strategy for outlier removal is employed. As mentioned before, the outlier values have already been graphically displayed. The same function used for this graphical display allows saving the data in the global environment

and extracting the outlier values. The implications of outlying values and missing values has been studied and several functions created to deal with this kinds of values using R exist (Bren et al.)

02. GROUPS

1. Iterative statistics
2. Creation of the subsets - declaring the groups
3. Labeling of the groups
4. Group Membership Probabilities

The second section of the workflow consists on defining the compositional groups after the statistical iterative process, according to the observations that have been made during the exploratory analysis. For instance, the decision of removing the TiO_2, confirms that GA4 is grouped within Gloucester ceramics. A dendrogram is newly obtained where this separation is clear (see Figure 4.7).

At this point, subsets can be created and labels can be given to the different individuals according to a new proposed compositional group. For this procedure a script is included, which extracts the groups from the cluster according to the number of groups included (k) or height to cut (h). In this case, it is clear that there are three clades, therefore k is set to 3. Therefore, three subset of the dataset can be automatically created. Nevertheless, for this step an equal variability among the groups is being assumed, which would be translated into the same ultra-metric fusion distance. However, this is not necessarily the case and there may be groups with widely dispersed variability due, for example, to the standardization of the paste preparation processes and/or the natural variability of the raw materials. In such cases, a manual assignation of the groups could be performed following the basic R function (an example is also provided).

Once these subsets have been created, the exploratory analysis of each compositional group can be performed for each group. Tools such as those seen for the exploration of the whole dataset (e.g. CVM and heatmap) will allow assessing the variability within each compositional group. The total variation for each group should be low, according to their monogenic nature (Buxeda i Garrigós and Kilikoglou, 2003). Nevertheless, high varying elements (e.g. Pb, As, P_2O_5...) might elevate this value significantly.

The HTML report generated in this step is of great utility to illustrate the reality of the dataset, which along with other archaeological data (e.g. chronology, site or production, etc.), will lead to working hypotheses.

Finally, the code to assess the group membership probability is included. It calculates the variance-covariance matrix and the centroid for any group of specimens. Then it determines from these the Mahalanobis distances expressed from an univariate mean in standard deviation units (i.e. from the centroid of the group for all members of the group) (Sayre, E.V., Harbottle, G., Bieber, A.M., Brooks, 1976; Baxter, 2015). For any additional specimens one might wish to compare to the group and it can be applied in a loop directly to the list of compositional groups created before. Thus, when Mahalanobis distance are converted into probabilities the potential membership for each individual in group can be assessed (Sayre, E.V., Harbottle, G., Bieber, A.M., Brooks, 1976; Glascock, 1992). These can also be cross-validated; by removing each specimen from its presumed group before calculating its own Mahalanobis distance from the centroid of the group and checking its actual correspondence to the group, as is reported in literature (Blomster et al., 2005). The limitation that Mahalanobis distance calculations present are that there must be two more individuals in comparison to the variables taken into account. Thus, if the compositional groups are of small size, the variables to be used must be reduced if possible. However, this may bias the results. Therefore, it is not advisable.

03. REPORT

This section includes a tex type file were called Report.tex which can be compiled directly from RStudio and creates a pdf including the CVM table (see Table 4.2) and the summary table (see Table 4.1) of each defined compositional groups. The purpose is to paste here the output tex code automatically generated in the previous steps (GROUPS).

	N	Mean	St. Dev	RSD
Al_2O_3	22	16.94	1.5	9
BaO	22	0.02	0.0	15
CaO	22	0.94	0.3	30
Fe_2O_3	22	7.43	0.7	9
K2O	22	3.11	0.2	7
MgO	22	1.84	0.2	11
MnO	22	0.07	0.0	26
Na_2O	22	0.35	0.2	46
TiO_2	22	0.90	0.2	23

Table 4.1: GR-GLO summary table

	Al_2O_3	Fe_2O_3	MgO	CaO	Na_2O	K_2O	TiO_2	MnO	BaO
Al_2O_3	0	0.005	0.005	0.085	0.245	0.006	0.552	0.074	0.024
Fe_2O_3	0.005	0	0.008	0.079	0.213	0.005	0.544	0.061	0.022
MgO	0.005	0.008	0	0.084	0.247	0.009	0.525	0.070	0.027
CaO	0.085	0.079	0.084	0	0.290	0.066	0.646	0.114	0.065
Na_2O	0.245	0.213	0.247	0.290	0	0.224	0.835	0.117	0.187
K_2O	0.006	0.005	0.009	0.066	0.224	0	0.547	0.065	0.020
TiO_2	0.552	0.544	0.525	0.646	0.835	0.547	0	0.668	0.559
MnO	0.074	0.061	0.070	0.114	0.117	0.065	0.668	0	0.062
BaO	0.024	0.022	0.027	0.065	0.187	0.020	0.559	0.062	0
τ_i	0.995	0.935	0.975	1.430	2.358	0.942	4.877	1.231	0.966
ν_τ/τ_i	0.821	0.874	0.838	0.572	0.347	0.867	0.168	0.664	0.846
R ν,τ	0.996	0.999	0.994	0.999	0.970	0.998	0.969	0.963	0.998
vt	0.817	0	0	0	0	0	0	0	0

Table 4.2: Compositional Variation Matrix of the GR-GLO group. Each column i (i = 1,$\cdots$S) shows the variances after a log-ratio transformation using the component x_i as divisor. vt = total variation. τ_i = total sum of the variances in column i. vt/τ_i = percentage of variance in the log-ratio covariance matrix using the component x_i, as divisor due to the total variation. $r_{v.\tau}$ = correlation between the values $\tau_{ij}(i \neq j)$ and the corresponding values τ_i (j = 1,$\cdots$,i-1, i+1,$\cdots$,S).$\Sigma_{\tau_{.i}}$ sum of the $\tau_{.i}$ values.

Final Remarks

After following the methodology presented in this section, 3 reference compositional groups were established for a set of 48 Ic-s matching the results published by Tubb et al. (1980). The variability of the different elements was evaluated according to different chemically distinguishable marks and their correlation with the archaeological data was assessed thanks to the different data visualization options. Moreover, the outlying Ic-s and problematic variables were easily detected thanks to different tools.

The idea of using the popular dataset validates the current proposed workflow, showing how can be performed the protocol from the data input to the output and output. The followed workflow covered from the data importation to the exportation of publishable figures (e.g. charts and tables). All the files of data and the routines involved on the process were stored in one single repository which can be cloned from the GitHub repository (Calparsoro, 2019) and rerun, thus the research becomes fully reproducible. Furthermore, the HTML report, allows saving an accessible file in order to keep the record of the results for interactive exploration at any moment.

The framework in which the current work was performed, —as an open method —is valid as starting point, for the beginner level, but it also allows the customization of the code in cases were the researcher is more confident with R environment and wants to deepen. The workflow includes the main tools used for the archaeometric approaches on compositional data analysis, but it is not limited to the field. Indeed, one remarkable advantage of the current work is that can be extended to other data types involving chemical compositions.

In view of the above, the implementation carried out of computer tools for the compositional analysis of archaeological ceramics aims to contribute substantially and thus settle a basis for the development of collaborative software around a line that has only just begun and which allows other users to contribute and make further improvements. These changes, or "commits" might be applied through "pull request"[2] to the present repository published in GitHub (Calparsoro, 2019) and we hope that these improvements will be reflected in the next versions of the repository presented in this doctoral thesis.

[2]"commit" and "pull request" are terms widely used in the GitHub environment. The first involves any change applied to the code and the second is used when the collaborator of a project wishes to implement those commits to the master project

Lo que este barro esconde y muestra es el transito del ser en el tiempo y su paso por los espacios, las señales de los dedos, los arañazos de las unas, las cenizas y los tizones de las hogueras apagadas, los huesos propios y ajenos, los caminos que eternamente se bifurcan y se han distanciado y perdido los unos de los otros. Este grano que aflora a la superficie es una memoria".

Jose Saramago. La Caverna

Chapter 5

Archaeometric Characterization of Pottery Production Centers from La Rioja and The Basque Country

5.1 Analytical considerations

For the archaeometric analysis of pottery, all the specimens presented in this doctoral thesis were subjected to ICP-MS analysis (n = 340) and, in addition, a subsample of them (n = 105) was analyzed by NAA (for further details on the methodologies, see Section 3.3). The nature of both techniques is very different and, in consequence, so are the possibilities they can offer. In general terms, NAA provides more precise and accurate information in comparison to ICP-MS. Moreover, the Archaeometry Lab at MURR, where NAA analyses were carried out, has been dedicated for decades to the analysis of archaeological ceramics. Therefore, apart from a high level of expertise, it contains the largest database of pottery NAA data, including most important majolica production centers of the Iberian Peninsula (Iñañez et al., 2008). This was, indeed, one of the main motivations for conducting these analyses. However, the installations required for NAA make this technique very limited. Thus, only a subsample of the individuals were subjected to NAA. Those analyses served to identify exogenous provenances as well as to support ICP-MS results as is addressed later. In addition, the experimental advantages and limitations concerning ED-XRF analyses performed in this doctoral thesis are widely discussed in the Chapter 6.

In the routines followed during this work, 33 and 43 chemical elements were detected by NAA and ICP-MS, respectively. The variables obtained with both techniques (n=29) are the following: Al, Rb, Sr, Zr, Cs, Ba, La, Ce, Nd, Sm, Eu, Tb, Dy, Yb, Lu, Hf, Ta,

Th, U, Na, K, Ca, Ti, V, Cr, Mn, Fe, Co and Zn. In contrast, by ICP-MS, concentrations were obtained for a wider element selection, extending to Cu, Er, Gd, Ho, Mg, Nb, P, Si, Sn and Tm. In the MURRs protocol, the reason for not quantifying Si, relies on the quartz vials used for the sample handling for irradiation (for more details see pag. 54 in the Section 3.3 of Methodology).

ICP-MS analyses were carried out in different batches (one batch per each archaeological site), whereas all NAA were carried out simultaneously. For this reason, NAA could be used to check the precision of ICP-MS results. The elements with the best correlation between NAA and ICP-MS was Co ($R^2 = 0.98$), however it was not used in statistical analyses for the reasons explained later. In addition, La, Ce, Mn, V and AlO_3 showed values above $R^2 = 0.88$), whereas the remaining where lower with the worst case in Cr ($R^2 = 0.12$). Nevertheless, no different tendencies were detected for each batch analyzed by ICP-MS (see Figure 5.1).

NAA also provided concentrations of As, Sb and Sc. By ICP-MS, Sc was no quantified since it was used as an internal standard (see Section 3.3) and, As and Sb were not quantified because the current protocol did not yield satisfactory results during the first trials. However, their quantification is not primordial because they often show high variabilities in Pb-rich matrices (such as the ceramics under this study) since they occur naturally together associated to Pb. With regard to NAA, the uranium concentrations are prone to be overestimated by the influence of Zr (Glascock et al., 1986), since the γ-ray emissions of both elements are of the same energy. However, regarding the low the concentrations in the studied individuals with a mean concentration of 3.4 ± 0.9 μg/g, these were considered insufficient to produce an experimental bias. In addition, both techniques failed to provide sufficient procedural quantification limits for Ni concentrations.

In the method followed in this work, JA-2, JG-1a, JG-2 and JB-3 were employed as external standard(Ando et al., 1989), whereas only SRM-1633b was used for NAA (Henry and Knapp, 1980). The CRMs selected for ICP-MS routines (which heavily relies on the calibration standards), involved restrictions on the use of some elements for the current study. For instance, Ni, Zn and Na_2O showed concentrations below Limit of Quantification (LOQ), together with high expanded uncertainties (see Table A.3 in Appendix 1). Therefore, these elements could not be employed in the chemometric analyses, especially in the case of Ni, where the 93% of the observations were below LOQ.

In addition, Sn and Pb concentrations showed values between LOD and LOQ in some cases. Furthermore, they presented concentrations that significantly exceeded their regression limits and they showed the most heterogeneously distributed values, especially for Pb (see Figure 5.2). Moreover, for the concentrations of Sn the expanded uncertainties were very elevated. Thus, their concentrations were considered semi-quantitative in the best of the scenarios. As is addressed later, their concentration

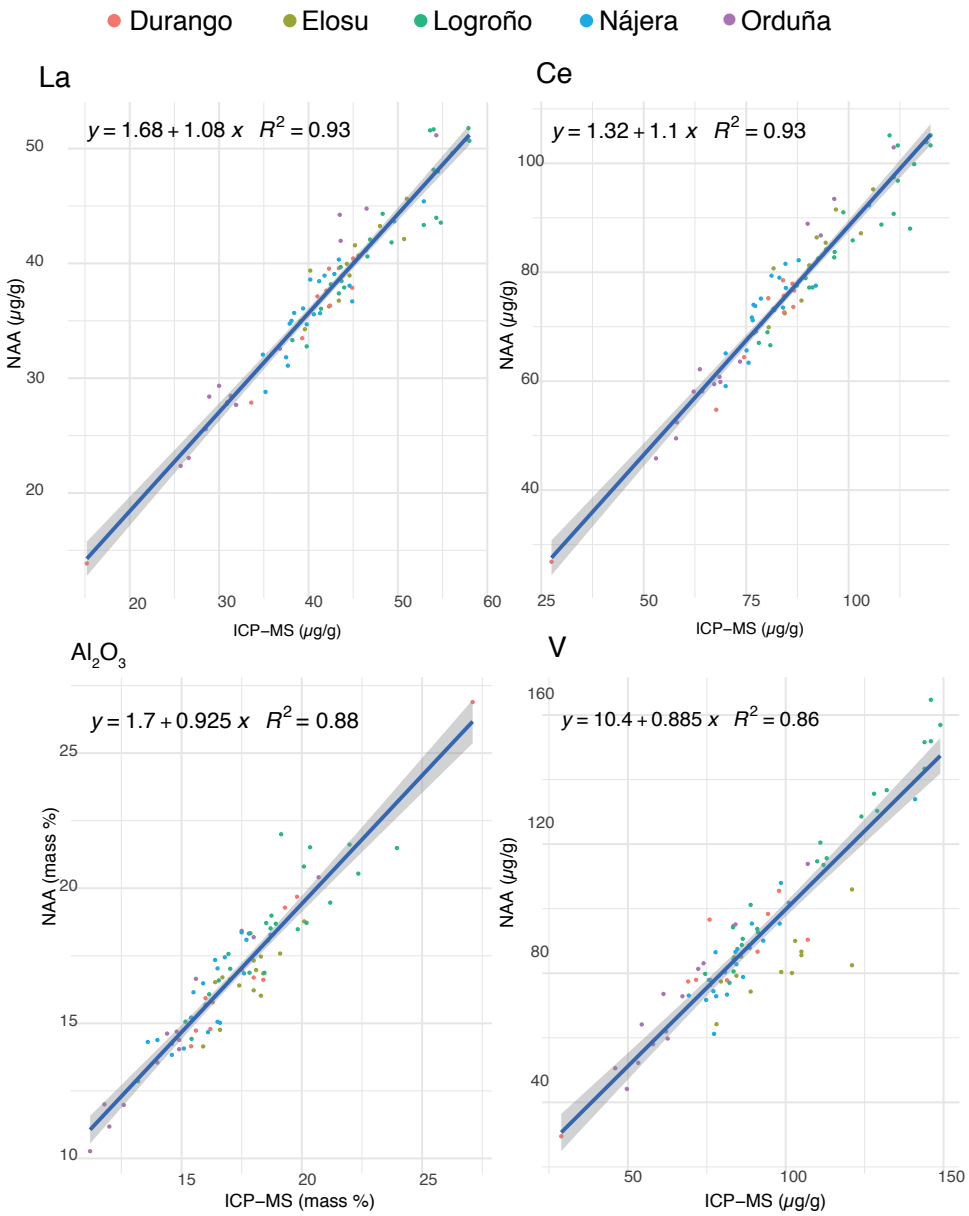

Figure 5.1: ICP-MS vs NAA regressions of Al_2O_3, V, Ce and La.

is subjected to alterations by the influence of the lead glazes. Interestingly, the linearity of which ICP-MS presumes, could be assessed in the extreme case of Pb, which shows

the widest range of concentrations. The ICP-MS instrument was still capable of providing a linear response far beyond the highest CMR concentration for this element (see the Figure 5.3).

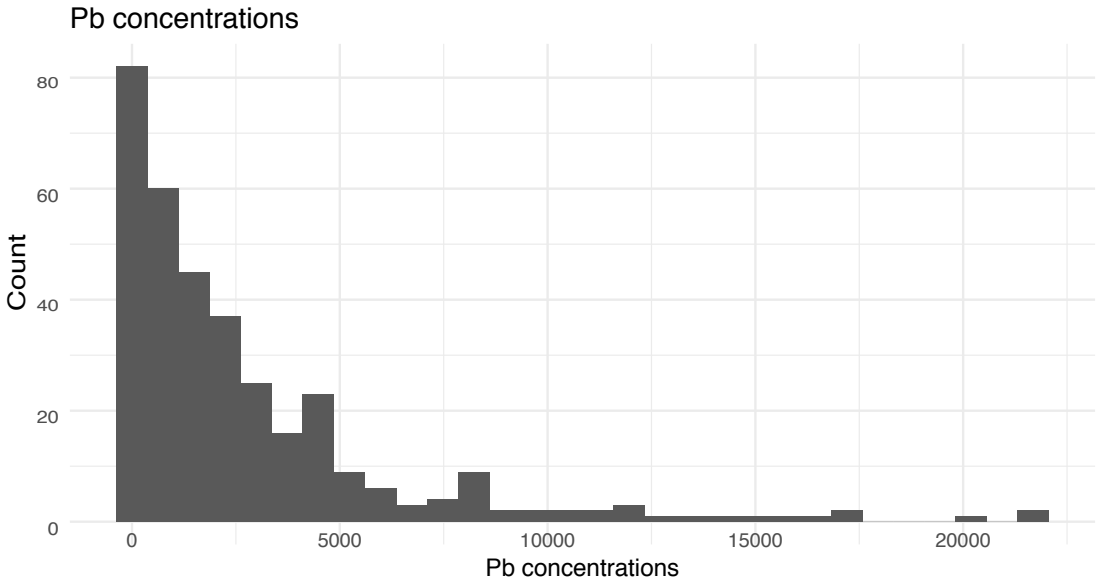

Figure 5.2: Histogram with the concentrations of Pb in μg/g for 347 samples

Furthermore, Cu showed very elevated uncertainties, which were probably due to the proximity of concentration values of the CRMs used to obtain the calibrates. Moreover, several outlying values were observed for this element. Thus it was also excluded from the statistical analyses. In light of the limitations exposed above, NAA concentrations were used to support and validate the concentrations of all commonly quantified elements obtained by ICP-MS.

Concerning the ceramics with micaceous pastes the expanded uncertainties of ICP-MS for some elements showed triplicated values (V, Cr and Ti) and duplicated ones (Sr, Th, Al, MgO, Fe_2O_3 and CaO) in comparison to the non-micaceous matrices. This increment is most probably explained by the low concentrations shown by those elements for micaceous matrices, especially in the cases of Ti, V, Cr and Th. In light of this, a critical treatment of the micaceous ceramics results and the necessity of a more suitable routine for their quantification was revealed. Thus, for these ceramic types the concentration of the above mentioned elements were only regarded as indicative and they were used with certain restrictions in the chemometric analyses.

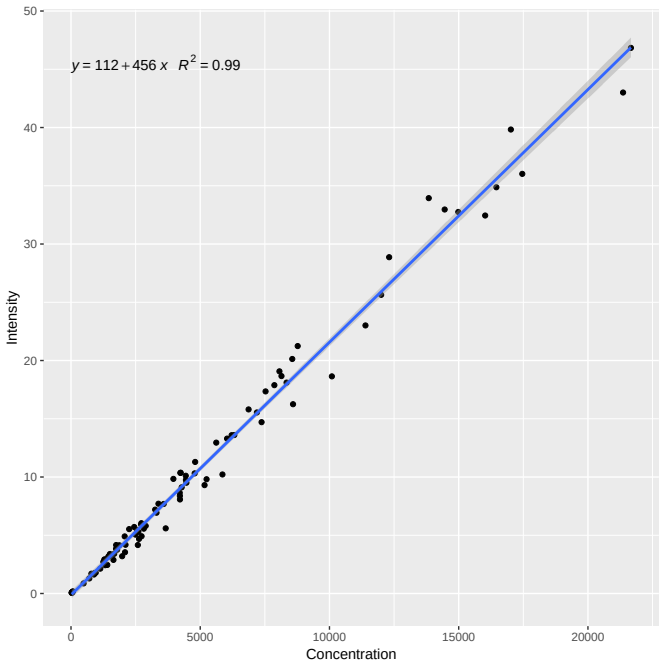

Figure 5.3: Normalized Intensity vs Concentration of Pb for a sample of 100 ceramics showing the good linearity obtained in a wide range of concentrations

Alterations and Contaminations

Regarding the *chaine operatoire* of ceramics addressed in the introduction (see pag. 1.1, these can undergo alterations and contaminations which occur mainly in two stages: during the firing process and during the post-depositional period. Moreover, the sample preparation process also have a direct influence depending on methodology used (Boulanger et al., 2013b). These alterations will introduce a chemical variability which does not represent the original chemical composition of the paste. In consequence, some elements will not be valid for statistical analysis in terms of discriminating among compositional groups because.

Alterations of glaze components: Pb and Sn

On the one hand, Pb and Sn are elements that are ubiquitous in tin-lead glazes and are prone to diffuse from the glaze into the clay body during firing process (Molera et al., 2001). As the names indicates, Pb is the major constituent of the plumbiferous glazes. In the present case, the variability of these elements is the highest observed in the whole dataset (see Figure 5.7). The influence of Pb and Sn from the glaze in the

concentrations of the ceramic bodies can be observed in Figure 5.4. The PCA depicts a clear discrimination based on these two elements, which by no means represent the natural variability of the ceramic assemblage. In the plot three trends are depicted: the unglazed ceramics, the lead glazed ceramics showing strikingly higher concentrations of Pb, and the tin-lead glazed ceramics, that show a clear enrichment of Sn. In addition, the high concentration of Pb in archaeological ceramics involves specific challenges regarding ED-XRF analyses. This point was addressed in the Chapter 6.

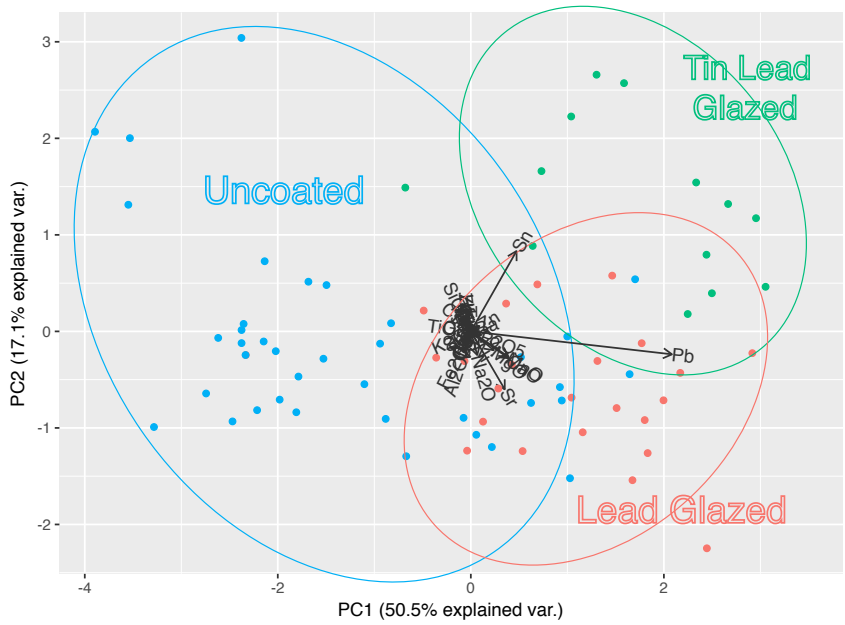

Figure 5.4: PCA showing the influence of Pb and Sn in the ceramic pastes.

Post-Depositional contaminations: P_2O_5 and Cu

Furthermore, post-depositional contaminations can occur due to P-compounds occurring in the soil waters. Thus, the concentration of this element in the ceramic pastes might vary depending on the exact burial location of the ceramics(Freestone, 1984). In consequence, random concentrations of P are obtained. The influence of P could be assessed by SEM-EDS analyses in two main levels: (i) spread through the glaze and forming liesegang rings-like degradation (see Figure 5.5) and (ii) taking advantage of one crack to penetrate into the ceramic body (see Figure 5.6).

Moreover, Cu concentrations can be a altered due to post-depositional contamination (Buxeda i Garrigós, 1999).

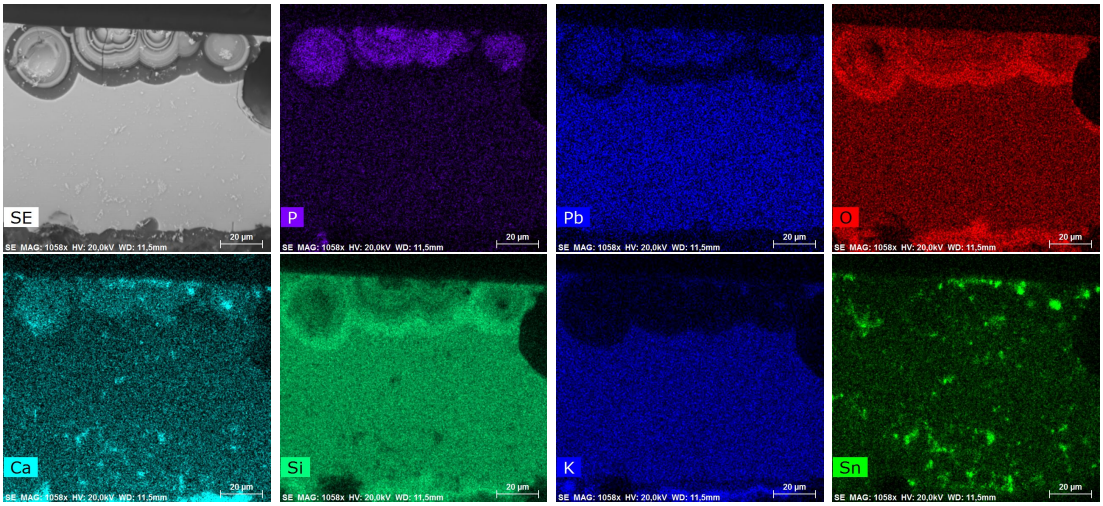

Figure 5.5: EDS maps of NAJ092 showing glaze alterations caused by P in form of liesegang rings.

Analcime driven Alteration: Na_2O, K_2O and Rb

Furthermore, some ceramics presented a double process of alteration of the vitreous phase of the ceramic paste with leaching of K_2O and Rb, and the subsequent crystallization of analcime ($NaAlSi_2O_6{\cdot}H_2O$), a sodium zeolite with the fixation of Na_2O from the water circulating in the soil (Buxeda i Garrigós et al., 2002; Schwedt et al., 2006). In this way, the contribution of this double process of alteration and contamination is difficult to quantify, thus as a general basis K_2O and Rb were also omitted from the statistical analyses. The identification of analcime was confirmed by XRD analysis and are listed in the summarizing tables of each case study. Moreover, the Ca variant of this zeolite, wairakite ($Ca(Si_4Al_2)O_{12}{\cdot}_2H_2O$), can also be found in ceramics. Additionally, CaO concentrations can be subjected to changes that do not respond to the natural variability of the clays. These are addressed in the following section.

Alterations due to sampling preparation

The sample preparation process can be another source of chemical variability. The use of a tungsten carbide cell for milling the ceramic pastes can alter Co and Ta concentrations since these are present in the alloy of the cell. Thus, they can be transferred to the ceramic paste when milling (Boulanger et al., 2013a). For this reason, Co and Ta were not used in the statistical analyses. Furthermore, prior to ICP-MS analyses, the milled

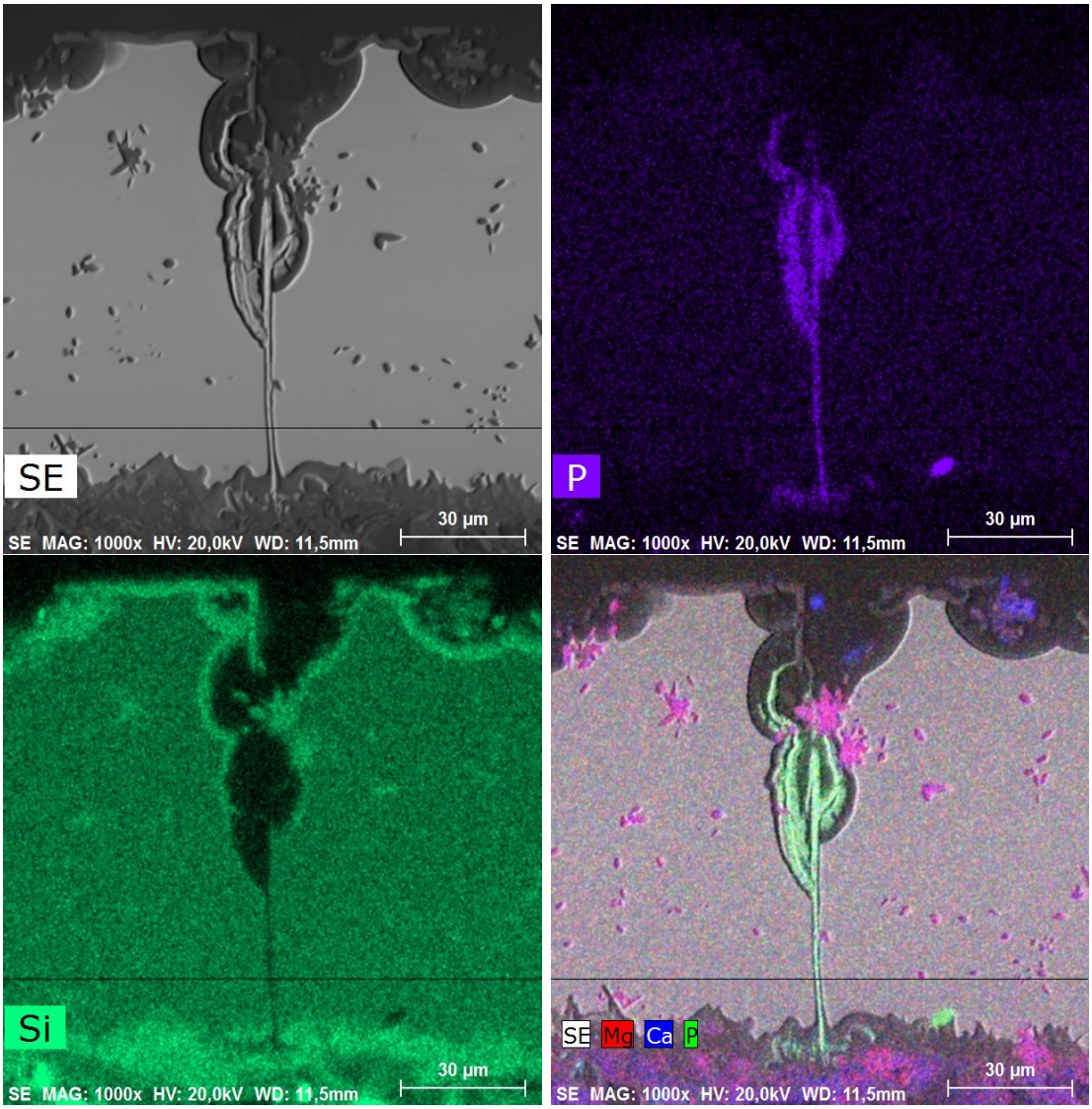

Figure 5.6: EDS map of LOG037 showing how P penetrates into the clay ceramic through a breach in the glaze.

pastes were mixed with the fluxer $LiBO_2$ and fused in Pt-Au crucibles (see Section 3.3). In consequence, non of these metals (Li, Pt and Au) could be determined.

REGION	SITE	GROUP	N	PROVENANCE
LA RIOJA				
	LOGROÑO	LOG-A	6	Local
		LOG-B	27	Local
		LOG-C	26	Local
		LOG-D	2	Undetermined
		LOG-E	3	Undetermined
		TER	6	Exogenous
	NAJERA	NAJ-A	56	Local
		NAJ-B	14	Local
		TAL	4	Exogenous
		MUEL	6	Exogenous
		NAJ-MIC	7	Exogenous
THE BASQUE COUNTRY				
	ORDUÑA	ORD-A	39	Local
		ORD-B	17	Local
		ORD-C	5	Local
		ORD-D	4	Local
		ORD-MEL-A	9	Local
		ORD-MEL-B	6	Local
		ORD-MIC	3	Exogenous
	DURANGO	DUR	18	Local
		DUR-MIC	4	Exogenous
	ELOSU	ELS	50	Local
TOTAL		21	312	

Table 5.1: Summary table of all the compositional groups defined in this Doctoral Thesis.

A broad perspective by ICP-MS

This section provides a general overview on the compositional characteristics of the ceramic assemblage under study. In order to extract the compositional groups present in the ceramic assemblage. First of all, the chemical variability of all elements was explored by means of compositional variation matrix (see A.8 in Appendix A). As a reference a list of all the established groups is displayed in the Table 5.1. As can be observed 312 samples were successfully ascribed to different groups (local, exogenous and undetermined). In addition, the number of samples constituting each group was very variable (N 2-56).

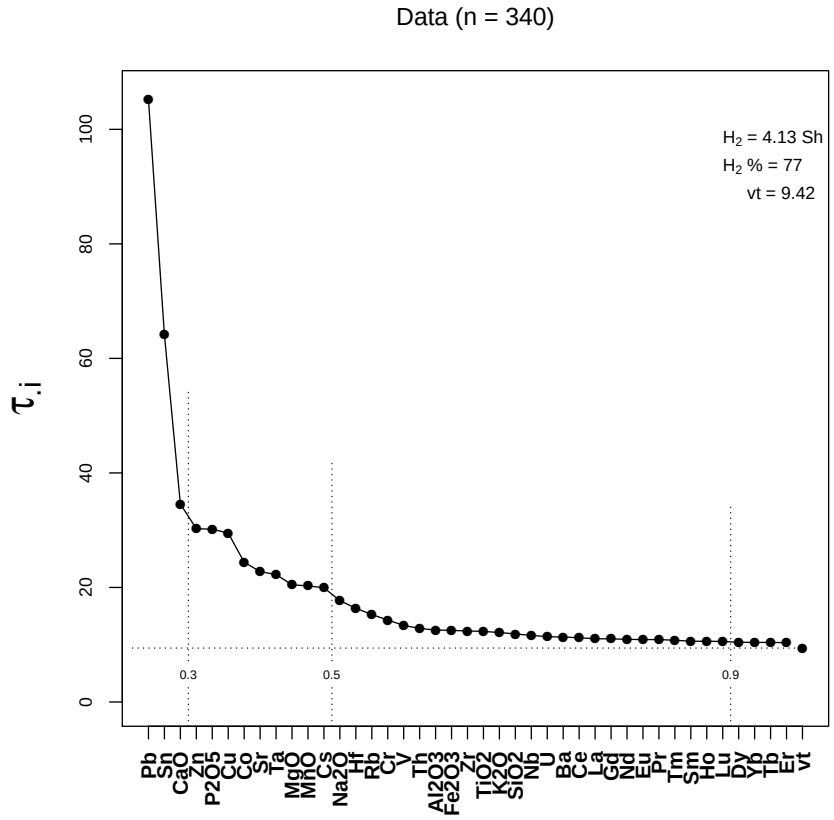

Figure 5.7: Graphical representation of the compositional variation matrix for 340 Ic (concentrations obtained by ICP-MS). vt = Total variation, H_2 = information entropy, $H_2\%$ = percentage of information entropy over the maximum possible, n = number of specimens

The CVM graph displays the individual variability introduced by each variable to the entire dataset (regarding all the Ic-s analyzed by ICP-MS). It can be observed how Pb is the component adding the highest variability to the dataset, whereas Er is the least varying one (see Figure 5.7). The total variation (vt) describes the extent of variability of the ceramic set. According to this measure, the polygenic or monogenic nature of the compositional data was hypothesized (Buxeda i Garrigós and Kilikoglou, 2003). Among the 347 individuals, the total variation of the whole dataset was very high (9.42). It was highlighted that the contribution of elements varying due to non-meaningful sources (contaminations and/or alterations) was very significant. Nevertheless, the omission of elements that are subjected the external variabilities (Pb, Sn, Co, Ta,...) still yielded a high total variation of 1.92 (see Figure 5.8). This high value, suggests a polygenic nature

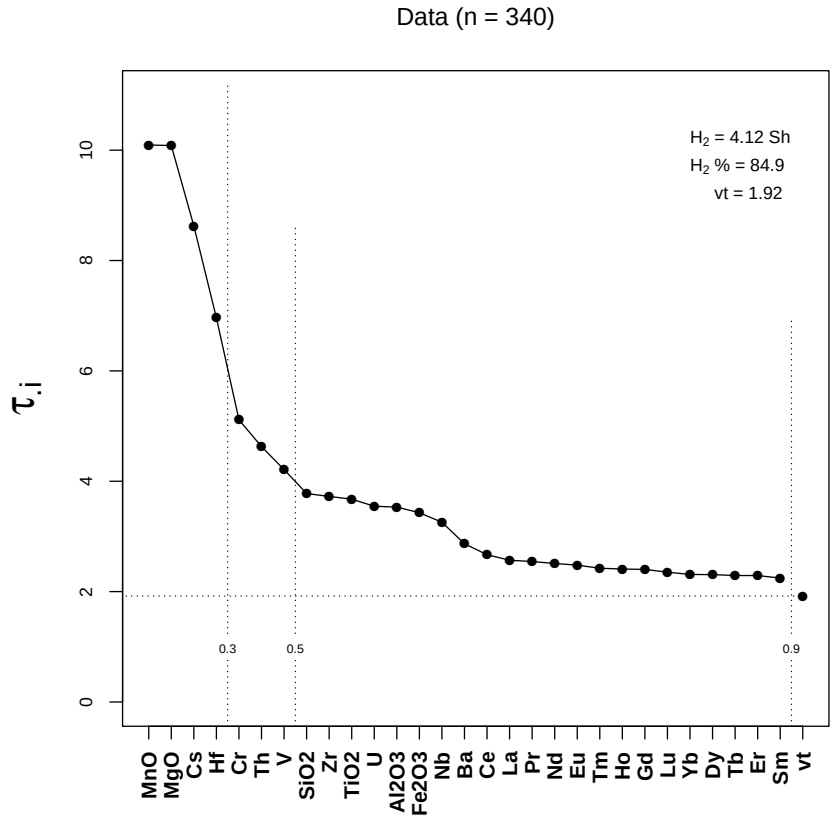

Figure 5.8: Graphical representation of the compositional variation matrix for 340 Ic based on concentrations obtained by ICP-MS. vt = Total variation, H_2 = information entropy, $H_2\%$ = percentage of information entropy over the maximum possible, n = number of specimens

of the set. Thus, anticipating that there are different compositional groups within this dataset.

After Pb and Sn, CaO was the most varying compound (see Figure 5.7). In archaeological ceramics, the influence of the technological choices on the concentrations of CaO and Sr should be critically addressed. In clays, the presence of Ca is usually accompanied by Sr. In Archaeology, ceramics are often referred to as calcareous or low-calcareous, according to their reddish or buffer color appearance, which mainly depends on the CaO concentration, among other factors (firing atmosphere, temperature, clay composition, etc.). Thus, the concentration of CaO is relevant as they can determine the final appearance. Nevertheless, CaO can never be the main

marker for provenance studies as it could provide spurious classifications. An increment of the concentration of CaO could be due to the use of clay mixtures, including more calcareous pastes, or to the addition of calcite grains like tempers to the ceramic paste (Fabbri et al., 2014). Depending on the nature of the carbonates present in the potsherd (primary, secondary, reformed, precipitated, etc.) it can affect the chemical composition of the paste (Fabbri et al., 2014; Buxeda i Garrigós, 1999; Schwedt et al., 2006). Moreover, the trace elements associated with the calcite could be another source of variability. For instance, in the case of Elosu, ethnographic works reported the mixing in the respective proportion 25/75 of two types of clays extracted nearby the ceramic kiln: the so-called "white" (high calcareous) and "red" (low-calcareous) clays (Ibabe, 1995a, p. 16). The light color is frequently obtained by the decomposition of calcite, the formation of pyroxenes and the low presence of iron oxides in oxidizing firings (Maniatis and Tite, 1981; Molera et al., 1998). In tin-lead glazes, these buffered colors are seek to minimize the Sn quantity used for the glaze opacification.

With regard to the manufacturing technique of ceramics, the division of high-calcareous (CaO > 20%), calcareous (20 %> CaO < 6%) and low-calcareous (CaO < 6%) is crucial. Normally, high concentrations of CaO are due to the presence of calcite ($CaCO_3$), which at high temperatures (ca. 650 °C) decomposes according to the following reaction 5.1. These, often are present as undesired inclusions, which are named as lime and known in the literature as *caliche* in Spanish, *kare-pikor* in Basque and *grain de chaux* in French (Astarloa et al., 2016).

$$CaCO_3 \longrightarrow CaO + CO_{2(g)} \tag{5.1}$$

In calcareous ceramics, this decomposition favors, on the one hand, the crystallization of high-temperature Ca-silicates and Ca-Al-silicates after the reaction of free CaO with the compounds of the ceramic paste and, on the other hand, gas emissions of CO_2 . The latter, makes a characteristic cellular microstructure. If there were remnant CaO, it can be re-carbonated, causing damage to the ceramic and according to the following two step reaction (5.2 and 5.3). The volume increases 2.5 with respect to the original CaO volume, causing tensions and it may fracture the ceramic piece (Traoré et al., 2007). For this reason, the calcareous pastes are traditionally fired in low-firing-temperatures (Maniatis and Tite, 1981; Picon, 1973).

$$CaO + H_2O \longrightarrow Ca(OH)_2 \tag{5.2}$$

$$Ca(OH)_2 + CO_2 \longrightarrow CaCO_3 + H_2O \tag{5.3}$$

The Fe_2O_3+MgO+CaO-Al_2O_3-SiO_2 ternary system (see Figure 5.9) presents the situation of the 340 Ic analyzed in this work. It can be observed how most of the

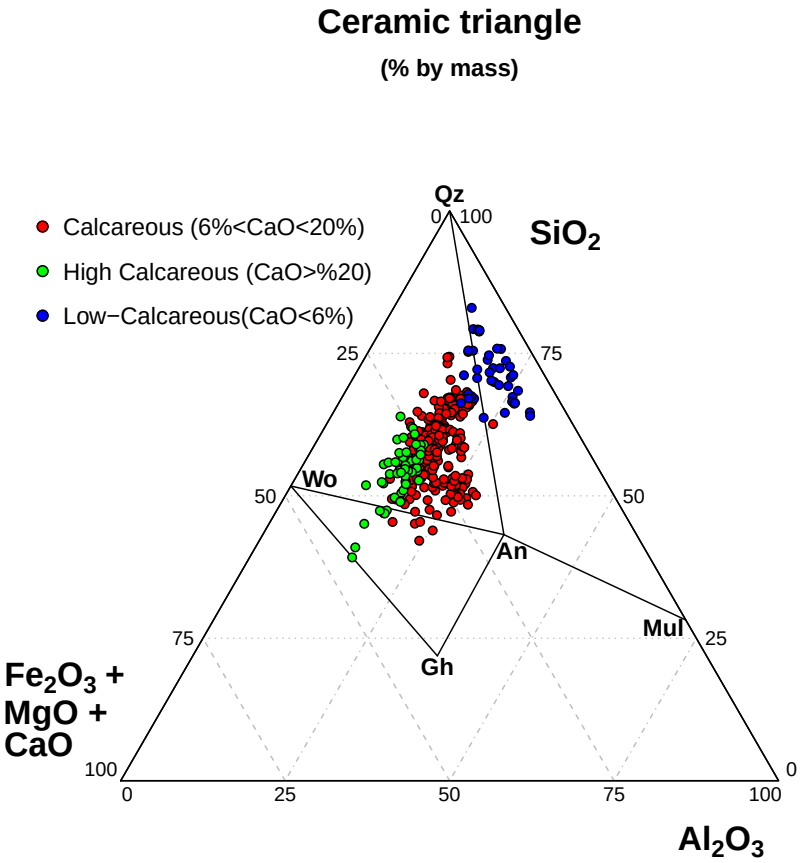

Figure 5.9: Diagram showing the Fe_2O_3+MgO+CaO-Al_2O_3-SiO_2 ternary system for 105individuals analyzed by ICP-MS. An:Anorthite, Gh:Gehlenite, Mul:mullite, Qz:quartz and Wo: Wollastonite (abbreviations after (Whitney and Evans, 2010))

classified as calcareous and high calcareous ceramics are situated in the thermodynamical-balance triangle of quartz-wollastonite-anorthite. These typologies comprises the largest fraction of within the ceramic assemblage. Moreover, some low-calcareous ceramics appear in the system of Anorthite-Quartz-Mullite. These correspond to the low-calcareous productions of Orduña (ORD-MEL-A and ORD-MEL-2). In the other extreme, two ceramics from Logroño showing 30% of CaO are situated in the boarder line of the Gehlenite-Wollastonite-Anorthite system, whereas some high-calcareous ceramics are contained within this thermodynamical-balance system characteristic of these paste typology.

From a given magma or fluid with the chemical composition of these Ic-s, they would crystallize in such minerals during cooling. However, ceramics do not come from a magma but from a clayey matrix with, sometimes, other type of mineral and organic inclusions. Therefore, with the increase of temperature during firing, primary mineral phases will begin to decompose resulting, eventually, in a glassy matrix with the crystallization of high temperature mineral phases. Thus, the higher the temperature is reached during firing, it can be suggested that the crystallized mineral phases found in the ceramic will be the ones that shows the thermodynamic ceramic phase diagram (Heinmann, 1989).

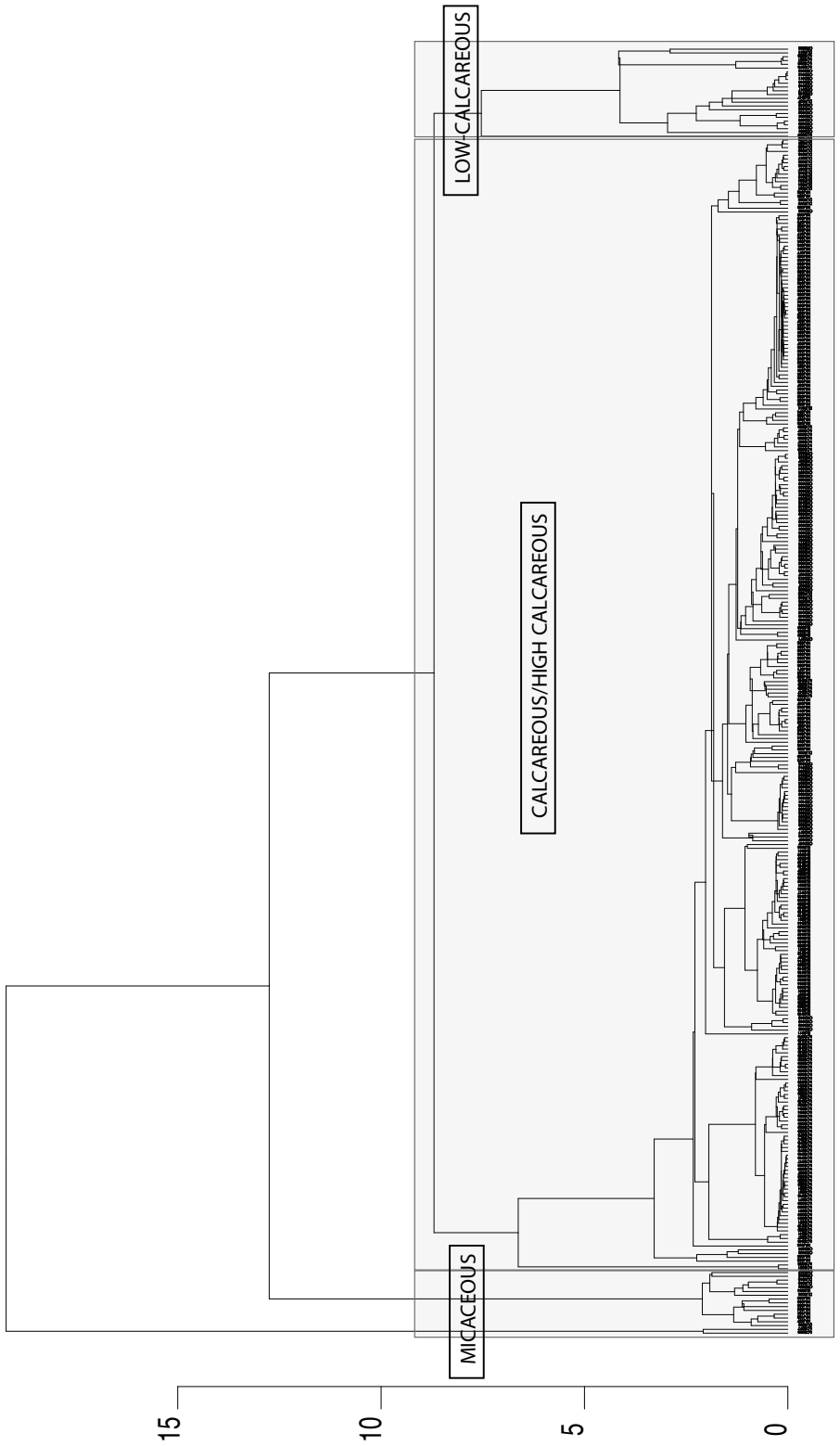

Figure 5.10: Dendrogram of euclidean squared distances using centroid algorithm of 340 Ic on the subcomposition of: Al_2O_3, Sr, Zr, Nb, Cs, Ba, La, Ce, Pr, Nd, Sm, Eu, Gd, Tb, Dy, Ho, Er, Tm, Yb, Lu, Hf, Th, U, MgO, SiO_2, CaO, TiO_2, V, Cr, MnO, Fe_2O_3

The hierarchical clustering analysis (see Figure 5.10) shows the main clusters of the 340 Ic studied, which clearly correspond to three ceramic paste typologies: micaceous, low-calcareous and calcareous. The largest cluster (n =297) was formed by unglazed and glazed ceramics (either lead or tin-lead glazes), which were manufactured with calcareous or high-calcareous pastes. Their CaO concentrations varIed from 6.5 and 31.3 mass % CaO and two sherds (LOG081 and LOG083) presented very high CaO concentrations (ca. 30 mass %).

Moreover, the most differentiated cluster corresponded to micaceous pastes (n=31), which are characterized by the highest concentrations of Rb, showing 500-600 μg/g, while the all the other Ic constituting the ceramic assemblage showed concentrations between 100-200 μg/g), Cs, showing 40-60 μg/g, whereas all the other sherds ranged between 10-30 μg/g and slightly lower concentrations of SiO_2 and U. Moreover, Al_2O_3 showing different tendencies among The Basque Country (TBC) and La Rioja (LR) (ca. 22 and 28 mass % Al_2O_3 respectively, for a concentration range of ca. 14-18 mass % Al_2O_3 for all the remaining ceramic pastes. Likewise Ta presented high concentrations of ca. 5 μg/g in LR and ca. 12 μg/g in TBC, contrasting to a range of 2-4 μg/g shown by the remaining micaceous sherds. Contrarily, marked lower concentrations of La, Pr, Nd, Sm, Eu, Gd, Th, Na_2O, Ti, Cr, Ba and Zr were detected in micaceous pastes. Their CaO and Sr concentrations were also very poor, as they present low-calcareous pastes (see A.6.

Finally, the third cluster (n=28) corresponds to low-calcareous pastes, characterized by a low concentration CaO (0.4-5.8 mass %), together with an increment of iron oxides proportions with respect to the more calcareous pastes. This combination leads to reddish colored clay bodies as mentioned before.

Chemical Differences between The Basque Country and La Rioja observed by NAA

The Figure 5.11 presents the chemical differences observed by NAA between LR and TBC. The micaceous and low-calcareous groups were omitted from this representation to better identify the main discriminant variables of the calcareous pastes which represent the ca. 90% of the total sample. Likewise the contribution of Ca and Sr were omitted in order to observe the chemical differences connected to the raw materials and not to the technological choices (as has been discussed before). According to the PCA, the ceramics from LR presented overall lower concentrations of most of the trace elements, as well as Al, K and Fe, whereas TBC ceramics showed higher concentrations of Hf and Zr. Nevertheless, it can be stated that the chemical differences were very subtle because the separation between the two groups was not clearly defined (see Figure 5.11).

These subtle chemical differences could be partially explained by the different geological spots from LR and TBC. Whereas the sites located in the Basque Country

lie on a geological strata from the tertiary period, Logroño and Nájera are located by the middle Ebro valley on a phacie from the mesozoic period.

Pastes with low content of calcite inclusions and a matrix characterized by autigenic quartz as well as pyroxenes (compositionally associated to clays from the Triassic period, can be found in Orduña and are also present in Maeztu, Murguia, Salinas de Añaña, Salinillas de Buradon and Peñacerrada (Solaun, 2005)

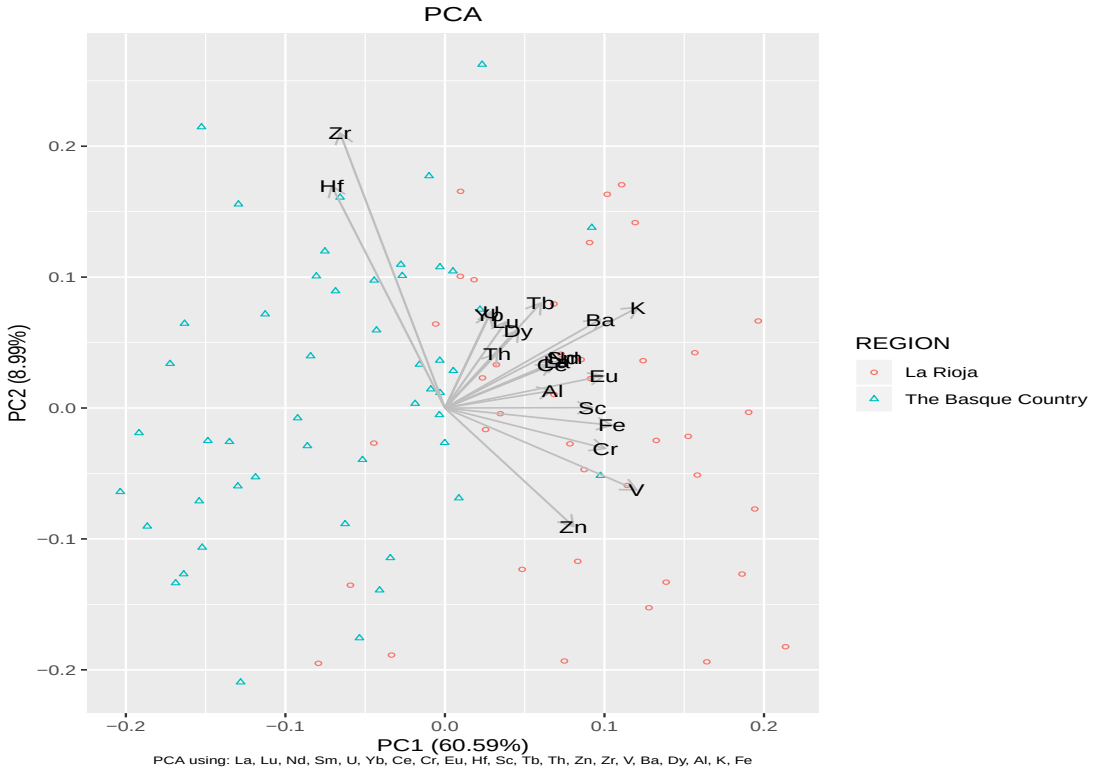

Figure 5.11: PCA from concentrations obtained by NAA for 105 Ic

The nature of this work served to contribute filling the knowledge-gaps on the puzzle of the ceramic productions of post-Medieval northern Iberian Peninsula. A priori, the geological ores from which the clays were extracted permitted to chemically discern between the two regions (LR and TBC). Nevertheless, taken as a basis the different range of chronologies, as well as the archaeological questions and heterogeneity of documentation, the ceramics unearthed in each of the archaeological sites were studied as a separate case studies.

5.2 Archaeometric characterization of pottery from Logroño

Abstract

In the archaeological intervention performed in the Hospital Viejo street from Logroño (La Rioja, Spain), pottery production evidence dating back from the 13^{th} to the 15^{th} centuries was discovered. Within the totally unexpected findings, three ceramic kilns and a dump were unearthed, including numerous ceramic sherds. Among the material recovered from the site, several kiln utensils, ceramic wastes and tableware, including glazed and unglazed pieces, as well as fired clay pellets were classified. These materials were thoroughly studied, contextualized and documented from a purely archaeological perspective by Milagros Martinez in her Doctoral Thesis (Martínez González, 2013). For the present work, a sample of 76 ceramics was archaeometrically characterized by a multi-analytical approach, by means of inductively coupled plasma mass spectrometry (ICP-MS), X-ray diffraction (XRD) and scanning electron microscopy (SEM-EDS), and a subsample of 25 sherds was further analyzed by neutron activation analysis (NAA), in order to characterize the chemical fingerprint of the pottery from Logroño pottery produced during the Late Medieval period. The archaeometric assessment enabled establishing several compositional reference groups that could be linked to a local origin production as well as several exogenous provenances. The complexity of ceramic production in pre-industrial eras was highlighted in terms of archaeometric characterization, showing different chemical reference groups diachronically within the same production center. The present archaeological characterization aims to serve to shed more light on the pottery activity and trade networks within northern Spain during Late Medieval and Post-medieval periods by providing the chemical characterization of these productions.

Background

Logroño is the capital city of the autonomous community of La Rioja and is located in the middle Ebro valley (northern Iberian Peninsula). Due to its strategic location, the urban nucleus known as *Gronnio* during the Roman period (which means ford or passage) functioned throughout centuries as a communication-node. The territory of La Rioja went from being a peripheral area of Al-Andalus to nucleus nerve of the life in the Kingdom of Pamplona, along these lines, Logroño became one of the most important urban centers of medieval Navarre and Castile, both culturally and economically (Moya Valgañón, 1994).

A significant boost in the city's importance took place in the 11^{th} century, when the king Sancho Garcés of Pamplona included the city in the Way of Saint James. Logroño's inclusion into the most important medieval route in Europe lead it to flourish

Figure 5.12: Image of the archaeological intervention in Hospital Viejo Street of Logroño. ArqueoRioja ©

economically. Moreover, the prominence of the city was increased when Alfonso VI decreed that only two bridges could cross the Ebro river in that region, one at Logroño and the other at Miranda de Ebro. These events, along with the transfer of the frontier with Islamic territory to the peninsular interior, allowed Logroño to gain status and to gradually displace Nájera and Viguera (the only cities of the territory documented in the 10^{th} century) from the geopolitical order (Martínez González, 2013).

In the 12^{th} century, the territory of La Rioja became a fluctuating frontier between Castilians, Navarre and Aragonese. However, the area prospered and was enriched by the interchange of people and merchandise with a heterogeneous population where former neighbors of Logroño, people from nearby villages, as well as Franks, Jews and Mudejars in a minor extent coexisted. Nevertheless, several events, including the modification of the Saint James Way at the end of the 13^{th} century impacted negatively its economy. Moreover the city experienced a severe economical decline traversed by the episodes of plague that lashed the city during the 14^{th} century(Martínez González, 2013).

Due to its strategic location as a military plaza, Logroño obtained several benefits and it was granted with two annual fairs by Alfonso XI (1314). Moreover, it obtained

the titles of "city" (1431) and of "very noble and very loyal" (1444). Later on, the city was granted with the right to vote in the Courts (1494), as well as to have a free market. These three centuries (13^{th}-15^{th}) with their socio-political up and downs, encompassed the operational period of the ceramic workshops under the present study, which supplied the population with ceramics.

Previous Ceramologic Research

On the one hand, the archaeological records and historical documentation attest to a wide chronological range of ceramic production in La Rioja, from Roman times to the Medieval Ages, including amphorae and dolia (large earthen jars) for the transport and storage of wine (Luezas Pascual, 2014). On the other hand, the discovery of potters' dump sites in the city of Logroño is a potential evidence of the existence of differentiated pottery nuclei (Martínez Glera, 1994; Martínez González, 2013). Furthermore, post-medieval pottery production evidence was discovered in Ollerías street (Gil Zubillaga and Luezas Pascual, 2018). In addition, based on the historical documentation, Enrique Martínez Glera provided a general and detailed panorama of the regional post-Medieval pottery activity of La Rioja (Martínez Glera, 1994). The information was mainly extracted from the Cadastre of Ensenada. Seemingly, Haro would have dominated the pottery production, being gradually replaced by Navarrete. The exchange of personnel that took place over the centuries between pottery workshops was also documented. Non surprisingly, the most intense pottery activity would have also occurred in Haro, where apprentices from diverse places were received (for more details see Martínez Glera (1994).

Alternatively, material unearthed in Hospital Viejo street of Logroño was addressed in the present work, that is, the first ever archaeological site in which direct evidence of pottery production has been documented. For the specific case of Logroño, the reception of potters from Zamora in the 16^{th} century was documented by Martínez Glera (1994). The origin of the potters expands to cities or villages such as Burgos, Viguera, Muel and Zaragoza, and regions such as Navarre and Alava during the 17^{th} century. Moreover, according to the registered news, there were familiar relationships that connected Logroño with Muel, a link that considerably increased during the 18^{th} century (Martínez Glera, 1994). Anecdotally, the work of Glera also mentions that Jose Bernardino del Busto (born in 1742) and neighbor of Logroño was the secretary of the Holy Inquisition, as well as the administrator of the lead and "lead alcohol" [1] of his party and in 1792 he granted to Manuel Blazo of Arnedo the administration and sale of both substances. These substances were necessary to obtain lead-glazes used for the ceramic coatings.

It can be said that in comparison with other sectors, the activity regarding pottery production in the Riojan territory is still relatively unexplored, especially corresponding

[1] A form in which galena or lead sulfide (PbS) was referred. Also known elsewhere as leaf alcohol, because of the laminar form in which the galena occurs (Martínez Glera, 1994).

to late medieval and post-Medieval periods. Although, this situation dramatically changed when the workshops of Hospital Viejo street were discovered (2009), unearthing the first structure associated with this type of economic activity (Martínez González, 2013). Moreover, Ceniceros Herreros (2004, 2012) provided the first typological approach to the significant findings of tin-lead glaze pottery unearthed in the site of the Alcázar of Nájera[2], which is located 28 km away from Logroño. In any case, none of the investigations to date were conducted from a multi-analytical and archaeometric perspective.

Concerning the diachronic production of Logroño, two streets are documented of being dedicated to pottery activity during the 16^{th} century, namely, *Ollerías altas* and *Ollerías Bajas* (Martínez Glera, 1994). These correspond to current *San Juan* and *Ollerías* street, respectively. The toponymy of *Ollerías* —meaning the place of the pottery workshops— and located *extramuros* and very close to Hospital Viejo street, denoted the tentative presence of ceramic workshops, which was recently confirmed by the unearthing of a ceramic kiln that occurred during the summer of 2018 (Gil Zubillaga and Luezas Pascual, 2018). The kiln was ascribed to the 16^{th} century, constituting the first ever evidence of the local pottery production of post-Medieval chronology. Along these lines, the study of them, as well as from the Riojan materials addressed in this doctoral thesis, play a key role for the understanding of post-Medieval pottery production in the northern Iberian Peninsula, as well as to understand how the pottery activity evolved from the production of Hospital Viejo street's workshops to the *Ollerías* street. That is to say, from the workshops located in the peripheral areas of the city and run by the Mudejar potters, to the workshops articulated in guilds as can be inferred from the toponymy.

The pottery workshops of Hospital Viejo street

The excavation performed in the archaeological site of Hospital Viejo street (see Figure 5.12), provided the largest assemblage related to ceramic production in Logroño until now, which includes three ceramic kilns and a potter's dump. The extensive collection of ceramic includes, kiln utensils, ceramic wastes, pieces related to storage, cookware, tableware, with glazed and unglazed coatings, as well as fired clay pellets.

[2]The archaeometric study of these ceramics is covered in the Section 5.3.

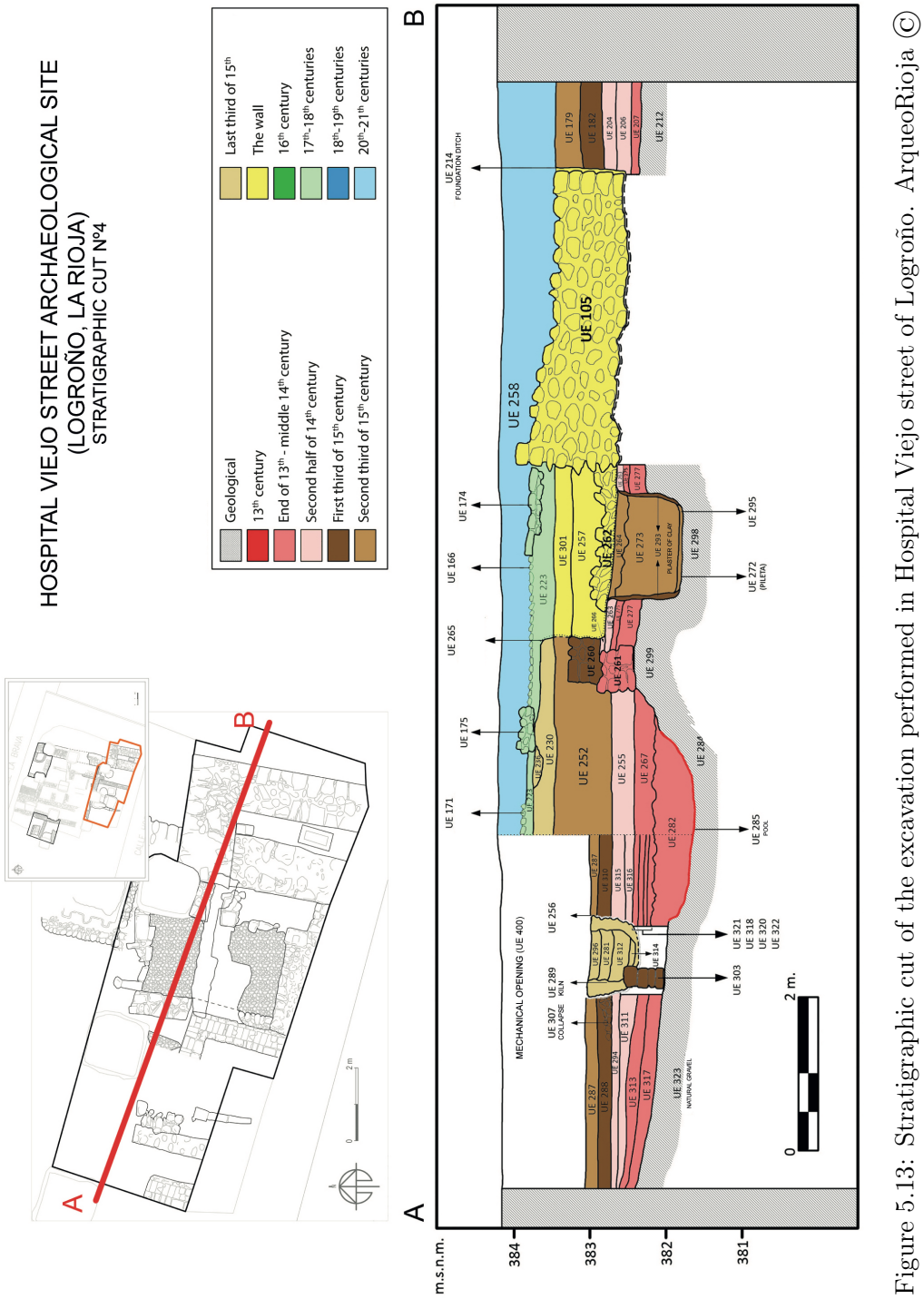

Figure 5.13: Stratigraphic cut of the excavation performed in Hospital Viejo street of Logroño. ArqueoRioja ©

Pottery production was regarded as a nuisance activity. Therefore, usually was carried out be in the outskirts of the urban nuclei (e.g in Roman times *Lex Ursonensis*, Montelupo, Seville...). Thus, the first workshop was located *extramuros* with regard to the first wall of this city, in the are called "Villanueva" (meaning the new village). In 1492, Ferdinand II of Aragón (The Catholic) ordered to erect the second fortification that was Wall of Revellín (part of which delimits the pottery workshops under this study).

Up to three superimposed workplaces were identified, operating during the 13^{th}, 14^{th} and 15^{th} centuries in the site of Hospital Viejo from Logroño, as well as a large collection of ceramic and other related materials (kiln utensils, clayey pellets, etc.). The pottery kilns were built with the purpose of serving to 2 to 3 generations and the workshops discovered in Hospital Viejo street, had a life cycle of ca. 50 years each (Martínez González, 2013). Moreover, the study of the stratigraphic sequence (see Figure 5.13) permitted to identify two different occupation phases (A and B) in each of the three workshop. According to the type and volume of materials, as well as the structures associated with the workshops, these were directly influenced by the socio-political conjunctures. The installations of the first workshop, were expanded in the second, which would have functioned more abundantly, but at some point, could have been abruptly disrupted by the influence of the plague (reporting the use of the kiln for calcination of the households). Finally, production of the third workshop would have diminished both in volume and quality, being finally abandoned.

According to the extensive archaeological investigation carried out in this site, the workshops would have been run by Islamic potters, being abandoned after the pragmatic[3] against the Mudejar community of 1502. As mentioned before, different communities coexisted in the medieval Logroño, including Catholics, Mudejars, Jews and Franks. The finding of *hanukkah* type pottery pieces [4], pointed out that the Jews were the customer of the Mudejar pottery, since they would not normally run these type of activities (Martínez González, 2013).

Ceramic Sample of Logroño

The pieces were selected from the well documented archaeological site of Logroño (Martínez González, 2013). The sampling strategy focused on kiln-related materials, such as pieces from kiln dumps, to achieve the highest probability on matching the provenance of materials with the respective workshops within the archaeological.

[3]Pragmatics of forced conversion is a term that could be applied to several pragmatics or other legal texts issued at the beginning of the 16^{th} century during the reign of the Catholic Monarchs and Charles V. It is the name that historiography gives especially to the Pragmatics of February 14, 1502 Apparently the subject Muslims (Mudejars) were given the choice between exile or conversion to Christianity (Artola and Ledesma, 1991).

[4]A type of oil lamp utilized by Jews in the Hanukkah festivity

The set of ceramics (n = 76) consists principally of kiln utensils, ceramic wastes, pieces related to storage, cookware, tableware, with glazed and unglazed coatings, as well as clay pellets (fired) ascribed from the 13^{th} to the 15^{th} centuries. In addition, ceramics corresponding to later chronologies (16^{th}-18^{th} centuries) were also selected in order to assess their compatibility with previously produced ceramic pastes and/or to ascribe them to exogenous provenances (see Appendix B). In the present work the ceramics unearthed in the second intervention of the Hospital Viejo street were analyzed. An archaeological examination and documentation of a subsample of them (e.g. archaeological profiles) was previously conducted (Angulo and Porres, 2015). Moreover, a Doctoral Thesis was conducted concerning the materials from the first intervention (Martínez González, 2013) and a summary, including the 35 ceramic forms identified in the mentioned Doctoral Thesis was also published (Martínez González, 2015).

Experimental

In order to characterize the compositions and mineralogical phases of the pastes, the whole set of ceramics was analyzed by means of inductively coupled plasma mass spectrometry (ICP-MS) and X-ray diffraction (XRD). Moreover, a subsample of them (n = 25) was analyzed by NAA. In addition, a subsample (n = 15) was analyzed by means of scanning electron microscopy coupled to energy dispersive spectrometry (SEM-EDS) in order to better understand the technology used by the potters. For more details about methodology, see Section 3.3. Likewise, NAA data from the main majolica production centers of Iberian Peninsula (Iñañez et al., 2008) were employed in order to identify exogenous provenances.

Results and Discussion

First Approach by NAA and Identification of Exogenous Provenances

The first approach by NAA performed on a subsample of 25 individuals from Logroño pointed out two main compositional groups (LOG-C and LOG-B) with regard to the Riojan pottery production (see Figure 5.14). Moreover, both LOG037 and LOG038 showed chemical dissimilarities in comparison with all the remaining sherds.

In addition, the sub-classification formed by LOG042, LOG043, LOG044 and LOG048 showed a differentiated chemical fingerprint. These four ceramics were highly compatible with the provenance of Teruel as can be observed in the dendrogram shown in Figure 5.15. Moreover, some of these sherds include green and black decorations that are very characteristic of the workshops from Teruel (for more details see the section of of compositional groups).

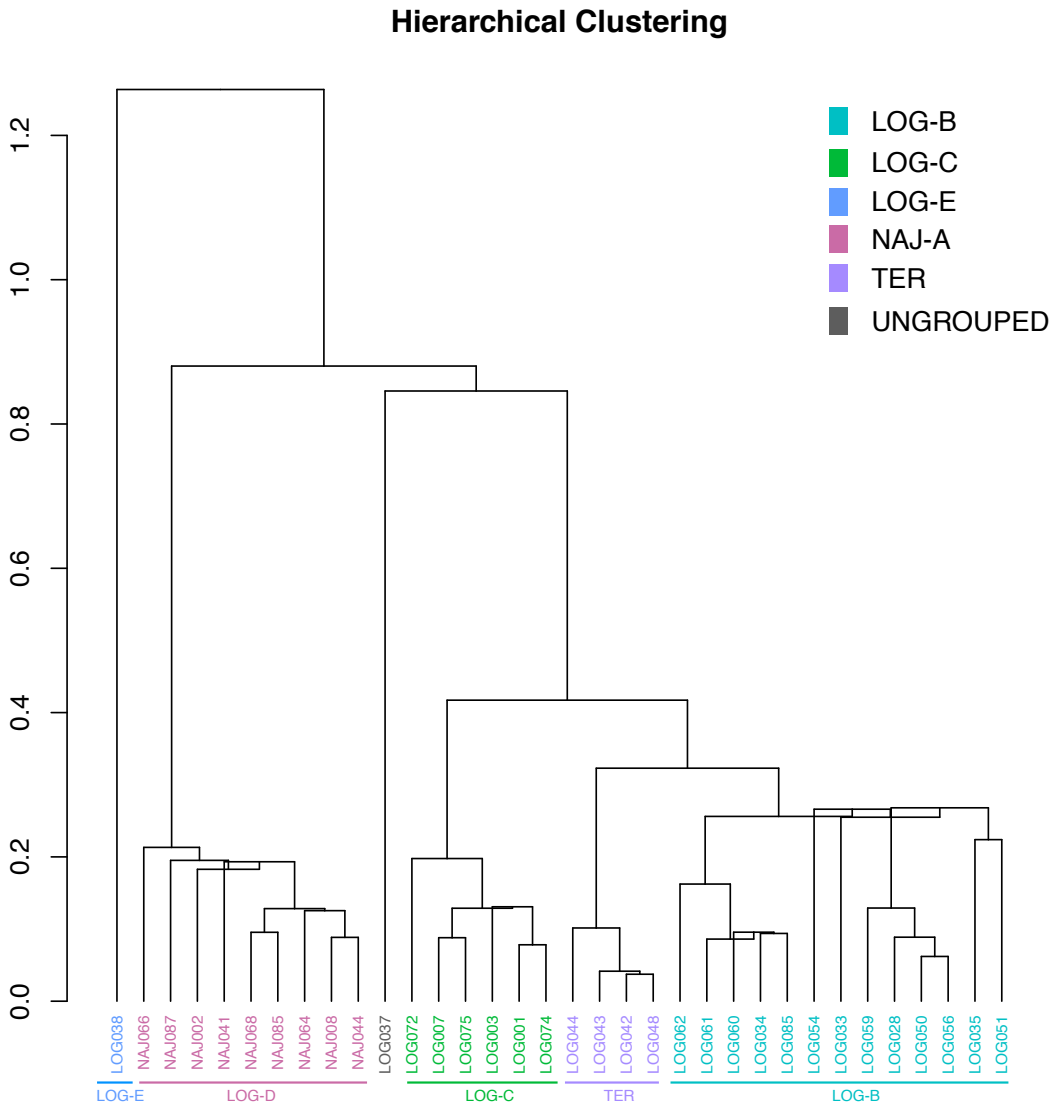

Figure 5.14: Dendrogram of Euclidean squared distances using centroid algorithm of 25 individuals from Logroño and other production centers, on the sub-composition of La, Lu, Nd, Sm, U, Yb, Ce, Cr, Cs, Eu, Fe, Hf, Sc, Tb, Th, Zr, Al, Ba, Dy, Mn, Ti and V.

In the mentioned dendrogram, a comparison with other contemporary majolica productions centers (Iñañez et al., 2008) was carried out. As a result the situation of the ceramics from Logroño is presented within a broader perspective. One the one hand, the two compositional groups identified from Logroño constituted two differentiated clades, which according to the Euclidean squared distances, cannot be

ascribed to any of the other production centers tested. The array of the productions centers tested was the following: Barcelona (BCN-B1B2, BCN-B3), Lleida, Manises, Muel, Paterna, Puente Arzobispo, Reus, Sevilla, Talavera, Teruel, Villafranca de Penedes, Villafeliche and Nájera. Whereas in all cases the matches were negatives, for the sake of clarity only a subsample was included the Figure 5.15.

On the other hand, the individuals LOG037 and LOG038 still present differentiated composition with respect to this broader sample. The former shows a composition strikingly different from all the majolica compositional group (due to the higher concentration of Ba and other minor and trace elements). The decoration it exhibits a Lis Flower that is generally associated to French productions. According to the HCA show in Figure 5.15, LOG038 showed a composition slightly compatible with the one of Sevilla. However, this chemical association is not very tight (see Figure 5.15), and its decoration and typology, a possible provenance from Paterna is suggested. Unfortunately, the available chemical data from Paterna could not confirm this hypothesis. The nuances of both ceramics and their tentative provenances are addressed in the ICP-MS discussion.

Finally, both HCA (Figures 5.14 and 5.15) showed that none of the ceramics from this site analyzed by NAA could be ascribed to the NAJ-A compositional group defined within the production of Nájera, as addressed in the Section 5.3.

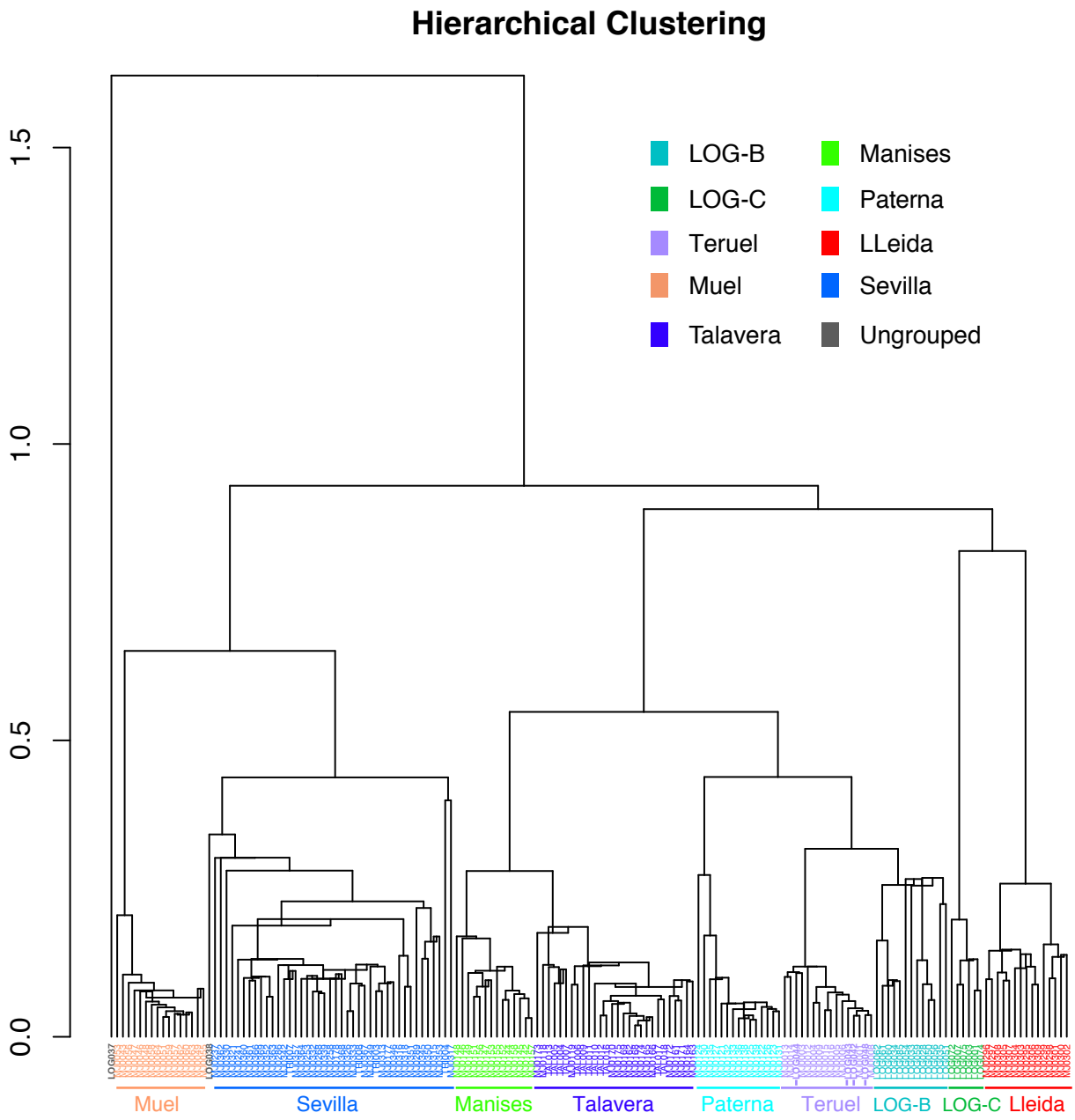

Figure 5.15: Dendrogram of Euclidean squared distances using centroid algorithm of 25 individuals from Logroño and other production centers on the sub-composition La, Lu, Nd, Sm, U, Yb, Ce, Cr, Cs, Eu, Fe, Hf, Sc, Tb, Th, Zr, Al, Ba, Dy, Mn, Ti and V.

Compositional Groups

In Table 5.2 the mean concentrations of each compositional group obtained by ICP-MS are presented. Ideally, for the statistical analysis, the analytical variance should be minimized in such a way that it is originated by natural sources and not because of experimental errors and/or alterations arising from post-depositional processes. Therefore, in this work, several elements were not regarded for the statistical analysis. These are addressed in the Section 5.1.

The compositional heterogeneity was assessed by calculating the compositional variation matrix (CVM), which provides information about the variability introduced by each element into the dataset (see Figure 5.16). Generally speaking, a large value of the total variation vt indicates greater variability and suggests that the dataset is polygenic (i.e. the presence of several compositional groups). In contrast, a small value for vt indicates a possible monogenic nature of the dataset (Buxeda i Garrigós and Kilikoglou, 2003). In this case, the set shows a very high vt (6.72), which reveals the high contribution of the elements (Pb, Sn, P, Co, Ta Na, K and Rb). The vt drops down to 0.95 when these are omitted (see Figure 5.16). From this vt several compositional groups can be expected.

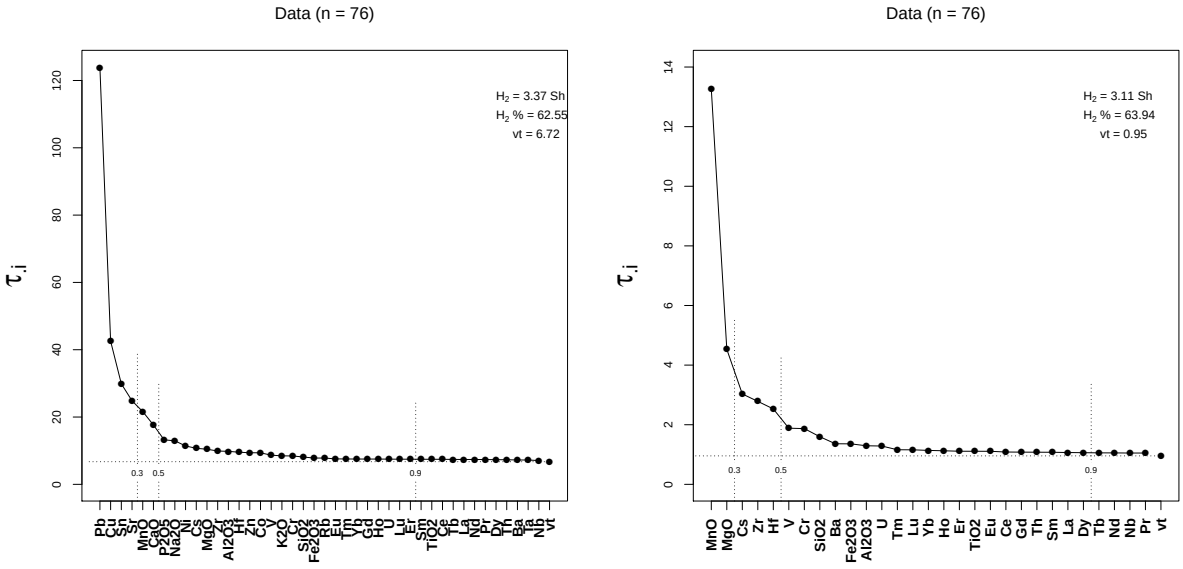

Figure 5.16: Graphical representation compositional variation matrix including all quantified elements (left) and excluding non-meaningful elements (right) of ceramics from Logroño

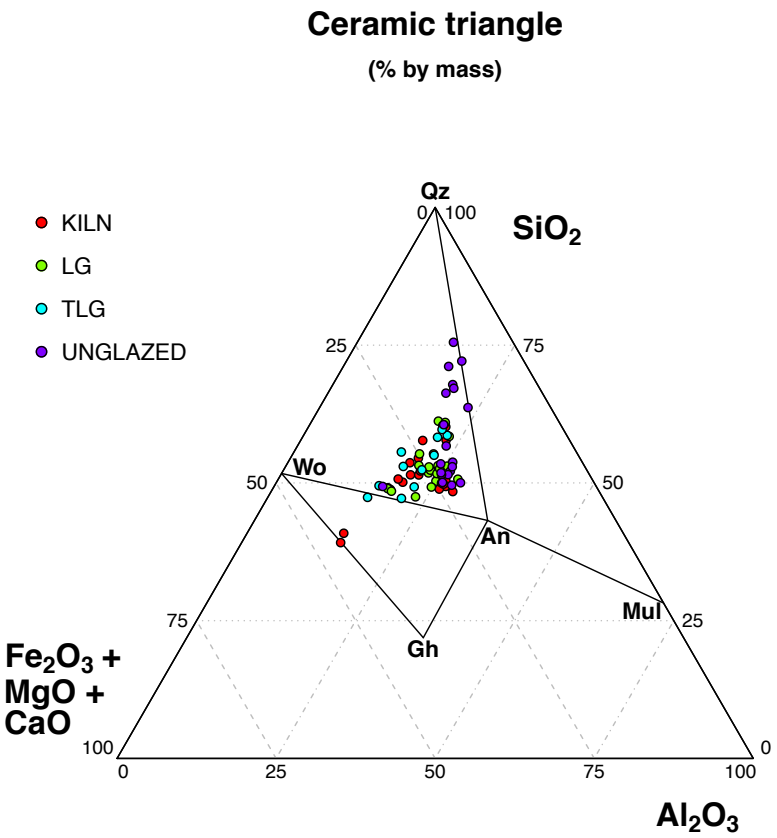

Figure 5.17: Ternary diagram showing the compositions of SiO_2, CaO and Al_2O_3 of the 76 potsherds from the archaeological site of Logroño. TLG: tin-lead glazed. An:Anorthite, Gh:Gehlenite, Mul: mullite, Qz: quartz and Wo: Wollastonite (abbreviations after (Whitney and Evans, 2010)

According to the ternary diagram (see Figure 5.17), all the pieces, which include, unglazed, tin-lead glazed and kiln utensils fall completely in the Wollastonite-quartz-anorthite triangle with exception of three. Among these three, two sherds fall within the gehlenite-anorthite-wollastonite triangle, due to their striking high concentration of CaO, and the other remains in the borderline between the two mentioned thermodynamic systems.

The statistical analysis performed on the 76 samples identified 6 compositional groups. The details for each individual and the compositional group are listed in the Table B of the Appendix B and the mean values with the standard deviation values of each compositional group are summarized in the Table 5.2. The compositional characterization of each group is discussed below.

Element	LOG-A	SD	LOG-B	SD	LOG-C	SD	LOG-D	SD	LOG-E	SD	TER	SD
Al_2O_3	14.0	0.8	16.9	1.7	21.6	1.5	12.7	0.1	14.1	1.5	17.8	0.8
CaO	3.7	1.1	12.9	4.5	9.3	1.1	30.8	0.7	19.8	4.0	8.5	0.7
Fe_2O_3	5.1	0.7	5.8	0.7	7.7	0.4	3.4	0.1	4.9	0.5	6.0	1.2
K_2O	2.3	0.2	3.1	0.4	3.5	0.2	2.1	0.1	2.1	0.5	3.7	0.3
MgO	0.9	0.19	1.92	0.22	2.18	0.15	2.59	0.05	2.82	0.27	1.61	0.08
MnO	0.025	0.019	0.045	0.012	0.039	0.004	0.01	0.001	0.056	0.003	0.032	0.008
Na_2O	0.75	0.1	0.8	0.14	0.72	0.07	0.61	0.2	0.72	0.56	0.29	0.04
P_2O_5	0.18	0.07	0.25	0.07	0.35	0.19	0.19	0.01	0.47	0.18	0.24	0.06
SiO_2	55.5	4.9	43.9	4.1	43.1	2.7	33.1	1.3	41.6	3.2	48.3	1.6
TiO_2	0.75	0.05	0.69	0.08	0.82	0.03	0.46	0.01	0.72	0.1	0.71	0.02
Ba	474	53	537	71	572	44	322	38	562	132	566	25
Ce	92	6	95	12	119	5	53	1	88	9	89	3
Co	16	2	20	7	24	7	9	1	18	1	22	5
Cr	69	15	82	10	102	16	69	2	67	7	76	25
Cs	27	5	21	4	22	3	11	2	9	3	29	3
Cu	63	107	30	17	25	25	23	16	106	66	118	88
Dy	5.7	0.3	5.2	0.6	5.8	0.2	2.8	0.1	5.5	0.3	5.3	0.3
Er	3.1	0.2	2.7	0.3	3.0	0.1	1.5	0.1	2.9	0.1	2.7	0.1
Eu	1.5	0.1	1.5	0.2	1.8	0.1	0.7	0.1	1.4	0.2	1.4	0.1
Gd	8.3	0.3	7.6	0.9	9.1	0.4	3.8	0.1	7.6	0.4	7.3	0.3
Hf	5.1	0.6	3.3	0.6	2.9	0.4	2.0	0.1	4.0	0.3	3.4	0.2
Ho	1.1	0.07	0.93	0.1	1.05	0.05	0.5	0.01	1.05	0.05	0.94	0.04
La	45	3	46	6	58	3	27	1	44	4	43	1
Lu	0.47	0.02	0.41	0.06	0.44	0.02	0.22	0.02	0.44	0.04	0.42	0.02
Nb	17	1	18	2	20	1	13	0	17	1	19	1
Nd	38	1	39	5	48	2	21	1	37	2	37	2
Pb	48	17	(81-4001)*		(24-12077)*		1052	876	3534	893	934	464
Pr	10	0	10	1	12	0	6	0	9	1	9	0
Rb	120	11	143	14	156	10	104	14	89	9	186	10
Sm	8.0	0.3	7.8	1.0	9.6	0.4	4.0	0.1	7.5	0.5	7.5	0.4
Sn	5	0	(4-49)*		5	1	5	1	23	2	43	40
Sr	129	85	622	256	499	65	1930	175	527	123	235	55
Ta	1.1	0.1	1.1	0.1	1.2	0.1	0.9	0.1	1.0	0.1	1.3	0.1
Tb	0.99	0.05	0.90	0.11	1.03	0.04	0.48	0.10	0.90	0.04	0.88	0.03
Th	9	1	9	1	11	1	6	1	9	1	9	1
Tm	0.54	0.04	0.48	0.06	0.52	0.02	0.24	0.10	0.52	0.03	0.47	0.02
U	2.4	0.2	2.9	0.2	3.1	0.2	2.0	0.1	2.5	0.1	2.4	0.1
V	76	5	101	15	139	9	73	10	78	8	85	2
Yb	3.2	0.2	2.7	0.3	3.0	0.2	1.5	0.1	3.0	0.2	2.8	0.1
Zn	86	6	101	30	101	14	92	14	91	7	159	160
Zr	363	48	217	41	189	21	125	9	267	22	230	9

Table 5.2: Mean concentrations and standard deviation values (SD) of each compositional group from the Hospital Viejo archaeological site. TER: Teruel (exogenous). Concentrations obtained by ICP-MS. Oxides are expressed in mass % and the rest in μg/g. *Pb and Sn ranges are given because they contain SD values higher than mean values due to their heterogeneous distribution.

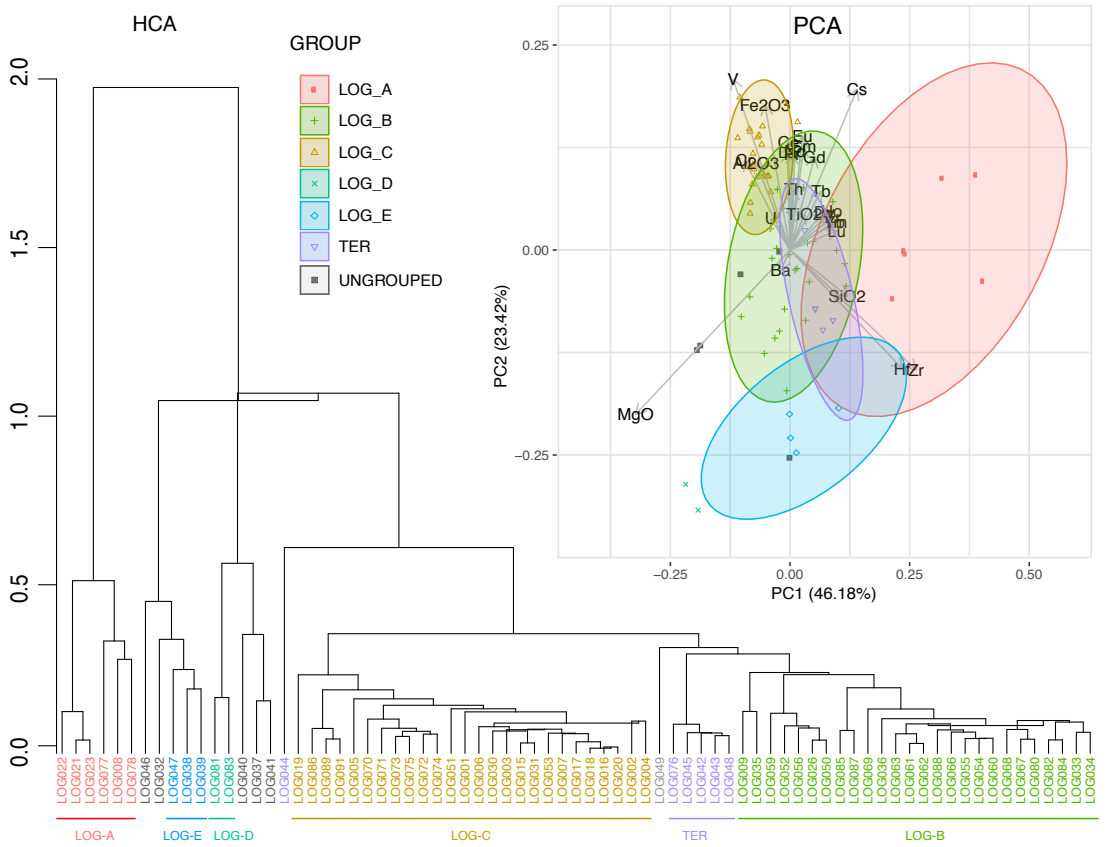

Figure 5.18: Dendrogram of Euclidean squared distances using centroid algorithm of 75 individuals from Logroño and other production centers (Talavera de la Reina (TAL) Manises and Muel), on the sub-composition of Al_2O_3, Zr, Nb, Cs, Ba, La, Ce, Pr, Nd, Sm, Eu, Gd, Tb, Dy, Ho, Er, Tm, Yb, Lu, Hf, U, MgO, SiO_2, TiO_2, V, Cr, Fe_2O_3

LOG-A Compositional Group

A lowest CaO concentration of 3.7 ± 1 mass % characterizes this group formed by 6 individuals. The forms include unglazed pots and lids used for cookware or storage. Chronologically, the ceramics of this group correspond to two periods, 1290-1350 and first third of the 15^{th} century, being all the cookware pieces from the former and the storage from the latter. This group presents two tendencies in MnO concentrations ranging from (0.0250 ± 0.19 mass %), whereas the specimens LOG008 and LOG078 show concentrations 7 times below the other sherds. For this reason, the RSD for this compound in this group is very elevated and if is regarded in the HCA, the group splits into two subgroups. However, on the basis of the chemical homogeneity shown by all the

Figure 5.19: A representative ceramic from the group LOG-A

remaining elements, as well as the technotypologic features these, two subgroups were considered as a single compositional group.

Moreover, this groups exhibits the highest concentration of Zr and Hf, with values of 363 ± 48 μg/g and 5 ± 1 μg/g, respectively. According to the mineralogical analysis performed by XRD, all of the sherds from this compositional group exhibit the same fabric type, F- I (see Table 5.3). The presence of illite-muscovite phases along withe the presence of K-feldspars (microcline peak is shown) and plagioclases (albite peak is shown), allowed estimating the EFT at 850-900 °C (see Figure 5.24). Moreover, the abundant quartz identified by XRD is in accordance with the high concentrations of Zr and Hf, which are associated to the sandy phases in the ceramic body.

LOG-B Compositional Group

The highest Al_2O_3 concentration (21 ± 1 mass %) of the dataset characterizes this group (see Table 5.2), which exhibits calcareous pastes (CaO 13 ± 5 mass %).

The 27 individuals that form this group depict a wide range of forms, which would have been presumably produced during the whole life-cycle of the three pottery workshop (13^{th}-15^{th} centuries). These include jars, porringers, small jugs and cups unglazed or coated by translucent greenish of honey glazes as well as plenty of kiln utensils such as trivets or roof tiles that were used. Moreover, some of the sherds identified in this group correspond to strata of the later chronologies (17^{th}-18^{th} centuries). Their compositional compatibility was taken as a basis to include them in the compositional group. Nonetheless, note that their chronologies go beyond the functioning time of the unearthed kilns. These, include a mortar with heraldic decoration, some ceramic pastes an a tin-lead glazed sherd and were most probably

manufactured in the ceramic workshop located very close to the archaeological site in the street called "Ollerias"[5].

As for LOG009 ascribed to 1290-1350 and which shows manganese bearing decorations. According to Martínez González (2013), the use of decoration painted with manganese since the mid-fourteenth century was attested, first in jugs of common tableware and, later, from the beginning of the 15^{th} on pitchers and small jugs. Parallel ceramics from nearby locations, can be found in the medieval pottery workshop discovered in Calahorra (Luezas Pascual, 2014), whereas Mn decorations were ubiquitous after the 14^{th} century.

After the mineralogical evaluation (see Table 5.3), two fabric types (F-I and F-II) were identified in LOG-B compositional group. Both showed the existence of quartz along with firing phases such as plagioclases (albite peak is shown) and pyroxenes (diopside peak is shown). Their coexistence with the lack of illite-muscovite phases and mullite and the presence of K-feldspars (microcline peak is shown), in the case of F-I, permits estimating the EFT at ca. 900 °C for this fabric. K-feldspars start decomposing at 850-900 °C approximately, therefore, their absence in the F-II accompanied by an enrichment of plagioclases and gehlenite (a sub-product of calcite) suggested a higher EFT than F-I, thus, ca. 950 °C. Moreover, the detection of hematite in F-I and calcite in F-II are connected with the different Fe_2O_3 CaO content of both fabrics, respectively. LOG052 has 8.2 mass % while LOG087 has 19.3 mass % CaO, while the Fe_2O_3 drops from 6.5 mass % to 5.4 mass % in the respective individuals.).

Most of the pieces from this group correspond to kiln utensils, therefore, they do not bear glazes, whereas the coated pieces bear a lead glaze of varying PbO concentrations, as observed by SEM-EDS analyses A.10. The influence of the high-calcareous pastes can be also observed floating in the glaze (see Figure 5.20).

The composition of the clay body influences the final composition of the glaze. The molten glass reacts with the body and diffusion of the elements from into the glaze and vice versa occurs, while the phases of the clay body are transformed(Molera et al., 2001). Figure 5.20 shows Ca-rich pyroxenes formed due to the high concentration of CaO. Likewise, the K and Al-feldspars growing from the clay body to the glaze. In calcareous clays such as LOG085, Ca cations are incorporated into the glaze and Ca rich pyroxenes are formed, but they do not enhance the interface formation because they appear floating on the glaze. Moreover, the growth of the K-Al rich crystallites on the interface has been observed in some of the samples, especially those rich in K-feldspars (see Figure 4). These interface crystallite formations play a role in the final stability of the ceramic coating (Molera et al., 2001). Furthermore, the nature of the interface is usually taken as indicative of single or double firing. According to this indicator, most

[5]as mentioned in the introduction, the findings of this pottery workshop took place in the summer of 2018 and the materials are now under study.

GROUP	Fab.	EFT (°C)	Qz	Ilt-Ms	Mul	Afs	Cal	Hem	Gh	Pl	Px	Spl	Anl
LOG-A	F-I	850-900	xxxx	xx		x				x			
LOG-B	F-I	900	xxxx			x		x		xx	x		
	F-II	950	xx				x		xxx	xx	x		
LOG-C	F-I	850-950	xx	x		x		x	x	xxx			
LOG-D	F-I	1000-1050	x		x		xxx	x	xxx		x	x	
LOG-E	F-I	900-1000	xxx			xxx	x	x	xx	x	x		
TER	F-I	900-1000	xxxx			x				xx	x		x

Table 5.3: Fabrics identified in each compositional group and their main mineralogical phases and EFTs. Qz: Quartz; Ilt-Ms: Illite-Muscovite; Afs: alkali-feldspars; Cal: Calcite; Gh: Gehlenite; Hem: Hematite; Pl: plagioclases; Px: Pyroxenes; Mul: Mullite; Spl: spinels; Gp: Gypsum, Anl: Analcime. Abbreviations after (Whitney and Evans, 2010).

of the ceramics subjected to analysis, showed a single firing for the lead glazed pottery, while the polychromatic decorations would have been applied on bisque ceramics.

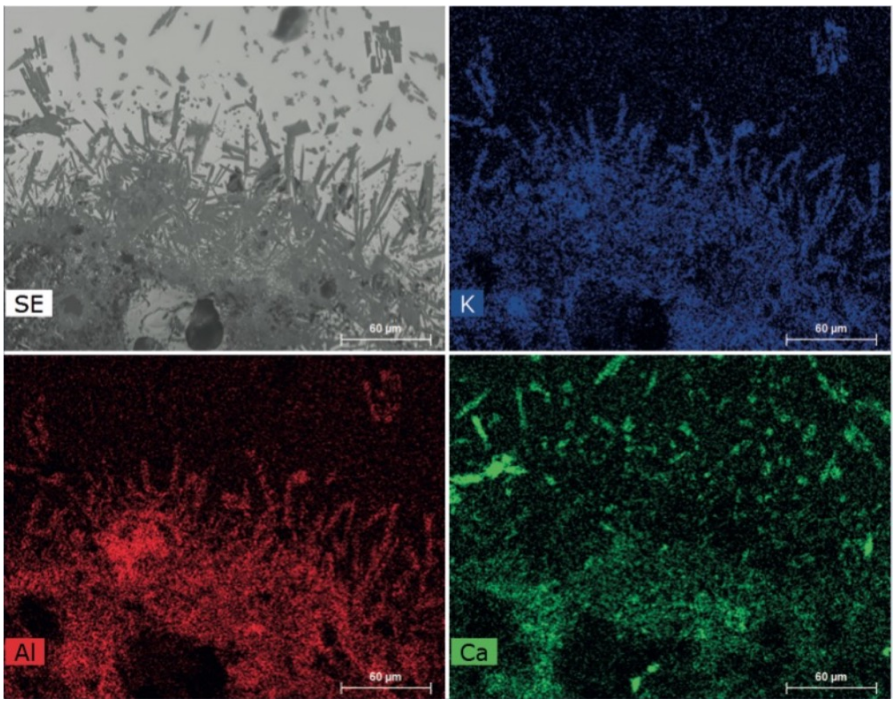

Figure 5.20: A representative ceramic (LOG059) from the group LOG-B (ArqueoRioja ©) and SEM-EDS images and Ca, Al and K elemental maps showing the growth of crystallites in ceramic body and diffusing into the glaze.

LOG-C Compositional Group

Provided its size (n= 25) LOG-C is the most compact compositional group found in Logroño, in chemical terms. It is highlighted by high concentrations of Al_2O_3, Fe_2O_3 and V, as well as other minor and trace elements such as Cr, Eu, Gd, Sm, La and U. They are medium-high-calcareous (CaO 9 ± 1 mass %) and very rich in iron (7.7 ± 0.4 mass %), which lead to orange-red colored pastes. These are unglazed in most of the cases and the forms include mostly jars and kiln utensils. Half of the ceramics from this group were most probably manufactured in the period of 1290-1350, whereas the later chronologies oft he remaining half including the late 14^{th} and the 15^{th} centuries suggest that they were manufactured by extracting very similar clays during, at least, during that period.

The compactness of this group was also evident in the fabric types as observed by XRD analysis, where only one fabric type was identified (F-I). The fabric shows the presence of quartz, along with plagioclases and K-feldspars, together with hematite and gehlenite (see Figure 5.24). The coexistence of these phases, in combination with the incipient peak of illite-muscovite indicated a low firing temperature ranging between 850-950 °C. In this case, the low sintering level can be observed in the microstructure of the ceramic body (see Figure 5.21). With regard to the decorations, like for the LOG-B group, most of the sherds do not show any kind of coating (see Figure 5.21), whereas those coated are obtained by glazes of high concentrations of PbO.

Figure 5.21: A representative ceramic (LOG004) from the group LOG-C and SEM images showing the low vitrification level of the paste and the influence of high-calcareous pastes.

Figure 5.22: Roof tile from LOG-D, showing drops of glaze (LOG081)

.

LOG-D Compositional Group

LOG-D is a very small group, only containing two individuals, which are roof tiles (see Figure 5.22). According to both statistical representations in Figure 5.18, the differentiation of these specimens is provided by the strikingly high CaO content (CaO 31 ± 1 mass %) and also shows the lowest Al_2O_3 concentration (12± 0.1 mass %). Apart from CaO concentration, it showed very low concentrations of most minor and trace elements, as well as the lowest Zr and Hf concentrations (125 and 2 μg/g respectively). Thus, the omission of CaO with its related Sr from the statistical analysis still showed clear differences that responsible for separate this group. According to the XRD analyses, both pastes showed F-I type fabric types, that were characterized by the lack of a high peak corresponding to quartz and at the same time, a very prominent peak of calcite and gehlenite. This F-I fabric is the only one in which spinel phases (that only appear after 1000 °C) were identified among the Ic-s from this assemblage. Therefore, the coexistence of spinels, mullite and the secondary phases, such as gehlenite and mullite, delimit the EFT between 1000-1050 °C. Roof tiles were extensively used as kiln tools for separation purposes. However, unlike with the trivets that were manufactured with the specific purpose as kiln utensil, the possibility that the roof tiles were recycled from somewhere else, must be regarded. In consequence, the link to a local origin cannot be performed with total certainty and the group was considered as undetermined.

LOG-E Compositional Group

This group includes three individuals that are characterized by bearing a tin-lead glazed coatings with colored decorations with buffer colored calcareous clay bodies (CaO 16 ± 2 mass %). Both HCA and PCA (see Figure 5.18) showed the clear compositional differences of these individuals with respect to the others, which are manifested by the higher MgO, Hf and Zr concentrations, while, Cr, V, Al_2O_3 and Fe_2O_3 exhibit lower concentrations, along with an overall lower concentration of minor and trace elements. Two of the individuals are from the latest chronologies (16-18th centuries), while the other (LOG047) dates backs to previous chronologies (15th century).

The individual LOG038 (see Figure 5.23), shows geometric strokes painted with cobalt blue on a white tin lead glaze (see Table A.10 in Appendix A). This bowl has a parallel in the documented local dump of Molí located in Paterna (Valencian area) in the 14th century (Mesquida García, 2002). Furthermore, a very similar piece to this one whose Valencian origin is suggested was document in the same archaeological site of Hospital Viejo with the inventory number N.441 (S. LHV.003.54) (Martínez González, 2013). Unfortunately, the comparative study performed by NAA with the main production centers of the Iberian Peninsula, could not confirm this provenance, and showed a possible compatibility with Sevillan productions. Nonetheless, it was not possible to find a parallel in the recently presented Doctoral Thesis concerning the Sevillan post-Medieval pottery production (Fernández de Marcos, 2018). In addition, the luster decoration of LOG039, can be associated to Valencian area (Pérez-Arantegui et al., 2001a; Conesa, 2008). Thus, the most probable provenance of this group would be Valencia (it is very difficult to distinguish between the productions from Manises and Paterna). However, further analyses should be performed to confirm this hypothesis.

According to mineralogical evaluation, the three sherds show F-I type fabric (see Table 5.3 and Figure 5.24). The F-I fabric, presents high peaks of gehlenite and calcite. The lack of illite and presence of gehlenite, a decomposition product of calcite places the firing temperature of this fabric between 900-1000 °C.

Figure 5.23: Representative ceramics from LOG-E and TER groups

.

TER

Finally, TER group is also formed by majolica pottery, including of bowls with tin-lead glazed decorations from different periods between the early 15^{th} to the early 16^{th}th centuries. According to the study and comparison performed by NAA, the origin of LOG042, LOG043, LOG044 and LOG048 is clearly associated to Teruel (see Figure 5.15). The pastes are characterized by reddish color and by medium-high-calcareous concentrations (CaO 9 ± 1 mass %), in combination with iron-rich pastes (6 ± 3 mass % 1.2). The decoration of green and manganese that LOG042 and LOG043 shows are associated to Teruel (see Figure 5.23), according to the archaeological and historical documentation (Conesa, 2008).

Among the individuals of TER group, F-I type fabric was identified. The mineral phases identified were quartz, K-feldspars, plagioclases and pyroxenes. The concurrence of all these phases permits estimating the EFT at 900-1000 °C.

Overall, the ceramics show high concentrations of Fe_2O_3 (4-8 mass %). Excluding LOG-A (MgO 0.9 mass %), and TER (MgO 1.6 mass %) all groups show MgO rich pastes (1.9-2.7 mass %). MnO exhibits an important variabilities within compositional groups (especially in LOG-A). Therefore, as in the cases of micaceous ceramics, the striking differences in composition do not allows properly determining the contribution of other elements in the variabilities. For this reason, MnO has been used with certain restrictions in the HCA and PCA.

Ungrouped Individuals

In addition, there were some sherds that could not be grouped. LOG037 is a piece with decoration showing castles and possibly a lis flower, the HCA obtained after NAA analysis

shows that this is the most differentiated ceramic in terms of chemical composition, due especially to a striking Ba concentration (755 μg/g). According to ICP-MS this sherd is chemically similar to LOG041 (tin-lead glazed decorated by blue) and LOG040, which shows a Mn-decoration applied on a whitish layer, being the only sherd bearing this kind of decoration. Although, they are chemically similar, their different typologies suggested that they most probably corresponded to different workshops.

LOG032 and LOG046, were not ascribed to LOG-E, since they exhibit differences in most of the trace and minor elements, as well as presenting significantly higher concentration of Ba, MgO and in a lesser extent U, while they also differ between each other in trace elements such as Tm, Lu and Sm. Moreover, they do not keep any typological or chronological accordance with the other sherds of LOG-E. Therefore, they could not be grouped to any other group. For a proper archaeological interpretation more sherd of the same chemical features should be analyzed. Additionally, LOG090 remained ungrouped due to its very low MnO concentration (0.003 mass %). This sherd showed a clear distinction within the ceramic assemblage even when MnO was not considered in the statistical analyses. Finally, LOG049 showed a different chemical fingerprint, as well as appearance in comparison to all the remaining studies ceramics.

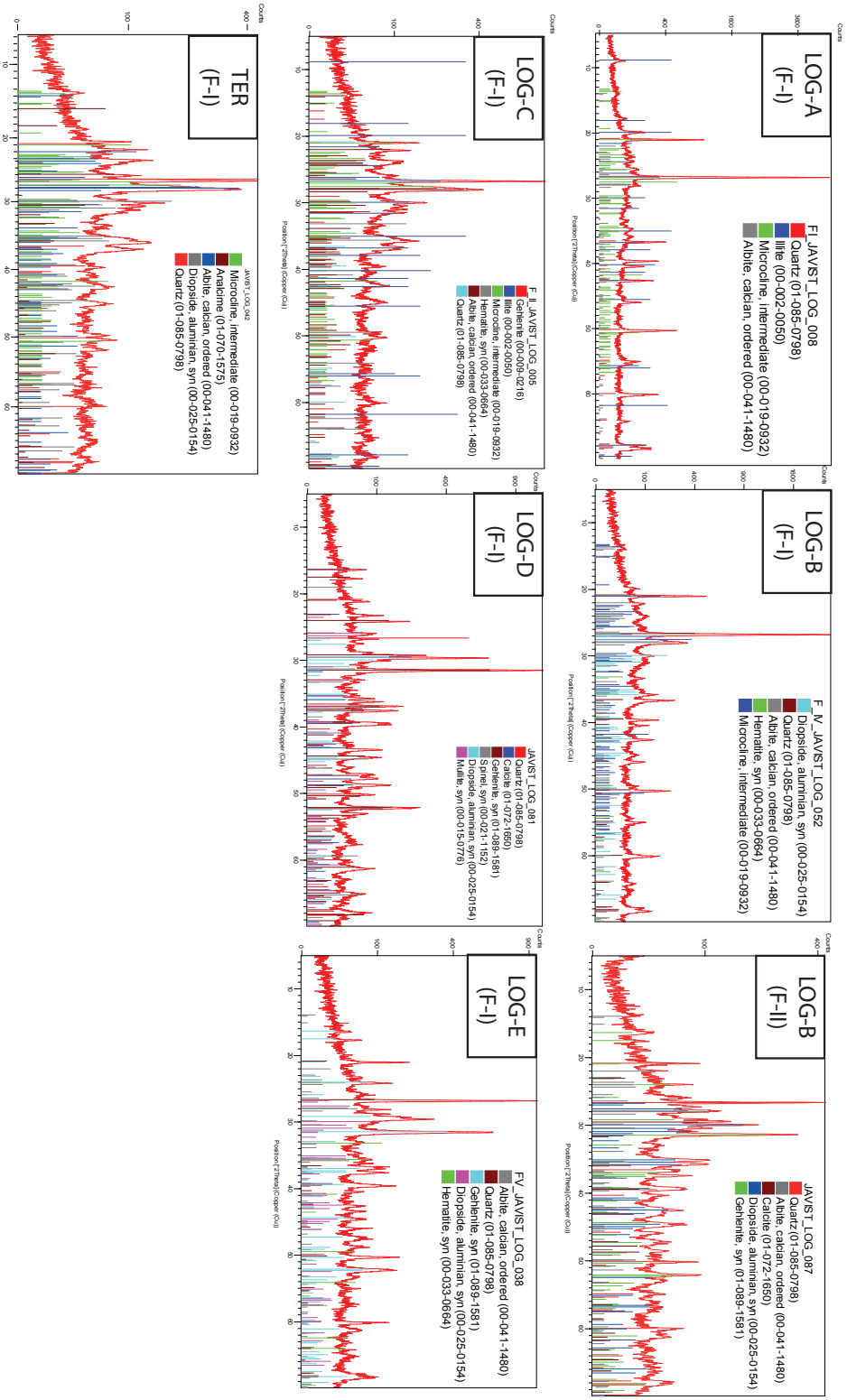

Figure 5.24: XRD diffractograms of the fabrics from Logroño

Final Remarks

The archaeometric analysis carried out in the 76 individuals from Hospital Viejo street, enabled to establish 6 compositional groups: 3 linked to a local production (LOG-A, LOG-B and LOG-C), one ascribed to Teruel (TER), as demonstrated after NAA , and two more undetermined (LOG-D and LOG-E). These groups could not be ascribed neither to a local origin nor to a known exogenous production center (see Figure 5.18). Along these lines, the complexity of Riojan ceramic production in pre-industrial eras was highlighted in terms of archaeometric characterization, showing different chemical reference groups diachronically within the same production center.

According to the multi-analytical approach on the samples studied in this work, the unglazed and lead glazed pottery would have been produced locally, whereas an exogenous origin for the tin lead glazed pieces is suggested. The group LOG-B depicts the continuity of manufacture of pottery from 1290 to 1500 with little modification in terms of pastes, showing ceramics fired at 900 °C. Whereas, the LOG-C group was the most extensive and compositionally compact, showing ceramics fired at 850-950°C, which seem to have remained in the posterior chronologies, beyond the operational period of the kilns. Furthermore, compositionally very different groups were identified ascribed to local origin, such as the non-calcareous cookware (LOG- A) and a high-calcareous group of roof tiles used as kiln tools (LOG-D). However, they could have also been transported from somewhere else, thus they cannot be linked to the local origin.

The majority of the production from Hospital Viejo from Logroño is unglazed or lead glazed. Those lead glazed provide a translucent glaze which gave them a final honey colored appearance.The polychromies include blue, black and green colors. All the opaque glazes were obtained through SnO_2 from concentrations ranging 3.26 to 7.41 mass % SnO_2. To obtain the final colors, traditional recipes based on different metallic oxides were used, thus the blue was acquired by CoO, while CuO was used to obtain the green color and MnO for the black. Interestingly, the tin lead glazed pieces that included poly-chromatic decorations were those whose provenance identified as exogenous (LOG-E and TER).The underrepresentation of the locally produced tin lead glazed ceramics, coincides with the slow adoption of tin-lead glazing technology which was more widely extended in other parts of the Iberian Peninsula (Molera et al., 1997).

5.3 Archaeometric characterization of pottery from Nájera

Abstract

The city of Nájera, located in the north of the Iberian Peninsula, hosts an alcazar of Arab origin, which became the residence of the king of Pamplona-Nájera and later of the duke and duchess of Nájera. From this last period (1500-1600), date the ceramics that were unearthed during the recent excavations of the Alcazar of Nájera. These findings constitute the largest post-Medieval assemblage of ceramic unearthed in the city. They include a large set of plain tin-lead glazed pieces of tableware, as well as some mono or polychrome decorated sherds. In this chapter, an archaeometric characterization was carried out on a sample of these ceramics (n = 94) by means of a multi-analytical strategy. The clayey pastes were analyzed chemically and mineralogically by ICP-MS and XRD, respectively. Further evaluation by SEM-EDS and Raman microscopy were carried out on a subsample of the ceramic glazes. The preliminary results enabled establishing a main large compositional group (NAJ-A) and a smaller one (NAJ-B) which could tentatively be linked to a local production origin. Moreover, exogenous provenances such as Muel and Talavera were identified after the comparison with data from other Spanish contemporary majolica pottery productions, both by NAA and ICP-MS.

Figure 5.25: Image of the Alcázar de Nájera.LDGP

Background

Located in the Autonomous Community of La Rioja (Iberian Peninsula), in the middle valley of the Ebro, the city of Nájera was the royal and episcopal see of the kingdom of Pamplona from the Christian conquest (c. 923) until its incorporation into the kingdom of León-Castilla in 1076. In the following centuries, despite the appearance of other cities such as Calahorra, Logroño or Santo Domingo de la Calzada, Nájera continued to be an important economic, political and religious center of the region (Ceniceros Herreros and Montejo López de Alda, 2006).

During Roman times, the place where medieval Nájera would emerge was located in a suburban area of *Tritium Magallum*, one of the main production centers of *Terra Sigillata* pottery from Hispania. Indeed, many remains pottery typology have been found in its vicinity. Their study has revealed an important pottery activity that began in the 1^{st} century CE and lasted at least during the 2^{nd} and 3^{rd} centuries CE (Garabito Gómez et al., 1978). The decline of the *Tritium Magallum* that occurred in the Andalusian period and the rise of Nájera to the status of political and military center of the upper Rioja is not yet fully understood.

Recent research has dealt with the daily life and artisan activity of medieval Nájera (Goicolea Julián, 2001, 2002, 2007), although little is known about a local pottery activity that seemingly must have been considerable, judging by various indirect references. The investigations carried out by Sánchez Trujillano on the decoration of the fortress, showed a wide range of ceramic typologies of Moorish influence. A sample of them are the tiles of the *cuerda seca* or *cuenca y arista*, characterized among the materials recovered in the decade of 1930. In the same way, the ostentation that housed the Alcázar is reflected in the imports from the main majolica producing centers, such as 14^{th} century Aragonese monochrome tiles and other architectonic decorated features, 15^{th} century Sevillan tiles with reliefs or 15^{th}century Valencian painted tiles (Sanchez Trujillano, 1991). These production centers were among the most technologically advanced in terms of ceramic production at the time (Iñañez et al., 2008).

In contrast to these well-studied sites, the centers of the north of the Iberian Peninsula and in the periphery of Al-Andalus where Nájera was located, barely dragged the attention of ceramologists and archaeometrists, due to their presupposed trade limited to the regional or local scale and beyond of the main long-distance exchange networks. Furthermore, the lack of research about pottery activity in Nájera in the post-Medieval period is even more dramatic. With regard to local pottery production, historical documentation revealed that in Nájera there were at least four active potters during the 16^{th} and 17^{th} centuries, namely: Pedro García (1589), Pedro García de Luis (1597), Pedro Gómez (1597), and Francisco de Sagastia (1661). Moreover, potters from the neighbor town of Navarrete going to Nájera as apprentices were also identified (Martínez Glera, 1994).

From the ethnographic and art history point of view, the research on the pottery workshops in Rioja carried out by Martínez (Martínez Glera, 1994) has attributed ceramic styles to a Nájera origin. The materials studied in his work came from the prospections of the fortress and the Las Viudas street in Nájera. In addition, the study also mentions a landfill corresponding to a possible local ceramic workshop located in San Lázaro (a land lot within Nájera municipality). However, the origin of these ceramics cannot be unequivocally attributed to Nájera due to the lack of more detailed archaeological or archaeometric studies. Therefore, their tentative production is not discarded in the most active contemporary workshops such as Haro or other Riojan cities such as Logroño (Martínez Glera, 1994). Additionally, the study of the ceramic record found in Alava, a northern adjacent region, includes a ceramic group (XLVII) whose provenance is tentatively attributed to Nájera or Logroño (Escribano, 2014). Therefore, until now, there is no direct archaeological evidence of ceramic production in Nájera, such as ceramic kilns or any other equipment required for production, unlike Logroño; where recently, kilns from the 13^{th}-15^{th} period (Martínez González, 2013) and a kiln from the 16^{th} period (Gil Zubillaga and Luezas Pascual, 2018) were discovered.

However, in the excavation carried out in the Alcázar de Nájera in 2002, hundreds of ceramic fragments were unearthed. The chronological framework is given by the

reconstruction of the Alcázar after the revolts that took place (1520) and until the abandonment of the construction (Ceniceros Herreros, 2004). The modification of the strata that were leveled to cover a difference in level of 12 m to use them as plots implies that the pieces found in this place correspond to those consumed during the Duchy of Nájera and until the moment when the occupants ceased to use the fortress as a residence (end of the 16^{th} century). The large number of pieces of similar appearance suggests that many of the fragments could be linked to a local production. In light of this, in the Museo Najerillense a first approximation and typological classification based on stylistic features was carried out (Ceniceros Herreros, 2012).

In the current work, an archaeometric approach has been carried in order to characterize the tentative ceramic productions of Nájera. The ceramic assemblage under study is mainly composed by plain tin-lead glazed earthenware. With such a scarce variety of typologies and decorations, it is especially interesting to carry out an approach based on the compositions of the pastes. In this way, it is possible to shed light on their provenance and technological features, and thus be able to obtain better understanding of the local ceramic production as well as the trade of valuable exogenous productions.

Along these lines, it is known that during the 16^{th} century a local market was held every Thursday in Nájera, where pieces from Valencia, Bilbao and Seville were sold (Martínez Glera, 1994). In addition, on a regional scale, Martínez preliminary identified the connections of ceramic workshops in La Rioja with other production centers reporting ceramic exchange. On the one hand, a regional and international provision from Flanders, Zamora and Pisa during the 16^{th} century (Martínez Glera, 1994); while on the other hand, a trend towards a regional provision of ceramics from Zamora, Talavera de la Reina, Agreda and Aragón during the 17^{th} century. This last link of Aragón, was especially intensified during the 18^{th} century, when connections with Talavera de la Reina and Alcora were also reported.

The ceramics under this study were unearthed in the interventions on the alcazar of Nájera (see Figure 5.25). The term alcazar refers to a type of fortification linked to the crown, which must be considered in its double aspect of military and palatial architecture. Thus, the fortress of Nájera, of Islamic origin and whose construction dates back to the 9^{th} century, served as a residence for the kings of Pamplona and maintained its status as a royal fortress until the end of the Middle Ages, when it was ceded to Pedro Manrique (1465). The lineage of the Manrique family reconstructed the ensemble, accentuating its palatial character. However, the assault by the communal rebels in 1520 shows that it maintained its military value even at the beginning of the 16^{th} century. It was later transformed into a luxurious Renaissance palace, despite which it was abandoned at the end of the 16^{th} century and went into ruin in the following century (Ceniceros Herreros, 2004).

Ceramic sample of Nájera

The set of ceramics (n = 94) consists principally of white plain tin-lead glazed pieces of tableware (27 porringers, 25 plates, 17 jars, 3 pots, and 22 others) from the 16^{th} century. Some of the glazes also include blue, green, yellow, black and luster decorations. The ceramics are glazed completely in the interior and either completely, partially or unglazed in the exterior (Ceniceros Herreros, 2004). Other tin-lead glazed forms include sauce boats, salt shakers, etc. Moreover, unglazed cooking pots and lids were also analyzed.

Experimental

In order to characterize the compositions and mineralogical phases of the pastes, the whole set of ceramics was analyzed by means of inductively coupled plasma mass spectrometry (ICP-MS) and X-ray diffraction (XRD). Moreover, a subsample of them (n = 25) was analyzed by NAA. In addition, a subsample (n = 15) was analyzed by means of scanning electron microscopy coupled to energy dispersive spectrometry (SEM-EDS) and Raman microscopy in order to better understand the technology used by the potters. Additionally, some μ-XRF and UV-Vis reflectance analyses were performed. For more details about methodology, see Section 3.3.

Results and Discussion

Identification of Exogenous Provenances

For the identification of the exogenous provenances, 14 reference groups obtained after NAA analyses (Iñañez et al., 2008) and corresponding to the main majolica production centers of the Iberian Peninsula were employed. These were, BCN-B1B2 and BCN-B3 from Barcelona, Lleida, Manises, Muel, Paterna, Puente, Puente Arzobispo, Reus, Sevilla, Talavera, Teruel, Villafranca de Penedes (VdP) and Villafeliche, in addition to those groups analyzed in the present work (Elosu, Durango, Orduña, Nájera, LoLogroñogrono). The Figure 5.71 presents the first approach by NAA omitting micaceous samples from Nájera and including the exogenous provenances from to sherds were ascribed to. These were Talavera for NAJ029 and NAJ033 and Muel for NAJ093 and NAJ092. Productions from Muel were divided into two subgroups as reported in the literature (Iñañez et al., 2008) and each one was compatible to each of the ceramics ascribed to this provenance.

In addition, these preliminary results on the subset of ceramics from Nájera, depicted a group of ceramics sharing strong similarities (NAJ-A), whereas, the NAJ076 and NAJ014 can be clearly differentiated fro those. These were ascribed to the NAJ-B

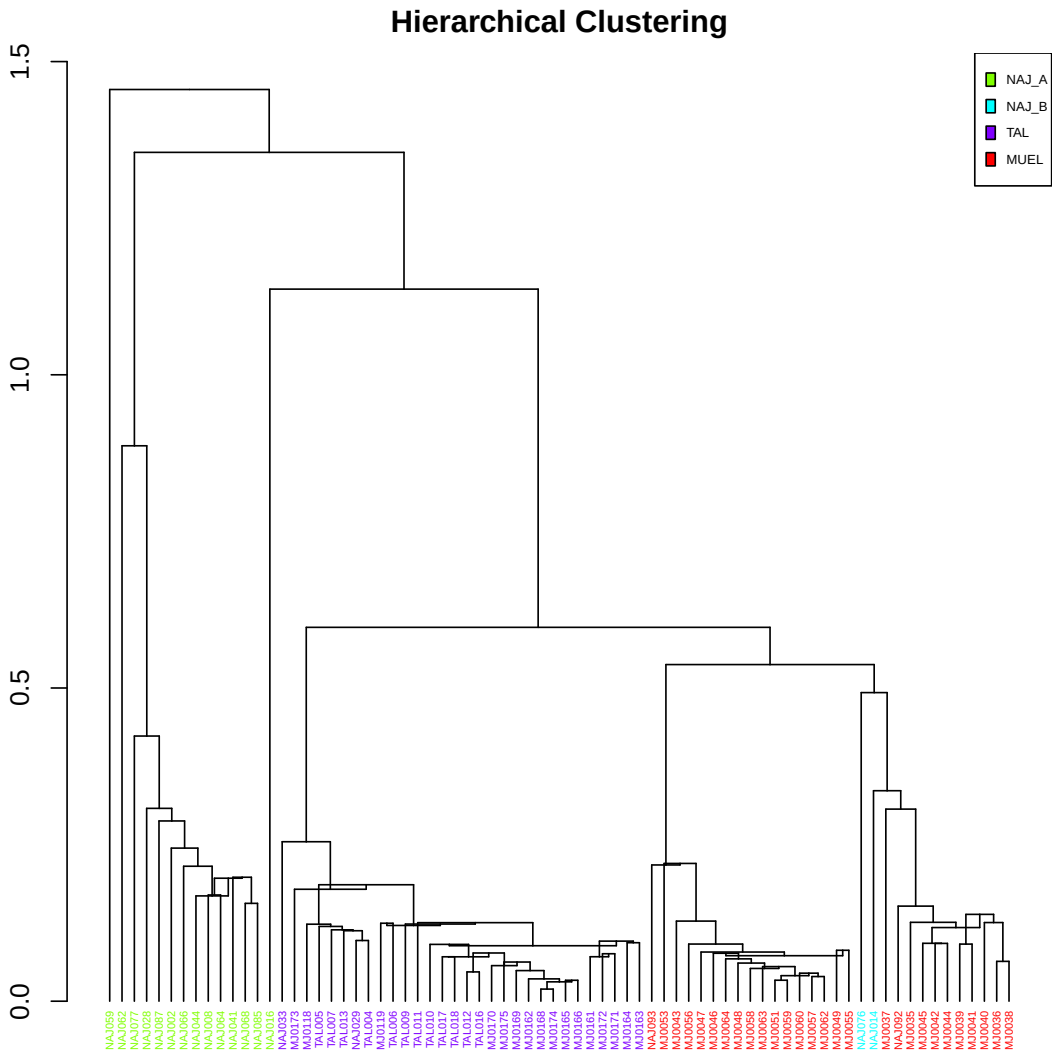

Figure 5.26: Dendrogram of Euclidean squared distances using centroid algorithm of 25 individuals from Nájera and other production centers (Talavera de la Reina (TAL) Manises and Muel), on the sub-composition obtained by NAA of La, Lu, Nd, Sm, U, Yb, Ce, Cr, Eu, Fe, Hf, Sc, Tb, Th, Zn, Zr, Al, Ba, Dy, Mn, Ti and V

group as is addressed later. A wider discussion on these groups, as well as the provenances identified was performed with the ICP-MS analyses performed on a wider sample.

Element	NAJ-A	SD	NAJ-B	SD	MUEL	SD	TAL	SD	NAJ-MIC	SD
Al2O3	16.5	1.2	17.6	1.2	13.7	1.3	15.3	0.53	21.8	1.4
CaO	18.2	3.1	15.0	4.5	18.8	3.9	17.8	1.9	3.75	1.5
Fe2O3	3.24	0.38	5.02	0.62	4.06	0.29	4.17	0.41	2.20	0.086
K2O	3.13	0.60	3.51	0.54	2.98	0.32	3.47	0.21	3.37	0.28
MgO	1.83	1.0	2.15	0.34	2.41	0.33	3.86	0.55	0.944	0.072
MnO	0.0244	0.0060	0.0674	0.013	0.0616	0.0050	0.0642	0.0040	0,0379	0,0070
Na2O	0.736	0.20	0.819	0.22	0.41	0.13	0.946	0.14	0.475	0.21
P2O5	0.216	0.057	0.191	0.038	0.179	0.065	0.259	0.054	0.17	0.037
SiO2	57.7	7.0	52.6	11	49.9	4.1	59.1	1.6	70.40	4
TiO2	0.703	0.043	0.757	0.064	0.665	0.078	0.742	0.035	0.271	0.064
Ba	425	47.1	495	36	435	78	454	23	256	30
Ce	78.0	5.1	89.6	9.3	77.5	4.7	93.0	3.7	38.5	7.0
Co	21.5	10	24.1	6.9	18.3	5.9	19.4	3.5	21.1	5.5
Cr	69.3	28	77.5	12	59.8	5.6	48.3	9.2	23.6	6.6
Cs	13.7	3.5	13.1	2.7	7.98	2.1	9.84	1.3	53.4	9.7
Cu	35.9	21	33.7	13	23.8	7.6	42.9	18	6.95	2.5
Dy	4.55	0.31	4.99	0.4	4.88	0.27	5.74	0.35	5.63	0.41
Er	2.39	0.16	2.59	0.18	2.64	0.15	2.96	0.22	2.85	0.24
Eu	1.24	0.10	1.5	0.17	1.30	0.099	1.35	0.039	0.741	0.076
Gd	5.35	0.38	6.04	0.56	5.65	0.28	6.64	0.31	4.61	0.28
Hf	4.07	0.35	3.81	0.36	4.29	0.41	5.26	0.92	4.08	0.66
Ho	0.789	0.048	0.845	0.053	0.845	0.045	0.96	0.047	0.963	0.075
La	38.9	2.4	45.3	4.9	41.1	2.1	45.4	1.9	19.5	2.3
Lu	0.337	0.025	0.374	0.033	0.362	0.033	0.448	0.037	0.38	0.046
Nb	17.0	1.4	16.4	0.91	15.6	1.4	17.3	0.66	26.0	1.7
Nd	33.6	2.3	38.5	4.0	35.3	1.73	40.9	2.5	19.3	2.0
Pb	(487 -	21.7x10^3)	(700 -	1.50x10^3)	(3.96x10^3 -	8.8x10^3)	(2.89x10^3 -	8.59x10^3)	(27.6 -	70.5)
Pr	9.00	0,59	10,3	1,1	9.29	0.44	10.9	0.63	4.87	0.51
Rb	170	35	180	23	136	21	161	11	528	43
Sm	6.24	0.50	7.07	0.69	6.52	0.32	7.61	0.50	4.47	0.43
Sn	(15.1 -	1240)	(12.7 -	220)	(16.3 -	68.3)	(16.7 -	61.6)	(69.8 -	110)
Sr	779	1.6x10^2	584	15x10^2	413	83	389	85	126	20
Ta	1.73	0.32	1.31	0.28	1.33	0.084	1.76	0.10	8.38	3.8
Tb	0.810	0.057	0.883	0.065	0.849	0.039	1.01	0.079	0.917	0.058
Th	13.0	1.0	13.5	0.82	12	0.79	15.7	1.3	6.47	1.1
Tm	0.362	0.025	0.399	0.032	0.387	0.03	0.475	0.042	0.441	0.046
U	3.63	0.35	3.94	0.42	3.24	0.24	4.87	0.35	4.61	0.87
V	82.6	9.7	107	19	77.4	6.8	73.4	101	24.7	3.9
Yb	2.41	0.14	2.61	0.18	2.6	0.16	3.04	0.25	2.87	0.27
Zr	197	24	184	22	228	27	264	61	171	39

Table 5.4: Mean concentrations standard deviation values (SD) of each compositional group from the Alcazar of Nájera site. Talavera (TAL) and Muel (MUEL) are exogenous. Concentrations obtained by ICP-MS. Oxides are expressed in mass % and the rest in μg/g. *Pb and Sn ranges are given because they contain SD values higher than mean values due to their heterogeneous distribution

Compositional Groups

In Table 5.4 the mean concentrations of each compositional group obtained by ICP-MS are presented. Ideally, for the statistical analysis, the analytical variance should be minimized in such a way that it is originated by natural sources and not because of experimental errors and/or alterations arising from post-depositional processes. Therefore, in this work, several elements were not regarded for the statistical analysis. These are addressed in the section 5.1.

The compositional heterogeneity was assessed by calculating the compositional variation matrix (CVM), which provides information about the variability introduced by each element into the dataset (see Figure 5.27). Generally speaking, a large value of the total variation vt indicates greater variability and suggests that the dataset is polygenic (i.e. the presence of several compositional groups). In contrast, a small value for vt indicates a possible monogenic nature of the dataset (Buxeda i Garrigós and Kilikoglou, 2003). In this case, the set shows a very high vt (5.75), which reveals the high contribution of the aforementioned (Pb, Sn, P, Co, Ta Na, K and Rb). The vt drops down to 0.75 when these are omitted (see Figure 5.28). This vt can be considered relatively low expecting a low number of compositional groups.

According to the ternary diagram (see Figure 5.29), the six micaceous sherds are strongly differentiated by a higher concentration of Al_2O_3 and SiO_2. Their provenance might be ascribed to Zamora according to historic trades of that ceramic typology as is later addressed. The remaining pieces (all tin-lead glazed, some of which include several decorations), fall mostly in the Wollastonite, quartz, anorthite triangle, whereas, some sherds fall within the gehlenite, anorthite, wollastonite triangle, in which a high concentration of CaO can be expected.

PCA and HCA were carried out in order to extract the compositional groups existing in the dataset (see Figure 5.30). Moreover, a comparison was performed to test the possible exogenous provenances. Thus, compositions of ceramics from Seville, Manises and Talavera de La Reina/Puente del Arzobispo were included in the multivariate statistics. These productions correspond to the main majolica production centers during the 14^{th} to the 18^{th} centuries and were previously characterized archaeometrically (Iñañez et al., 2008).

On the one hand, the results permitted identifying two main compositional groups (NAJ-A and NAJ-B), which are not mixed with exogenous provenances and could be tentatively ascribed to a local origin (see Figure 5.30). Micaceous sherds, which are compositionally distinctive, were defined as NAJ-MIC group and is addressed later. On the other hand, ceramics compatible with Talavera reference group were identified. Additionally, some of the sherds showing luster decoration were ascribed to Muel (NAJ088-NAJ093). Despite no ICP-MS reference data from Muel was available, previous comparative NAA analyses performed in the ongoing research, pointed out

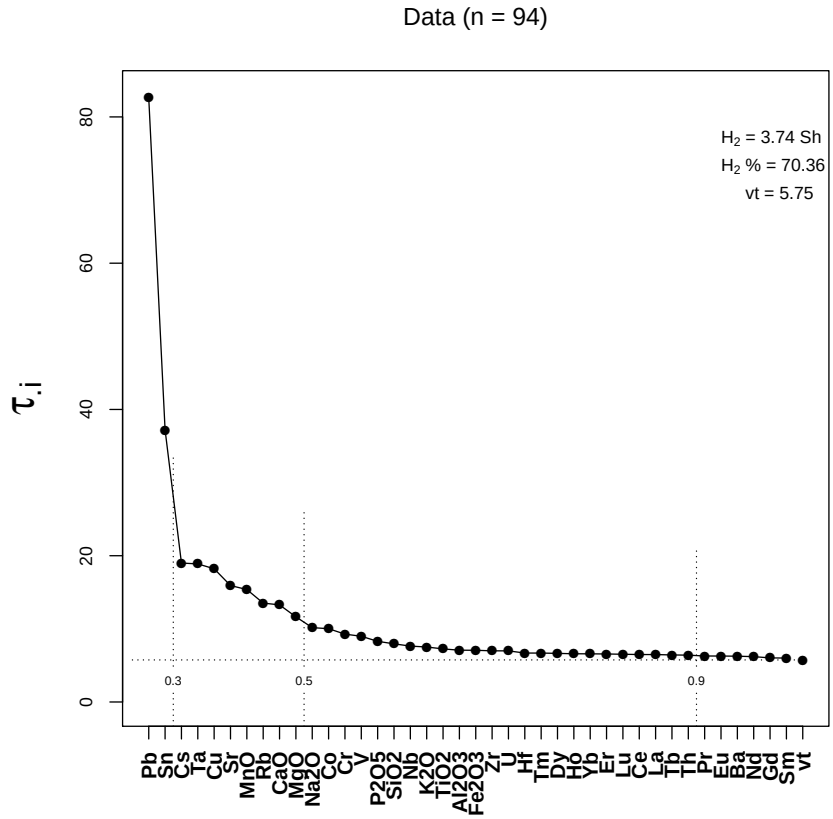

Figure 5.27: Graphical representation compositional variation matrix including all quantified elements

this provenance for NAJ092 and NAJ093. Thus, the compositional compatibility of the remaining sherds observed by ICP-MS and their coherence in luster decorations suggested that these could also be ascribed to Muel (Zaragoza). Finally, some sherds could not be ascribed to any provenance due to the lack of a larger sample to compare with. They could neither constitute a compositional group because they showed differing compositions among each other. Thus, NAJ024, NAJ026, NAJ035, NAJ042, NAJ043, NAJ048, and NAJ053 were all tin-lead glazed, whereas NAJ048 and NAJ053 were highlighted by a reddish paste and a very fine coating, which resulted in a glaze with a very poorly white appearance.

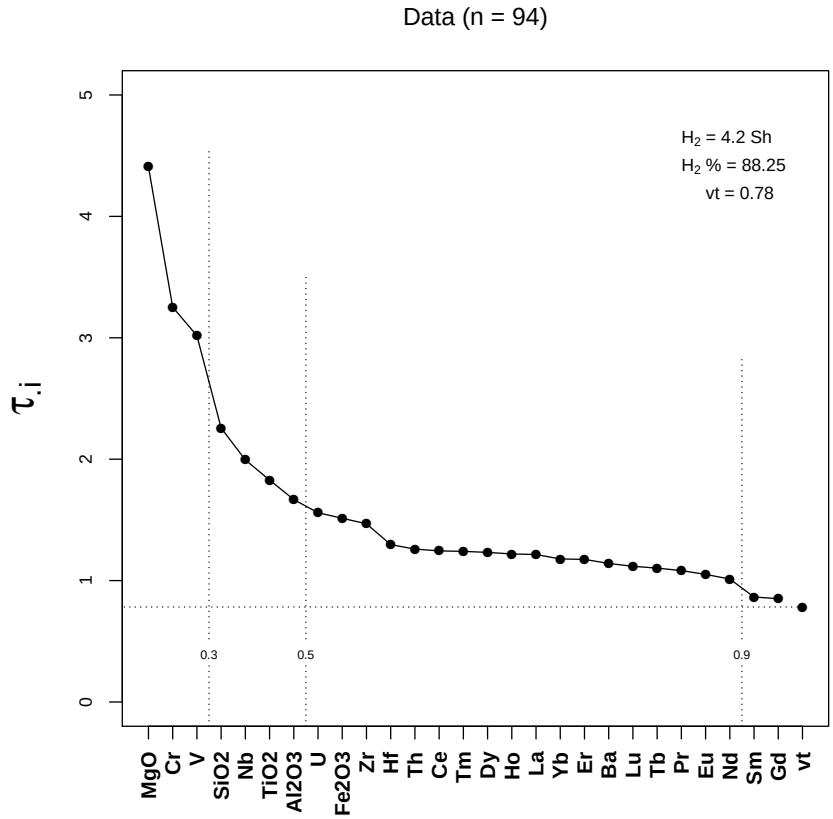

Figure 5.28: Graphical representation compositional variation excluding non-meaningful variables.

NAJ-A group

The main compositional group called NAJ-A is the largest (n = 56) and include CaO rich (18 ± 3 mass %) pastes. The forms dominating in this group are porringers, jars, plates and bowls, corresponding to tin-lead glazed tableware. Some ataifors used for the household are also present in the group. Compositionally, some of the sherds of this group showed differing concentrations of MgO (NAJ075, NAJ059, NAJ055 and NAJ073). Thus, they remain distanced from this group if MgO is considered in the statistics, but omitting it regroups them within NAJ-A (see the contribution of MgO in the PCA in Figure 5.30). Moreover, NAJ016 presents an outlying value of Cr and, likewise, omitting this element regroups the sample within the NAJ-A group.

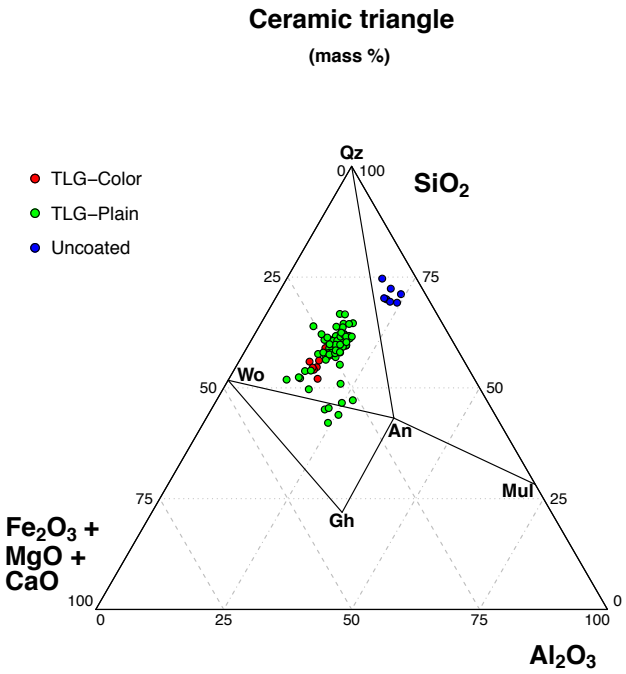

Figure 5.29: Ternary diagram showing the compositions of SiO_2, CaO and Al_2O_3 of the 94 potsherds. TLG: tin-lead glazed. An: Anorthite, Gh: Gehlenite, Mul: mullite, Qz: quartz and Wo: Wollastonite (abbreviations after (Whitney and Evans, 2010)

According to the XRD analysis, four main fabric types were identified in NAJ-A compositional group. Each specific fabric type and compositional groups are listed in the Appendix B and their representative diffractograms are shown in Figure 5.32.

The main phases of NAJ-A fabrics are quartz, K-feldspars, plagioclases and pyroxenes. The presence of calcite and gehlenite, a phase arising from the reaction of the carbonates with CaO in the clay paste, is also ubiquitous among all sherds. In Figure 5.32, NAJ001 is shown as representative diffractogram of F-I (n = 9). The incipient presence of plagioclases and pyroxenes and the illite-muscovite basal peak at 7Å detected in all the samples indicates that the ceramics of F-I group were fired at low temperature ranging, between 800-900°C. Moreover, this fabric showed the presence of gypsum, which can be formed due to the reaction between calcite and sulfates. While F-II fabric (n = 20) is mineralogically very similar to F-I, the illite basal peak is completely absent, whereas the non basal peak can be still observed at (19 Å). Additionally , a more abundant presence of firing phases such as plagioclases and

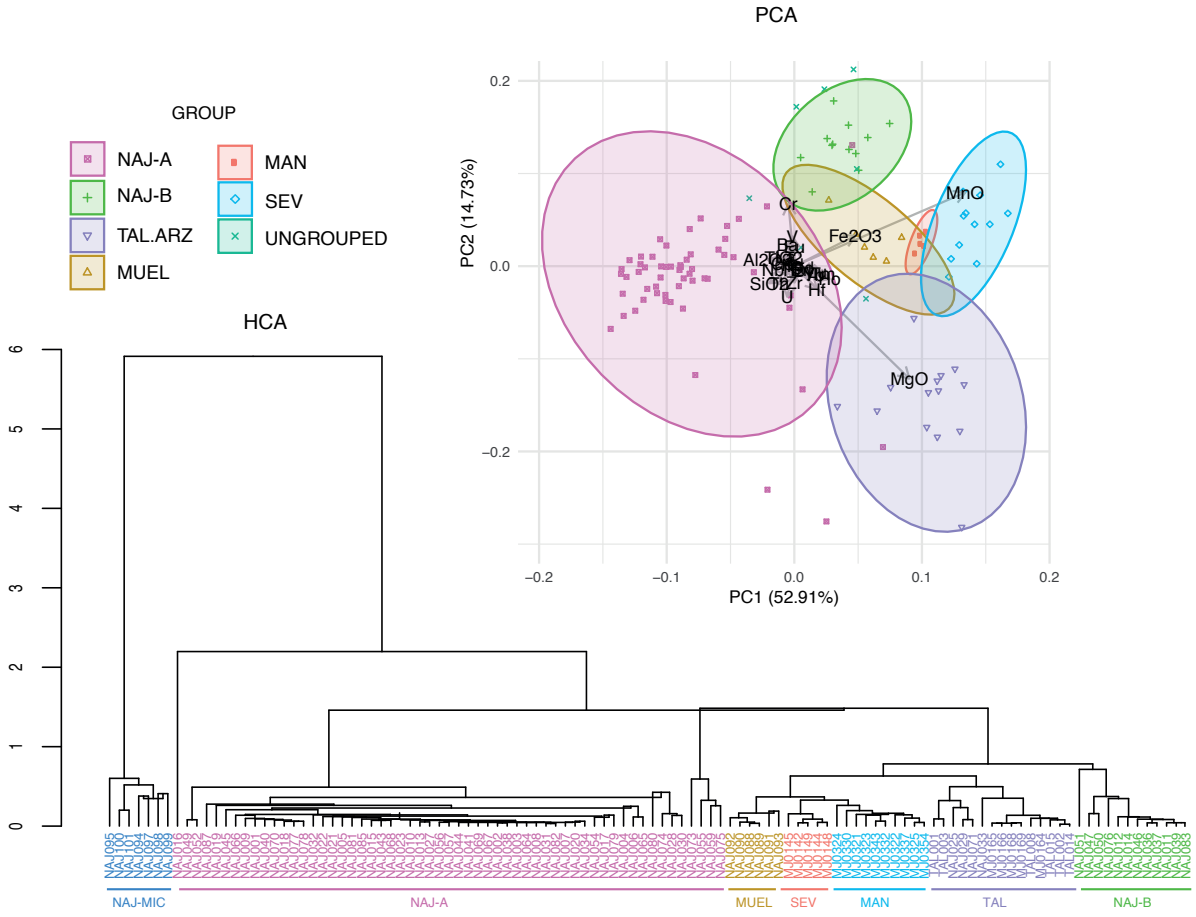

Figure 5.30: Dendrogram of Euclidean squared distances using centroid algorithm of 94 individuals from Nájera and other production centers (SEV:Seville, TAL.ARZ: Talavera de la Reina, MAN: Manises and Muel), on the sub-composition of Al_2O_3, Zr, Nb, Cs, Ba, La, Ce, Pr, Nd, Eu, Gd, Tb, Dy, Ho, Er, Tm, Yb, Lu, Hf, Th, U, TiO_2, V, Cr, MnO, Fe_2O_3 and SiO_2. Gd was used as divisor for the PCA.

Figure 5.31: Examples of tin-lead glazed and blue decorated ceramics from group NAJ-A.

pyroxenes in coexistence with K-feldspars that have not been fully decomposed permitted estimating the equivalent firing temperature above 850 °C.

According to the mineralogical phases identified, most of the ceramics of NAJ-A show a F-III fabric type (n = 27). This fabric is very similar to the previous ones, but with a equivalent firing temperature (EFT) higher because the lack of non-basal peaks of illite and K-feldspars indicates that phyllosilicates and K-feldspars have been completely decomposed. Moreover, spinels presence was also detected, which occurs at high temperatures. However, the lack of mullite indicates that the TCE would be at maximum of ca. 950 °C. Additionally, some of the sherds showed the presence of analcime.

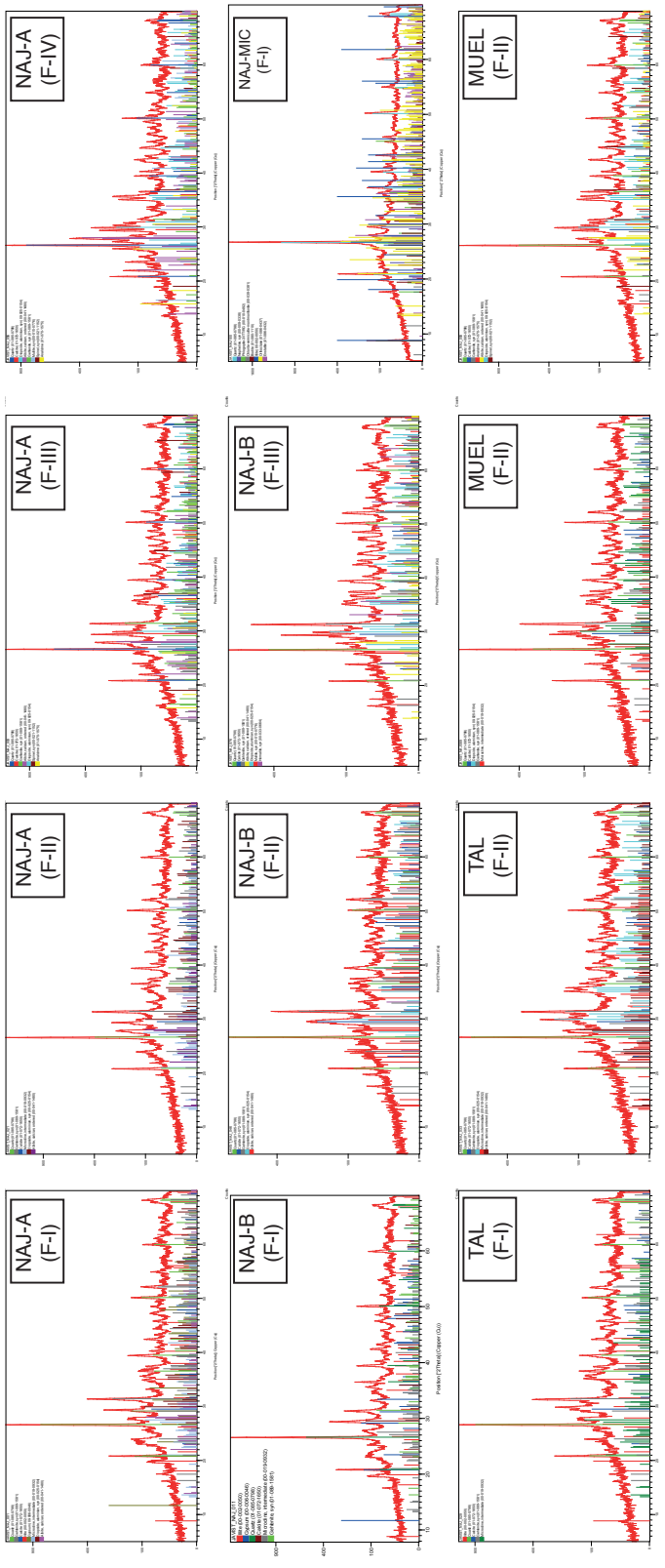

Figure 5.32: Representative XRD diffractogram of each fabric identified in each compositional group.

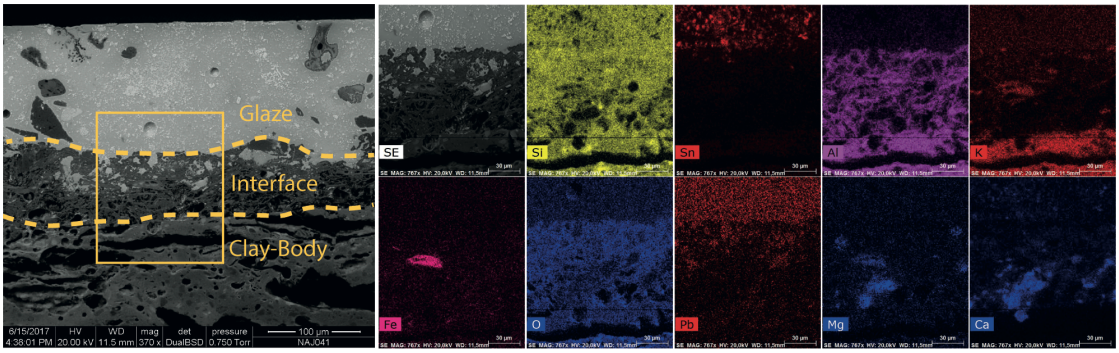

Figure 5.33: SEM-EDS image and elemental distribution maps of the selected area inside NAJ041 glaze-ceramic body interface area.

There is one sample (NAJ056) showing F-IV fabric type, also with similar mineralogical composition to previous ones, but characterized by the presence of mullite. Unless it is not a primary phase, the occurrence of this silicate indicates that a temperature of at least. 1000°C was reached during firing. This is in accordance with the more significant presence of firing phases such as pyroxenes and plagioclases observed in this sample. Moreover, an intense detection of analcime was detected. As mentioned before, all the pieces of NAJ-A group were coated by white glazes that were opacified by cassiterite (SnO_2). The coating was applied either partially or completely (see Figure 5.31). In addition, some ceramics (NAJ074, NAJ075, NAJ077-NAJ082 and NAJ085) include decorative blue motifs (both geometric and vegetal). NAJ085 shows a jasper blue decoration. There is also one with green decoration (NAJ087). From the SEM-EDS evaluation it can be concluded that the glazes were applied following two step technology, namely, applying a second firing for the glaze on the bisque ceramic. During this process, the compounds from the glaze are still diffused into the clay body and vice versa. The Pb clearly diffuses into the clay body, while Sn tends to be retained in the glaze (see Figure 5.33). In addition, the Al-silicates interact highly with the glazes in comparison to K-bearing phases, as the penetration depth is higher in the former case. Moreover, the observed Ca-Mg accumulations constitute a part of the clay body and most probably correspond to diopsides ($CaMgSi_2O_6$) that were previously identified by XRD.

Overall, the glazes of NAJ-A present elevated concentrations of SnO_2, being the case of NAJ064 strikingly high one (22.06 mass %). The use of high concentration of SnO_2 is normally found in the glazes of the so-called "proto-majolica" pottery, because sometimes the pastes were darker than the common majolica pottery and the opacifying know-how had not been completely achieved by artisans (Iñañez et al., 2008, 2009). However, this is not the cases of NAJ064, which shows a buffer colored ceramic body, and is even less common regarding the period under study (16^{th} century). NAJ015 shows the thickest glaze of the whole set of ceramics (0.6 mm), with a 10 mass % of SnO_2, ensuring a high

GROUP	Fab.	EFT (°C)	Qz	Ilt-Ms	Afs	Cal	Gh	Hem	Pl	Px	Mul	Spl	Gp	Anl	Phyllo-Si
NAJ-A	F-I	800-900	xx	xx	x	x	x		x	x			x		
	F-II	>850	xx		x	x	x		x	x					
	F-III	ca. 950	xx			x	x		x	x		x		x	
	F-IV	ca. 1000	xx			x	x		xx	x	x	x		x	
NAJ-B	F-I	ca. 850	xx	xx	x	x	x						x		
	F-II	ca. 900	xx			x	x		x	x					
	F-III	>1000	xx			x	x	x	x	x	x				
MIC	F-I	ca. 850	xx	xx	x										x
TAL	F-I	800-900	xx	x	x	x	x								
	F-II	ca. 900	xx		x	x	x		x	x					
MUEL	F-I	800-900	xx		x	x	x			x					
	F-II	900-1000	xx			x	x		x	x		x		x	

Table 5.5: Fabrics identified in each compositional group and their main mineralogical phases and EFTs. Qz: Quartz; Ilt-Ms: Illite-Muscovite; Afs: alkali-feldspars; Cal: Calcite; Gh: Gehlenite; Hem: Hematite; Pl: plagioglases; Px: Pyroxenes; Mul: Mullite; Spl: spinels; Gp:Gypsum, Anl:Analcime. Abbreviations after (Whitney and Evans, 2010). Phyllo-Si Group (Phyllosilicates): nepheline, phlogopite, chlorite-vermiculite-montmorillonite, biotite, enstatite, orthoclase).

opacity in the glaze (Molera et al., 1997). In contrast, the thickness of the NAJ044 glaze is smaller (0.11 mm). According to SEM-EDS evaluation, it can be suggested that the use of inclusions in NAJ-A glazes was scarce, although with some exceptions. In any case, these were not very abundant (see Figure 5.33). No evident correlation was observed among the coating-type (partial or complete), the SnO_2 concentration and other factors of glazing technology (inclusions, thickness, etc.). To achieve the mentioned decorations, traditional recipes were used: CoO to obtain the blue and CuO based mixtures for the greens were identified (see Table A.10 in Appendix A). Many of the sherds (NAJ016, NAJ020, NAJ025, NAJ049, NAJ055-NAJ057) present marks of trivet (i.e. the utensil used to separate the ceramic pieces in the kiln that are to be glazed. Moreover, some sherds present drops of honey-glaze (NAJ005, NAJ021, NAJ65). Interestingly, this decoration has not been identified in any of the ceramics. Nonetheless, it can be concluded, that the firing of honey-glazed sherds with tin-lead glazed was performed simultaneously.

NAJ-B group

NAJ-B is composed by 14 ceramics and is characterized by a reddish colored clay paste. This color is given by the increment of Fe_2O_3 (5.0 mass %) with respect to NAJ-A, whereas the CaO content is still high (15.0±4 mass %). Likewise, the higher concentration of metals such as V, Cr and Mn was observed in this group (see Table 5.4 and PCA in

Figure 5.30). The forms comprising NAJ-B are tableware: mainly plates, porringers and others (ataifor, bowl and jar). Beyond the compositional discrimination, the decorations were similar to NAJ-A group, including, largely, plain tin-lead glazes. In contrast, one of the sherds of this group (NAJ076) outlies due to its tricolor decoration, showing the typical decorative motif known as *cenefa castellana*, which includes blue, yellow and black geometric patterns (see Figure 5.34 top-right). Furthermore, NAJ083 shows blue colored decorations.

Ceramics showing very similar decoration to these of NAJ-B (especially NAJ076) and described as of "reddish pastes" have been previously reported in the literature (Ceniceros Herreros, 2004). In the mentioned work, their provenance is tentatively ascribed to Haro or Logroño, where these kinds of reddish pastes were more abundant. Nonetheless, preliminary comparisons with productions of Logroño performed in the current research could not confirm this hypothesis(Calparsoro et al., 2016). Therefore, its exact provenance remains unclear. However, according to the high compositional similarity with NAJ-A group, it can be suggested a local origin or a nearby producing location that were exploiting geochemically similar clay beds in the Najerilla basin.

NAJ-B shows three types of fabrics (see XRD results in Table 5.5). Their common main phases are quartz and silicates that clearly differ according to their EFT. F-I fabric (n=6) shows a significant presence of illite coexisting with calcite, gehlenite and K-feldspars. Since the latter start decomposing after 850 °C, the EFT should be close to that temperature (see Figure 5.32, where NAJ011 is shown as a representative diffractogram of the fabric). Additionally, gypsum was detected in some of the sherds showing this fabric.

F-II fabric (n = 6) present similar mineralogical composition to F-II. In contrast, it shows a complete absence of illite-muscovite, together with a total decomposition of K-feldspars and presence of pyroxenes and plagioclases. The concurrence of these phases places the EFT at ca. 900 °C. In addition, NAJ076 and NAJ063 show an F-III fabric type, which is highlighted by the very incipient presence of mullite and plagioclases together with a higher concentration of pyroxenes. Their concurrence allows estimating the EFT above 1000°C.

In a similar way to NAJ-A, the coatings of this group present tin-lead glazes with infrequent inclusions. Exceptionally, NAJ076 showed abundant inclusions (see Figure 5.35). Moreover, an overall lower concentration of SnO_2 was detected with values that drop down to 5.3 mass % (see the Table A.10 in Appendix A).

With regard to the tricolor decoration on NAJ076, the spectroscopic characterization by Raman revealed that yellow color was obtained by $Pb_2Sb_2O_7$, known as Naples yellow (see Figure 5.34), the yellow layer is evident to the naked eye since antimony does not dissolve into the glaze, unlike CuO greens and or CoO based pigments. Moreover, the presence of quartz particles and iron oxides which give the reddish hue to the yellow

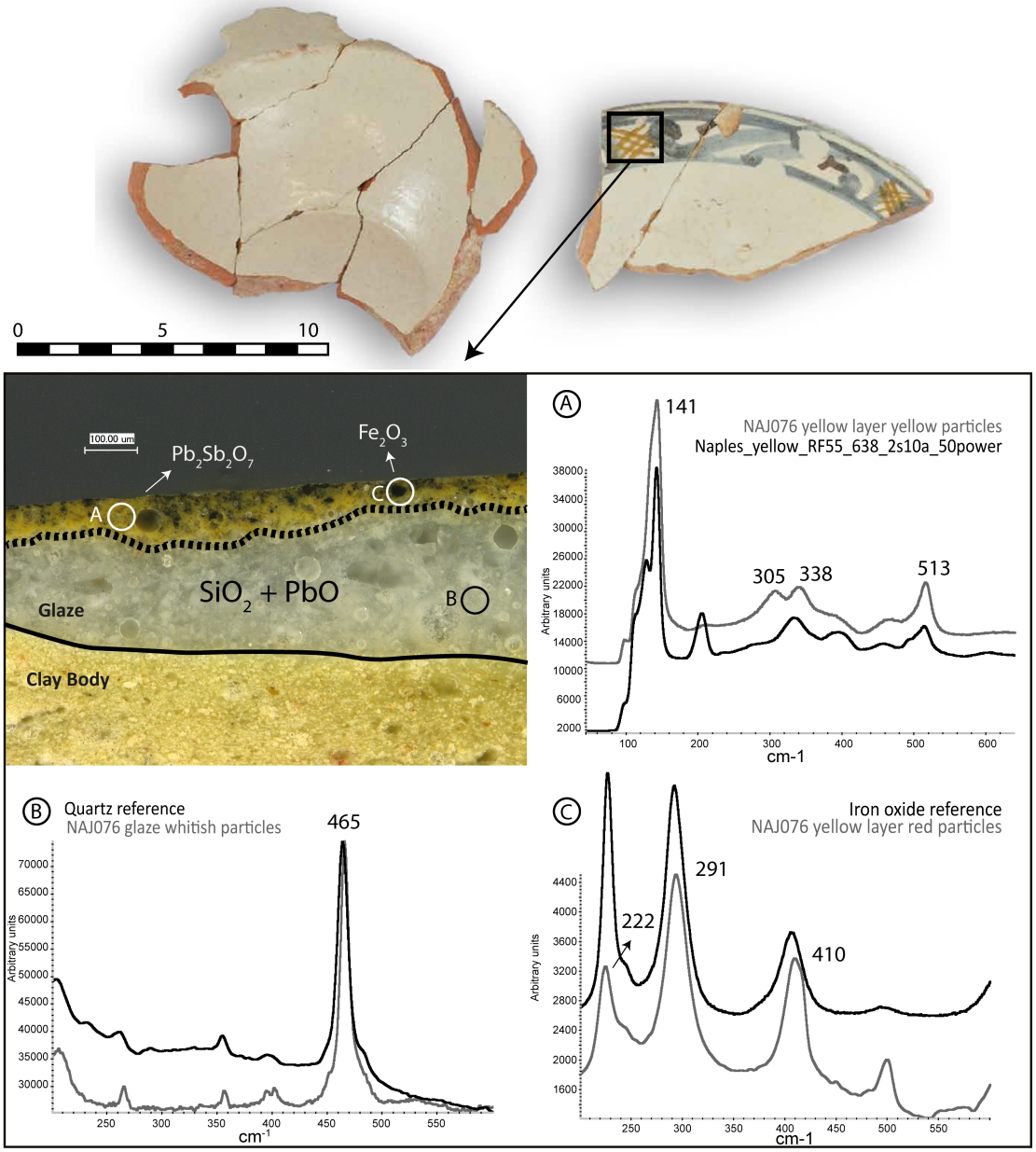

Figure 5.34: NAJ011 representative sample from group NAJ-B (upper-left). NAJ076 (upper-right), its micro-photograph and Raman spectra corresponding to yellow part of the glaze showing Naples yellow ($Pb_2Sb_2O_7$), α-quartz (SiO_2) and iron oxides.

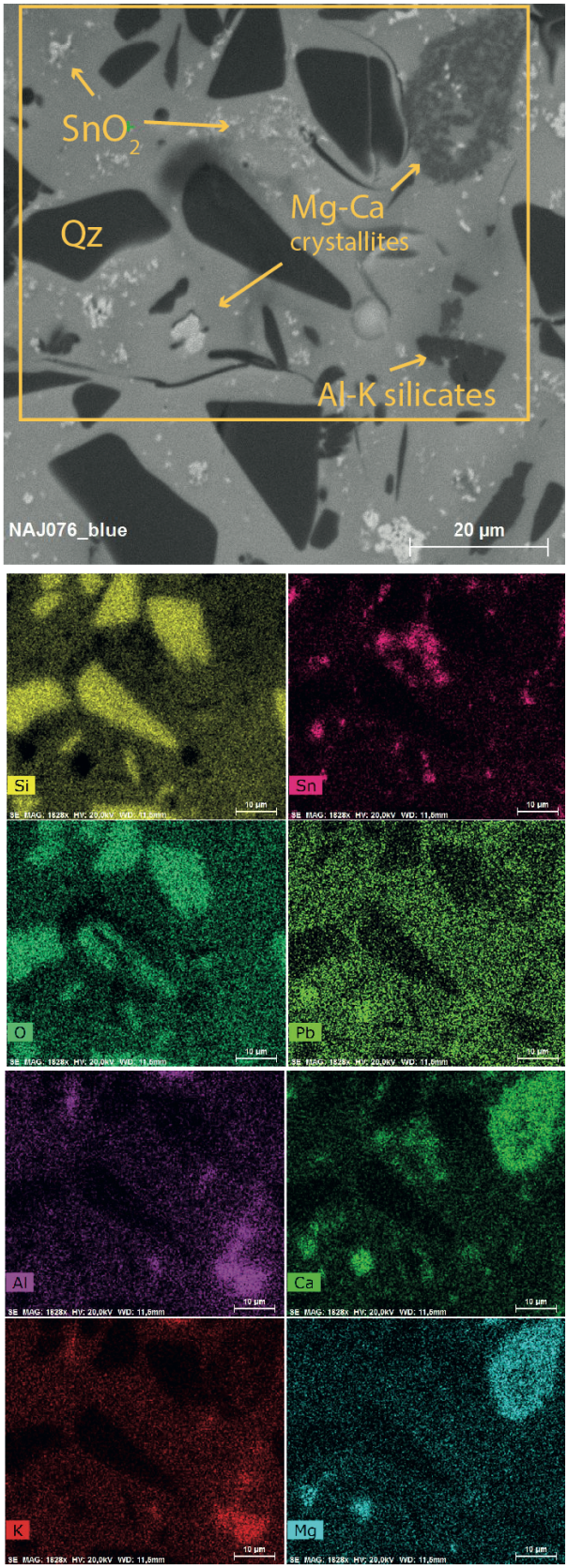

Figure 5.35: SEM-EDS image and mapping of NAJ076 glaze showing inclusions.

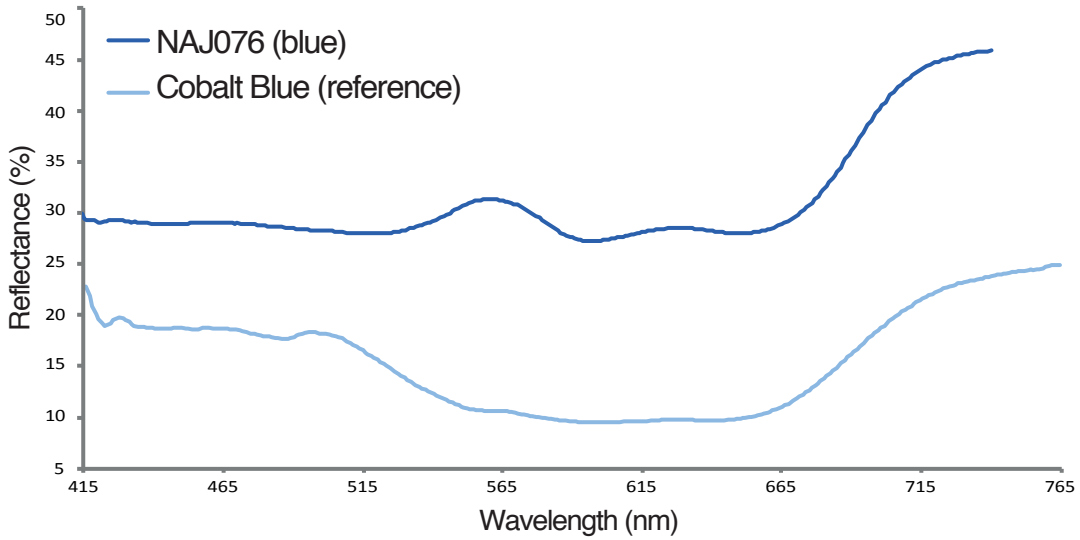

Figure 5.36: UV-Vis reflectance spectrum of NAJ076 blue and reference spectrum of cobalt blue.

colorant was observed. Naples yellow is light-fast and chemically stable, but may darken with high temperatures (e.g. during the glaze firing), and also with the exposure to iron compounds, which is the case of NAJ076. The presence of iron oxides along with Naples yellow is ubiquitous among majolica pottery from Renascence.

Interestingly, the blue colorant analyzed in this sample revealed the presence of Mn, As and Ni beyond, Co (see Table and Figure 5.36 and 5.37). Their presence was only observed in this case and suggest differences in the raw material employed, which must be different to cobalt blue used in the other cases, as confirmed by UV-Vis reflectance, (see Figure 5.36). According to the elements observed, the alternatives can include asbolan ($(Ni, Co)_{2-x}Mn^{4+}(O, OH)_4 \cdot H_2O$), cobaltite (CoAsS), skutterudite ($(Co, Ni)As_{3-x)}$ or erythrite ($(Co_3(AsO_4)_2 \cdot 8H_2O$). Unfortunately, Raman microscopy did not offer any Raman band related with this cobalt compounds due to the high fluorescence registered in the spectra.

NAJ-MIC group

The HCA depicts clearly a subset, which is dramatically different from the remaining sherds (see Figure 5.30). These ceramics constituted the group called NAJ-MIC (n = 6). They are de visu recognizable (see Figure 5.38) for their heterogeneous pastes showing big sized inclusions (< 1 mm). The compositional differences with respect to

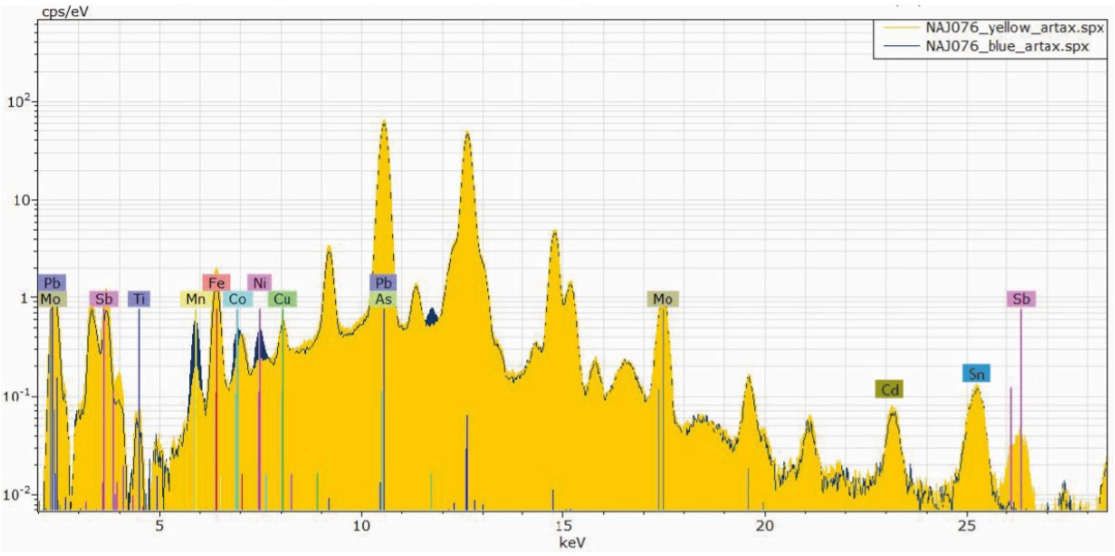

Figure 5.37: μ-XRF spectra of blue and yellow pigments in NAJ076.

the other compositional groups, are mainly given by major elements, especially Al_2O_3, but also most of the trace elements (highlight Cr and Ta) show an important decrease (see Table 5.4). The pastes of this group are highly micaceous, thus, bearing high Al2O3 concentrations. As stated in the literature, Al_2O_3 can be positively correlated with the relative abundance of clay minerals and/or the quantity of monomineralic granules of feldspars and mica in the coarser granulometric fractions (Hunt, 2016). For such a study, however, further analyses should be performed of the clay samples and their respective comparison. According to the literature, the most likely origin of these ceramics would be in Zamora.

The region hosts abundant deposits of highly micaceous clays, which show very good refractory properties. For this reason, Zamora has a long-lasting tradition on the production of kitchen ceramics. In the NAJ-MIC group, it can be observed how several ceramics show blackish parts as a result of their exposition to fire, confirming they utility as kitchen utility.

The XRD results were in accordance with the chemical composition showing a very distinctive geochemical situation (see Table 5.4). These pastes show very big sized inclusions (order of mm), which according to the diffractogram (see Figure 5.39) correspond to micaceous particles such as chlorite-vermiculite-montmorillonite and biotite, and other phyllosilicates such as nepheline, phlogopite, and enstatite. The presence of muscovite and K-feldspars (orthoclase) which are related to low firing temperatures situate the equivalent firing temperature around 850 °C. The use of

Figure 5.38: Images of micaceous sherds from NAJ-MIC group (NAJ098 and NAJ101).

phyllosilicates in cooking pots is related to their non-swelling property when exposed to temperature changes. This property, in addition to the higher grain-size distribution and other inclusions such as quartz, is very relevant in pieces that are to be subjected to heating-cooling cycles, such as some kitchenware, thus showing very good thermal-shock resistance. With regard to the coating, none of the micaceous sherds presented glaze or any other decoration.

Characterization of TAL group

NAJ029, NAJ033, NAJ025 and NAJ071 showed compatible compositions with the productions of Talavera de La Reina (see Figure 5.30). Majolica productions of Talavera have been archaeometrically studied by several authors (Iñañez et al., 2008; Buxeda i Garrigós et al., 2011; Guirao et al., 2014; Fernández de Marcos, 2018). Compositionally, they are characterized by a high MgO concentration. MgO was, indeed, the main discriminant element within the current dataset. Besides MgO, a higher concentration was observed in trace elements such as Dy, Er, Gd, Hf, Lu, Nd, Sm, Tb, Y, Zr and especially Th (see Table 5.4). Along these lines, NAJ029 and NAJ033 ceramics showed chemical compatibility with Talaveran productions when compared with the NAA data published by Iñañez et. al (Iñañez et al., 2008). In addition, from the stylistic perspective, similar pieces produced in Talavera were reported in the literature (Conesa, 2011), including both complete glazed and half glazed pieces (see Figure 5.39).

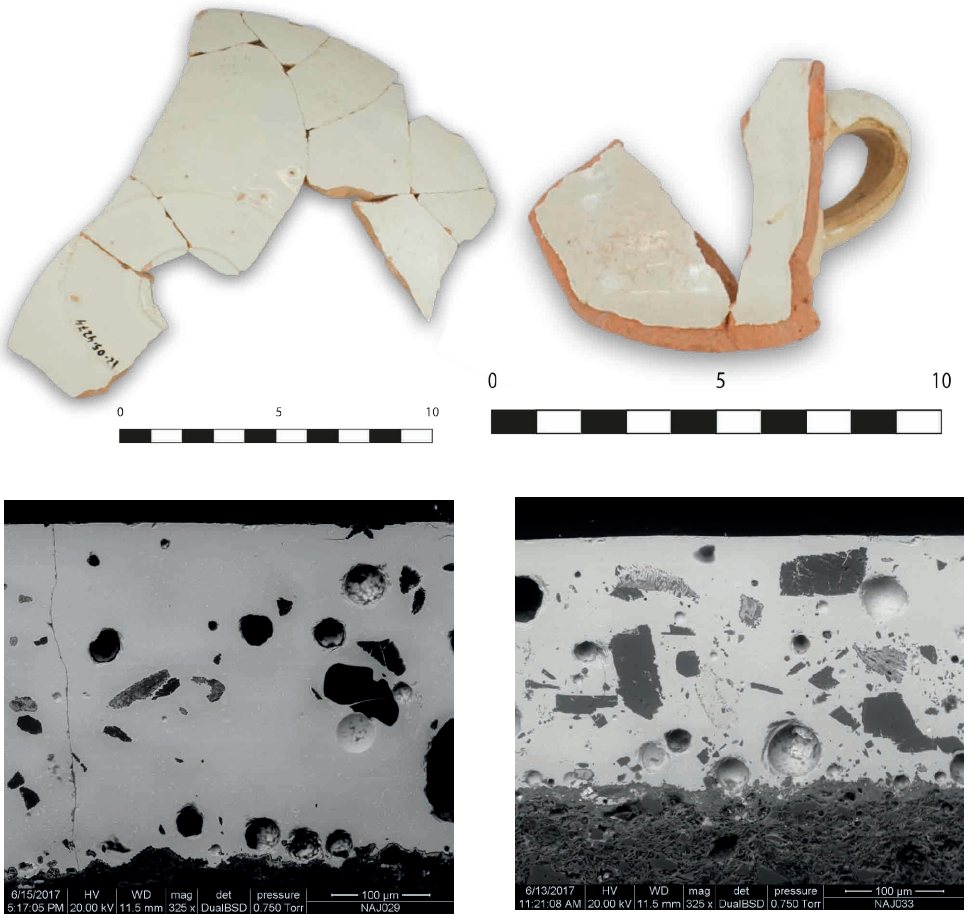

Figure 5.39: NAJ029 and NAJ033 and the SEM images of their glazes.

In the group of Talavera (TAL) two different fabrics were observed (see Figure 5.32 and 5.38). On the one hand, F-I has two ceramics (NAJ029 and NAJ025) and an illite peak at 7Åand the K-feldspars characterize its mineralogical association. Thus, its EFT can be established between 800-900 °C, as no firing phases were detected in significant manner. In contrast, F-II, composed by NAJ033 and NAJ071, shows the lack of illite basal peak and present significant differences on calcite and gehlenite peaks. Therefore, the EFT should slightly higher (ca. 900 °C). These sherds are pieces of tableware that show a finely applied tin-lead glaze resulting in a highly opaque coating. The EDS analysis showed that the white glaze in NAJ029 contained 36 mass % of PbO and 9 mass % of SnO_2 respectively. The glaze thicknesses (0.3-04 mm) are the among the biggest of the studied collection. The 20 μm narrow interface between the ceramic body and the glaze depicts that the glaze was applied on the bisque ceramics, according to the

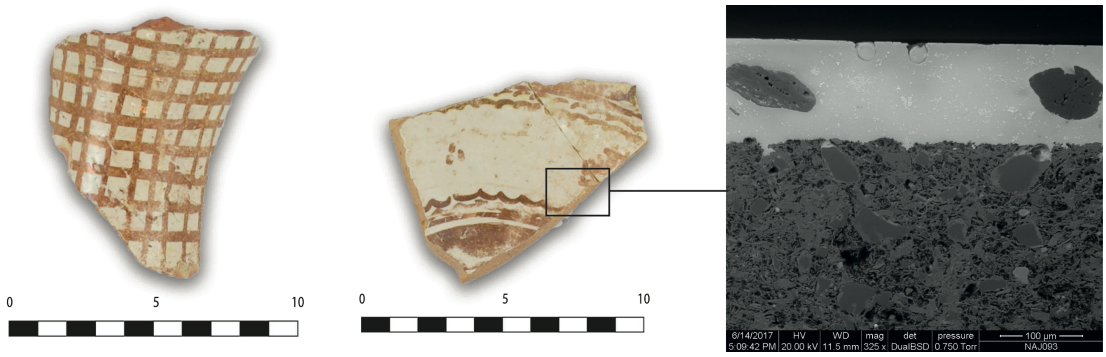

Figure 5.40: Samples from Muel (NAJ092 and NAJ093) and the SEM image of the NAJ093 glaze-ceramic body interface.

procedures reported in the literature (Conesa, 2008, 2011). Remarkably, the recipes used in the glazes from Talavera show abundant inclusions and a low concentration of bubbles.

Characterization of MUEL group

The statistical analysis (see Figure 5.30 and the Table 5.4) disclosed a group of ceramics (MUEL group) showing the lowest Al2O3 concentration of the whole dataset (13.7 mass %). These sherds, were not compatible with any other of the tested provenances. Due to the absence of ICP-MS data for Muel production center ceramics, it was not possible to assess unequivocally its provenance to this reference group for these ceramics. Nonetheless, parallel preliminary NAA results performed on NAJ092 and NAJ093 allowed establishing their provenance in Muel, according to the NAA data published in the literature (Iñañez et al., 2008). Thus, their compositional similarity with respect to the remaining sherds of the present group was used as a basis to consider them as a production from Muel. Furthermore, the luster decorations that some of the sherds of this group show are in accordance with the productions of Muel reported in the literature, reinforcing the hypothesis of their Zaragozan provenance (Conesa, 2008, 2011).

According to XRD analysis, ceramics from Muel presented two fabric types (see Figure 5.32). NAJ089 is representative of F-I fabric (n = 3) and NAJ093 F-II fabric (n = 2). Both contain the common phases of quartz, calcite, gehlenite and diopsides. In F-I fabric the K-feldspars have not yet fully decomposed, thus the EFT correspond to between 800-900°C. In contrast, in F-II, the lack of the K-feldspars, and the presence of firing plagioclasic phases together with the incipient K-spinels observed, allow estimating the EFT between 900-1000°C. The differences among these temperature not necessarily must suggest an intentional modification in the firing technology. A temperature gradient

within the chamber could be responsible of the different mineralogical situations, as well as the original temper fraction of the clay.

The ceramics ascribed to Muel show mainly luster decorations including also blue painting (see Figure 5.40). As all the cases observed before, the tin-lead glazes were applied on the bisque ceramic. However, in order to obtain the luster decoration, historically a third firing was applied (Conesa, 2008, 2011). The luster decoration is obtained by the use of a very thin CuO on the outer layer of the glaze, which highly tends to dissolve in the glaze mixture and to be eroded during postdepositional phase (Pérez-Arantegui et al., 2001b).

Final Remarks

The work concerning ceramics of Nájera constitutes the first archaeometric approach about post-medieval pottery productions of Nájera. The archaeometric characterization performed on the 94 ceramics by ICP-MS, XRD, SEM-EDS and other spectroscopic techniques, with the subsequent chemometric treatment (PCA and HCA), allowed identifying one main compositional group linked to the local pottery production of Nájera during the 16^{th} century (NAJ-A), a second group whose provenance could be tentatively ascribed to Nájera (NAJ-B), and three exogenous groups (NAJ-MIC, MUEL and TAL). All of them were tin-lead glazed, except for the micaceous ceramics (NAJ-MIC). With regard to the productions ascribed to a local origin (NAJ-A and NAJ-B), calcareous pastes (showing abundant calcite and gehlenite) were detected in all cases. Moreover, NAJ-B showed a reddish paste which is the result of a higher presence of iron oxides. According to XRD analysis, the EFTs ranged between 800-1000°C. However, in NAJ-A dominated those closer to 900°C and in NAJ-B those fired at lower temperatures (850°C). This difference could be connected to a different workshop, kiln or artisan. However, they compositional similarity suggests that NAJ-B was produced nearby, if not in Nájera itself. The elemental compositions responsible for the different decorations, as well as the identification of the chemical compounds that play a main role in those pigments dissolved into the glaze coat were also identified. The use of traditional recipes, such as CuO base greens and lusters, MnO base blacks, CoO blues and opacification by means of SnO_2 on PbO rich glazes was determined. In addition, the characterization of Naples yellow pigment used to obtain the yellowish color was performed in NAJ076's *cenefa castellana* decoration. This sample also showed a different recipe used to obtain the blue, which includes, Mn, Ni and As. Thus, a marked difference in the raw material employed can be inferred.

In brief, the results allowed to link a great part of the ceramics set that was unearthed in the Alcazar of Nájera to a local origin related to the ceramic productions during 16^{th} century. Moreover, the reception of prestigious ceramics from Talavera and Muel was identified, as well as, most tentatively cooking pots from Zamora. The presence

of ceramics from Muel is not surprising when it is known that the neighboring city of Logroño maintained close relations (family ties) with this Zaragozan city, documented as early as the 17^{th} century as reported in the literature (Martínez Glera, 1994).

5.4 Urduñako Buztingintzaren Ezaugarritze Arkeometrikoa

Abstract

Urduña Iberiar penintsulako iparraldean kokatuta dago eta mendeetan zehar elkartruke-gune garrantzitsua izan da, Gaztelako goi-ordokia euskal kostaldeko herriekin konektatzen baitu. Gainera, hainbat akordioek merkataritza-zentro garrantzitsu bihurtu zuten herria XIII. mendetik aurrera. Nahiz eta herri honek garrantzi historiko nabarmena izan, erabat murriztua da bertako buztingintza-jarduera eta bere bilakaera diakronikoari buruzko ezagutza. Jarduera horrek eraldaketa nabarmena jasango zuen XVIII. mendean zehar. Duela gutxi, bertako ekoizpen-zeramikoa agerian uzten zuten lehenengo aztarnak aurkitu ziren indusketa arkeologiko batzuetan; bertan, XVI. eta XIX. mendeetako zeramikazko pieza ugari atera ziren, hala nola, zeramika-labe bat. Aurkikuntza horiek aurrekaririk gabeko erreferentzia eta paradigma izan ziren; hiribilduko beste lurzatietako material zeramikoak, zein, beste euskal hiribildu batzuk aztertzeko. Lan honetan, aurkitutako tipologia zeramiko ezberdinen artean 97 pieza adierazgarri aztertu dira, NAA, ICP-MS, XRD eta SEM-EDSren bidez; batetik, material zeramiko horiei buruzko ezagutzan sakontzeko eta, bestetik, eskualdeko mailako merkataritza-jarduerarekiko eta haien lotura historikoak hobeto ulertzeko helburuarekin. Ondorioz, zazpi konposizio-multzo ezarri dira. Horiek; alde batetik, teknotipo desberdinekin bat datoz; eta, bestetik, zeramikaren ekoizpenaren bilakaera diakronikoa erakusten dute, denboran zehar konposizio-multzo desberdinen agerpena erakutsiz. Bestalde, alderdi teknologikoak ere aztertu dira; horrela, erabilitako pigmentu nagusiak eta biratu motak zehaztuz.

Aurrekariak

Urduña Iberiar penintsulako erdi-iparraldean kokatuta dago (ikus 5.41. irudia). Historia ekonomiko eta komertzial luzea izan du hiribilduak; merkataritza-ibilbide handienetik hurbil egoteagatik, eta bere aduana-sistemek erakusten duten moduan (Salazar Arechalde and Llano Hernaiz, 2006). Bailara batean murgildurik dago, 1000 m-ra iristen diren mendiz inguratuta. Bai bere kokapen estrategikoak, bai bere topografiak, Gaztelako goi-ordokia euskal itsasertzeko herriekin lotzeko funtsezko rola izan dute (Salazar Arechalde and Llano Hernaiz, 2006; Angulo, 1995). Gainera, XIII. mendeko lehen Erdi Aroko asentamenduetatik, hainbat merkataritza-akordioek ziurtatu zuten hiribilduaren izaera ondasun-trukerako puntu garrantzitsu gisa (Salazar Arechalde, 1995).

Oraindik ere, herriko buztingintza jardueren jatorria eta garapena nahiko gutxi ezagutzen da. Hala ere, berebiziko garrantzia izan omen zuen herriaren eraketan, izan ere, hura artisautzaren espezializazioarekin bat etorri zen, zeina beste euskal eskualde batzuetan IX. mendetik aurrera ematen hasi zen (Solaun, 2005). Urduñako zeramiken salerosketa VIII. mendetik XVII. mendera arte dokumentatuta dago (Solaun, 2005; Escribano, 2014). Hala ere, ekoizpenari dagokionez, lehen aztarna sendoak ez dira lortzen Urduñako *Zaharra 2-4*, *Zaharra 24-30* eta *Tras-Santiago* kaleetan egindako esku-hartze arkeologikoetara arte. Bertan, zeramikazko labe bat eta XVII-XIX mende bitarteko pieza ugari atera ziren lurpetik (Cajigas Panera et al., 2004). Eskualde mailako buztingintza jarduerak garapen garrantzitsua izan zuen XVIII. mendearen amaieran eta XIX. mendean zehar (Escribano, 2013). Urduñan, bereziki bi gertaera historiko garrantzitsuekin batera eman ziren aldaketa horiek. Batetik, Gaztela goi-ordokirako bidearen irekiera 1774an, horren eraginez, merkataritza-trafiko guztia Balmasedatik Urduñara bideratuko zen eta; bestetik, aduana-gune baten irekiera 1792an, horrela merkantziak kudeatzeko eta gordetzeko aukera emanez, bertatik gero eta era nabarmenagoan igarotzen hasiak zirenak (Salazar Arechalde, 1995). Bi gertakari horiek baldintza ekonomiko berriak sustatu zituzten hirian, hala nola, negozio aukera berriak, buztingintza barne.

Buztingintza jarduerak herriaren konfigurazioaren heinean garatu ziren eta, oraindik, toponimiaren bidez haien aztarna nabaria da. Eginkizun historikoa izan duten arren, orain arte egindako zeramika-azterketa guztiak ikuspegi etnografiko edota teknotipologikoetatik soilik jorratu dira. Dokumentu-iturriei dagokienez, Ibabe (1995a) etnografoak bertako buztingileen jardueraren berri ematen du XVII. eta XVIII. mendeetan zehar. Bestalde, Erdi Aroko Euskal erregistro zeramikoaren lehen azterketa zabalean (Solaun, 2005) aipatzen da Urduñan hainbat zeramika-tipologia jaso zirela eta haien balizko birbanatzeari buruz hitz egiten da, batez ere, da 1228 ondoren. Izan ere, urte horretan erregearen pribilegioa jaso zuten hiria merkataritza-gune bezala suspertuz, gaztelaniaz *mercado franco* bezala ezagutzen den aukera emanez. Tipologia horiek sukaldeko eltzeak, xukagailuak, pitxer eta ontzi handiak biltzen dituzte eta kronologikoki VIII-XIII mendeen bitartean kokatzen dira (Solaun, 2005).

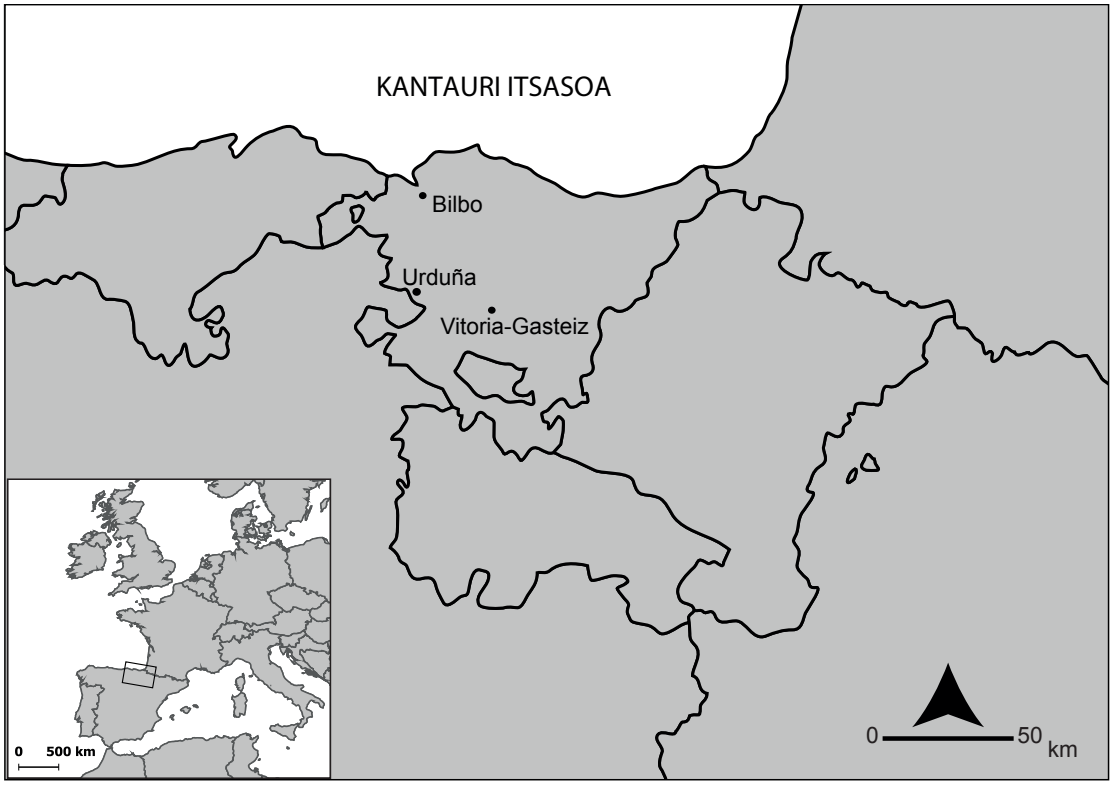

Figure 5.41: Urduñaren kokalekua

Azterlan berean, Urduñako jatorria izan dezakeen zeramika multzo bat iradokitzen da; zehazki, VIII-X. mende bitartean agertzen dena eta itxuraz pareta meheko zeramika trauskila tipologiari dagokiona (II-Multzoa). Proposamen hori egiteko zeramiken pastak hartzen dira oinarritzat, zeinak Urduñako buztinen konposizio-ezaugarri makroskopikoekin bat etortzen diren. Horiek, kaltzita inklusio gutxiko pastak izango lirateke, hala nola, kuartzo eta piroxeno autigeniko ugari (Solaun, 2005). Hala ere, hipotesi hori babesten duen froga gehiago ez da ematen. Gainera II-Multzoaren jatorriari erreparatuz, ez dira baztertzen garai Triasikora lotutako buztinak dituzten beste kokaleku batzuk (adib., Maeztu, Murgia, Gesaltza Añana, Buradon Gatzatza edo Urizaharra), horiek guztiak Euskal Herriko hegoaldean kokaturik daudela (Solaun, 2005). Ildo horretan, Arabako zeramika-erregistroari buruzko azterlanean (Escribano, 2014), eskualdeko kontsumoaren analisi zabal bat garatzen da. Lan horretan ere, ez da agertzen produktu zeramikoen ekoizpenaren ebidentziarik Urduñako kasurako (XIV-XVII. mendeen artean). Antza denez, Araban jasotzen ziren zeramika-produktuen gehiengoa Bilbo, Buradon Gatzaga, Ollerietan edo Egiletan ekoiztutakoak ziren. Izan ere, aipatutako lantegien produktuak Euskal Herriko eskualde-mailako ekoizpenaren zati handi bat hartzen zuten.

Gune horietan ekoiztutako zeramika, berriz, Urduñan salerosten zuten, dokumentatzen den moduan (Escribano, 2014).

Azterlan arkeometrikoei dagokionez, existitzen diren ikerketa urriak kontsumo ikuspegitik landu dira eta *Euskal zeramika herrikoia* deritzonaren hedapenaren aurreko garaiei dagokie; hain zuzen, XIV eta XVI mende tarteari (Puig, 2016). Beraz, lan honen ikerketa-esparrutik at geratzen dira. *Euskal zeramika herrikoia* bezala ezagutzen den tipologia, euskal eltzegileek ekoiztu zutena da. Industrializazioaren aurretik oso zabaldua zegoen Euskal gizartean zehar (gehien bat ontziteriako piezak). Gainera, buztin gorrixka batez bereizten da. Pastari eztainu-berunezko beiratu txuri bat partzialki aplikatzen zaio. Hautapen murritz baten gainean egindako analisi arkeometriko horietan (12 zatiki), bi multzo iradokitzen dira (PB10a eta PB10b). Denak kare-altukoak dira (15-20 masa % CaO), Fe_2O_3 kontzentrazio baxukoak ($\approx$3.5 masa %) eta MgO kontzentrazio ertainak dituzte (1-5 masa %), eta bere artean Ce-ren kontzentrazioaren bidez bereizten dira. Hortaz gain, Euskal Herriko gainerako zeramikekin alderatuta, Pb eduki altua dute. Detektatutako elementu horren agerpena ekoizpenerako erabilitako buztinaren inklusioekin erlazionatzen da. Hala ere, berun-beiratuaren balizko ekarpena ez da baztertzen. Haien ekoizpen-jatorria Bilbon (PB10a) eta Gasteizen (PB10b) iradokitzen da Puig (2016).

Arestian aipatu den bezala, zeramika-ekoizpen sistemek eraldaketa nabarmenak jasan zituzten XVIII. mendean zehar. Horrela, XIV. eta XV. mendeetan soilik gizartearen gutxiengo batentzako lorgarriak ziren zeramikak, jendartera zabaldu ziren askoz ere eskuragarriagoak bilakatuz (Escribano, 2013, 2014). Urduñako kasu espezifikoan, eraldaketa hauek, esan bezala, aduana-gune berriaren irekiarekin batera (1774) eta Gaztelarako bidearen desbideratzearekin batera gertatu ziren. Horrela, pixkanaka-pixkanaka Euskal zeramika herrikoiaren materializazioa ekarri zuten aldaketa horiek, eskuz ekoiztutako zeramikaren amaiera arte jarraitu zuena. Espainiako gerra zibilak gogor jo zuen zeramika-ekoizpen hori, eta, XX. mendearen bigarren erdialdera arte iraun zuen (Ibabe, 1995a).

Nahiz eta Urduña merkataritza-gune gisa paper garrantzitsua jokatu izan duen, buztingintzaren jarduerei dagokionez, arreta eskasa jaso du. Buztingintza jarduera horien gaineko ezagutza urria da iparraldean, penintsulako beste gune batzuetan ez bezala (Iñañez et al., 2008; Fernández de Marcos, 2018). Lan honen bidez, ikerketa horren egoera asimetrikoa orakatu nahi da, batez ere, arkeometriaren ikuspegitik. Era horretan, ezagutza sakonagoa lortuz, horren gutxi ezagutzen diren bertako zeramika ekoizpen-gune horiei buruz; hala nola, erabilitako teknologiari buruz. Bestalde, Urduñako merkataritza elkar-trukeei Euskal Herriko beste tokiekin edota Espainiako iparraldearekin hobeto ulertzea da helburua.

Urduñako esku-hartze arkeologikoa

Buztingintza-labe bat eta hainbat zeramika zatiki aurkitu ziren 2001 eta 2002 urteen artean Urduñan egindako indusketa arkeologikoetan, XVII. eta XVIII. mendeei dagozkienak (Cajigas Panera et al., 2004). Lurpetik ateratako zeramikaren aurretiazko azterketetan (Cajigas Panera et al., 2004), teknotipologian oinarritutako hurbilketa bat gauzatu zen (forma, dekorazioak, etab. aztertuz), baina karakterizazio arkemoetrikorik egin gabe. Hala ere, interes handikoa izan zen azterlan hori. Izan ere, *Tras-Santiago* eta Kale Zaharreko aztarnategietan aurkitutako zeramikazko multzoa XIII. mendetik XIX. mendera arte etenik gabeko aldi kronologiko bat eskaini zuen, eta horrek zeramika tipologia ugari berreraikitzea ahalbidetu zuen. Azken batean, Urduñan aurkitutako zeramika bilduma erreferentziazko testuinguru bat eskaintzen du bertako eta Euskal Herriko beste gune batzuetako materialak aztertzeko. Lan honetan aztertutako material zeramikoak hiriko hiru aztarnategietatik datoz: *Zaharra Kalea 2-4*, *Zaharra kalea 24-30* eta *Tras-Santiago* kaleetan kokatzen direnak, hain zuzen ere. Unitate estratigrafikoak (SU) ekoizpen-jarduerarekin zerikusia duen materiala aurkezten dute, batik bat, eta eraikina eraiki aurretik hutsuneak bete eta lurra nibelatzeko erabili ziren. Hori dela eta, aztarnategi hauetan agertutako zeramika zatiki asko labeko tresneriari dagokio (adibidez, treberak eta matoiak), hala nola, zeramika akastunak, bertan izandako ekoizpenaren isla zuzena direnak. Gainera, eguneroko erabilerarekin zerikusia duten zeramikak ere agertu ziren (ontziteria gehien bat). Kronologiak eta aztarnategi bakoitzaren zeramika kopurua eta estaldura mota, 5.42. irudian ikus daitezke.

Urduñako Zeramika Lagina

Ikerketa arkeometrikorako, XVII-XIX. mende bitarteko 97 zatiki-zeramiko hautatu ziren, hainbat tipologia barne, besteak beste: platerak, goporrak, ontziak, pitxerrak, askak eta labe-lanabesak (ikus 5.42. irudia eta B Eranskina). Zatiki guztiak Bizkaiko Arkeologia Museoan gordetakoak ziren eta, hautaketa egiteko, labe-lanabesei lehentasuna eman zitzaien —tokiko produkzioarekin lotu daitezkeelako—, hala nola, zeramiken ugaritasunari eta tipologia adierazgarrienei ere.

Esperimentala

Pasten konposizio eta fase mineralogikoak karakterizatzeko, zeramikazko multzo osoa aztertu zen, indukziozko plasma-masen espektrometriaren bidez (ICP-MS) eta X izpien difrakzioa (XRD) erabiliz. Gainera, horietako batzuk (n = 25) NAA bidez aztertu ziren. Horrez gain, hautapen bat aukeratu zen (n = 15), SEM-EDS bidez ebaluatzeko, buztingileek erabiltzen zuten teknologia hobeto ulertzeko helburuarekin. Metodologiari buruzko xehetasun gehiagorako (ikus 3.3. atala).

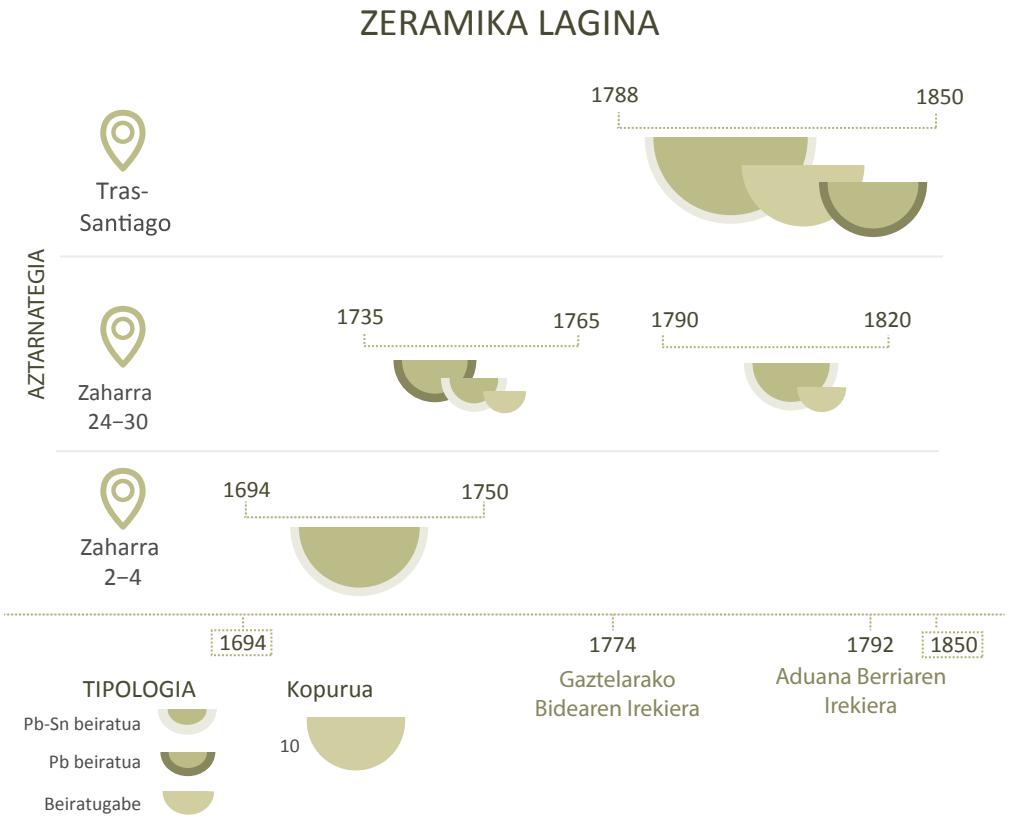

Figure 5.42: Urduñako Zeramika lagina, kronologia, kokapena, tipologia eta kopurua adieraziz

Lehen Hurbilketa NAA bidez

NAA bidez egindako azterketan, bi multzo nagusi identifikatu ziren 25 zatikien gainean egindako analisian (ikus 5.43. irudia). Multzo bakoitza zeramika karedun eta ez-karedunei dagokie eta itxuraz argiagoak eta ilunagoak diren pastak erakusten dituzte, hurrenez hurren. Hala ere, Ca eta Sr elementuak analisi-estatistikoetatik baztertzerakoan sailkapen bera eskuratzen zen. Beraz moldaketa teknologikoak alde batera utzita, kimikoki benetan desberdinak diren bi pasta identifikatzen dira. Multzo kareduna beste bi multzotan banatzen da eta horiek erabat ICP-MSren bidez definitutako multzoekin bat datoz, aurrerago eztabaidatuko den moduan. Bi multzo horiek, ORD-A eta ORD-B bezala izendatu ziren eta kronologia desberdinekoak dira, ORD-B zaharrena izanik (1694-1788). Gainera, kluster txikienak, ez-karedunenak, alegia, ORD-MEL-A eta ORD-MEL-B multzoen arteko konposizio desberdinak erakutsi

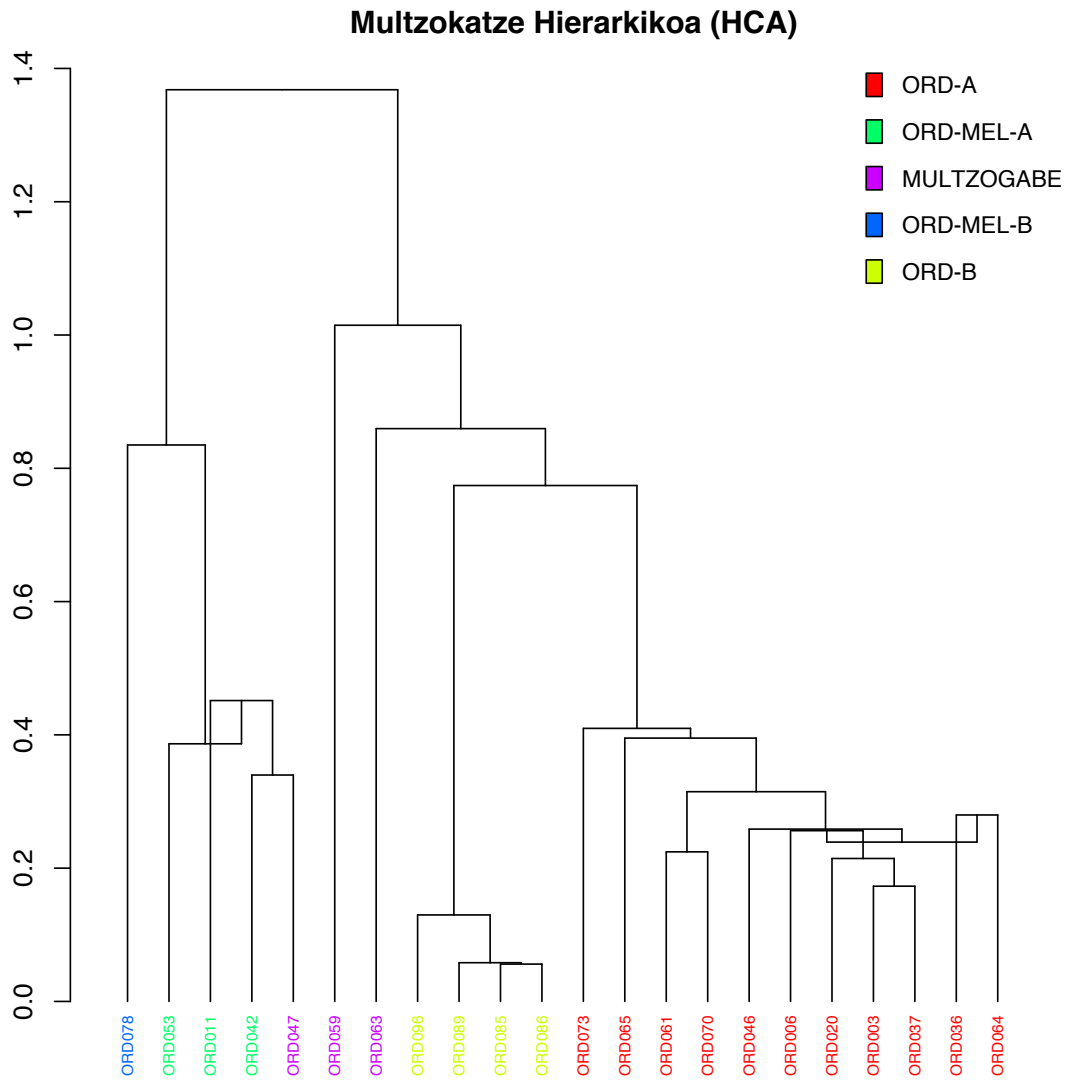

Figure 5.43: Euklidear distantzia karratua eta zentroidearen algoritmoa erabiliz lortutako dendrograma. Datuak NAA bidez aztertutako Urduñako 25 Ic-ei dagokie eta clr bidez eraldatu dira hurrengo azpi-konposizioa kontuan hartuz: La, Lu, Nd, Sm, U, Yb, Ce, Cr, Eu, Fe, Hf, Sc, Tb, Th, Zn, Zr, Al, Ba, Dy, Mn, Ti eta V

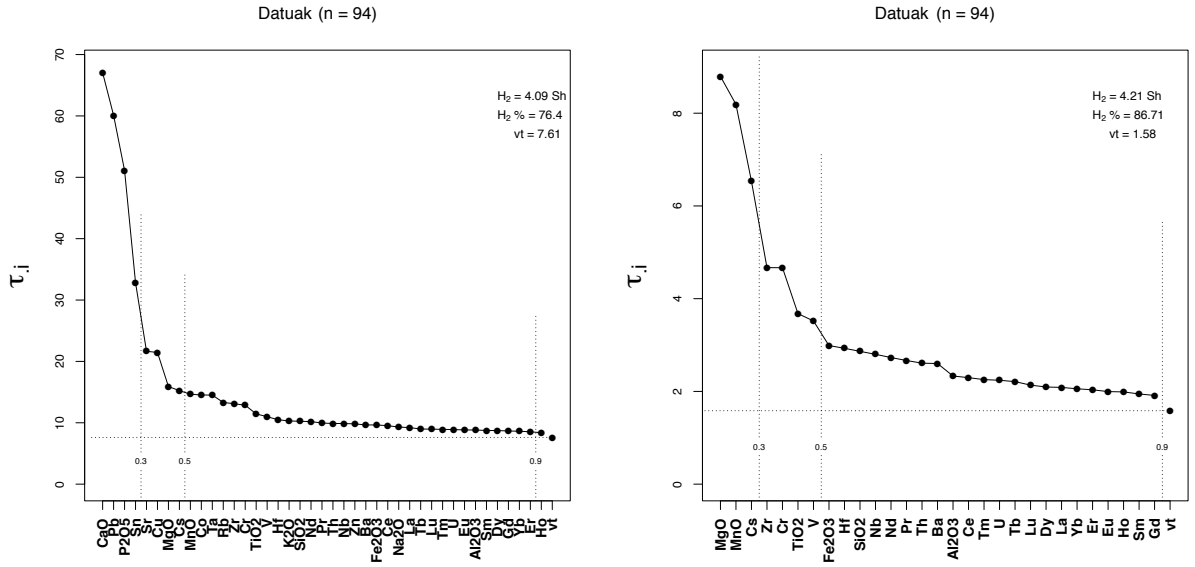

Figure 5.44: Urduñako konposizio-aldakortasunaren matrizea erakusten duen irudikapena ICP-MS bidez lortutako datu guztiekin (ezkerrean) eta soilik esanguratsuak ez diren aldagaiak erabiliz (eskuinean).

zituen, horrela, beste bi multzo horietan banatuz. Nahiz eta ORD-MEL-B multzotik banako bakarra egon, ezberdintasun kimikoak argi eta garbi bereizten dira. Aitzitik, ORD047 ORD-MEL-A multzoren barne agertu zen. Baina, ICP-MS bidez lortutako datuak kontuan hartuz, non lagin zabalago bat aztertu den. zeramika hori ezin izan zen multzo horren barne sartu ezaugarri kimiko oso desberdinak erakusten dituelako. Gainera, tipologikoki ere oso desberdina da, itxurari erreparatuz. Kasu bera aplikatzen zaie ORD059 eta ORD063 laginei. Ezaugarri kimiko bereiziak erakutsi dituzte, nahiz eta lagin-kopuru handiagoa erabili ICP-MS analisian, bere horretan mantentzen dira. Azkenik, irudian aipatzen den bezala, zeramikak mikatsuak ez dira agertzen, baina hirugarren kluster definitu bat erakutsiko luke, aurrerago eztabaidatuko den moduan.

Urduñako Konposizio-Multzoak (ICP-MS)

Lehenik eta behin, osagai kimiko bakoitzaren aldakortasuna ebaluatu zen konposizioaren aldakortasun-matrizea kalkulatuz, elementu bakoitzak datu multzoari gehitzen dion aldakortasunari buruzko informazioa ematen duena (ikus 5.44. irudia). Idealki, bariantza analitikoa minimizatu egin beharko litzateke, bariantzaren zatirik handiena iturri naturalen araberakoa izan dadin, eta ez akats esperimentalei edota jalkitze-ondoko prozesuen kutsadurak eragindako aldaketena.

Pb eta Sn beiratuarekin erlazionatutako aldakortasuna izateagatik baztertu egin ziren. Gainera, kasu honetan aldakortasun-totalaren % 30a gehitzen dute (ikus 5.44. irudia). Aztertutako datu-multzorako, Ta-ren aldakortasun handia bi faktoreek emana dator. Alde batetik, zatiki mikatsuek erakutsitako desberdintasun handiak (11-16 μg/g) gainerako zeramika guztiekiko (1-4 μg/g). Bestalde, laginak prestatzeko erabili den metodoaren ondorioak ere kontuan hartu behar dira, izan ere, gure kasuan, ehotzerakoan wolframio karburozko zelda bat erabili zen eta aleazio horretan dauden Co eta Ta aztarnak zeramika-matrizera transferitu daitezke (Boulanger et al., 2013a). Beraz bi elementu hauek ere ez ziren kontuan hartu analisia-estatistikoetarako. Aipatutako elementuez gain, Na, K, Rb, P eta Zn ez ziren estatistika-analisietan erabili 5.1. atalean azaldutako arrazoiengatik.

Hortaz gain, CaO eta MgOk aldakortasun handia gehitzen diote datu-multzo osoari (ikus 5.44. irudia). Hala ere, CaOk eta MgO konposatuek teknologiarekin zuzenean loturik egon litezke, edota zeramika horiek ekoizpenerako artisauen banakako edo taldeko ekintzen ondorioz aldatu daitezke (eztabaida sakonago baterako ikus (Buxeda i Garrigós, 2008). Beraz, elementu horiek zenbait murriztapenekin erabili ziren. Hala ere, emaitzek erakutsi zuten moduan, MgOk funtsezko papera jokatzen du zenbait konposizio-multzo bereizi ahal izateko, edota banako zehatz batzuentzako (adibidez, ORD007). Kasu honetan, datu multzoaren aldakortasun-totala (vt) oso balio handia du: vt 7.61 (ikus 5.44. irudia). Hala ere, esanguratsuak ez diren aldagaiak baztertzean (Pb, P_2O_5, CaO, Sn, Zn, Sr, MgO, Cs,Co, Ta eta Cu), balioa nahiko altua izaten jarraitzen du (1.58). Hori dela eta, hainbat zeramika-multzo desberdinen presentzia aurresan daiteke (Buxeda i Garrigós and Kilikoglou, 2003).

Multzo desberdinak identifikatzeko helburuarekin multzokatze hierarkikoaren azterketa burutu zen (ikus 5.45 irudia). Horretarako Euklidear distantzia karratua kalkulatu zen zentroide algoritmoa erabiliz. Lortutako dendrogramaren bidez hiru teknotipo nagusirekin bat datozen hiru multzo identifikatu ahal izan ziren: zeramika mikatsuak (MIC), zeramika beiratu gardenak (LG) eta nagusiki eztainu-beruna duten beiratutako zeramikak (TLG), pasta kareduna erakusten dituztenak. Garbien isolatzen den klusterra, konposizio-multzo bat osatzen du (ORD-MIC). Bigarren multzoa (LG) berun-beiraz estalitako pieza guztiak biltzen ditu (ORD-MEL, erdaratik *meladas*) eta bi konposizio-multzotan banatzen da (ORD-MEL-A eta ORD-MEL-B). Gainera, hirugarren multzo (TLG) lau konposizio-multzotan banatzen da (ORD-A, ORD-B, ORD-C eta ORD-D).

Identifikatutako multzo guztiek, beiratu gabeko labe-lanabesak hartzen dituzte barne (treberak eta zeramika akastunak), material zaharrenak (ORD-B) eta mikatsuak (ORD-MIC) izan ezik (ikus 5.42 irudia). Azkenengo hauek Zamorako jatorria edukiko lukete, geroago eztabaidatuko den moduan. Labe-tresneriaren agerpena pista fidagarriena da, karakterizazio arkeometrikoa tokiko ekoizpenari dagokiola ziurtatzeko. Gainera, labe zeramikoen presentziak hipotesi hori berresten du erabat. Aitzitik, zaharragoak diren piezentzat, ezin dira ziurtasun berdinarekin esleitu, ekoizpen proba

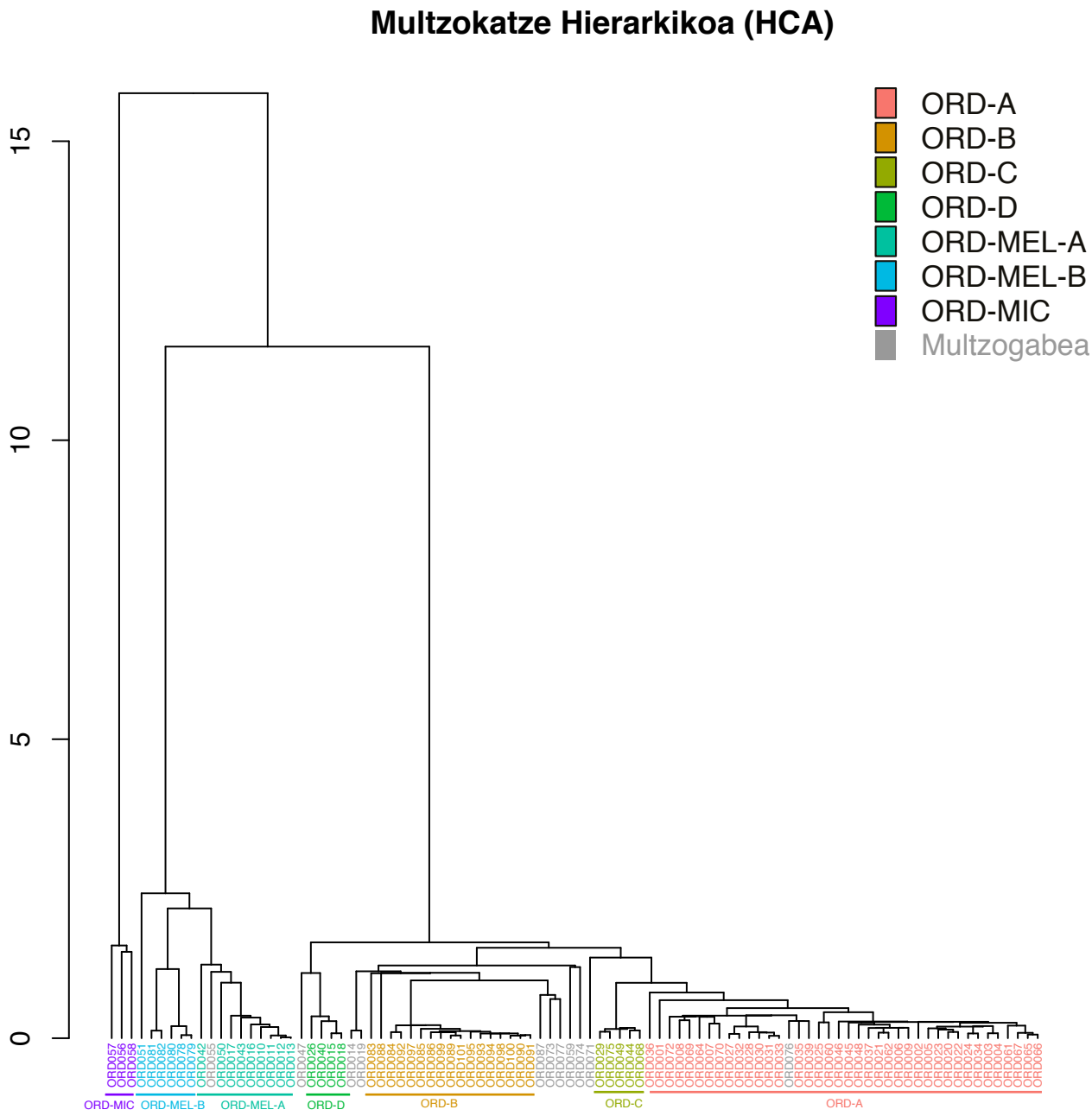

Figure 5.45: Euklidear distantzia karratua irudikatzen duen dendrograma, zentroidearen algoritmoa erabiliz eta Urduñako 91 zeramika barne hartuz lortu dena azpi-konposizio honetarako: Al_2O_3, Zr, Nb, Cs, Ba, La, Ce, Pr, Nd, Sm, Eu, Gd, Tb, Dy, Ho, Er, Tm, Yb, Lu, Hf, Th, U, SiO_2, TiO_2, V, Cr, MnO eta Fe_2O_3.

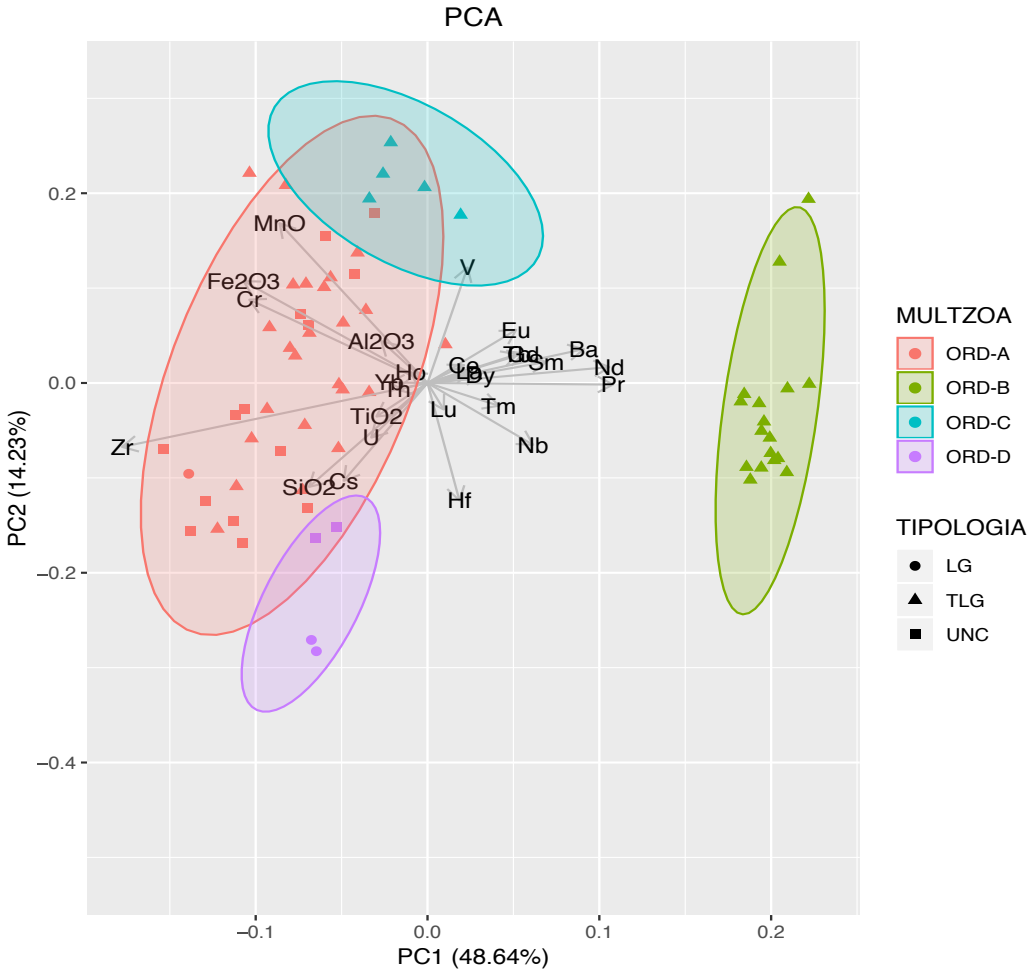

Figure 5.46: ORD-A, ORD-B, ORD-C eta ORD-D multzoen Osagai Nagusien Analisia (PCA) alr transformazioa erabiliz hurrengo azpi-konposiziorako: Al_2O_3, Zr, Nb, Cs, Ba, La, Ce, Pr, Nd, Sm, Eu, Tb, Dy, Ho, Er, Tm, Yb, Lu, Hf, Th, U, SiO_2, TiO_2, V, Cr, MnO eta Fe_2O_3

.

espliziturik ez baitago. Kasu honetan haien tokiko ekoizpena, soilik iradoki daiteke, zeramika-labe eta zeramikazko beste pieza batzuen gertutasunean oinarrituta. Ideia hori literaturan aipatzen den hiribilduaren iraupen luzeko buztingintza jarduerak babesten du (Solaun, 2005; Escribano, 2014). Hala ere, ikerketa sakonago bat beharko litzake hipotesi hori frogatzeko.

ORD-MIC eta ORD-MEL multzoek heterogeneotasun handian gehitzen diote datu-multzoari. Horren eraginez, karedun multzoak estatistika-emaitzetan beraien

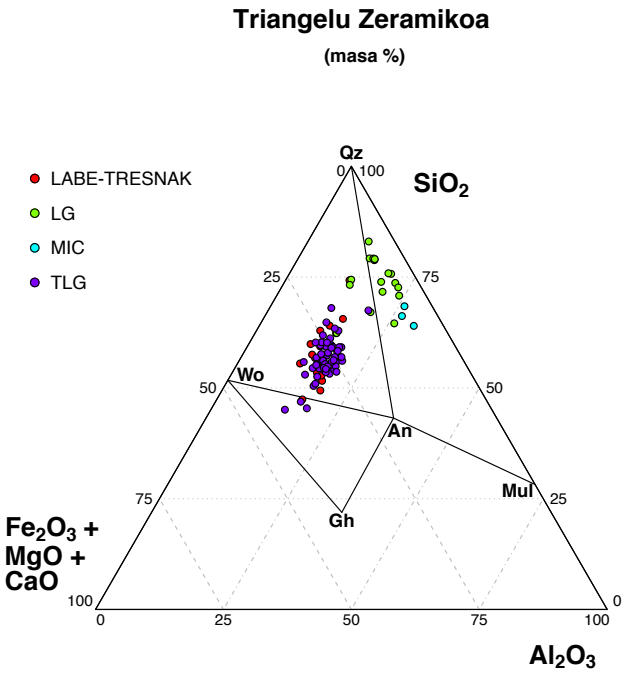

Figure 5.47: Diagrama hirutarra Fe_2O_3+MgO+CaO - Al_2O_3 - SiO_2 sistema erakutsiz Urduña-ko 94 zeramika-zatikiei dagokienak. An:Anortita, Gh:Gehlenita, Mu: Mullita, Qtz: kuartzoa, Wo: Wollastonita

artean multzokatzera behartzen ditu eta horrek zaildu egiten du multzoen horien arteko desberdintasun kimikoak behar bezala identifikatzea. Beraz, karedun multzoak era sakonago batean ebaluatzeko, PCA bat burutu zen soilik ORD-A, ORD-B, ORD-C, ORD-D multzoak barne hartuz. Gainera, kasu honetan, ez ziren CaO, Sr eta MgO kontuan hartu multzo bakoitzaren barneko aukera teknologikoek sartutako aldakortasunaren saihesteko. Karedun multzoen artean, aldakortasun baxuena erakusten zuen elementua Gd izan zen, eta, beraz, hura erabili zen zatiki gisa alr transformaziorako (ikus 5.46. irudia).

Fe_2O_3+MgO+CaO - Al_2O_3 - SiO_2 sistema hirutarraren diagramak aztertutako piezen egoera azaltzen du (ikus 5.47. irudia). TLGren lagin guztiak eta pasta bera daukaten labeko altzariak Wollastonita-Kuartzo-Anorthita oreka-sistema hirutarraren barruan daude; LG eta MIC multzok, berriz, Anorthita-Mullita-Kuartzo oreka hirutarraren sistemaren barruan daude. Analisi kimikoek erakusten dutenez, LG eta MIC-eko zatikiak oso ongi bereizten dira TLG zatiki guztiengandik, hain zuzen,

erakusten dituzten konposizio desberdintasun nabariengatik, SiO_2 eta Al_2O_3an, hurrenez hurren.

	ORD-A	SD	ORD-B	SD	ORD-C	SD	ORD-D	SD	ORD-MEL-A	SD	ORD-MEL-B	SD	ORD-MIC	SD
Al_2O_3	14.2	1.5	14.0	0.74	17.0	0.61	13.0	0.69	15.4	1.7	19.9	2.2	27.4	1.4
CaO	19.7	2.8	15.5	2.2	15.8	1.3	9.31	1.8	1.11	0.39	0.960	1.1	2.26	1.1
Fe_2O_3	3.89	0.45	2.84	0.39	5.24	0.24	3.76	0.19	4.49	0.61	3.06	0.30	2.89	0.54
K_2O	1.72	0.27	2.49	0.42	2.07	0.32	2.00	0.066	2.70	0.48	3.59	0.12	3.82	0.17
MgO	1.20	0.25	2.43	0.47	1.55	0.15	0.990	0.34	0.73	0.17	0.806	0.37	0.837	0.10
MnO	0.0320	0.0010	0.0250	0.0087	0.0305	0.0029	0.0227	0.0052	0.0145	0.0030	0.0116	9.810^{-4}	0.0347	0.0017
Na_2O	1.42	0.19	<LOD	<LOD	1.49	0.24	1.36	0.11	1.46	0.17	1.56	0.21	6.01	8.3
P_2O_5	1.59	5.5	0.425	0.11	1.13	1.7	0.379	0.25	0.133	0.12	0.0761	0.078	0.219	0.16
SiO_2	51.7	8.0	46.7	6.3	50.1	3.0	69.7	7.3	78.2	8.1	64.6	6.4	65.6	6.3
TiO_2	0.607	0.071	0.625	0.047	0.749	0.029	0.725	0.087	0.835	0.10	0.832	0.066	0.145	0.013
Ba	274	36	431	93	399	22	294	41	381	74	538	48	349	$1.2{\cdot}10^2$
Ce	64.8	7.7	76.9	6.1	79.2	2.1	72.4	3.9	89.4	11	110	5.6	30.2	2
Co	18.7	11	15.6	3.8	21.8	3.7	23.9	8.6	35.3	11	14.3	4.9	22.5	11
Cr	93.4	13	71.7	6.0	156	21	103	7.6	123	12	140	41	27.4	6.1
Cs	9.55	2.8	8.99	2.1	9.20	1.2	10.1	0.62	12.1	2.0	16.4	0.54	47.1	7.1
Cu	44.4	33	71.3	31	103	49	84.1	123	32.1	10	49.1	18	43.6	13
Dy	3.66	0.49	4.50	0.33	4.53	0.16	4.31	0.42	4.96	0.80	5.68	0.23	7.45	0.70
Er	2.16	0.26	2.37	0.15	2.56	0.091	2.49	0.20	2.80	0.36	3.00	0.18	4.12	0.44
Eu	0.882	0.14	1.15	0.097	1.26	0.055	0.990	0.040	1.22	0.22	1.57	0.17	0.781	0.14
Gd	4.15	0.66	5.53	0.47	5.42	0.15	4.73	0.26	5.75	1.0	7.34	0.51	5.64	0.81
Hf	5.97	1.0	7.42	1.2	5.62	0.24	8.23	1.3	9.79	1.3	8.65	2.5	4.26	0.30
Ho	0.699	0.085	0.737	0.043	0.814	0.028	0.758	0.057	0.840	0.090	0.916	0.070	1.24	0.12
La	30.3	3.3	36.6	2.9	38.0	0.86	34.2	2.2	42.4	4.7	53.0	3.0	17.1	3.4
Lu	0.314	0.043	0.365	0.028	0.387	0.033	0.408	0.054	0.471	0.082	0.466	0.021	0.618	0.057
Nb	16.0	2.2	22.7	1.4	16.8	0.67	17.1	1.5	18.5	2.2	33.6	8.4	28.3	3.7
Nd	26.8	4.0	43.5	3.7	36.2	0.89	32.1	2.4	41.4	7.2	54.9	4.6	16.8	5.5
Ni	19.7	3.7	14.9	2.4	32.7	7.2	29.2	26	19.3	3.9	24.6	10.	12.1	3.7
Pb	(196 -	10^3)*	$3{\cdot}10^3$	$2{\cdot}10^3$	$2{\cdot}10^3$	10^3	973	$3{\cdot}10^2$	(95 -$5{\cdot}10^3$)*		301	10^2	(21-472)*	
Pr	6.96	0.89	11.5	1.0	9.01	0.31	8.12	0.57	10.1	1.5	13.9	1.8	4.39	1.1
Rb	110	25	142	25	153	35	128	4.6	160	19	213	5.4	616	35
Sm	4.72	0.73	6.63	0.45	6.15	0.33	5.56	0.31	6.57	1.1	8.34	0.4	4.61	0.84
Sn	34.3	32	58.1	61	31.4	28	17.9	7.5	12.5	4.1	11.1	2.8	59.1	19
Sr	545	$1.4{\cdot}10^2$	321	40	960	$1{\cdot}10^2$	222	22	143	45	173	12	205	13
Ta	2.32	0.37	1.62	0.11	2.09	0.18	2.52	0.36	2.83	0.44	3.24	0.71	12.8	2.9
Tb	0.613	0.11	0.804	0.074	0.802	0.033	0.717	0.054	0.866	0.17	1.06	0.071	1.19	0.16
Th	12.4	1.4	12.9	0.92	13.8	0.41	13.4	0.86	16.7	1.1	17.0	0.47	4.71	0.41
Tm	0.308	0.042	0.401	0.033	0.380	0.020	0.390	0.045	0.436	0.073	0.462	0.013	0.681	0.073
U	3.08	0.34	3.08	0.21	3.19	0.14	3.52	0.33	3.84	0.40	4.23	0.34	5.78	1.4
V	61.2	11	73.0	6.4	105	14	53.6	3.6	74.2	9.2	103	6.4	21.6	3.2
Yb	2.25	0.28	2.29	0.15	2.65	0.093	2.64	0.25	2.97	0.38	3.02	0.25	4.11	0.34
Zn	38.0	7.5	9.69	1.8	37.6	2.9	36.2	7.4	37.5	6.2	26.3	15	45.5	5.0
Zr	231	40	135	11	219	9.8	327	54	384	48	247	63	123	15

Table 5.6: Urduñako konposizio-multzo bakoitzaren ICP-MS bidez lortutako kontzentrazio kimikoen batez bestekoak eta desbiderapen estandarrak (SD). Unitateak μg/g dira eta oxidoen kasuan masa %-ak aurkezten dira. <LOD: detekzio muga azpitik.(*) Pb eta Sn-rentzako kontzentrazio tarteak ematen dira SDak batez bestekoak baino handiagoak diren kasuetan.

Gainera, alde batetik, multzo bakoitzean hainbat ehundura-mota identifikatu ziren, eta horien erreketa tenperatura baliokideak ere (ingeleseko laburduran EFT). Horretarako XRD bidez lortutako difraktogramak erakusten dituzten fase mineralogikoak oinarritzat hartuz (ikus 5.56. irudia). Hala nola, haustura freskoak SEM bidez aztertu ziren, beiratze-maila ebaluatzeko haiek erakutsitako mikro-egituraren bidez (ikus 5.52. irudia). Azkenik, beiratuen karakterizaziorako konposizio-multzo bakoitzeko pieza adierazgarrienetarikoak aukeratu ziren,

koloratzaileak eta moldaketa teknologikoak identifikatuz. Ondorengo lerroetan, konposizio-multzo bakoitzaren eztabaida aurkezten da, besteak beste, konposizioaren alderdi aipagarrienak, XRD bidez identifikatutako ehundura motak eta SEM-EDX bidezko beiratuen karakterizazioa. 5.6 taulan, multzo bakoitzaren batez besteko kontzentrazioak eta SD balioak kontsulta daitezke. Multzo bakoitzaren zeramika adierazgarrien irudiak aurkezten dira, bai eta 3D berreraikitzeak ere, zeramika zatikietatik abiatuta egin direnak, artikulu honetan jasotzen den bezala (Rodríguez Miranda et al., 2017).

ORD-A

Multzo honetan, *Tras-Santiago* (n = 32) eta *Zaharra 24-30* (n = 7) guneetako 39 zatiki daude. Beraz, kronologikoki 1788-1850 bitartean definituta daude, nahiz eta bi pieza aurreko kronologia batekoak diren (1735-1760). Labeko tresneriaren ehuneko handi batek osatzen du konposizio-multzo hau, kare-eduki handiko pastak erakusten dituena (CaO $\approx$ 20 masa %). Gainera piezak eztainu-berunezko beiratuez estaliak daude eta kasu batzuetan apaindura berdeak erakusten dituzte (ikus 5.48. irudia).

Pasta honekin, batez ere, baxera formak sortu ziren: goporrak, platerak eta, neurri txikiagoan, txarroak. Hala ere, forma handiagoko aska batzuk ere pasta berarekin ekoitzi ziren (horietako bat, ORD030ak berunezko beiratu bat baino ez du erakusten, beste guztiak eztainu-berunezkoa izanik). Bestalde, ORD048 kolore urdinez apaindutako zatiki bakarra da. Geroago ikusiko den moduan, ORD-C, dekorazio urdinak ezaugarritzen dituen multzoa da. Hala ere, kasu honetan, konposizio aldetik ORD048 zatikia bat dator ORD-A multzoarekin (ikus 5.6. taula), berdeaz apaindutako piezak erakusten dituena. Urduñako datu multzo osoa kontuan hartuta, ORD-A multzoan gutxiengo elementuen kontzentrazio orokor baxuagoa hautemanen da; besteak beste Dy, Gd, Ho, Lu, Nb, Nd, Pr, Th, Tm, Yb eta Sm-ren kasuetan (ikus 5.6). CaO, MgO eta Sr bezalako elementu gehiengoetan aldakortasun altuek heterogeneotasun bat eragiten dute, konposizio-multzoaren barruko aldaketa teknologikoak iradokiko lituzkeena. Horrela, multzoa bitan banatzen da, MgOaren arabera. Hala ere, bere kontzentrazioa tarte estu baten barruan mantentzen da ORD-A multzo osoan zehar (1.2 $\pm$ 0.25 masa %). MgOn kontzentrazio baxuak dituztenak Sr kontzentrazio altuak erakusten dituzte eta alderantziz; kasu guztietan, CaOren kontzentrazio altuak mantenduz. MgOren kontzentrazio altuek zerikusia izan dezakete erabilitako buztinen fase dolomitikoekin.

Azkenik, ORD048 zatikiaren bereizpena ORD-A multzoaren barnean Al_2O_3 kontzentrazio altuago bati zor zaio (ikus 5.46. irudia). Izan ere, 11.7 masa % Al_2O_3 du, non gainerako zeramikek 4.2 $\pm$ 1.6 masa % erakusten dute. Hala nola, Th-a 9 μg/g -ko kontzentrazioa du eta gainerako zeramikek 12 $\pm$ 1 μg/g duten bitartean.

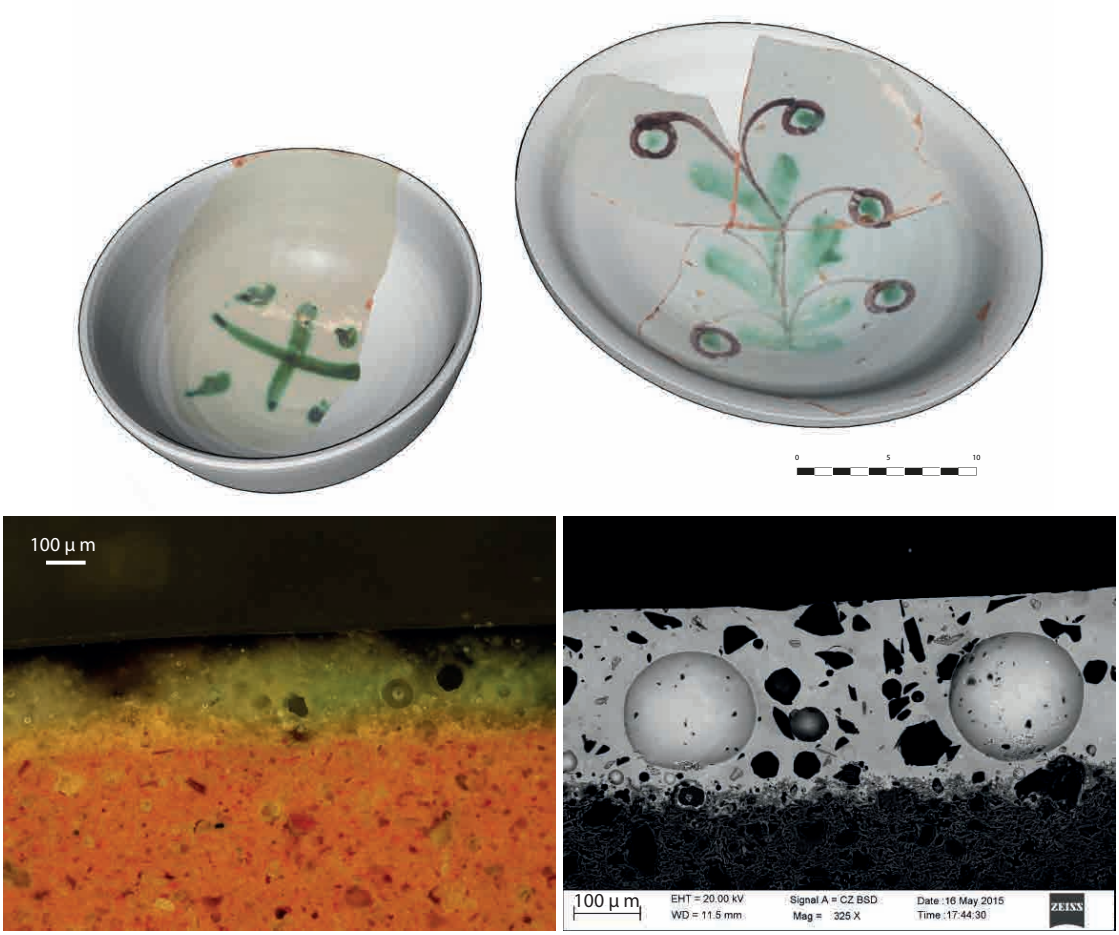

Figure 5.48: ORD-A multzoko zeramika adierazgarrien 3D berreraikitzea (goian). ORD-A multzo beiratuen eredu bat SEM-EDS eta mikroargazkia erakutsiz (behean).

Desberdintasun kimiko horietaz gain, gainerako elementuen kontzentrazioa eta HCAk iradokitzen duen bezala, ORD-A multzoaren barne geratuko litzake zatikia.

Multzo honek bi ehundura mota aurkezten ditu: F-I eta F-II (ikus 5.56. irudia). Kuartzo, gehlenita, plagioklasak (albita erakusten da) eta piroxeno (diopsidoa erakusten da) fase nagusiak dituzte biak. F-I fasean, mullitaren $Al_{4+2x}Si_{2-2x}O_{10-x}$ ($x \approx 0.4$) agerpen hasiberria hauteman daiteke (ORD020 erakusten da eredu gisa). Fase horien konkurrentziak, haren EFTa 900-1000°C artean kokatuko luke. Bigarren ehundura (F-II), berriz, aurrekoaren oso antzekoa izanik, erreketa-tenperatura altuko fase gehiago erakusten ditu (ORD003 erakusten da eredu gisa). Hala nola, mullita, eta espinelen agerpen hasiberria sumatzen da ehundura honetan. Beraz, haren EFTa 1050-1100°C tartean kokatuko litzateke, aurrekoa baino zertxobait altuagoa izanik.

EFTaren diferentzia horiek, pastaren sinterizazio maila desberdinekin bat datoz, haustura-freskoan antzeman daitekeen moduan (ikus 5.52. irudia). Irudi horretan, F-II ehunduraren sinterizazio maila aurreratuago bat hautematen da F-I-rekin alderatuz. CaOren eduki handia, multzo honen ezaugarria da eta difraktogrametan identifikatutako kaltzitarekin bat dator. Hala ere Kaltzita 650°C ondoren deskonposatzen da; beraz, presente dagoen kaltzio guztia birkarbonatazio- edota kutsadura-prozesuen emaitzaren bidez sortutakoa izan behar du.

Zenbait zeramikek aldaketa txikiak erakusten dituzte zenbait fase mineralogikoetan. Esaterako, ORD022 kaltzita eta feldespato-potasiko gehiago erakusten ditu. Hori dela eta, EFT baxuago batekoa izango litzakeela pentsa daiteke. Aitzitik, ORD021 zeramikan ez da kaltzitarik identifikatu, eta hori ez da ohikoa, kontuan hartuta F-II ehunduran konposatu hau nabaria dela. Bestalde, ORD006 eta ORD077 zatikien plagioklasen gailurrak oso baxuak dira F-II-rako nagusitzen den joerarako. Horregatik, tenperatura baxuago batera iritsi direla iradoki daiteke. Gainera, bi labe-tresna daude ORD024 eta ORD031, tenperatura altuagoak jasan zituztela antzeman daitekela (≈1100°C), haiek erakusten dituzten erreketa-faseen aberastasuna dela eta (bereziki plagioklasena). Kontuan hartuta pieza horiek erreketa anitzak jasaten zituztela, behin eta berriro erabiltzen zirelako, zentzua dauka pentsatzeak uneren batean tenperatura hori jasan izana, labearen bizi-ziklo osoan zehar.

Zeramika-gorputzen eta beiraduren interakzioaren arabera, zeramikak bi erreketa-prozesuko teknologiaren bidez egin zirela baieztatzen da. Lehenengo erreketa batean bizkotxoa lortuko zen, XRDk erakutsitako EFT maximoetara helduz (ikus 5.56. irudia), eta bigarren erreketa batean beiratua aplikatuko litzake, eskuarki, tenperatura baxuagoetara. Estaldurek beiratu zuriak erakusten zituzten, SnO_2 oinarri hartuta, kasu gehienetan, eta apaindutako piezek, berriz, beiratu gainean MnO bidez lortutako kolore beltzak edota CuO bidez lortutako berdeak erakusten zituzten (ikus 5.48 irudia).

Multzo honetan dauden labeko tresna guztiez gain, erreketa-akatsak dituzten beiratu batzuk daude, multzoa tokiko ekoizpenari lotzea ahalbidetzen dutenak (adibidez, ORD061, akatsak dituen beiratu bat erakusten duena, oso litekeena izanik gainberotze-prozesu bat gertatu izana.

ORD-B

ORD-B multzoa 17 zeramika-zatikiek osatzen dute, guztiak eztainu-berun zuria eta apaindurarik gabeko beiratua aurkezten dutelarik. Tipologikoki bi forma nagusi daude multzo honetan: plater eta katilu txikiak, txarro bakarra barne. Multzo honen ezaugarririk esanguratsuena denak kronologikoa berekoak direla da; izan ere, zatiki guztiak *Zaharra 2-4* aztarnategiko unitate estratigrafikoari dagozkio (SU 80). Beraz, zeramika hauek pieza goiztiarrenak irudikatzen dituzte (1694-1750), zeramika-multzo osoaren kronologia kontuan hartuta (1694-1850).

MULTZOA	Ehund.	EFT(°C)	Qz	Ilt-Ms	Afs	Cal	Gh	Goet	Hem	Pl	Px	Mul	K-Sp	Phyllo-Si
ORD-A	F-I	900-1000	xx			x	x			x	x	x		
ORD-A	F-II	1050-1100	xx			xx	x			x	x	xx	x	
ORD-B	F-I	850-900	xx	x	x		x							
ORD-B	F-II	900-1000	xx		x		x			x	x	x		
ORD-B	F-III	950-1000	xx		x		x	x		xx	x	x		
ORD-C	F-I	900	xx		x	x	x			x	x			
ORD-C	F-II	1000-1050	xx			x	x				x		x	
ORD-D	F-I	<950	xx	x	x	x	x		x	x				
ORD-D	F-II	>950	xx		x	x	x		x	x				
ORD-MEL-A	F-I	850-900	xx	x	xx		x	x		x				
ORD-MEL-B	F-I	>900	xx	x	xx		x	x		x				
ORD-MIC	F-I	850	xx	xx	x									x

Table 5.7: Urduñako multzoan identifikatu diren konposizio-multzo bakoitzaren ehundura desberdinak. Qz: Kuartzoa; Ilt-Ms: Illita-Muskovita; Afs: alkali-feldespatoak; Cal: Kaltzita; Gh: Gehlenita; Hem: Hematitea; Pl: plagioklasak; Px: Piroxenoak; Mul: Mulita. Laburdurak (Whitney and Evans, 2010) ondoren. Phyllo-Si Taldea (filosilikatoak): nephelinea, phlogopitea, klorita-bermikulita-montmorillonita, biotita, enstatita, ortoklasa).

PCAk ORD-B eta TLG multzoen arteko bereizketa argia erakusten du (ikus 5.46. irudia). Izan ere, multzo honek Fe_2O_3 kontzentrazio baxuak erakusten ditu, TLGko gainerako multzoekin alderatuta. Beste gehiengo aldagai batzuk, hala nola, Zr (135 ± 11 μg/g) eta SiO_2 (46.7 ± 6.3 masa %) ere kontzentrazio apalagoak aurkezten dituzte. Hori dela eta, garai horri esleitutako zeramikazko pastei dagokienez, nahasketa desberdinen erabilera iradoki daiteke. Hipotesi hau sendotzen da, aztarna eta gutxiengo elementu askok erakusten dituzten kontzentrazio aberatsagoak ikusita; besteak beste, Dy, Gd, Nb, Nd, Pr, Tm eta Sm.

Elementu horiek ez daude loturik aukera teknologikoekin, jatorrizko lehengaien konposizioarekin baizik (Glascock, 2016). Hori dela eta, buztin-horniketaren aldaketa batean pentsa genezake. Hori gutxi balitz, ORD-B multzoak aberastasun altuago bat aurkezten du MgOren kontzentrazioan, beste TLG multzoekin alderatuz (2.43 ± 0.43 masa %). MgOren aldaketa horiek, maiz, fase dolomitiko ugariko zeramikekin erlazionatzen dira. Aberastasun hori azaltzeko, karbonatoak nahita gehitzea aukera posible bat da. Hala ere, beste TLG-multzoekin alderatuz gero erakusten duten CaOren kontzentrazio baxuagoak (15.5 ± 2.2 masa %), pasten hareazko frakzioan egon daitezkeen Mg-an aberatsak diren silikatoen presentziarekin zerikusia eduki dezake; adibidez, XRD bidez identifikatu diren piroxenoak (ikus 5.56. irudia).

Konposizio mineralogikoaren arabera, hiru ehundura-mota nagusi identifikatu ziren konposizio multzo honetan. ORD095 eta ORD097, F-I motakoa aurkezten dute. Zeramika hauek illita gailur bat erakusten dute, 9Å-an. Mineral honen presentzia,

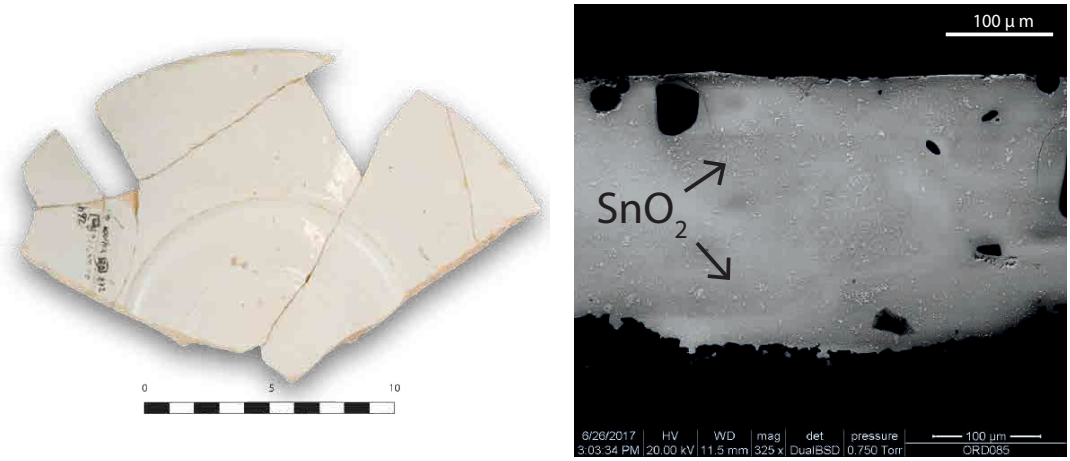

Figure 5.49: ORD-B multzoko zeramika-zatiki eredu bat (ezkerrean). SEM irudia beiratua erakutsiz zeharkako azaleran. Kasiterita partikula opakutzaileak nabariak dira.

K-feldespatoekin batera 850-900°C-tako EFTa iradokitzen du. Gainera piroxenoen presentzia apala ere hautematen da (diopsidoak erakusten dira), horiek tenperatura altuagokoak izanik, jatorrizko sendagarrien frakzioaren ere izan litezke. Bestalde, EFT baxu honi dagokion sinterizazio-maila baxua ere SEM bidez hauteman daiteke (ikus 5.52. irudia).

ORD084ren difraktograma erakusten da F-II-ehunduraren eredu gisa. Bere osagai mineralogiko nagusiak kuartzoak eta zenbait erreketa-faseak osatzen dute. Gainera feldespato alkalinoak era nabari dira (mikroklina erakusten da) neurri txikiago batean. plagioklasen presentzia dauka (albita erakusten da), alde batetik, eta, gehlenita $Ca_2Al(AlSi)O_7$ bestetik, diopsidoekin batera ($Ca(Mg,Al)(Si,Al)_2O_6$). Horiek denak silikatoen eta karbonatoen tenperatura altuetara ematen diren erreakzioen ondorio dira. Gainera, mullitaren identifikazioa, nahiz eta neurri txikian, eta, batez ere, illitaren erabateko desagerpenak, EFTa 900-1000°C-tan kokatzen dute.

F-III ehundura, berriz F-II-aren oso antzekoa da, baina plagioklasa, diopsido eta gehlenitaren gailur altuagoak erakusten ditu, hala nola, feldespatoei dagokien gailurrak ia erabat desagertu dira. Horrek, mullitaren presentziarekin batera, EFTa 950-1000°C artean dagoela iradokitzen du. Sinterizazio-maila handiena ere nabarmena da SEM mikroargazkien bidez (ikus 5.52. irudia). Goetitaren presentzia ere ($\alpha-Fe^{3+}O(OH)$) atzematen da. Burdin oxidoaren forma hidratatua, normalean 300°C-tatik aurrera deskonposatzen da. Beraz, jalkitze-ondoko errehidratazio batek bakarrik azal dezake bere presentzia.

Pieza batzuk osagai mineralogiko zertxobait desberdinak aurkezten dituzte. Hala nola, ORD091 zatikiak, gailentzen den gehlenita gailur bat du erakusten du, eta horrek

adieraziko luke zeramika horrek tenperatura altuagoa lortu zuela. Aitzitik, ORD088 kaltzitaren gailur nabarmen bat aurkezten du 30Å inguruan. Arestian aipatu den bezala, alterazio produktu bat izan behar du, kaltzita 650°C-etara deskonposatzen baita (Fabbri et al., 2014).

ORD-B multzoak ez du inolako dekorazio kromatikorik, soilik eztainu-berunezko estaldura zuriak aurkezten ditu (ikus 5.49. irudia). SEM-EDS emaitzek SnO_2 kontzentrazio nahiko altuen erabilera erakutsi zuten ($\approx$ 10 masa %). Literaturan agertzen den moduan, konposatu honen kontzentrazio altuak teknika opakutzailearen erabateko kontrola ez izateraerkin erlazionatzen dira. Horrela, nahiz eta eltzegileek beharrezko lehengaiak ahalik eta gutxien murriztea bilatzen duen, ezagutza horren faltan behar baino baino askoz kasiterita gehiago erabiliko lukete (Iñañez et al., 2008)

Gainera, ez dira ikusten bestelako beiradura baliabideen laguntzarik, hala nola kuartzozko partikulak ugariak eta burbuilak, modernoagoa den ORD-A multzoan gertatzen denaren aldean. Beiratuan identifikatutako desberdintasun hauek, 1694tik 1850ra emango zen teknologia moldaketa garapen batekin erlazionatu daitezke. Era horretan, eztainu kopuru txikiak erabiltzea ere merkatuan beharrezkoa den konposatu horren erabilgarritasunarekin loturik egongo litzake, eta XVIII. mendean gutxitu egiten da, gerra-industriaren beharrak direla eta. Beraz, buztingileek pixkanaka ezarri zituzten aldaketa teknologikoak, adibidez, kuartzoa eta feldespato pikorren erabilera, beiradura-prozeduretan eztainu erabilera gutxitzea helburu zutenak.

ORD-C

ORD-C multzoa 5 zatikiek osatzen dute. Apaindura urdinak daramaten eztainu-berunezko estaldurak dituzte. Formen artean, bi plater, katilu bat, ontzi bat eta ur bedeinkatuko ontzi bat aurki dezakegu. Azkenengo hau, etxean nahiz elizan ur bedeinkatua gordetzeko erabiltzen den ontzi mota berezi bat da. Kronologikoki aldi desberdinketakoak dira: hiru pieza 1785etik 1850erakoak, beste bat goiztiarragoa, 1735-1765koa da eta pieza erlijiosoa berantiarragoa da (1790-1820). Konposizio kimikoari dagokionez, CaO kontzentrazio altuek ezaugarritzen dute multzo hau (19.2 $\pm$ 3.7 masa %). Nahiz eta datu-multzo hau ORD-Aren oso antzekoa izan, HCA era PCAk, zeramika hauek bere osotasunean multzo bat osatzeko desberdintasun haina dutela iradokitzen dute. Gainera, kanpoko itxura ere ezberdinarekin koherenteak dira, multzo honen estaldura guztiek urdinez apaindutako eztainu-beruna duten beiratuak erakusten baitituzte.

XRD analisien arabera, ORD-C multzoak bi ehundura bereizgarri erakusten ditu. F-I-rako, ORD075 eredu gisa erakusten da. Bertan, kuartzoa eta erreketa faseak identifikatu ziren, piroxeno (diopsidoa) eta plagioklasak (albita) bezala. Gainera kaltzita identifikatu zen, zeina jalkitzen-ondoko prozesuen ondoriozkoa, hau da, bigarren mailako izan behar dena, aurretik azaldutako arrazoien arabera. Hala ere,

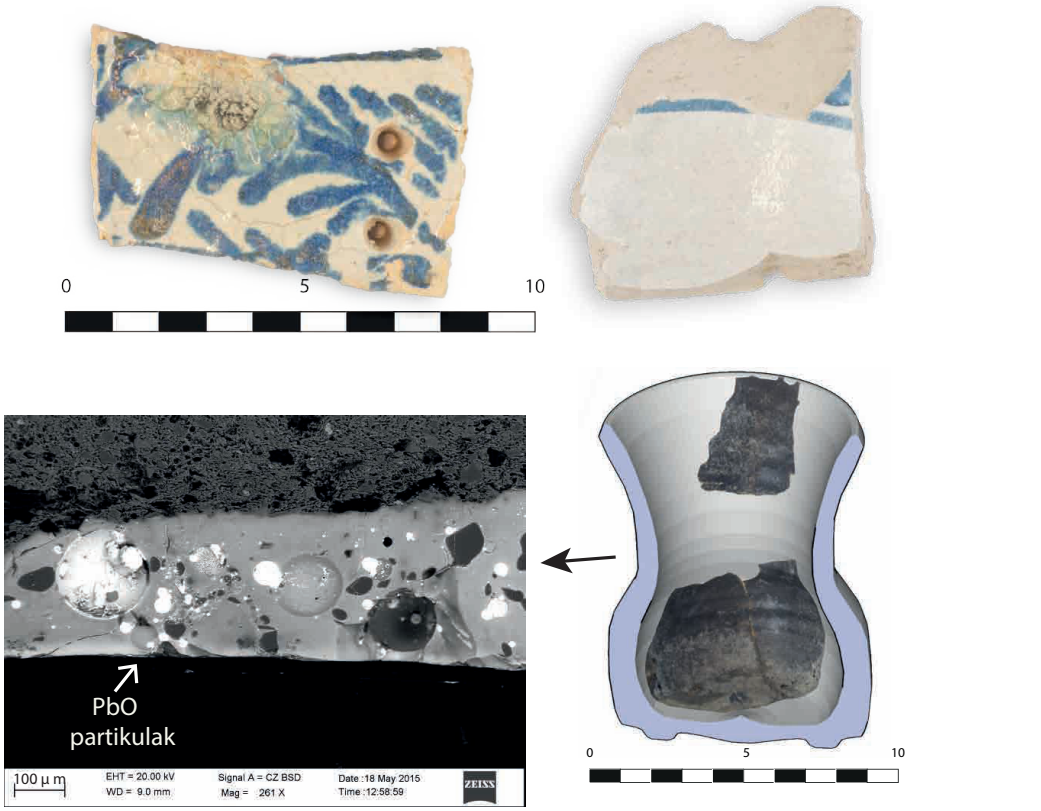

Figure 5.50: ORD-C multzoko zeramika-zatiki adibideak. Ezkerreko zatikiak erreketa-akatsak aurkezten ditu (goian). SEM irudia beiratua erakutsiz zeharkako azaleran (behean).

gehlenitaren presentzia, kaltzitaren deskonposizioan sortzen dena, hain zuzen (Fabbri et al., 2014), iradokitzen du lehenengo mailako kaltzita ere bazegoela jatorriz. Erreketa-fase hauen eta bigarren mailako fase hauek batera agertzeak EFT 900°C inguruan kokatzen du. Hala ere, feldespato alkalinoen (adib., mikroklina) erabateko deskonposizio eza, zeina 850°C-tik aurrera gertatzen den, iradokitzen du tenperatura 900°C-tik gertu dagoela. F-I ehundurarekiko oso desberdina ez izan arren, bigarren ehundurak (F-II) erreketa-tenperatura altuagoak jasan zituen. Alde batetik, feldespato alkalinoen deskonposizio osoa (≈14 Å gailurra desagertu egiten da); eta, bestetik, erreketa-faseen agerpena ezaugarritzen dute ehundura hau. Gehlenita, diopsidoak eta plagioklasen (albita) presentzia, eta hare gehiago, espinelen gailur hasiberriek (19 Å), EFT altuen adierazle izaten dira. Beraz, 950-1050°C-ko EFT bat iradokitzen da.

ORD-C multzoaren estaldura bereizgarriek eztainu-berunezko beiratuen gainean aplikatutako CoO-an oinarritutako apaindura urdinak erakusten dituzte (ikus 5.50.

irudia). Historikoki, kolore urdinak beiratutako zeramiketan prozedura tekniko berriak ekarri zituen; izan ere, CoO-ren bidez lortutako pigmentu urdinak, disoluzio kontzentratuagoak eskatzen ditu, konposatu hori oso hegazkortasun handia baitauka. Dekorazio urdinak Iberiar penintsulako beste tailer batzuetan (adib., Manises eta Paterna) erabiliak izan ziren mende batzuk lehenagotik (Conesa, 2008, 2011). Hala ere, iparraldeari dagokionez, horrelako eraldaketa teknologikoek denbora gehiago behar izan zuten. Horrela, XVIII. mendean, soilik berdeak zabaldu ondoren hedatu zen urdinaren erabilera, hala ere, pieza berezientzako erreserbatzen zen (adib., ur bedeinkatuaren ontzia). Gainera, hain zuzen, aipatutako piezak beiratuetan erakusten duen akatsa (ikus 5.50. irudia), eltzegileen erabateko trebetasunik ez zutela iradoki lezake. Hala ere nahiko ohikoa zen erreketa-aldi bakoitzean pieza akastun ehuneko finko bat izatea. Nolanahi ere, mugatuagoa zegoen pigmentu urdinaren erabilera, pieza honen izaera erlijiosoa bezala, helburu finagotarako erreserbatutako ekoizpen esklusiboa iradokitzen dute, ORD-B pastarekin. Emaitza horietatik abiatuta, buztin-nahasketak nahita hautatzea iradoki genezake, kolore urdinekin apaindutako zeramikarako bakarrik. Urdinez egindako apainketez gain, (ikus 5.50. irudia) ORD-B arekin bateragarria den pasta bat identifikatu zen. SEM-EDS irudiak txarroaren beiratua erakusten du. Kasu berezi honetan, ez zuen eztainu-berunezko estaldura bat erakusten, berunezkoa baizik. Gainera estaldura honetan Pb pikor handiak ikusten dira eta kuartzozko inklusio txikiak.

ORD-D

Multzo txiki hau (n = 4) beiratu gabe eta berun-beiratua daramaten zatikiek osatzen dute (ikus B Eranskina). Berun-beiratuak dituzten beste zeramikak ez bezala (geroago aurkezten direnak), ORD-D multzoak CaO kontzentrazio nahiko altua erakusten dute (9.3 $\pm$ 1.9 masa %). Multzo honetan, zeramika-akastunak aurkitzen dira eta labe-lanabesak ere, 1788-1850 garaiari esleitzen zaizkionak. Gainera, eltze bat dago (ikus 5.51. irudia) kronologia berekoa eta kolore marroi-zeharrargia duen beiratua erakusten duena. Euskal Herrian eltzeen merkataritzari dagokionez, litekeena da Zamoratik inportatu izana, hori baita XIV. mendetik aurrera ematen den joera.

Hemengo buztinak ez dutenez ezaugarri erregogorrak erakusten, jatorri horretakoak egokiagotzat jo ziren eta horrela, Zamorako eltzeen salmentak euskal zeramika-merkatura guztiz zabaldurik zeuden XVIII. mendea iritsi zenerako (Solaun, 2005). Zamorako ekoizpenak, historikoki, pasta trauskil eta mikatsuek ezaugarritzen dituzte. Horiek Al_2O_3 kontzentrazio altuak erakusten dituzte (Sanchez-Garmendia et al., 2018). Oso baloratuak izan dira, erreketak burutzeko erakusten duten txoke-termikorako erresistentzia dela eta. Hala ere, ORD015ren kasua ez dator bat deskribapen honekin. Izan ere, dekantatutako pastak erakusten ditu eta hemengo buztinekin eginda egongo litzake, pasta dekantatuak eta pikor finek iradokitzen duten bezala. Bestalde, ORD018k ere espero baino CaO kontzentrazio altuagoak erakusten

Figure 5.51: ORD-D multzoko zeramika-zatiki adibideak. Eltze baten irudiak agertzen dira, erreketa zantzuak erakutsiz (goian) eta bere beiratuaren SEM irudia trebera baten ondoan (behean).

ditu (8.56 masa %), izan ere estaldura hori (marroi-zeharrargia) dituzten beste zeramikek oso CaO kontzentrazio baxuak erakusten dituzte (ORD-MEL-A eta ORD-MEL-B).

Zatiki horren forma, katilu bati dagokio, deformazio bat erakusten duena labeko beste piezek eragindako tentsioarengatik. Laburbilduz, tipologikoki heterogeneoa den multzo honek aparteko piezak erakusten ditu. Besteak beste, marroi-zeharrargia eta kare-eduki handiko zeramika; mikatsua ez den eltzea; edota salmentarako erabiltzen ez diren piezak; akastunak eta labe-lanabesak (trebera).

Kanpoko itxurari dagokionez, ORD-D multzoak ez dauka apaindurarik, berunezko estaldura marroi-zeharrargiaz haratago. Labe tresnak ez daude beiraturik eta, bestalde, ORD015 eltzeak erreketa-zantzuak aurkezten ditu lehen aipatu den bezala (ikus 5.51. irudia). ORD-D multzoa konposizio aldetik, ORD-Aren antzekoa da; eta, aldiz,

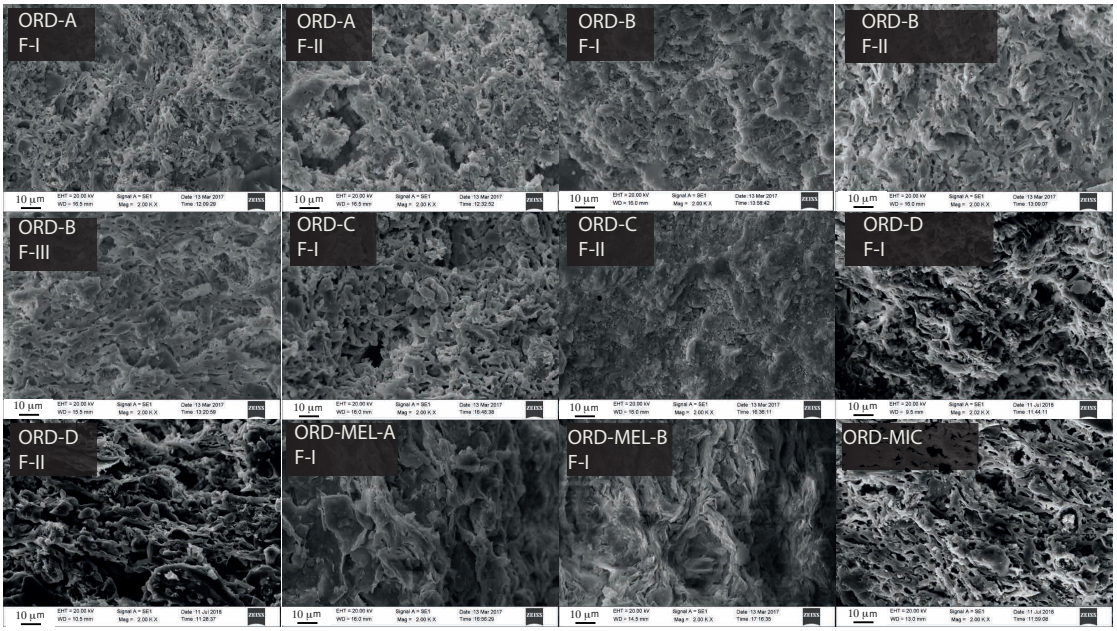

Figure 5.52: Urduñako zatikien mikroegituren SEM irudiak sinterizazio maila desberdinak erakutsiz. Eskuinetik ezkerrera eta goitik behera: ORD020, ORD003, ORD075, ORD049, ORD084, ORD099, ORD012 eta ORD078.

tipologikoki budinean aberatsa den ORD-MEL multzora gerturatzen da. Erlazio hori XRD bidez ikusitako emaitzekin bat dator, non F-I eta F-II ehun-motak identifikatu diren (ikus 5.7. taula). F-I-ak kaltzita eta hematitearen agerpena erakusten du, ORD018 laginak adibide gisa erakusten da (ikus 5.56. irudia). Illita eta feldespato alkalinoen agerpen txikiak EFT baxu bat adierazten dute. Beste fase batzuen presentzia kontuan hartuta, hala nola, gehlenita, eta plagioklasak, beraz, EFTa ez luke 950 °C baino handiagoa izan behar. F-II-ari dagokionez, ORD015 adibide gisa erakusten da (ikus 5.56. irudia eta 5.7. taula), oso pasta antzekoa erakusten du. Hala ere, illitaren erabateko desagerpena eta fase plagioklasiko aberatsagoak EFT 950°C baino altuago izan beharko lukeela iradokitzen dute.

ORD-MEL-A

Multzo honek 9 zatiki ditu. Denak kronologia berekoak dira (1788-1850) eta *Tras-Santiago* aztarnategian topatu ziren. Haien konposizioa ez-kareduna (CaO 1.1 ± 0.39 masa %) eta burdin oxidoan oso aberatsa (Fe_2O_3 4.49 ± 0.61 masa %) izateagatik ezaugarritzen da. Bibliografiaren arabera, mineral buztintsuetan kristalinotasun baxua duten oxido/hidroxidoen partikula koloidalen ugaritasunak menderatzen du masa

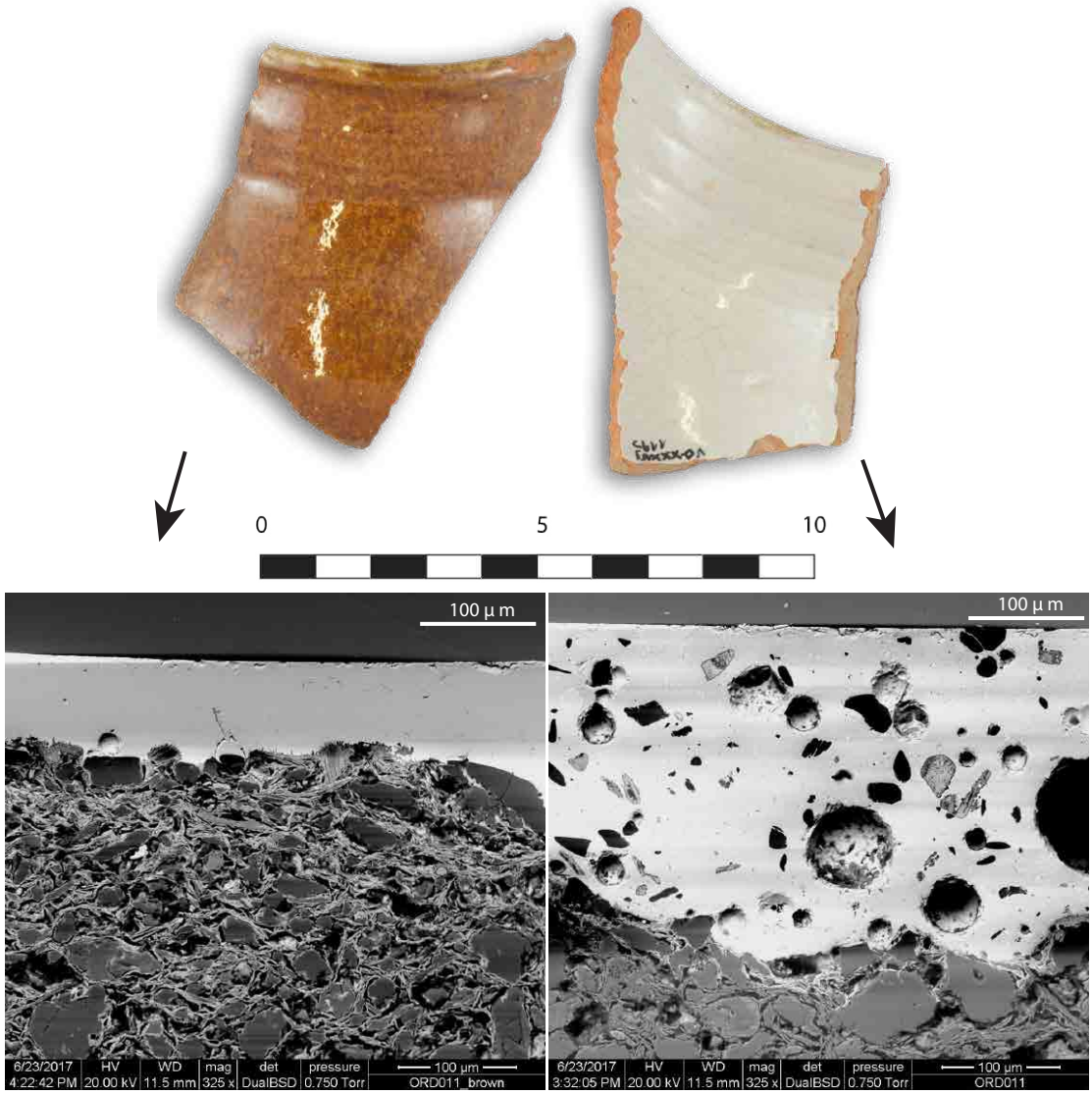

Figure 5.53: ORD-MEL-A multzoko zeramika-zatiki baten adibidea. Kanpoaldeko eta barrualdeko beiratuak erakusten dituen zatikia (goian) eta bakoitzaren beiratuaren SEM irudia (behean).

osoaren Fe_2O_3 kontzentrazioa, oro har, partikula horiek jalkitze sedimentarioetan agertzen dira, non 0.002 mm baino diametro txikiagoa duten partikulak nagusi diren, limo eta areetan (Montana, 2016). Beraz, buztinezko pastetan ikusitako Fe_2O_3 kontzentrazio aberatsagoa, bertako zeramikak ekoizteko buztina erauzteko gunearen aldaketarekin zerikusia izan dezake. Horrek buztingilearen hautapen teknologiko garbia adierazten du, nahi dituen propietateak lortzeko kare gutxiko buztinak bilatuz.

Konposizio multzo honen forma nagusia katiluarena da, txarro bat ere barne hartzen duelarik. Lagin guztiek kanpoaldeko estaldura zeharrargia dute, eztiaren kolorea hartzen duena. Gainera, piezetako batzuk barrualdean berun-eztainuzko beiratuak erakusten dituzte. Pentsa daiteke, arrazoi estetikoengatik ez ezik, eztainu-berun estaldura partziala, arrazoi ekonomikoekin ere zer ikusia daukala. Horrela, lehengai opakutzailearen kantitate beharra murrizten baita. Azkenik, ORD050 laginak multzoaren barruko oinarrizko konposizioan bariazio txikiak erakusten ditu, pieza hau berunezko beiratu erdi bat erakusten du kanpoaldean; barrualdea, berriz, soilik piezaren ezpainetik gertu beiratuta dago.

ORD-MEL-A multzoak (baita ORD-MEL-B ere) sinterizazio-maila txikiko pasta erakusten du. Egoera hori SEM irudian behatu daiteke; bertan, argi eta garbi antzematen da bitrifikazio baxuko pasta baten morfologia eta buztin-egitura (ORD012 adibide gisa erakusten da, ikus 5.53. irudia). F-I ehunak kuartzozko eta illita-muskovita faseak ezaugarritzen ditu, horiek, feldespato alkalinoekin batera (mikroklina) erreketa-tenperatura baxua adierazten dute (ikus 5.56. irudia eta 5.7. taula). Filosilikatoen hiru gailur nagusiak oso nabariak dira, eta horrek adierazten du fase horiek oraindik ez direla deskonposatzen hasi ere egin. Gainera, plagioklasak eta gehlenita bezalako erreketa-faseak ere badaude, eta, beraz, tenperatura 850-900°C-koa dela iradoki daiteke. Goethita ere identifikatu da, pasta gorrixka horien ezaugarri diren lehen mailako burdin oxidoen forma errrehidratatuari dagokiona.

Beiratuen zeharkako sekzioek erakusten duten bezala, bi beiratuen arteko mikroegituren desberdintasunak antzeman daitezke SEM irudien bidez (ikus 5.53. irudia). Berun beiratua meheagoa da eta eztainu-berun beiratua lodiagoa, gainera, atzenengoak 100 μm beherako inklusio txikiak agertzen ditu. Gorputz zeramikoa eta beiratuaren interakzio txikian oinarrituta, esan daiteke beiratuak bizkotxoaren gainean aplikatu zirela, bi urratseko-erreketaren bidez. Kanpoko ezti kolorea zeharrargia lortzeko, berun beiratuari burdin oxidoak gehitu zitzaizkion. Barruko aldean estaldura zuria erakusten duten kasuetan, berriz, kasiterita erabili zen opakutzaile gisa (ikus A.10. taula A Eranskinean).

ORD-MEL-B

Urduñako indusketetan aurkitutako ezti kolorez beiratutako piezen artean, ORD-MEL-B izendatutako beste multzo bat dago, 6 zatikiek osatzen dutena. Multzo

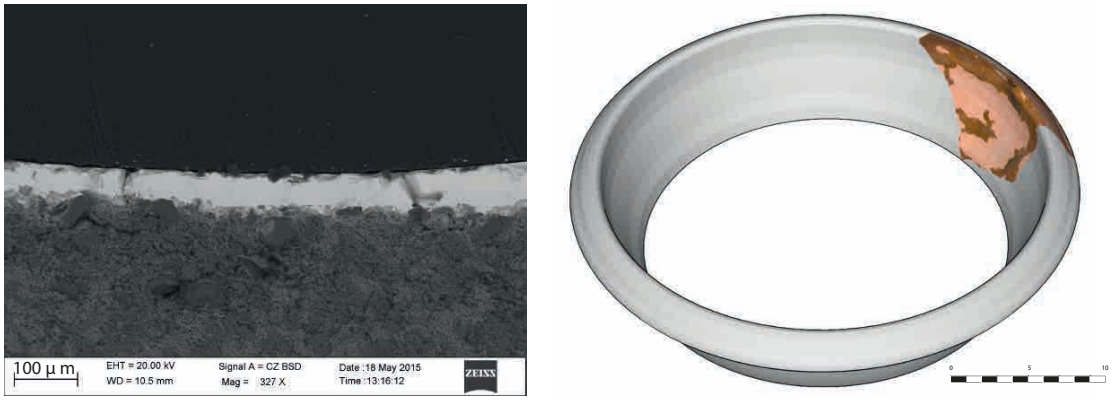

Figure 5.54: ORD-MEL-B multzoko berun-beiratu baten zeharkako sekzioaren SEM irudia (ezkerrean) eta zeramika-zatiki adibide bat, 3D bidez berreraikia (eskuinean)

honen barneko ezberdintasun kimikoak oso txikiak dira, ORD-MEL-A multzoaren aldean; beraz, oso multzo konpaktua dela esan daiteke. Ezberdintasun horiek CaOren kontzentrazio txikiago batek emana dator (0.51 ±0.07 masa %) (kontuan hartu gabe ORD051, zeinak CaOren eta MgOren aberastasun partikular bat erakusten duen) eta beste aldaketa batzuk elementu gutxi batzuetan bereizten direnak (Mn, Nb eta Zr) dira. Gainera, multzo honek Urduñan azterturiko lagin guztien artean Al_2O_3 kontzentraziorik altuenak erakusten ditu (19.9 ± 2.3 masa %), zeramika mikatsuak kontuan hartu gabe (ORD-MIC multzoa). Lagin hauen homogeneotasun kimikoa oso handia da (ikus 5.46. irudia). Halaber, multzo honek tipologia bakarra aurkezten du: tamaina desberdinetako askak (pieza bera izateko aukera baztertu da, perimetro desberdineko piezak baitira). Gainera, kronologikoki, multzo hau modu homogeneoan esleitzen da 1735-1765 aldi laburrera. Beraz, mota honetako piezen ekoizpena ekoizpena ORD-MEL-Aren multzokoarena (1788-1850) baino lehenagokoa izango litzateke. Gainera, zatiki horiek guztiak *Kale Zaharra 24-30* aztarnategian berreskuratuak izan ziren. Beste ezti koloreko beiratuak (ORD-MEL-A), aldiz, *Tras-Santiagon* aurkitu ziren. ORD-MEL-A eta ORD-MEL-B arteko antzekotasun kimikoak gorabehera, gunearen ezaugarri arkeologiko trinkoak eta kronologia puntu indartsu gisa hartu dira, erreferentziazko bi multzo horiek zehazteko orduan. ORD-MEL-B multzoak ehundura-mota bakarra erakusten dute, F-I-ari dagokiona, hain zuzen ere, eta ORD-MEL-A multzoaren F-I ehunduraren oso antzekoa dena. Eredugarria den ORD078ri dagokion difraktograma bat 5.56. irudian erakusten da. ORD-MEL-Arekin alderatuz, aldaketa txikiak aurkezten ditu, gehien bat filosilikatoei dagozkien faseetan ematen dena, batez ere, 7Å inguruko illitaren gailurrean, kasu honetan handiagoa dena. Beraz, zeramika horien erreketa-tenperatura 900°C-tik beherakoa izan litekeela pentsa daiteke. ORD-MEL-B pastak askak sortzeko erabili zen, 3Dn berreraikitako piezaren antzekoak (ikus 5.54. irudia). SEM irudiaren bidez, hauteman daiteke, zeramika mota

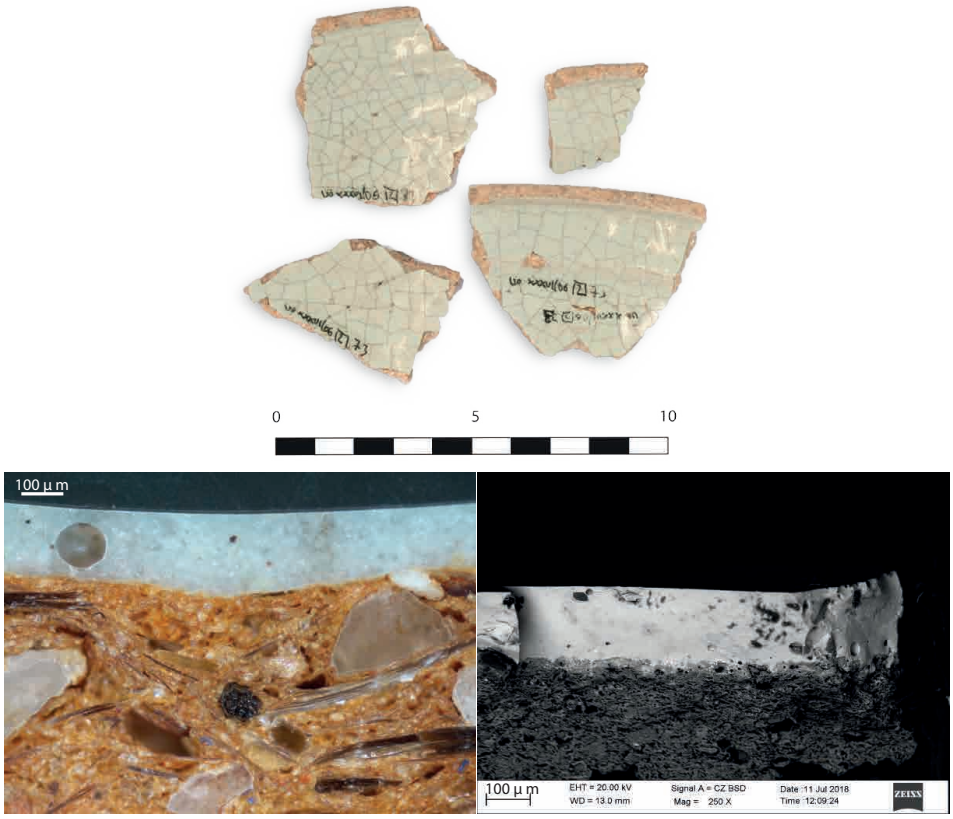

Figure 5.55: ORD-MIC multzoko zatikiak (goian), haietako baten mikroargazkia (behian, ezkerrean) eta SEM argazkia zeharkako sekzioari dagokiona beiratua erakutsiz.

horiek erreketa-bakarrarekin egiten zirela, berunezko beiratua eta gorputz zeramikoa aldi berean errez.

ORD-MIC

HCAk, garbi erakusten du gainerako piezez bestelakoa den azpimultzo bat (ikus 5.45. irudia). Zeramika horiek ORD-MIC izeneko multzoa osatzen dute (n = 3). Pasta oso heterogeneoa dute ezaugarri nagusitzat eta tamaina handiko inklusioak erakusten dituzte (<1 mm). Elementu nagusiek gehitzen dute konposizio-aldakortasun nabarmenenak. Batez ere Al_2O_3, baina aztarna eta elementu minoritario gehienak ere beherakada nabarmena erakusten dute (ikus 5.6. taula), gainerako konposizio-multzoekin alderatuz. Cs-ren eta Ta-ren kontzentrazio zeharo desberdinak ere azpimarratu behar dira. Multzo honen pastak oso mikatsuak dira, beraz, Al_2O_3

kontzentrazio altuak erakusten dituzte. Literaturan adierazten den bezala Al_2O_3, modu positiboan koerlazionatu daiteke buztin-mineralen ugaritasun erlatiboarekin edota feldespato eta mikaren mineral-bakarreko granuloen kopuruarekin, frakzio granulometriko trauskiletan (Hunt, 2016). Horrelako baieztapen bat egiteko, hala ere, ikerketa sakonago bat burutu beharko litzakete.

Euskal Herrian aurkitutako zeramika mikatsuen kasuan, eztabaida arkeologiko ireki bat dago haien jatorriari buruzkoa. Lehen aipatu dugun bezala, sukaldeko zeramika ekoizteko propietate erregogorrak behar dira (buztin mikatsuekin lortzen direnak adibidez). Produktuak jasango dituzten hozte-berotze zikloekiko erresistentzia handiagoa erakusten dute horrelako buztinak. Helburu hauetarako euskal buztinak ez dira egokiak, horregatik, beste jatorri batzuetatik ekartzen ziren (Solaun, 2005). Hain zuzen ere, ekoizpen horien agerpenak tokiko ekoizpenaren merkatua eraldatu zuen, batez ere XIV. mendean zehar. Prozesu horretan, buztingileek eltzeen ekoizpena pixkanaka baztertu zuten, atzerriko ekoizpenen eskari eta kalitate handiagoaren aurrean. Prozesu honen berrespena Zamorako eltze famatuen kasuan ikusten da. Horiek XVIII. mendean Euskal Herriko sukaldaritza-zeramikaren merkatuaren zati handi bat osatzen zuten (Solaun, 2005).

Beraz, literaturaren arabera, zeramika horien jatorria Zamoran egongo litzateke, eta, mendebaldera 368 km-tara kokatuta dagoen zeramika-ekoizle gune garrantzitsu bat (Sanchez-Garmendia et al., 2018). Bitxia bada ere, pieza bat (ORD056) eztainu-berunezko beiratu batez estalita dago, eta antzeko piezak topatu dira Durangon. Garai bereko beste euskal zeramika ekoizpen gune bat dena, Urduñatik 56 km-tik kokatua dagoena (Ibabe, 1995a).

XRD emaitzak konposizio kimikoarekin bat etorri ziren, egoera geokimikoaren antzera, fase mineralogiko oso desberdina erakutsiz, gainerako multzoekin alderatuz. Pasta horiek tamaina handiko (mm-ko ordena) inklusioak dituzte eta difraktogramaren arabera (ikus 5.56. irudia), klorita-bermikulita-montmorillonita eta biotita, edota nefelina, phlogopita, eta enstatita bezalako partikula mikatsuei dagokie. Pastek ere magnetita erakutsi zuten (ikus 5.7. taula). K-feldespatoak (ortoklasak) eta illita-muskovitaren presentziak EFT baxuekin erlazionatzen direnez, 850°C inguruan estimatzen da horien EFTa.

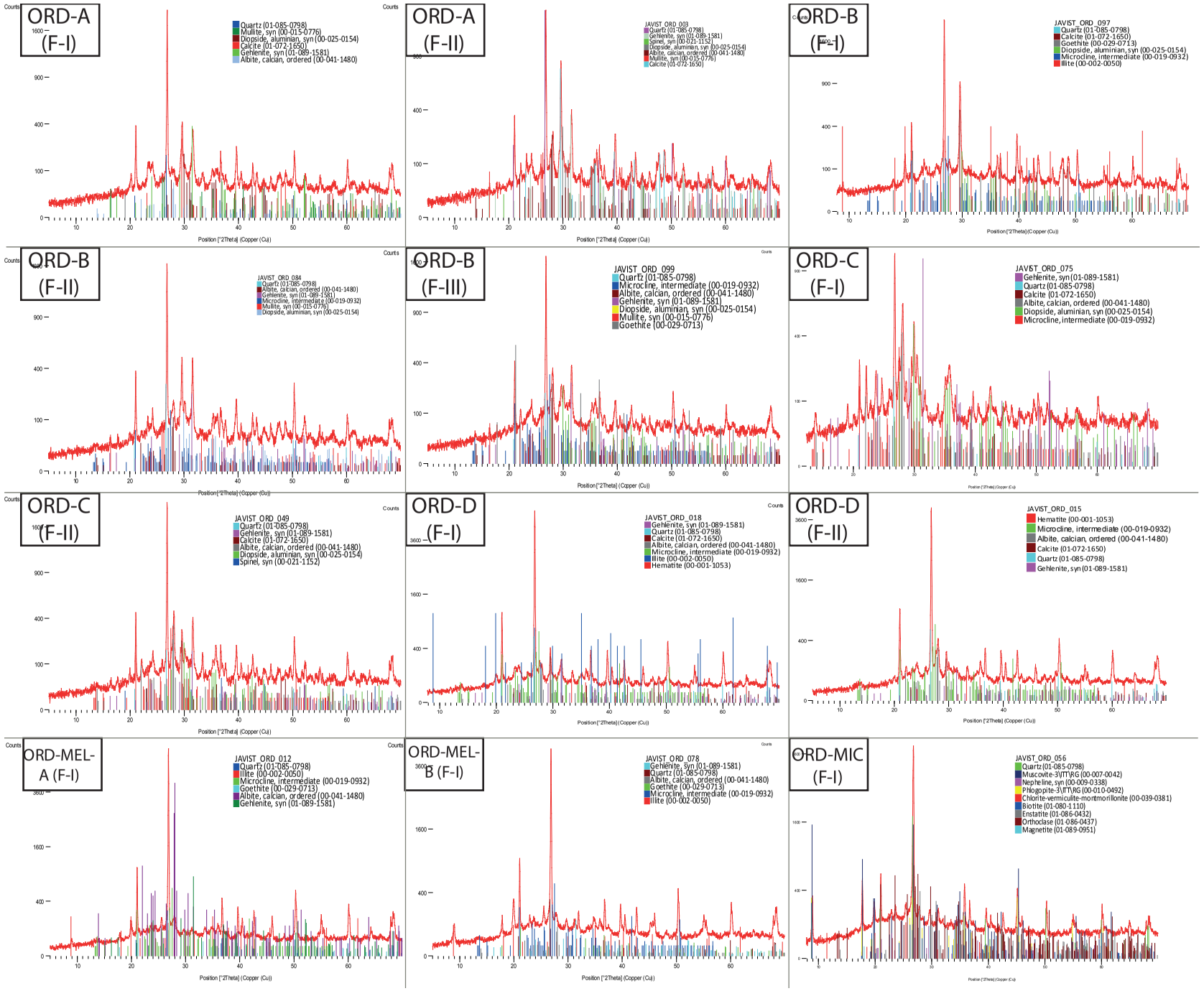

Figure 5.56: XRD bidez lortutako difraktogramak ORD-A, ORD-B, ORD-C, ORD-MEL-A eta ORD-MEL-B multzoei dagokienak.

Multzokatu gabeko laginak

Gainera, banako batzuk ezin izan ziren multzokatu (n = 11). Nahiz eta ezaugarri arkeologiko eta tipologikoen arabera, seguruenik Urduñan ekoiztuko ziren, lagin horiek ausazko aldakortasunak dituzte beren kontzentrazioetan, eta ez datoz bat identifikatutako beste konposizio-multzoekin. Hori dela eta, lehentasuna eman zitzaion konposizio esanguratsuei buruzko datuak eskaintzeari, gehien bereizitako multzoentzat kontuan hartuz eta beste lagin horiek multzokatu gabe utzi ziren.

Lagin horiek muturreko balioak erakusten zituzten, hainbat arrazoirengatik. ORD014 eta ORD019 laginek oso kontzentrazio handia dute (3.42 masa % MgO) baina konposatu hori erabiltzen ez zenean analisi estatistikoetan, ez ziren beste multzoekin bateratu. Nahiz eta haien pastak ORD-B multzoarekin alderatuz oso antzekoak diren; beraz, ezin da hipotesi sendo bat eskaini jatorriari buruz. Gainera, ORD047 beira berdexka duen txarroa da, eta tipologikoki, azterturiko zeramika guztiaz oso bestelakoa da. ORD057, CoO bidezko marra urdin ilunak erakusten dituena, Cu-aren kontzentrazio altua du, eta litekeena da jalkitze-ondorengo kutsadura batekin lotuta egotea. Hala ere, elementu hori saihestean, beste zeramikekin bateratu gabe jarraitzen zuen. Azkenik, ORD055k tipologia berezia aurkezten du (berunezko beiratu bat itxura horixka duena). Gainera, MgO eta V- aren kontzentrazio desberdinak aurkezten zituzten besteekin alderatura, horregatik, ezin izan zen bateratu beste multzoekin. Era berean, ORD071, ORD073, ORD074, ORD076, ORD087 eta ORD077 zatikiak ezin izan ziren multzokatu. Dendrograman ikus daitekeenez, zeramika horiek desberdintasun kimiko diskriminatzaileak aurkezten dituzte beste multzo guztiekin alderatuta, baina baita beraien artean ere, eta horrek ezinezkoa egiten du edozein multzotara atxikitzea (5.45. irudia)

Eztabaida atala eta Ondorioak

Lan honetan identifikatutako sei konposizio-multzoen karakterizazio arkeometrikoak, Urduñan aurkitutako zeramikak bertako ekoizpenarekin erlazionatzeko aukera eman du, XVII. eta XIX. mende bitarteari dagokiena. Hala nola, Zamorari (Iberiar penintsulako mendebaldean) esleitzen zaion ORD-MIC multzoa ere identifikatu da. Horrela, XVIII. eta XIX. mendeetako ekoizpenak tradizioari eutsi zioten bertako aurreko ekoizpenetan ikusten diren kare-pastak erabiliz. Hala ere, ORD- B multzoak azaldutako konposizio-ezberdintasunak kontuan hartuta, aldakortasun kimiko bat antzeman zen, ziurrenik erauzketa-leku aldaketaren ondorioz. Horrela, gertaera honek aldaketa bat islatu dezake, azterturiko lehen periodotik (1694) hurrengo mendera bitartean.

Gainera, identifikatutako konposizio-multzoen itxura zeramikoa ekoizpenaren eraldaketarekin lotu daiteke; dekoratu gabeko piezetatik (ORD-B), asko zabaldu ziren

berde eta berde/beltzez apainduriko formetara (ORD-A), gainera ORD-B, helburu esklusiboagoetarako erabili zena ere identifikatu zen.

Bestalde, zeramika tipologia berri baten ekoizpena identifikatzen da: ezti koloreko beiratua duena eta 1788 (ORD-MEL-B) ondoren hasten dena. Azken ekoizpen honetan pasta ez-karedunak baino ez dira erabiltzen, kanpoaldeko beiratu zeharrargiekin eta eztainu-berunez beiratutako barrualdeekin batera. Zamorako azterlan honetan aurkeztutako inportazioen garrantzia ere nabarmendu behar da, bere tokiko ekoizpena Urduñan argi eta garbi baztertuz.

Ildo beretik, ikuspegi multi-analitikoaren interpretazio integratuak hainbat patroi kimiko eta teknologiko erakutsi zituen Urduñako zeramika ekoizpenari dagokionez. Alde batetik, buztingileek buztinen propietateei dagokienez erakusten duten trebetasuna nabarmentzen da. Lehengaiak nahita hautatzen zituzten akaberaren arabera. Adibidez, buztingileek kare kontzentrazio altuko edo baxuko buztinak aukeratzen zituzten aplikatu nahi zuten estalduraren arabera (adibidez, eztainu-beruna beiratua, zeharrargia edo urdinez apaindua).

Bestalde, beiratuei dagokionez, ohiko errezeten erabilera berretsi zen. Horrela, SnO_2 erabiltzen zuten beiratuak opakutzeko, eta, haien gainean, CuO erabiltze zuten berdearentzat, MnO beltzarentzat eta CoO urdinak lortzeko. Apaingarriek landare- edo geometria-motiboak erakusten zituzten, eta aipatutako kolore-paleta erabiliz, kolore bat edo bi konbinatuz, gehienez ere. Dekorazio horiek nahiko xumeak, batez ere Iberiar penintsulako maiolikako aurreko tailerrekin alderatuta (Manises, Sevilla, etab.). Leku horietan, dekorazio polikromatuak oso hedatuta zeuden aurreko kronologietan (Coll Conesa, 2009). Beraz, iradoki genezake XVII eta XIX urte bitarteko zeramika landuagoak urdinez apainduak izan zirela (ORD-B). Pieza horiek, hain zuzen, helburu berezietarako erreserbatuta zeuden, eta buztingileen hautaketa teknologikoak kontsumitzaileen gustu aldakorren eskakizunak asetzeko egokitzeko saiakerari erantzuten diete.

Lan honetan aztertutako zeramikaren testuinguru historikoa Ibabe etnografoak euskal zeramikari buruz egindako ikerketekin bat dator kronologiari dagokionez (Ibabe, 1995a). Antza denez, XVIII. eta XIX. mendeetan zehar, lau familiek Urduñako tokiko produkzioa menderatu zuten. Hasiera batean, Lazkano familia jardun zen, ondoren (1780), Martin eta Martinez familiak hari jarraitu ziotelarik. Ondoren, Ibañez jardun zen (1841ean jaioa), eta haren azkenengo arrastoa Elosun galtzen da, hain zuzen euskal industriaurreko azken ekoizpen guneetako batean. Hala ere, dokumentazio historikoaren arabera, argudiatu da Urduñako buztingintza jarduera tokiko oligarkia garrantzitsuen esku egon zitekeela, hala nola, Ortes de Velasco, jarduera Arabako buztingileei errentan emanez edo bere zerbitzuak zuzenean kontratatuz (Cajigas Panera et al., 2004).

1694-1850 bitarteko tokiko zeramika ekoizpenari buruz egindako erradiografiak aldaketa sozial eraldatzailea islatzen du aztertutako aldian. Horrela, ORD-A multzoa,

azkenean, biztanleriaren sektore gehienetara zabaldu zen zeramikaren adibide bat da. Ekitaldi hau periodo luze baten ondoren bakarrik gertatu zen, zeinetan zeramika mota horiek soilik bezero dirudunentzako ziren eskuragarriak (Escribano, 2014).

Laburbilduz, ICP-MS, XRD eta SEM-EDS tekniken bidez burututako karakterizazio arkeometrikoa, ondorengo tratamendu kimiometrikoarekin batera, XVII. eta XIX. mendeetan Urduñako zeramikazko tokiko produkzioarekin lotutako sei konposizio-multzoa identifikatzea ahalbidetu du eta bat kanpokoa, XVII. eta XIX. mendeen bitarteko ekoizpenei dagokionez. Horietatik, lau eztainu-berun beiratuko (TLG) motakoak dira: ORD-A, ORD- B, ORD-C eta ORD-D. Gainera, beste multzo kare-baxukoak (ORD-MEL-A eta ORD-MEL-B) eta, azkenik, exogenoa den multzo mikatsua (ORD-MIC). Eztainu-berunez beiratutako zeramika guztiek CaO aberatsa duten pastak erakutsi dituzte (9.3-19.7masa %) eta gainerako multzoek CaO oso kontzentrazio txikiak dituzte.

Gainera, multzoen konposizio-aldakortasunak zeramikaren bilakaera diakronikoa agerian utzi du denboran zehar. *Zaharra 2-4ko* aztarnategiko zatikiak konposizio-multzo goiztiarrenari esleitzen zaizkio (ORD-B), eta, aldiz, eztainu-berun beiratua dutenak, ORD-A, ORD-C eta ORD-MEL-B gutxienez 1735. urtetik aurrera ekoiztuak izango ziren. Nolanahi ere, 1788tik aurrera multzo guztietako ekoizpenak emango ziren (ORD-B ezik). Hortik aurrera, bi ekoizpen berri nabarmenduz: ORD-D eta ORD-MEL-A. Azken honek, lehen aldiz, eztainu-berun beiratu bat dauka barneko estalduran eta berunezko beiratu bat aurkezten du kanpoaldean.

Gainera, XRD analisiak adierazi dutenez, konposizio-multzo gehienek hainbat ehundura mineralogiko osatzen dituzte. Horrela, aztertutako zeramika guztiak 850 eta 1050 °C bitarteko EFTak aurkezten dituzte. Ildo horretatik, ehundura mota ezberdinek ez dute beste faktore batzuekin inolako korrelaziorik erakutsi eltzegileen aukera teknologikoetatik harago, beren desberdintasun nagusiak direla medio, bai EFTak edota konposizio-ezaugarriak. Hori da Zamoran ORD-MIC multzoaren kasua, desberdintasun mineralogikoak oso lotuta baitaude konposizio kimikoarekin, gainerako multzoekin alderatuta.

5.5 Durangoko Buztingintzaren Ezaugarritze Arkeometrikoa

Abstract

Durangok XVI. mendetik aurrera buztingintza ohitura luzea izan du, euskal zeramika herrikoiaren historiaren amaiera arte iraun duena, alegia, XX. mendeko bigarren erdialdera arte. Herriak jarduera komertzial bizia izan du, Bilborako iparraldeko bidean duen kokapen estrategikoagatik. Nahiz eta buztingintza jarduera nabarmena egon den herri honetan, arkeologoentzat lan nekeza izan da bertako ekoizpenak ezagutzea, erregistro arkeologikoan oso material gutxi baitago tokiko ekoizpenarekin erlazionatu daitekeen. Bestalde, Ibabe etnografoak informazio garrantzitsua jaso zuen XX. mendean Euskal Herrian funtzionatu zuen azkenetariko zeramika-gune honi buruz. Kasu honetan, dokumentazio-lanez gain, ekoizpenari lotutako material zeramikoak ere jaso zituen (treberak eta matoiak), baita etxerako baxera eta zeramika anitzak ere. Antza denez, mendeetan zehar Gerediaga inguruko buztinen ustiapena mantendu da, Durangoko eta inguruko guneetako buztingileak hornituz. Lan honetan ezaugarritze arkeometrikoa burutu da aztarnategi honetako 26 zatiki zeramikoetan oinarrituz. Zatikiak estrategia multi-analitiko baten bidez aztertu ziren, horretarako ICP-MS, NAA, XRD eta SEM-EDS erabiliz. Emaitzek tokiko ekoizpenarekin lotutako konposizio-multzo bat zehaztea ahalbidetu zuten (DUR) eta kanpoko jatorria duen beste bat (DUR-MIC). Azken horrek, pasta mikatsuak ditu eta baliteke erakusten duen eztainu-berunezko estaldura Durangon bertan aplikatu izana, aurretik iradoki den moduan. Atal honetan, Durangoko ekoizpenei buruzko erreferentzia historikoak berrikusten dira; eta, bide batez, Durangoko ekoizpenaren ezaugarri den aztarna kimiko bat ematen da, bertako eta inguruko eskualdeko azken mendeetako buztingintza ekoizpena hobeto ulertzen laguntzeko helburuarekin.

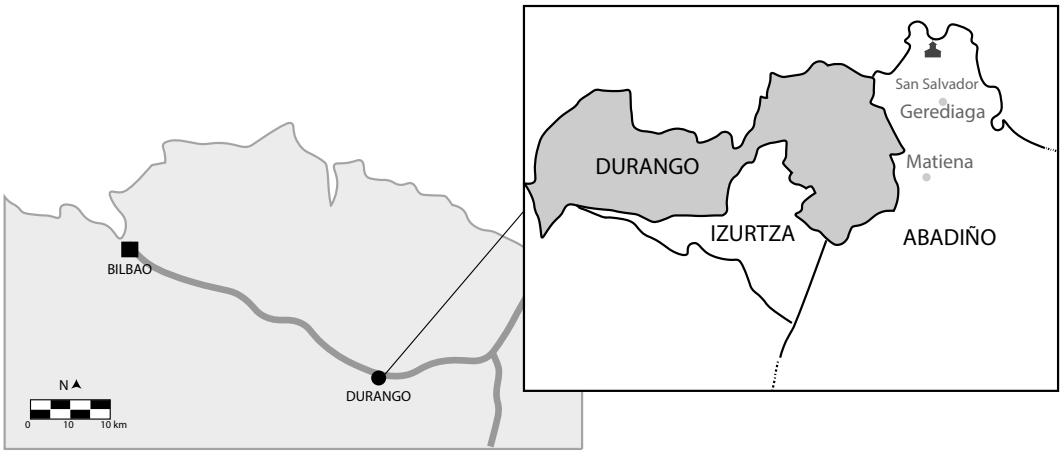

Figure 5.57: Durangoko kokapena eta testuan aipatzen diren guneak.

Aurrekariak

Durango Bizkaiko lurralde historikoan eta probintzian dago. Jarduera ekonomikoaren eta biztanle-kopuruaren arabera, Bizkaiko herririk garrantzitsuena da Bilbo Handia osatzen duten horien ondoren. Bilbora doan iparraldeko bidean dago eta kokapen estrategiko horrek, denbora luzez, onurak ekarri dizkio bertako jarduera komertziala sustatuz.

Dokumentazio historikoaren arabera, hiribildu honetan ekoizpen-zeramikoa XVI. mendetik aurrera ezagutzen da. Horrela, buztingintza jarduera nabarmena garatuko zen hainbat mendetan zehar, zeramika lantegi desberdinetan antolatuz. Dokumentatutako azken buztingintza lantegiak, hain zuzen, Aretxagako Lópezena eta Bizkarra-Markiegirenak izan ziren (Ibabe, 1995a; Lardizabal, 2008). Idatzizko beste iturri batzuek ebidentzia ez-zuzenak ematen dizkigute, XVI. mendetik aurrerako buztingintza-jarduerari dagokionez. Esate baterako, Gestosok XIV. eta XIX. mendeen artean Sevillan jardun ziren buztingileen zerrenda osatu zuen (Gestoso y Pérez, 1904), Durangoko Juan Martínez (1528) eta Nicolás Martínez (1525-1534) buztingileak aipatuz. Buztingitza jardueraren beste zantzu bat *Notas históricas de la Villa de Durango (IV) (9-2-1652)* testuan jasotzen da, kasu honetan, eraikin bat aipatzen da XVII. mendean teilak, adreiluak eta antzeko piezen ekoizpenerako erabiltzen zena (Larracoechea Bengoa, 1992).

Buztingintza ohitura luzea izan arren, Durangoko zeramika ekoizpenari buruzko erreferentziak oso urriak dira literaturan. Gainera, bertan dokumentatuta dagoen zeramika kontsumo handia, tokiko ekoizpenen ezagutzarekin, zeharo kontrastatzen du. Erreferentziako azterlan batean buztingintza jardueraren panorama orokorra eskaintzen da Euskal Herrian, VIII-XIII. mendeen bitartean Solaun (2005). Durangori dagokionez,

Figure 5.58: Markiegi anaien argazkia beren lantegian (Ibabe, 1995a). BBK Fundazioa©

aipatutako lanean ezin izan zen bertako ekoizpen zeramikorik identifikatu, zailtasun nagusia inguru horretan aurkitutako material urria izanik (Solaun, 2005).

Bestalde, aurreko lanari jarraipena ematen dion beste erreferentziazko lanean, XIV-XVII mendeen arteko jarduera jorratzen dira (Escribano, 2014). Nahiz eta azterlan hori Araban zentratzen den, Durangon hainbat jatorri exogenoko eta eskualde-mailako zeramika jaso izana dokumentatzen da, horien artean hainbat multzo identifikatuz: V, VI, X, XXV, XXIX, XXX, XXV, XXXIII, XXXIV, XXXVII, XXXIII, XXXIV, XXXVII, XXXIII eta LVI, hau da, definitutako 33 multzoetatik 11 multzoetan Durangon kontsumitutako zeramika aurkitzen da. Aitzitik, euskal zeramikaren koadro zabal honetan, tokiko multzorik ez zen arkeologikoki esleitu Durangoko ekoizpenari. Egile berdinak, kontsumoaren ikuspegitik aztertu zituen Durangoko zatiki batzuk. Besteak beste, Durangoko bi aztarnategietatik ateratako 10 banako (*Komentukale* eta *Kale Barria*). Material horiek abiapuntu gisa hartu ziren, arkeologikoki ezaugarritzeko Ollierietako (Elosu) ekoizpena. Antza denez, Ollerietako lantegiek era nabarmen batean hornitzen zituzten Durango eta Gasteizko hiribilduak, izan ere, biak ziren merkataritza-ibilbideen gune garrantzitsuak (Escribano, 2013). Kontuan hartu beharra dago, XVIII. mendean, Balmaseda eta Durango izan zirela Bilboraino iristeko lekurik garrantzitsuenetarikoak, Pancorbotik Bilbora eramaten zuen bidea Urduñatik pasarazi

zen arte, Bizkaiko Jaurerriko esku-hartze handienetakoa izan omen zena (Gómez-Cambronero Puyuelo, 2003).

Aipatu den moduan, historikoki eta arkeologikoki Durangoko material zeramikoak oso gutxi aztertu izan dira. Arkeologikoki, azterlanak urriak badira ere, arkeometriaren ikuspuntutik oraindik eskasia handiagoa sumatzen da. Existitzen diren analisi gutxi horien artean, nabarmentzekoa da, berriki, *Komentukaleko* zenbait banakoen ezaugarritze arkeometrikoa (Puig, 2016). Hala ere, kontsumo-testuinguru bat izanik, eta ez ekoizpenekoa, ezin izan zen tokiko jatorrik egotzi. Aldiz, Ibabe etnografoari esker, buztingintza lantegiek utzitako zantzua pixkat hobeto ezagutzen dugu (Ibabe, 1995a). Bere ikerketen arabera, bertan erabiltzen zituzten buztinak bi motakoak ziren, eta ia beti langunetik oso gertu kokatutako lekuetatik lortzen ziren. Erauzketa, oro har, azalekoa izaten zen, Durangon 5 metroko sakonera duten putzuak egiten zituztelarik, Gerediagako San Salbador elizatik hurbil (ikus 5.57. irudia). Behaketa honetatik, ekoizpenaren bolumen handia ondoriozta daiteke. Toki batzuetan, buztina hura ateratzen zen lekutik gertu uzten zen urtebetez, eurite, izozte eta abarrekin, lokatza esponjatu eta lan egiteko egokiagoa izan zedin. Beste lan batzuetan jasotzen da, XIX. mendean Bizkarra-Markiegi lantegian ere, bi buztin mota erabiltzen zirela (Lardizabal, 2008). Alde batetik buztin zuria, Matienatik lortzen zena, bertan 10 m-rainoko putzuak zulatzen zituztelarik. Bestalde, gorria, eltze eta pitxerrentzako erabiltzen zena. Antza denez, azken hori lantegitik gertu edota Izurtzako lurretatik ateratzen zuten (ikus 5.57. irudia). Bi buztin motak 4:1 zuri-gorri proportzioan nahasten ziren, eta deskribatu den bezala, zeramikak beiratu zuriekin estaltzen ziren. Batzuetan, aldiz, berunezko beiratuak ere erabiltzen ziren. Bestalde, aipatzen da, Aretxaga eta Mentxakaren lantegiek Matienatik ateratako buztinak erabiltzen zituztela (Lardizabal, 2008).

Lan etnografikoei esker, zeramika ekoizpenaren beste alderdi batzuk ezagutzen ditugu, esaterako beiratuen errezetak. Dirudienez, Mariano Markieguik honako errezetak erabiltzen zituen beiraztatuentzako: 150 kg berun, 20 kg eztainu eta 150 kg harea (Ibabe, 1995a). Kasu honetan, Markiegi anaien tailerretan erabiltzen den labeari buruzko dokumentazioa ere eskaintzen da (ikus 5.58. irudia), egile berdinak Elosun dokumentatutakoaren labe baino pixka bat txikiagoa izanik (ikus 5.70. irudia). Elosuko ekoizpen gunea hurrengo atalean jorratzen da (ikus 5.6. atala).

Lan honetan aztertutako zeramiken bilduman bederatzi labe-tresna daude. Materiala Ibabek berak hartu zuen Gerediaga auzoko partzeletatik eta ondoren Euskal Buztingitza Museoan gordea izan zen. Zeramikazko pieza horiek, Bizkarra-Markiegiren ekoizpenari lotuta daude, arestian aurkeztutako dokumentazio historikoa abiapuntutzat hartuz. Hala ere, esku-hartze arkeologiko ezagatik, ezin da tokiko jatorria hori bermatu, eta soilik proposamen bat egitera mugatzen gaitu. Horrela, labe-lanabesen aztarna kimikoa funtsezko elementu bihurtzen da bertako ekoizpenak, ekoizpen exogenoetaz bereizteko, kasu honetan bereziki, zeramikaren ekoizpenari lotutako erreferentzia historikoak edo egiturak hain urriak direnean.

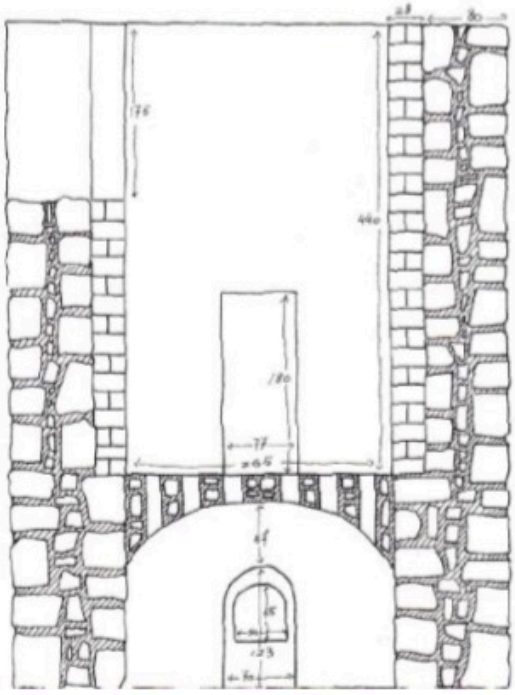

Figure 5.59: Ibabek Durangon dokumentatutako labea (1995). BBK Fundazioa©

Durangoko zeramika lagina

Lan honetarako hautatutako materialen artean (n = 26), bederatzi labe-lanabes, hamabi katilu, aska bat, eltze bat, plater bat, estalki bat eta loreontzi bat daude (ikus B.1 zerrenda B Eranskinean, argazkiak C Eranskinean eta profil arkeologikoak D Eranskinean). Kronologiak 1900-1960 bitartekoak dira, eta horien tipologietan eta erauzitako lurraren muga naturaletan oinarritzen da. Zeramikazko multzoa, zeramika eztainu-berunezko beiratuak barne hartzen ditu, eta zenbait kasutan kolore berdeko dekorazioak erakusten ditu. Gainera, zeramikazko dekorazio bat dago jaspeatu urdinarekin eta beste bat ezti-kolore beiratu zeharrargiarekin. Halaber, labe-lanabesak eta zeramika mikatsuetako bat ez daude estalirik. Aitzitik, gune honetan aurkitutako zeramikazko hiru zatiki mikatsuek, eztainu-berunezko beiratua daramate. Katiluetako batzuek buztingileen markak erakusten dituzte. Zeramika beiratu gehienak soilik barrualdea dute estalirik; horietako hiruk kanpoaldea ere (DUR004, DUR006 eta DUR013).

Esperimentala

Pasten konposizio eta fase mineralogikoak ezaugarritzeko, zeramikazko multzo osoa aztertu zen, ICP-MS eta XRD erabiliz. Gainera, horietako pieza batzuk (n = 15) NAA bidez aztertu ziren eta beste azpi-lagin bat (n = 5), SEM-EDS bidez aztertu zen. Metodologiari buruzko xehetasun gehiagorako ikus 3.3. atala.

Emaitzak eta Eztabaida

NAAren bidezko lehenengo hurbilketa

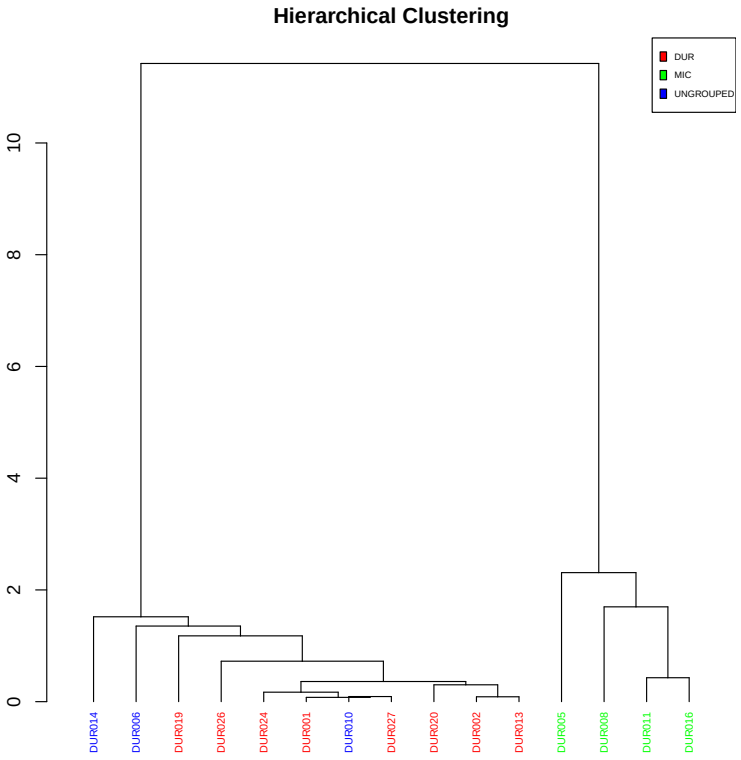

Figure 5.60: Euklidear distantzia karratua irudikatzen duen dendrograma, zentroidearen algoritmoa erabiliz eta NAA bidez aztertutako Durangoko banakoen datuak clr bidez transformatuak ondorengo azpi-konposizioari dagokienak: La, Lu, Nd, Sm, U, Yb, Ce, Cr, Eu, Fe, Hf, Sc, Tb, Th, Zn, Zr, Al, Ba, Dy, Mn, Ti eta V

NAA bidez lortutako emaitzak 5.60. irudian erakusten dira, 15 banakoen hautaketa kontuan hartuz. Zatiki mikatsuen bereizpena nabarmena da, eta gainerako zatikiak,

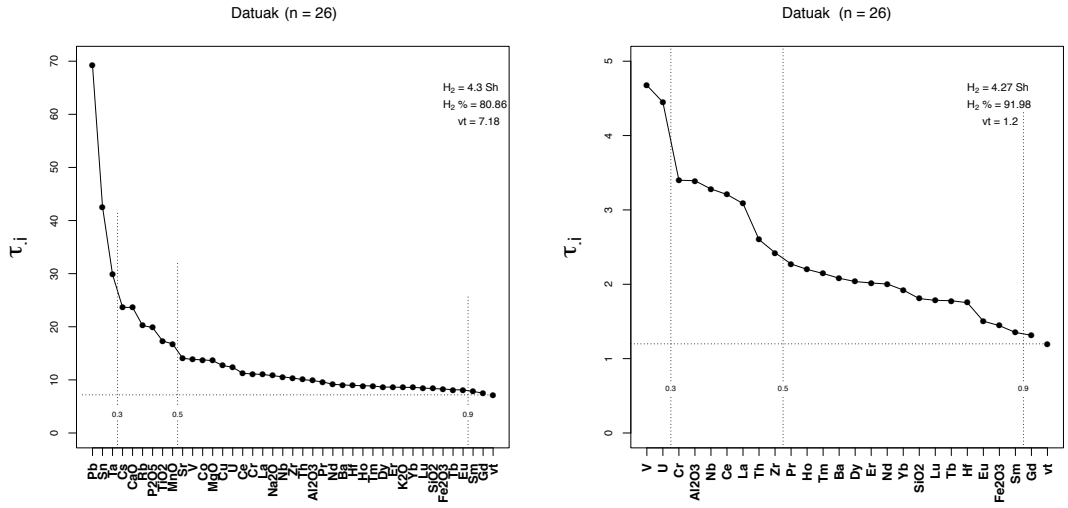

Figure 5.61: Durangoko konposizio-aldakortasunaren matrizea erakusten duen irudikapena ICP-MS bidez lortutako datu guztiekin (ezkerrean) eta soilik esanguratsuak ez diren aldagaiak erabiliz (eskuinean).

berriz, konposizio-bateragarritasun handia erakusten dute. Hala ere, DUR014 eta DUR006 laginek erakutsitako desberdintasun kimikoak oinarri gisa balio dute, DUR multzo nagusiarekin ez bateratzeko. Sailkapen hori neurri handi batean mantendu zen ondoren ICP-MS bidezko analisiek erakutsi zuten bezala, bi banako horiek multzo nagusiarekin bateratu gabe utziz. Aldiz, NAAren bidez DUR010 banakoa multzo nagusiarekin bateratzen da, baina ICP-MS bidez lortutako emaitzak —lagin handiago bat kontuan hartuz—, ez datoz bat multzokatze honekin. Desberdintasun horiek, Zr, Hf, Mn eta MgOren kontzentrazio kimikoen aldakortasunei erantzuten diete.

Durangoko konposizio-multzoak

ICP-MS bidez lortutako konposizio-multzo bakoitzaren batez besteko kontzentrazioak aurkezten dira 5.8. taulan. Azterketa estatistikorako idealki, bariantza analitikoa minimizatu egin behar da iturri naturaletatik sortzen den aldakortasuna adierazteko, eta ez akats esperimentalengatik edota jalkitze-osteko prozesuetan sortzen diren aldaketengatik. Beraz, lan honetan ez ziren hainbat elementu kontuan hartu estatistika-analisirako: Pb, Sn, Na_2O, K_2O, Rb, Co, Ta, Zn eta Cu. Horiei buruzko eztabaida eta xehetasun gehiagorako ikus 5.1. kapituluaren hasieran. Era berean, Cao eta Sr zenbait murrizketarekin erabili ziren.

Element	DUR	SD	DUR-MIC	SD
Al_2O_3	17.2	1.2	26.9	0.4
CaO	11.7	2.6	2.3	0.3
Fe_2O_3	5.2	0.3	3.8	0.1
K_2O	2.1	0.2	2.2	0.1
MgO	1.39	0.31	1.03	0.17
MnO	0.067	0.03	0.032	0.002
Na_2O	0.65	0.18	0.31	0.1
P_2O_5	0.2	0.18	0.13	0.03
SiO_2	63.9	5.5	68.4	2.5
TiO_2	0.75	0.05	0.14	0.01
Ba	439	42	206	1
Ce	83	4	26	1
Co	101	44	114	33
Cr	84	6	42	27
Cs	12	2	36	2
Cu	43	23	39	28
Dy	4.7	0.3	5.8	0.4
Er	2.4	0.1	2.9	0.2
Eu	1.3	0.1	0.8	0.1
Gd	5.9	0.3	5	0.1
Hf	6.6	0.9	3.8	0.1
Ho	0.72	0.04	0.94	0.07
La	43	2	14	1
Lu	0.43	0.04	0.48	0.05
Nb	25	4	36	2
Nd	37	1	16	1
Pb	1474	1401	124	74
Pr	10	0	4	0
Rb	175	18	545	5
Sm	6.6	0.3	4	0.2
Sn	(9-381)*		93	3
Sr	316	154	128	7
Ta	2.6	0.4	16	1.3
Tb	0.83	0.05	0.94	0.04
Th	15	1	5	0
Tm	0.43	0.03	0.55	0.04
U	3.6	0.3	7.7	1
V	84	10	25	4
Yb	2.5	0.1	3	0.3
Zn	117	75	55	14
Zr	239	37	105	6

Table 5.8: Durangoko konposizio-multzo bakoitzaren ICP-MS bidez lortutako kontzentrazio kimikoen batez bestekoak eta desbiderapen estandarrak (SD). Unitateak μg/g dira eta oxidoen kasuan masa %-ak aurkezten dira. (*) Pb eta Sn-rentzat kontzentrazio tarteak ematen dira SDak batez bestekoak baino handiagoak diren kasuetan.

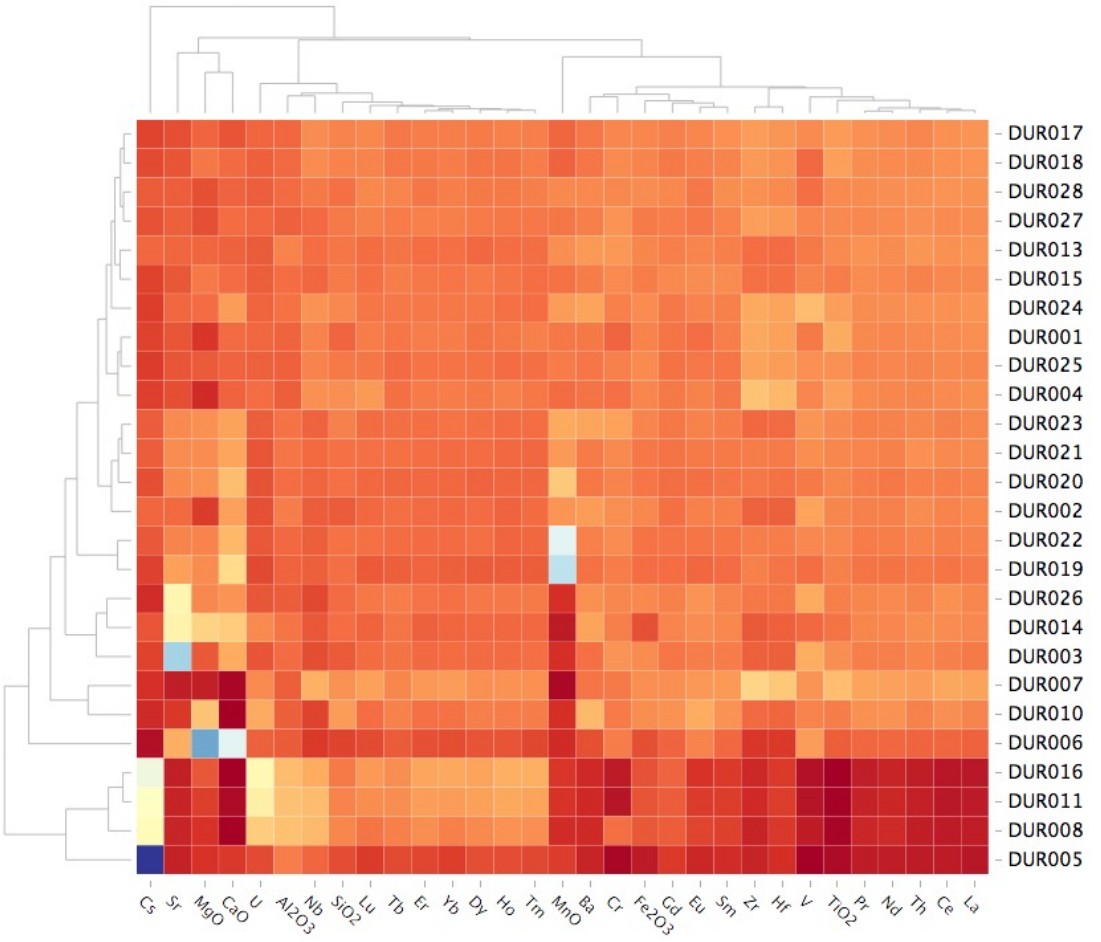

Figure 5.62: Durangoko bero mapa zeramiken konposizio kimikoetan dauden desberdintasunak adieraziz, kolore-gradientearen arabera (kolore hotzek kontzentrazio altuak adierazten ditu eta beroek kontzentrazio baxuak.

Lehenik eta behin, konposizio-heterogeneotasuna ebaluatu zen konposizio-aldakortasun matrizea (CVM) kalkulatuz, elementu bakoitzak datu-multzoan sartutako aldakortasunari buruzko informazioa ematen duena (ikus 5.61. irudia). Oro har, aldakortasun-totalaren (vt) balio handi batek aldakortasun datu multzoa poligenikoa dela iradokitzen du, hau da, hainbat konposizio-multzoren presentzia. Aitzitik, balio txiki batek datu-multzoaren izaera monogenikoa adierazten du (Buxeda i Garrigós and Kilikoglou, 2003). Kasu honetan, lortutako vt balio hori oso altua da (7.18), eta horrek agerian uzten du arestian aipatutako elementuen ekarpen handia. Aldiz, beherakada handia jasaten du, 1.2-ra, elementu horiek baztertzerakoan.

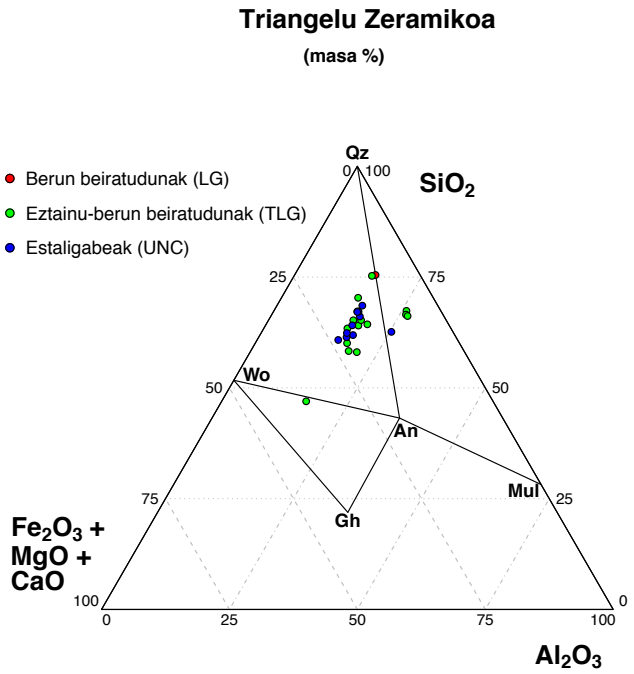

Figure 5.63: Diagram hirutarra Fe_2O_3+MgO+CaO - Al_2O_3 - SiO_2 sistema erakutsiz Durangoko 26 zeramika-zatikiei dagokienak. An:Anortita, Gh:Gelehenita, Mu:Mullita, Qtz:kuartzoa, Wo:Wollastonita. Laburdurak Whitney and Evans (2010), ondoren.

Diagramaren hirutarraren arabera (ikus 5.63. irudia), lau zatiki mikatsuak nabarmenki bereizten dira Al_2O_3 eta SiO_2 kontzentrazio altuagoengatik. Horrela, anortita-kuartzoan-mullita triangeluan agertzen da. Hala ere, mikatsuen artean alde nabarmena dago: beiratu gabe eta eztainu-berunarekin beiratuen artekoa (DUR005).

Horrelako pasta mikatsuak daramaten piezen jatorria Zamorarekin lotuta egon ohi diren arren, kasu honetan eztainu-berunezko beiratua Euskal Herrian aplikatua izan zitekeela iradoki da (Escribano, 2013). Bestalde, berunezko beiratua duen zeramika bakarra (DUR007) ere triangelu honen mugan dago. Gainerako piezei dagokienez (beiratuak eta beiratu gabeak), batez ere, wollastonita, kuartzo anortita, triangeluan aurkitzen dira, eta, gainera, CaO kontzentrazio oso altua duen zatiki bakarra DUR006, (CaOren masa % 25) gehlenita, anortita, wollastonita triangeluaren barruan geratzen da.

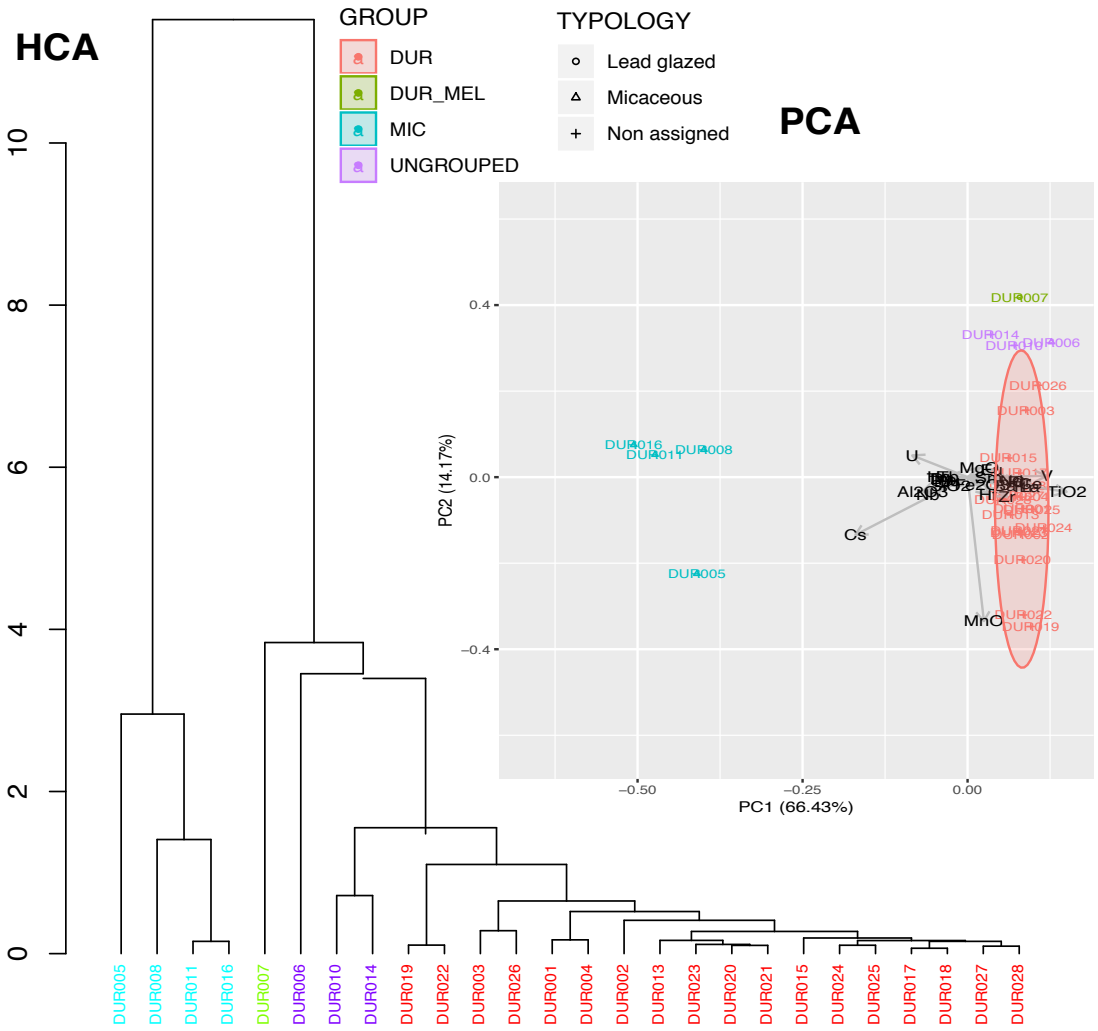

Figure 5.64: Euklidear distantzia karratua eta zentroidearen algoritmoa erabiliz lortutako dendrogram. Datuak ICP-MS bidez aztertutako Durangoko 26 Ic-ei dagokie, clr bidez eraldatuta hurrengo azpi-konposiziorako: Al_2O_3, Zr, Nb, Cs, Ba, La, Ce, Pr, Nd, Eu, Sm,Tb, Gd , Dy, Ho, Er, Tm, Yb, Lu, Hf, Th, U, TiO_2, V, Cr, MnO, Fe_2O_3 and SiO_2. PCAan alr eraldaketa aplikatu zen Gd zatitzaile gisa erabiliz.

PCA eta HCA burutu ziren mihiztatze zeramikoaren konposizio-multzoak identifikatzeko (ikus 5.64. irudia). Alde batetik, emaitzek konposizio-multzo nagusi bat (DUR) identifikatzea ahalbidetu zuten. Bestalde, konposizioaren ikuspegitik oso bereizgarriak ziren pasta mikatsuak dituen MIC multzoa definitu zen. Multzo horretako banakako batek (DUR005), besteekiko desberdintasun nabarmenak erakutsi zituen. Gainera, DUR007 adierazpen estatistiko guztietan bereizten da, CaOk eta Fe_2O_3k

ageritako kontzentrazio baxuen ondorioz. Zatiki honek berunezko beiratu bat dauka pasta gorrixka baten gainean (DUR-MEL). Bestalde, aztertutako zatiki batzuk ezin izan ziren multzoren bati esleitu. Halaber, beren artean konposizio ezberdinak aurkezten zituzten, beraz multzokatu gabe geratu ziren. Alde batetik, DUR006 jaspeatu urdina erakusten duen zeramika bakarra da. Bestetik, DUR010, eztainu-berunezko beiratuaren dekorazio partziala agertzen duen tapa bat da. Gainera, belarri hiru-gilgilduna erakusten duen goporrari dagokio DUR014. Kontuan izan behar da, ikuspuntu tipologikotik, zeramika horiek guztiz desberdinak direla. Laburbilduz, bi multzo definitu ziren aztertutako datu-multzoaren barruan: DUR eta DUR-MIC. Denak eztainu-berunezko beiratuekin estalirik, DUR005 izan ezik.

DUR

Multzo hau 18 zatikiez osatuta dago, labe-lanabes zati handi bat barne hartzen duelarik (9/18). Multzoa karedun pastek ezaugarritzen dute (CaO 11.7 ± 2.6 masa %). Gainera, 17 ± 1.1 masa % Al_2O_3 eta 2 ± 0.2 masa % Fe_2O_3-ko kontzentrazioak erakusten ditu. DUR019 eta DUR022 zatiek barne-aldakortasuna nabarmenki igotzen dute (ikus 5.62. irudia) MnO oso kontzentrazio handiak dituztelako (0.150 masa % eta 0.134 masa %, hurrenez, hurren). Balio horiek bikoiztu egiten dute DUR multzoaren batez besteko kontzentrazioa, alegia, 0.067 ± 0.03 masa %.

Durangoko mihiztatze zeramikoan bi labe tresna mota nagusi identifikatu ziren (ikus 5.65. irudia). Lehenengoa trebera bati dagokio, Urduñako, Logroñoko eta Elosuko ekoizpenetan ikusi direnen antzerakoak. Bigarrena, berriz, matoi[6] bati dagokio, eta Elosun agertu direnaren antzekoa da. Matoiak, labean bertikalki ipintzen diren zilindro-formako pieza hutsak dira, labearen barrualdean pisu desberdinak eraikitzeko erabiltzen zirenak. Erreketa bakoitzaren premien arabera erabil daitezke, erretzen diren objektuen tamaina kontuan hartuta.

Pieza apainduei dagokienez, multzo honetan eztainu-berunezko estaldura beiratuak aurkitzen dira, eta formei dagokienez, baxera eta platerak dira nagusi. Katiluetako batzuek motibo geometrikoak erakusten dituzte, eta beste batzuek, berriz, Markiegi buztingileen markari lotuta egon daitezkeen beste bi marra (ikus 5.66. irudia). Beiratuak SnO_2 opakutzailearen bidez lortu ziren eta kolore berdeak, CuO erabiliz (ikus A.10. taula).

Multzo honetan bi ehundura mota daude, F-I eta F-II. Lehena, F-I (n = 4), kuartzo eta feldespato alkalinoak erakusten ditu (ortoklasa erakusten da) plagioklasa bezalako erreketa faseekin batera (anortita erakusten da). Gainera, ehundurak kaltzita, hematitea eta igeltsua erakusten ditu. Mineral horiek guztiak batera egoteak, illita-muskovitarekin batera, EFTa 850-900°C-tan kokatzen du (DUR001 difraktograma

[6]Frantzesez, *tuyere*; ingelesez, *kiln-tube*; eta gaztelaniaz, *bodoque* bezala itzultzen da.

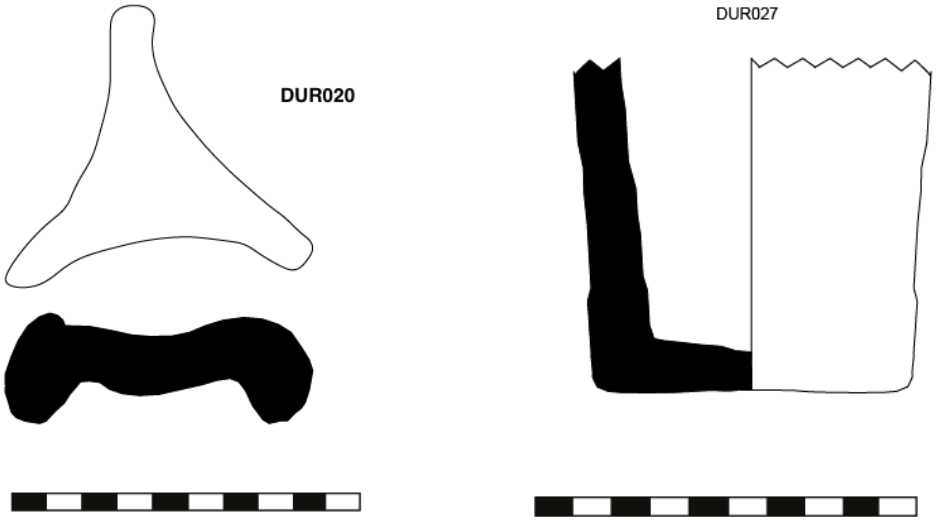

Figure 5.65: Durangon erabilitako labe-lanabesen profil arkeologikoak. Trebera bat (ezkerrean) eta matoi bat (eskubian).

erakusten da ehundura honen eredu bezala 5.68. irudian). Gainera, EFT horrekin bat datorren sinterizazio maila baxu bat erakusten du mikroegiturak (ikus 5.66. irudia). Dena den, DUR multzoko zeramika gehienek F-II motako ehundura dute. Ehundura honen fase mineralogikoen zati handi bat kuartzoa, kaltzita eta gehlenita da. F-I ehundurarekin alderatuta, CaO-ren kontzentrazio handiagoa erakusten dute zeramika gehienek. Horrek azal lezake kaltzioaren presentzia eta bere azpiproduktua den gehlenita izatea. Gainera, plagioklasen presentzia handiagoa eta piroxenoen identifikazioa EFTa 950°C-etan kokatzen dute. Tenperatura horien arteko ezberdintasunak ez dira nahitaez erreketa teknologiaren isla zuzena izan behar. Kontuan hartu beharra dago, labearen barruko tenperatura-gradientea egoera mineralogikoen erantzule ere izan daitekeela, hala nola jatorrizko balizko sendogarrien gehitzea ere.

Ehundura mota bakoitzari dagozkion SEM-EDS irudiak ikus daitezke 5.66. irudian. Lehenak, hainbat kuartzo pikor eta burbuila ugariko beiratu bat erakusten du. Besteak berriz, beiratu homogeneo bat erakusten du.

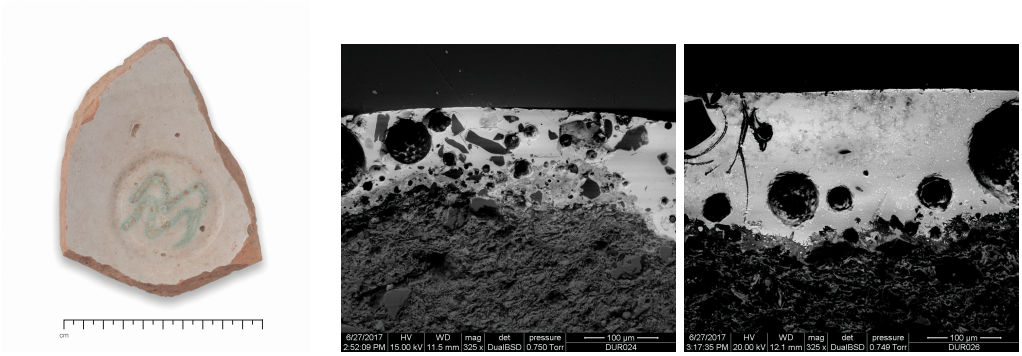

Figure 5.66: DUR multzoko eztainu-berunarekin beiratutako katilua berdez apainduta, eta DUR024 (F-I) eta DUR036 (F-II)-ren SEM-EDS irudiak beiratua eta gorputz zeramikoaren interfazea erakutsiz.

DUR-MIC

DUR-MIC multzoa hiru zatikiek osatzen dute. Zeramika mikatsuaren ohiko ezaugarri kimikoak aurkezten dute, horrela, Al_2O_3 kontzentrazio altuak erakutsiz (26.9 $\pm$ 0.4 masa %). Halaber, gainerako zatikiek baino hiru aldiz Cs kontzentrazioa altuagoak erakusten dituzte. Gainera, elementu hauetarako kontzentrazio handiagoak erakusten dituzte: U, Nb, SiO_2, Lu, Tb, Ho, Tm, Dy, Er eta Yb. Aitzitik, honako elementuetarako kontzentrazio baxuagoak erakusten dituzte: Sr, MgO, CaO, MnO, Ba, Cr, Sm, Eu, Fe_2O_3, Gd, Zr, Hf, V, TiO_2, Pr, Nd, Th, La eta Ce. Desberdintasun kimiko horiek argi eta garbi behatu daitezke bero mapan (ikus 5.62. irudia).

Euskal Herrian eztabaida arkeologiko ireki bat dago horrelako zeramika mikatsuen jatorriari buruz. Lehenago aipatu dugun bezala, sukaldeko zeramikak ekoizteko propietate erregogorrak behar dira, hala nola, buztin mikatsuak eskaintzen dutenak bezala). Izan ere, buztin horiek, bizitza baliagarrian zehar espero diren berotze-hozte-zikloekiko erresistentzia handiagoa erakutsiko dute.

Euskal buztinak, oro har ez dira egokitzen behar hauetara (Lardizabal, 2008), eta horregatik, mendeetan zehar beste gune batzuetatik ekarri izan dira horrelako piezak (Solaun, 2005). Are gehiago, beste leku batzuetatik ekarritako produktu horien agerpenak, guztiz eragingo zuten XIV. mendeetako merkatuan. Horrenbestez, atzerriko ekoizpenen eskari eta kalitate handiagoaren aurrean, Euskal Herriko buztingintzako jarduera hori pixkanaka baztertuko zuten. Prozesu honen adierazpiderik onena Zamorako eltze famatuak dira, XVIII. mendean Euskal Herriko sukalde-zeramikaren merkatuaren zati zabal bat osatzen baitzuten (Solaun, 2005).

Beraz, literaturaren arabera, zeramika horien jatorririk seguruena Zamoran izango litzateke, 378 km-ra kokatuta dagoen zeramika-ezkoizpen handiko hiribildua, hain zuzen. Ildo horretan, Urduñan aurkitutako zatiki bat (ORD056) DUR-MICen tankerako beiratua aurkezten du. Egile batzuek atzerritik ekarritako piezen gainean estaldura beiratuak euskal lantegietan aplikatu izan zitezkeela iradokitzen dute (Escribano, 2013). Hala ere, hipotesi hori oraindik ez da baieztatua izan eta ikerketa gehiago burutu beharko litzateke. SEM-EDS analisiek erakutsi duten moduan, beiratuek inklusio txiki asko dauzkate, baita burbuilak ere (ikusi 5.67. irudia). Gainera, zeramika gorputzaren eta beiratuaren arteko elkarrekintza baxuak ikusita, argi adierazten dute beiratua bizkotxoaren gainean aplikatu zela, alegia, bi urratseko teknologia erabiliz.

XRD emaitzek, konposizio-multzo honetarako ehundura bat erakutsi dute (F-I), pasta mikatsuak tamaina handiko inklusioak dituena (mm-ko ordena). Difraktogramaren arabera (ikus 5.56. irudia), klorita-bermikulita-montmorillonita edo biotita faseak identifikatzen dira, hala nola, beste filosilikato batzuk, nefelina eta flogopita ere (ikus 5.9. taula). Ilita-muskobita faseak, feldespato alkalinoekin (ortokasa erakusten da) batera agertzeak EFT a 850-950 °C-etan kokatzen du. Tenperatura horietara iritsitako sinterizazio baxua agerikoa da gorputz zeramikoan (ikus 5.67. irudia).

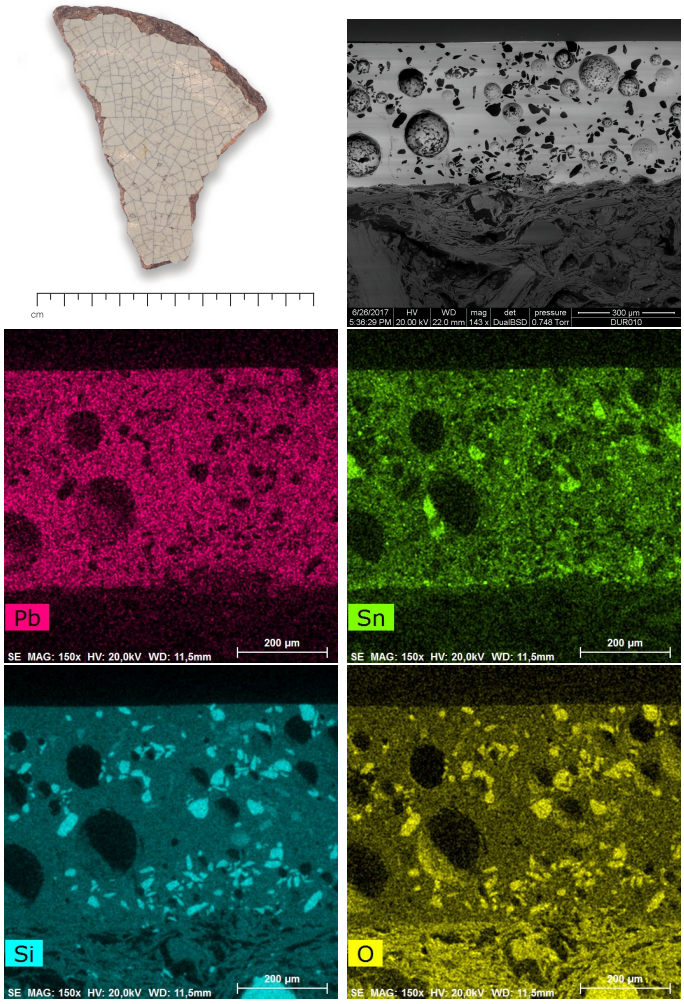

Figure 5.67: DUR-MIC Multzoa. Eztainu-berunezko beiratua duen zeramika (DUR008), eta SEM-EDS irudiak beiratua eta gorputz zeramikoaren arteko interfazea erakutsiz.

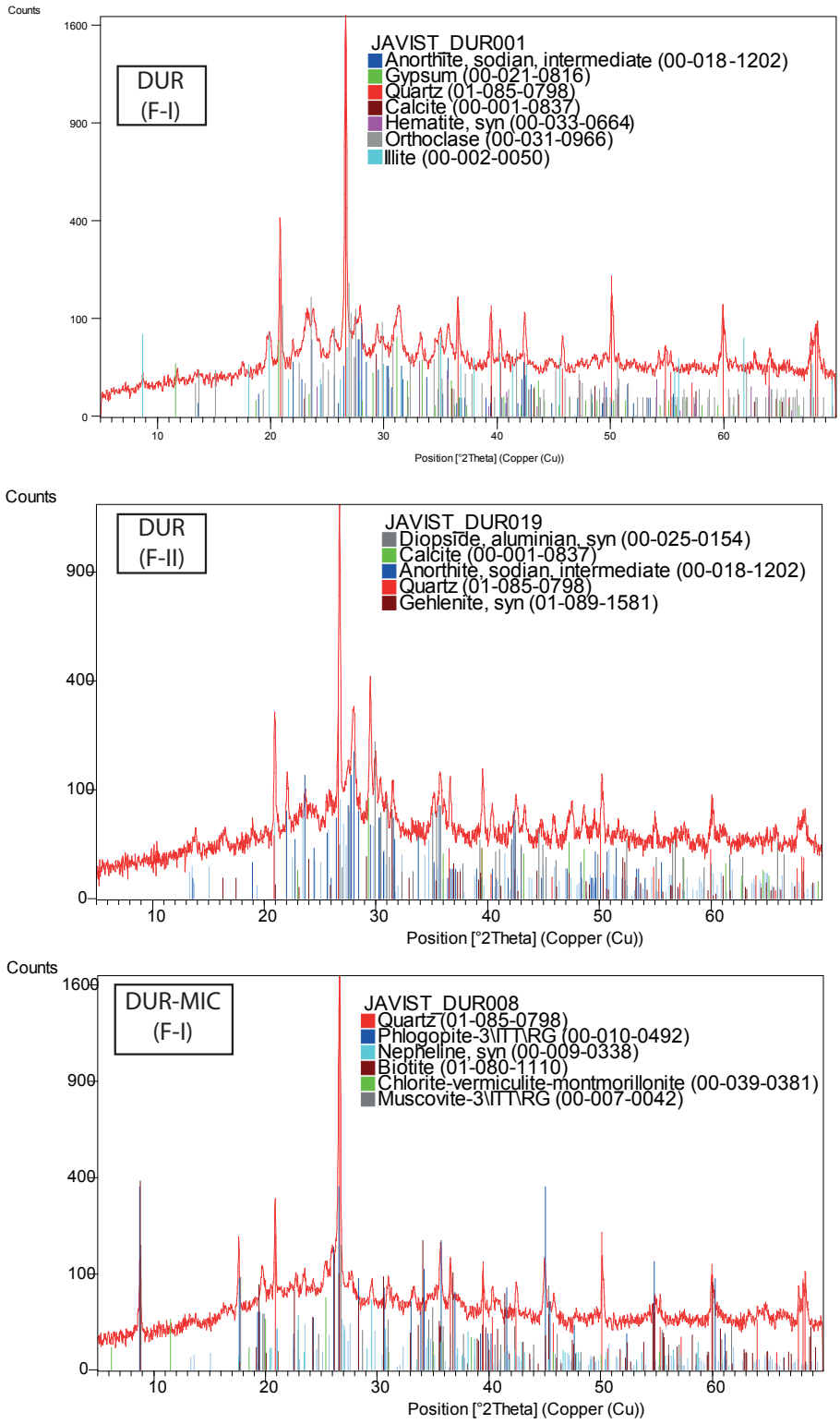

Figure 5.68: DUR eta DUR-MIC multzoen XRD difraktograma adierazgarriak.

MULTZOA	Fab.	ANID	EFT (°C)	Qz	Ilt-Mus	Afs	Cal	Gh	Hem	Pl	Px	Gy	Phyllo-Si
DUR	F-I	DUR001	850-900	x	x	x	x		x	x		x	
	F-II	DUR019	950	x			x	x		x	x		
DUR-MIC	F-I	DUR008	850-950	x	x	x							x

Table 5.9: Durangoko multzoan identifikatu diren konposizio-multzo bakoitzaren ehundura desberdinak. Qz: Quartz; Ilt-Ms: Illita-Muskobita; Afs: alkali-feldspatoak; Cal: Kaltzita; Gh: Gehlenita; Hem: Hematitea; Pl: Plagioklasak; Px: Piroxenoak; Mul: Mulita. Laburdurak (Whitney and Evans, 2010) ondoren. Phyllo-Si multzoa (filosilikatoak): nephelinea, phlogopitea, klorita-bermikulita-montmorillonita, biotita, enstatita, ortoklasa).

Multzokatu gabeko banakoak

Lehen aipatu den bezala, zatiki horietako lauk ezin dira esleitu identifikatu diren bi multzo nagusiei, DUR005 delakoa barne, DUR-MICekin bateragarria ez dena. Zatiki horrek itxura desberdina erakusten du beste zati mikatsuen aldean. Gainontzekoak beiratuta daude eta pasta ilun bat dute, DUR005, berriz, beiratu gabeko kolore argiko pasta. Gainera, bi eraztun zentrokide dituen dekorazio baten aplikazioa erakusten du. Alde batetik, DUR006, Durangoko datu multzoari dagokionez, MgO kontzentrazio handiagoa aurkezten du (5.00 masa %). Gainera, bere CaOren kontzentrazio altua ere nabarmentzekoa da (25 masa %). Konposizio desberdinaz haratago, jaspeatu urdineko dekorazio bat aurkezten du, horrelako apaindura daraman bakarra izanik. Lehen aipatu dugun bezala, DUR007 kare gutxiko pasta dauka eta berunezko beiratu zeharrargi bat erakusten du, alegia, Durangoko mihiztatzean identifikatutako ezti-koloreko beiratua erakusten duen bakarra izan da. Bestalde, DUR multzoaren kontzentrazioak kontuan hartuz (MgO 1.39 $\pm$ 0.31), DUR010 eta DUR014 banakoek MgO kontzentrazio altuak erakusten dute (2.22 masa % eta 2.46 masa %, hurrenez, hurren). MgOren kontzentrazioez harago, ICP-MS emaitzek bi zeramika horien aztarna kimiko desberdindua adierazi dute (ikus 5.64. irudia).

Eztabaida eta Ondorioak

Burututako ikerketa honek, Durangoko ekoizpen-zeramikoei buruzko lehen hurbilketa arkeometrikoa litzateke. Bertan ekoizpenari lotutako material ugari nabarmentzen dira (adibidez, treberak edo matoiak). Erreferentzia historikoen arabera, Durangoko lantegietako zeramikak ekoizteko Gerediaga auzoko buztin-iturrien ustiapen luzeaz hornitu dira. Aztarnategi honetan ekoizpen zeramikoaren ebidentzia ez-zuzen ugariarekin alderatuz, orain arte oso material gutxi aurkitu da, tokiko zeramika ekoizpenarekin zuzenean lotuta egon litekeena.

Lan honetan, 26 zatikien ezaugarritze arkeometrikoaren bidez bi konposizio-multzo identifikatu dira. Alde batetik, DUR multzoa (n = 18), non piezen erdiak labe-tresnak diren. Horrela, multzo hau tokiko jatorriari lotuta egon liteke, XX. mendeko zeramika-ekoizpenari dagokionez. Gainera, ustiapen-iturriaren kokapen finkoak DUR multzoaren aztarna kimikoa kontuan hartzeko aukera ematen du, aurreko mendeetako zeramikak aztertzeko erreferentzia gisa, oraindik deskubritzeke daudenak. XRDren analisien arabera, EFTak 850°C eta 950°C artean kokatzen dira, eta, zentzu horretan, bi ehundura mota identifikatu dira DUR multzoan. Gainera, SEM-EDS analisiak, kasiterita opakutzaile gisaren erabilera erakutsi dute. Koloreei dagokienez, berdea baino ez da identifikatzen, eta CuOn oinarritutako pigmentuen erabilera erakusten du. Gainera, DUR-MIC multzoa definitu zen, eta horren jatorria Zamorari esleitu zaio, zeramika mikatsuak inportatzeko tradizio luzearen arabera (Solaun, 2005). Kasu berezi honetan, zeramika mikatsuak eztainu-berunez beiratu diren, baina oraindik ez dakigu estalki horiek lokalki aplikatu diren ala ez.

5.6 Archaeometric characterization of pottery from Elosu

Abstract

Elosu, which belongs to the town of Legutio (The Basque Country) and is located 20 km north from Vitoria-Gasteiz, hosts the district called Ollerías (which means pottery workshops). The toponymy of the district clearly reflects its historical pottery manufacturing tradition, which according to the historical documentation, was articulated in different workshops and has been very active during centuries until the construction of a dam in 1958, which totally covered the clay source from which the potters were supplied. The center produced the so called Basque Traditional Pottery, characterized by tin-lead glazes partially covering the ceramic pieces. In the present work, 51 ceramics from this site, including tableware and kiln utensils and dating back from the 18^{th} century until the ceasing of the activity, were archaeometrically characterized. The multi-analytical approach consisted on the evaluation of the pastes by ICP-MS, NAA and XRD and the evaluation of the glazing technology by means of SEM-EDS. The results revealed one main ceramic group (ELS) that could be linked to the local production of Ollerías. The compositional group, which covers the ceramics production of more than two centuries, showed internal differences in CaO, which could be linked to the mixing of the clays documented in the literature. Nonetheless, the diachronic evolution showed marked differences regarding the glazing technology as well as new typologies. This modification was given after a disruption of the ceramic production caused by the Spanish Civil war, after which the potters had to adapt their production to continue obtaining white glazes, but with the scarcity of metals such as tin. In consequence, the use of slips was introduced.

Background

Elosu is one of the councils from the town of Legutio (Alava, The Basque Country) and includes the district of Ollerías, which as its toponymy reflects, has an historical pottery production tradition. In comparison to the previously studied cases in this doctoral thesis, Elosu did not have any strategic location regarding its location or topography which would had given the place a relevant geopolitical role. In contrast, it had the ingredients for hosting an intense pottery activity during centuries, which made this place one of the most active centers of The Basque Country during the preindustrial period. On the one hand, the geological outcroppings of the site involved the abundance of clay sources that were suitable for pottery manufacturing. On the other hand, the urban nucleus did not experienced any important growth. Thus it did not find any restriction to the proliferation of the ceramic workshops.

Note that, as mentioned in the case of Logroño, pottery production had been regarded as a nuisance activity during different periods of the history, especially in the Modern Period. Therefore, usually was carried out be in the outskirts of the urban nuclei (e.g in Roman times *Lex Ursonensis*, Montelupo, Seville...).

Ollerías manufactured in its workshops the so-called Traditional Basque Pottery, which is characterized by tin-lead partial glazes on reddish decanted pastes. The forms included typologies for household or tableware. For instance, the famous *pedarra* or *pegarra*, which is a recipient with a little tube which for water transportation. The ceramic form was designed to bring it over the head and such task was carry out mainly by women. The relevance of such ceramic typologies remain in the collective memory and are still used in artworks nowadays (see the mural paining carried out in 2018 in Vitoria-Gasteiz in Figure 5.69). On the basis of historical and ethnographic data, the district of Ollerías of Elosu, along with Egileta and Hijona, was among the most important pottery production centers of the Basque Country in the pre-industrial period (Escribano, 2014).

In addition, its location ensured a regional network for trading. For instance, 20 km separated Elosu from Vitoria-Gasteiz and 29 km from Durango. Thus, the productions from this site were extensively consumed in both places, as documented in the literature. Indeed, the productions from Ollerías were archaeologically characterized based on the consumption materials recovered in the sites from Vitoria-Gasteiz and Durango (Escribano, 2013). Along these lines, this is a reflection of the important distributions that the products from Ollerías had at a regional level.

The district, had several pottery workshops, including several kilns that were active until the arrival of the Spanish Civil War (1936-1939), where the production was disrupted (Ibabe, 1995a). Later on, the creation of a water dam completely covered the clay extraction sites from which the workshops were supplied, involving the permanent cessation of the traditional Basque pottery production. Nowadays, the district of

Figure 5.69: Mural painting "La Pegarra" by Manolo Mesa in Errekaleor neighborhood of Vitoria-Gasteiz, painte in 2018. Asier Iturralde Sarasola .

Ollerías hosts the Museum of Basque Pottery run by Blanka Gómez de Segura, in which the only ceramic kiln that still stands can be visited (see Figure 5.70).

Previous Ceramologic Studies

From ethnographic view, the beginning of the popular pottery activity in Elosu is established in the 18^{th} century (Ibabe, 1995a). Nevertheless, some historians relate the

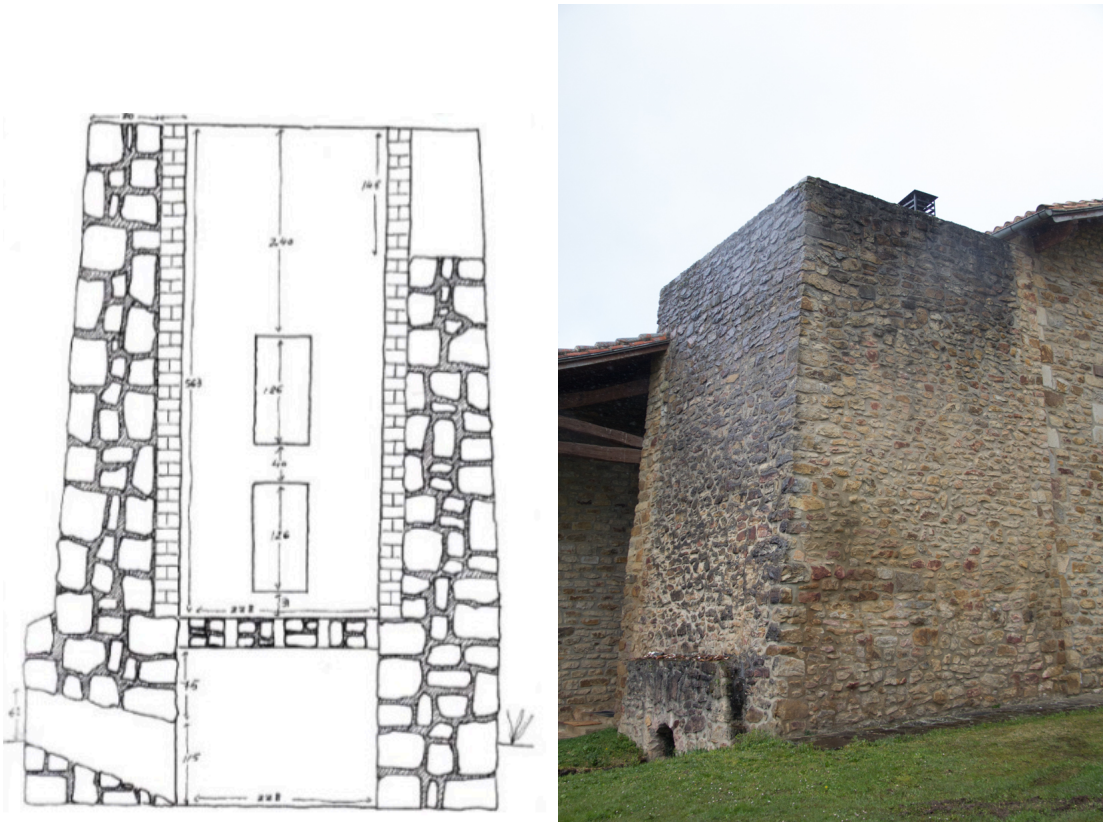

Figure 5.70: Ceramic kiln of Elosu documented by (Ibabe, 1995a) (left), Fundación BBK© and photo of the current status (right), E. Calparsoro

village of Olleros cited in the *Reja de San Millán*[7] with the current Ollerías district in Elosu, which implies that the ceramic tradition of this place could date back to the 11^{th} century.

The production of certain type of ceramics characterized by decanted micaceous pastes has been ascribed to Ollerías in the literature (Solaun, 2005). The geological compatibilities of the Ollerías area, which presents alluvial and alluvial-colluvial soils belonging to the flood basin of the Santa Engracia river, were taken as a basis to ascribe the Group V to a local origin (Solaun, 2005). Seemingly, although the production of this group dates back to the 8^{th} century, its consumption became widespread in the 12^{th}century and achieved the highest rate in the ceramic register as early as the 13^{th}century lasting during the late Medieval period (Solaun, 2005). In the 16^{th} and 17^{th} centuries, parallel to the increase in number of glazed types, and as a

[7]A document written in 1025 with a list of towns in Alava that gave the monastery of San Millán certain iron bars as a tribute. It involves the earliest register of the names of the town of Alava

direct consequence of this situation, the percentages observed of the Group V, but it remained as one of the main types with a continuous production at least until the 18^{th} century (Escribano, 2014).

The use of tin lead glazed ceramics in Alava dates back to the 16^{th} century, whereas in Ollerías, lead glazed ceramics would have been manufactured since the 15^{th} century (Escribano, 2013). Beyond the Group V of micaceous ceramics identified in the work from Solaun (2005), further ceramic groups were archaeologically ascribed to the local production of Ollerías in the of 14^{th} -17^{th} centuries (Escribano, 2014): Glazed ceramics of undecanted and micaceous sandy pastes (Group XXXVII), glazed ceramics of decanted red pastes (Group XXXI) and ceramic of reddish-orange pastes with abundant carbonates and glazed in white (Group LVI).In addition, the production evidence recovered in this site indicated that this pottery workshop was dedicated to produce ceramics either with lead glazes or with tin glaze, sometimes decorated in green and, very likely, to apply this same cover to the ceramics of Zamoran origin (Escribano, 2009).

The documentation we have about the current existing kiln and its functioning is mainly thanks to Ibabe (1995b,a), but also to Blanka Gómez de Segura, who spend 15 years learning the craft with the last preindustrial potter, Jose Ortiz de Zarate. Regarding the only ceramic kiln preserved, its construction dates back to 1711. It is of 9 m of height and quadrangular base and includes two chambers. The first one on the upper part for firing and the second one, underground with brick cladding for combustion purposes. The main chamber is rigged by masonry and has two different accesses to load the ceramics from the lower part to the upper part, which is open. On the top, ceramic remains wastes were used to protect the ceramic pieces during the firing. In the busiest periods, up to 8000 ceramic pieces were introduced every two months. For the combustion the bushes of *Ulex Europaeus*[8] were loaded under control, which provides a rapid combustion. The firing process was controlled by one professional who would be in charge of checking the firing conditions such as temperature, atmosphere, time, etc. in an uninterrupted period of 20-24 hours approximately. Once it was verified that the pieces were well fired, the kiln was turned off, covering the mouth of the chamber, with adobe or with an iron plate. This also prevented the entry of fresh air that could spoil the fired pieces. It could take up to 5-6 days both to load the kiln with the unfired pieces and to unload it, so that it could have enough time to cold down. In every firing, there could be approximately 20% of defective pieces (also called as "reuses"). These defective pieces, were normally kept out from the selling ones, therefore, their presence is an indicative of the local production. Nevertheless, in the cases of Elosu, the interchange of the lower quality pieces for other goods (e.g. apples), were carried out. Some potters had the habit of celebrating the end of the batch with a "festive meal". The clays were extracted from the same area, and the kiln has served to fire the ceramics manufacture in the different workshops located in Ollerías, as not all of them could afford to have a kiln.

[8]Known as *ote zuri* in Basque and *argoma* in Spanish

The last known preindustrial potter in active was José Ortiz de Zarate, who learned the craft from his family. The civil war lashed severely the area of Elosu, damaging the kiln and the attached farm. Along these lines, the potter activity suffered a disruption which was only recovered after 1941. Later on, the provision of tin from Cornwall was interrupted or diminished, and priority was given for the manufacture of arms. However, the traditional white glazes were replaced by the introduction of a slip. The clays for the slips were obtained from Miribilla area in Bilbao, from where iron was extracted in the metallurgy. The potter's activity was considered second class job after mining. Thus, the potters could extract the scarce and white clays which would appear in the geologic veins during the free of the miners (Ibabe, 1995a).

With regard to the archaeometric characterization, certain aspects that can hinder the proper interpretation must be taken into consideration. For instance, the mixing of the clays can have a direct influence on the compositions of the pastes. In the case of Elosu, ethnographic works reported the mixing in the respective proportion 25/75 of two types of clays: the so-called "white" (high calcareous) and "red" clays (Ibabe, 1995a, p. 16). Whereas, the red clays were extracted nearby the ceramic kiln, the white ones were obtained from Miribillla (Bilbao).

In addition, other centers, such as Narbaiza or Amorebieta-Etxano, also used the same clays (Ibabe, 1995a, p. 81). This fact could lead to confusion because several workshops could have a very similar chemical fingerprint. In consequence, the whitish productions that can appear in Elosu must be regarded with caution.

Moreover, seemingly, in after the flooding of the clay source in Elosu, Jose Ortiz de Zarate tried to continue the activity by carrying the clays from Navarrete (located in La Rioja and separated by a distance of 93.5 km), but the increase of transportation costs, the uncomfortable situation and other circumstances made him close the workshop definitively (Martínez Glera, 1994). Finally, he shifted forcedly his work to cattle breeding, however, he followed teaching until he died in 2008. Nowadays, in the National Pottery Museum of Chinchilla from Montearagón (Albacete), his pieces can be consulted (as of course, in the Museum of Ollerías in Elosu. Other potters from Elosu, such as Garmendia or Fernandez of Larrinoa families opted to move to Narbaiza (located 20 km west from Elosu). In consequence, this regional mobility of potters, could hinders the process of the characterization of local pottery production.

With awareness of the issues posed before, the collection of 51 ceramics collected nearby the current Museum of Basque Pottery were subjected to archaeometric characterization in order to provide a chemical fingerprint which could serve as a reference for future studies involving the pottery production of Elosu.

Ceramic sample of Elosu

The set of ceramics (n = 51) consists mainly of white plain glazed pieces of tableware (17 bowls, 13 kiln utensils, 10 flowerpots, 7 plates, 1 fired paste, 1 vase and 2 undetermined pieces). The detailed can be consulted in the Table B.1 of the Annex B, as well as the photographs in the Annex C and the archaeological profiles in the Annex D. Chronologically they range from the 18^{th} century until 1960 approximately (coinciding with the cessation of the activity. The ceramics were glazed completely in the interior and either completely, partially or unglazed in the exterior. Among the sherds, 15 contain slip, and were ascribed to the period after the Spanish Civil war, that is from the 1940s to 1960.

Experimental

In order to characterize the compositions and mineralogical phases of the pastes, the whole set of ceramics was analyzed by means of inductively coupled plasma mass spectrometry (ICP-MS) and X-ray diffraction (XRD). Moreover, a subsample of them (n = 15) was analyzed by NAA. In addition, a subsample (n = 6) was analyzed by means of scanning electron microscopy coupled to energy dispersive spectrometry (SEM-EDS). For more details about methodology, see Section 3.3.

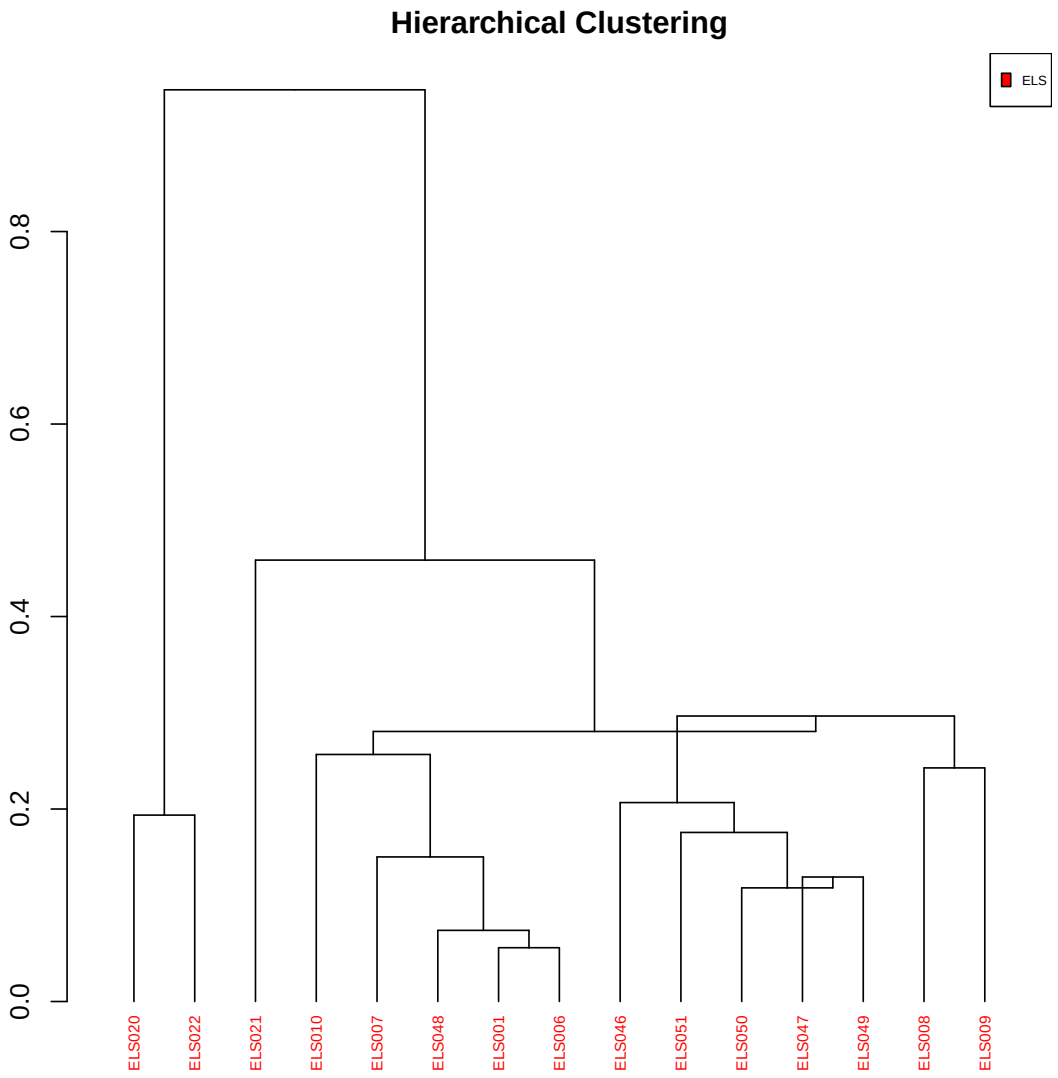

Figure 5.71: Dendrogram of Euclidean squared distances using centroid algorithm of 15 individuals from Elosu, on the sub-composition obtained by NAA of La, Lu, Nd, Sm, U, Yb, Ce, Cr, Eu, Fe, Hf, Sc, Tb, Th, Zn, Zr, Al, Ba, Dy, Mn, Ti and V

Element	ELS	SD
Al_2O_3	17.2	0.9
CaO	16.1	4.7
Fe_2O_3	5	0.2
K_2O	2.5	0.2
MgO	0.7	0.07
MnO	0.026	0.011
Na_2O	0.81	0.09
P_2O_5	0.09	0.06
SiO_2	58.7	3.6
TiO_2	0.7	0.12
Ba	412	37
Ce	86	7
Co	49	27
Cr	103	20
Cs	14	2
Cu	38	39
Dy	4.5	0.4
Er	2.4	0.2
Eu	1.2	0.2
Gd	5.7	0.5
Hf	6.6	0.8
Ho	0.72	0.06
La	43	3
Lu	0.41	0.05
Nb	20	2
Nd	38	3
Pb	(79-12909)*	
Pr	10	1
Rb	178	16
Sm	6.9	0.8
Sn	(15-1725)*	
Sr	517	89
Ta	2.4	0.3
Tb	0.82	0.08
Th	19	1
Tm	0.4	0.06
U	3.6	0.4
V	94	17
Yb	2.4	0.2
Zn	56	47
Zr	229	29

Table 5.10: Mean concentrations standard deviation values (SD) of each compositional group from the Elosu. Concentrations obtained by ICP-MS. Oxides are expressed in mass % and the rest in μg/g.

Compositional Groups

Results and Discussion

In Table 5.10 the mean concentrations of the compositional group obtained by ICP-MS are presented. Ideally, for the statistical analysis, the analytical variance should be minimized in such a way that it is originated by natural sources and not because of experimental errors and/or alterations arising from post-depositional processes. Therefore, in this work, several elements were not regarded for the statistical analysis. These are Pb, Sn, Na_2O, K_2O,Rb, Co, Ta, Zn, Ni and Cu and were addressed at the beginning of the present chapter (see pag. 102). Likewise, CaO and Sr were used with certain restrictions.

The compositional heterogeneity was assessed by calculating the compositional variation matrix (CVM), which provides information about the variability introduced by each element into the dataset (see Figure 5.72). Generally speaking, a large value of the total variation vt indicates greater variability and suggests that the dataset is polygenic (i.e. the presence of several compositional groups). In contrast, a small value for vt indicates a possible monogenic nature of the dataset (Buxeda i Garrigós and Kilikoglou, 2003). In this case, the set shows a very high vt (4.98), which reveals the high contribution of the aforementioned. The vt drops down to 0.62 when these are

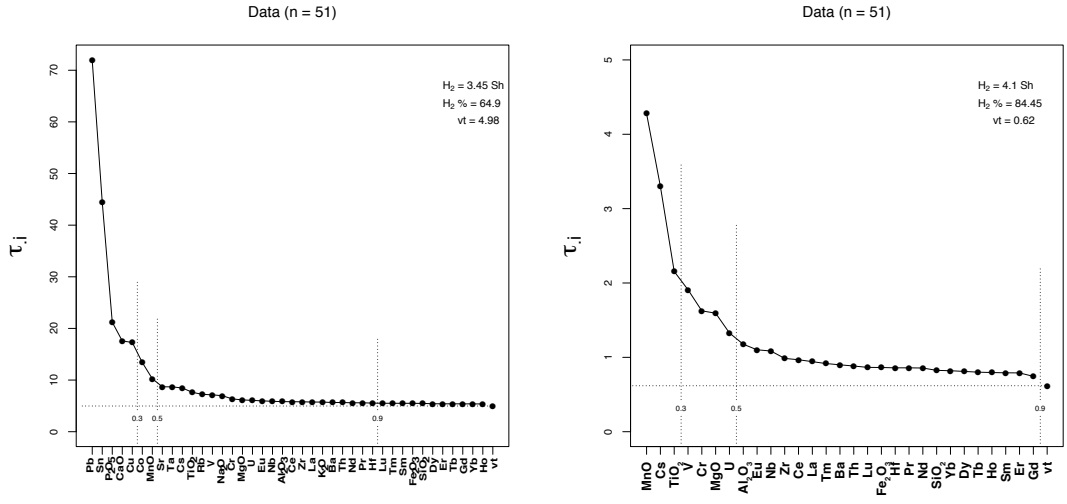

Figure 5.72: Graphical representation compositional variation matrix including all quantified elements (left) and only meaningful elements (right).

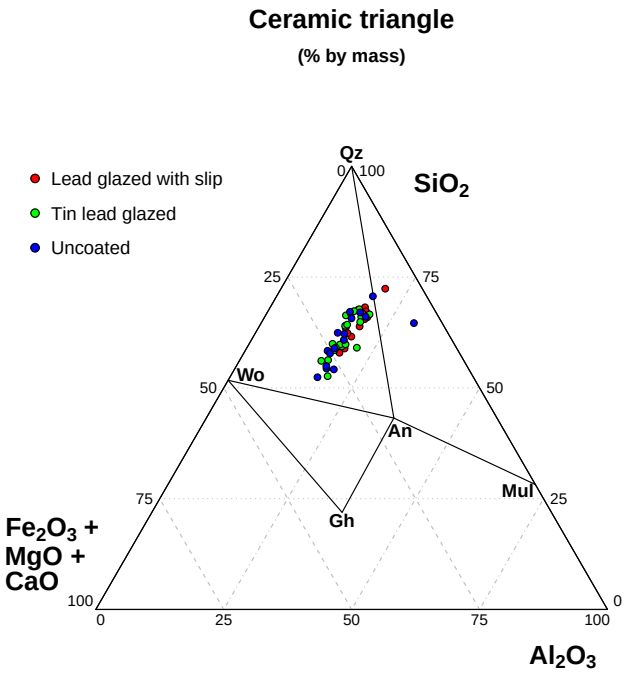

Figure 5.73: Ternary diagram showing the compositions of SiO_2, CaO and Al_2O_3 of the 51 potsherds. TLG: tin-lead glazed. An: Anorthite, Gh: Gehlenite, Mul: mullite, Qz: quartz and Wo: Wollastonite (abbreviations after (Whitney and Evans, 2010)

omitted (see Figure 5.72). This vt can be considered relatively low expecting a low number of compositional groups.

According to the ternary diagram (see Figure 5.73), one micaceous sherd is strongly differentiated by a higher concentration of Al_2O_3 and SiO_2, while lower concentration of CaO. Moreover, another sherd (ELS047) situates in the same ternary system of anorthite, quartz, mullite. Concerning the remaining pieces all fall in the Wollastonite, quartz, anorthite triangle, which is the expectable for medium-high calcareous pastes.

PCA and HCA were carried out in order to identify the compositional groups existing in the dataset (see Figure 5.74). Apart from the micaceous sherd observed in the ternary diagram, which is evidently different, the results permitted identifying one main compositional group (ELS), which could be tentatively ascribed to a local origin (see Figure 5.74).

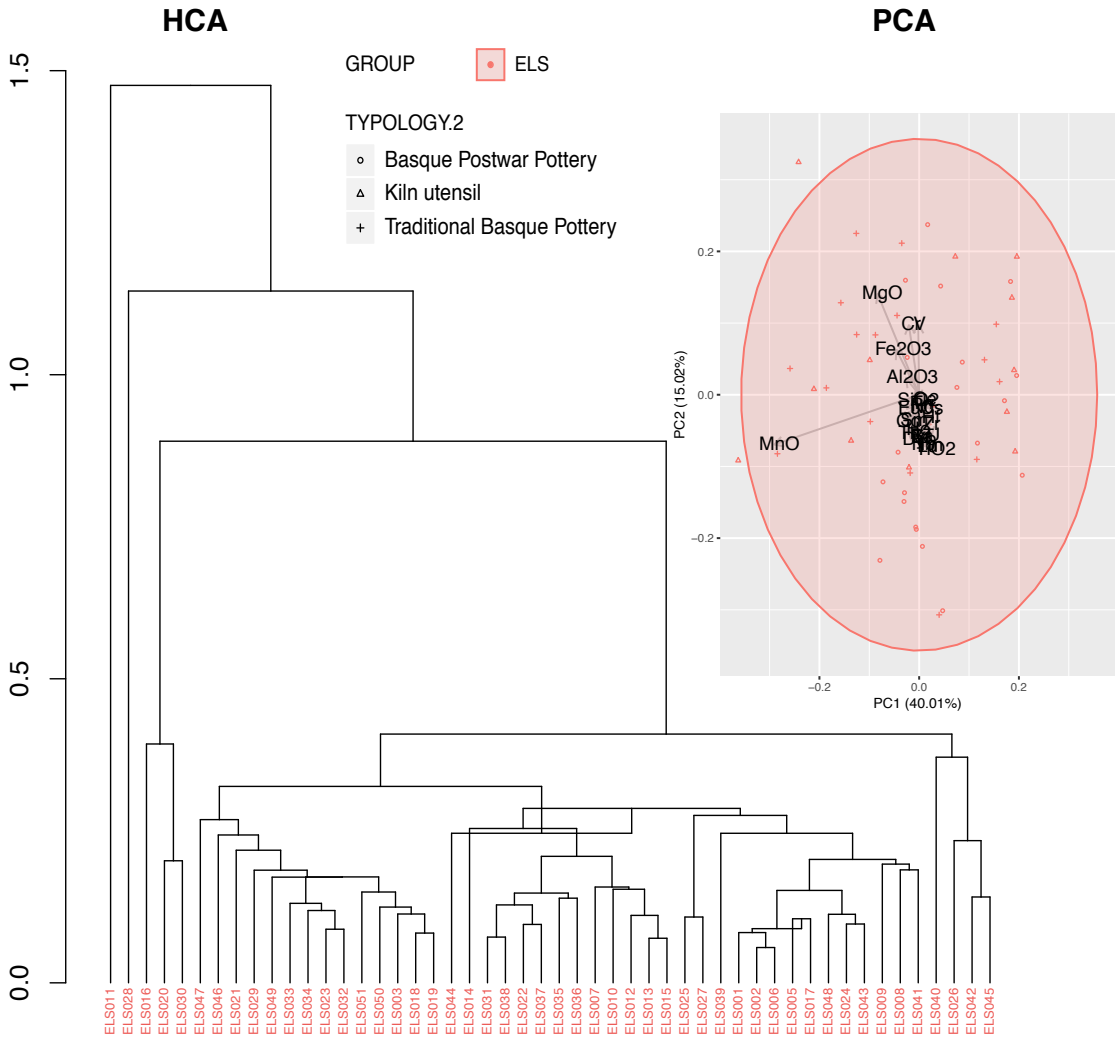

Figure 5.74: Dendrogram of Euclidean squared distances using centroid algorithm of 51 individuals from Elosu and other production centers on the sub-composition obtained by ICP-MS of Al_2O_3, Zr, Nb, Cs, Ba, La, Ce, Pr, Nd, Eu, Sm,Tb, Dy, Ho, Er, Tm, Yb, Lu, Hf, Th, U, TiO_2, V, Cr, MnO, Fe_2O_3 and SiO_2. La was used as divisor for the PCA. The micaceous sherd ELS004 is not shown.

ELS Group

This group is formed by 50 potsherds, including an important fraction of kiln furniture (13/50). The group is characterized by calcareous pastes (16.1 ± 4.7) which is varies considerably reaching down to 1.5 mass % CaO in some sherds and up to 24.5 mass % CaO in others (see 5.75). In contrast, concentrations such as Al_2O_3 (17.2 ± 0.9 mass %) and Fe_2O_3 (5.0 ± 0.2 mass % shows more constant concentrations among the ceramic assemblage. Furthermore, some sherds contribute to the internal chemical variability due to the outlying concentration of certain elements, such as MnO in the case of ELS016, ELS020, ELS022, ELS030 and ELS037; and, Cs in the case of ELS011. For this reason, the latter appears separated in the dendrogram (see Figure 5.74). However, if Cs is removed from the statistical analysis ELS011 clusters perfectly, since regarding all the remaining elements shows a very high compositional compatibility. Likewise, ELS028 shows the highest concentrations of MgO (0.93 mass %) and Cr (175 $\mu g/g$) and for this reason, a separation could be perceived in the HCA as well as in the PCA plots (see Figure 5.74).

The main chemical difference is observed in the CaO concentration, which varies significantly within the defined compositional group and its variation is not correlated to the variabilities of the remaining chemical elements. In contrast, it can be observed how the classified as postwar pottery contains a lower CaO concentration than the other groups (see Table 5.75). If the clay mixtures were carried out, the lower addition of white clays is suggested with regard to the postwar period.

Regarding the decoration, the ceramics exhibit coatings of tin-lead glazes which were used for the manufacture of tableware forms such as bowls, and plates until the arrival of the war. These partially white decorated pieces were considered the main exponent of the so-called Basque traditional pottery. One of the pieces show motifs in green and black, which according to the elemental semiquantitative analysis were obtained by CuO and MnO, respectively. Moreover, the SEM-EDS analyses showed the presence and lack of cassiterite (SnO_2) depending on the use of slip or not. The concentration of SnO_2 observed in the tin-lead glazed ceramics range between 7-11 mass %, and clearly the use of slips was introduced to substitute the white glaze obtained by the opacifier of cassiterite. Nevertheless, the most significant changes with regard to the appearance were observed in the use of slips in combination with transparent glazes lacking of Sn, in order to obtain the appearance obtained previously (see Figures 5.77 and 5.78). The same Figures serve to assess the visual influence of the CaO concentration the ceramic pastes containing 7.8 mass % (ELS005) and obtaining a reddish paste and 17.5 mass % (ELS007) obtaining a buffered color paste. Both of them correspond to the same compositional group, as they have the same chemical fingerprint. In this case, they even correspond to the same typology as both show slipped coatings. However, if a classification was performed only attending to the color pastes, spurious results would be obtained.

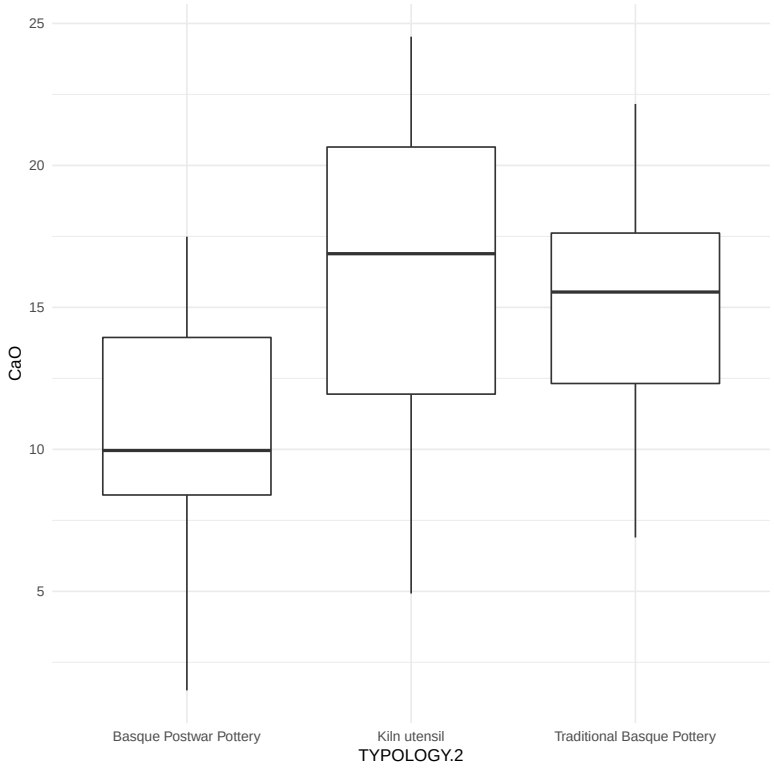

Figure 5.75: Box-plot showing the differences in the CaO compositions of the ceramics from Elosu

With regard to the postwar period, the introduction of flowerpot forms was observed. Moreover, the decorations included concentrated greens and blues that were applied to fully cover the pieces with homogeneous coatings.

The slips were obtained by applying a kaolinitic clays, obtained in accordance with the historical data about the extraction site of Miribilla (Bilbao). Attending to the interaction from the interface and the ceramic body observed in the SEM-EDS images (see Figure 5.77), it could be suggested that the the firing were applied once, however different factors can lead to obtain the same interface with other conditions Molera et al. (1997). Nevertheless, it could not be difficult to think that in postwar times they were saving resources, such as the combustible required for the firing of the pottery. Moreover, quartz inclusions, which could be related to a mixing of sand for obtaining the slips is also attested by the Si elemental maps (see Figure 5.78).

Regarding the mineralogical phases, the ELS group showed three type of fabrics, F-I and F-II and F-III (see Figure 5.76 and Table 5.11). A total of 16 samples presented the F-I fabric, in which the presence of illite along with incipient presence of albite places

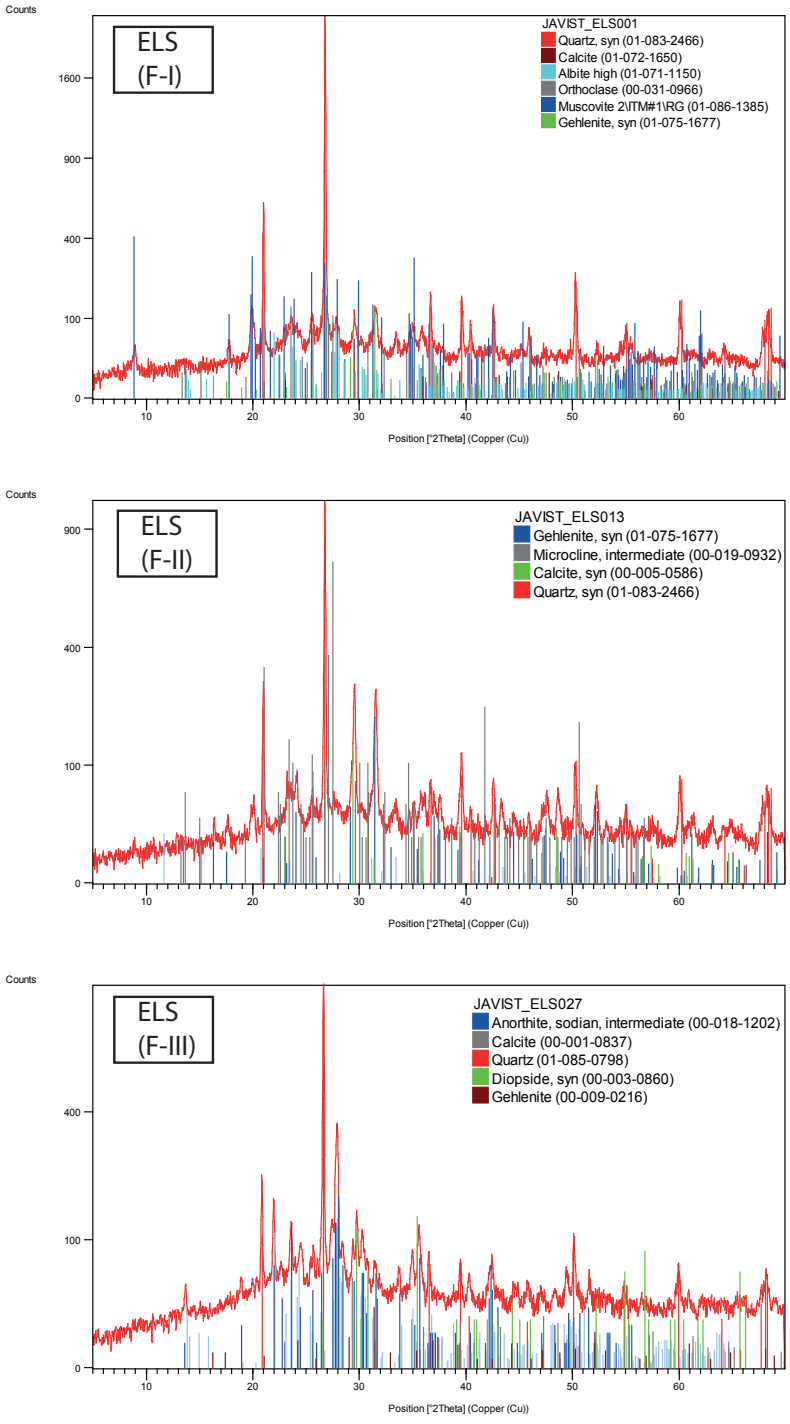

Figure 5.76: Representative XRD diffractogram of each fabric identified in each compositional group.

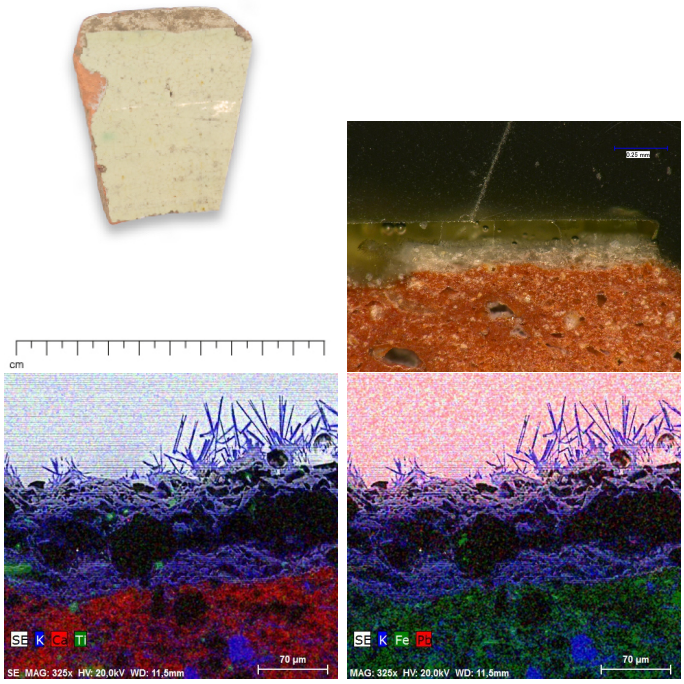

Figure 5.77: Images of piece from ELS005 showing the slip and elemental mappings by SEM-EDS showing K, Ca, Fe, Ti and Pb distributions.

the EFT in 850-900°C. Interestingly 12 out of 20 postwar pieces showed this low firing temperature that until now it has not been observed in any white opacified ceramics (in this case via slip). This could suggest a lower temperature reached in the postwar period, although the uneven distribution of the heat inside the kiln chamber could also show similar results.

Most of the ceramics show F-II type fabric (n=25), which was characterized by the presence of calcite and can be connected by their higher CaO concentration, because all of these sherds show higher than 10 mass % concentrations of CaO. The fabric show also important peaks of gehlenite which is a byproduct of calcite. The concurrence of this phase, along with K-feldspars, but at the same time the lack of illitic phases of plagioclasic ones, places the EFT at ca. 900 °C.

Finally, F-III fabric (n =9) was present in the ceramics showing CaO concentrations lower than ≈ 10 mass % In this case, the peaks of Ca were not that evident, but the presence of more phases of plagioclases, places a higher temperature at ≈ 950 °C. (see Figure 5.76).

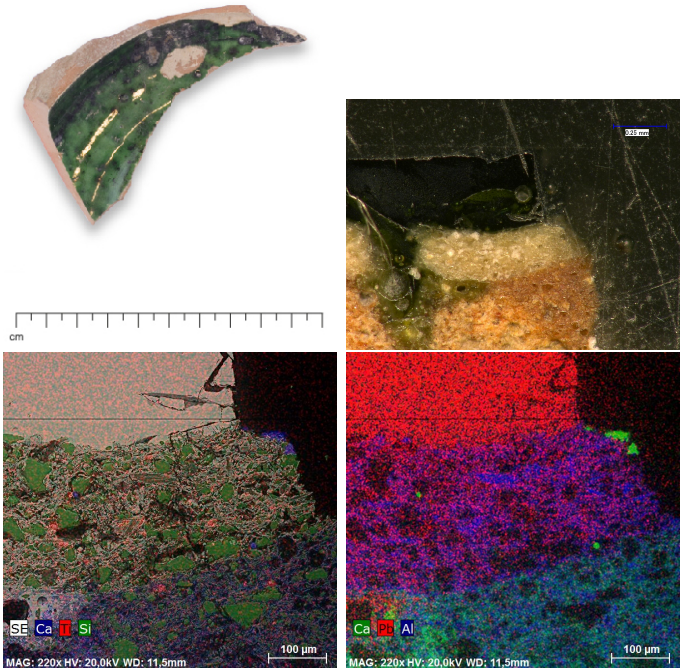

Figure 5.78: Images of piece from ELS007 showing the slip and elemental mappings by SEM-EDS showing K, Ca, Fe, Ti and Pb distributions.

GROUP	Fab.	ANID	EFT	Qz	Ilt-Mus	Afs	Cal	Gh	Hem	Pl
ELS	F-I	ELS001	850-900	x	x	x	x	x		x
	F-II	ELS013	900	x		x	x			
	F-III	ELS027	950	x		x	x	x		x

Table 5.11: Fabrics identified in each compositional group and their main mineralogical phases and EFTs. Qz: Quartz; Ilt-Ms: Illite-Muscovite; Afs: alkali-feldspars; Cal: Calcite; Gh: Gehlenite; Hem: Hematite; Pl: Plagioclases; Px: Pyroxenes. Abbreviations after (Whitney and Evans, 2010).

Final Remarks

The archaeometric characterization of the 51 sherds from Elosu permitted identifying one main compositional group, which could be tentatively linked to a local origin, in connection to the ceramic productions diachronically from the 18^{th} to the 20^{th} centuries. Additionally, a micaceous sherd whose provenance was tentatively ascribed to Zamora in accordance with the tradition of exporting micaceous ceramics was observed. The main differences in ELS group were linked to the technology that had to be adapted to the lack of raw materials during the postwar period, such as tin in this case. According to the mineralogical analysis performed by XRD, the ceramics were all fired between 850 °C and 950 °. Nevertheless, a trend for lower temperatures seems to dominate the postwar ceramic production.

Chapter 6

ED-XRFan oinarritutako *screening* metodologia ez-suntsitzaile baten garapena Erdi Aro eta Erdi Aro osteko zeramika arkeologikoen sailkapenerako

Abstract

Zeramikaren konposizio-analisiak berebiziko garrantzia du arkeologian, metodologia egokia jarraituz gero, iraganeko giza portaerari buruzko ezagutza lortzea ahalbidetzen baitu. Ildo horretan, X izpien fluoreszentziaren espektrometriak (XRF) aukera anitzak eman ditzake analisi ez-suntsitzaileari dagokionez. Hala ere, oraindik hainbat erronka gainditu behar ditu (adib., detekzio-mugak, zehaztasuna, prezisioa etab.), ICP-MS edo NAA bezalako ohiko teknikekin alderatuz. Kapitulu honetan aurkeztutako lanaren helburu zehatza, ED-XRFean oinarrituko puntu-anitzeko estrategia bat garatzea izan zen; halaber, ebaluatzea zenbat gerturatzen ziren modu ez-suntsitzailean lortutako emaitzak, aurretik ICP-MSren bidez modu suntsitzailean lortutako sailkapenari. Aipaturiko prozesua Iberiar penintsulako 4 gune arkeologikoetako 47 zeramikei aplikatu zitzaien. Bi metodo horien emaitzak estatistikoki aztertu ondoren, ICP-MS bidez eta era ez-suntsitzailean lortutako sailkapenek alde gutxi zutela ikusi zen, metodologiaren bahetze ahalmena frogatuz. Era berean, karakterizazio

geokimikoan zerikusia duten faktoreak jorratu ziren, hala nola, parametro instrumentalak, tipologia zeramiko horien kontzentrazio-tarteak, heterogeneotasuna eta berunezko beiratuen eragina.

Lan honen testuingurua 1. atalean eztabaidatzen da. Bertan, historian zehar zeramiken konposizio-analisiak egiteko erabili diren teknika analitiko desberdinak aipatzen dira. Besteak beste, NAA, ICP-AES, ICP-MS eta XRF-an oinarritu diren tresna desberdinak: WD-XRF, TXRF, ED-XRF eta pXRF. Azkenengo hauek, aurrekoekin alderatuz analisi ez-suntsitzailerako aukera eman dezakete. Hala ere, oraindik ere gainditu beharreko arazoak aurkezten dituzte; alegia, detekzio-mugak eta heterogeneitatearekin zer ikusia dutenak.

Atal honetan, hurbilketa ez-suntsitzaile bat garatu zen, automatikoki aldakorra den kolimazio bikoitzeko sistema batekin ekipatutako ED-XRF gailu finko bat erabiliz, 1 mm-ko eta 25 μm-ko albo-ebazpenak eskaintzen dituenak. Proposatutako bahetze-metodologia honen helburua, metodo analitiko tradizionalekiko hainbat abantaila eskaintzen dituen alternatiba sendo eta fidagarria aurkeztea da, hala nola, laginak prestatzeko prozesua nabarmen laburtzea eta analisi automatiko ez-suntsitzailea burutzeko aukera ematea. Teknika ez-suntsitzailearen diskriminazio-gaitasuna aztertzeko, lehendabizi ICP-MS bidezko analisiak egin ziren eta konposizio-multzo desberdinak identifikatu ziren. Proiektu hau garatzeko zeramika arkeologikoak hautatu ziren, beraien artean hainbat mailatako konposizio-desberdintasuna erakusten dutenak (elementu nagusi eta/edo gutxiengoetan), eta hainbat konposizio-multzori dagozkienak, aurreko kapituluetan jorratu den bezala; era horretan, metodologia ez-suntsitzailearen bidez lortutako sailkapenaren ebazpen-maila ebaluatu ahal izateko. Gainera, Iberiar penintsulako zeramika-lantegietan ekoiztutako Erdi Aroko eta Erdi Aro osteko zeramika tipologia desberdinei eragiten dieten arazo espezifikoak landu ziren, hala nola berunezko beiratuak edota zeramikazko-gorputzean erakusten duten heterogeneotasun-maila.

Jatorria	Akronimoa	Erakundea	N	Erreferentziak
Logroño	LOG	ArqueoRioja	n= 12	(Angulo and Porres, 2015)
Urduña	ORD	Bizkaiko Arkeologia Museoa	n= 10	(Calparsoro et al., 2019a; Rodríguez Miranda et al., 2017)
Durango	DUR	Euskal Buztingintza Museoa	n= 5	(Ibabe, 1995a; Calparsoro et al., 2016)
Elosu	ELS	Euskal Buztingintza Museoa	n=20	(Ibabe, 1995a; Calparsoro et al., 2016)

Table 6.1: Zeramiken jatorrizko gune arkeologikoen deskribapena.

Zeramika lagina

Iberiar penintsulako iparraldean kokatzen diren lau gune arkeologiko ezberdinetan aurkitutako 47 zeramika hautatu ziren lan honetarako. Gune arkeologikoak Euskal Herriko (TBC) Durango, Elosu eta Urduña; eta, Errioxako (LR) Logroñoko hirietan kokatzen dira eta XIII-XX. mende bitarteko kronologiak dituzte (ikus 6.1. taula eta 6.1. irudia). Zeramika hauek tipologia desberdinketakoak dira: alde batetik, ekoizpenerako tresnak (treberak), eta; bestetik, ontziteria (katiluak, ontziak, pitxarrak,

etab.). Apaindura anitzak erakusten dituzte, beiratu gabe edo beiratu zeharrargiak dituzten piezetatik berun-eztainuzko beiratu zurietara (ikus B Eranskina).

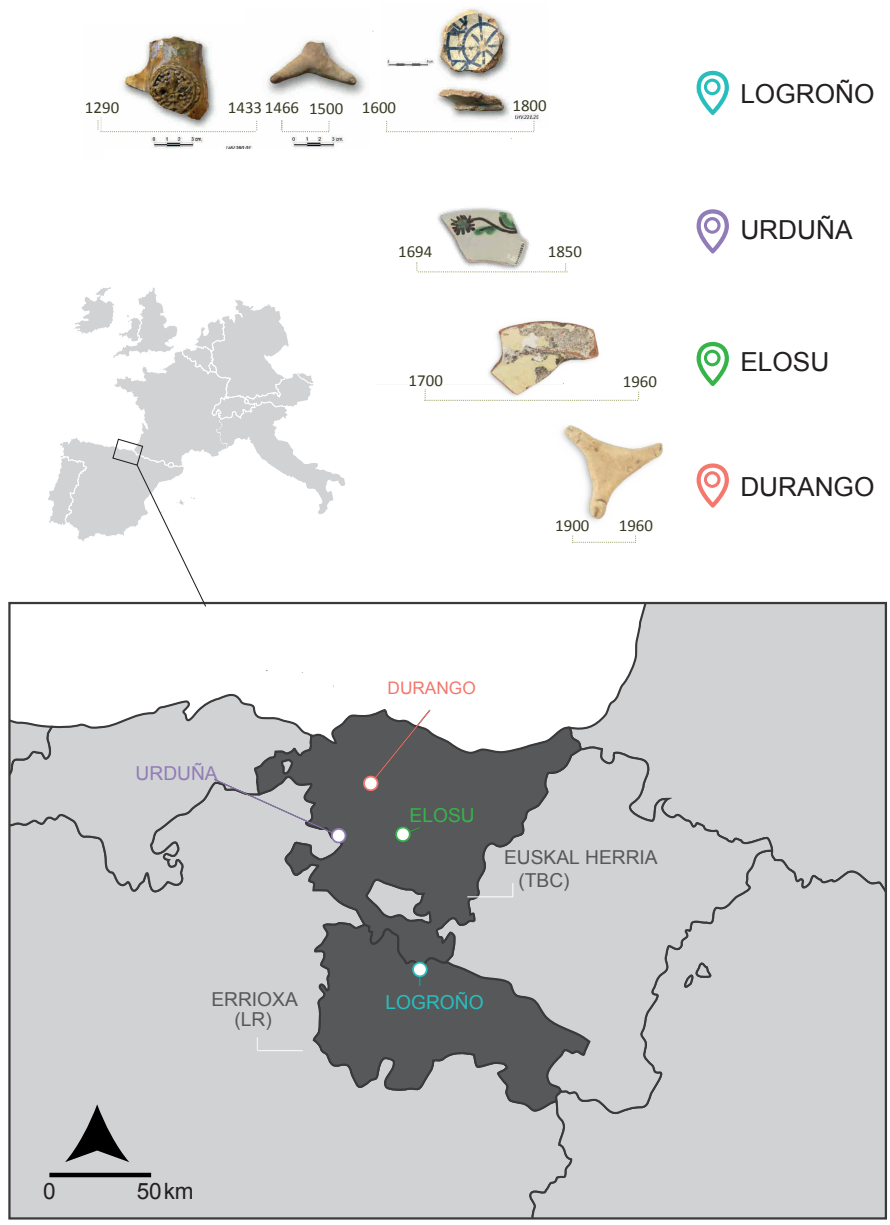

Figure 6.1: ED-XRF Bidez aztertutako laginen deskribapena, kronologia eta jatorria zehaztuz.

Esperimentala

Induktiboki Akoplatutako Plasma Masa Espektrometria (ICP-MS)

ICP-MS analisiak 3.3. atalean azaltzen den metodologia jarraituz egin ziren.

Energia sakabanatzaileko X-izpien Fluoreszentzia Espektrometria (ED-XRF)

Pasta zeramikoen eta CRMen konposizio-karakterizaziorako ED-XRF M4 Tornado espektrometroa erabili zen (Bruker Nano GmbH, Berlin, Alemania). Analisiak zuzenean zeramiken ebakiduran egin ziren, prezisiozko-ebakitzaile baten bidez moztu ondoren, espektrometroaren ganberan jarri zirelarik zuzenean. Espektrometroan 33 x 17 cm eta 5 kg arteko laginak sar daitezkeen arren, laginak moztea erabaki zen analisirako azalera laua lortzeko, kanpoko kutsadurak dituzten eremuen analisia saihesteko eta laginen azalera gehiengora iritsi ahal izateko. Tresna honen konfigurazioak bi albo-ebazpenetan neurtu dezake; 1 mm, eta 25 μm instrumentuan ezarritako optika-polikapilarraren bidez.

Gailuak duen X izpien hodia mikro-fokozko albo-leihoko Rh hodi bat da, potentzia baxuko HV sorgailu batek eraginda eta airez hozten dena. X izpien hodi honek gehienez ere 50 kV-ko tentsioa izan dezake, eta 700 μAko gehienezko korrontea 1mm-ko kolimazioarekin, non 600 μA-etara iris daiteke $25\mu m$ albo-ebazpenarekin. Fluoreszentzia erradiazioa detektatzeko, XFlash ® siliziozko detektagailu baten bidez egiten da, 30 mm^2-ko eremu sentikorrarekin eta 145 eV-ko energia-ebazpenarekin Mn-K_α-arentzat. Elementu arinenen detekzioa hobetzeko (Z <11), ez zen iragazkirik erabili eta hutsean hartu ziren neurriak (20 mbar). Hutsa lortzeko, MV 10n VARIO-B mintz-bonba bat erabili zen. Neurriak hartzerako garaian, enfokatzeko bi bideo-mikroskopio erabili ziren; horietako bat laginak aztertzeko erabili zen magnifikazio-txikietan (1 cm^2-ko azalera), eta bestea, berriz, amaierako fokuratzea egiteko (1 mm^2 azalera).

Espektroak eta haien tratamendua Brukerren M4 softwarearen bidez lortu ziren. Neurketa baldintzei buruzko xehetasun gehiagorako, adibidez, neurketa-denborak, kolimadore-mota eta analisi-kopurua (ikus 6.2. atala) Lortutako espektroetan oinarritutako matrizearen efektuek eragindako interferentziak eta pilaketa-zuzenketak (ingelesez *pile ups* deritzona) softwarearen bidez zuzenduak izan ziren. Softwareak matrizearen konposizioa kanpotik ezartzeko ere aukera ematen du.

Lan honetan aurkeztutako Hyper-Mapak optika-polikapilarra erabiliz lortu ziren ($25\mu m$-ra arte). Hyper-Mapak lortu aurretik, esleipen elementala eta espektroen

informazioaren dekonboluzioak burutu ziren aztertutako elementu bakoitzaren K_α-an oinarrituta. CRM SRM679-aren elementu bakoitzaren LODa kalkulatu zen, prentsatutako pellet-etan hartutako neurriak kontuan hartuz eta formula honi jarraiki:

$$LOD = 3C\sqrt{\frac{Inguru\ Intentsitatea}{Intentsitate\ Netoa}} \tag{6.1}$$

non C kontzentrazio erreala den eta iturburuko intentsitate-espektroetatik lortu zen. Formula honetan, intentsitate netoa jatorrizko intentsitatea (zenbaketetan) eta elementu bakoitzaren intentsitatearen kenketaren bidez lortu zen. Zertifikatu gabeko elementuetan, LODak Brukerrek emandako balio teorikoen hurbilketa bat eginez kalkulatu ziren.

Datuen tratamendua

Hemen aurkezten den lanean aplikatutako analisi estatistikoa Aitchisonen ikuspegian eta ondoren Buxedak konposizio-datuei buruz egindako behaketetan oinarritzen da (Buxeda i Garrigós, 1999; Aitchison, 1982; Buxeda i Garrigós and Kilikoglou, 2003).

Lehenik eta behin, elementu nagusien eta aztarna elementuen arteko eskala absolutuen desberdintasunak orekatzeko, eraldaketa logaritmikoa aplikatu zen, aukera hori literaturan gehien erabiltzen dena izanik (Bishop and Neff, 1989; Shennan, 1988; Sayre, E.V., Harbottle, G., Bieber, A.M., Brooks, 1976; Neff, 2000). Eraldaketa honekin aztarna elementuen eragina gutxiestea saihesten da (konposizio-multzo batzuk bereizteko funtsezko eginkizuna izan dezakete elementua hauek) (Glascock, 2016).

Alderaketak, Aitchisonen behaketen arabera egin ziren (Aitchison, 1986) logaritmoak erabiliz eta osagai kimiko guztien zatiketa eginez hautatutako osagai batekin. Konposizio datuetan, aldagaiek beraien arteko menpekotasuna dutenez, alegia, osagai kimiko guztien batuketak 100 % ematera behartuta dago, aipatutako eraldaketa aplikatuz unitatearen batuketaren arazoa hori konpontzen da (Buxeda i Garrigós and Kilikoglou, 2003).

Zatitzaile bezala erabilitako elementua desberdina izan zen aplikatutako analisi estatistikoaren arabera. Alde batetik, osagai nagusien analisian (ingelesetik PCA), aldakortasun txikieneko elementua aukeratu zen. Eraldaketa honi, ingelesetik additive log ratio (alr) deritzo. Bestalde, multzokatze hierarkikoaren analisietarako (HCA), batez besteko geometrikoa erabili zen zatitzailea gisa, centered log ratio (clr) eraldaketa deritzona. HCAn Euklidear distantzia grafikoki irudikatzen da zentroide algoritmo aglomeratzailea erabiliz. Eraldaketa horiek ICP-MS bidez lortutako kontzentrazioei eta ED-XRFren bidez eskuratutako intentsitate gordinei aplikatu zitzaizkien.

Eraldaketa guztietarako, hala nola, analisi estatistikorako eta datuak bistaratzerako erabilitako softwarea R (Core Team, 2013) izan zen. Lehenago jorratu den moduan,

programazio-lengoaia hori kode irekikoa da eta analisi estatistikorako diseinatua dago (ikus 4. kapitulua). Instalatutako paketeen artean, "Compositions" erabili zen, Van de Boogartek garatutakoa (Boogaart et al., 2010) eta Buxeda i Garrigósek idatzitako errutinak ere erabili ziren, GitHub webgunean argitaratutako biltegian kontsultatu daitekeen metodo irekiari jarraituz (Calparsoro, 2019).

6.1 *ICP-MS Emaitzak*

Aldagaia	ELS	SD	DUR	SD	ORD	SD	LOG	SD	LOG033	LOG038
Al_2O_3	18	1	17	1	15	2	20	3	16	13
CaO	13	4	15	2	19	2	9	1	13	24
Fe_2O_3	4.8	0.2	4.9	0.2	4.1	0.4	7.5	0.3	5.3	4.7
K_2O	2.6	0.2	2.1	0.2	1.9	0.3	3.2	0.1	2.8	2.4
MgO	0.67	0.08	1.72	0.05	1.20	0.30	2.10	0.20	1.77	2.53
MnO	0.024	0.009	0.100	0.040	0.032	0.007	0.038	0.004	0.042	0.057
Na_2O	0.81	0.08	0.67	0.06	1.50	0.30	0.70	0.06	0.65	0.36
P_2O_5	0.18	0.20	0.14	0.01	0.70	0.91	0.46	0.24	0.28	0.39
SiO_2	60	5	64	3	51	10	43	2	38	40
TiO_2	0.75	0.12	0.72	0.01	0.63	0.10	0.81	0.03	0.63	0.67
Ba	452	34	436	49	300	53	586	57	517	487
Ce	89	6	79	3	68	9	117	4	91	80
Co	49	20	95	23	18	7	23	6	16	18
Cr	100	14	85	6	98	9	96	19	65	62
Cs	15	2	13	1	11	3	20	3	18	6
Cu	47	49	54	41	45	22	36	35	28	161
Dy	4.8	0.5	4.4	0.3	3.9	0.6	5.7	0.2	5.2	5.2
Er	2.6	0.2	2.3	0.1	2.3	0.4	2.9	0.1	2.8	2.7
Eu	1.2	0.2	1.2	0.1	0.9	0.2	1.8	0.1	1.4	1.4
Gd	5.8	0.6	5.7	0.1	4.5	0.8	9.1	0.4	7.4	7.2
Hf	6.9	0.7	6.1	0.2	6.4	1.7	2.8	0.2	3.4	3.6
Ho	0.76	0.08	0.67	0.03	0.74	0.10	1.00	0.04	0.92	0.94
La	44	3	41	1	32	4	57	2	44	41
Lu	0.46	0.05	0.40	0.03	0.34	0.06	0.43	0.01	0.42	0.39
Nb	21	2	23	1	17	3	20	1	18	16
Nd	40	4	35	1	28	4	47	1	38	35
Ni	20	3	<LOD		20	4	68	17	63	49
Pb	(204 - 12x10^3)*		(377 - 5.5x10^3)*		(339 - 10.1x10^3)*		(37 - 2.65x10^3)*		1.73 x10^3	2.58 x10^3
Pr	11.0	0.7	9.1	0.3	7.5	1.0	12.0	0.4	9.6	8.8
Rb	186	12	189	17	122	32	149	7	132	80
Sm	7.3	0.8	6.3	0.2	5.1	0.8	9.4	0.3	7.7	7.0
Sn	(165 - 377)*		62	30	35	24	5	1	49	22
Sr	473	97	329	18	523	108	494	57	677	644
Ta	2.5	0.3	2.5	0.08	2.5	0.4	1.2	0.1	1.1	1.0
Tb	0.87	0.10	0.78	0.04	0.67	0.12	1.01	0.04	0.89	0.86
Th	20	1	14	1	13	1	11	1	8	8
Tm	0.44	0.05	0.40	0.02	0.33	0.06	0.51	0.02	0.47	0.50
U	3.9	0.4	3.3	0.2	3.3	0.6	3.0	0.1	2.9	2.5
V	89	18	81	7	65	9	139	7	83	74
Yb	2.6	0.3	2.3	0.1	2.4	0.4	3.0	0.2	2.9	2.8
Zn	<LOD	<LOD	100	51	94	14	94	14	93	83
Zr	237	26	219	11	250	67	191	15	222	252

Table 6.2: Konposizio-multzo bakoitzaren ICP-MS bidez lortutako kontzentrazio kimikoen batez bestekoak eta desbiderapen estandarra (SD). Unitateak μg/g dira eta oxidoen kasuan masa %-ak aurkezten dira. <LOD: detekzio muga azpitik.(*) Pb eta Sn-rentzako kontzentrazio tarteak ematen dira SDak batez bestekoak baino handiagoak diren kasuetan.

ICP-MS bidez, 42 elementuen kuantifikazioa burutu zen. Konposizioaren aldakortasun-matrizearen grafikoa aurkezten da 6.2. irudian. Bertan, elementu bakoitzak datu multzo osoari gehitutako banakako aldakortasuna erakusten da, altuenetik txikienera. Grafiko honen arabera Pb da 47 banako dituen datu-multzoaren elementurik aldakorrena; ondoren, Sn, eta aldaketa gutxien erakusten duen elementua Lu da. Aldakortasun-totalak (vt) multzo zeramikoaren uniformetasuna erakusten du, eta, metrika horren arabera, konposizio-datuen izaera poligenikoa edo monogenikoa definitzen da (Buxeda i Garrigós and Kilikoglou, 2003).

Aldakortasun-iturriak

Aztertutako laginen aldakortasun-totala (vt) 7.69 da (ikus 6.2. irudia). Eskuarki, datu multzoaren izaera poligeniko argi baten zeinua da horrelako balore handi bat, hau da, multzo kimiko bat baino gehiagoren agerpena adierazten du (Buxeda i Garrigós and Kilikoglou, 2003). Nolanahi ere, azterketa estatistiko egokia egiteko, aldakortasunaren jatorriarekin loturiko hainbat arazo hartu behar dira kontuan. Ondorioz, kuantifikatutako elementu guztiak ez dira erabiliko azterketa kimiometrikorako.

Zeramika arkeologikoek azken konposizioan eragina duten eraldaketa edo kutsadura prozesuak jasan ditzakete (Molera et al., 2001). Honen inguruko eztabaida zabalago batentzako ikus 5.1. atala. Alde batetik, Pb eta Sn ohiko osagaiak dira, eztainu-berunezko beiratuetan, eta hauek erreketa-prozesuan zehar barreiatu daitezke beiratutik buztin gorputzera. Gure kasuan, bi elementu horiek erakusten dute aldakortasun handiena (ikus 6.2. irudia) eta, gainera, beraien artean oso koerlazionatuak agertzen dira (ikus 6.2. irudia). Azkenengo irudi honetan, aldagai bakoitzaren erlazioa aurkezten da hauek agertzen duten aldakortasunaren arabera (informazio gehiago 4. atalean).

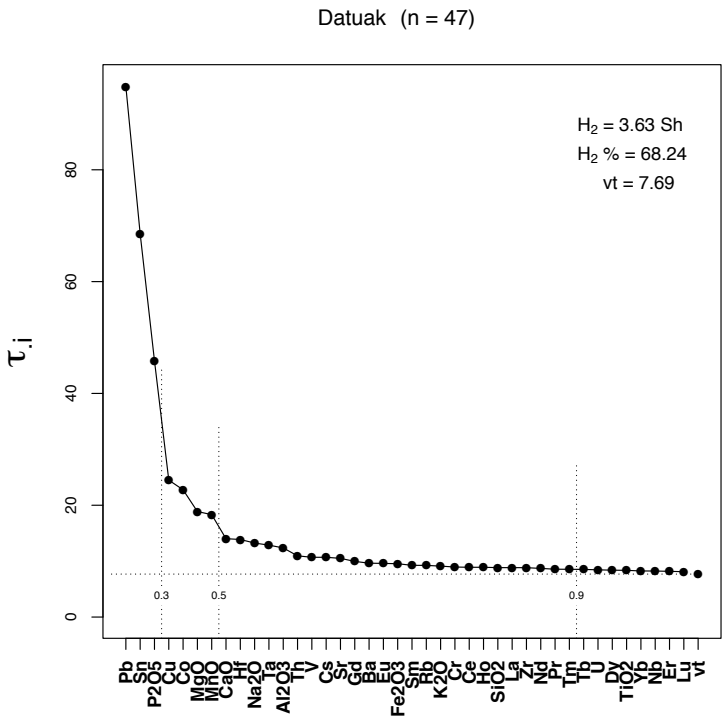

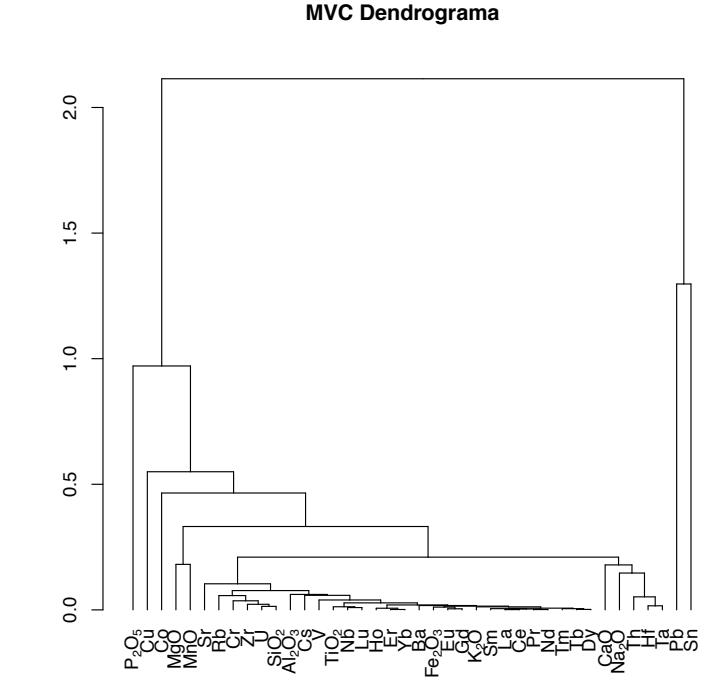

Figure 6.2: Eskuinean elementu bakoitzak duen aldakortasunaren erlazioa aurkezten duen dendrograma, aztertutako 47 zeramikentzat eta ICP-MS bidez lortutako datuetatik abiatuz. Eskerrean 47 banakoen konposizioaren aldakortasun-matrizearen Irudikapen grafikoa. vt =aldakortasun-totala, H_2 = informazio-entropia, $H_2\%$ = Informazio-entropiak izan dezakeen gehienezko balioarekiko ehunekoa, n = banakoen kopurua.

Aldakortasun altuaz haratago, azpimarratzekoa da aztertutako eskualdeetako zeramikek Pb kontzentrazio orokor handiak erakusten dituztela, μg/g gutxi batzuetatik 10^3 μg/g-rainoko tarteak erakutsiz, aztertutako laginentzat. Berunezko beiratuen ekarpena, beiratu gabeko zeramiken kasuan argi geratzen da, hauek Pb kontzentrazio txikienak aurkezten baitute (adib., LOG006, LOG019, LOG003 eta LOG002). Beste muturrean, beiratuak dituzten zeramikak, Pb aberatsak dituzten pastak aurkezten dituzte (LOG0072, LOG074 eta, neurri txikiagoan, LOG075). Kasu honetan, arau hori saihesten duten bi salbuespen daude: Pb kontzentrazio handienak erakusten dituzten pasta zeramikoak ORD065 eta ELS038 dira. Lehenengoa beiratu gabeko trebera bat da eta 10.1x10^3 μg/g Pb-ko kontzentrazioa du. Bigarrenak, eztainu-berunezko beiratu bat dauka eta 12.9x10^3 μg/g Pb aurkezten du (xehetasun gehiagorako ikus A Eranskina).

Gainera, zeramikak lurperatuta egon diren denboran, kutsadurak jasan ditzakete. Adibidez, lurzoruko uretan dagoen P_2O_5, haren kontzentrazioa alda dezake, zeramika lurperatua izan den kokapen zehatzaren arabera aldatuz. Beraz, bere aldakortasuna ez dago hasierako pastarekin lotuta, baizik eta aipatutako kutsadurarekin. Horregatik, konposatu honen kontzentrazioa ausaz agertzen dira. Aztertutako banakoen artean, Pb eta Sn ondoren, gehien aldatzen den konposatua da P_2O_5 (ikusi 6.2. irudia).

Ildo horretan, Cu da hurrengo elementurik aldagarrirena, toki bakoitzeko laginetan ohiz-kanpoko balioei erantzuten dien aldakortasun handia erakutsiz zeramika multzo-honetarako. Aldakortasun horren iturria jalkitze-ondoko kutsadura ere izan daiteke (Buxeda i Garrigós, 1999). Gainera, kasu zehatz honetarako ziurgabetasun balio handiak lortu ziren elementu honentzako, aldakortasun handi horiekin erlazionatuta egon litekeena. Beraz, Cu-ren aldagarritasun desberdinari dagokionez, ez da aintzat hartzen estatistika-analisirako.

Gainera, lagina prestatzeko prozesua beste aldakortasun-iturri bat izan daiteke. Laginak ehotzeko wolframio karburozko zelda bat erabiltzeak, Co eta Ta-ren kontzentrazioetan aldaketak eragin ditzake. Esandako elementuak zeldaren aleazioan daudenez ehotze-prozesuan laginetara transferitu daitezke (Boulanger et al., 2013a). Azkenik, Zn eta Ni ez ziren kontuan hartu, balio batzuk detekzio mugatik (LOD) gertu edo azpitik baitzeuden.

Horrez gain, Rb, Na_2O eta K_2O kontzentrazioak estatistika-azterketatik kanpo utzi ziren. Aldagai horiek erlazioa dute zeramika pastaren beira-fasean gertatzen den balizko eraldaketa-prozesu bikoitz batekin. Eraldaketa horretan K_2O eta Rb-aren lixibiazioa gertatzen da, analzimaren kristalizazioarekin eta lurrean topatzen den uretan dagoen Na_2Oaren finkatzearekin batera (Buxeda i Garrigós et al., 2002; Schwedt et al., 2006). Analzima, sodioaren zeolita bat da eta haren kaltzio baliokidea wairakita litzateke. Horrela, zaila da kuantifikatzea kutsadura eta eraldaketa-prozesu bikoitz honen ekarpena. X izpien difrakzioaren bidez egindako aurretiazko analisiek ez zuten

hemen azterturiko zeramiketan analzimarik erakutsi. Hala ere, elementu horiek ez erabiltzea erabaki zen, lurperatze ondoko kutsadurak ahalik eta gehien saihesteko.

Azkenik, CaO kontzentrazioei dagokienez, hautaketa teknologikoen eragina aintzat hartu zen. Buztinetan CaO-ren presentzia Sr-rekin agertzen da normalean. Zeramika arkeologikoak, karedun edo ez-karedun bezala sailkatu daitezke, beraien kolore argia edo gorriaren arabera. Kolorea, batez ere CaO kontzentrazioaren mende dago, besteak beste (erreketa-giroa, tenperatura, buztinaren osaera, etab.). Beraz, CaO kontzentrazioak garrantzitsuak dira, azken itxura zehaztu dezaketelako. Hala ere, CaO ezin da inoiz izan zeramiken jatorria zehazteko adierazle nagusia, sailkapen okerrak eman ditzakeelako. CaO eta Sr kontzentrazio igoera batek buztin desberdinen nahasketarekin zerikusia izan dezake, karedun pastak edota karbonatoen inklusioak gehitu litezkeelako pasta zeramikoan (Fabbri et al., 2014).

Zeramiketan dauden karbonatoen izaera anitza izan daiteke: lehen edo bigarren mailakoa, formazio-berrikoa, hauspeatutakoak eta abar. Karbonatoen izaeraren arabera eragin desberdinak izan ditzakete pastaren konposizio kimikoan, baita kaltzioarekin lotutako elementu minoritarioetan ere (Fabbri et al., 2014; Buxeda i Garrigós, 1999; Schwedt et al., 2006). Esate baterako, Elosuren kasuan, lan etnografikoek, zeramikazko labetik hurbil dauden bi buztin moten nahastea aipatzen zuten 25/75 buztin gorri eta buztin zuri proportzioan (Ibabe, 1995a, 16. or.). Hala nola, Durangon *buztin surise* eta *buztin gorrise* aipatzen dira (Ibabe, 1995a, 112. or.). Hemen aztertzen diren 47 banakoen artean, ICP-MS emaitzek erakutsi zuten bezala, sailkapen berdina izaten jarraitzen du CaO eta Sr, estatistiketan erabili edo ez, horrela garbi geratzen da lortutako multzoak ez daudela elementu horiengatik eraginduta, aurrerago eztabaidatzen den bezala.

ICP-MS bidezko sailkapena

HCAren bidez sortutako dendrogramak (ikus 6.3. irudia) Errioxa (LR) eta Euskal Herriko (TBC) zeramika-multzoen arteko desberdintasun argia erakusten du, bai eta aurrerago aztertuko diren bi kasu ere (LOG038 eta LOG033). Multzo bakoitzaren batez besteko kontzentrazioak 6.2. taulan aurkezten dira. LR multzoak aberastasun orokorra du elementu minoritarioetan eta aztarna elementuetan, bai eta Fe_2O_3n ere, alegia, 7.5 masa %-koa, non beste guztiek 4.0-5.4 masa %-ko kontzentrazioak aurkezten dituzten. Aitzitik, euskal multzoak (TBC), Th, Zr eta Hf bezalako elementu minoritarioetan, orokorrean, kontzentrazio altuagoa aurkezten du (ikus 6.3. irudia eta 6.2. taula). Gainera, TBC multzoa, oro har CaO kontzentrazio altuagoak erakusten ditu eta hiru multzo txikiagoetan banatzen da: ORD (Urduña), ELS (Elosu) eta DUR (Durango).

HCA eta PCAk adierazi dutenez, TBCko multzoen artean, Durangoko laginak ezberdintasun kimikoak agertzen ditu MnO eta MgOaren kontzentrazioari dagokionez. Alde batetik, DUR multzoak MnO oso altua du (0.10 masa %), zeinak beste guztien

kontzentrazioak (0.025-0.040 masa %) bikoizten duen. Bestalde, TBCko multzoen artean MgO kontzentraziorik handiena agertzen du (1.7 masa %), non beste guztiek honako tartea agertzen duten: 0.67-12 masa %. Horregatik, elementu honek DUR multzoa bereizteko gakoa da. Ondorioz, MgOren paper erabakigarria nabarmentzen da TBC multzoaren barruan DUR multzoaren bereizpenari dagokionez.

Gainera, ORDren bereizpena TBCren barruan, Al_2O_3 kontzentrazio baxuagoak (15 masa %) eta CaO altuagoak (19 masa %) emana dator. Halaber, aztarna elementuen murrizte orokor bat erakusten du. Kontraste gisa, ELSko zeramikak aberatsagoak dira zenbait aztarna eta elementu minoritario, esaterako Cr, Lu, Sm, Tb, Tm, U, V eta Yb-n, eta bereziki Th, 20 μg/g-ko kontzentrazioa erakutsiz, non TBCko beste guztien Th kontzentrazioak 12-14 μg/g-ko tartean aurkitzen dira (ikus 6.2. taula).

Lehen aipatu den moduan, Logroñoko bi zeramikek konposizio desberdinak erakusten dituzte LOG multzo nagusiarekin alderatuz. Hauek LOG033 eta LOG038 dira. Doktorego-tesi honetan aurretik jorratu den bezala, LOG033 LOG-B multzoari dagokio eta ELS038 LOG-E multzoari (ikus 5.2. atala), non hemen LOG deritzogun multzoa LOG-A multzoari dagokio. Hala ere, atal honetan, LOG deituko diogu azkenengo honi eta beste bi zeramikak beraien identifikazioaren bidez izendatuko ditugu. Zeramika multzo honekin (n=47) burututako sailkapenean, bai HCAk bai PCAk bi banako horien izaera bereizia adierazten dute. LOG033, kimikoki berdintasun gehiago erakusten du LOG multzoarekiko LOG038 baino. Hala ere, aztarna eta elementu minoritarioen desberdintasun orokorrak eta, bereziki, MgOren kontzentrazio baxuagoa da (1.8 masa %) multzo horretatik banantzearen erantzule nagusia, non beste zeramika guztiek 2.1-2.5 masa %-ko kontzentrazio tarteak erakusten dituzten.

Aipatutako beste zeramikari dagokionez (LOG038) gainerako pieza guztiez bestelakoa da, aztarna eta elementu minoritarioak kontzentrazio altuagoak dituelako (ikus 6.2. taula). Aipatu beharra dago, multzo zeramiko osoko pieza karedunena dela (23.8 masa % CaO). Doktorego-tesi honen 5.2. atalean jorratzen den moduan, ezaugarri teknologikoen ebaluazioaren eta NAAren bidez jatorri-azterketetan oinarrituz (Calparsoro et al., 2016), pieza honen jatorria Valentzian dagoela proposatzen da. Izan ere, bertako oso ezaugarrikoak den apaindura urdin mota erakusten du (Mesquida García, 2002; Coll Conesa, 2009; Pérez-Arantegui et al., 2008).

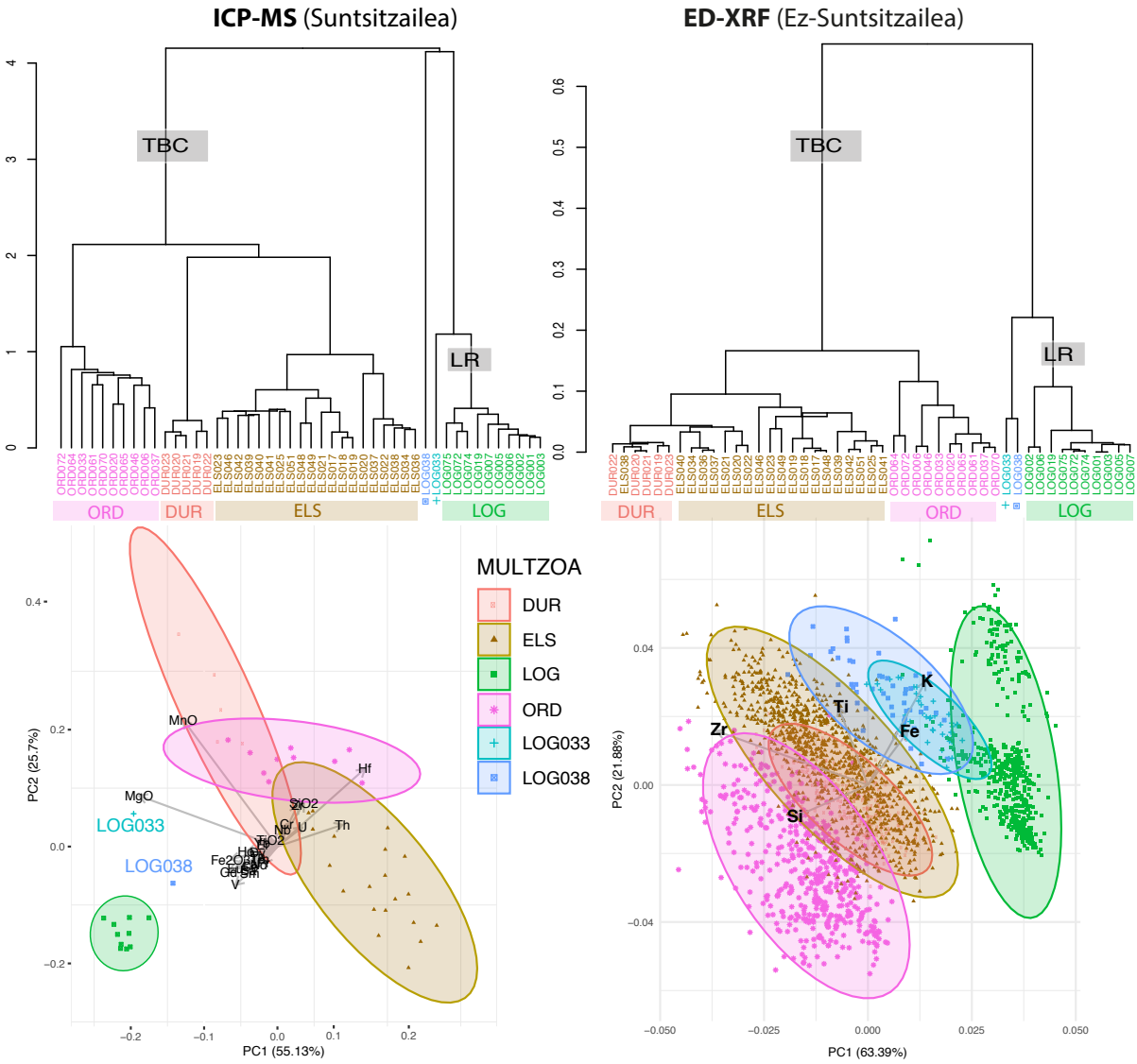

Figure 6.3: HCA eta PCA, bi tekniken bidez lortutako datuekin: ICP-MS (ezker) eta ED-XRF (eskuin). clr eta alr transformazioak aplikatu ziren HCA eta PCAn, hurrenez hurren ondorengo aldagaiei: MgO, Al_2O_3, SiO_2, TiO_2, Fe_2O_3, MnO, V, Cr, Zr, Nb, Ba, Hf, La, Ce, Pr, Nd, Sm, Eu, Gd, Tb, Dy, Ho, Er, Er, Tm, Yb, Th eta U. ED-XRFan: Si, Ti, Fe, Zr eta K. PCArako Lu eta Al erabili ziren zatitzaile moduan ICP-MS eta ED-XRFrako hurrenez hurren. Elipseak 95%- konfiantza tartea adierazten dute.

6.2 *ED-XRF Emaitzak*

Neurketa Parametroak

Instrumentuan konfiguratu daitezkeen aukeretatik abiatuta, lehenik eta behin hiru aldagai optimizatu ziren: (i) neurketa-denbora, (ii) tentsioa eta (iii) Rh hodiari aplikatutako korrontea. Seinale/zarataren erlazioa (SNR ingelesetik) hobetzerik ez dagoen neurketa-denbora zehazteko, eta, beraz, detekzio-muga, denbora-tarte desberdinetako neurketak burutu ziren (100 s, 150 s, 200 s, 250 s eta 300 s) hainbat zeramiketan (multzo bakoitzeko bat). Hildako-denbora (ingelesez *dead time* deritzona) zeramika guztietan berdina zela ikusita ($\approx 1\%$), denbora erreala neurtu zen neurketa guztietan.

Lagin bakoitzeko aztarna elementuentzat SNRak kalkulatu ziren (μg/g maila). Ondorioz, 200 s-etara, hiru baino balio askoz handiagoak lortu ziren aztertutako kasu guztietan. *American Chemical Society*ak SNRak hiru edo gehiagokoa izan behar duela gomendatzen du espektro-gailur bat elementu/konposatu espezifiko baten presentziari lotu daitekeela egiaztatzeko (Keith et al., 1983).

Gure neurketetan eta zenbait elementu zehatzetarako, SNRak hiru baino gutxiago izan ziren 100 s edota 150 s-tan. Horrenbestez, 200 s ezartzea erabaki zen neurketa-denborarik egokiena bezala. Neurketa-denbora horrek lagin bakoitzaren balio adierazgarriak eskuratzeko aukera eman zigun (50 puntu neurtuta), lagin bakoitzeko 3 ordu baino gutxiagotan.

X izpien hodiak gehienez 50 KV-ko tentsioan egin dezake lan, eta, gehienez ere, 700 μA-ko korrontearekin. Hauek, baldintza optimotzat jo ziren, 1 mm-ko albo-ebazpena duten espektroak eskuratzeko. Tentsio baxuagoetan eta korronte baxuagoetan erregistratutako zenbaketa-netoen (*net counts*) kopurua jaisteaz gain, inguru-espektrala ez zen hobetzen.

Espektroak interpretatzeko erabiltzen den software komertzialak ematen dituen kalkulu aukerei dagokienez, funtsezko parametroetan (FP) oinarritutako zenbait hurbilketa semi-kuantitatibo eskaintzen ditu. CRM-arekin (SRM679) egindako frogatan, "Oxido-metodoa" eta "espektroko elementuak" oinarri hartuta, lehenengoak emaitza hobeak eman zituen, elementuak oxido egoeran daudela asumitzen duelako, horrela era hobeago batean islatzen du zeramikaren errealitatea (adibidez silizio oxidoak eta burdin oxidoak).

Hala ere, bi FP-metodoak ez daude diseinatuta matrize mota jakin batentzat, eta metodo horietako edozein erabilita lortutako balio kuantitatiboak balio errealekiko

desbideratze handiak erakutsi zituzten, analitikoki onargarriak diren mugen gainetik. Beraz, kontzentrazioekin lana egin beharrean, hurbilketa semi-kuantitatibo batekin lana egitera beharturik gaude. Hurbilketa semi-kuantitatibo honetan, ED-XRFren oinarritutako sailkapen-eredua eraikitzeko zenbaketa-netoak erabili ziren. Balio absolutuen ordez, balio erlatiboetan oinarritzen den sailkapen bat lortzea denean helburua, zenbaketa netoak erabiltzea gomendatzen da, baldintza berdinetan egindako analisietan balio fidagarriagoak ematen baitituzte. Aitzitik, emaitza kuantitatiboak beharrezkoak izaten dira laborategietan lortutako emaitzak konparatzeko.

Hala ere, kontuan izan behar da, kontzentrazio jakin baterako, ED-XRFren intentsitateak askoz txikiagoak izango direla elementu arinentzat, elementu astunekin alderatuz. Ionizazioaren zeharkako-azalera askoz txikiagoa da elementu arinentzat, eta horregatik energia baxuko X izpien xurgapena handiagoa da elementu hauentzat, islapena murriztuz. Islapena txikiagoa izanik, ED-XRF detektoreak jasoko duen seinalea ere txikiagoa izango da. Horrek eragina izan dezake, bereziki, elementu arinen bidez (Al edo Si) bereizten diren laginen diskriminazioan. Beraz, muga horiek direla eta, hemen aurkezten den metodologia bahetze helburuetarako bakarrik erabili daiteke.

Albo-ebazpena

Energia-fluxua batez ere hautatutako optikak arautzen duena, handiagoa izango da optika polikapilarra erabiliz (25 μm vs 1 mm albo-ebazpena). Horrela, 25 μm-etara, lagineko elementu arinenen detekzioa hobetuko litzateke. Horregatik, zentzuzkoa izan liteke albo-ebazpen hau aukeratzea ED-XRF eredua eraikitzeko. Hala ere, lan honetan erabilitako CRMen partikula-tamaina 75 μm-tik gorakoa da. Beraz, pellet moduan edo Mylar filmarekin aurre-prentsatutako CRMak ez dira era homogeneoan aurkituko 25 μm-ko albo-ebazpenarekin, are gehiago, CRMak bola bidez ehotuak izan direla eta bahe batetik iragaziak izan direla kontuan hartuz, kontsideratu daiteke benetako zeramika-matrizea askoz ere heterogeneoagoa izango dela albo-ebazpen txiki honetara neurtuta. Behaketa hau, hurrengo ataletan baieztatuko da.

CRMak pellet gisa eta Mylar filmarekin ematen dituzten neurketen desbideratze estandarrak (% RSD) kalkulatu ziren 1 mm eta 25 μm-ko albo-ebazpenak erabilita (ikus 6.3. taula). Ikus daitekeen bezala, elementu guztietarako 1 mm-ko kolimadoreak RSD baxuagoak eskaini zituen. Horrela, 1 mm-ko albo-ebazpena erabiliz lortutako balio gehienak 25 μm-etara lortutakoen erdiak izan ziren, 15-20%-ko tarteko RSDak emanez gutxi gora behera, Cl, As eta Pb salbuespen izanik. Pb-arentzako lortutako RSD balio handiek, iradokitzen dute elementu hori oso era sakabanatuan aurkitzen dela pellet-ean zehar. Gainera, Cl-a eta As-arentzat lortutako RSD balio altua elementu horien LOD-arekin erlaziona daiteke, erabilitako gailuarekin, Rh-zko X-izpiaren hodi batekin, alegia. Kasu batzuetan, % RSD baxuagoak lortu ziren 1 mm-rekin Mylar filma erabiliz, pelletekin lortutako balioekin alderatuz. Horrekin ulertzen dugu, CRM-a pellet moduan

prentsatutakoan ez zegoela 25 μm-etara neurtutako pellet-a bezain beste homogeneizatuta. Emaitza hauetatik abiatuz, ED-XRFean oinarritutako modelo ez-suntsitzaile bat eraikitzeko 1 mm-ko albo-ebazpenera neurtu ziren zeramikak. Matrizearen heterogeneotasuna kontuan hartuz, albo-ebazpen bakoitzak estalitako eremuen konparazioa burutu zen (ikus 6.4. irudia). Behatu daitekeen moduan inklusio-tamaina ohikoenak 1 mm-ko diametroaren barnean geratzen dira.

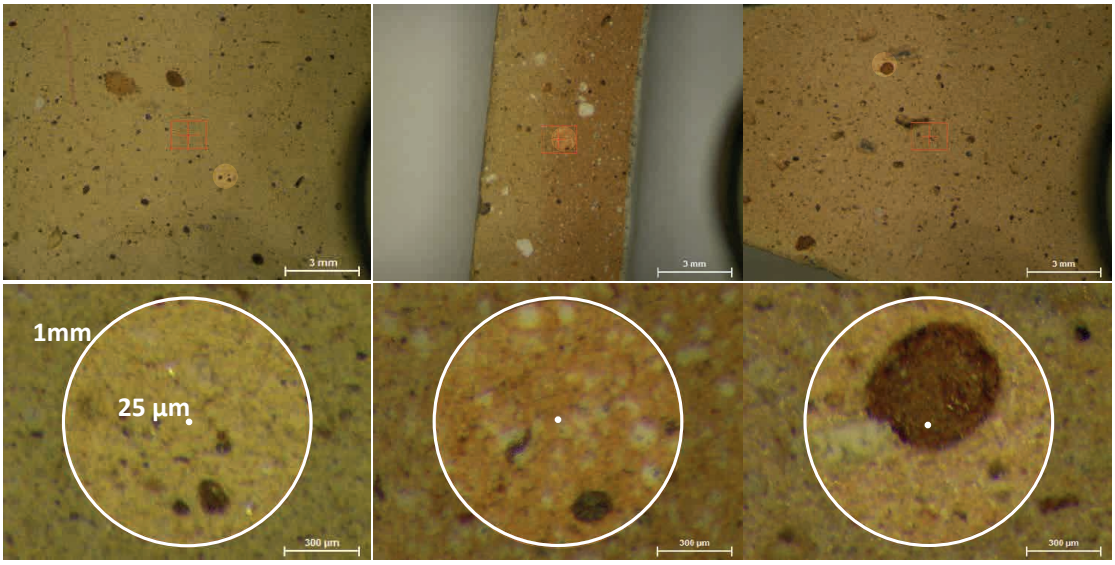

Figure 6.4: Zeramiken heterogeneotasun desberdinak eta albo-ebazpen bakoitzak estalitako azalera 25 μm eta1 mm-etara.

Laginaren adierazgarritasuna

Lagin bakoitzeko 50 erreplika-analisi egitea erabaki zen, aztertutako zeramika-zatikien ohiko morfologiak kontuan hartuz, 4 cm-ko luzera maximoak dituztenak, alegia. Analisi-kopuru hau (bakoitza 1 mm-ko albo-ebazpenarekin), nahikoa zela kontsideratu zen. Horrela, aztertutako azalerak estaltzeko eta, beraz, lagin bakoitzaren geokimika behar bezala adierazteko, hau da, prezisio-zerra batekin ebakitako zeharkako-azalerak.

Hala ere, analisi-kopurua erraz egokitu daiteke zeramika-multzo bakoitzaren premietara. Gainera, ED-XRF softwareak neurketa-puntu zehatzak eskuz edo automatikoki hautatzea ahalbidetzen du, hautaketa-aukera desberdinak ahalbidetuz. Hala nola, ausazkoak edo uniformeki sakabanatutako puntuak hartuz. Beraz, analistak zehatz-mehatz aukeratu ditzake analisi puntuak, azalera zailak dituzten zeramiketarako bereziki erabilgarria dena (adibidez, inklusio handiak dituztenak, beiratuak etab.).

Table 6.3: ED-XRF bidez lortutako %RSD balioak SRM679-CRMan, Mylar filmean prentsatuta eta zenbaketa-netoak neurtuta 1 mm- eta 25 μm-ko albo-ebazpenekin. CRMen balioak pellet-gisa prestaturik parentesi arten aurkezten dira.

Elementua RSD (%)	25 μm	1 mm
Al	8	2 (2)
Si	9	1 (1)
Cl	26	50 (45)
K	13	1 (1)
Ca	54	6 (4)
Ti	9	2 (1)
V	16	7 (7)
Cr	14	16 (11)
Mn	16	5 (5)
Fe	22	2 (1)
Ni	34	19 (10)
Cu	37	16 (16)
Zn	38	7 (4)
Ga	42	13 (13)
As	80	28 (15)
Rb	47	4 (2)
Sr	51	8 (4)
Y	39	12 (9)
Zr	40	5 (4)
Pb	183	83 (75)

Hemen aztertzen den zeramika-multzoan, zeramika gehienak beiraztatuak direnez, neurketa-puntuak eskuz zehaztu ziren, eta horrek erraztu egin zuen zeramiken morfologia anitzetara erraz egokitzea. Aldiz, laginaren azalera laukizuzena edo karratua izan daitekeen kasuetan, sistema automatikoa egokiagoa izan daiteke, baina zeramika arkeologikoetan hautaketa-automatiko bat zeramikaren adierazgarriak izan daitezkeen guneak alde batera uzteko arriskua dakar.

Begi-bistakoa izan zen, analisi-puntuak beiratuetatik gertu egiten ziren kasuetan Pb kontzentrazioak izugarri handitzen zirela. Izan ere, erreketa garaian, elementu hau beiratutik zeramika-gorputzera barreiatzen da (Molera et al., 2001). Gainera, ED-XRF softwareak auto-fokatze aukera ematen du. Hori dela eta, automatikoki burutu liteke lagin anitzen analisia, sistemak lagin batetik bestera automatikoki pasatzeko ahalmena daukalako. Gaitasun honek, analisiak aldez aurretik programatzeko aukera ematen du.

Tarte-Dinamikoak, LOD eta LOQak

$Z < 20$ Elementuak

Oro har, ED-XRFren LOD-ak hobeak dira elementuen zenbaki atomikoak (Z) handitzen diren heinean. Nahiz eta arau hori lineala ez izan, Na (Z=11) beherako elementuak detektaezinak izango dira (Speakman et al., 2011; Beckhoff et al., 2007). Aztertutako zeramiketan Na_2O-ren kontzentrazioak 0.7 eta 1.5 masa % tartekoak ziren. Beraz, zeramika-arkeologikoetan dagoen Na birtualki ikusezina izango da Rh-zko kitzikatzailea duen ED-XRFaren detektorearentzako. Aitzitik, W-zko kitzikatzailea egokiagoa izango litzake elementu arinen detekziorako. Era berean, Mg, P eta S-ren ekarpenak ingurumen-intentsitateagatik bereiztea zaila da bi oztopo nagusiengatik: (i) haien kontzentrazio baxuak zeramika arkeologikoetan, eta (ii) isuritako fluoreszentziaren energia baxua, zeina xurgatua izan daiteke era erraz batean zeramika-matrizeagatik, detektorearen-leihoagatik eta edota Si-ko geruz-hilarengatik (ingelesez *dead-layer* deritzona) (Hunt and Speakman, 2015). Detekzioak are okerragoak dira kolimazio mekanikoa erabiltzen bada, lehenago adierazi den bezala. Gainera, P-ren kasuan, Ca-ren ihes-gailurrak (ingelesez *scape-peak*) arazoak ekar ditzake. Hori dela eta, dekonboluzio egokia egiten ez bada, P-ren ekarpena erreala baino handiagoa izango da. Hala ere, zenbait kasuetan S eta P baztertuak izan daitezke karakterizazio-arkeometrikoan, haiek erakusten duten ausazko aldakortasunaren ondorioz. Izan ere, lehenago azaldu den moduan (ikus 5.1. atala) kanpo-faktoreen mende egon daiteke, eta, beraz, ez dira zeramika-pasten ezaugarrien adierazle izango. Aitzitik, Mg-a atzematea oso zaila da, baina elementu honek paper garrantzitsu bat joka dezake konposizio-multzo batzuen bereizketan. Hala nola, DUR multzoaren bereizgarritasunean; zeina Mg-aren (Mn-az gain) bidez, ELS multzotik bereizia izan daitekeen, ICP-MS emaitzak adierazi duten moduan. Halaber, LOG033ren LOG multzotik bereizten da Mg kontzentrazio baxuagoa erakusten duelako (ikus 6.2. taula).

Horrela, zeramika arkeologikoetan adierazgarriak izan daitezkeen Z baxu edo ertaineko elementuetatik, alegia, Na, Mg, Al, Si, Mg, Al, Si, P, S, K eta Ca (Speakman et al., 2011), erabilitako ED-XRF konfigurazioarekin, Al, Si, K eta Ca-k erakusten dute atzemateko behar besteko kontzentrazio nahikoa.

$Z > 20$ Elementuak

ED-XRF-an LODak askoz hobeak dira, batez ere Z >15 elementuetarako. Lan honetan erabilitako ED-XRF tresnarako estimatutako LODak (μg/g-tan) honakoak dira: 100 Ti-rentzat, 80 Cr-rentzat, 50 Mn-rentzat, 40 Fe-rentzat, 30 Ni-rentzat, 20 Cu eta Zn-rentzat. Gainera, 300 eta 200 Sn eta Pb-rentzat.

Beraz, ICP-MS emaitzen arabera, Ti, Mn, Fe eta Pb bezalako elementuak, nahiko kontzentrazio aberatsetan daude, baldintza horietan balio semi-kuantitatibo adierazgarriak emateko. Aitzitik, Sn-aren balioak 200 μg/g-tik behera geratzen dira. Gainera, Fe-an aberatsak diren matrizeetan ihes-gailurren (4.660 keV) ekarpena kontu handiz landu behar dira, Ti-aren K_α (4.508 keV) lerroari gainjartzeko arriskua baitago.

Era berean, Ti, V, Cr, Mn, Fe eta Co-ren espektro-lerroak kontu handiz hautatu behar dira dekonboluzio egoki bat lortzeko, haien K_α lerroak, elementu horien aurreko Z daraman K_β-lerroarekin gainjartzen baitira. V, Cr, Mn eta Co-ren kontzentrazioak Ti eta Fe-renak baino asko baxuagoak dira. Halere, elementu horiek Ti eta Fe seinaleetan eragin dezaketen ekarpena ekiditua izan behar da seinaleen dekonboluzio egoki baten bidez. Aztertutako zeramika multzoan V, Cr, Co, Ni, Cu eta Zn-k aurkezten dituzten kontzentrazioak LODaren edota LOQaren azpitik geratzen dira, aztertutako zeramika multzorentzat. Sr-arentzako, konposizio-multzo bakoitzaren batez bestekoa 329 eta 677 μg/g bitartekoa da. Beraz, ED-XRF metodoarekin atzemateko arazorik ez litzake izan behar. Hala ere, bere presentzia Ca-rekin batera aurkitzen da, eta, beraz, aukera teknologikoen ondorio izan daiteke zeramikaren hatz-marka kimikoarena izan beharrean, lehen eztabaidatu den bezala. Horregatik, estatistika-analisian duen eragina kontu handiz tratatu behar da. Rb-rentzako estimatutako LODa 30 μg/g-koa da, gutxi gora behera, zeramiketan topaturiko kontzentrazioak (80 - 189 μg/g) aise gainditzen dutelarik. Rb, Ga eta Y-ren kasuetan, oso zenbaketa-baxuak erakusteaz gain, Pb-aren presentziak elementu hauen atzematean duen eragina nabarmendu behar da, aurrerago ikusiko dugun bezala. Laburbilduz, hemen erabilitako ED-XRF konfigurazioarekin arkeologia-zeramikaren kontzentrazioen arabera, ondorengo elementu hauek bakarrik hartu daitezke kontuan azterketa estatistikorako: Ti, Mn, Fe eta Zr. Sr-a ere erabil daiteke, baina zenbait murriztapenekin.

Heterogeneotasun zeramika arkeologikoetan

Zeramika arkeologikoak material sintetiko eta heterogeneo gisa ulertzea nahitaezkoa da. Izan ere, XRF bidezko azterketa ez-suntsitzailea egiteko erronka multzo berezi bat aurkezten dute. Horrela, orain arte aipatutako faktoreez haratago (ihes-gailurrak, LODak, atenuazioak, etab.), zeramika-matrizeekin zerikusia duten beste aldakortasun-iturri batzuk, haien geokimika behar bezala karakterizatzea oztopatu dezakete. Muga horietatik garrantzitsuenak hauek dira: zeramikaren heterogeneotasun, ale-tamaina eta efektu mineralogikoak (Hunt and Speakman, 2015; Forster et al., 2011; Frahm, 2013). Faseen nahasketa heterogeneoak, beste faktore batzuez gain, X izpien interakzioak biziki eragin ditzake. Gainera, alearen tamainak X izpi sortaren barneratze sakoneran eragina izango du. Horrela, ale txikiagoak barneratze sakonagoa ahalbidetuko dute. Handienek, berriz, sortarekin zuzenean elkarreragin dezakete, eta horretaz gain, berez aztertzen den konposizioaren masa mugatu (Hunt and Speakman, 2015). Gainera, ale horien kristal-egiturak, dentsitateak eta konposizioak X izpi

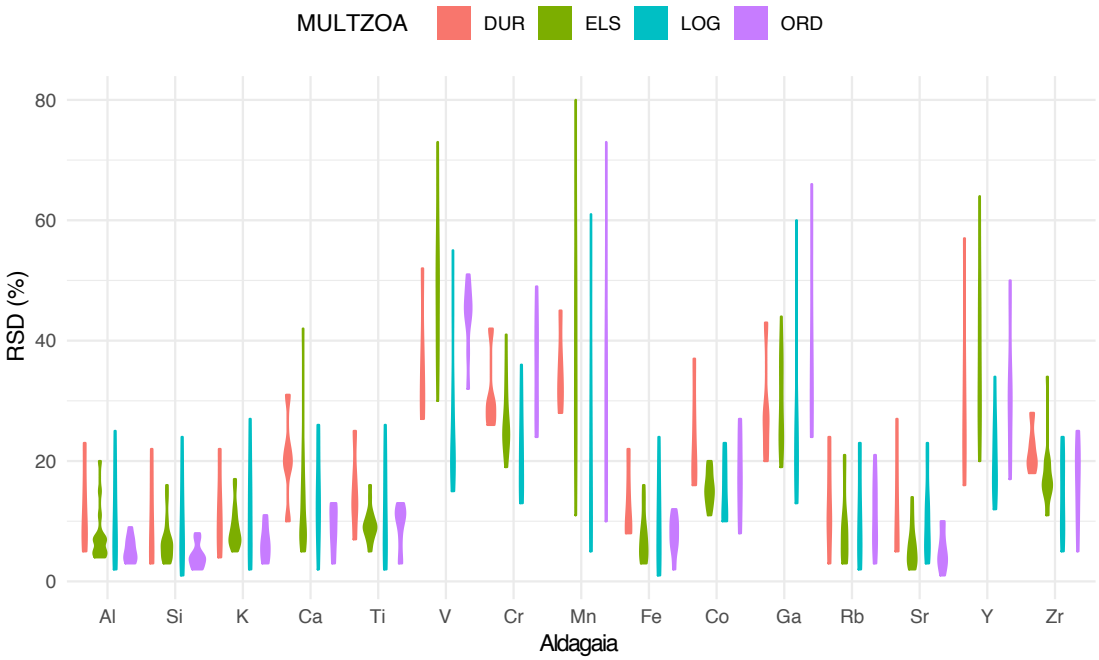

Figure 6.5: Biolin diagrama ED-XRF bidez lortutako RSD (%) balioekin. Elementu bakoitzaren 50 erreplika-analisiak erakusten dira. Pb-a 200% gorako RSDa aurkeztu zuen eta ez da grafikoan erakusten, gainera elementu batzuk LOD edota LOQren azpitik geratzen dira, beraz haien balioak orientagarriak dira.

sortarekin edukiko duten interakzioan eragin zuzena edukiko dute. Zeramika arkeologikoak hainbat tamainatako mineralez osatutako buztinak dituzte, eta horiek ez dira ehotzen era ez suntsitzailean egindako analisietan. Horregatik, zeramiken heterogeneotasuna erronka eztabaidatuenetako bat da.

Ohiko zeramika arkeologikoen heterogeneotasuna ebaluatzeko, lagin bakoitzeko 50 analisi-punturi dagozkien zenbaketa netoen balioen ondoriozko RSDak hartu ziren kontuan (ikus 6.5. irudia). Grafikoak datuen sakabanaketa ebaluatzeko aukera ematen du, zeina kasurik onenetan % 5 baino baxuagoa den (Al eta Si) eta %100-etara iristen den Ga bezalako elementurako. Pb-a salbuespena litzake, % 200-etik gorako balioak emanez. Oro har, zenbat eta heterogeneoagoak izan zeramikak, orduan eta handiagoak izango dira RSD balioak. Hala ere, RSD altua duten zenbait elementuk, beste arrazoi bati erantzun diezaiekete, hala nola, detektoreak haien zenbaketa neto murriztuak erregistratzeko duen zailtasunari (RSDen zerrenda A. Eranskinaren A.9. taulan aurkezten da).

Bi joera hauteman ziren 6.5. irudiaren arabera: batez ere 1-25 % tarteko RSDak zituzten elementuak (Al, Si, K, Ca, Ti, Fe, Rb, Sr, Zr) eta horren gaineko balioak

erakusten zituztenak % 80-ra iritsiz (V, Cr, Mn, Co, Zn, Ga eta Y). Azken elementu zerrenda honetatik, berriz, Mn izan zen kontzentrazio-tarte egokiak aurkezten zituen elementu bakarra ED-XRF analisirako. Hala ere, elementu horren heterogeneotasuna altuegia da estatistika-analisian aintzat hartzeko. Kontuan izan beharra dago, elementu batzuk ez zirela kontuan hartu emandako seinale baxuen ondorioz (Cr, V, Co, Ga eta Y) edo Pb-aren eraginagatik (Ga, Rb eta Y). Hala ere, haien RSDak, banaketari buruzko informazioa eman ditzakete.

Emaitza horien arabera, %RSD balorerik onenak Al, Si eta Fe-k eskaini zituzten. Gainera, grafikoan ikus daiteke nola aldatzen den heterogeneotasuna konposizio-multzo batetik beste batera, analizatutako piezen kopuruaz haratago (ikus 6.5. irudia). Esate baterako, DUR (n = 5) multzoak ORD (n = 10) baino askoz % RSD handiagoa bat erakutsi zuen, naiz eta zeramika-kopuru erdia izan. Beraz, argi dago %RSDa aldakortasuna ez dela lagin kopuruaren araberakoa, baizik eta multzo bakoitzaren konposizio banaketaren araberakoa. Gainera, elementu bakoitzaren distribuzioa aztertzeko asmoarekin, ED-XRF gailu honek ahalbidetzen duen *imaging* analisia burutu zen 25 μm-ko albo-ebazpenarekin. Hori dena, aurreko analisiak burutu diren txanda berdinean, hau da, inolako aldaketarik egin behar izan gabe. Azterketan honen emaitzak 6.6. irudian behatu daitezke, non ELS020-ren kasu aurkezten da adibide moduan.

Mapeatutako eremuaren azalera 36 x 13.4 mm-koa izan zen zen (1803 x 671 pixelekoa). Espektro bakoitza lortzeko 50 ms eta 4 ziklo erabili ziren. Puntu gorriek Ca metaketak adierazten dituzte. Horiek, kaltzita bezalako karbonatoren bat izan daitezke eta Ca-ren %RSD a handitzea eragiten dute. Puntu berdeak berriz, Fe adierazten dute, eta dentsitate handiagoa adierazten dute. Horiek hematiteekin lotuta egoten ohi dira. Bi inklusio mota hauek, aurkitzen diren ohikoenak izaten dira zeramika arkeologikoetan.

Pb kontzentrazio altuek zeramika arkeologikoetan duten eragina

Pb zeramika-arkeologikoetan bi lekutan aurkitzen da: buztinezko gorputzetan eta beiratuetan nabarmenki (horren osagai nagusi bat izanik). Pb-a beiratutik buztinezko gorputzerako zabaltze-frontea oso aurreratua baldin bada, haren kontzentrazioa nabarmenki igotzen da beiratuen inguruan (Molera et al., 2001) .Esperimentu honetan erregistratutako Pb kontzentrazioak oso distribuzio irregularra ageri zuten lagin desberdinen artean. Zenbaketa-netoen tarteak $1x10^3$-tik $3x10^5$-ra igarotzen ziren. Gainera, haien %RSDak 200%tik gora egiten zuten, beste elementu guztiek erakutsitakoak baino askoz altuagoak izanik (ikus 6.5. irudia).

Gainera, $2x10^6$-ko muturreko balio bat erregistratu zen ELS049 kasurako. Lagin honen salbuespenarekin, ICP-MS bidez lortutako kontzentrazioak ED-XRFarekin lortutakoekin bat datoz. Bi teknikek, ELS038 irudikatzen dute Pb-an aberatsagoan den lagina bezala (12.9 $x10^3$ μg/g). Aitzitik, ELS049, ez zuen balio bereziki alturik eskaini

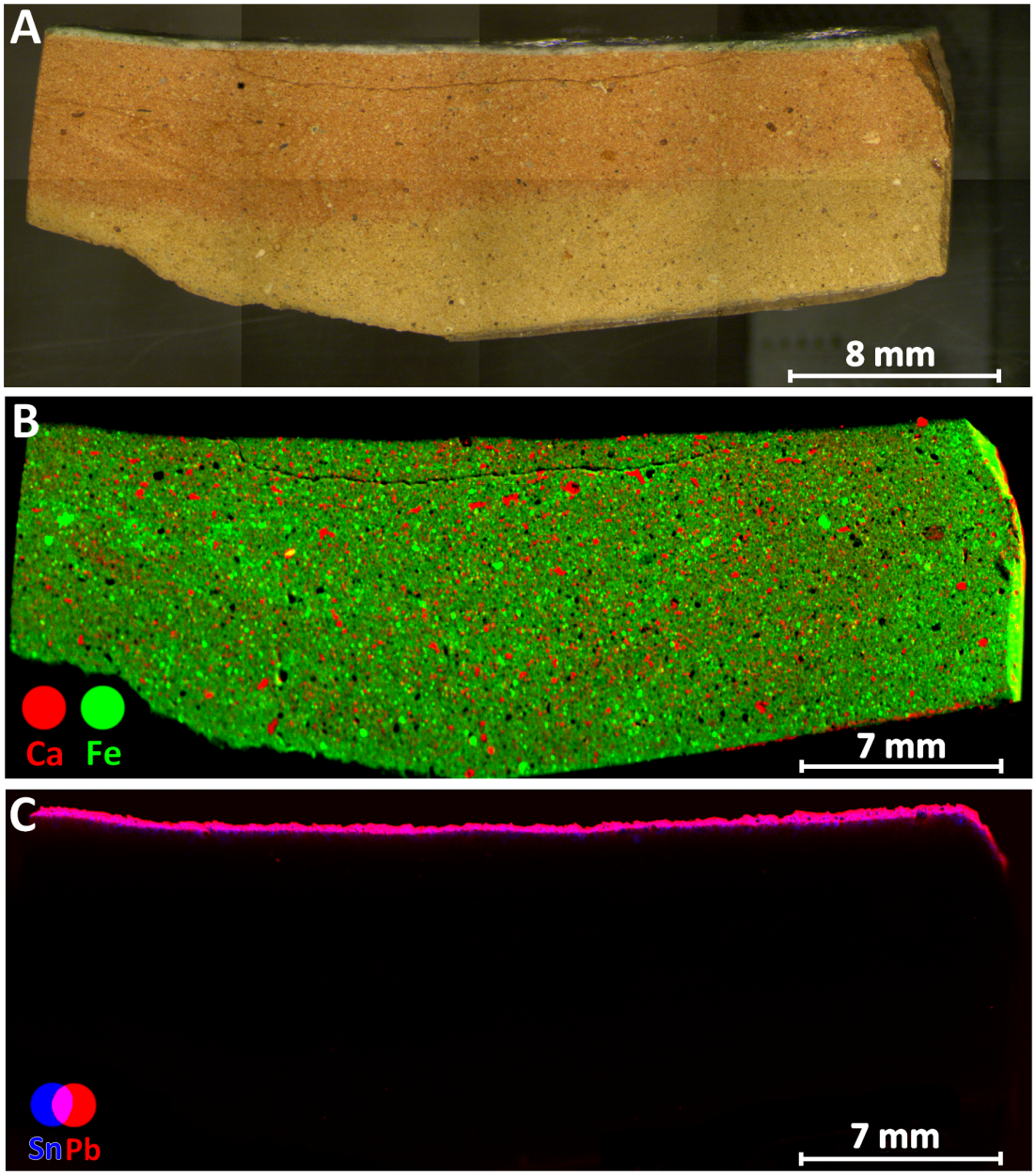

Figure 6.6: ELS020 zeramikaren irudia (A) eta ED-XRF bidezko mapa elementala 25μm-tara,Ca eta Fe elementuen distribuzioak erakutsiz (B) eta Sn eta Pb elementuak, beiratuekin loturik daudenak (C).

Pb kontzentrazioari dagokionez ICP-MS bidez ($11.4x10^3$ μg/g). Beraz, nahiz eta beiratuaren inguruko analisi-puntuak biziki saihestu ziren, emaitza altu hau azaltzeko modu bakarra, analisi-puntuen berunezko beiratuaren gertutasuna da. ED-XRFri

dagokionez, matrize zeramikoetan Pb-aren presentzia modu kritikoan jorratu behar da; izan ere, Ga eta Rb seinaleekin interferentziak eragiten ditu, era horretan, balizko elementu diskriminatzaileak murriztuz (Forster and Grave, 2013). Ga eta Y murrizketaren arrazoia, ziurrenik, Pb-aren eragina da. Bai ELS049ko zenbaketa netoetan eta oro har lagin guztiek erakusten dituzten %RSD altuetan ere (20-60%-koa). Eragin hau bereziki handia da Pb kontzentrazio altuak erakutsi dituzten laginetan (ikus 6.5. irudia). Gainera, elementu hauek LODeiko oso gertuko kontzentrazio-balio erakutsi zituzten, eta, beraz, ez ziren baliozkoak izan estatistika-analisirako. Aitzitik, Rb laginak, oro har, RSDen balio baxuagoak erakusten ditu (<25 %) Pb-aren interferentzia txikiago bat adieraziz, hala nola, kontzentrazio-tarte hobeagoak (LOD gainetik). Hala ere, zenbaketa-netoek adierazten dutenez, ELS049ren Pb altuenaren seinalea Rb seinale baxuenarekin lotuta egongo litzake. Nahiz eta erlazio hori lineala ez izan, Rb-ren balioak kontu handiz erabili behako lirateke analisi-estatistikoetan; eta, bereziki Pb-an aberatsak diren matrizeetan.

ED-XRF bidezko sailkapena

Zeramika guztiak neurtu ondoren, honako 24 elementu hauek detektatu ziren: Mg, Al, Si, P, S, K, Ca, Ti, V, Cr, Mn, Fe, Co, Ni, Cu, Zn, Ga, As, Rb, Sr, Y, Zr eta Pb. Kasu guztietan, elementu bakoitzaren Kα lerroa hartu zen kontuan, Pb kasuan izan ezik, non Lα lerroa aukeratu zen. Hala ere, detektatutako elementu asko ez ziren baliozkoak analisi-estatistikoetarako honako arrazoiengatik: (i) ED-XRF laginak modu egokian detektatzea ez zen posiblea, hain zuzen ere, kontzentrazio txiki eta zenbaketa-kopuru txikien ondorioz, (ii) zeramiken kontzentrazioak LOD edo LOQren azpitik geratzen ziren (iii) %RSDak altuegiak ziren zeramika matrizeak ondo adierazi ahal izateko eta (iv), Pb-kontzentrazio altuek beste elementuen seinaletan eragiten zuten.

Arestian aipatutako oztopoak kontuan hartuta, honako elementu hauek erabilgarritzat jo ziren estatistika-tratamendurako: Al, Si, Ca, Ti, Fe, Zr, K eta Sr. Oinarrizko azterketa egiteko kontzentrazio-eremu egokietan egon ziren, eta RSD muga onargarriak aurkeztu zituzten.

Sailkapen zehatzena, ordea, azterketa-estatistikoan Ca eta Sr baztertzen zirenean lortu zen (Ikus 6.3. irudia). Elementu horientzat aurretik eztabaidatutako oztopoez gain, elementu diskriminatzaileen kopuru murriztuak sailkapena desbideratzen zuten elementu nagusi horiei lehentasuna emanez eta haien kontzentrazioari neurri handiagoan eusten dioten multzoak sortuz. Beraz, Ca eta Sr azterketa estatistikoan barne hartuz, LOG033 eta LOG038, era okerrean TBC multzoei lotuak agertzen ziren. Aldi berean, TBC hiru kluster berritan banatu zen, non hiru multzo euskaldunak (ELS, ORD eta DUR) bereizezinak zirelarik. Bestalde, LOG multzoa hobeto definituta zegoen, Ca kontzentrazio txikiagoa oso nabarmena baita, beste multzo guztiekin alderatuz.

Horrenbestez, hobekuntza nabarmena lortu zen, azterketa estatistikotik Ca eta Sr baztertzean. Ezabatu arren, adierazi behar da egungo metodologia ez dela gai elementu horiek beste elementu batzuen seinaleetan izan dezaketen eragina zuzentzeko. Hori kontuan hartu behar den beste joera bat izan liteke, batez ere Ca-n pasta aberatsak dituzten zeramiketan.

Erabilgarriak diren 6 aldagaiekin HCA eta PCA burutu ziren (ikus 6.3. irudia). ED-XRFaren kasuan, 50 neurketen batez besteko balioak erabili ziren HCArako. PCArako, berriz, behaketa guztiak hartu ziren kontuan. Era horretan, lagin bakoitzari dagozkion puntuen banaketa ere ebaluatu daiteke. ED-XRFk lortutako dendrogramak arrakasta handiz erreproduzitzen du TBC eta LR arteko banaketa nagusia. Gainera, TBC hiru multzo txikiagoetan banatzen da, nahiz eta hierarkia orain desberdina den. Kasu honetan, DUR multzoaren ordez isolamendu handiagoa erakusten du ORD multzoak. PCAren arabera, ORD multzoa, Si-ren ekarpen handiagoaren eraginez separatzen da. Gainera, bi kasuetan LOG038 eta LOG033, LOG multzotik kanpo agertzen dira, nahiz eta distantziak ere aldatu diren. Oker sailkatuta agertzen den lagin bakarra ELS038 da; hau da, Pb gehien duena eta DUR multzoari lotuta agertuz kasu honetan.

Azpimarratzekoa da K-a funtsezkoa elementua izan zela sailkapen hau lortzeko. Batzuetan, elementu hori estatistika-analisietatik saihestu egiten da, analzimarekin lotutako eraldaketa dela eta (ikus 5.1. atala). Nahiz eta zeramika-multzo honetarako XRD bidezko analisiek ez zuten horrelakorik identifikatu, metodologia hau mugatua egongo litzake analzima bidez eraldatutako zeramikentzat. Adibidez, DUR multzoa, bereziki Mn zein Mg-ren bidez bereizten da gainontzeko multzoetatik, ICP-MS emaitzek erakutsi zuten bezala, baina elementu horiek ezin dira ED-XRFren bidez erabili. Beraz, K-ren erabilera nahitaezkoa izan zen multzo hori behar bezala identifikatzeko. Analisi-estatistikoetan K kontuan hartuz, LOG multzoan elementu honetan oinarrituriko bi multzo bereizten ziren, ICP-MS bidez ikusten ez zirenak, HCA eta PCA behatu daitezkeenak (ikus 6.3. irudia).

Esan daiteke korrespondentzia-maila handia dagoela lortutako sailkapena suntsitzailea eta ez-suntsitzailearen artean (ikus 6.3. irudi). Nolanahi ere, Pb-ren kontzentrazio altuek eragina dute azken emaitzetan. Hala ere, eragin hori ez zen nahikoa izan ELS049 era oker batean sailkatzeko, izan ere, bi sailkapenetan ELS multzoaren barruan bateratu zen.

6.3 *Eztabaida eta Ondorioak*

Lan honetan, ED-XRFren bidez, era ez-suntsitzailean lortutako datuak aldagai anitzeko metodo estatistikoekin tratatu ziren. Horrela, teknika ez-suntsitzailearen gaitasuna ebaluatu zen ICP-MS bidez eta era suntsitzailean lortutako konposizio-multzo

desberdinen artean diskriminatzeko. 1 mm-ko albo-ebazpenarekin burututako analisi puntualek estrategia ez-suntsitzailea jarraituz (50 erreplika-analisi), agerian utzi dute ED-XRF errutinen potentziala Erdi Aroko eta Erdi Aro osteko zeramiken helburu diskriminatzailerako. Zeramika-tipologia horiek oso pasta dekantatuak izaten ohi dituzte (karedun edo ez-karedun), eta haien inklusioen tamaina 1 mm baina txikiagoa izan ohi da (ikusi 6.4. irudia). Nolanahi ere, buztin-gorputzak gutxieneko pasta homogeneoa aurkeztu behar du, metodologia honek aplikagarritasuna izan dezan. Beraz, matrize guztiak ez lirateke egokiak izango; esate baterako, sendogarri asko dituzten zeramikak, aipatutako Zamorako eltze ezagunak, edota ez-dekantatutako pastak, adibidez, zeramika-ekoizpenaren lehen etapakoak.

Elementu bakoitzak erakutsitako kontzentrazio eta heterogeneotasun-tarteei erreparatuz, honako aldagai hauek erabil daitezke estatistika-analisirako: Al, Si, K, Ti, Fe, Zr, Ca eta Sr. Hala ere, azken biak ez ziren erabili ondoren azaltzen diren arrazoiengatik. Gainera, elementu ugari LODaren azpitik geratzen ziren, hori izanik gainditu beharreko oztopo nagusietako bat.

Emaitzek korrespondentzia positiboa erakutsi zuten era suntsitzailean eta ez-suntsitzailearen bidez lortutako sailkapenen artean, bigarrenak zeramika-pastaren geokimikaren hurbilketa nahiko ona eskaintzen duela adieraziz. Hala ere, azpimarratu beharra dago ICP-MS bidez lortutako multzoak zehatzagoak izan zirela, ebazpen maila altuagoa erakutsiz. Dendrogramaren distantziek, y-ardatzean irudikatzen direnak, ezberdintasun horiek irudiztatzeko balio dezakete. Horrela, metodologia suntsitzailean 3-ra arteko distantziak lortzen dira. Bestean, 0.6-ra arte baino ez dira iristen (ikus 6.3. irudia). Beraz, lan honetan aurkeztutako metodologia arrakastaz erabil daiteke *screening* edo bahetze helburuetarako.

Ca eta Sr ezin izan ziren erabili, sailkapen okerrak eman ditzaketelako. Gehien bat, hautaketa-teknologikoak nabarmenak direnean (adibidez, karbonatoen gehikuntza nabarmena pastetan). Kasu horietan, sailkapena elementu nagusi horien menpe egon liteke; izan ere, hain elementu diskriminatzaile gutxi egonda, elementu nagusiek pisu handia hartzen dute analisi-estatistikoaren emaitzetan. Aitzitik, ICP-MS bidezko sailkapena askoz egokiagoa suertatzen da, elementu sorta zabalagoa eskaintzen duelako, non nahiz eta elementu horiek kontuan hartu, ez diren aldaketa nabarmenak gertatzen. Gainera, analzimaren bidez eragindua egon litekeen K erabili behar izan zen sailkapen egokiak lortu ahal izateko, elementu diskriminatzaile nahikorik ez zegoelako. Beraz, metodo hau baliogabea izan daiteke analzima duten laginen kasuetarako.

Metodologia honen abantaila nagusia azterketa ez suntsitzailea da. Zeramikaren ebaketa teknika inbasiboa da, baina pauso hori funtsezkoa da jalkitze-ondoko kutsadurak saihesteko eta jatorrizko zeramika matrizetik datuak ateratzeko. Hala ere, pausu horrek inbasibitate maila oso baxua hartzen du, laginen ehotzearekin konparatuta; izan ere, zatikiak berriro erabil daitezke analisi gehiago egiteko edo gordetzeko. Gainera, egungo metodologiak instalazio merkeagoa eta eskuragarriagoa

eskatzen du ICP-MS analisia egiteko behar diren ekipoekin alderatuta, lagina prestatzeko (urgarria, produktu kimikoak, etab.) eta ekipo-analizatzailearentzat beharrezkoa den gela zuriarekin alderatuta. Beste abantaila batzuen artean nabarmendu beharra dago, konfigurazioak eskaintzen duen automatizazio aukera. Haren bidez eta auto-enfokeari esker, lagin-sorta handiak (bai puntualak, bai mapping modukoak) etengabe aztertzea ahalbidetzen da.

Analisi hau, lehenengo hurbilketa gisa erabili daiteke zeramikazko materialentzat. Horren bidez zeramika adierazgarrien hautaketa bat egiteko aukera legoke, ondoren, analisi suntsitzailearen bidez analizatu ahal izateko. Era horretan, denbora eta kostuak aurrezteaz gain, ordezkaezinak diren material zeramikoak eraldatu edo suntsitu gabe gordetzea ahalbidetzen du.

Hemen proposatzen den metodologiak, atariko hurbilketa bat eskaintzen du testuinguru zehatz batzuetako zeramika arkeologikoentzako. Konfigurazio honekin, horrela lortutako sailkapenek, aldez aurreko sailkapen bat egitea ahalbidetuko luke. Aitzitik, jatorri-ikerketak, aztarna eta elementu gutxiengoen kontzentrazioetan gehiago oinarritzen direnak teknikaren lantze handiago bat beharko lukete.

Chapter 7

Conclusions

The results obtained in the present Doctoral Thesis constitute an important progress in the development of tools for archaeometric study of pottery, both regarding the computational aspect of the compositional analysis, as is addressed in Chapter 4, and the non-destructiveness of the techniques used to acquire the compositional data, as is addressed in Chapter 6. Along these lines, the study of the pottery production centers of Logroño, Nájera, Orduña, Durango and Elosu, allowed to conduct these methodological developments. In addition, it entailed an important contribution to the archaeometric knowledge about the ceramic productions of the Basque Country and La Rioja in medieval and post-medieval periods, as is addressed in Chapter 5.

The development of an *open source* methodology based in R (Calparsoro, 2019) has provided all the necessary code to apply the routines involved in statistical analysis of compositional data. In consequence, the repository can be cloned and/or the code it contains can be executed guaranteeing 100% of reproducibility. In addition, the HTML reports generated automatically during the process, allow to keep the record of the results for interactive exploration at any time. The framework in which the current work has been carried out —as an *open method*— allows to follow the workflow from a beginner level, but also permits the customization of the code according to the specific requirements and skills of the user. In addition, the chunks of code included in the Rmarkdown files of this proposal involves a high user-friendly environment. It is therefore a particularly useful method for pedagogical purposes, which, at the same time, intends to engage the scientific community using such tools. Moreover, the workflow includes the main tools used for archaeometric analysis of compositional data, but is not limited exclusively to this field. In fact, a notable advantage of the current methodology is that it can be extended to other types of analyses involving compositional data.

In the academic scenario, current general understanding about concepts that have been addressed in the Chapter 4, such as *open source*, *open method*, *open data* and *open access* seems to be still fuzzy. In contrast, these formulas are increasingly been employed in the guidelines of the most important research funding organizations, such as the Horizon 2020 Framework program on Research and Innovation of the European Commission (Guedj and Ramjoué, 2015; Wilkinson et al., 2016). In consequence, the open publication of data and results has started to be rather generalized, as evidences the obligation to publish in *open access* imposed by this organization in the projects financed by it. Moreover, the concept of *Open Science* can be extended to the software and methods as has been highlighted in this Doctoral Thesis. Nonetheless, many research projects funded by public money still employ privative softwares to carry out investigations and a wide array of everyday task (e.g. Microsoft Office or Matlab). Part of the reason for this scenario relies on the easiness that these software provide, in comparison to open source programs (e.g. R, LaTeX or Open Office) and the ignorance about their real implications. Therefore, this matter should not be ignored in scientific works since it has serious implications in the current and future societies. In this regard initiatives are being carried out extend the use of *open source* tools in organizations receiving public funding[1]. However, to promote *Open Science*, more resources should be provided, along with a more strategical election of software by organizations where the research is carried out.

Concerning the underlying processes employed in statistical analysis, until now, these processes were characterized by the inherent difficulty of being shared. For this reason, it is very important to counteract with more open initiatives that are aimed to engage the research community in using these kinds of tools. Thus, the methodology proposed here partially intends to alleviates this problem. In light of this, the implementation carried out of computer tools for the compositional analysis of archaeological ceramics aims to contribute substantially and establish a basis for the development of collaborative software for compositional analysis, allowing other users to contribute and make further improvements. These changes have to be applied to the current repository published in GitHub (Calparsoro, 2019) and we hope that these improvements will be reflected in the next versions of the repository presented in this Doctoral Thesis.

With regard to the non-destructive analyses based on ED-XRF (addressed in Chapter 5), the research conducted has provided a screening methodology that allows to conduct a preliminary classification of archaeological ceramics of medieval and post-medieval periods (Calparsoro et al., 2019b). After the different experiments carried out, the proposed strategy involves a multi-point analysis by acquiring 50 measurements with a lateral resolution of 1 mm, for which the optimum conditions were found at a voltage of 50KV and a current of 700 μA. The measurement time was optimized at 200 s, which involves approximately 3 hours per sample. Moreover, the instrument used allows introducing samples up to 33 x 17 cm and 5 kg, including a

[1] `https://publiccode.eu/es/`

stage that permit the automatic analysis of the sherd along with the auto-focus option. These kind of approaches permit to envision strategies for the massive analysis of ceramics, which can give rise to a great database of compositional data of ceramics. In this way, if a large volume of compositional data is shared in a inter-operable manner, it could be subjected to strategies of Big Data analysis such as machine learning, which would place the compositional analysis of ceramics straight into the third revolution of the Archaeology ((Kristiansen, 2014), giving rise to new characterization formulas. Similar approaches are being already applied in the case of ceramic profiles, such as the one of the ARCHAIDE project[2].

Nevertheless, with regard to the compositional analysis by ED-XRF the potential of the proposed methodology for provenance analysis has been demonstrated to be limited due mainly to two issues: the restrictions imposed by the heterogeneity of the ceramic matrices and the limits of detection. As for the detection limits observed for some of the elements, these have proved to be crucial in the chemical discrimination of the compositional groups, such as MgO in order to discern DUR group from the rest of Basque groups.In spite of this, and as has been evidenced, the high coincidence between the two approaches (non-destructive and destructive), has allowed to use the method presented for screening purposes prior to a destructive analysis, which allows us to reduce costs considerably. In addition, its non-destructive character is of great interest in the same line as the previous methodological contribution (open source methodology for compositional data analysis), since by keeping the samples practically intact, it allows these materials to be reanalyzed and reinterpreted by future generations.

At the same time, to support the methodological contributions carried out in this Doctoral Thesis an archaeometric characterization has been carried out, which is addressed in the Chapter 5. The multi-analytical evaluation employing mainly, but not only, ICP-MS, NAA, XRD and SEM-EDS has been applied to 347 ceramics from archaeological sites from the Basque Country (Orduña, Durango and Elosu) and from La Rioja (Logroño and Nájera). These analyses have provided the first systematic archaeometric characterization, approached from the production perspective, of late-medieval and post-medieval period conducted in this region. In conclusion, the results has permitted establishing 21 compositional groups, among which, 13 have been related to a local origin, 6 have been ascribed to an exogenous origin and 2 has remained undetermined (see the Figure 7.1).

Conditioned to the existing material reality, the study of these five production centers has involved an important advancement in the fragmented knowledge of the ceramic production of the north center of the Iberian Peninsula during the studied chronologies. In the case of Logroño, the study performed on materials from production contexts corresponding to the 13^{th}-15^{th} centuries, has allowed establishing reference groups (LOG-A, LOG-B and LOG-C) of lead-glazed and unglazed ceramics that would have been

[2] http://www.archaide.eu/

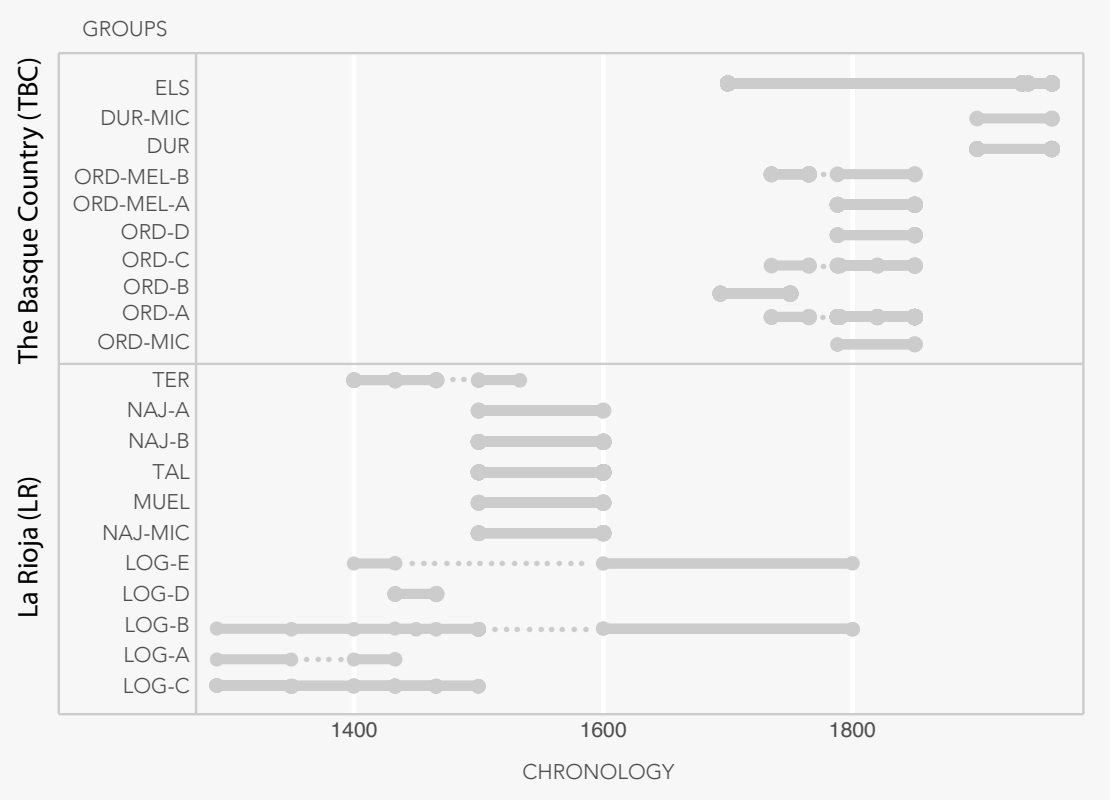

Figure 7.1: All the compositional groups defined according to their chronology

produced locally. In contrast, an exogenous origin has been suggested for tin-lead glazed pieces, either decorated with green or green and black polychromies, after the collation with NAA data from contemporary majolica producing centers (Calparsoro et al., 2016). Moreover, in this case, the TER group identified is composed by pieces where CuO based greens and MnO based blacks were identified, which is in accordance with the traditional decorations documented in the pottery workshops from Teruel.

With regard to Nájera, the chemical fingerprint has been provided for tin-lead glazed ceramics that have been ascribed to a local origin linked to a possible local production during the 16^{th} century. These include a set of mainly plates and porringers that show two type of pastes: buffer colored (NAJ-A) and a reddish one highlighted by being more rich in iron oxides (NAJ-B). Both groups show some sherds decorated by little strokes of CuO based greens and CoO based blues, as SEM-EDS results showed. In addition, the Naples yellow pigment has been identified by Raman spectroscopy in a decoration known as *cenefa castellana*, while the blue present it shows include Ni and Mn. Therefore, the use of other type of blue pigments employed in the manufacture (e.g. asbolan) is suggested. Interestingly, most of the ceramics from this site show similar typologies (tin-lead glazes

applied completely or partially). However, according to the NAA analyses some of these white tin-lead glazes correspond to Talavera de la Reina. In this case, the validity of the archaeometric analyses has highlighted its potential to provide supporting data for provenance studies, whereas according to traditional taxonomic criteria would have all these sherds would have clustered together. In contrast, by means of NAA collation, ceramics from Muel were also identified in this site, which is in accordance with the CuO based luster decorations they identified in this site.

In the case of Orduña, the compositional variability of the ceramic assemblage together with the periodization of the deposits has revealed the diachronic evolution of ceramic production during the 17^{th}-19^{th} centuries revealing very differentiated groups. In consequence, four groups of calcareous pastes with tin-lead glazes (ORD-A, ORD-B, ORD-C, ORD-D), two groups with honey-glazes or mixed glaze with tin-lead and non-calcareous pastes (ORD-MEL-A and ORD-MEL-B) were characterized, in addition to one showing tin-lead glazes with micaceous pastes (ORD-MIC). Some of the tin-lead glazed show decorations including, greens, blacks and blues and blacks that were applied using tradition recipes. Regarding Durango, the results revealed two compositional groups: the first linked to a local production (DUR) and one exogenous of micaceous pastes (DUR-MIC). In addition, in the ceramic assemblage from Elosu, a main ceramic group (ELS) was defined that presents internal differences in CaO. However, the main differences has been observed in the modification of the glazing technology, as well as the typologies. The interruption observed in ceramics is related to the Spanish Civil War. Due to the scarcity of raw materials, such as tin, the ceramists of Elosu chose to use slips to achieve an appearance similar to that of tin-lead ceramics. In addition, XRD results revealed three types of fabrics in for the ELS group. The first is characterized by a lower firing temperature (850-900 °C) while the other two are 900-950 °C respectively, owing their main differences to the presence of gehlenite. It should be noted that the first fabric is present in most post-war pastes, which invites us to think about a more limited use of fuel.

The XRD analyses showed that most of the ceramics groups include different fabric types. The results depicted that the firings temperatures ranged between 800°C and 1050°C. Although, most of the are closer to 900 °C. Typologically, all the ceramics evaluated range from unglazed ceramics or glazed only with lead to glazed with tin and lead, which reflect the evolution of the ceramic technology transference from the Islamic world in the Iberian Peninsula. Thus, the evolution from non-glazed during the late medieval to the spreading of tin-lead glazed ceramic typologies could be indirectly spotted throughout the five case studies. The complexity of ceramic production in pre-industrial times has become relevant in terms of archaeometric characterization, showing different chemical reference groups diachronically within the same production centers. This archaeometric characterization aims to shed more light on the activity of pottery and commercial networks within northern Spain during the Late Medieval and Post-Medieval periods by providing the chemical footprint of these productions.

The results obtained in this research have given rise to several publications and communications arising from the completion of this Doctoral Thesis, which have served to structure and give continuity to it. However, this work has only gone one step further in this research-path. Ceramics are complex, heterogeneous by nature and by anthropic influence, and there are several factors that intervene in their *chaine operatoire*. In addition, Archaeology is a active field in which more and more materials are continuously being discovered, which in many cases accumulate in museum deposits awaiting investigation. Therefore, research into the systematization of low-cost efficient archaeometric analyses is a task that needs to be continued.

In future approaches, the investigation could be extended by using a wider array of CRMs, both in ICP-MS analyses to obtain better accuracy and ED-XRF analyses. In the latter case, a more accurate method, would allow to evolve from "Screening" analysis to a properly non-destructive analysis for the classification and provenance analysis of Medieval and Post-Medieval Archaeological Pottery.

Bibliography

R is for Archaeology, 2017. URL `https://github.com/benmarwick/ctv-archaeology`.

GPL License, 2019. URL `https://www.gnu.org/licenses/licenses.html`.

MIT License, 2019. URL `https://opensource.org/licenses/MIT`.

Creative Commons website, 2019. URL `https://es.creativecommons.org/`.

Aitchison, J. The Statistical Analysis of Compositional Data. In *Monographs on Statistics and Applied Probability*. Chapman & Hall Ltd., 1986.

Aitchison, J., Barceló-Vidal, C., Martín-Fernández, J. A., and Pawlowsky-Glahn, V. Logratio analysis and compositional distance. *Mathematical Geology*, 32(3):271–275, 2000. ISSN 08828121. doi: 10.1023/A:1007529726302.

Aitchison, J. The Statistical Analysis of Compositional Data. *Journal of the Royal Statistical Society. Series B. Methodological*, 44(2):139–177, 1982. ISSN 0035-9246. doi: 10.2307/2345821.

Alberti, G. An R script to facilitate Correspondance Analysis. A guide to the use and the interpretation of results from an archaeological perspective. *Archaeologia e Calcolatori*, 24(April):25–53, 2013.

Alvárez Clavijo, P. Contextos Arqueológicos para cerámicas deñ siglo XVII EN Logroño. In *XV congreso anual de la asociación de ceramología. La cerámica en el mundo del vino y del aceite*, pages 185–204, Navarrete, 2012.

Ando, A., Kamioka, H., Terashima, S., and Itoh, S. 1988 values for GSJ rock reference samples,"Igneous rock series". *Geochemical Journal*, 23(3):143–148, 1989.

Angourakis, A., Martínez Ferreras, V., Torrano, A., Gurt Esparraguera, J. M., Ferreras, V. M., Torrano, A., and Esparraguera, J. M. G. Presenting multivariate statistical protocols in R using Roman wine amphorae productions in Catalonia, Spain. *Journal of Archaeological Science*, 93(March):150–165, 2018. ISSN 03054403. doi: 10.1016/j.jas.2018.03.007.

Angulo, A. *Las puertas de la vida y la muerte. La administración aduanera en las provincias vascas (1690-1780).* Servicio Editorial de la Universidad del País Vasco, Bilbao, 1995.

Angulo, T. and Porres, F. Acondicionamiento del solar municipal de la C/ Hospital Viejo, nº 11, de Logroño (La Rioja). Technical report, ArqueoRioja, Logroño, 2015.

Arantegui, J. P. Métodos analíticos para el estudio de materiales de patrimonio histórico y artístico. In *Arqueometría de los materiales cerámicos de época medieval en España*, pages 39–45. Universidad del País Vasco/Euskal Herriko Unibertsitatea, 2018.

Artola, M. and Ledesma, M. P. *Enciclopedia de historia de España.* Alianza editorial, 1991.

Astarloa, E., Aranburu, I., Arrate, B., Laskibar, N., Baztarrika, P., and Gomez, B. *Zeramika Hiztegia.* Eusko Jarurlaritzaren Argitalpen Zerbitzu Nagusia, Vitoria-Gasteiz, 2016. ISBN 978-84-457-3400-1.

Baxter, M. Notes on Quantitative Archaeology and R. (May):289, 2015.

Beckhoff, B., Kanngiesser, B., Langhoff, N., Wedell, R., and Wolff, H. *Handbook of Practical X-Ray Fluorescence Analysis.* Springer Science & Business Media., 2007. ISBN 9783540367222.

Bishop, R. L. and Neff, H. Compositional data analysis in archaeology. In *Archaeological chemistry IV*, pages 57–86. 1989. ISBN 0-8412-1449-2. doi: doi:10.1021/ba-1988-0220.ch004.

Bishop, R. L., Rands, R. L., and Holley, G. R. *Advances in Archaeological Method and Theory.* Elsevier, 1982. ISBN 9780120031054. doi: 10.1016/B978-0-12-003105-4.50012-1.

Blanco-Zubiaguirre, L., Olivares, M., Castro, K., Iñañez, J. G., and Madariaga, J. M. An alternative analytical method based on ultrasound micro bath hydrolysis and GC-MS analysis for the characterization of organic biomarkers in archaeological ceramics. *Analytical and Bioanalytical Chemistry*, 408(28):8001–8012, 2016. ISSN 16182650. doi: 10.1007/s00216-016-9898-9.

Blanco-Zubiaguirre, L., Ribechini, E., Degano, I., La Nasa, J., Carrero, J. A., Iñañez, J., Olivares, M., and Castro, K. GC–MS and HPLC-ESI-QToF characterization of organic lipid residues from ceramic vessels used by Basque whalers from 16th to 17th centuries. *Microchemical Journal*, 137:190–203, 2018. ISSN 0026265X. doi: 10.1016/j.microc.2017.10.017.

Blomster, J. P., Neff, H., and Glascock, M. D. Olmec pottery production and export in ancient Mexico determined through elemental analysis. *Science*, 307(5712):1068–1072, 2005. ISSN 00368075. doi: 10.1126/science.1107599.

Boogaart, K. G., Tolosana, R., and Bren, M. Compositions: compositional data analysis. *R package version*, pages 1–10, 2010.

Boulanger, M. T., Fehrenbach, S. S., and Glascock, M. D. Experimental evaluation of sample-extraction methods and the potential for contamination in ceramic specimens. *Archaeometry*, 55(5):880–892, 2013a. ISSN 0003813X. doi: 10.1111/j.1475-4754.2012.00706.x.

Boulanger, M. T., Fehrenbach, S. S., and Glascock, M. D. Experimental evaluation of sample-extraction methods and the potential for contamination in ceramic specimens. *Archaeometry*, 55(5):880–892, 2013b. ISSN 0003813X. doi: 10.1111/j.1475-4754.2012.00706.x.

Boulanger, M. Recycling Data: Working with published and unpublished ceramic-compositional data. In Hunt, A. M., editor, *The Oxford Handbook of Archaeological Ceramics*, volume 1. Oxford University Press, 2017. ISBN 9780199681532. doi: 10.1093/oxfordhb/9780199681532.013.6.

Bren, M., Tolosana-Delgado, R., and Boogaart, K. G. News from "compositions", the R package.

Buxeda i Garrigós, J. Alteration and Contamination of Archaeological Ceramics: The Perturbation Problem. *Journal of Archaeological Science*, 26(3):295–313, mar 1999. ISSN 03054403.

Buxeda i Garrigós, J. and Kilikoglou, V. Total Variation as a Measure of Variability in Chemical Data Sets. In van Zelst, L., editor, *Patterns and Process. A Festchrift in honor to Dr. Edward Sayre*, pages 185–198. Smithsonian Center for Materials Research and Education, Suitland, Maryland, 2003.

Buxeda i Garrigós, J. and Madrid i Fernández, M. Designing Rigorous Research: Integrating Science and Archaeology. In *The Oxford Handbook of Archaeological Ceramics*, chapter Part II. R, pages 19–47. Oxford University Press, Oxford, oxford han edition, 2017.

Buxeda i Garrigós, J., Madrid i Fernández, M., Iñañez, J. G., and Vila Socias, L. Mayor Conocimiento, Mejores Interpretaciones: La Arqueometría Cerámica. *CVDAS Revista de arqueología e historia*.

Buxeda i Garrigós, J., Cau, M., Gurt, J. M., and Tuset, F. Análisis tradicional y análisis arqueométrico en el estudio de las cerámicas comunes de época romana. *Monografies Empuritanes*, 8:39–60, 1995.

Buxeda i Garrigós, J., Mommsen, H., and Tsolakidou, A. Alterations of Na, K and Rb concentrations in Mycenaean pottery and a proposed explanation using X-ray diffraction. *Archaeometry*, 44(2):187–198, 2002. ISSN 0003-813X.

Buxeda i Garrigós, J., Cau Ontiveros, M. A., and Kilikoglou, V. Chemical variability in clays and pottery from a traditional cooking pot production village: Testing assumptions in Pereruela. *Archaeometry*, 45(1):1–17, 2003. ISSN 0003813X. doi: 10.1111/1475-4754.00093.

Buxeda i Garrigós, J. *La caracterització arqueomètrica de la ceràmica de Terra Sigillata Hispanica Avançada de la ciutat romana de Clunia i la seva contrastació amb la Terra Sigillata Hispanica d'un centre productor contemporani, el taller d'Abella.* Universitat de Barcelona, 1994.

Buxeda i Garrigós, J. Análisis tradicional y análisis arqueométrico en el estudio de las cerámicas comunes de la época romana, 1995.

Buxeda i Garrigós, J. Revisiting the compositional data. Some fundamental questions and new prospects in Archaeometry and Archaeology. *Proceedings of CODAWORK08 The 3rd Compositional Data Analysis Workshop May 2730 University of Girona Girona Spain*, pages 1–18, 2008.

Buxeda i Garrigós, J., Madrid i Madrid, M., Iñañez, J. G., and Vila Socias, L. Arqueometria ceràmica: una arqueologia ceràmica amb més informació. *Cota Zero. Revista d'Arqueologia i Ciència*, 23:38–53, 2008.

Buxeda i Garrigós, J., Garcia Iñañez, J., Madrid Fernández, M., and Beltrán de Heredia Bercero, J. La ceramique de Barcelone. Organisation et production entre les XIIIe et XVIIIe siècles à travers sa caracterisation archeometrique, 2011. ISSN 1699-793X.

Cajigas Panera, S., Martinez Izquierdo, D., and Savanti, F. Excavación en Zaharra Nº2-4 de la antigua ciudad de Orduña. Resultados, evolución y usos del solar desde el siglo XIII al XIX. *KOBIE (Paleoantrología)*, XXVII:231–300, 2004.

Calparsoro, E., Glascock, M., Angulo, T., Porres, F., Ceniceros, J., and Garcia Iñañez, J. An Archaeometric Approach to Pottery from the Basque Country and La Rioja (13th-18th) by Means of NAA. In *World Archaeological Congress (WAC8), 2016*, Kyoto, Japan, 2016.

Calparsoro, E., Arana, G., and Iñañez, J. Pottery from Orduña Village in the 17th–19th centuries: An archaeometrical approach. *Journal of Archaeological Science: Reports*, 23(July):304–323, 2019a. ISSN 2352409X. doi: 10.1016/j.jasrep.2018.10.019.

Calparsoro, E. GitHub Website, 2019. URL `https://github.com/esteful/arch_flow`.

Calparsoro, E., Iñañez, J. G., Arana Momoitio, G., Porres, F., and Angulo, T. Shedding light on the pottery activity from Logroño (La Rioja, Spain) during the Late Medieval period: an archaeometric approach. In *14th European Meeting on Ancient Ceramics*, Bordeaux, 2017a.

Calparsoro, E., Maguregui, M., Iñañez, J. G., and Madariaga, J. M. Towards non-destructive analysis of archaeological ceramics by micro X-ray fluorescence spectrometry. In *Technart. Non-destructive and Microanalytical Techniques in Art and Cultural Heritage*, Bilbao, 2017b.

Calparsoro, E., Maguregui, M., Iñañez, J. G., and Madariaga, J. M. Optimización de estudio no destructivo para el análisis elemental de cerámicas arqueológicas a través de micro-XRF. In *XII Congreso Ibérico de Arqueometría*, Burgos, 2018.

Calparsoro, E., Maguregui, M., Morillas, H., Arana, G., and Iñañez, J. G. Non-destructive Screening Methodology based on ED-XRF for the classification of Medieval and post-Medieval Archaeological Ceramics. *Ceramics International*, 45(8):10672–10683, 2019b. doi: https://doi.org/10.1016/j.ceramint.2019.02.138.

Calparsoro, E., Morales-Merino, C., and Iñañez, J. G. Characterization of Medieval and Modern Glazes from Archaeological sites in Logroño and Nájera. In Coll Conesa, J., editor, *Vidriados medievales en España. Investigaciones recientes.*, pages In–press. 2019c.

Calparsoro, E., Sanchez-garmendia, U., Arana, G., Maguregui, M., and Iñañez, J. G. An Archaeometrical Approach to the Majolica Pottery from Alcazar of Nájera Archaeological Site. *Heritage Science*, In press, 2019d.

Calparsoro Forcada, E., Garcia Iñañez, J., Arana Momoitio, G., Castro Pinedo, K., and Escribano, S. Basque glazed pottery through 16th-18th centuries: a revisited archaeometrical approach, 2016.

Campbell, G. *The Grove Encyclopedia of Decorative Arts: Two-volume Set*, volume 1. Oxford University Press, 2006.

Cariati, F., Fermo, P., Gilardoni, S., Galli, A., and Milazzo, M. A new approach for archaeological ceramics analysis using total reflection X-ray fluorescence spectrometry. *Spectrochimica Acta - Part B Atomic Spectroscopy*, 58(2):177–184, 2003. ISSN 05848547. doi: 10.1016/S0584-8547(02)00253-7.

Carlson, D. L. An R Companion to Quantifying Archaeology by Stephen Shennan. pages 1–43, 2012.

Carlson, D. L. and Roth, G. *archdata: Example Datasets from Archaeological Research*, 2016. URL `https://cran.r-project.org/package=archdata`.

Ceniceros Herreros, J. Alcázar de Nájera: primeras investigaciones arqueológicas. *Conflictos sociales, políticos e intelectuales en la España de los siglos XIV y XV : XIV Semana de Estudios Medievales, Nájera, del 4 al 8 de agosto de 2003*, pages 519–530, 2004.

Ceniceros Herreros, J. Cerámica con vidriado estannífero del Alcázar de Nájera (La Rioja). In *XV congreso anual de la asociación de ceramología. La cerámica en el mundo del vino y del aceite*, pages 168–183, Navarrete, 2012.

Ceniceros Herreros, J. and Montejo López de Alda, P. El Alcázar de Nájera. In *Castillos de La Rioja. Base documental para su plan de protección.*, pages 503–519. Gobierno de La Rioja Asociación Española de Amigos de Castillos en La Rioja, 2006.

Chapoulie, R., Delery, C., Daniel, F., and Vendrell-Saz, M. Cuerda seca ceramics from Al-Andalus, Islamic Spain and Portugal (10th-12th centuries AD): Investigation with SEM-EDX and cathodoluminescence. *Archaeometry*, 47(3):519–534, 2005. ISSN 0003813X. doi: 10.1111/j.1475-4754.2005.00217.x.

Chiarantini, L., Gallo, F., Rimondi, V., Benvenuti, M., Costagliola, P., and Dini, A. Early Renaissance production recipes for Naples Yellow pigment: A mineralogical and lead isotope study of Italian Majolica from Montelupo (Florence). *Archaeometry*, 57 (5):879–896, 2015. ISSN 14754754. doi: 10.1111/arcm.12146.

Coll Conesa, J. La cerámica valenciana (apuntes para una sintesis). page 306, 2009.

Colomban, P., Milande, V., and Lucas, H. On-site Raman analysis of Medici porcelain. *Journal of Raman Spectroscopy*, 35(1):68–72, 2004. ISSN 03770486. doi: 10.1002/jrs.1085.

Colomban, P. Polymerization degree and Raman identification of ancient glasses used for jewelry, ceramic enamels and mosaics. *Journal of Non-Crystalline Solids*, 323(1-3): 180–187, aug 2003. ISSN 00223093.

Colomban, P. On-site Raman identification and dating of ancient glasses: A review of procedures and tools, 2008. ISSN 12962074.

Colomban, P. and Treppoz, F. Identification and differentiation of ancient and modern European porcelains by Raman macro- and micro-spectroscopy. *Journal of Raman Spectroscopy*, 32(2):93–102, 2001. ISSN 03770486. doi: 10.1002/jrs.678.

Conesa, J. C. *Manual de cerámica medieval y moderna*. Cursos de formación permanante para arqueólogos. Museo Arqueológico Regional, 2011. ISBN 9788445133750.

Conesa, J. C. La loza decorada en España. *ARS Longa*, (17):151–168, 2008.

Criado-Boado, F., Alonso-Pablos, D., Blanco, M. J., Porto, Y., Rodríguez-Paz, A., Cabrejas, E., del Barrio-Álvarez, E., and Martínez, L. M. Coevolution of visual behaviour, the material world and social complexity, depicted by the eye-tracking of archaeological objects in humans. *Scientific Reports 2019 9:1*, 9(1):3985, 2019. ISSN 2045-2322. doi: 10.1038/s41598-019-39661-w.

De Vleeschouwer, F., Renson, V., Claeys, P., Nys, K., and Bindler, R. Quantitative WD-XRF calibration for small ceramic samples and their source material. *Geoarchaeology*, 26(3):440–450, 2011. ISSN 08836353. doi: 10.1002/gea.20353.

Escribano, S. Los Antecedentes de la Cerámica Popular Vasca. Consideraciones desde el Consumo Cerámico de Durango y Vitoria-Gasteiz (siglos XIV y XVII). *Siglos de Alfarería en Ollerías*, pages 34–61, 2013.

Escribano, S. Alfares alaveses (Alegría-Dulantzi, Elburgo, Labastida, Legutiano, Vitoria-Gasteiz) Dirección:. *Arkeoikuska*, 2008:216–223, 2009.

Escribano, S. *Genealogía del registro cerámico alavés de época preindustrial*. PhD thesis, Universidad del País Vasco UPV/EHU, 2014.

Escribano, S. Estrategias cuantitativas para el estudio de cerámica arqueológica. Una propuesta desde el caso de la cerámica histórica alavesa. *Munibe Antropologia-Arkeologia*, 2017(1):289–300, 2017a. ISSN 11322217. doi: 10.21630/maa.2017.68.07.

Escribano, S. Estrategias cuantitativas para el estudio de cerámica arqueológica. Una propuesta desde el caso de la cerámica histórica alavesa. *Munibe Antropologia-Arkeologia*, 68(1):289–300, 2017b.

Fabbri, B., Gualtieri, S., and Shoval, S. The presence of calcite in archeological ceramics. *Journal of the European Ceramic Society*, 34(7):1899–1911, 2014.

Fernández de Marcos, C. *Sevilla i l'expansió atlàntica en els s. XVI i XVII. Un estudi arqueomètric i arqueològic del principal centre productor ceràmic d'Europa*. PhD thesis, Universitat de Barcelona, 2018.

Fernández-Ruiz, R. and García-Heras, M. Study of archaeological ceramics by total-reflection X-ray fluorescence spectrometry: Semi-quantitative approach. *Spectrochimica Acta - Part B Atomic Spectroscopy*, 2007. ISSN 05848547. doi: 10.1016/j.sab.2007.06.015.

Forster, N. and Grave, P. Effects of elevated levels of lead in ceramics on provenancing studies using non-destructive PXRF: A case study in byzantine cypriot glazed ceramics. *X-Ray Spectrometry*, 42(6):480–486, 2013. ISSN 00498246. doi: 10.1002/xrs.2507.

Forster, N., Grave, P., Vickery, N., and Kealhofer, L. Non-destructive analysis using PXRF: methodology and application to archaeological ceramics. *X-Ray Spectrometry*, 40(5):389–398, sep 2011. ISSN 00498246. doi: 10.1002/xrs.1360. URL `http://doi.wiley.com/10.1002/xrs.1360`.

Fowler, K. D., Middleton, E., and Fayek, M. The human element: discerning the effects of potter's behavior on the chemical composition of ceramics. *Archaeological and Anthropological Sciences*, 11(1):171–198, 2019. ISSN 18669565. doi: 10.1007/s12520-017-0535-0.

Frahm, E. Validity of "off-the-shelf" handheld portable XRF for sourcing Near Eastern obsidian chip debris. *Journal of Archaeological Science*, 40(2):1080–1092, feb 2013. ISSN 03054403. doi: 10.1016/j.jas.2012.06.038.

Freestone, I. Retention of Phosphate in Buried Ceramics: An electron microbeam approach. *Archaeomtery*, 27(2), 1984.

Garabito Gómez, T., Solovera, M. E., and Pradales, D. *Los Alfares Romanos de Tricio y Arenzana de Arriba: Estado de la cuestión*. Universidad de Valladolid, Valladolid, 1978. ISBN 84-600-8640-2.

García-Florentino, C., Maguregui, M., Marguí, E., Torrent, L., Queralt, I., and Madariaga, J. M. Development of Total Reflection X-ray fluorescence spectrometry quantitative methodologies for elemental characterization of building materials and their degradation products. *Spectrochimica Acta - Part B Atomic Spectroscopy*, 143: 18–25, 2018. ISSN 05848547. doi: 10.1016/j.sab.2018.02.008.

García-Heras, M., Blackman, M. J., Fernández-Ruiz, R., and Bishop, R. L. Assessing Ceramic Compositional Data: A Comparison of Total Reflection X-ray Fluorescence and Instrumental Neutron Activation Analysis On Late Iron Age Spanish Celtiberian Ceramics. *Archaeometry*, 43(3):325–347, 2001. doi: 10.1111/1475-4754.00020.

Gestoso y Pérez, J. Historia de los Barros Vidriados Sevillanos desde sus origenes hasta nuestros dias. 1904.

Gil Zubillaga, L. and Luezas Pascual, R. A. El resurgir de las viejas Ollerias: Excavación de un Horno en La Calle Ollerias De Logroño. *Belezos: Revista de cultura popular y tradiciones de La Rioja,*, 38:64–71, 2018.

Giussani, B., Monticelli, D., and Rampazzi, L. Role of laser ablation-inductively coupled plasma-mass spectrometry in cultural heritage research: A review. *Analytica Chimica Acta*, 635(1):6–21, 2009. ISSN 00032670. doi: 10.1016/j.aca.2008.12.040.

Glascock, M. D., Nabelek, P. I., Weinrich, D. D., and Coveney, R. M. Correcting for uranium fission in instrumental neutron activation analysis of high-uranium rocks. *Journal of Radioanalytical and Nuclear Chemistry Articles*, 99(1):121–131, 1986. ISSN 02365731. doi: 10.1007/BF02060832.

Glascock, M. D. Characterization of Archaeological Ceramics at MURR by Neutron Activation Analysis and Multivariate Statistics. In *Chemical Characterization of Ceramic Pastes in Archaeology*, number August. Prehistory Press, 1992. ISBN 1055-2316.

Glascock, M. D. Compositional Analysis in Archaeology. In *Oxford Handbooks*, pages 1–25. Oxford Handbooks Online, Oxford, 2016. doi: 10.1093/oxfordhb/9780199935413.013.8Abstract.

Glascock, M. D. Geochemical Sourcing. In *Encyclopedia of Geoarchaeology*, pages 303–308. Springer, 2017.

Glascock Michael D, S. R. J. and Neff, H. Archaeometry at the University of Missouri Research Reactor and the provenance of obsidian artefacts in North America. *Archaeometry*, 49(2):343–357, 2007.

Goicolea Julián, F. J. La vida cotidiana en la ciudad de Nájera a fines de la Edad Media: una aproximación. *En la España Medieval*, 24:171–194, 2001.

Goicolea Julián, F. J. La ciudad de Nájera en la Baja Edad Media como espacio de poder político y social. *Los espacios de poder en la España medieval : XII Semana de Estudios Medievales, Nájera, del 30 de julio al 3 de agosto de 2001*, pages 149–179, 2002.

Goicolea Julián, F. J. Mercaderes y hombres de negocio: el poder del dinero en el mundo urbano riojano de fines de la Edad Media e inicios de la Edad Moderna. *Hispania Revista Española De Historia*, 67(227):947–992, 2007. ISSN 00182141.

Gómez-Cambronero Puyuelo, M. *Bizkaiko Hiribilduetan Zehar = Un paseo por las Villas de Bizkaia*. Bizkaiko Foru Aldundia = Diputación Foral de Bizkaia, Bilbao, 2003. ISBN 84-7752-344-4.

González-Ruibal, A. Archaeological revolution (s). *Current Swedish Archaeology*, pages 41–45, 2014.

González-Ruibal, A. and Ayán Vila, X. *Arqueología. Una introducción al estudio de la materialidad del pasado*. Alianza Editorial, Madrid, 2018. ISBN 9788491812357.

Goodman, S. N., Fanelli, D., and Ioannidis, J. P. A. What does research reproducibility mean? *Science Translational Medicine*, 8(341):341ps12–341ps12, 2016. ISSN 1946-6234. doi: 10.1126/scitranslmed.aaf5027.

Grassi, F. and Quirós, J. A. *Arqueometría de los materiales cerámicos de época medieval en España (Documentos de Arqueología Medieval 12)*. 2018. ISBN 9788490829073.

Grugel, A. *Zuni, Pueblo und Laguna Pueblo: Ökonomische Entwicklung und kulturelle Perspektiven,*. Bonner geographische Abhandlungen. Asgard-Verlag Sankt Augustin, 2005.

Guedj, D. and Ramjoué, C. European Commission Policy on Open-Access to Scientific Publications and Research Data in Horizon 2020. *Biomed Data J*, 1(1), 2015.

Guirao, D., Pla, F., and Acosta, A. The archaeometric characterization of majolica ceramics from Talavera de la Reina and El Puente del Arzobispo (Toledo, Spain). *Archaeometry*, 56(5):746–763, 2014. ISSN 14754754. doi: 10.1111/arcm.12048.

Habicht-Mauche, J. a., Glenn, S. T., Schmidt, M. P., Franks, R., Milford, H., and Flegal, a. R. Stable lead isotope analysis of Rio Grande glaze paints and ores using ICP-MS: a comparison of acid dissolution and laser ablation techniques. *Journal of Archaeological Science*, 29(October 2015):1043–1053, 2002. ISSN 03054403. doi: 10.1006/jasc.2001.0804.

Hein, A. and Kilikoglou, V. Compositional variability of archaeological ceramics in the eastern Mediterranean and implications for the design of provenance studies. *Journal of Archaeological Science: Reports*, 2015. ISSN 2352409X. doi: 10.1016/j.jasrep.2017.03.020.

Heinmann, R. B. Assesing the Technology of Ancient Pottery: The Use of Ceramic Phase Diagrams. *Archaeomaterials*, (3):123–148, 1989.

Henry, W. M. and Knapp, K. T. Compound forms of fossil fuel fly ash emissions. *Environmental science & technology*, 14(4):450–456, 1980.

Hunt, A. M. W. *The Oxford handbook of archaeological ceramic analysis*. 2016. ISBN 9780199681532.

Hunt, A. M. W. and Speakman, R. J. Portable XRF analysis of archaeological sediments and ceramics. *Journal of Archaeological Science*, 53:626–638, 2015. ISSN 03054403. doi: 10.1016/j.jas.2014.11.031.

Ibabe, E. *Ceramica popular vasca*. Fundación BBK, 1995a. ISBN 84-89476-09-8.

Ibabe, E. *Notas sobre Ceramica Popular Vasca*. Auman, Bilbao, 1995b. ISBN 8430024506.

Iñañez, J. G., Speakman, R. J., Buxeda i Garrigós, J., and Glascock, M. D. Chemical characterization of tin-lead glazed pottery from the Iberian Peninsula and the Canary Islands: Initial steps toward a better understanding of Spanish Colonial pottery in the Americas. *Archaeometry*, 51(4):546–567, 2009. ISSN 0003813X. doi: 10.1111/j.1475-4754.2008.00431.x.

Iñañez, J. G., Bellucci, J. J., Rodríguez-Alegría, E., Ash, R., McDonough, W., and Speakman, R. J. Romita pottery revisited: A reassessment of the provenance of ceramics from Colonial Mexico by LA-MC-ICP-MS. *Journal of Archaeological Science*, 37(11):2698–2704, 2010. ISSN 03054403. doi: 10.1016/j.jas.2010.06.005.

Iñañez, J. G., Madrid-Fernández, M., Molera, J., Speakman, R. J., and Pradell, T. Potters and pigments: Preliminary technological assessment of pigment recipes of American majolica by synchrotron radiation micro-X-ray diffraction (Sr-μXRD). *Journal of Archaeological Science*, 40(2):1408–1415, 2013. ISSN 03054403.

Iñañez, J. G., Speakman, R. J., Buxeda i Garrigós, J., and Glascock, M. D. Chemical characterization of majolica from 14th-18th century production centers on the Iberian

Peninsula: a preliminary neutron activation study. *Journal of Archaeological Science*, 35(2):425–440, 2008. ISSN 03054403. doi: 10.1016/j.jas.2007.04.007.

Keith, L. H., Crummett, W., Deegan, J., Libby, R. A., Taylor, J. K., and Wentler, G. Principles of environmental analysis. *Analytical chemistry*, 55(14):2210–2218, 1983.

Kristiansen, K. Archaeological revolution(s). *Current Swedish Archaeology*, 22(Barrett): 11–34, 2014. ISSN 11027355.

Kuhn, R. D. and Sempowski, M. L. A new approach to dating the League of the Iroquois. *American Antiquity*, 66(2):301–314, 2001. doi: 10.2307/2694610.

Lardizabal, A. M. M. *Arcillas del lugar y su incidencia en producciones cerámicas de Euskal Herria*. Colección Tesis doctorales. Universidad del País Vasco, Servicio Editorial = Euskal Herriko Unibertsitatea, Argitalpen Zerbitzua, 2008. ISBN 9788498600629.

Larracoechea Bengoa, J. M. *Notas históricas de la villa de Durango*. Kurutzeaga Congreg. Mariana, Durango, 1992. ISBN 8427117450.

López de Heredia, J. *La Cerámica de la Segunda Edad del Hierro en el País Vasco: Estudio Tecnológico, Funcional y Social*. PhD thesis, Universidad del País Vasco UPV/EHU, 2014.

Luezas Pascual, R. A. Evidencias de producción alfarera medieval en Calahorra. *Kalakorikos*, 19:95–120, 2014.

Madinabeitia, S. G. D., Lorda, M. E. S., and Ibarguchi, J. I. G. Simultaneous determination of major to ultratrace elements in geological samples by fusion-dissolution and inductively coupled plasma mass spectrometry techniques. *Analytica Chimica Acta*, 625(2):117–130, 2008. ISSN 00032670. doi: 10.1016/j.aca.2008.07.024.

Maggetti, M. Composition of Roman pottery from Lousonna (Switzerland). In *Scientific studies in ancient ceramics*. British Museum Research Laboratory, London, 1981.

Maniatis, Y. and Tite, M. S. Technological examination of Neolithic-Bronze Age pottery from central and southeast Europe and from the Near East. *Journal of Archaeological Science*, 8(1):59–76, 1981. ISSN 10959238. doi: 10.1016/0305-4403(81)90012-1.

Maritan, L., Nodari, L., Mazzoli, C., Milano, A., and Russo, U. Influence of firing conditions on ceramic products: Experimental study on clay rich in organic matter. *Applied Clay Science*, 31(1-2):1–15, 2006. ISSN 01691317. doi: 10.1016/j.clay.2005.08.007.

Martín-Fernández, J. A., Buxeda i Garrigós, J., and Pawlowsky-Glahn, V. Logratio Analysis in Archeometry: Principles and Methods. In *Mathematics and Archaeology*, volume Science Pu, pages 178–189. Science Publishers, Boca Raton., bogdanovic edition, 2015.

Martínez Glera, E. *La Alfarería en La Rioja: Siglos XVI-XX*. Consejería de Cultura, Deportes y Juventud, Logroño, Logroño, consejería edition, 1994. ISBN 84-7359-428-2.

Martínez Glera, E. and Álvarez González, T. Origen y formación de la Colección de alfarería de La Rioja - Bodegas Darien. *XV Congreso anual de la Asociación de Ceramología. La cerámica en el mundo del vino y del aceite. La Rioja 2010*, pages 240–249, 2012.

Martínez González, M. M. *La producción cerámica en la Baja Edad Media: el alfar de la calle Hospital Viejo de Logroño (La Rioja)*. PhD thesis, Universidad de la Rioja, 2013.

Martínez González, M. M. *Arqueología en La Villanueva. Los alfares meievales de la calle Hospital Viejo de Logroño*. Instituto de Estudios Riojanos, Logroño, 2015. ISBN 978-84-9960-072-7.

Martinón-Torres, M. and Killick, D. Oxford Handbooks Online Archaeological Theories and Archaeological Sciences. (March 2017):1–28, 2015. doi: 10.1093/oxfordhb/9780199567942.013.004.

Marwick, B. Computational Reproducibility in Archaeological Research: Basic Principles and a Case Study of Their Implementation. *Journal of Archaeological Method and Theory*, 24(2):424–450, 2017. ISSN 15737764. doi: 10.1007/s10816-015-9272-9.

Marwick, B., Guedes, A., Barton, C. M., Bates, L. A., Baxter, M., Bevan, A., Bollwerk, E. A., Bocinsky, R. K., Brughmans, T., Carter, A. K., Conrad, C., Contreras, D. A., Costa, S., Crema, E. R., Daggett, A., Davies, B., Drake, B. L., Dye, T. S., France, P., Fullagar, R., Graham, S., Harris, M. D., Hawks, J., Heath, S., Huffer, D., Kansa, C., Kansa, S. W., Madsen, M. E., Melcher, J., Negre, J., Fraser, D., Opitz, R., Orton, D. C., Przystupa, P., Raviele, M., Riel-salvatore, J., Riris, P., Romanowska, I., Strupler, N., Ullah, I. I., Vlack, H. G. V., Ethan, C., Webster, C., Wells, J., Winters, J., and Wren, C. D. The SAA Archaeological Record 17 (4), 2017.

Mesquida García, M. *La Vajilla Azul en La Cerámica de Paterna*. Number V-3127-2002. Escuela de Arte Francisco Alcántara, 2002.

Millhauser, J. K., Rodríguez-Alegría, E., and Glascock, M. D. Testing the accuracy of portable X-ray fluorescence to study Aztec and Colonial obsidian supply at Xaltocan, Mexico. *Journal of Archaeological Science*, 38(11):3141–3152, 2011. ISSN 03054403. doi: 10.1016/j.jas.2011.07.018. URL `http://dx.doi.org/10.1016/j.jas.2011.07.018`.

Molera, J., Vendrell-Saz, M., García-Vallés, M., and Pradell, T. Technology and colour development of Hispano-Moresque lead-glazed pottery. *Archaeometry*, 39(1):23–39, 1997. ISSN 0003813X.

Molera, J., Pradell, T., and Vendrell-Saz, M. The colours of Ca-rich ceramic pastes: Origin and characterization. *Applied Clay Science*, 13(3):187–202, 1998. ISSN 01691317. doi: 10.1016/S0169-1317(98)00024-6.

Molera, J., Pradell, T., and Salvado, N. Interactions between clay bodies and lead glazes. *Journal of the American Ceramic Society*, 84(5):1120–1128, 2001. ISSN 0002-7820. doi: 10.1111/j.1151-2916.2001.tb00799.x.

Molera, J., Pradell, T., Salvado, N., and Vendrell-Saz, M. Evidence of tin oxide recrystallization in opacified lead glazes. *Journal of the American Ceramic Society*, 82(10):2871–2875, 1999. ISSN 00027820. doi: 10.1111/j.1151-2916.1999.tb02170.x. URL [PDF].

Montana, G. *Ceramic Raw Materials*. Oxford University Press, 2016. ISBN 9780199681532.

Montero Ruiz, I., García Heras, M., and López-Romero, E. Archaeometry: changes and current trends. *Trabajos de Prehistoria*, 64(1):23–40, 2008. ISSN 0082-5638. doi: 10.3989/tp.2007.v64.i1.92.

Mounier, A., Lazare, S., Le Bourdon, G., Aupetit, C., Servant, L., and Daniel, F. LEDμSF: A new portable device for fragile artworks analyses. Application on medieval pigments. *Microchemical Journal*, 126:480–487, 2016. ISSN 0026265X. doi: 10.1016/j.microc.2016.01.008. URL http://dx.doi.org/10.1016/j.microc.2016.01.008.

Moya Valgañón, J. G. *Historia de la ciudad de Logroño*. Ibercaja, Logroño, 1994. ISBN 8488793316.

Munafò, M. R., Nosek, B. A., Bishop, D. V. M., Button, K. S., Chambers, C. D., Percie du Sert, N., Simonsohn, U., Wagenmakers, E.-J., Ware, J. J., and Ioannidis, J. P. A. A manifesto for reproducible science. *Nature Human Behaviour*, 1(1):21, 2017. ISSN 2397-3374. doi: 10.1038/s41562-016-0021.

Neff, H. Neutron activation analysis for provenance determination in archaeology. In John, W., editor, *Modern Analytical Methods in Art and Archaeology*. Wiley, New York, 2000.

Neff, H. Analysis of Mesoamerican Plumbate Pottery Surfaces by Laser Ablation-Inductively Coupled Plasma-Mass Spectrometry (LA-ICP-MS). *Journal of Archaeological Science*, 30(1):21–35, 2003. ISSN 03054403. doi: 10.1006/jasc.2001.0801.

Neff, H. Laser Ablation ICP-MS in Archaeology. In *Handbook of Mass Spectrometry*. John Wiley & Sons., New York, 2012.

Neff, H. and Bishop, R. L. Plumbate Origins and Development. *American Antiquity*, 53 (03):505–522, jul 1988. ISSN 0002-7316. doi: 10.2307/281214.

Neustupny, E. *Whiter Archaeology?*, volume 45, pages 34–39. Antiquity, 1971.

Ohmori, T., Hatayama, M., Ohchi, T., Ito, H., Takenaka, H., and Tsuji, K. Development of X-ray 2D dispersive device for WD-XRF imaging spectrometer. *Powder Diffraction*, 27(2):71–74, 2012.

Olaetxea, C. *La tecnología cerámica en la protohistoria vasca.* PhD thesis, 2000.

Palumbo, S., Golitko, M., Christensen, S., and Tietzer, G. Basalt source characterization in the highlands of western panama using portable X-ray fluorescence (pXRF) analysis. *Journal of Archaeological Science: Reports*, 2:61–68, jun 2015. ISSN 2352409X. doi: 10.1016/j.jasrep.2015.01.006.

Pawlowsky-Glahn, V. and Egozcue, J. Exploring Compositional Data with the CoDa-Dendrogram. *Austrian Journal of Statistics*, 40(1-2):103–113, 2011. doi: 10.17713/ajs.v40i1&2.202.

Peacock, D. P. S. *Pottery in the Roman world: an ethnoarchaeological approach.* Longman Publishing Group, London, 1982.

Pearson, K. Mathematical Contributions to the Theory of Evolution. - On a Form of Spurious Correlation Which May Arise When Indices Are Used in the Measurement of Organs. *Proceedings of the Royal Society of London*, 60:489–498, 1897. ISSN 0370-1662. doi: 10.1098/rspl.1896.0076.

Peng, R. D. Reproducible research in computational science. *Science*, 334(6060):1226–1227, 2011.

Pérez-Arantegui, J. *Pottery Analysis: Chemical.* Cambridge University Press, Cambridge, 2008.

Pérez-Arantegui, J., Resano, M., García-Ruiz, E., Vanhaecke, F., Roldán, C., Ferrero, J., and Coll, J. Characterization of cobalt pigments found in traditional Valencian ceramics by means of laser ablation-inductively coupled plasma mass spectrometry and portable X-ray fluorescence spectrometry. *Talanta*, 74(5):1271–1280, 2008. ISSN 00399140. doi: 10.1016/j.talanta.2007.08.044.

Pérez-Arantegui, J., Molera, J., Larrea, A., Pradell, T., and Vendrell-Saz, M. Luster Pottery from the Thirteenth Century to the Sixteenth Century : A Nanostructured Thin Metallic Film. *Journal of the American Ceramic Society*, 84(2):442–446, 2001a. ISSN 00027820. doi: 10.1111/j.1151-2916.2001.tb00674.x.

Pérez-Arantegui, J., Molera, J., Larrea, A., Pradell, T., and Vendrell-Saz, M. Luster Pottery from the Thirteenth Century to the Sixteenth Century : A Nanostructured Thin Metallic Film. *Journal of the American Ceramic Society*, 84(2):442–446, 2001b. ISSN 00027820. doi: 10.1111/j.1151-2916.2001.tb00674.x.

Perlman, I. and Asaron, F. Pottery Analysis by Neutron Activa. *Archaeometry*, 11(1): 21–38, jun 1969. ISSN 0003-813X. doi: 10.1111/j.1475-4754.1969.tb00627.x.

Picon, M. *Introduction à l'étude technique des céramiques sigillées de Lezoux*, volume 2. Centre de Recherches sur les techniques Gréco-romaines, 1973.

Pleguezuelo, A. Barros con alma alfarería andaluza en la colección de Luis Porcuna Jurado (siglos XVI-XX). *Cuadersno de los amigos de los Museos de Osuna*, 18:110–111, 2016.

Pollard, A. M. *Analytical Chemistry in Archaeology*. Cambridge University Press, Cambridge, 2007.

Pollard, A. M., Heron, C., and Britain, R. S. o. C. G. *Archaeological Chemistry*. 2008. ISBN 0854042628.

Possolo, A. Simple Guide for Evaluating and Expressing the Uncertainty of NIST Measurement Results. *National Institute of Standards and Technology*, 1297:1–20, 2015. ISSN 17426596. doi: 10.6028/NIST.TN.1900.

Puig, C. *Les produccions ceràmiques del País Basc durant l'època baixmedieval i moderna. Una aproximació arqueomètrica*. PhD thesis, Universitat de Barcelona, 2016.

Puig, C. and Escribano, S. Las producciones cerámicas vascas de época moderna: un caso práctico de arqueología histórica. In *JIA 2011. IV Jornadas de Jovens em Investigaçao Arqueológica*, pages 219–224, 2011.

Resano, M., Perez-Arantegui, J., Garcia-Ruiz, E., and Vanhaecke, F. Laser ablation-inductively coupled plasma mass spectrometry for the fast and direct characterization of antique glazed ceramics. *Journal of Analytical Atomic Spectrometry*, 20(6):508–514, 2005.

Rice, P. M. Recent ceramic analysis: 2. Composition, production, and theory. *Journal of Archaeological Research*, 4(3):165–202, 1996. ISSN 1059-0161. doi: 10.1007/BF02228880.

Rice, P. M. *Pottery analysis: a sourcebook*. University of Chicago Press, Chicago, 2015.

Rodríguez Miranda, A., Valle Melón, J., Calparsoro, E., and Iñañez, J. G. Study, revalorization and virtual musealization of a ceramic kiln based on information gathered from old excavations. *Digital Applications in Archaeology and Cultural Heritage*, 7, 2017. ISSN 22120548. doi: 10.1016/j.daach.2017.08.003.

Roux, V. Introduction to Ceramic Technology. In *Ceramics and Society*, pages 1–14. Springer, Berlin, 2019.

Salazar Arechalde, J. I. *Urbanismo e historia, la ciudad de Orduña*. Instituto Vasco de Administración Pública = Herri-Arduralaritzaren Euskal Erakundea,, 1995. ISBN 8477771324.

Salazar Arechalde, J. I. and Llano Hernaiz, J. M. *Orduña: Camino y Frontera, Urduña: Muga eta Bidea*. Tecnos, 2006. ISBN 8460970124.

Salinas, E. and Pradell, T. Primeros resultados del proyecto «La introducción del vidriado en al-Andalus: olas tecnológicas e influencias orientales», a partir de análisis arqueométricos. In *Arqueometría de los Materiales Cerámicos en España*, pages 241–252. Servicio Editorial de la Universidad del País Vasco, 2018. ISBN 978-84-9082-907-3.

Sanchez-Garmendia, U., Estefania, C., Arana, G., and Iñañez, J. G. Beneath sacred land : glazed pottery from the old Church of La Concepción in Zamora. In *Glaze Art Lisbon*, pages 361–379, Lisbon, Portugal, 2018. Laboratorio Nacional de Engenharia Civil. doi: 978-972-49-2301-7.

Sanchez Trujillano, M. T. La Decoración Mudéjar del Alcázar de Nájera. *II Semana de Estudios Medievales. Nájera*, (1):663–681, 1991.

Sandve, G. K., Nekrutenko, A., Taylor, J., and Hovig, E. Ten Simple Rules for Reproducible Computational Research. *PLoS Computational Biology*, 9(10):1–4, 2013. ISSN 1553734X. doi: 10.1371/journal.pcbi.1003285.

Sayre, E.V., Harbottle, G., Bieber, A.M., Brooks, D. Application of Multivariative Techniques to Analytical Data on Aegean Ceramics. *Archaeometry*, 18(1):59–74, feb 1976. ISSN 0003-813X. doi: 10.1111/j.1475-4754.1976.tb00145.x.

Schwedt, A., Mommsen, H., Zacharias, N., and Buxeda i Garrigós, J. Analcime crystallization and compositional profiles - Comparing approaches to detect post-depositional alterations in archaeological pottery. *Archaeometry*, 48(2):237–251, 2006. ISSN 0003813X. doi: 10.1111/j.1475-4754.2006.00254.x.

Shennan, S. *Quantifiying Archaeology*. Edinburgh University Press, Edinburgh, 1988. ISBN 0126398607.

Shepard, A. O. *Plumbate, a Mesoamerican trade ware*. Number 573. Carnegie Institution of Washington, 1948.

Shepard, A. O. *Ceramics for the Archaeologist*. Number 609. Carnegie Institution of Washington Washington, 1956.

Sheppard, P. J., Irwin, G. J., Lin, S. C., and McCaffrey, C. P. Characterization of New Zealand obsidian using PXRF. *Journal of Archaeological Science*, 38(1):45–56, 2011. ISSN 03054403. doi: 10.1016/j.jas.2010.08.007.

Silvan, L. *Cerámica del País Vasco*. Ediciones de la Caja de Ahorros Provincial de Guipuzcoa, 1982. ISBN 84-7231-621-1.

Solaun, J. L. *Erdi Aroko Zeramika Euskal Herrian*. Eusko Jarurlaritzaren Argitalpen Zerbitzu Nagusia, 2005. ISBN 844572410X.

Speakman, R. J. and Steven Shackley, M. Silo science and portable XRF in archaeology: a response to Frahm. *Journal of Archaeological Science*, 40(2):1435–1443, feb 2013. ISSN 03054403. doi: 10.1016/j.jas.2012.09.033.

Speakman, R. J., Little, N. C., Creel, D., Miller, M. R., and Iñañez, J. G. Sourcing ceramics with portable XRF spectrometers? A comparison with INAA using Mimbres pottery from the American Southwest. *Journal of Archaeological Science*, 38(12):3483–3496, 2011. ISSN 03054403. doi: 10.1016/j.jas.2011.08.011.

Steele, T. E. and Weaver, T. D. The modified triangular graph: A refined method for comparing mortality profiles in archaeological samples. *Journal of Archaeological Science*, 29(3):317–322, 2002. ISSN 03054403. doi: 10.1006/jasc.2001.0733.

Stodden, V. and Miguez, S. Best Practices for Computational Science: Software Infrastructure and Environments for Reproducible and Extensible Research. *Journal of Open Research Software*, 2(1):21, 2014. ISSN 2049-9647. doi: 10.5334/jors.ay.

Tite, M. S. Pottery Production, Distribution, and Consumption. The Contribution of the Physical Sciences. *Journal of Archaeological Method and Theory*, 6(3):181–233, 1999. ISSN 10725369. doi: 10.1023/a:1021947302609. URL `http://www.jstor.org/stable/20177403`.

Tite, M. S., Freestone, I., Mason, R., Molera, J., Vendrell-Saz, M., and Wood, N. Lead glazes in antiquity - Methods of production and reasons for use. *Archaeometry*, 1998. ISSN 0003813X. doi: 10.1111/j.1475-4754.1998.tb00836.x.

Tite, M. S., Kilikoglou, V., and Vekinis, G. Strength, toughness and thermal shock resistance of ancient ceramics, and their influence on technological choice. *Archaeometry*, 43(3):301–324, 2001. ISSN 0003813X. doi: 10.1111/1475-4754.00019.

Tite, M., Pradell, T., and Shortland, A. Discovery, production and use of tin-based opacifiers in glasses, enamels and glazes from the Late Iron Age onwards: A reassessment. *Archaeometry*, 50(1):67–84, 2008. ISSN 0003813X. doi: 10.1111/j.1475-4754.2007.00339.x.

Traoré, K., Ouédraogo, G. V., Blanchart, P., Jernot, J. P., and Gomina, M. Influence of calcite on the microstructure and mechanical properties of pottery ceramics obtained from a kaolinite-rich clay from Burkina Faso. *Journal of the European Ceramic Society*, 27(2-3):1677–1681, 2007. ISSN 09552219. doi: 10.1016/j.jeurceramsoc.2006.04.147.

Tubb, A., Parker, A. J., and Nickless, G. The analysis of Romano-British pottery by atomic absorption spectrophotometry. *Archaeometry*, 22(2):153–171, 1980. ISSN 1475-4754. doi: 10.1111/j.1475-4754.1980.tb00939.x.

Vanhoof, C., Bacon, J. R., Ellis, A. T., Vincze, L., and Wobrauschek, P. 2018 atomic spectrometry update – a review of advances in X-ray fluorescence spectrometry and its special applications. *Journal of Analytical Atomic Spectrometry*, pages 1413–1431, 2018. ISSN 0267-9477. doi: 10.1039/C8JA90030B.

Vendrell, M., Molera, J., and Tite, M. S. Optical Properties of Tin-Opacified Glazes. *Archaeometry*, 42(2):325–340, 2000. ISSN 1475-4754. doi: 10.1111/j.1475-4754.2000.tb00885.x.

Whitney, D. L. and Evans, B. W. Abbreviations for names of rock-forming minerals. *American Mineralogist*, 95(1):185–187, 2010. ISSN 0003004X. doi: 10.2138/am.2010.3371.

Wilkinson, M. D., Dumontier, M., Aalbersberg, I. J., Appleton, G., Axton, M., Baak, A., Blomberg, N., Boiten, J.-W., da Silva Santos, L. B., Bourne, P. E., and Others. The FAIR Guiding Principles for scientific data management and stewardship. *Scientific data*, 3, 2016.

Yuste, A., Luzón, A., and Bauluz, B. Provenance of Oligocene-Miocene alluvial and fluvial fans of the northern Ebro Basin (NE Spain): An XRD, petrographic and SEM study. *Sedimentary Geology*, 2004. ISSN 00370738. doi: 10.1016/j.sedgeo.2004.10.001.

Zhang, C., Manheim, F. T., Hinde, J., and Grossman, J. N. Statistical characterization of a large geochemical database and effect of sample size. *Applied Geochemistry*, 20 (10):1857–1874, 2005. doi: 10.1016/j.apgeochem.2005.06.006.

Part III

Appendices - *Eranskinak*

Appendix A

Data Tables

Table A.1: Experimental Conditions for ICP-MS analyses

Exp. Conditions for ICP-MS	
Nebulizer Flow	0.90-1.00 L/min
Plasma Flow	$18L/min$
Auxiliary Flow	$1.2L/min$
RF Power	1600 W
Helium Flow	4.0 mL/min
Dwell time	50 ms
Sweeps	20
Integration Time	1000 ms
Readings	1
Replicates	3

Precision and Accuracy of NAA and ICP-MS

Table A.2: Concentrations and LOD in SRM-1633b Fly-ash used as the standard for NAA of ceramics at MURR

Element	SRM-1633b	LOD
short-lived		
Al_2O_3 (mass %)	28.44 ±0.51	0.8
CaO (mass %)	2.11 ± 0.08	0.1
Dy (μg/g)	17 ± 1	0.19
K_2O (mass %)	2.35 ± 0.04	0.19
MnO (mass %)	0.017 ± 0.001	0.01
Na_2O (mass %)	0.1971 ± 0.004	0.007
TiO_2 (mass %)	1.319 ± 0.023	0.17
V (μg/g)	296 ± 4	2
medium-lived		
As (μg/g)	136 ± 3	2
Ba (μg/g)	709 ± 27	25
La (μg/g)	86 ± 1	0.1
Lu (μg/g)	1.05 ± 0.04	0.04
Nd (μg/g)	82 ± 7	2.5
Sm (μg/g)	18.6 ± 0.7	0.02
U (μg/g)	8.8 ± 0.8	0.5
Yb (μg/g)	7.43 ± 0.34	0.1
long-lived		
Ce (μg/g)	184 ± 2	2
Co (μg/g)	48.6 ± 0.7	0.05
Cr (μg/g)	197 ± 4	2
Cs (μg/g)	10.5 ± 0.19	0.3
Eu (μg/g)	3.93 ± 0.09	0.005
Fe_2O_3 (mass %)	11.02 ± 0.17	0.07
Hf (μg/g)	6.76 ± 0.190	0.19
Ni (μg/g)	116 ± 35	50
Rb (μg/g)	138 ± 6	5
Sb (μg/g)	4.85 ± 0.16	0.05
Sc (μg/g)	40.19 ± 0.6	0.001
Sr (μg/g)	1036 ± 97	50
Ta (μg/g)	1.84 ± 0.09	0.05
Tb (μg/g)	2.73 ± 0.194	0.19
Th (μg/g)	24.4 ± 0.4	0.19
Zn (μg/g)	206 ± 18	5
Zr (μg/g)	223 ± 37	40

Table A.3: Concentrations ranges of the JA-2. JG-1a. JG-2 and JB-3 standards used in ICP-MS analyses. LOQs for the current method and mean expanded uncertainties $\overline{U}(\%)$ of the obtained results on the non-micaceous (NM) and micaceous samples (M).The coverage factor is k=2. Therefore, these data are expressed with a 95% of confidence interval. The uncertainty is not expressed for those cases showing values <LOQ and/or being greater than 50% (see Analytical Considerations in Section 5.1 for more details).

Measurand	Isotope	Range	LOQ	$\overline{U}(\%)$-NM	$\overline{U}(\%)$M
Na_2O (%)	^{23}Na	2.73 - 3.54	0.54	-	-
MgO (%)	^{25}Mg	0.037 - 7.6	0.15	7	14
Al_2O_3 (%)	^{27}Al	12.47 - 17.2	1.2	10	21
SiO_2 (%)	^{28}Si	50.96 - 76.83	4.0	17	11
P_2O_5 (%)	^{31}P	0.002 - 0.1994	0.190	21	23
K_2O (%)	^{39}K	0.78 - 4.71	0.1	3	3
CaO (%)	^{44}Ca	0.7 - 9.79	0.4	10	16
TiO_2 (%)	^{47}Ti	0.044 - 1.44	0.11	7	21
V (μg/g)	^{51}V	3.78 - 372	10	8	30
Cr (μg/g)	^{52}Cr	6.37 - 450	15	11	34
Fe_2O_3 (%)	^{54}Fe	0.97 - 11.82	0.19	1	2
MnO (%)	^{55}Mn	0.016 - 0.177	0.010	27	21
Co (μg/g)	^{59}Co	3.62 - 34.3	8	11	11
Ni (μg/g)	^{60}Ni	4.35 - 134	72	-	-
Cu (μg/g)	^{63}Cu	0.49 - 194	2	-	-
Zn (μg/g)	^{66}Zn	13.6 - 100	116	-	-
Rb (μg/g)	^{85}Rb	15.1 - 301	2	8	6
Sr (μg/g)	^{88}Sr	17.9 - 403	17	5	12
Zr (μg/g)	^{90}Zr	97.6 - 118	75	29	33
Nb (μg/g)	^{93}Nb	2.47 - 14.7	5	8	9
Sn (μg/g)	^{118}Sn	0.94 - 4.47	11	-	-
Cs (μg/g)	^{133}Cs	0.94 - 10.6	8	12	14
Ba (μg/g)	^{138}Ba	81 - 470	26	10	14
La (μg/g)	^{139}La	8.81 - 21.3	4	18	18
Ce (μg/g)	^{140}Ce	21.5 - 48.3	17	15	12
Pr (μg/g)	^{141}Pr	3.11 - 6.2	1	9	7
Nd (μg/g)	^{146}Nd	14.2 - 26.4	4.24	8	6
Sm (μg/g)	^{147}Sm	3.1 - 7.78	0.95	6	8
Eu (μg/g)	^{153}Eu	0.1 - 1.32	0.19	12	18
Gd (μg/g)	^{157}Gd	3 - 8.01	0.5	11	14
Tb (μg/g)	^{159}Tb	0.48 - 1.62	0.07	10	9
Dy (μg/g)	^{163}Dy	2.9 - 10.5	0.3	11	10
Ho (μg/g)	^{165}Ho	0.61 - 1.67	0.08	9	7
Er (μg/g)	^{166}Er	1.7 - 6.04	0.3	10	9
Tm (μg/g)	^{169}Tm	0.196 - 1.16	0.06	23	19
Yb (μg/g)	^{172}Yb	1.68 - 6.85	0.3	11	9
Lu (μg/g)	^{175}Lu	0.195 - 1.22	0.07	17	16
Hf (μg/g)	^{178}Hf	2.67 - 4.73	1	9	9
Ta (μg/g)	^{181}Ta	0.15 - 2.76	0.1	24	19
Pb (μg/g)	^{208}Pb	5.58 - 31.5	239	12	8
Th (μg/g)	^{232}Th	1.27 - 31.6	4	7	15
U (μg/g)	$^{208+238}$	0.48 - 11.3	0.19	11	9

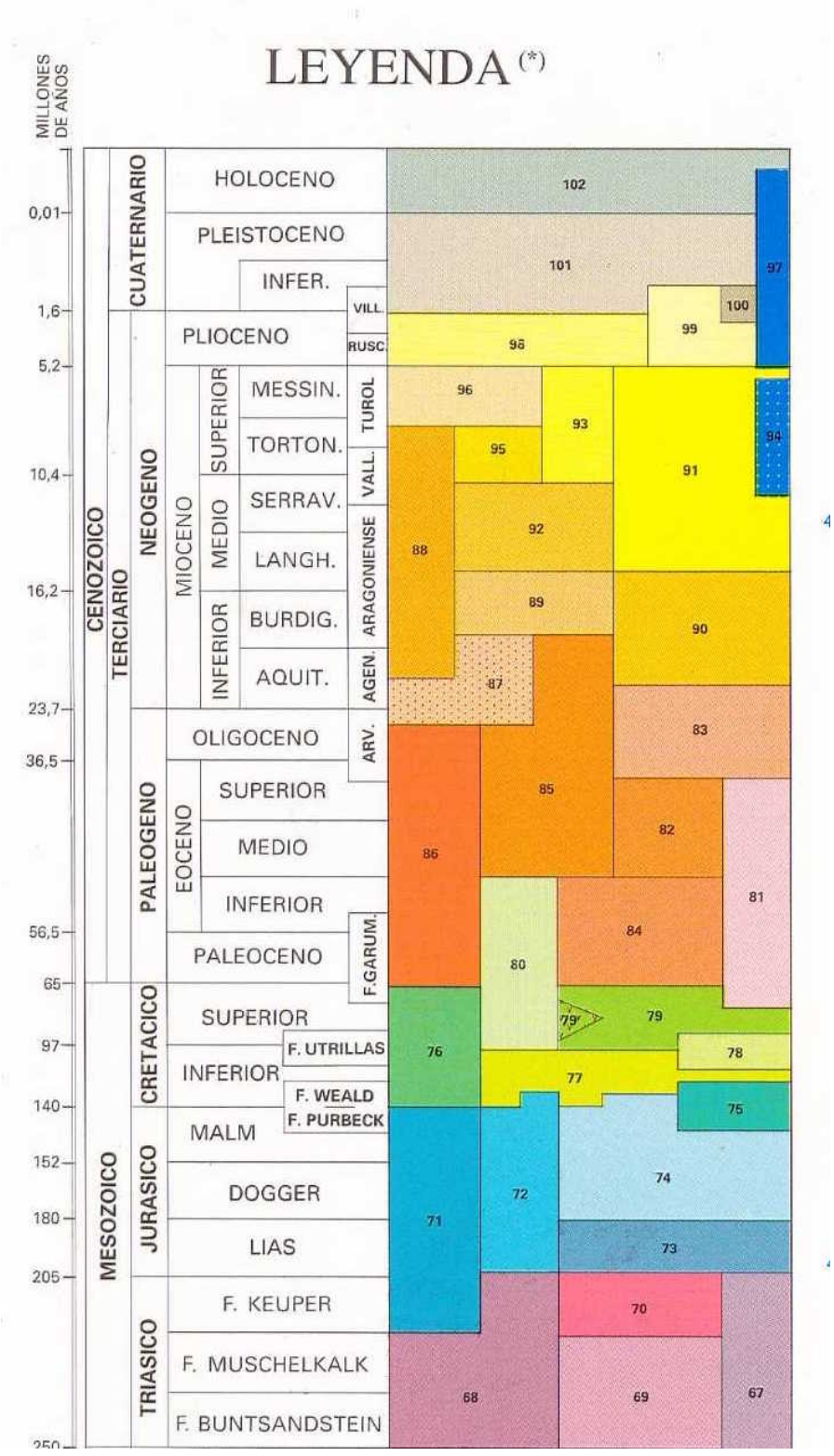

Figure A.1: Legend of the geologic map shown in the Figure 3.4

Concentrations on ceramic samples obtained by NAA

Table A.4: Concentrations obtained by NAA (Al_2O_3 - MnO)

ANID	Al_2O_3	As	Ba	CaO	Ce	Co	Cr	Cs	Dy	Eu	Fe_2O_3	Hf	K_2O	La	Lu	MnO
ELS001	16.53	10	359	6.62	81	44.2	71	13.3	5	1.12	4.82	6.44	2.84	39	0.38	0.033
ELS006	16.97	12	426	7.97	81	56.2	73	14.5	5	1.14	5.02	6.73	2.65	40	0.36	0.031
ELS007	16.85	10	368	15.52	72	23.1	66	14.3	4	0.96	4.87	5.60	2.46	36	0.34	0.026
ELS008	14.76	13	419	8.25	84	23.5	65	10.9	5	1.16	4.07	7.92	2.94	41	0.45	0.027
ELS009	14.15	12	351	10.19	70	26.4	53	11.7	5	1.01	4.10	7.00	2.31	34	0.37	0.024
ELS010	16.22	15	365	14.08	75	49.2	59	14.0	5	1.08	4.64	5.55	2.75	37	0.30	0.026
ELS020	14.95	12	407	17.86	66	54.8	58	13.0	4	1.01	4.87	4.91	2.25	34	0.20	0.048
ELS021	17.66	6	383	10.11	86	40.0	77	16.2	5	1.22	5.04	6.20	2.86	42	0.34	0.016
ELS022	16.02	14	426	16.50	69	28.9	69	14.5	4	1.00	4.73	5.17	2.53	35	0.20	0.038
ELS046	16.70	8	413	11.28	86	78.3	75	15.7	5	1.17	4.96	7.09	2.74	42	0.37	0.023
ELS047	18.77	14	505	0.77	95	71.7	83	16.4	5	1.24	4.91	7.46	3.20	46	0.41	0.019
ELS048	17.32	10	400	7.04	81	47.6	71	13.5	5	1.15	4.84	6.64	2.79	39	0.38	0.033
ELS049	17.59	6	467	5.51	92	74.6	76	14.6	6	1.15	4.49	7.52	3.12	43	0.41	0.016
ELS050	17.47	8	452	7.07	87	70.1	75	14.8	5	1.22	4.76	7.34	2.85	42	0.38	0.019
ELS051	16.40	7	421	9.16	85	81.9	71	13.4	5	1.04	4.51	8.10	2.56	41	0.38	0.019
DUR001	15.78	9	436	8.66	76	76.5	68	11.4	5	1.07	4.69	7.28	2.78	39	0.38	0.060
DUR002	19.28	11	499	13.16	75	63.6	79	15.9	5	1.15	5.05	4.86	3.40	40	0.32	0.069
DUR005	22.11	2	141	5.06	29	94.3	14	60.0	5	0.49	1.83	4.20	2.65	13	0.19	0.040
DUR006	14.15	19	249	23.56	55	46.4	66	5.2	3	0.92	3.06	3.06	1.39	28	0.19	0.029
DUR008	26.89	26	226	1.30	27	155.0	65	37.9	6	0.70	3.65	3.43	3.40	14	0.38	0.031
DUR010	16.96	9	421	7.51	79	92.4	72	12.3	5	0.19	4.89	7.53	3.13	40	0.36	0.055
DUR011	27.36	19	246	1.14	28	91.5	21	38.9	6	0.65	3.70	3.62	3.22	14	0.43	0.036
DUR013	19.68	11	467	9.48	78	101.3	85	16.2	5	1.14	5.21	5.82	3.50	40	0.33	0.067
DUR014	16.61	13	474	15.03	73	100.8	74	16.0	4	1.10	3.34	4.72	3.52	36	0.20	0.021
DUR016	23.84	31	182	1.23	24	105.9	17	36.0	6	0.58	3.36	3.30	3.04	11	0.64	0.034
DUR019	14.79	9	367	15.91	64	115.1	65	11.8	4	0.97	4.13	5.67	2.84	33	0.30	0.156
DUR020	16.98	9	364	13.86	71	87.2	73	13.3	5	1.04	4.49	5.85	3.06	37	0.32	0.093
DUR024	16.69	12	449	11.96	74	68.3	65	12.0	4	1.07	4.61	6.41	2.98	38	0.34	0.066
DUR026	14.73	18	440	11.24	77	64.6	78	8.9	5	1.24	4.83	5.73	3.44	38	0.34	0.033
DUR027	15.93	12	405	9.27	79	219.7	71	11.9	5	0.19	4.52	7.73	2.68	40	0.32	0.058
ORD003	11.98	8	204	21.03	50	78.5	45	10.0	3	0.65	3.25	4.64	1.65	23	0.19	0.033
ORD006	14.05	11	313	18.10	61	15.2	51	6.0	4	0.80	4.17	5.25	1.55	28	0.20	0.030
ORD011	16.65	15	405	1.24	87	44.4	67	12.8	6	1.22	4.29	9.47	2.93	42	0.40	0.017
ORD020	14.69	12	237	19.68	59	28.1	50	11.3	4	0.79	4.02	4.94	1.86	28	0.20	0.028
ORD033	13.55	10	204	20.82	52	13.7	54	11.0	3	0.66	3.58	6.16	1.79	26	0.30	0.022
ORD036	10.19	9	208	25.93	46	8.9	41	4.6	3	0.63	2.75	5.07	1.09	22	0.20	0.028
ORD037	14.62	10	325	21.20	62	20.6	57	10.8	4	0.88	4.24	5.69	1.85	29	0.20	0.043
ORD042	18.42	13	421	0.55	89	30.4	76	18.1	6	1.30	5.48	7.44	3.97	44	0.44	0.021
ORD046	14.24	12	239	20.63	60	11.4	52	9.2	4	0.87	3.77	5.04	1.47	28	0.32	0.034
ORD047	18.19	9	474	6.11	93	34.7	77	15.3	5	1.28	5.04	7.30	3.37	45	0.35	0.014
ORD053	17.28	15	392	1.12	89	85.4	75	13.5	5	1.14	5.54	9.29	2.85	43	0.37	0.010
ORD056	26.81	14	260	1.47	30	16.2	18	50.8	8	0.92	2.86	3.91	3.88	19	0.74	0.035
ORD058	27.90	18	213	1.19	28	32.4	17	53.7	7	0.61	3.18	4.00	4.07	14	0.54	0.035
ORD059	10.19	11	371	24.99	64	25.1	48	4.0	4	1.07	3.90	5.38	2.17	33	0.33	0.063
ORD061	14.39	14	242	21.09	58	12.3	56	14.3	4	0.85	4.00	5.01	1.99	28	0.33	0.043
ORD063	13.22	11	313	11.93	64	19.4	49	11.8	5	0.91	3.52	7.71	2.24	31	0.38	0.024
ORD064	12.47	11	276	15.05	60	23.2	53	10.6	4	0.85	3.55	6.72	1.93	29	0.34	0.030
ORD065	12.96	14	215	21.15	56	20.3	60	11.0	4	0.75	3.87	4.59	1.88	26	0.19	0.027
ORD070	15.54	9	255	15.59	59	12.3	64	14.3	4	0.84	4.01	5.60	2.32	28	0.20	0.041
ORD073	12.01	10	191	16.11	58	9.3	50	10.0	4	0.88	3.41	5.66	1.72	28	0.32	0.033
ORD078	20.41	10	489	0.61	103	9.5	92	15.5	6	1.46	3.22	7.19	3.75	51	0.53	0.012
ORD085	15.14	14	341	16.32	72	17.9	75	8.6	5	1.14	2.98	4.97	2.51	35	0.35	0.022
ORD086	16.86	16	391	16.36	79	20.3	84	10.6	5	1.30	3.32	4.68	2.50	38	0.35	0.026
ORD089	17.08	14	410	16.04	77	17.3	82	12.2	5	1.29	3.41	5.12	2.65	38	0.38	0.030
ORD096	13.59	13	334	18.19	65	11.5	57	8.8	4	1.11	2.67	4.07	2.55	31	0.33	0.023
NAJ002	18.28	16	391	16.01	73	22.1	75	17.2	5	1.12	3.66	4.14	3.80	36	0.33	0.024

Continued

ANID	Al_2O_3	As	Ba	CaO	Ce	Co	Cr	Cs	Dy	Eu	Fe_2O_3	Hf	K_2O	La	Lu	MnO
NAJ008	18.36	16	453	15.24	79	13.2	76	15.0	5	1.19	3.67	5.02	3.55	39	0.46	0.027
NAJ014	18.07	28	479	8.98	92	17.3	85	7.6	5	1.49	6.47	4.58	4.15	45	0.37	0.085
NAJ015	16.33	8	238	15.92	38	3.6	20	54.3	5	0.74	2.60	4.85	2.61	19	0.65	0.023
NAJ016	15.06	17	396	15.14	66	32.7	52	13.0	5	1.15	3.52	4.53	2.90	32	0.40	0.055
NAJ028	13.83	13	336	24.33	59	12.6	60	8.8	4	0.90	3.33	3.95	1.51	29	0.20	0.028
NAJ029	14.07	17	381	18.07	78	16.4	47	7.8	6	1.10	4.21	6.35	2.95	37	0.39	0.061
NAJ033	16.48	18	447	16.69	82	22.6	64	8.9	6	1.22	5.35	5.22	3.70	39	0.38	0.070
NAJ041	18.32	12	406	19.02	73	37.8	74	14.1	5	1.24	3.48	4.43	3.16	36	0.33	0.025
NAJ044	17.04	14	420	18.09	71	21.3	68	15.4	5	1.05	3.49	4.60	3.17	35	0.40	0.023
NAJ053	15.69	21	462	12.50	77	16.9	82	13.7	6	1.41	5.20	5.90	3.66	44	0.40	0.088
NAJ059	14.67	17	337	17.93	63	12.7	55	3.5	4	1.05	3.08	3.74	1.66	31	0.30	0.025
NAJ062	15.53	20	354	18.59	70	25.6	78	9.7	4	1.13	5.17	4.01	1.97	35	0.20	0.044
NAJ064	17.45	15	471	16.62	74	25.1	70	15.8	5	1.13	3.61	4.38	3.51	36	0.32	0.026
NAJ066	15.21	14	382	17.89	65	26.2	61	12.1	4	1.00	3.15	4.48	2.85	32	0.30	0.032
NAJ068	18.09	17	425	13.46	79	29.3	73	15.2	5	1.27	3.77	5.00	3.96	38	0.20	0.024
NAJ076	15.02	20	421	22.52	74	17.1	70	10.6	5	1.24	5.25	3.98	3.03	38	0.33	0.074
NAJ077	16.85	19	414	15.97	69	19.5	70	15.1	4	1.05	4.28	4.32	3.33	35	0.34	0.036
NAJ085	16.15	16	381	16.57	72	24.7	66	13.5	4	1.06	3.09	4.81	2.35	35	0.30	0.020
NAJ087	17.35	15	411	14.01	75	15.7	67	14.1	5	1.26	3.02	5.16	2.94	36	0.33	0.028
NAJ092	14.38	18	418	19.54	74	17.8	68	7.4	5	1.29	5.16	4.76	3.69	39	0.35	0.078
NAJ093	14.31	18	602	16.78	82	29.1	68	7.1	5	1.39	4.98	6.15	2.28	40	0.35	0.064
NAJ095	24.43	17	404	3.16	63	31.7	50	12.5	7	1.09	3.45	4.44	3.57	31	0.33	0.033
NAJ096	20.62	11	267	5.06	30	3.0	16	60.4	5	0.60	2.10	3.49	3.41	15	0.47	0.043
NAJ100	23.87	5	235	5.00	30	3.2	15	67.3	7	0.79	2.22	3.98	3.08	17	0.51	0.038
LOG001	21.62	23	636	8.58	103	19.4	108	13.6	5	1.66	7.45	3.80	4.30	52	0.37	0.053
LOG003	21.49	28	554	9.00	105	23.0	109	14.3	6	1.69	7.63	3.83	4.15	52	0.49	0.053
LOG007	20.54	10	473	10.11	100	28.4	103	13.7	5	1.58	7.20	3.84	3.93	50	0.36	0.055
LOG028	15.74	7	412	5.28	87	58.4	87	12.2	5	1.36	5.99	5.79	3.44	42	0.31	0.052
LOG033	16.08	26	482	14.31	77	19.0	76	10.5	5	1.29	5.49	4.09	4.01	38	0.44	0.061
LOG034	16.62	17	493	12.81	83	23.9	86	12.2	5	1.38	6.04	4.37	3.68	41	0.36	0.068
LOG035	15.06	10	404	20.88	67	15.6	76	11.2	4	1.06	4.82	3.41	2.95	33	0.20	0.045
LOG037	18.52	26	755	12.84	84	28.9	96	18.0	4	1.29	5.97	3.59	3.38	42	0.20	0.083
LOG038	12.86	18	417	24.65	69	18.8	62	4.9	4	1.19	4.47	4.72	3.10	36	0.33	0.065
LOG042	18.71	21	533	7.98	81	32.6	79	19.3	5	1.30	5.94	4.83	4.73	40	0.36	0.046
LOG043	17.57	16	506	8.44	78	27.4	72	18.0	5	1.29	5.46	5.02	4.40	38	0.34	0.046
LOG044	18.69	19	460	9.55	79	23.4	79	19.3	5	1.36	5.90	4.71	4.38	38	0.35	0.048
LOG048	16.88	14	471	8.29	77	27.2	71	17.5	5	1.24	5.27	5.11	4.33	37	0.34	0.044
LOG050	18.99	8	521	6.90	97	50.4	95	13.9	5	1.60	6.65	5.68	3.99	48	0.38	0.050
LOG051	19.47	25	521	9.98	88	27.9	93	13.2	5	1.43	6.41	4.30	3.87	44	0.36	0.051
LOG054	18.72	11	447	11.99	97	48.3	102	13.2	5	1.58	7.07	4.25	3.77	48	0.31	0.068
LOG056	16.87	8	498	6.50	89	36.5	85	12.1	5	1.42	6.00	5.57	3.36	43	0.38	0.049
LOG059	17.02	13	484	6.77	86	32.9	82	14.5	5	1.37	5.86	6.03	3.83	42	0.39	0.059
LOG060	18.33	17	475	12.02	91	33.0	97	13.6	5	1.46	6.76	4.01	3.99	44	0.36	0.072
LOG061	18.48	21	613	10.34	91	26.6	94	13.8	5	1.47	6.62	4.44	3.73	44	0.38	0.074
LOG062	16.59	21	554	13.27	83	25.2	85	12.2	5	1.33	5.87	4.27	3.39	40	0.35	0.076
LOG072	22.00	28	493	9.91	105	38.0	108	14.2	6	1.70	7.53	3.75	4.16	52	0.41	0.052
LOG074	21.52	25	529	9.09	103	36.3	109	13.9	5	1.65	7.35	3.71	4.24	51	0.42	0.049
LOG075	20.80	28	422	9.85	104	25.8	108	14.1	5	1.66	7.46	3.82	4.37	51	0.42	0.051

Table A.5: Concentrations obtained by NAA (Na_2O - Zr)

ANID	Na_2O	Nd	Rb	Sb	Sc	Sm	Sr	Ta	Tb	Th	TiO_2	U	V	Yb	Zn	Zr
ELS001	0.867	32	168	1.48	12.6	6.7	303	2.15	0.77	15.4	0.883	4.2	85	2.92	81	181
ELS006	0.895	31	172	1.23	12.5	6.8	378	2.17	0.77	15.7	0.829	4.3	85	2.99	80	175
ELS007	0.748	31	159	1.01	11.7	5.8	549	1.67	0.74	14.2	0.621	3.9	80	2.36	67	147
ELS008	0.622	34	144	1.22	11.9	6.9	363	2.11	1.07	15.6	0.923	3.6	79	3.33	80	205
ELS009	0.810	30	142	0.98	10.9	6.1	752	1.97	0.77	13.7	0.770	4.3	64	2.64	82	203
ELS010	0.666	29	159	1.04	11.8	6.3	436	1.61	0.99	14.0	0.632	2.9	90	2.44	74	156
ELS020	0.683	29	160	1.92	11.0	5.7	619	1.51	0.78	12.5	0.588	2.3	60	2.27	95	130
ELS021	0.827	37	183	10.05	13.3	7.2	484	1.87	0.82	15.9	0.712	2.8	89	2.79	100	173
ELS022	0.746	28	173	6.90	11.6	6.0	648	1.59	0.72	13.2	0.624	2.2	77	2.33	109	122
ELS046	0.781	36	184	1.27	12.8	7.1	449	2.05	0.84	16.1	0.809	3.4	82	3.07	88	179
ELS047	0.753	40	190	1.45	14.0	7.6	204	2.37	0.83	17.7	1.025	4.8	106	3.41	85	205
ELS048	0.873	35	168	1.44	12.6	6.7	382	2.16	0.96	15.5	0.853	4.1	86	2.79	74	197
ELS049	0.753	39	183	1.40	12.7	7.0	405	2.37	0.77	17.1	0.803	4.9	80	3.14	94	186
ELS050	0.777	35	173	1.10	13.1	7.3	405	2.02	0.90	16.2	0.961	4.4	74	3.10	92	213
ELS051	0.897	34	162	1.45	11.8	6.4	369	2.17	1.04	16.2	0.866	4.8	87	3.07	71	230
DUR001	0.607	30	151	1.28	11.9	6.1	194	2.05	0.89	13.2	0.844	3.5	76	2.90	86	173
DUR002	0.590	32	191	1.24	14.2	6.3	248	1.78	0.84	13.5	0.622	3.2	98	2.71	84	160
DUR005	0.195	15	457	0.46	4.7	3.4	116	7.71	0.65	5.2	0.191	6.3	15	2.16	70	102
DUR006	0.192	23	68	1.38	10.3	5.0	369	1.10	0.54	9.4	0.434	2.9	87	2.07	57	70
DUR008	0.407	14	521	0.94	6.1	4.3	98	10.91	1.03	5.1	0.162	10.6	30	3.02	81	106
DUR010	0.730	34	161	1.36	12.7	6.6	202	1.99	1.01	13.6	0.776	3.3	73	3.21	80	193
DUR011	0.346	14	528	1.00	5.9	4.5	108	11.03	0.99	5.2	0.132	12.4	24	3.41	78	104
DUR013	0.609	34	195	3.71	14.8	6.3	174	1.89	0.80	14.4	0.740	3.4	97	2.81	89	148
DUR014	0.397	31	169	2.03	12.4	6.4	582	1.63	0.78	13.2	0.661	3.5	77	2.36	62	112
DUR016	0.194	13	464	0.94	5.1	3.9	91	11.13	0.88	4.4	0.136	11.9	19	3.15	61	116
DUR019	0.567	30	157	1.56	11.3	5.5	363	1.57	0.72	11.8	0.554	2.9	78	2.50	53	176
DUR020	0.680	29	179	1.48	12.5	5.8	320	1.77	0.69	12.8	0.694	2.9	78	2.63	74	135
DUR024	0.540	30	159	1.35	12.5	5.9	211	1.93	0.95	13.1	0.705	2.8	90	2.75	77	167
DUR026	0.561	33	144	1.36	12.4	6.6	606	1.32	0.88	12.5	0.681	2.9	106	2.82	88	171
DUR027	0.636	32	154	1.37	12.3	6.5	192	2.21	0.83	14.2	0.829	3.1	78	2.83	79	196
ORD003	0.532	20	98	1.09	7.9	3.9	691	1.52	0.46	10.1	0.500	2.2	51	1.62	56	120
ORD006	0.445	22	64	1.41	10.1	4.7	629	1.42	0.57	12.0	0.526	3.6	52	2.09	69	126
ORD011	1.001	38	157	1.47	11.5	7.3	146	2.04	1.13	16.3	0.843	3.4	83	3.38	88	248
ORD020	0.568	25	117	1.99	9.9	4.7	587	1.39	0.63	12.0	0.569	2.3	62	2.13	72	138
ORD033	0.780	21	112	1.53	8.8	4.0	378	1.62	0.45	11.9	0.627	4.2	60	2.04	67	161
ORD036	0.804	17	52	0.97	7.1	3.7	353	1.24	0.51	9.4	0.481	2.3	44	1.67	53	76
ORD037	0.738	22	125	3.34	10	5.2	594	1.57	0.73	12.6	0.603	3.0	64	2.04	74	156
ORD042	0.193	34	195	2.19	14.2	7.5	0	1.78	0.99	16.9	0.802	4.0	95	3.57	81	169
ORD046	0.509	24	85	1.20	9.4	5.0	461	1.38	0.70	11.5	0.518	2.5	81	2.25	78	109
ORD047	0.912	37	193	1.55	13.5	7.2	342	1.88	1.02	17.0	0.776	3.5	95	2.71	91	149
ORD053	0.803	38	170	1.26	12.6	6.7	127	2.09	0.84	16.9	0.836	3.9	94	3.22	75	205
ORD056	0.195	21	617	1.00	6.4	5.4	170	9.81	1.34	5.0	0.118	8.2	21	4.28	88	104
ORD058	0.199	15	580	0.47	6.3	4.3	160	7.87	1.08	5.1	0.144	9.7	21	3.59	81	85
ORD059	0.313	28	85	1.36	9.5	5.9	386	1.09	0.79	10.4	0.546	3.2	58	2.38	53	112
ORD061	0.853	23	125	3.52	10	5.0	609	1.49	0.64	11.9	0.597	3.0	73	2.02	134	104
ORD063	0.795	26	122	1.08	9.2	5.5	275	1.64	0.70	12.6	0.649	3.9	47	2.73	58	180
ORD064	0.879	23	114	1.98	9.1	5.1	337	1.58	0.77	12.0	0.570	2.9	58	2.51	90	143
ORD065	0.669	23	113	6.19	9.2	4.5	703	1.28	0.57	11.3	0.539	2.7	85	1.83	97	116
ORD070	0.885	24	144	1.62	10.4	4.8	394	1.69	0.60	12.6	0.676	2.6	72	2.30	105	127
ORD073	0.596	23	104	0.80	8.5	5.2	241	1.29	0.65	11.1	0.525	3.0	74	2.35	59	159
ORD078	1.096	40	196	2.40	15.8	8.2	143	2.37	0.91	16.5	0.834	4.3	114	3.63	60	160
ORD085	0.176	30	122	2.08	12.0	6.2	329	1.32	0.81	12.2	0.694	3.0	87	2.48	82	134
ORD086	0.199	34	143	1.48	13.6	7.0	347	1.44	0.86	13.0	0.741	3.4	102	2.73	90	139
ORD089	0.459	32	177	1.90	13.4	6.9	314	1.42	0.83	13.1	0.693	3.4	100	2.71	87	156
ORD096	0.166	27	118	1.45	10.9	5.8	356	1.14	0.73	10.6	0.588	2.6	88	2.36	56	117
NAJ002	0.492	29	189	1.14	13.3	6.3	581	1.58	0.76	13.4	0.612	3.5	95	2.44	99	95
NAJ008	0.546	33	166	1.03	13.5	6.8	670	1.58	0.85	14.4	0.631	4.0	95	2.65	113	138
NAJ014	0.424	38	138	2.31	15.3	7.6	429	1.10	0.79	14.4	0.682	3.3	134	2.65	95	121

Continued

ANID	Na_2O	Nd	Rb	Sb	Sc	Sm	Sr	Ta	Tb	Th	TiO_2	U	V	Yb	Zn	Zr
NAJ015	0.756	19	511	0.51	6.4	5.0	133	6.80	1.11	6.4	0.676	7.9	86	3.63	74	113
NAJ016	0.412	28	143	0.87	11.2	6.2	673	1.42	0.91	12.4	0.617	3.3	73	2.34	160	140
NAJ028	0.698	26	91	0.95	9.8	5.2	825	1.27	0.60	10.9	0.602	2.5	79	2.16	63	98
NAJ029	0.728	34	118	1.00	10.5	7.2	438	1.34	0.89	14.5	0.572	4.3	61	2.93	77	170
NAJ033	0.601	33	148	1.31	12.8	7.3	422	1.37	0.92	14.9	0.654	4.6	83	2.75	86	126
NAJ041	0.658	30	162	1.06	12.7	6.8	1002	1.53	1.00	13.3	0.660	3.0	88	2.52	79	118
NAJ044	0.804	29	179	1.08	12.2	6.2	741	1.57	0.67	13.3	0.613	3.7	72	2.27	68	130
NAJ053	0.197	35	167	2.13	13.9	7.3	234	1.31	0.97	13.1	0.852	2.6	102	3.15	87	142
NAJ059	0.190	26	53	1.28	11.4	5.6	318	1.14	0.66	10.9	0.600	2.6	90	2.20	74	92
NAJ062	1.056	29	121	1.82	12.5	6.1	795	1.15	0.69	11.8	0.576	3.6	114	2.15	80	91
NAJ064	0.495	31	181	0.86	12.7	6.5	603	1.51	0.77	13.2	0.571	3.7	73	2.51	99	134
NAJ066	0.646	28	136	1.01	11.4	5.8	683	1.50	0.72	12.2	0.601	3.6	73	2.63	74	130
NAJ068	0.509	35	170	1.13	13.4	7.1	791	1.62	0.83	14.4	0.679	3.9	87	2.56	85	130
NAJ076	0.317	30	143	1.89	12.4	6.5	438	1.19	0.76	12.3	0.635	2.2	74	2.57	79	86
NAJ077	0.723	30	171	0.93	12.4	6.0	729	1.50	1.02	13.1	0.606	3.4	80	2.38	98	89
NAJ085	0.666	30	143	1.03	11.5	6.4	661	1.59	0.69	13.0	0.587	3.2	87	2.25	59	136
NAJ087	0.607	35	157	0.97	11.8	7.2	636	1.62	0.87	14.1	0.728	4.2	108	2.67	62	127
NAJ092	0.195	33	131	1.21	12.1	6.9	413	1.17	0.86	11.9	0.621	2.9	78	2.62	77	118
NAJ093	0.590	34	121	3.37	12.1	6.9	311	1.27	1.06	13.1	0.683	3.8	89	2.87	70	163
NAJ095	0.383	28	139	0.86	10.9	6.2	655	1.33	0.83	12.0	0.190	2.8	21	2.54	152	119
NAJ096	0.505	17	473	0.44	5.4	4.1	125	6.22	0.85	5.1	0.190	6.0	21	2.60	88	87
NAJ100	0.197	18	515	0.46	6.7	4.7	146	7.55	1.02	5.4	0.161	6.3	17	2.76	80	93
LOG001	0.608	45	186	2.29	17.8	8.5	483	1.29	0.89	16.1	0.738	4.0	152	2.91	106	98
LOG003	0.533	45	186	2.38	18.2	8.8	474	1.36	1.21	16.4	0.735	3.9	137	2.83	111	100
LOG007	0.582	44	181	2.13	17.1	8.4	486	1.34	0.89	15.7	0.757	3.5	143	2.88	106	120
LOG028	0.574	36	161	2.34	14.0	7.3	185	1.40	0.83	13.9	0.718	3.1	109	2.80	92	155
LOG033	0.600	32	150	2.28	13.2	6.8	507	0.19	0.78	12.5	0.670	3.3	94	2.53	85	135
LOG034	0.721	39	172	2.29	14.5	7.2	497	1.24	0.79	13.5	0.611	4.0	91	2.60	94	97
LOG035	0.808	28	156	1.58	11.8	5.8	822	1.12	0.83	11.2	0.536	3.4	94	2.06	76	111
LOG037	1.323	34	195	2.63	15.7	7.2	712	1.29	0.74	14.1	0.637	5.3	121	2.17	105	106
LOG038	0.197	30	101	1.10	10.8	6.3	512	1.13	0.77	11.3	0.575	2.9	80	2.51	64	120
LOG042	0.198	34	235	2.04	14.5	7.0	214	1.57	0.89	13.7	0.649	3.8	89	2.77	75	125
LOG043	0.194	33	216	1.57	13.2	6.9	191	1.51	0.81	13.4	0.615	3.1	77	2.73	79	125
LOG044	0.194	34	231	1.69	14.2	7.0	172	1.57	0.86	13.3	0.622	2.9	88	2.47	82	146
LOG048	0.198	32	220	1.51	12.8	6.8	227	1.51	0.86	13.1	0.599	3.4	84	2.59	68	116
LOG050	0.611	43	172	2.36	15.9	8.4	278	1.47	0.94	15.5	0.770	4.1	130	3.15	95	158
LOG051	0.638	39	177	2.00	15.6	7.6	499	1.28	1.35	14.3	0.697	3.3	152	2.80	120	133
LOG054	0.642	38	176	8.42	16.8	8.0	537	1.35	0.85	15.4	0.629	3.5	129	2.56	104	141
LOG056	0.492	39	158	1.93	14.2	7.7	314	1.28	0.87	14.1	0.704	3.1	116	2.80	88	146
LOG059	0.526	37	171	2.31	13.7	7.4	247	1.40	0.86	13.6	0.688	3.3	101	2.90	139	130
LOG060	0.610	35	176	2.29	16.1	7.7	449	1.32	0.91	14.5	0.632	3.7	115	2.94	99	96
LOG061	0.603	38	176	3.31	15.8	7.7	438	1.37	0.91	14.7	0.675	3.5	114	2.89	94	87
LOG062	0.698	34	159	3.28	14.1	7.1	497	1.26	0.83	13.3	0.728	3.5	93	2.84	227	121
LOG072	0.609	46	182	2.72	18.1	8.3	455	1.38	1.07	16.4	0.724	4.2	165	3.15	115	72
LOG074	0.550	41	184	2.55	17.8	8.1	358	1.37	0.96	16.1	0.759	4.0	157	2.74	110	93
LOG075	0.595	44	182	2.57	17.9	8.8	453	1.34	0.94	16.3	0.766	4.1	136	2.69	110	120
LOG085	0.820	26	145	1.82	11.8	5.7	832	1.10	0.72	11.2	0.531	3.2	81	2.12	75	75

ICP-MS concentrations tables

Table A.6: Major elements and sum values with loss on ignition (LOI) values

ANID	Na_2O	MgO	Al_2O_3	SiO_2	P_2O_5	K_2O	CaO	MnO	TiO_2	Fe_2O_3	$\Sigma(\mu g/g)$	$\Sigma(\%)$	LOI	Σ
ELS001	0.85	0.55	16.4	60.4	0.10	2.4	6.5	0.029	0.79	4.7	0.30	92.7	3.05	96.1
ELS002	0.93	0.57	18.2	64.0	0.14	2.6	7.4	0.030	0.82	4.9	0.37	99.7	3.21	103.3
ELS003	1.01	0.58	18.4	59.1	0.13	2.5	13	0.020	0.78	4.9	0.45	100.5	4.16	105.1
ELS004	<LOD	0.72	29.6	64.1	0.04	3.2	1.6	0.023	0.13	3.1	0.20	103	0.43	103.6
ELS005	0.80	0.49	18.8	61.8	0.10	2.8	7.8	0.030	0.84	4.9	0.20	98.3	3.23	101.8
ELS006	0.90	0.54	18.1	63.3	0.19	2.5	8.9	0.029	0.78	5.1	0.20	100.4	1.17	101.8
ELS007	0.80	0.70	18.4	58.3	0.10	2.5	17.5	0.025	0.67	5.2	0.19	104.2	5.11	109.5
ELS008	0.64	0.50	16.6	64.3	0.13	2.6	9.5	0.026	0.87	4.2	0.19	99.3	4.9	104.4
ELS009	0.89	0.62	15.9	67.1	0.14	2.3	13.1	0.023	0.84	4.4	0.19	105.4	4.86	110.4
ELS010	0.71	0.69	18.0	58.3	0.06	2.4	16.1	0.026	0.68	5.1	0.19	102.2	6.51	108.9
ELS011	2.37	0.77	17.1	55.8	0.10	1.3	20.5	0.021	0.66	5.0	0.19	103.7	2.83	106.7
ELS012	0.76	0.70	17.2	57.6	0.03	2.4	15.6	0.030	0.65	5.3	0.19	100.2	8.03	108.4
ELS013	0.73	0.71	16.1	56.5	0.09	2.4	22.2	0.034	0.64	5.2	0.19	104.7	8.64	113.5
ELS014	0.89	0.80	19.0	58.4	0.03	2.6	15.6	0.021	0.69	5.4	0.19	103.3	3.96	107.5
ELS015	0.82	0.75	16.5	63.3	0.11	2.6	13.1	0.033	0.71	5.2	0.19	103.1	5.02	108.4
ELS016	0.77	0.72	16.1	59.0	0.06	2.4	17.6	0.049	0.68	5.1	0.20	102.4	7.24	110.0
ELS017	0.84	0.55	18.7	63.0	0.19	2.5	9.8	0.027	0.77	5.0	0.19	101.4	2.62	104.2
ELS018	0.82	0.60	18.4	59.8	0.07	2.8	9.7	0.017	0.84	5.1	0.66	98.3	14.4	113.3
ELS019	0.77	0.56	18.3	65.0	0.92	2.9	8.6	0.020	0.82	5.0	0.49	102.8	2.91	106.2
ELS020	0.70	0.81	18.0	50.0	0.19	2.3	21.0	0.047	0.60	5.1	0.30	98.7	8.05	107.1
ELS021	0.83	0.69	19.9	54.8	0.17	2.8	12.5	0.014	0.68	4.9	1.20	97.3	1.41	99.9
ELS022	0.77	0.70	18.3	51.0	0.19	2.5	19.4	0.037	0.58	4.7	0.73	98.2	6.24	105.2
ELS023	0.95	0.81	17.9	60.2	0.02	2.8	14.8	0.021	0.71	5.2	0.19	103.4	1.23	104.9
ELS024	0.95	0.63	18.4	69.0	0.19	2.9	4.9	0.025	0.90	4.7	0.19	102.6	1.76	104.5
ELS025	1.02	0.66	16.4	68.4	0.12	2.6	11.9	0.027	0.93	4.5	0.60	106.6	1.70	108.9
ELS026	0.80	0.66	15.8	61.5	0.09	2.5	15.4	0.013	0.77	5.2	0.50	102.7	5.70	108.9
ELS027	0.92	0.65	17.1	65.8	0.13	2.7	12.1	0.026	0.95	4.5	0.67	104.8	1.81	107.3
ELS028	1.04	0.93	17.2	62.3	0.14	2.8	21.0	0.034	0.66	5.3	0.87	111.4	6.24	118.5
ELS029	1.00	0.64	16.7	59.5	0.03	2.4	14.1	0.014	0.66	4.7	0.57	99.7	0.68	100.9
ELS030	0.73	0.68	16.8	51.6	0.16	2.2	24.5	0.058	0.56	4.8	0.43	102.2	8.82	111.4
ELS031	0.76	0.71	17.4	52.8	0.09	2.4	21.4	0.026	0.57	4.8	0.78	100.9	7.18	108.9
ELS032	0.86	0.64	17.0	58.1	0.07	2.5	19.6	0.018	0.60	5.3	0.63	104.6	0.74	106.0
ELS033	0.72	0.59	17.1	58.8	0.09	2.3	18.4	0.015	0.63	4.9	0.35	103.6	1.91	105.9
ELS034	0.78	0.63	18.0	58.4	0.06	2.6	15.1	0.019	0.62	5.1	0.31	101.3	3.78	105.3
ELS035	0.75	0.74	17.2	53.7	0.09	2.2	21.3	0.029	0.58	4.9	0.37	101.5	7.89	109.8
ELS036	0.74	0.72	17.8	55.4	0.05	2.6	16.7	0.024	0.61	5.0	0.19	99.7	5.67	105.6
ELS037	0.74	0.69	16.7	56.3	0.08	2.5	17.6	0.037	0.60	4.8	0.19	100.1	6.59	106.9
ELS038	0.79	0.74	16.8	57.4	0.07	2.6	17.4	0.028	0.65	4.8	1.69	101.2	5.77	108.7
ELS039	0.74	0.57	16.4	61.0	0.51	2.4	13.7	0.032	0.80	4.4	0.19	100.5	4.85	105.6
ELS040	0.78	0.66	18.3	58.1	0.13	2.8	15.5	0.015	0.68	4.5	0.30	101.5	3.99	105.8
ELS041	0.74	0.61	16.1	65.3	0.13	2.4	11.1	0.023	0.89	4.7	0.19	102.0	2.70	104.9
ELS042	0.80	0.64	16.1	61.0	0.11	2.4	12.7	0.017	0.87	4.4	0.19	99.2	3.33	102.8
ELS043	0.98	0.63	16.0	64.8	0.10	2.4	10.3	0.024	0.90	4.8	0.34	101.0	1.92	103.3
ELS044	0.96	0.69	17.8	68.3	0.09	2.5	9.1	0.034	1.00	5.0	0.74	105.4	0.75	106.9
ELS045	0.81	0.66	16.4	65.6	0.07	2.5	10.1	0.015	0.92	4.7	0.35	101.7	1.53	103.5
ELS046	0.83	0.70	16.7	57.7	0.10	2.5	12.7	0.021	0.99	4.8	0.44	97.1	3.41	100.9
ELS047	0.79	0.50	20.1	71.4	0.07	3.1	1.5	0.018	0.99	5.1	0.20	103.6	1.45	105.3
ELS048	0.95	0.65	18.0	59.5	0.08	2.6	7.9	0.029	0.81	4.8	0.33	95.3	3.19	98.8
ELS049	0.81	0.74	19.1	63.1	0.10	2.9	6.9	0.016	0.81	4.9	0.35	99.3	2.00	101.7
ELS050	0.83	0.60	18.3	61.3	0.30	2.9	7.8	0.017	0.93	4.8	1.14	97.8	2.94	101.9
ELS051	0.91	0.60	17.4	64.3	0.19	2.5	9.0	0.017	0.79	4.6	0.62	100.4	1.70	102.7
DUR001	1.30	0.91	16.3	57.6	0.15	1.9	9.8	0.056	0.87	5.2	0.19	94.3	2.13	96.6
DUR002	0.62	0.97	19.3	53.7	0.13	2.3	13.1	0.065	0.72	5.4	0.19	96.2	1.73	98.1
DUR003	0.55	1.24	17.4	53.1	0.86	2.0	13.8	0.031	0.75	5.5	0.30	95.3	5.89	101.5
DUR004	0.54	0.79	15.7	73.8	0.14	1.9	9.3	0.052	0.83	5.3	0.19	108.4	2.79	111.5
DUR005	<LOD	0.88	19.2	47.5	0.34	1.9	6.4	0.035	0.17	1.9	0.15	78.6	2.61	81.3

Continued

Table A.6 – *Continued*

ANID	Na_2O	MgO	Al_2O_3	SiO_2	P_2O_5	K_2O	CaO	MnO	TiO_2	Fe_2O_3	$\Sigma(\mu g/g)$	$\Sigma(\%)$	LOI	Σ
DUR006	<LOD	4.99	15.4	43.8	0.44	1.2	25.4	0.029	0.56	3.7	0.45	95.6	14.97	111.0
DUR007	0.50	0.63	15.7	74.9	0.07	1.9	2.4	0.013	0.95	5.6	0.19	102.7	1.94	104.8
DUR008	0.41	0.88	27.1	70.5	0.16	2.3	2.2	0.029	0.15	4.0	0.19	107.7	3.64	111.5
DUR010	0.52	2.29	15.9	78.8	0.13	2.6	2.1	0.031	0.69	5.6	0.19	108.7	1.19	110.1
DUR011	<LOD	1.00	27.2	69.0	0.14	2.1	2.7	0.032	0.14	3.8	0.16	106.5	2.66	109.4
DUR013	0.60	1.38	19.8	64.3	0.20	2.3	9.1	0.063	0.74	5.3	0.42	103.8	1.44	105.7
DUR014	0.44	2.47	18.4	61.5	0.20	2.3	16.3	0.021	0.65	3.7	0.53	106.0	8.07	114.6
DUR015	0.41	1.57	17.5	66.4	0.10	1.9	9.9	0.054	0.69	5.1	0.41	103.6	3.09	107.1
DUR016	<LOD	1.22	26.5	65.6	0.10	2.1	2.0	0.033	0.13	3.8	0.17	101.6	11.53	113.3
DUR017	0.60	1.37	16.8	69.1	0.10	2.0	8.2	0.050	0.80	5.3	0.39	104.4	0.85	105.6
DUR018	0.68	1.54	17.1	69.0	0.14	2.0	9.8	0.049	0.82	5.3	0.20	106.4	0.96	107.6
DUR019	0.60	1.72	16.2	62.3	0.15	1.9	17.5	0.150	0.70	4.7	0.47	105.9	7.03	113.4
DUR020	0.69	1.77	17.5	62.7	0.15	2.0	15.2	0.085	0.72	4.9	0.52	105.7	4.10	110.4
DUR021	0.73	1.73	18.3	62.4	0.12	1.9	13.4	0.067	0.72	4.9	0.39	104.3	2.98	107.7
DUR022	0.72	1.64	17.0	63.2	0.13	2.1	14.7	0.134	0.73	4.8	0.76	105.1	4.94	110.8
DUR023	0.60	1.76	18.1	68.6	0.14	2.4	13.2	0.072	0.73	5.3	0.20	111.0	4.42	115.6
DUR024	0.60	1.45	18.0	71.0	0.19	2.2	12.8	0.068	0.81	5.5	0.19	112.7	4.69	117.6
DUR025	0.56	1.26	15.9	65.5	0.19	2.0	9.2	0.057	0.76	5.5	0.19	100.9	2.84	103.9
DUR026	0.55	1.68	15.6	60.4	0.42	2.4	12.2	0.031	0.69	5.4	0.19	99.3	5.24	104.8
DUR027	0.61	1.14	16.0	65.4	0.13	2.1	9.9	0.055	0.73	5.0	0.35	101.0	1.45	102.8
DUR028	0.73	1.16	17.3	62.3	0.14	2.2	9.2	0.061	0.74	5.5	0.36	99.4	1.89	101.7
ORD001	1.42	1.04	13.5	52.1	0.06	1.5	21.4	0.028	0.59	3.6	0.34	95.2	10.88	106.5
ORD002	1.31	1.22	14.9	57.3	0.07	1.7	18.9	0.029	0.61	4.3	0.19	100.4	8.78	109.4
ORD003	1.33	1.02	12.6	53.1	0.07	1.5	18.9	0.033	0.52	3.4	0.19	92.5	11.10	103.8
ORD004	1.36	1.05	13.2	56.8	0.07	1.6	19.4	0.028	0.58	3.7	0.35	97.7	10.55	108.6
ORD005	1.50	1.15	15.3	53.0	0.08	1.8	18.8	0.046	0.64	4.2	0.35	96.5	7.66	104.5
ORD006	1.23	1.17	14.9	59.7	0.12	1.6	17.4	0.029	0.59	4.4	0.20	101.2	8.73	110.2
ORD007	1.40	1.97	15.2	59.7	0.08	2.3	13.7	0.032	0.65	4.3	0.19	99.3	5.09	104.6
ORD008	1.38	1.07	15.3	44.7	0.09	1.8	15.3	0.037	0.58	3.7	0.19	83.9	7.50	91.7
ORD009	1.16	1.46	14.7	67.4	0.15	1.5	20.9	0.029	0.60	4.5	0.19	112.4	1.10	113.7
ORD010	1.54	0.68	15.6	88.6	0.04	2.7	1.7	0.014	0.99	5.2	0.36	117.1	0.91	118.4
ORD011	1.57	0.69	15.6	81.6	0.15	2.7	1.3	0.017	0.89	4.3	0.65	108.9	0.90	110.4
ORD012	1.58	0.67	15.6	82.8	0.17	2.8	1.3	0.016	0.84	4.3	0.19	110.1	0.95	111.2
ORD013	1.50	0.66	15.5	81.4	0.13	2.7	1.4	0.017	0.83	4.2	0.43	108.4	0.97	109.8
ORD014	1.26	3.42	16.5	52.0	2.02	2.1	20.9	0.025	0.77	3.2	1.02	102.2	4.24	107.4
ORD015	1.43	0.78	12.8	74.7	0.65	2.0	8.4	0.021	0.81	3.7	0.31	105.3	2.62	108.2
ORD016	1.31	0.59	15.1	81.4	0.42	2.4	0.9	0.013	0.84	4.8	0.19	107.7	0.62	108.5
ORD017	1.59	0.63	14.3	75.2	0.07	2.6	0.8	0.014	0.88	4.2	0.19	100.1	0.84	101.1
ORD018	1.38	0.82	12.6	70.7	0.53	2.0	8.6	0.021	0.79	3.8	0.19	101.3	3.25	104.8
ORD019	0.98	4.46	16.5	56.2	1.65	2.3	19.3	0.029	0.73	3.6	0.32	105.8	8.44	114.6
ORD020	1.22	1.44	14.8	52.5	0.89	1.9	21.8	0.030	0.60	4.3	0.36	99.4	8.51	108.3
ORD021	1.24	1.27	14.6	50.0	0.69	1.4	19.3	0.028	0.52	3.8	0.19	92.8	7.56	100.6
ORD022	1.27	1.55	14.7	48.5	0.44	1.7	20.4	0.028	0.56	4.0	0.31	93.1	9.18	102.6
ORD023	1.73	1.13	14.9	53.4	0.51	2.0	23.8	0.075	0.66	4.8	0.59	103.0	8.54	112.1
ORD024	1.37	1.25	13.8	53.9	0.34	1.9	22.2	0.033	0.58	3.8	0.30	99.3	9.88	109.5
ORD025	1.34	1.31	14.7	41.7	0.15	1.7	25.9	0.034	0.56	4.3	0.90	91.6	9.36	101.9
ORD026	1.20	1.49	12.5	74.3	0.19	2.1	8.2	0.019	0.62	3.5	0.19	104.1	3.71	108.1
ORD027	1.26	0.80	11.9	60.1	0.20	1.8	19.6	0.023	0.60	3.1	0.17	99.4	10.33	109.9
ORD028	1.44	1.07	14.4	67.1	0.10	2.1	18.2	0.032	0.76	4.0	0.19	109.1	7.40	116.7
ORD029	1.36	1.50	16.1	53.0	0.20	2.2	14.7	0.031	0.73	5.2	0.40	95.1	3.97	99.4
ORD030	1.40	0.94	14.6	57.2	0.14	1.8	15.3	0.029	0.70	3.7	0.19	95.7	2.64	98.5
ORD031	1.52	1.02	14.4	56.4	0.06	1.8	18.5	0.025	0.71	3.9	0.46	98.3	7.79	106.6
ORD032	1.29	0.86	11.9	60.6	0.13	1.7	17.1	0.025	0.61	3.1	0.19	97.2	9.55	107.0
ORD033	1.44	0.93	14.0	51.9	0.05	1.9	19.7	0.021	0.69	3.7	0.40	94.3	7.58	102.3
ORD034	1.25	1.35	12.5	52.2	0.12	1.7	18.5	0.023	0.55	3.3	1.04	91.6	9.39	102.0
ORD035	1.27	0.91	11.0	54.5	0.10	1.5	21.7	0.023	0.56	2.9	0.60	94.3	11.74	106.7
ORD036	1.48	0.96	11.2	50.9	0.10	1.1	25.7	0.029	0.55	2.9	0.34	95.0	11.26	106.6
ORD037	1.32	0.91	14.4	40.2	0.08	1.6	18.6	0.037	0.56	3.8	0.19	81.5	7.28	89.0
ORD039	1.41	1.05	12.2	51.7	0.05	1.7	21.3	0.032	0.64	3.6	0.56	93.7	9.41	103.7
ORD040	1.45	0.86	14.0	59.0	0.14	1.9	12.1	0.030	0.68	4.0	0.19	94.2	4.71	99.1
ORD042	1.11	0.97	17.5	68.6	0.07	3.7	0.6	0.019	0.82	5.2	0.19	98.5	1.09	99.8

Continued

Table A.6 – *Continued*

ANID	Na_2O	MgO	Al_2O_3	SiO_2	P_2O_5	K_2O	CaO	MnO	TiO_2	Fe_2O_3	$\Sigma(\mu g/g)$	$\Sigma(\%)$	LOI	Σ
ORD043	1.63	0.64	17.6	62.3	0.12	3.0	1.4	0.011	0.81	5.0	0.19	92.3	1.93	94.5
ORD044	1.46	1.62	16.8	46.7	0.69	1.8	17.3	0.031	0.77	5.4	0.62	92.6	4.94	98.1
ORD045	1.30	1.23	13.9	40.3	0.08	1.4	20.6	0.025	0.55	3.8	0.19	83.3	8.09	91.6
ORD046	1.30	1.33	14.6	45.0	0.09	1.4	20.8	0.032	0.54	3.9	0.19	89.0	10.14	99.3
ORD048	1.40	1.46	11.7	51.2	0.32	1.6	23.4	0.047	0.61	3.9	0.64	95.6	2.61	98.9
ORD047	1.58	0.77	18.0	59.8	0.19	2.9	5.8	0.014	0.74	4.8	2.23	94.5	10.52	107.3
ORD049	1.24	1.31	17.5	48.2	0.53	2.4	16.8	0.035	0.76	5.4	0.35	94.1	4.79	99.2
ORD050	1.33	1.08	11.7	81.9	0.03	1.8	0.7	0.010	0.61	3.3	0.14	102.4	0.98	103.5
ORD051	1.15	1.54	21.1	52.2	0.19	3.5	3.2	0.012	0.88	2.8	0.19	86.6	1.92	88.8
ORD055	1.43	5.01	19.1	65.8	0.09	2.9	2.1	0.036	0.97	5.5	0.63	103	1.04	104.6
ORD056	1.23	0.72	28.5	60.4	0.14	3.7	1.8	0.033	0.13	2.9	0.19	99.6	1.16	101.0
ORD057	0.55	0.86	25.8	63.8	0.40	3.7	3.5	0.037	0.15	2.3	0.19	101.1	1.71	103.0
ORD058	1.20	0.92	27.8	72.7	0.11	4.0	1.4	0.034	0.16	3.4	0.17	111.7	1.41	113.3
ORD059	1.36	2.53	12.0	37.4	0.14	2.0	26.9	0.062	0.63	4.1	0.67	87.2	1.88	89.7
ORD060	1.38	1.24	14.4	40.5	0.15	1.5	26.3	0.028	0.53	3.9	0.20	90.0	6.10	96.4
ORD061	1.59	1.67	14.9	43.4	0.13	2.0	21.2	0.043	0.59	4.0	0.39	89.5	1.16	91.0
ORD062	1.30	1.20	14.4	45.4	0.13	1.2	18.1	0.030	0.53	3.9	0.19	86.1	9.83	96.2
ORD064	2.23	1.47	18.8	74.0	2.58	2.5	19.5	0.041	0.85	4.9	0.76	126.9	1.63	129.3
ORD065	1.44	1.10	14.1	45.6	0.38	1.9	20.6	0.027	0.54	3.9	1.20	89.5	7.45	98.1
ORD066	1.47	1.24	14.9	44.3	0.82	1.8	19.5	0.027	0.55	4.0	0.92	88.6	9.09	98.6
ORD067	1.71	1.24	15.2	39.1	1.88	1.7	19.6	0.040	0.59	4.0	1.02	85.0	5.77	91.8
ORD068	1.89	1.68	17.6	49.0	4.14	1.7	14.2	0.028	0.71	4.8	0.39	95.8	4.36	100.5
ORD069	1.61	1.42	16.4	46.3	1.95	1.9	15.9	0.052	0.69	4.3	0.19	90.5	9.46	100.19
ORD070	1.60	1.47	17.5	50.9	0.93	2.2	15.3	0.039	0.70	4.2	0.19	94.7	8.23	103.2
ORD071	0.47	1.49	14.6	47.1	0.12	1.4	17.3	0.027	0.67	4.6	0.45	87.2	13.45	101.1
ORD072	1.54	0.80	14.8	45.4	0.60	1.8	16.5	0.026	0.63	3.7	0.19	85.8	4.94	91.0
ORD073	<LOD	0.99	11.8	66.5	0.07	1.7	15.1	0.030	0.54	3.4	0.14	100.1	1.81	102.1
ORD074	<LOD	2.08	11.2	41.1	0.13	2.0	19.5	0.056	0.57	3.7	0.64	80.3	1.49	82.4
ORD075	1.49	1.64	17.2	53.6	0.04	2.2	16.2	0.028	0.78	5.4	0.72	98.7	6.22	105.6
ORD076	1.56	1.16	12.0	56.1	0.04	1.5	20.8	0.030	0.60	3.1	0.20	96.8	7.88	105
ORD077	<LOD	1.67	12.4	44.0	0.19	1.8	18.3	0.031	0.48	3.4	0.14	82.3	1.82	84.2
ORD078	1.8	0.68	20.7	70.2	0.03	3.8	0.5	0.011	0.90	3.2	0.19	101.7	3.90	105.9
ORD079	1.55	0.66	21.1	67.2	0.03	3.6	0.4	0.011	0.87	3.1	0.19	98.5	2.69	101.4
ORD080	1.66	0.75	22.3	66.0	0.04	3.7	0.6	0.013	0.85	3.6	0.20	99.5	8.71	108.5
ORD081	<LOD	0.55	16.9	64.3	0.07	3.4	0.4	0.010	0.76	2.7	0.19	89.1	1.61	90.9
ORD082	<LOD	0.64	17.2	67.6	0.05	3.5	0.6	0.013	0.74	3.1	0.19	93.4	1.66	95.3
ORD083	<LOD	1.84	13.6	43.6	0.41	2.9	10.4	0.057	0.66	4.2	0.52	77.8	3.23	81.5
ORD084	<LOD	1.90	13.0	40.9	0.39	2.3	16.7	0.020	0.55	2.5	0.32	78.2	9.16	87.7
ORD085	<LOD	2.79	13.3	48.8	0.19	2.4	14.2	0.019	0.60	2.7	0.33	85.0	8.49	93.9
ORD086	<LOD	2.72	14.2	37.6	0.63	2.3	12.8	0.022	0.62	2.8	0.56	73.6	4.09	78.3
ORD087	<LOD	0.99	13.8	40.6	0.20	2.1	16.8	0.040	0.54	3.6	0.55	78.7	8.02	87.3
ORD088	<LOD	3.60	13.2	32.2	0.39	1.5	19.3	0.025	0.50	2.6	0.47	73.4	14.92	88.8
ORD089	<LOD	3.10	14.1	43.1	0.37	2.3	13.3	0.026	0.65	3.0	0.39	80.1	3.90	84.4
ORD090	<LOD	2.22	14.1	43.1	0.35	2.7	16.4	0.025	0.61	2.7	0.20	82.3	8.98	91.5
ORD091	<LOD	2.75	14.5	50.9	0.59	2.1	16.8	0.024	0.69	2.9	0.44	91.2	5.87	97.5
ORD092	<LOD	2.11	13.3	50.1	0.37	2.3	18.8	0.020	0.62	2.6	0.56	90.19	9.62	100.4
ORD093	<LOD	2.45	14.0	42.5	0.34	2.5	16.6	0.024	0.63	2.7	0.59	81.8	8.94	91.4
ORD094	<LOD	2.00	13.1	52.2	0.34	1.9	16.8	0.020	0.60	2.6	1.10	89.6	6.47	97.2
ORD095	<LOD	2.37	13.6	57.3	0.44	3.1	14.3	0.025	0.61	2.8	0.41	94.6	11.44	106.5
ORD097	<LOD	2.03	13.6	47.9	0.41	2.7	16.4	0.024	0.61	2.7	0.33	86.4	16.41	103.1
ORD098	<LOD	2.17	14.7	52.0	0.51	2.7	16.1	0.020	0.61	2.8	0.49	91.6	8.94	101.1
ORD099	<LOD	2.75	15.7	51.5	0.61	3.1	13.8	0.029	0.68	3.2	0.38	91.4	5.64	97.4
ORD100	<LOD	2.17	14.4	51.3	0.51	2.7	16.3	0.024	0.68	2.7	0.41	90.8	6.75	97.9
ORD101	<LOD	2.28	15.1	48.5	0.30	2.8	14.5	0.023	0.70	2.7	0.42	87.0	6.30	93.7
LOG001	0.73	2.00	22.0	45.6	1.02	3.5	7.9	0.037	0.81	7.3	0.19	106.8	2.64	109.6
LOG002	0.83	2.28	23.7	46.9	0.39	3.5	8.9	0.040	0.85	8.2	0.19	114.1	1.35	115.7
LOG003	0.61	2.12	23.9	43.0	0.71	3.4	8.1	0.039	0.80	7.7	0.19	109.6	1.97	111.8
LOG004	0.68	1.91	20.4	49.5	0.53	3.5	7.6	0.046	0.86	7.8	0.19	106	4.89	111.1
LOG005	0.68	2.10	23.5	42.0	0.45	3.3	9.8	0.036	0.79	7.3	0.19	108.3	1.45	110.0
LOG006	0.70	1.86	22.1	43.3	0.48	3.7	9.3	0.037	0.86	7.6	0.19	105.7	3.62	109.6
LOG007	0.74	2.35	22.3	45.7	0.34	3.6	10.4	0.045	0.84	7.9	0.19	110.6	1.64	112.5

Continued

Table A.6 – *Continued*

ANID	Na_2O	MgO	Al_2O_3	SiO_2	P_2O_5	K_2O	CaO	MnO	TiO_2	Fe_2O_3	$\Sigma(\mu g/g)$	$\Sigma(\%)$	LOI	Σ
LOG008	0.60	0.65	13.7	54.6	0.09	2.0	2.1	0.001	0.74	4.6	0.16	80.9	0.89	81.9
LOG009	1.03	1.76	13.1	37.8	0.40	2.7	19.8	0.020	0.57	4.1	0.19	82.1	7.57	89.9
LOG015	0.73	2.25	24.1	41.7	0.45	3.4	7.6	0.039	0.81	7.6	0.19	108.1	0.33	108.7
LOG016	0.73	2.30	23.2	42.4	0.19	3.6	10.1	0.039	0.84	8.0	0.19	109.1	0.75	110.1
LOG017	0.67	2.36	22.2	42.7	0.20	3.5	10.3	0.040	0.86	7.8	0.19	106.9	0.60	107.8
LOG018	0.76	2.36	23.1	44.0	0.30	3.8	9.9	0.038	0.86	8.0	0.19	110.7	1.96	112.9
LOG019	0.64	1.76	21.0	42.4	0.54	3.4	8.0	0.044	0.82	7.0	0.19	99.8	2.98	103
LOG020	0.70	2.23	22.1	42.5	0.20	3.7	10.1	0.038	0.85	7.9	0.19	106.2	2.59	109
LOG021	0.77	1.04	14.2	51.0	0.19	2.5	4.2	0.041	0.78	4.7	0.19	82.0	1.74	83.9
LOG022	0.70	1.05	14.9	53.1	0.19	2.4	5.1	0.043	0.77	6.0	0.19	88.0	1.79	89.9
LOG023	0.72	1.11	15.0	52.0	0.20	2.5	4.5	0.037	0.77	4.9	0.19	85.6	2.17	87.9
LOG026	0.69	1.73	18.3	46.4	0.19	3.1	7.3	0.035	0.80	6.5	0.19	94.7	1.40	96.4
LOG030	0.80	2.21	21.5	40.1	0.30	3.3	10.0	0.044	0.77	8.3	0.56	102.4	0.64	103.6
LOG031	0.61	2.10	22.1	37.5	0.20	3.2	8.6	0.031	0.78	7.1	0.33	98.2	0.95	99.5
LOG032	0.73	3.03	17.0	42.9	0.40	2.4	14.9	0.062	0.73	5.5	0.87	95.1	2.65	98.6
LOG033	0.65	1.77	16.1	38.3	0.20	2.9	12.8	0.042	0.63	5.4	0.39	84.8	6.36	91.6
LOG034	0.86	1.99	17.0	41.2	0.32	3.1	12.8	0.053	0.68	5.9	0.34	91.3	4.89	96.6
LOG035	1.06	2.16	15.2	39.9	0.20	2.4	19.7	0.030	0.63	4.8	0.20	90.4	6.86	97.5
LOG036	0.65	1.61	15.6	46.7	0.20	3.1	12.1	0.034	0.60	5.0	0.19	90.4	12.00	102.7
LOG037	1.47	5.13	18.7	38.4	0.99	2.7	12.7	0.069	0.71	5.8	0.54	97.1	3.73	101.3
LOG038	0.36	2.53	13.2	39.8	0.39	2.4	23.8	0.057	0.67	4.7	0.47	88.8	7.85	97.1
LOG039	1.36	3.06	15.8	45.3	0.34	1.5	15.8	0.052	0.83	5.5	0.58	95.0	4.51	100.1
LOG040	2.09	3.92	17.8	39.8	0.20	1.8	12.9	0.067	0.71	6.4	0.54	94.5	1.37	96.4
LOG041	1.7	6.44	17.6	39.3	0.51	2.0	14.2	0.062	0.71	5.7	0.72	96.6	1.59	98.9
LOG042	<LOD	1.66	18.5	48.1	0.34	4.1	7.8	0.031	0.73	5.9	0.35	97.3	3.53	101.2
LOG043	<LOD	1.50	16.9	48.8	0.19	3.5	8.2	0.030	0.69	5.3	0.37	92.7	2.13	95.2
LOG044	0.34	1.72	18.9	46.6	0.19	3.8	9.0	0.048	0.71	8.5	0.30	100.4	2.23	103
LOG045	<LOD	1.65	17.4	47.9	0.20	3.5	9.8	0.024	0.72	5.4	0.30	94.9	3.36	98.6
LOG046	0.6	1.90	13.5	44.3	0.65	2.4	15.4	0.051	0.70	4.7	0.47	85.5	4.43	90.4
LOG047	0.44	2.86	13.2	39.6	0.68	2.2	19.9	0.059	0.66	4.5	0.64	84.9	10.8	96.4
LOG048	<LOD	1.59	17.8	51.1	0.19	3.9	8.4	0.032	0.72	5.5	0.20	98.3	2.65	101.3
LOG049	0.87	2.23	18.7	42.0	0.19	3.0	11.7	0.051	0.75	6.5	1.38	96.2	0.79	98.4
LOG050	0.72	1.77	18.7	47.6	0.19	3.1	6.6	0.035	0.82	6.7	0.31	96.6	0.91	97.8
LOG051	0.76	2.17	21.2	44.3	0.19	3.3	10.3	0.039	0.80	7.3	1.49	105.0	0.58	107.1
LOG052	0.77	1.66	17.3	53.2	0.19	3.2	8.2	0.049	0.86	6.5	0.32	99.8	1.24	101.4
LOG053	0.80	2.25	21.7	46.5	0.30	3.8	10.3	0.043	0.89	8.6	0.31	110.3	1.12	111.7
LOG054	0.80	2.38	20.2	45.8	0.39	3.4	12.1	0.059	0.79	7.1	0.46	105.8	2.22	108.5
LOG055	0.98	1.96	18.6	46.4	0.19	3.7	11.2	0.033	0.67	5.8	0.19	99.4	9.87	109.5
LOG056	0.69	1.58	18.5	53.1	0.19	3.1	8.3	0.039	0.77	6.3	0.19	102.3	1.23	103.7
LOG059	0.59	1.64	17.0	49.2	0.19	3.0	7.1	0.044	0.71	5.7	0.32	92.6	2.28	95.2
LOG060	0.70	2.21	17.9	41.8	0.19	3.3	10.7	0.057	0.70	6.4	0.19	92.8	3.65	96.7
LOG061	0.70	2.10	19.8	43.4	0.19	3.4	10	0.061	0.75	6.6	0.60	99.3	1.98	101.9
LOG062	0.76	1.85	16.6	39.9	0.30	2.7	12.3	0.058	0.63	5.6	0.56	87.3	4.98	92.8
LOG063	0.67	2.00	19.9	41.9	0.48	3.3	9.4	0.053	0.70	6.7	0.31	97.3	1.57	99.2
LOG066	1.09	2.19	16.8	42.9	0.19	2.7	12.2	0.054	0.72	6.5	0.61	92.3	0.87	93.8
LOG067	0.74	1.98	16.2	41.0	0.19	2.9	17.2	0.034	0.62	5.4	0.19	92.4	5.44	98.0
LOG068	0.76	1.94	15.9	42.9	0.19	3.1	17.7	0.043	0.64	6.1	0.19	94.8	7.05	102.1
LOG069	0.86	1.69	17.4	48.4	0.19	3.7	7.1	0.027	0.64	5.9	0.19	93.7	6.11	100.0
LOG070	0.68	2.16	21.5	40.6	0.20	3.8	9.4	0.040	0.81	7.9	0.51	102.2	1.53	104.3
LOG071	0.67	2.34	21.5	44.6	0.19	3.8	9.1	0.042	0.85	8.4	0.19	106.5	1.51	108.2
LOG072	0.68	2.22	19.1	40.0	0.19	3.3	6.9	0.034	0.75	7.1	0.43	91.4	0.86	92.7
LOG073	0.73	2.17	20.1	40.5	0.19	3.4	10.5	0.034	0.77	7.2	0.73	98.3	0.61	99.6
LOG074	0.66	2.19	20.3	43.0	0.20	3.5	10.19	0.035	0.81	7.5	0.48	101.5	1.32	103.3
LOG075	0.74	2.22	20.1	40.0	0.19	3.4	11.4	0.036	0.80	7.5	0.20	99.0	0.71	100.0
LOG076	<LOD	1.53	16.9	47.6	0.17	3.6	8.0	0.026	0.68	5.6	0.19	91.4	2.04	93.7
LOG077	0.89	0.78	12.8	64.1	0.13	2.0	2.8	0.003	0.78	4.4	0.16	88.9	0.72	89.8
LOG078	0.80	0.76	13.5	57.9	0.12	2.2	3.3	0.025	0.65	5.9	0.19	86.4	2.27	88.9
LOG080	0.83	1.90	14.9	40.6	0.19	2.7	20.4	0.033	0.59	4.9	0.32	90.7	8.49	99.5
LOG081	0.76	2.55	12.8	32.2	0.19	1.9	31.3	0.011	0.46	3.3	0.35	85.7	12.2	98.2
LOG082	0.66	1.94	16.1	44.9	0.20	3.4	14.8	0.066	0.70	5.9	0.20	94.5	3.34	98.2
LOG083	0.47	2.62	12.6	34.0	0.19	2.2	30.3	0.010	0.47	3.5	0.45	86.3	10.00	96.8

Continued

Table A.6 – *Continued*

ANID	Na_2O	MgO	Al_2O_3	SiO_2	P_2O_5	K_2O	CaO	MnO	TiO_2	Fe_2O_3	$\Sigma(\mu g/g)$	$\Sigma(\%)$	LOI	Σ
LOG084	0.91	1.77	15.7	42.5	0.19	2.6	12.4	0.063	0.68	5.6	0.20	87.6	2.58	90.5
LOG085	1.02	2.29	15.4	41.8	0.19	2.2	20.8	0.045	0.61	5.1	0.30	94.3	6.73	101.3
LOG086	0.96	2.11	18.5	41.1	0.19	3.5	8.6	0.032	0.80	7.1	0.77	92.7	0.197	93.8
LOG087	0.83	2.15	15.6	40.0	0.19	2.6	19.3	0.037	0.63	5.4	0.41	91.8	4.26	96.5
LOG088	0.68	1.98	15.9	44.1	0.19	3.1	12.1	0.057	0.68	5.7	0.20	90.0	4.79	95.1
LOG089	0.69	2.23	20.2	43.5	0.19	3.5	9.1	0.035	0.79	7.7	0.43	100.8	1.12	102.3
LOG090	0.33	1.91	18.7	51.1	0.16	4.4	1.9	0.003	0.97	6.6	0.19	96.3	4.72	101.2
LOG091	0.72	2.36	21.0	46.6	0.19	3.7	8.9	0.040	0.81	8.2	0.19	106.6	0.10	106.9
NAJ001	0.79	1.71	18.6	51.2	0.19	3.8	17.1	0.030	0.76	4.1	0.51	98.4	5.89	104.8
NAJ002	0.64	1.59	18.7	61.0	0.20	4.O	18.0	0.024	0.75	3.5	0.45	108.5	5.8	114.7
NAJ003	0.90	1.89	18.7	66.5	0.19	3.3	21.8	0.028	0.77	3.8	0.64	118	6.25	124.9
NAJ004	0.53	1.25	15.0	57.7	0.19	3.4	19.0	0.022	0.64	2.9	0.19	100.7	8.11	109.0
NAJ005	0.72	1.50	17.2	65.5	0.19	3.6	18.6	0.022	0.75	3.2	0.43	111.3	6.54	118.2
NAJ006	0.57	1.28	16.4	65.4	0.19	3.6	15.3	0.020	0.74	3.0	0.39	106.5	5.28	112.2
NAJ007	0.58	1.64	18.4	68.2	0.16	3.9	18.7	0.023	0.77	3.3	0.39	115.7	6.51	122.6
NAJ008	0.72	1.69	17.5	63.3	0.19	3.3	16.2	0.025	0.73	3.2	0.80	107.0	3.84	111.6
NAJ009	0.73	1.30	16.2	61.7	0.30	3.7	18.2	0.026	0.69	3.8	0.51	106.7	10.47	117.6
NAJ010	0.83	1.54	17.4	60.3	0.34	3.0	15.9	0.024	0.72	3.2	0.75	103.2	4.15	108.1
NAJ011	0.86	2.18	17.5	61.8	0.19	3.7	14.7	0.067	0.79	5.0	0.20	106.8	6.84	113.9
NAJ012	0.75	2.19	18.8	58.6	0.19	3.6	13.4	0.055	0.77	5.2	0.34	103.6	4.98	108.9
NAJ013	0.60	1.57	16.4	63.6	0.16	3.7	15.4	0.018	0.70	2.9	0.50	105.0	10.66	116.2
NAJ014	0.53	2.44	18.6	66.9	0.19	4.1	9.9	0.083	0.85	5.7	0.30	109.4	5.39	115.0
NAJ015	0.85	1.41	16.5	60.7	0.20	2.8	16.7	0.021	0.72	2.7	0.73	102.8	5.45	109.0
NAJ016	0.55	2.72	16.5	63.4	0.19	3.1	16.8	0.054	0.70	3.3	0.33	107.5	9.79	117.6
NAJ017	0.85	1.30	15.5	65.5	0.19	3.5	17.3	0.022	0.70	3.0	0.31	107.9	7.54	115.8
NAJ018	0.90	1.45	15.4	59.2	0.20	2.6	18.9	0.027	0.67	3.1	0.96	102.5	6.04	109.5
NAJ019	0.67	1.43	16.6	56.8	0.19	3.1	20.3	0.022	0.64	3.6	0.65	103.4	7.94	112.0
NAJ020	0.95	1.51	16.7	60.6	0.19	2.6	18.9	0.022	0.69	2.9	1.23	105.1	5.17	111.5
NAJ021	0.54	1.69	16.7	58.1	0.36	3.5	17.1	0.023	0.66	3.3	0.39	102.1	6.16	108.6
NAJ022	0.61	1.29	16.7	55.7	0.14	3.0	17.7	0.019	0.62	2.8	0.49	98.6	6.64	105.7
NAJ023	0.76	1.59	16.7	63.3	0.16	3.7	19.5	0.022	0.73	3.3	0.70	109.8	8.18	118.7
NAJ024	<LOD	1.44	15.1	70.2	0.15	3.6	14.1	0.075	0.80	4.4	0.40	110.1	6.53	117.1
NAJ025	1.05	3.07	14.7	60.7	0.19	3.5	17.7	0.059	0.72	3.7	0.47	105.3	8.64	114.4
NAJ026	0.87	6.83	11.8	53.9	0.19	2.5	28.1	0.050	0.57	3.3	0.20	108.1	3.56	111.9
NAJ027	0.75	1.61	16.6	59.8	0.19	2.6	17.7	0.020	0.66	2.8	1.35	102.7	5.17	109.3
NAJ028	0.86	1.89	14.6	56.2	0.12	1.8	28.5	0.028	0.65	3.2	1.97	107.8	8.01	117.8
NAJ029	1.00	4.28	15.1	59.6	0.33	3.3	20.4	0.062	0.72	4.0	1.06	108.8	7.88	117.7
NAJ030	1.10	2.37	14.7	55.4	0.12	2.3	30.1	0.030	0.63	3.6	1.82	110.3	8.04	120.1
NAJ031	0.78	1.63	17.1	62.5	0.19	3.6	21.5	0.025	0.74	3.3	0.50	111.4	6.11	118.0
NAJ032	1.28	1.55	14.3	61.0	0.19	1.6	20.8	0.020	0.69	2.6	2.38	104.1	4.35	110.8
NAJ033	0.74	4.19	15.9	56.8	0.20	3.8	17.3	0.068	0.73	4.6	0.53	104.4	5.91	110.9
NAJ034	0.56	1.56	18.2	65.0	0.32	4.0	16.4	0.025	0.77	3.4	0.40	110.2	3.15	113.8
NAJ035	0.64	1.72	10.7	64.7	0.19	2.5	21.1	0.050	0.57	3.0	0.52	105.3	3.56	109.3
NAJ036	0.88	2.48	18.2	58.1	0.16	3.7	15.2	0.079	0.73	5.1	0.51	104.7	2.51	107.7
NAJ037	0.82	2.47	18.5	59.4	0.17	3.9	11.5	0.075	0.78	5.2	0.47	102.9	6.04	109.5
NAJ038	0.64	1.65	16.9	58.8	0.16	3.4	20.5	0.023	0.72	3.6	0.68	106.5	3.84	111.0
NAJ039	0.75	2.37	19.3	64.0	0.20	4.4	12.2	0.073	0.85	5.8	0.20	110.0	6.94	117.2
NAJ040	0.78	1.52	17.9	56.9	0.19	3.8	16.2	0.032	0.69	3.5	0.38	101.5	5.15	107.0
NAJ041	0.74	1.74	17.8	55.1	0.30	3.1	19.0	0.022	0.69	3.1	0.87	101.6	6.64	109.1
NAJ042	0.56	1.51	17.0	57.4	0.19	3.6	19.6	0.044	0.69	3.6	0.46	104.2	5.57	110.3
NAJ043	0.60	1.32	16.8	60.8	0.17	3.7	16.5	0.022	0.73	3.3	0.38	103.9	5.75	110.0
NAJ044	0.87	1.45	16.5	58.1	0.17	3.1	18.0	0.021	0.70	3.2	0.41	102.1	6.21	108.7
NAJ045	0.63	1.35	17.7	40.3	0.15	3.5	16.7	0.019	0.64	3.1	0.39	84.0	9.15	93.5
NAJ046	0.54	1.95	15.5	45.9	0.19	3.2	24.7	0.044	0.61	4.3	0.64	96.9	2.46	100.1
NAJ047	0.93	2.38	18.6	33.0	0.19	3.7	10.4	0.062	0.77	5.5	0.69	75.5	4.88	81.1
NAJ048	<LOD	1.39	16.6	61.9	0.19	3.9	11.4	0.068	0.84	4.8	0.39	101.5	7.25	109.1
NAJ049	0.64	1.33	16.4	33.4	0.20	3.2	19.6	0.022	0.68	3.3	0.98	78.9	2.82	82.7
NAJ050	1.09	2.51	18.7	35.2	0.17	3.6	13.6	0.086	0.81	5.5	0.36	81.3	7.99	89.6
NAJ051	0.54	1.34	17.1	34.1	0.11	3.6	17.9	0.074	0.73	4.6	0.58	80.19	5.6	86.3
NAJ052	0.90	1.64	17.2	29.8	0.19	3.4	18.9	0.023	0.75	3.2	0.50	76.1	4.62	81.2
NAJ053	0.33	1.44	16.0	27.6	0.19	3.8	13.1	0.083	0.85	4.7	0.45	68.2	7.1	75.7

Continued

Table A.6 – *Continued*

ANID	Na_2O	MgO	Al_2O_3	SiO_2	P_2O_5	K_2O	CaO	MnO	TiO_2	Fe_2O_3	$\Sigma(\mu g/g)$	$\Sigma(\%)$	LOI	Σ
NAJ054	0.67	1.45	15.8	53.1	0.19	2.8	21.0	0.022	0.69	2.9	0.68	98.6	5.79	105.0
NAJ055	0.57	3.58	14.0	50.1	0.19	1.7	22.5	0.027	0.70	2.7	1.61	96.1	4.12	101.8
NAJ056	1.26	1.67	17.7	62.5	0.19	2.8	15.5	0.025	0.78	3.5	1.06	105.9	5.78	112.8
NAJ057	0.80	1.62	17.0	52.6	0.19	2.7	16.3	0.026	0.74	3.2	1.44	95.1	3.54	100.1
NAJ058	1.19	1.99	15.8	59.0	0.19	2.3	13.0	0.070	0.75	4.6	1.70	99.0	12.41	113.1
NAJ059	<LOD	6.44	16.1	60.4	0.14	1.9	18.2	0.025	0.73	3.0	0.20	107.2	7.08	114.5
NAJ063	1.08	1.71	16.0	54.6	0.19	2.7	19.0	0.042	0.67	3.5	0.86	99.5	6.19	106.6
NAJ064	0.57	1.48	16.8	56.2	0.19	3.4	16.4	0.023	0.69	3.1	0.36	99.0	6.92	106.3
NAJ065	0.60	1.24	14.7	63.6	0.19	3.8	13.4	0.017	0.71	2.6	0.48	100.8	3.72	105.0
NAJ066	0.70	1.37	15.4	49.9	0.20	2.8	16.7	0.029	0.65	2.9	1.00	90.8	3.94	95.7
NAJ067	0.96	1.57	17.6	59.8	0.19	3.4	14.8	0.021	0.78	3.3	1.08	102.4	5.83	109.3
NAJ068	0.56	1.33	17.7	56.7	0.33	3.8	13.1	0.021	0.73	3.2	0.95	97.5	6.53	105.0
NAJ069	0.85	1.67	17.3	55.5	0.19	3.5	14.5	0.021	0.70	3.0	0.48	97.4	6.05	103.9
NAJ070	0.62	1.56	17.2	57.0	0.14	3.7	17.8	0.038	0.73	3.9	1.08	102.6	5.46	109.2
NAJ071	1.00	3.92	15.6	59.3	0.19	3.4	15.9	0.068	0.79	4.3	0.89	104.5	3.01	108.4
NAJ073	0.39	3.45	13.1	62.3	0.19	3.3	19.0	0.019	0.70	2.4	0.31	105.0	5.66	110.9
NAJ074	1.08	2.38	15.0	51.8	0.20	2.5	22.1	0.028	0.66	3.4	2.40	99.3	5.41	107.1
NAJ075	0.43	5.88	13.8	55.9	0.16	2.6	21.0	0.029	0.66	3.4	1.39	103.8	8.72	113.9
NAJ076	0.55	1.86	16.6	49.9	0.16	3.1	22.8	0.071	0.73	4.7	0.64	100.4	6.28	107.3
NAJ077	0.82	1.47	17.6	59.9	0.19	3.3	16.6	0.034	0.65	3.8	0.67	104.4	5.36	110.4
NAJ078	0.59	1.53	17.2	60.1	0.19	3.8	17.3	0.032	0.72	3.6	0.47	104.9	4.47	109.8
NAJ079	0.77	1.35	15.1	58.0	0.19	3.1	20.5	0.024	0.64	3.3	0.66	103.1	1.64	105.4
NAJ080	0.98	2.86	18.0	58.4	0.19	2.6	14.5	0.019	0.74	3.8	1.92	102.0	12.49	116.4
NAJ081	1.05	1.36	16.7	62.0	0.13	2.6	16.0	0.019	0.69	3.5	1.95	104.0	2.73	108.6
NAJ082	0.54	1.46	16.2	54.7	0.13	3.7	20.1	0.022	0.66	3.1	0.56	100.6	4.73	105.8
NAJ083	0.96	2.22	18.0	56.0	0.16	3.6	12.3	0.060	0.77	5.5	0.76	99.6	4.82	105.2
NAJ085	0.73	1.56	15.5	54.5	0.19	2.5	17.1	0.018	0.65	2.7	1.60	95.5	3.72	100.8
NAJ087	0.65	1.58	16.4	54.9	0.15	2.8	13.3	0.024	0.77	4.4	0.40	95.0	7.88	103.3
NAJ088	0.33	2.49	13.9	48.3	0.16	3.1	20.6	0.061	0.62	4.0	0.66	93.5	4.11	98.3
NAJ089	<LOD	2.27	12.5	45.2	0.13	2.8	19.1	0.057	0.57	3.7	0.59	86.6	5.82	93.0
NAJ090	0.34	2.57	12.4	48.2	0.20	3.1	25.0	0.063	0.64	3.8	1.06	96.4	1.94	99.4
NAJ091	0.47	1.88	16.0	49.8	0.20	2.9	14.0	0.059	0.68	4.0	0.94	90.1	7.24	98.3
NAJ092	0.36	2.87	14.0	50.6	0.12	3.5	18.2	0.071	0.69	4.4	0.57	94.7	16.05	111.4
NAJ093	0.66	2.37	13.6	57.3	0.14	2.5	15.7	0.060	0.80	4.4	1.05	97.6	3.57	102.2
NAJ094	0.47	0.92	23.5	69.5	0.14	3.5	1.5	0.037	0.20	2.2	0.19	102.0	1.58	103.8
NAJ095	0.38	0.87	22.0	62.8	0.15	3.2	2.8	0.030	0.19	2.2	0.16	94.8	1.54	96.5
NAJ097	0.33	1.07	21.9	70.3	0.19	3.3	5.1	0.029	0.20	2.1	0.16	104.5	3.21	107.9
NAJ098	0.69	0.95	18.8	75.3	0.19	3.4	3.6	0.046	0.39	2.2	0.17	105.6	2.90	108.7
NAJ099	0.84	0.97	21.8	73.6	0.16	3.9	3.0	0.048	0.31	2.3	0.17	106.9	2.16	109.3
NAJ100	<LOD	0.85	22.7	69.2	0.13	3.2	4.8	0.036	0.19	2.1	0.15	103.5	2.37	106.0
NAJ101	<LOD	0.97	21.8	72.1	0.19	3.1	5.6	0.041	0.19	2.2	0.16	106.6	2.60	109.3

Table A.7: ICP-MS data (Minor and trace elements in μg/g)

ANID	V	Cr	Co	Cu	Zn	Rb	Sr	Zr	Nb	Sn	Cs	Ba	Lu	Hf	Ta	Pb	La	Ce	Pr	Nd	Sm	Eu	Gd	Tb	Dy	Ho	Er	Tm	Yb	Th	U
ELS001	84	84	41	18	<LOD	161	343	220	23	20	11	443	0.39	6.1	2.6	1130	40	82	10	35	6.9	1.1	5.4	0.78	4.5	0.69	2.3	0.39	2.4	18	3.5
ELS002	91	95	50	21	<LOD	180	370	289	25	20	13	469	0.44	8.0	2.8	1622	45	91	11	39	7.5	1.1	6.2	0.91	5.0	0.77	2.6	0.42	2.6	21	34.1
ELS003	85	102	35	28	<LOD	186	461	266	23	127	14	497	0.49	7.5	2.6	2196	47	97	12	44	7.7	1.2	6.7	0.91	5.2	0.85	2.8	0.46	2.8	22	34.4
ELS004	26	31	129	31	<LOD	565	109	118	32	165	48	186	0.47	4.7	14.0	816	15	30	4	16	4.1	0.4	4.1	0.80	5.1	0.84	2.8	0.49	2.8	8	37.1
ELS005	85	94	40	15	<LOD	193	351	248	25	19	14	537	0.48	7.0	2.9	388	48	97	12	44	7.8	1.2	6.4	0.92	5.3	0.80	2.8	0.46	2.8	23	34.3
ELS006	86	99	56	24	<LOD	183	393	250	25	16	14	450	0.45	7.0	2.9	659	44	90	11	40	7.3	1.1	6.1	0.89	5.0	0.79	2.5	0.44	2.5	21	34.0
ELS007	99	98	23	26	<LOD	171	563	258	20	18	13	396	0.38	6.8	2.4	104	42	84	10	37	6.5	1.0	5.2	0.74	4.2	0.68	2.3	0.36	2.2	20	33.4
ELS008	84	87	24	14	<LOD	158	340	287	24	51	11	507	0.52	8.2	2.8	188	46	95	11	42	7.5	1.2	6.2	0.91	5.4	0.87	3.0	0.48	2.9	21	34.3
ELS009	78	82	28	85	85	146	420	254	23	20	10	397	0.43	7.4	2.7	<LOD	40	80	9	37	6.9	1.0	5.5	0.83	4.7	0.76	2.4	0.40	2.5	19	33.9
ELS011	103	93	52	26	<LOD	168	477	212	19	28	12	433	0.40	6.3	2.4	98	43	89	10	40	7.3	1.2	5.8	0.83	4.7	0.71	2.3	0.39	2.4	19	33.4
ELS012	106	105	31	21	<LOD	161	528	200	19	22	12	372	0.34	6.0	2.2	196	40	80	9	34	6.1	1.1	5.1	0.71	4.0	0.66	2.1	0.34	2.1	18	33.2
ELS013	97	101	18	24	<LOD	150	627	226	19	34	10	376	0.38	6.4	2.0	282	41	83	10	36	6.7	1.3	5.5	0.75	4.2	0.68	2.3	0.34	2.3	18	33.3
ELS014	97	114	42	69	69	178	541	214	21	16	14	379	0.42	6.4	2.4	117	43	85	10	37	6.6	1.2	5.5	0.75	4.1	0.69	2.4	0.36	2.2	20	33.5
ELS015	112	111	42	19	<LOD	169	535	256	20	85	13	383	0.45	7.3	2.2	385	43	89	11	38	7.0	1.3	6.2	0.85	4.5	0.74	2.5	0.39	2.4	20	33.5
ELS016	110	88	30	20	<LOD	156	551	231	19	107	12	380	0.39	6.5	2.0	694	42	86	10	35	6.9	1.3	5.5	0.81	4.4	0.70	2.4	0.39	2.3	18	33.3
ELS017	91	82	29	26	<LOD	188	416	232	25	20	13	460	0.49	6.5	3.0	204	45	92	11	42	7.7	1.3	6.3	0.92	5.0	0.77	2.7	0.48	2.8	21	34.2
ELS018	107	113	35	42	42	199	424	248	23	62	17	484	0.50	7.0	2.6	4342	47	95	11	44	7.7	1.2	6.0	0.93	5.1	0.80	2.7	0.50	2.8	22	34.3
ELS019	99	111	29	35	35	191	434	242	24	88	15	533	0.49	7.0	2.8	2444	47	95	12	44	7.7	1.2	6.2	0.87	5.0	0.78	2.7	0.48	2.8	22	34.4
ELS020	63	88	55	56	56	187	682	202	18	44	15	453	0.40	5.9	2.2	543	40	77	10	38	7.3	1.1	5.7	0.88	4.7	0.72	2.4	0.42	2.4	19	33.0
ELS021	87	104	37	165	165	204	529	227	21	29	18	499	0.50	6.9	2.3	9534	47	97	12	46	8.7	1.3	6.7	1.04	5.5	0.83	2.7	0.49	2.8	22	33.7
ELS022	80	100	28	38	38	190	651	197	18	169	14	424	0.37	5.5	2.1	4711	39	77	10	37	6.9	1.1	5.7	0.81	4.5	0.65	2.2	0.40	2.3	19	33.2
ELS023	109	98	72	28	<LOD	180	471	230	20	17	15	429	0.41	6.8	2.3	330	45	92	11	42	7.6	1.2	6.0	0.92	4.9	0.78	2.5	0.42	2.4	21	33.6
ELS024	109	113	72	13	<LOD	206	298	239	26	22	17	459	0.43	7.0	3.0	<LOD	45	93	11	43	7.4	1.3	6.0	0.91	5.2	0.77	2.6	0.42	2.6	22	34.0
ELS025	112	139	67	20	<LOD	169	397	282	25	171	11	435	0.45	8.4	2.9	3740	44	90	11	42	7.6	1.2	5.8	0.93	5.5	0.89	2.8	0.46	2.8	21	34.5
ELS026	89	108	42	49	49	167	389	285	20	72	12	397	0.39	8.2	2.3	2966	41	84	10	38	6.3	1.0	4.8	0.73	4.1	0.73	2.3	0.37	2.3	20	33.9
ELS027	126	138	81	24	<LOD	190	403	280	26	306	14	462	0.45	8.1	3.0	4240	47	98	11	44	7.8	1.3	5.9	0.93	5.2	0.88	2.7	0.43	2.7	22	34.6
ELS028	117	175	36	46	46	188	560	180	19	83	13	372	0.34	5.4	2.2	6487	38	76	9	36	6.4	1.1	5.1	0.78	4.4	0.68	2.0	0.33	2.0	18	33.2
ELS029	104	83	50	22	<LOD	167	533	260	19	152	14	401	0.45	7.5	2.3	3467	45	91	11	41	7.7	1.3	6.2	0.91	5.1	0.80	2.7	0.45	2.7	21	33.5
ELS030	72	86	40	17	<LOD	185	695	186	18	96	12	407	0.38	5.6	2.0	2135	38	74	9	34	6.4	1.1	5.7	0.82	4.5	0.69	2.3	0.36	2.3	17	33.2
ELS031	78	95	37	27	<LOD	184	598	212	18	185	14	388	0.38	6.1	2.2	5604	39	76	9	35	6.5	1.1	5.6	0.79	4.4	0.68	2.3	0.37	2.2	18	33.2
ELS032	95	100	54	42	42	172	530	211	18	191	14	400	0.38	6.4	2.2	4095	43	86	10	38	6.4	1.1	5.6	0.77	4.3	0.69	2.2	0.39	2.3	19	33.4
ELS033	91	104	78	16	<LOD	165	533	239	19	74	13	417	0.39	7.0	2.4	1357	46	91	11	40	6.8	1.1	5.8	0.78	4.3	0.68	2.3	0.41	2.4	20	33.7
ELS034	85	98	23	50	50	183	507	229	19	92	15	429	0.44	6.9	2.3	956	45	92	11	40	7.5	1.3	6.1	0.84	4.8	0.75	2.5	0.45	2.6	20	33.7
ELS035	65	74	45	23	<LOD	195	590	199	18	16	14	385	0.37	5.8	2.2	1771	39	76	9	35	7.0	1.2	5.9	0.87	4.8	0.73	2.4	0.39	2.2	18	33.1
ELS036	71	80	22	24	<LOD	180	547	213	20	64	14	416	0.37	6.2	2.3	425	43	88	10	38	7.7	1.3	5.9	0.88	4.4	0.68	2.4	0.38	2.2	20	33.4
ELS037	71	90	38	28	<LOD	167	559	212	19	21	14	404	0.36	6.1	2.2	242	40	83	10	35	6.7	1.2	5.5	0.82	4.3	0.67	2.2	0.37	2.1	19	33.3
ELS038	73	104	21	204	204	171	634	211	19	1725	15	411	0.37	6.1	2.3	12910	41	83	10	35	6.6	1.2	5.2	0.79	4.2	0.68	2.3	0.36	2.3	19	33.4
ELS039	65	100	61	31	<LOD	170	393	260	22	41	15	469	0.43	7.6	2.6	270	41	85	10	36	6.8	1.2	5.2	0.81	4.7	0.73	2.6	0.41	2.6	20	34.0
ELS040	68	103	57	38	38	200	403	235	20	15	18	470	0.36	6.8	2.4	1040	41	84	10	33	6.1	1.0	4.7	0.68	4.1	0.64	2.4	0.38	2.2	20	33.8
ELS041	79	80	73	26	<LOD	175	449	283	23	35	14	465	0.50	7.8	2.8	301	44	89	11	41	7.6	1.3	6.5	1.00	5.7	0.90	3.0	0.50	3.0	21	34.2
ELS042	85	90	64	18	<LOD	177	340	262	21	75	14	421	0.39	7.7	2.5	395	41	82	9	34	5.4	0.9	4.5	0.62	3.7	0.67	2.3	0.38	2.4	20	34.0
ELS043	98	97	59	30	<LOD	172	383	221	23	314	14	420	0.43	6.4	2.6	1172	41	84	10	38	6.6	1.2	6.0	0.88	4.8	0.76	2.6	0.43	2.6	20	33.9
ELS044	132	108	92	14	<LOD	188	380	216	26	42	15	443	0.46	6.4	3.1	5324	45	91	11	42	6.8	1.3	6.3	0.87	5.0	0.77	2.7	0.43	2.7	21	34.0
ELS045	117	104	140	27	<LOD	188	354	275	22	150	15	428	0.39	7.4	2.8	1270	43	86	10	36	5.2	0.9	4.5	0.67	3.9	0.67	2.4	0.39	2.5	20	34.0
ELS046	121	104	72	19	<LOD	201	434	232	22	363	18	464	0.46	6.6	2.5	1917	45	92	11	42	6.8	1.2	6.3	0.87	5.0	0.77	2.7	0.45	2.7	21	34.1
ELS047	121	111	72	15	<LOD	228	233	256	27	23	20	557	0.52	7.5	3.3	677	51	106	12	46	8.8	1.6	6.6	1.01	5.6	0.87	3.0	0.50	2.9	23	34.7
ELS048	105	93	46	18	<LOD	195	398	219	25	27	17	458	0.47	6.4	2.9	1306	45	91	10	41	7.6	1.4	6.0	0.91	5.0	0.81	2.6	0.42	2.5	21	34.1
ELS049	102	115	68	32	<LOD	208	404	248	24	81	19	491	0.47	7.1	2.9	1139	48	97	11	44	8.5	1.7	6.5	0.99	5.4	0.87	2.8	0.52	2.9	22	34.3
ELS050	89	120	74	16	<LOD	212	391	257	25	110	18	515	0.54	7.6	3.2	8960	51	103	12	45	8.5	1.5	6.5	0.99	5.7	0.88	3.0	0.51	2.9	23	34.4
ELS051	105	105	78	42	42	179	384	278	24	145	14	422	0.51	8.0	3.0	3976	46	94	11	40	7.7	1.4	5.6	0.87	4.8	0.78	2.6	0.51	2.8	21	4.6
DUR001	76	68	77	38	38	161	228	280	28	50	11	414	0.45	7.6	2.4	615	44	84	10	37	6.6	1.2	5.8	0.84	4.8	0.76	2.5	0.47	2.6	15	3.9
DUR002	94	87	60	53	53	201	269	190	22	24	15	499	0.40	5.3	2.3	344	42	80	9	36	6.6	1.3	5.6	0.81	4.5	0.66	2.3	0.42	2.3	15	3.2
DUR003	99	89	72	61	61	169	834	187	19	57	11	396	0.41	5.2	2.0	643	39	80	9	35	6.6	1.3	5.8	0.83	4.5	0.69	2.2	0.42	2.4	15	3.4
DUR004	81	74	80	36	36	150	218	322	30	53	11	403	0.52	8.6	3.1	532	44	84	10	37	6.3	1.3	5.9	0.82	4.9	0.78	2.5	0.44	2.6	15	4.0
DUR005	15	18	88	23	<LOD	490	125	98	23	82	66	182	0.20	3.4	8.4	94	13	28	3	13	3.3	0.6	3.6	0.60	3.6	0.55	1.7	0.31	1.6	5	3.1
DUR006	91	79	50	59	59	69	388	132	16	129	5	309	0.31	3.8	1.8	2779	34	68	8	31	5.8	1.3	5.2	0.71	3.8	0.58	1.8	0.31	1.9	12	3.7
DUR007	88	77	205	32	<LOD	149	117	352	35	9	9	406	0.54	9.3	3.5	87	48	97	11	42	7.6	1.5	6.6	0.93	5.5	0.86	2.9	0.51	3.1	16	4.7
DUR008	29	74	151	71	71	542	134	98	37	93	34	208	0.43	3.7	17.1	210	15	28	4	17	4.2	0.8	4.9	0.89	5.3	0.86	2.7	0.50	2.7	5	6.6

Table A.7 – *Continued*

ANID	V	Cr	Co	Cu	Zn	Rb	Sr	Zr	Nb	Sn	Cs	Ba	Lu	Hf	Ta	Pb	La	Ce	Pr	Nd	Sm	Eu	Gd	Tb	Dy	Ho	Er	Tm	Yb	Th	U
DUR010	80	78	129	31	<LOD	162	178	201	18	10	8	578	0.41	5.5	2.0	302	41	86	10	39	7.3	1.6	6.7	0.90	5.0	0.78	2.3	0.46	2.5	14	5.6
DUR011	24	25	87	31	<LOD	551	131	111	37	90	35	205	0.49	3.9	16.3	<LOD	14	26	4	16	4.1	0.8	4.9	0.96	6.0	0.96	3.0	0.56	3.1	6	8.1
DUR013	76	91	92	58	58	201	260	207	25	276	15	493	0.41	5.8	2.7	1985	45	86	10	38	6.6	1.3	6.1	0.84	4.4	0.71	2.3	0.42	2.4	16	3.5
DUR014	69	80	99	51	51	173	561	177	21	381	13	518	0.38	5.3	2.6	2813	42	84	10	37	6.9	1.4	6.3	0.84	4.4	0.67	2.1	0.41	2.3	15	4.8
DUR015	81	85	87	35	35	161	234	209	23	35	11	427	0.42	5.9	2.5	2297	42	83	10	37	7.1	1.4	6.4	0.88	4.9	0.74	2.4	0.42	2.5	14	3.6
DUR016	22	29	105	16	<LOD	542	120	105	34	96	38	206	0.52	3.8	14.6	92	13	25	4	15	3.9	0.7	5.1	0.96	6.1	1.00	3.1	0.59	3.3	5	8.5
DUR017	84	83	162	34	34	162	218	264	29	28	11	409	0.47	7.2	3.2	2031	45	87	10	38	7.2	1.3	6.2	0.85	4.9	0.78	2.5	0.46	2.6	15	3.8
DUR018	69	85	155	30	<LOD	165	230	262	29	18	12	408	0.46	7.1	3.2	962	45	86	10	38	6.8	1.3	5.9	0.85	4.8	0.74	2.5	0.46	2.6	15	3.7
DUR019	72	79	117	40	40	170	360	228	22	65	11	399	0.36	6.1	2.6	2739	39	74	9	33	5.9	1.1	5.5	0.73	4.0	0.63	2.2	0.37	2.2	14	3.1
DUR020	76	82	84	32	<LOD	190	324	219	23	43	12	411	0.40	6.0	2.5	3339	41	79	9	34	6.2	1.2	5.6	0.76	4.3	0.67	2.2	0.40	2.3	14	3.3
DUR021	85	84	69	34	34	217	326	223	24	70	14	419	0.42	6.3	2.6	1933	43	83	9	36	6.4	1.3	5.7	0.82	4.5	0.69	2.3	0.40	2.4	16	3.4
DUR022	82	86	122	37	37	183	311	225	22	106	13	430	0.42	6.3	2.6	5545	41	79	9	35	6.3	1.2	5.7	0.80	4.6	0.67	2.3	0.40	2.4	14	3.4
DUR023	89	96	82	128	128	187	322	200	23	28	14	521	0.41	5.7	2.4	377	42	80	9	36	6.5	1.3	5.8	0.81	4.7	0.70	2.3	0.42	2.5	15	3.6
DUR024	107	80	73	38	38	167	263	282	30	26	11	518	0.43	7.7	2.9	201	45	86	10	38	6.7	1.3	5.9	0.85	4.9	0.72	2.4	0.42	2.5	15	3.8
DUR025	86	81	57	31	<LOD	155	228	273	28	25	11	409	0.43	7.4	2.5	116	42	82	9	37	6.3	1.2	5.6	0.79	4.7	0.70	2.4	0.42	2.5	15	3.7
DUR026	98	84	64	29	<LOD	162	571	217	18	10	9	468	0.44	6.1	1.7	191	42	87	10	37	6.8	1.4	6.1	0.88	4.9	0.75	2.4	0.45	2.5	15	3.4
DUR027	81	89	213	31	<LOD	168	249	267	24	38	13	428	0.46	7.3	2.8	1216	43	84	10	38	6.7	1.2	6.0	0.87	4.9	0.75	2.5	0.45	2.6	15	3.9
DUR028	72	84	154	32	<LOD	182	247	250	26	29	14	452	0.47	6.8	2.9	1471	45	87	10	38	7.1	1.2	6.4	0.92	4.9	0.75	2.4	0.46	2.7	16	3.6
ORD001	51	50	29	34	34	91	713	212	16	31	6	248	0.20	5.6	2.2	1673	28	60	6	23	4.2	0.8	3.7	0.52	3.5	0.66	2.1	0.20	2.1	11	3.2
ORD002	73	66	30	21	<LOD	103	593	224	16	19	8	266	0.31	5.9	2.3	196	31	68	7	28	4.8	0.9	4.3	0.60	3.6	0.69	2.2	0.31	2.2	13	3.1
ORD003	46	63	79	18	<LOD	93	662	202	15	25	7	234	0.20	5.1	2.5	604	27	58	6	22	3.9	0.8	3.5	0.44	3.2	0.62	1.9	0.20	1.9	11	3.1
ORD004	50	77	19	16	<LOD	103	626	210	16	30	9	243	0.20	5.5	2.2	1862	27	60	6	23	4.1	0.8	3.6	0.50	3.2	0.66	1.9	0.20	2.0	11	3.0
ORD005	56	86	28	31	<LOD	121	622	237	18	38	10	305	0.34	6.2	2.7	1694	32	69	8	30	5.1	1.0	4.6	0.62	3.8	0.72	2.2	0.34	2.3	13	3.1
ORD006	53	89	16	22	<LOD	71	628	211	16	19	6	327	0.30	5.5	2.3	954	31	69	7	27	4.7	0.9	4.3	0.61	3.6	0.69	2.1	0.30	2.2	13	2.8
ORD007	63	110	17	25	<LOD	147	353	219	17	18	14	308	0.35	5.8	2.5	768	35	74	8	33	5.5	1.1	4.9	0.73	4.1	0.77	2.4	0.34	2.4	14	3.3
ORD008	52	86	13	48	48	128	507	247	18	18	10	299	0.37	6.7	2.6	633	32	68	8	31	5.5	1.1	4.8	0.72	4.3	0.76	2.5	0.33	2.5	13	3.0
ORD009	71	97	20	30	<LOD	71	635	208	16	15	6	283	0.31	5.6	2.5	227	30	67	7	28	4.5	0.9	4.3	0.61	3.6	0.65	2.0	0.31	2.2	13	2.8
ORD010	86	145	54	48	48	162	171	425	20	17	13	399	0.50	11.2	3.2	1693	44	93	11	45	6.8	1.3	6.2	0.95	5.4	0.87	3.1	0.44	3.2	17	4.2
ORD011	74	135	44	44	44	156	149	404	20	16	11	398	0.50	10.5	3.1	4708	44	93	11	45	6.7	1.3	6.3	0.98	5.5	0.89	3.1	0.48	3.2	17	4.1
ORD012	68	118	37	27	<LOD	164	153	395	20	15	12	394	0.50	10.3	3.2	297	44	94	11	44	7.1	1.3	6.5	0.96	5.4	0.90	2.9	0.47	3.2	17	4.0
ORD013	68	117	42	27	<LOD	164	156	398	20	15	12	397	0.50	10.4	3.2	2530	44	93	11	45	6.8	1.3	6.2	0.95	5.3	0.87	3.0	0.47	3.1	17	3.9
ORD014	98	142	26	44	44	140	325	204	17	28	8	417	0.40	5.2	2.3	8388	41	85	10	40	7.1	1.4	5.9	0.92	4.8	0.84	2.8	0.41	2.8	13	3.8
ORD015	54	98	37	268	268	126	215	361	19	28	9	313	0.44	9.0	2.9	1260	34	72	8	32	5.4	1.0	4.7	0.71	4.3	0.76	2.6	0.42	2.8	13	3.7
ORD016	77	113	37	19	<LOD	151	159	460	19	12	11	382	0.54	11.3	2.9	119	43	91	10	42	7.0	1.3	6.2	0.98	5.2	0.82	3.0	0.50	3.1	17	4.1
ORD017	67	120	31	28	<LOD	156	130	357	17	12	14	365	0.46	9.0	2.9	244	40	84	9	36	6.0	1.0	4.8	0.73	4.4	0.80	2.7	0.44	2.8	16	3.9
ORD018	49	107	19	14	<LOD	134	229	326	17	15	11	319	0.40	8.3	2.7	619	35	73	8	32	5.4	1.0	4.7	0.70	4.3	0.75	2.6	0.41	2.8	14	3.8
ORD019	88	144	24	56	56	109	280	223	17	130	7	379	0.43	5.6	2.3	1400	41	85	10	41	6.8	1.3	6.1	0.92	5.0	0.81	2.5	0.42	2.8	14	3.8
ORD020	62	92	31	39	39	122	578	213	13	28	11	272	0.20	5.2	2.2	1909	31	67	7	28	4.8	0.8	4.2	0.65	3.7	0.66	2.1	0.31	2.2	13	2.9
ORD021	67	104	13	18	<LOD	70	610	201	15	18	6	287	0.31	5.0	2.1	632	30	64	7	26	4.6	0.8	4.0	0.61	3.5	0.65	2.1	0.30	2.2	12	2.9
ORD022	57	105	15	25	<LOD	120	595	213	15	18	10	273	0.20	5.4	2.2	1418	30	66	7	27	4.6	0.8	4.0	0.61	3.8	0.68	2.1	0.30	2.2	13	2.9
ORD023	65	102	27	60	60	122	612	245	16	28	9	277	0.35	6.3	2.6	4047	33	79	8	32	5.5	1.0	4.7	0.77	4.2	0.72	2.2	0.34	2.4	14	3.1
ORD024	51	93	13	35	35	123	665	208	16	43	12	254	0.30	5.5	2.3	1241	29	62	6	24	4.3	0.8	3.8	0.55	3.6	0.66	2.0	0.20	2.1	12	3.0
ORD025	63	108	16	74	74	98	739	206	11	21	9	272	0.33	5.3	1.8	7103	33	73	8	33	5.9	1.1	5.0	0.73	4.3	0.74	2.3	0.35	2.3	12	2.8
ORD026	58	111	22	30	<LOD	123	197	251	15	10	10	232	0.33	6.4	2.2	1153	31	68	7	30	5.3	1.0	4.4	0.66	3.8	0.69	2.2	0.32	2.3	12	3.1
ORD027	49	80	10	55	55	105	297	222	15	14	10	270	0.30	5.8	2.1	306	26	55	6	22	3.8	0.7	3.4	0.47	3.0	0.59	1.9	0.19	1.9	11	3.0
ORD028	72	111	12	43	43	124	374	260	18	25	12	259	0.32	6.8	2.7	420	29	60	6	25	4.2	0.8	3.8	0.52	3.3	0.65	2.0	0.20	2.2	13	3.2
ORD029	96	157	19	52	52	215	843	210	16	9	10	376	0.40	5.4	2.0	1702	37	76	9	35	5.6	1.2	5.2	0.75	4.4	0.78	2.4	0.37	2.5	13	3.1
ORD030	70	100	10	18	<LOD	123	384	273	19	21	11	272	0.32	7.0	2.7	330	28	57	6	23	4.0	0.8	3.6	0.52	3.3	0.65	2.1	0.31	2.2	12	3.3
ORD031	69	110	14	17	<LOD	122	404	280	18	16	12	272	0.32	7.3	2.5	2952	30	62	7	25	4.2	0.8	3.6	0.55	3.4	0.66	2.0	0.31	2.2	13	3.4
ORD032	49	91	9	24	<LOD	107	282	220	15	15	11	253	0.20	5.7	2.2	861	26	55	6	21	3.9	0.7	3.3	0.49	3.1	0.62	1.9	0.20	2.0	11	3.1
ORD033	63	109	15	20	<LOD	119	389	273	17	27	11	248	0.30	6.9	2.5	2423	29	58	6	23	3.9	0.7	3.4	0.54	3.3	0.63	2.0	0.31	2.1	13	3.6
ORD034	41	91	18	84	84	107	668	201	14	157	10	227	0.19	5.2	2.0	8556	26	56	6	22	4.0	0.7	3.4	0.51	3.1	0.59	1.8	0.20	1.8	11	2.8
ORD035	44	90	14	33	33	89	344	238	14	18	7	226	0.20	6.1	1.9	4664	25	54	6	21	3.7	0.7	3.3	0.52	3.1	0.62	1.9	0.30	1.9	10	3.1
ORD036	50	86	10	17	<LOD	54	378	241	15	52	4	212	0.20	6.1	2.0	2027	26	53	6	21	3.7	0.7	3.3	0.50	3.0	0.62	1.9	0.20	1.9	10	3.0
ORD037	54	85	19	39	39	99	598	220	16	22	6	287	0.31	5.7	2.2	760	30	64	7	28	4.8	0.9	4.3	0.62	3.7	0.68	2.1	0.31	2.1	13	2.9
ORD039	45	88	20	35	35	108	311	258	15	33	9	257	0.34	6.4	2.0	4175	30	63	7	27	4.8	0.8	4.3	0.60	4.0	0.72	2.2	0.31	2.3	11	3.0
ORD040	54	95	18	24	<LOD	127	248	369	17	19	10	314	0.46	9.2	2.3	863	37	77	9	35	6.0	1.1	5.1	0.79	4.9	0.83	2.6	0.41	2.7	14	3.5
ORD042	84	123	31	37	37	188	79	320	18	7	16	445	0.51	7.8	2.6	95	43	90	10	42	6.9	1.3	5.9	0.82	5.1	0.88	2.7	0.41	2.9	17	3.7
ORD043	83	128	19	37	37	182	220	386	19	12	13	453	0.48	9.8	2.6	205	49	102	12	49	8.0	1.4	6.3	0.94	5.4	0.91	2.9	0.46	3.1	18	3.7
ORD044	101	144	28	77	77	147	1,15	226	17	8	9	420	0.42	6.0	2.0	3514	39	81	9	36	6.3	1.3	5.3	0.81	4.8	0.85	2.6	0.39	2.7	14	3.0
ORD045	62	81	15	17	<LOD	71	636	198	14	11	6	245	0.19	5.1	2.0	414	27	58	6	21	3.9	0.7	3.2	0.46	3.0	0.63	1.9	0.19	2.0	12	2.8

Table A.7 – *Continued*

ANID	V	Cr	Co	Cu	Zn	Rb	Sr	Zr	Nb	Sn	Cs	Ba	Lu	Hf	Ta	Pb	La	Ce	Pr	Nd	Sm	Eu	Gd	Tb	Dy	Ho	Er	Tm	Yb	Th	U
ORD046	72	93	13	22	<LOD	84	462	223	15	14	9	267	0.32	5.8	2.2	339	32	69	7	29	5.5	1.0	4.9	0.72	4.1	0.76	2.2	0.32	2.4	13	3.1
ORD048	81	110	13	154	154	125	790	224	14	9	6	299	0.31	5.6	1.4	4343	30	61	7	27	4.7	0.9	4.2	0.59	3.6	0.74	2.2	0.30	2.3	9	2.6
ORD047	83	131	33	37	37	180	368	301	19	6	12	472	0.41	7.7	2.7	20314	46	97	11	46	7.3	1.3	6.0	0.91	4.8	0.91	2.7	0.43	2.9	17	4.0
ORD049	95	156	20	74	74	134	819	233	16	21	8	414	0.35	5.8	1.9	1153	38	79	9	36	6.0	1.3	5.5	0.79	4.5	0.81	2.6	0.41	2.6	14	3.2
ORD050	60	106	23	21	<LOD	119	72	308	13	<LOD	9	198	0.20	7.8	1.9	164	31	64	6	25	3.9	0.7	3.3	0.49	3.0	0.62	1.9	0.19	2.0	14	2.9
ORD051	100	165	22	81	81	209	156	248	20	13	17	466	0.46	6.4	2.5	346	50	105	12	51	8.1	1.7	7.2	1.14	5.8	0.94	3.0	0.48	3.2	17	4.2
ORD055	102	157	33	36	36	166	162	296	23	7	19	344	0.41	7.5	3.2	4581	42	91	10	39	6.1	1.1	5.3	0.79	4.7	0.84	2.7	0.42	2.8	17	4.2
ORD056	19	21	16	47	47	653	207	141	32	81	48	294	0.64	4.6	16.1	472	21	32	6	23	5.6	0.9	6.5	1.36	8.1	1.32	4.4	0.73	4.2	5	5.6
ORD057	20	29	16	54	54	583	216	113	24	45	39	494	0.66	4.1	10.5	<LOD	15	30	4	14	4.1	0.8	5.4	1.17	7.5	1.29	4.4	0.71	4.4	4	4.4
ORD058	25	33	35	29	<LOD	612	191	115	29	51	54	260	0.55	4.1	11.7	<LOD	15	28	4	14	4.2	0.6	5.0	1.05	6.7	1.10	3.6	0.60	3.7	5	7.3
ORD059	58	78	26	164	164	85	395	255	15	15	4	370	0.40	6.5	1.8	4933	37	74	9	36	6.0	1.1	5.5	0.85	4.7	0.83	2.7	0.36	2.7	11	3.4
ORD060	51	86	13	30	<LOD	111	761	200	14	11	11	284	0.34	5.3	1.9	879	33	74	8	33	5.8	1.1	5.1	0.78	4.2	0.78	2.4	0.33	2.4	12	2.8
ORD061	67	101	13	61	61	136	641	192	16	66	16	269	0.32	4.8	2.3	2038	31	64	7	28	4.8	0.9	4.5	0.67	3.8	0.74	2.3	0.31	2.3	12	3.0
ORD062	73	103	13	18	<LOD	69	573	204	15	33	6	264	0.30	5.3	2.1	685	31	69	7	27	5.0	0.9	4.4	0.66	3.7	0.75	2.2	0.32	2.4	12	2.9
ORD064	74	115	31	39	59	167	462	416	23	47	14	372	0.5	10.4	3.3	5411	44	93	10	39	7.1	1.3	6.6	0.97	5.5	1.10	3.3	0.50	3.5	17	4.7
ORD065	81	104	20	90	90	121	654	198	15	85	11	248	0.20	4.9	2.1	10061	29	64	7	25	4.8	0.9	4.2	0.58	3.4	0.67	2.1	0.20	2.2	12	2.8
ORD066	76	104	26	91	91	118	671	213	16	97	11	261	0.20	5.4	2.2	7258	30	65	7	27	4.6	0.9	4.1	0.64	3.5	0.70	2.2	0.20	2.3	12	3.0
ORD067	83	90	18	154	154	110	682	209	17	131	10	262	0.30	5.3	2.5	8148	31	62	7	27	5.0	1.0	4.3	0.64	3.6	0.71	2.2	0.20	2.3	12	2.9
ORD068	100	135	20	142	142	132	1,061	214	18	46	9	411	0.36	5.4	2.2	1273	39	81	9	37	6.5	1.3	5.6	0.84	4.4	0.81	2.6	0.37	2.7	14	3.3
ORD069	56	92	15	56	56	119	531	251	20	17	7	281	0.35	6.7	2.9	631	33	68	8	30	5.2	1.0	4.5	0.71	3.9	0.77	2.4	0.36	2.6	14	3.4
ORD070	63	98	14	55	55	168	459	257	20	16	16	304	0.37	6.8	3.3	726	35	72	8	30	5.6	1.1	4.7	0.76	4.2	0.77	2.5	0.34	2.6	15	3.5
ORD071	106	82	14	52	52	127	967	148	24	46	8	346	0.36	9.2	1.6	2305	36	76	11	41	6.3	1.1	5.2	0.78	4.4	0.72	2.3	0.40	2.3	14	3.0
ORD072	60	99	10	61	61	133	363	298	16	29	11	405	0.35	7.9	2.8	744	32	65	7	26	4.7	0.8	4.1	0.62	3.8	0.74	2.3	0.34	2.6	13	3.3
ORD073	61	51	9	62	62	109	227	162	21	15	9	196	0.34	10.3	1.6	233	29	62	9	32	5.3	0.8	4.5	0.65	3.8	0.67	2.1	0.34	2.0	12	2.8
ORD074	61	54	14	80	80	76	269	174	20	12	4	341	0.39	12.3	1.2	5098	35	71	11	43	6.1	1.0	5.3	0.77	4.4	0.74	2.4	0.39	2.4	12	3.2
ORD075	131	190	23	168	168	136	927	213	17	74	10	373	0.41	5.5	2.4	4617	38	80	9	37	6.3	1.3	5.4	0.82	4.6	0.82	2.6	0.36	2.7	14	3.4
ORD076	67	82	14	55	55	93	344	228	15	31	7	231	0.32	6.1	2.2	999	29	64	7	27	4.7	0.9	4.1	0.60	3.9	0.71	2.2	0.20	2.4	11	3.1
ORD077	60	49	9	23	<LOD	92	381	141	21	13	7	203	0.31	8.7	1.6	173	28	61	8	32	4.8	0.8	4.3	0.63	3.7	0.62	1.9	0.30	1.9	12	2.4
ORD078	107	180	10	58	58	213	176	305	32	13	16	532	0.48	7.6	3.9	228	54	111	13	51	8.1	1.6	7.0	1.03	5.7	0.95	3.1	0.47	3.2	17	4.6
ORD079	108	160	9	45	45	212	172	318	32	12	16	538	0.49	8.0	3.9	318	55	113	13	51	8.4	1.6	7.3	1.09	5.6	0.95	3.1	0.45	3.2	17	4.3
ORD080	110	160	18	44	44	223	193	266	33	9	17	602	0.47	6.4	3.9	459	58	119	14	55	9.1	1.8	8.3	1.13	6.0	1.00	3.2	0.45	3.2	17	4.5
ORD081	94	86	15	37	37	215	167	182	42	12	17	512	0.45	12.3	2.6	287	50	104	16	59	8.2	1.3	6.8	0.96	5.4	0.82	2.8	0.46	2.7	16	3.8
ORD082	99	90	12	30	<LOD	208	172	164	42	7	16	578	0.43	11.2	2.7	166	51	108	16	62	8.2	1.4	7.3	1.01	5.5	0.84	2.8	0.47	2.7	17	3.9
ORD083	66	63	17	64	64	148	284	162	24	35	8	723	0.42	10.7	1.5	3299	44	90	14	52	7.2	1.4	6.6	0.91	5.1	0.81	2.7	0.47	2.6	15	3.2
ORD084	56	64	16	59	59	125	342	133	21	25	7	370	0.35	7.4	1.5	1771	34	70	10	40	6.0	1.1	5.1	0.69	4.2	0.70	2.2	0.38	2.1	12	2.8
ORD085	67	68	15	37	37	117	276	137	22	81	7	329	0.37	8.2	1.6	1888	35	74	11	41	6.2	1.1	5.2	0.75	4.2	0.70	2.3	0.39	2.2	13	2.9
ORD086	78	75	15	87	87	140	297	130	23	17	10	386	0.35	6.6	1.6	4074	36	78	12	45	6.6	1.2	5.6	0.79	4.5	0.76	2.4	0.40	2.3	12	3.3
ORD087	55	56	30	217	217	130	386	142	25	63	13	245	0.20	8.7	2.2	3945	28	54	8	29	4.6	0.7	3.6	0.54	3.3	0.59	1.9	0.32	1.8	13	2.8
ORD088	68	73	12	58	58	85	409	113	20	249	4	511	0.30	5.1	1.4	2845	32	66	10	37	5.9	1.1	4.8	0.70	3.8	0.65	2.1	0.34	2.0	11	2.6
ORD089	76	76	14	62	62	177	254	137	23	83	11	389	0.35	7.6	1.7	2381	37	77	12	43	6.5	1.1	5.5	0.82	4.4	0.74	2.3	0.42	2.3	13	2.9
ORD090	71	72	13	51	51	154	328	132	23	44	10	399	0.36	7.5	1.7	1308	37	77	11	44	6.6	1.1	5.4	0.81	4.6	0.73	2.3	0.40	2.3	13	3.1
ORD091	78	84	14	38	38	180	330	146	24	23	10	452	0.38	8.6	1.7	2736	39	82	13	47	7.3	1.2	6.0	0.86	4.8	0.79	2.5	0.42	2.4	14	3.4
ORD092	69	65	17	128	128	113	347	132	22	16	7	377	0.38	7.2	1.7	4036	34	71	11	40	6.0	1.0	5.2	0.73	4.3	0.70	2.3	0.38	2.2	12	3.1
ORD093	75	69	16	69	69	129	337	129	22	154	8	369	0.36	6.2	1.6	4273	35	73	11	41	6.3	1.1	5.3	0.73	4.5	0.72	2.4	0.37	2.2	13	3.1
ORD094	78	68	14	149	149	114	308	131	21	27	8	376	0.38	7.2	1.6	9483	34	73	11	42	6.5	1.1	5.3	0.77	4.5	0.72	2.4	0.39	2.3	12	3.0
ORD095	81	67	15	50	50	142	320	132	22	76	10	460	0.36	7.0	1.6	2519	35	76	11	43	7.0	1.1	5.3	0.80	4.4	0.74	2.3	0.39	2.3	13	3.4
ORD097	80	69	12	56	56	142	384	129	22	46	10	547	0.35	6.6	1.5	1525	37	75	11	43	7.0	1.2	5.3	0.83	4.6	0.73	2.3	0.38	2.2	12	3.0
ORD098	71	69	17	93	93	148	344	127	23	60	10	393	0.33	6.7	1.6	3268	35	76	11	41	6.6	1.1	5.4	0.81	4.2	0.70	2.3	0.38	2.2	13	2.9
ORD099	75	81	16	98	98	178	310	140	25	21	13	447	0.37	7.5	1.8	2140	41	87	13	49	7.3	1.3	6.3	0.95	5.1	0.81	2.5	0.44	2.5	14	3.2
ORD100	73	75	16	49	49	160	315	143	24	7	11	406	0.40	8.2	1.7	2580	39	83	13	46	7.1	1.2	6.1	0.90	4.8	0.77	2.5	0.44	2.4	14	3.3
ORD101	79	79	28	64	65	154	271	148	24	24	11	389	0.38	8.0	1.8	2697	39	81	12	45	6.5	1.1	5.6	0.84	4.4	0.77	2.5	0.44	2.4	14	3.1
LOG001	146	116	17	73	73	143	490	177	20	<LOD	19	693	0.42	2.8	1.2	93	54	113	12	45	8.8	1.8	8.4	1.03	5.6	0.95	2.8	0.49	2.8	12	3.0
LOG002	140	119	23	28	<LOD	145	523	206	21	<LOD	18	568	0.44	3.1	1.3	<LOD	58	119	12	47	9.3	1.8	9.4	1.07	5.8	1.04	3.0	0.52	3.0	13	3.1
LOG003	132	111	20	23	<LOD	153	529	191	21	6	21	642	0.42	3.0	1.3	<LOD	58	121	12	48	9.4	1.8	9.5	1.06	5.8	1.04	3.0	0.51	3.1	13	3.1
LOG004	140	109	23	24	<LOD	140	466	207	20	6	19	575	0.41	3.1	1.2	<LOD	53	110	11	45	8.9	1.7	8.8	0.98	5.5	1.02	2.9	0.52	3.0	11	2.9
LOG005	134	103	18	21	<LOD	142	614	190	21	6	15	597	0.45	2.9	1.3	97	58	121	12	48	9.7	1.8	9.4	1.04	6.0	1.12	3.0	0.55	3.1	12	3.1
LOG006	143	104	19	12	<LOD	146	439	178	20	<LOD	19	571	0.43	2.6	1.2	<LOD	56	115	12	46	9.3	1.7	8.7	0.97	5.7	1.05	2.8	0.50	3.1	11	3.0
LOG007	144	113	26	13	<LOD	154	528	176	19	<LOD	23	557	0.43	2.7	1.2	86	56	117	12	47	9.5	1.8	9.0	1.01	5.6	1.05	2.8	0.49	3.0	11	3.1
LOG008	71	59	20	16	<LOD	117	26	357	16	6	34	443	0.49	4.9	1.1	<LOD	43	89	9	38	8.5	1.6	8.8	1.08	6.4	1.24	3.3	0.61	3.5	9	2.3
LOG009	69	62	14	13	<LOD	111	1,158	189	15	<LOD	12	392	0.20	2.8	1.0	119	34	70	7	29	5.7	1.1	5.6	0.68	3.9	0.75	2.0	0.35	2.1	7	2.4
LOG015	139	113	20	25	<LOD	167	493	215	22	6	23	628	0.47	3.5	1.3	<LOD	63	132	13	53	10.6	1.9	10	1.12	6.3	1.14	3.3	0.55	3.5	12	3.4

Table A.7 – *Continued*

ANID	V	Cr	Co	Cu	Zn	Rb	Sr	Zr	Nb	Sn	Cs	Ba	Lu	Hf	Ta	Pb	La	Ce	Pr	Nd	Sm	Eu	Gd	Tb	Dy	Ho	Er	Tm	Yb	Th	U
LOG016	143	113	25	13	<LOD	162	461	192	20	<LOD	24	546	0.45	3.1	1.2	85	60	123	12	50	9.9	1.9	9.4	1.02	5.8	1.05	3.1	0.53	3.2	11	3.2
LOG017	139	118	21	8	<LOD	156	469	199	19	<LOD	22	546	0.43	3.2	1.2	393	58	119	12	49	9.5	1.8	9.1	1.01	5.8	1.06	3.0	0.48	3.0	11	3.2
LOG018	146	117	22	11	<LOD	171	499	193	21	6	26	587	0.44	3.1	1.2	<LOD	61	126	13	51	9.7	2.0	9.4	1.06	5.9	1.11	3.0	0.53	3.2	12	3.4
LOG019	133	130	18	19	<LOD	165	498	225	20	6	26	642	0.46	3.4	1.2	<LOD	58	120	12	48	9.8	1.9	9.3	1.03	6.0	1.08	3.1	0.54	3.2	11	3.2
LOG020	141	117	21	9	<LOD	162	560	190	20	6	23	582	0.43	3.1	1.2	<LOD	59	122	12	48	9.7	1.9	9.1	1.00	5.8	1.02	3.0	0.49	3.1	11	3.3
LOG021	80	72	16	9	<LOD	133	168	330	17	<LOD	25	520	0.44	4.7	1.1	<LOD	46	95	10	39	7.8	1.5	8.1	0.96	5.6	1.06	3.0	0.51	3.0	9	2.4
LOG022	80	92	16	29	<LOD	127	224	379	17	6	22	509	0.48	5.3	1.1	<LOD	48	99	10	39	8.2	1.6	8.1	0.94	5.7	1.07	3.0	0.56	3.1	9	2.7
LOG023	81	73	14	12	<LOD	129	217	341	18	<LOD	22	532	0.45	5.0	1.1	<LOD	47	96	10	38	8.0	1.6	7.8	0.94	5.4	1.03	3.0	0.50	3.1	9	2.5
LOG026	118	94	19	9	<LOD	149	314	279	19	<LOD	25	548	0.47	4.3	1.2	845	54	110	11	44	9.1	1.8	8.8	1.00	5.9	1.07	3.1	0.55	3.2	11	2.9
LOG030	113	113	19	43	43	152	630	196	20	6	22	575	0.44	3.0	1.2	3190	57	119	12	47	9.5	1.9	9.0	1.05	5.8	1.04	3.0	0.53	3.0	11	2.9
LOG031	127	101	24	10	<LOD	152	449	185	20	<LOD	21	547	0.43	3.0	1.2	1156	58	119	12	48	9.6	1.8	9.1	1.05	5.7	1.00	2.9	0.50	3.1	11	3.1
LOG032	80	74	19	711	711	140	780	280	19	49	15	660	0.44	4.2	1.1	5484	48	98	10	40	8.3	1.6	8.0	0.97	5.5	0.97	2.9	0.49	2.9	10	2.3
LOG033	83	67	16	28	<LOD	132	678	223	18	49	18	517	0.42	3.4	1.1	1729	44	91	10	38	7.7	1.4	7.4	0.89	5.3	0.93	2.8	0.47	2.9	9	2.9
LOG034	86	76	21	52	52	154	633	233	18	6	23	557	0.42	3.7	1.1	1117	47	97	10	39	8.0	1.6	7.8	0.96	5.4	0.94	2.8	0.51	2.9	10	3.0
LOG035	91	73	14	15	<LOD	119	1,025	188	16	<LOD	13	435	0.33	2.9	1.0	362	38	78	8	32	6.3	1.2	6.2	0.74	4.3	0.76	2.2	0.42	2.2	8	2.5
LOG036	100	73	14	35	35	137	500	209	16	<LOD	19	510	0.38	3.2	1.0	158	44	91	9	37	7.5	1.4	7.2	0.83	4.9	0.87	2.5	0.45	2.6	9	2.6
LOG037	111	92	26	18	<LOD	150	902	183	19	8	22	892	0.37	2.8	1.2	2588	47	97	10	38	7.5	1.5	7.2	0.84	4.9	0.88	2.6	0.42	2.6	10	3.6
LOG038	75	62	18	161	161	80	644	252	16	22	6	487	0.39	3.6	1.0	2581	41	80	9	35	7.0	1.4	7.2	0.86	5.2	0.94	2.7	0.50	2.8	8	2.5
LOG039	86	74	17	33	33	98	398	292	19	21	10	714	0.46	4.3	1.0	3667	48	98	10	39	7.9	1.6	8.0	0.95	5.8	1.04	3.0	0.55	3.2	9	2.4
LOG040	94	106	16	59	59	163	587	192	17	30	24	576	0.37	3.0	1.1	3095	45	93	10	38	7.8	1.4	7.3	0.83	5.0	0.94	2.5	0.45	2.6	10	3.1
LOG041	106	87	20	114	114	146	856	180	17	22	21	696	0.37	2.9	1.1	4592	45	93	10	37	7.5	1.4	7.3	0.82	5.0	0.86	2.5	0.44	2.7	9	3.2
LOG042	86	75	28	119	119	194	268	226	19	122	30	613	0.43	3.5	1.4	968	44	90	9	37	7.6	1.4	7.4	0.86	5.2	0.98	2.7	0.48	2.8	9	2.4
LOG043	82	64	25	269	269	179	191	235	18	27	27	540	0.42	3.6	1.3	1679	43	87	9	38	7.2	1.4	7.3	0.89	5.3	0.96	2.6	0.47	2.9	9	2.4
LOG044	89	126	23	164	164	196	207	224	19	40	33	572	0.43	3.4	1.3	871	44	90	9	37	7.7	1.4	7.6	0.91	5.5	0.96	2.8	0.48	2.8	9	2.5
LOG045	85	70	16	49	49	178	331	221	19	13	28	564	0.44	3.3	1.3	972	45	91	10	39	8.0	1.4	7.6	0.89	5.3	0.97	2.8	0.47	2.9	9	2.4
LOG046	76	59	20	72	72	112	501	292	18	76	16	564	0.49	4.2	1.2	2526	45	92	10	39	8.2	1.4	7.7	0.92	5.6	1.04	2.9	0.55	3.1	9	2.4
LOG047	72	59	17	123	123	89	539	256	17	25	11	485	0.45	3.7	1.1	4351	43	85	9	37	7.5	1.3	7.4	0.90	5.4	1.03	2.9	0.50	2.9	8	2.7
LOG048	84	69	25	80	80	196	225	247	18	21	34	558	0.43	3.7	1.3	896	43	91	9	37	7.4	1.4	7.3	0.88	5.4	0.93	2.7	0.46	2.9	9	2.5
LOG049	126	85	24	59	59	149	487	225	20	6	23	963	0.45	3.4	1.2	11129	51	105	11	42	8.5	1.8	8.3	0.96	5.8	1.00	3.0	0.50	3.0	10	3.2
LOG050	129	88	44	6	<LOD	152	293	263	20	<LOD	25	532	0.47	3.9	1.3	1097	54	111	11	45	8.8	1.7	8.5	1.00	5.9	1.04	3.1	0.55	3.1	10	3.0
LOG051	144	98	42	6	<LOD	156	649	223	20	<LOD	25	541	0.44	3.6	1.3	12080	55	115	12	45	9.0	1.8	8.6	0.98	5.8	0.99	2.8	0.50	2.9	11	3.1
LOG052	109	90	32	43	43	148	337	311	19	11	25	531	0.49	4.6	1.3	1040	51	105	11	43	8.4	1.7	8.3	0.99	5.6	1.05	3.1	0.53	3.2	10	2.9
LOG053	145	118	20	23	<LOD	157	463	193	21	6	21	552	0.48	3.1	1.3	923	59	121	12	48	9.8	1.9	8.9	1.04	5.9	1.03	2.9	0.54	3.0	11	3.1
LOG054	124	101	26	45	45	160	562	231	21	6	23	663	0.47	3.5	1.3	2172	55	112	11	45	8.8	1.9	8.8	1.06	6.0	1.04	3.1	0.51	3.1	11	3.3
LOG055	114	90	15	51	51	152	516	199	19	6	21	567	0.42	3.0	1.1	270	48	100	10	41	8.1	1.6	7.6	0.88	5.3	0.90	2.7	0.46	2.7	10	2.8
LOG056	114	89	32	16	<LOD	145	396	293	20	<LOD	23	562	0.48	4.3	1.3	145	53	108	11	45	9.2	1.7	8.6	1.01	6.0	1.02	3.1	0.58	3.2	10	3.2
LOG059	89	80	27	14	<LOD	152	263	293	19	6	25	538	0.49	4.2	1.2	1287	49	101	11	43	8.9	1.7	8.6	1.04	5.8	1.02	3.1	0.57	3.1	9	2.9
LOG060	111	89	27	25	<LOD	150	508	190	19	7	23	560	0.43	2.9	1.1	314	48	99	10	42	8.4	1.6	8.0	0.92	5.3	0.93	2.7	0.49	2.8	10	3.0
LOG061	112	95	23	21	<LOD	166	454	231	21	6	26	720	0.50	3.6	1.3	3622	54	111	12	46	9.3	1.8	9.1	1.07	6.2	1.07	3.2	0.57	3.1	11	3.3
LOG062	91	78	21	48	48	139	541	209	18	46	22	574	0.41	3.0	1.1	3284	45	93	10	39	7.7	1.5	7.7	0.89	5.3	0.92	2.7	0.50	2.6	9	2.9
LOG063	107	89	17	65	65	166	524	212	20	7	27	688	0.47	3.3	1.2	692	55	113	12	47	9.3	1.8	8.9	1.04	5.9	1.05	3.0	0.50	3.1	11	3.2
LOG066	120	91	16	26	<LOD	156	459	202	17	6	23	538	0.43	3.0	1.1	4002	46	95	10	39	7.9	1.5	7.5	0.90	5.3	0.97	2.7	0.48	2.7	9	3.0
LOG067	95	78	12	18	<LOD	136	857	200	18	6	19	479	0.37	3.1	1.1	127	42	86	9	35	6.8	1.3	6.6	0.83	4.9	0.86	2.4	0.42	2.5	8	2.8
LOG068	92	78	13	35	35	141	912	207	17	6	21	505	0.36	3.2	1.1	121	42	87	9	35	7.0	1.3	6.8	0.80	4.7	0.89	2.4	0.42	2.4	9	2.7
LOG069	113	78	15	41	41	163	359	203	17	6	26	547	0.38	3.1	1.0	<LOD	50	101	11	41	8.1	1.5	7.7	0.89	5.1	0.92	2.7	0.44	2.6	10	2.9
LOG070	151	88	19	8	<LOD	180	494	215	20	<LOD	29	613	0.45	3.4	1.1	2753	63	128	13	52	10.7	2.0	9.8	1.06	6.2	1.11	3.1	0.55	3.2	12	3.4
LOG071	145	90	21	27	<LOD	166	502	180	21	6	25	573	0.47	2.8	1.2	<LOD	61	124	13	51	9.8	1.9	9.4	1.08	5.8	1.09	3.0	0.52	3.0	11	3.4
LOG072	146	71	32	123	123	145	418	190	19	<LOD	21	498	0.40	3.0	1.1	2225	54	110	11	45	9.1	1.7	8.6	0.93	5.2	1.00	2.8	0.50	2.7	11	2.9
LOG073	132	67	19	20	<LOD	154	524	177	20	<LOD	23	541	0.45	2.7	1.1	5156	58	119	12	49	10.1	1.9	9.0	1.01	5.7	1.08	3.0	0.52	2.9	11	3.0
LOG074	149	77	33	14	<LOD	148	440	189	20	<LOD	19	574	0.43	3.0	1.1	2654	58	120	12	47	9.8	1.8	9.4	0.97	5.6	1.01	2.9	0.53	2.9	11	3.2
LOG075	128	79	23	31	<LOD	153	471	190	19	<LOD	22	538	0.43	3.0	1.1	539	58	119	12	48	9.5	1.8	9.3	1.05	5.6	1.05	3.0	0.51	3.1	11	3.2
LOG076	85	56	17	29	<LOD	174	187	228	18	32	25	554	0.38	3.4	1.3	218	41	84	9	34	7.0	1.3	6.6	0.82	4.8	0.88	2.7	0.44	2.8	9	2.3
LOG077	69	48	17	30	<LOD	106	57	452	17	<LOD	32	413	0.49	6.1	1.1	<LOD	43	89	9	37	7.7	1.4	8.4	1.00	5.7	1.13	3.2	0.56	3.5	9	2.4
LOG078	75	66	16	280	281	109	80	321	16	6	27	424	0.46	4.5	1.0	<LOD	40	83	9	37	7.8	1.4	8.5	1.00	5.6	1.09	3.2	0.52	3.2	8	2.3
LOG080	89	72	14	21	<LOD	122	966	191	16	6	15	443	0.35	3.1	1.0	896	40	81	8	33	6.3	1.2	6.5	0.75	4.2	0.78	2.3	0.39	2.4	8	2.8
LOG081	66	66	8	34	34	94	2,052	131	13	6	10	295	0.19	2.0	0.8	432	26	53	5	21	4.0	0.7	3.8	0.48	2.8	0.49	1.5	0.19	1.5	6	2.1
LOG082	100	70	19	38	38	134	680	214	17	<LOD	20	546	0.40	3.2	1.0	623	46	94	10	38	7.4	1.4	8.0	0.89	5.1	0.97	2.7	0.47	2.8	9	3.0
LOG083	80	68	10	12	<LOD	113	1,805	119	13	<LOD	13	349	0.19	1.9	0.9	1670	27	54	6	22	4.0	0.7	3.8	0.48	2.8	0.51	1.4	0.19	1.5	6	1.9
LOG084	98	67	16	18	<LOD	138	554	203	17	<LOD	21	496	0.42	3.0	1.0	831	44	90	9	37	7.5	1.4	7.3	0.88	5.0	0.92	2.8	0.46	2.7	8	2.8
LOG085	84	79	17	14	<LOD	128	1,021	145	17	<LOD	18	485	0.34	2.1	1.1	637	40	81	9	33	6.7	1.2	6.5	0.76	4.4	0.82	2.3	0.40	2.4	7	2.5
LOG086	131	94	41	42	42	154	414	131	18	<LOD	25	503	0.41	1.9	1.2	5661	54	110	12	45	9.1	1.6	8.6	0.97	5.6	0.97	2.8	0.48	2.9	9	2.9

Table A.7 – *Continued*

ANID	V	Cr	Co	Cu	Zn	Rb	Sr	Zr	Nb	Sn	Cs	Ba	Lu	Hf	Ta	Pb	La	Ce	Pr	Nd	Sm	Eu	Gd	Tb	Dy	Ho	Er	Tm	Yb	Th	U
LOG087	91	72	14	66	66	131	726	152	16	<LOD	16	509	0.36	2.3	1.0	1961	41	84	9	34	7.0	1.3	6.7	0.77	4.5	0.83	2.4	0.41	2.4	8	2.6
LOG088	95	79	15	16	<LOD	139	933	170	17	<LOD	22	510	0.38	2.5	1.1	471	44	89	9	36	7.7	1.4	7.3	0.87	5.1	0.91	2.6	0.45	2.5	8	2.9
LOG089	136	104	22	19	<LOD	160	392	158	20	7	25	546	0.43	2.6	1.2	2176	58	119	12	49	9.7	1.8	9.3	1.04	5.8	1.07	3.0	0.52	3.1	10	3.2
LOG090	141	123	11	39	39	178	231	184	21	<LOD	40	588	0.42	2.8	1.2	<LOD	40	79	9	34	6.9	1.4	6.7	0.83	4.8	0.94	2.7	0.48	2.8	8	4.6
LOG091	150	113	27	8	<LOD	159	576	157	21	<LOD	24	544	0.47	2.5	1.3	<LOD	59	122	12	49	9.4	1.9	9.4	1.04	5.9	1.07	3.1	0.55	3.1	10	3.3
NAJ001	93	71	27	57	57	181	869	204	17	107	12	454	0.35	4.1	1.5	2586	42	84	10	35	6.5	1.3	5.4	0.83	4.7	0.81	2.5	0.38	2.5	14	3.9
NAJ002	98	79	26	54	54	203	640	198	19	339	16	466	0.35	4.1	1.9	1979	41	82	9	35	6.7	1.3	5.4	0.81	4.7	0.80	2.4	0.37	2.4	14	3.8
NAJ003	90	78	32	53	53	198	910	227	19	165	13	482	0.41	4.6	1.9	3664	42	87	10	37	6.9	1.4	6.1	0.95	5.3	0.90	2.7	0.41	2.6	15	4.1
NAJ004	70	80	14	37	37	155	653	236	17	22	11	376	0.20	4.5	1.7	487	36	73	8	31	5.9	1.1	5.0	0.72	4.1	0.68	2.1	0.31	2.2	13	3.1
NAJ005	80	87	18	43	43	169	642	234	18	76	12	455	0.39	4.6	1.8	2090	42	84	10	37	6.8	1.4	5.6	0.87	4.9	0.84	2.6	0.39	2.5	15	4.0
NAJ006	76	63	18	30	<LOD	175	790	242	18	45	14	405	0.32	4.6	1.8	1643	40	80	9	35	6.4	1.2	5.6	0.82	4.5	0.74	2.2	0.36	2.3	14	3.4
NAJ007	88	68	19	38	38	198	959	185	19	49	15	485	0.37	4.1	2.0	1404	43	86	10	38	7.3	1.4	5.9	0.86	5.0	0.86	2.6	0.38	2.7	14	3.5
NAJ008	89	69	18	35	35	162	692	171	18	42	12	453	0.37	3.9	1.9	5860	40	81	9	34	6.4	1.3	5.6	0.83	4.8	0.84	2.6	0.39	2.6	13	3.9
NAJ009	90	65	15	53	53	173	663	174	17	422	13	402	0.33	3.7	1.8	2633	36	73	8	32	5.9	1.2	5.1	0.76	4.5	0.78	2.4	0.35	2.4	12	3.6
NAJ010	72	71	75	27	<LOD	180	833	176	18	81	13	457	0.35	3.9	1.9	5168	39	80	9	34	6.4	1.2	5.7	0.85	5.0	0.83	2.6	0.41	2.6	13	3.7
NAJ011	115	79	24	24	<LOD	171	658	166	17	15	11	495	0.36	3.6	1.5	709	44	88	10	38	6.8	1.5	5.9	0.88	5.0	0.83	2.6	0.39	2.7	13	4.0
NAJ012	114	81	28	29	<LOD	177	546	143	17	25	11	504	0.36	3.3	1.5	1324	47	94	11	40	7.3	1.5	6.1	0.90	4.9	0.83	2.7	0.38	2.6	13	4.2
NAJ013	85	63	14	28	<LOD	169	856	185	18	19	13	451	0.35	4.0	1.8	2731	40	82	10	35	6.4	1.3	5.6	0.80	4.5	0.79	2.5	0.36	2.5	13	3.9
NAJ014	141	81	22	59	59	154	442	178	17	38	7	517	0.38	3.7	1.4	889	53	105	12	44	8.0	1.7	6.5	0.90	5.1	0.88	2.7	0.41	2.7	14	3.9
NAJ015	81	59	17	25	<LOD	169	683	192	18	69	13	416	0.36	4.1	2.0	5245	40	81	10	35	6.8	1.4	5.7	0.88	4.8	0.83	2.6	0.37	2.5	13	3.7
NAJ016	81	270	39	30	<LOD	163	727	181	18	53	12	419	0.37	3.9	1.8	911	38	75	9	32	6.2	1.3	5.8	0.91	5.1	0.87	2.6	0.41	2.6	12	3.6
NAJ017	64	52	17	28	<LOD	157	634	201	17	106	11	384	0.33	4.4	1.8	1133	39	79	9	34	6.2	1.2	5.4	0.79	4.3	0.78	2.4	0.34	2.4	12	3.5
NAJ018	71	59	21	26	<LOD	131	902	177	17	122	10	404	0.31	3.8	1.9	7373	36	72	8	30	5.6	1.1	4.8	0.75	4.1	0.75	2.1	0.34	2.3	12	3.4
NAJ019	73	64	18	36	36	150	951	171	17	90	11	375	0.20	3.7	1.8	4212	36	71	8	31	5.6	1.1	4.7	0.73	4.2	0.73	2.2	0.35	2.1	12	5.1
NAJ020	85	64	16	19	<LOD	171	767	177	17	56	14	429	0.34	4.0	1.8	10093	39	79	9	34	6.5	1.2	5.6	0.86	4.9	0.85	2.5	0.38	2.5	12	3.9
NAJ021	67	54	18	35	35	185	895	167	17	93	14	427	0.34	3.7	1.9	1557	39	78	9	34	6.2	1.2	5.3	0.84	4.4	0.77	2.3	0.35	2.3	12	3.7
NAJ022	70	64	13	19	<LOD	176	792	164	17	47	13	423	0.33	3.7	1.8	2817	40	81	9	35	6.4	1.3	5.5	0.86	4.5	0.77	2.4	0.36	2.5	12	4.0
NAJ023	83	68	15	35	35	180	1,108	163	18	226	13	462	0.33	3.7	1.9	4216	40	79	9	33	5.9	1.2	5.3	0.81	4.5	0.8	2.4	0.34	2.5	12	4.2
NAJ024	99	82	17	49	49	186	239	214	17	95	16	458	0.42	4.5	1.6	2110	47	83	10	39	7.1	1.5	6.3	0.95	5.3	0.93	2.7	0.42	2.8	12	3.2
NAJ025	58	38	15	35	35	161	315	306	17	17	9	429	0.48	6.0	1.9	2890	47	95	11	42	8.0	1.3	6.9	1.06	5.9	1.00	3.1	0.52	3.3	16	5.0
NAJ026	65	34	15	32	<LOD	80	448	210	13	6	3	370	0.35	4.4	1.2	956	35	70	8	30	5.9	1.1	5.0	0.79	4.6	0.82	2.4	0.36	2.5	11	3.7
NAJ027	84	61	15	23	<LOD	194	707	174	17	31	17	440	0.31	3.9	1.9	11393	41	84	10	36	6.4	1.3	5.5	0.82	4.3	0.78	2.3	0.33	2.4	13	3.6
NAJ028	87	64	16	98	98	105	933	157	15	69	9	381	0.31	3.4	1.6	17460	35	70	8	30	5.6	1.1	4.7	0.73	4.2	0.76	2.2	0.34	2.2	11	3.3
NAJ029	77	46	19	67	67	146	471	263	17	25	9	449	0.47	5.4	1.7	8590	45	92	11	41	7.9	1.4	6.6	0.99	5.8	0.99	3.0	0.48	3.1	15	5.0
NAJ030	92	65	31	91	91	93	982	151	16	28	5	348	0.30	3.4	1.6	16025	34	69	8	30	5.5	1.1	4.5	0.69	4.0	0.71	2.1	0.30	2.2	11	3.7
NAJ031	83	69	27	33	33	192	742	173	17	191	15	454	0.32	3.7	1.9	2608	39	79	9	34	6.3	1.3	5.5	0.84	4.7	0.83	2.4	0.36	2.5	13	3.5
NAJ032	77	64	16	45	45	89	948	197	16	96	10	531	0.34	4.1	1.6	21359	37	74	8	32	6.0	1.2	5.3	0.80	4.5	0.81	2.4	0.36	2.5	12	3.4
NAJ033	84	61	24	45	45	169	455	178	17	62	10	485	0.39	3.9	1.6	3308	43	88	10	37	6.9	1.4	6.2	0.91	5.2	0.89	2.6	0.42	2.7	14	4.4
NAJ034	85	69	23	41	41	202	661	193	18	158	17	458	0.34	4.1	2.0	1672	43	87	10	38	7.5	1.5	6.2	0.91	4.9	0.88	2.6	0.39	2.7	14	4.1
NAJ035	52	35	16	47	47	91	416	281	11	19	4	350	0.30	5.2	1.1	3588	31	62	7	28	5.2	1.1	4.5	0.65	3.8	0.73	2.0	0.30	2.2	9	2.8
NAJ036	109	82	25	39	39	191	672	195	17	47	14	518	0.35	3.9	1.5	2808	48	93	11	40	7.5	1.7	6.0	0.86	5.0	0.84	2.5	0.39	2.6	14	4.2
NAJ037	110	79	21	43	43	191	471	201	17	88	13	535	0.39	4.1	1.5	2495	49	97	11	41	7.4	1.6	6.5	0.93	5.4	0.92	2.7	0.42	2.7	14	4.3
NAJ038	90	75	14	95	95	177	808	193	17	217	14	453	0.34	4.1	1.7	4206	42	82	9	34	6.4	1.3	5.3	0.77	4.4	0.79	2.4	0.36	2.4	14	4.1
NAJ039	130	89	22	28	<LOD	213	456	188	18	13	17	538	0.43	3.9	1.5	788	51	100	12	43	8.1	1.7	6.7	0.94	5.4	0.89	2.7	0.42	2.8	15	4.4
NAJ040	86	65	24	26	<LOD	206	652	190	20	184	16	454	0.37	4.0	3.2	1507	41	82	9	36	7.0	1.4	5.7	0.90	5.0	0.85	2.5	0.38	2.5	14	3.7
NAJ041	85	67	41	27	<LOD	203	1,129	191	18	78	18	466	0.36	3.9	1.8	6039	41	82	9	36	7.1	1.4	6.0	0.85	4.8	0.82	2.5	0.36	2.5	14	3.7
NAJ042	74	62	26	38	38	186	800	198	17	115	15	594	0.36	4.0	1.7	1488	43	81	9	34	6.8	1.4	5.8	0.85	4.9	0.85	2.5	0.39	2.5	13	4.3
NAJ043	74	65	18	23	<LOD	193	631	225	17	56	18	416	0.35	4.5	1.7	1743	41	84	10	37	7.1	1.4	5.9	0.89	4.9	0.82	2.5	0.36	2.5	14	3.9
NAJ044	75	65	23	29	<LOD	210	751	201	17	117	17	447	0.33	4.1	1.8	1869	38	77	9	33	6.2	1.3	5.2	0.78	4.4	0.75	2.3	0.34	2.4	13	3.9
NAJ045	80	69	11	22	<LOD	205	639	191	17	105	19	453	0.31	4.1	1.2	1785	40	78	9	32	6.1	1.3	5.1	0.77	4.2	0.73	2.2	0.32	2.3	13	3.7
NAJ046	94	64	16	29	<LOD	156	834	150	14	26	10	416	0.20	3.3	1.2	4282	37	74	8	32	5.9	1.3	4.8	0.70	3.9	0.70	2.1	0.31	2.1	12	3.3
NAJ047	120	90	25	32	<LOD	207	414	184	16	62	17	509	0.40	3.9	0.8	4784	49	96	11	41	7.7	1.6	6.5	0.93	5.2	0.87	2.7	0.43	2.7	14	4.0
NAJ048	94	79	18	48	48	213	190	274	18	10	18	495	0.47	5.2	1.6	2077	50	88	11	41	7.7	1.7	6.8	1.02	5.9	0.93	3.0	0.50	3.1	14	3.3
NAJ049	66	59	12	34	34	184	1,001	223	16	1237	16	417	0.34	4.5	0.9	6214	38	77	9	34	6.5	1.3	5.5	0.81	4.6	0.81	2.5	0.38	2.4	13	3.6
NAJ050	101	98	20	27	<LOD	212	629	195	16	21	16	533	0.40	4.1	0.8	1251	48	95	11	41	7.4	1.6	6.7	0.93	5.2	0.85	2.6	0.43	2.8	14	4.2
NAJ051	87	68	45	22	<LOD	180	754	205	16	222	14	450	0.38	4.3	0.9	3257	39	82	9	35	7.0	1.4	6.2	0.95	5.5	0.91	2.7	0.44	2.8	14	4.2
NAJ052	70	68	12	28	<LOD	178	774	230	17	44	15	428	0.35	4.7	0.8	2723	40	81	9	36	6.8	1.4	5.8	0.84	4.6	0.84	2.4	0.42	2.6	14	3.7
NAJ053	101	80	19	32	<LOD	185	280	285	16	18	13	497	0.47	5.5	0.5	2554	50	85	11	40	7.6	1.6	6.6	1.00	5.8	0.99	3.1	0.50	3.2	14	3.2
NAJ054	71	57	15	20	<LOD	149	939	228	16	57	12	435	0.36	4.7	1.5	4447	37	76	9	33	6.3	1.2	5.5	0.82	4.6	0.81	2.3	0.40	2.5	13	3.6
NAJ055	97	66	18	35	35	124	384	184	15	128	9	322	0.31	3.8	1.3	14457	34	69	8	30	5.7	1.2	4.9	0.73	4.1	0.74	2.2	0.36	2.3	11	3.2
NAJ056	90	72	44	17	<LOD	250	866	234	19	38	20	500	0.38	4.6	1.8	8143	43	87	10	37	6.7	1.3	5.7	0.84	4.8	0.82	2.5	0.38	2.6	15	3.7

Table A.7 – *Continued*

ANID	V	Cr	Co	Cu	Zn	Rb	Sr	Zr	Nb	Sn	Cs	Ba	Lu	Hf	Ta	Pb	La	Ce	Pr	Nd	Sm	Eu	Gd	Tb	Dy	Ho	Er	Tm	Yb	Th	U
NAJ057	87	69	26	19	<LOD	193	880	220	17	31	16	444	0.34	4.5	1.7	12000	41	84	10	36	6.8	1.3	5.5	0.83	4.5	0.79	2.5	0.37	2.4	14	3.6
NAJ058	104	67	26	41	41	146	522	221	16	37	13	479	0.36	4.2	1.3	14984	42	84	10	35	6.7	1.4	5.7	0.83	4.8	0.84	2.5	0.41	2.5	13	3.9
NAJ059	93	56	15	8	<LOD	70	365	195	16	55	4	342	0.35	3.9	1.5	1289	38	76	9	32	6.1	1.2	5.1	0.78	4.5	0.79	2.4	0.38	2.4	13	3.3
NAJ063	79	54	22	23	<LOD	144	870	210	17	33	11	452	0.36	4.2	1.7	6319	37	74	8	30	5.8	1.2	5.1	0.82	4.5	0.80	2.4	0.38	2.5	13	3.8
NAJ064	78	64	25	25	<LOD	200	629	184	17	15	18	441	0.35	3.7	1.7	1441	38	77	9	33	5.9	1.2	5.2	0.81	4.4	0.76	2.4	0.36	2.4	13	3.9
NAJ065	69	49	36	10	<LOD	179	629	259	17	165	14	381	0.32	4.9	1.8	2712	39	77	9	34	6.1	1.1	5.2	0.73	3.9	0.72	2.1	0.34	2.2	14	3.2
NAJ066	69	54	27	22	<LOD	169	672	204	13	61	15	417	0.33	4.0	1.5	7869	35	70	8	30	5.5	1.1	4.8	0.74	4.2	0.74	2.3	0.34	2.3	12	3.4
NAJ067	97	71	20	21	<LOD	179	746	198	18	82	18	493	0.35	4.1	1.8	8341	40	79	9	34	6.4	1.3	5.6	0.85	4.8	0.81	2.5	0.37	2.4	14	3.6
NAJ068	84	64	29	28	<LOD	200	759	200	17	59	19	460	0.36	4.1	1.9	7193	41	83	10	37	6.7	1.4	5.7	0.87	4.6	0.82	2.5	0.37	2.5	14	3.7
NAJ069	85	65	24	15	<LOD	205	716	192	18	98	17	477	0.33	4.0	1.8	2446	40	80	9	35	6.3	1.3	5.4	0.83	4.6	0.78	2.4	0.37	2.4	14	3.7
NAJ070	88	69	27	17	<LOD	193	902	189	18	175	16	414	0.35	3.8	1.8	8065	38	75	9	33	6.0	1.3	5.4	0.85	4.9	0.79	2.4	0.37	2.6	13	3.7
NAJ071	74	49	20	25	<LOD	168	317	310	18	62	11	456	0.45	5.7	1.8	6871	47	96	11	43	7.6	1.3	6.8	1.09	6.1	0.96	3.1	0.49	3.1	17	5.1
NAJ073	77	49	13	34	34	111	497	244	14	62	6	291	0.33	4.5	1.3	1309	36	71	8	31	5.4	1.1	4.8	0.74	4.4	0.76	2.4	0.36	2.5	11	3.0
NAJ074	92	65	17	62	62	99	863	183	12	177	7	375	0.20	3.7	1.4	21663	36	70	8	31	5.4	1.1	4.8	0.73	4.2	0.73	2.2	0.32	2.2	12	3.3
NAJ075	99	69	21	58	58	125	352	174	14	64	9	323	0.30	3.6	1.2	12309	34	67	8	29	5.3	1.1	4.7	0.70	4.1	0.71	2.2	0.33	2.1	11	3.0
NAJ076	77	66	18	58	58	179	468	169	16	22	14	492	0.38	3.5	1.5	4466	45	84	10	37	6.4	1.4	6.1	0.88	5.0	0.85	2.7	0.40	2.6	13	2.8
NAJ077	81	62	20	33	33	201	741	193	17	36	18	447	0.31	3.9	1.8	4440	40	77	9	32	5.9	1.2	5.2	0.81	4.4	0.76	2.3	0.35	2.3	14	3.6
NAJ078	88	68	17	20	<LOD	196	899	203	18	63	16	457	0.34	4.0	1.7	2250	40	78	9	35	6.2	1.3	5.5	0.90	4.9	0.83	2.5	0.37	2.5	14	3.4
NAJ079	63	58	14	29	<LOD	170	1,032	209	16	67	15	387	0.31	4.2	1.7	4232	36	70	8	31	5.5	1.1	4.7	0.76	4.2	0.74	2.2	0.35	2.2	12	3.7
NAJ080	98	74	14	36	36	149	1,068	211	19	157	16	468	0.34	4.4	1.8	16458	42	83	10	37	6.7	1.3	5.6	0.87	5.0	0.81	2.6	0.37	2.5	15	3.5
NAJ081	96	72	13	102	102	157	642	207	17	358	17	426	0.34	4.1	1.8	17018	39	78	9	34	6.0	1.1	5.2	0.79	4.6	0.77	2.4	0.36	2.3	13	3.6
NAJ082	81	68	11	14	<LOD	189	835	174	16	49	17	417	0.30	3.7	1.5	3384	37	73	8	32	5.7	1.1	5.1	0.77	4.4	0.76	2.3	0.33	2.3	12	3.2
NAJ083	123	87	22	18	<LOD	194	452	171	16	13	15	498	0.38	3.5	1.3	5620	45	89	10	39	7.0	1.5	5.9	0.91	4.9	0.82	2.6	0.38	2.6	14	3.9
NAJ085	78	60	26	45	45	168	704	207	16	42	16	415	0.31	3.9	1.8	13841	38	76	9	34	6.5	1.1	5.3	0.77	4.2	0.74	2.2	0.34	2.3	13	3.2
NAJ087	98	74	18	44	44	166	814	240	17	43	12	365	0.36	4.6	1.6	1747	39	79	9	33	6.1	1.3	5.3	0.82	4.8	0.87	2.6	0.37	2.6	13	3.3
NAJ088	79	65	16	29	<LOD	139	429	232	16	32	8	409	0.39	4.3	1.3	4804	42	79	10	36	6.7	1.3	5.8	0.87	5.1	0.85	2.6	0.41	2.6	12	3.4
NAJ089	70	53	16	31	<LOD	110	384	215	14	29	5	365	0.33	4.1	1.2	4243	38	72	9	33	6.0	1.2	5.2	0.80	4.5	0.80	2.4	0.34	2.4	11	3.1
NAJ090	72	53	14	20	<LOD	116	570	211	14	68	7	369	0.34	4.0	1.3	8771	39	73	9	34	6.3	1.2	5.4	0.81	4.6	0.80	2.6	0.37	2.5	11	3.0
NAJ091	81	65	15	31	<LOD	166	344	245	18	53	11	466	0.37	4.6	1.5	7528	42	80	10	36	6.8	1.3	5.9	0.85	5.1	0.90	2.8	0.41	2.8	13	3.2
NAJ092	76	61	18	17	<LOD	148	408	199	16	23	9	429	0.34	3.8	1.3	3961	42	77	9	36	6.6	1.3	5.7	0.88	4.8	0.84	2.6	0.39	2.5	12	3.1
NAJ093	88	63	30	14	<LOD	135	348	266	16	16	9	575	0.41	4.9	1.3	8561	43	85	10	38	6.8	1.5	5.9	0.89	5.2	0.90	2.8	0.41	2.7	13	3.6
NAJ094	27	35	18	5	<LOD	589	117	185	29	97	66	275	0.38	4.2	16.8	<LOD	20	40	5	21	5.1	0.8	4.9	0.96	5.6	0.95	2.9	0.43	2.9	7	4.2
NAJ095	23	17	19	4	<LOD	531	122	160	27	96	50	236	0.47	3.7	7.0	<LOD	19	37	5	19	4.7	0.7	4.9	0.98	6.4	1.12	3.3	0.53	3.4	6	5.3
NAJ097	24	25	18	10	<LOD	508	142	172	26	87	48	277	0.37	4.1	7.6	<LOD	17	38	4	17	3.8	0.6	4.1	0.82	5.3	0.91	2.7	0.44	2.8	6	4.6
NAJ098	29	29	20	7	<LOD	456	113	233	24	75	42	295	0.38	5.0	5.2	<LOD	24	51	6	23	4.6	0.8	4.7	0.89	5.5	0.94	2.9	0.44	2.9	8	4.8
NAJ099	26	21	19	10	<LOD	568	94	200	24	70	46	267	0.40	4.9	6.2	<LOD	20	43	5	20	4.3	0.7	4.7	0.95	5.8	0.98	2.9	0.46	3.0	7	6.1
NAJ100	22	16	34	6	<LOD	518	145	127	27	110	57	211	0.34	3.4	8.4	<LOD	17	31	5	19	4.6	0.8	4.7	0.93	5.6	0.95	2.7	0.40	2.6	5	3.6
NAJ101	21	23	19	8	<LOD	526	148	125	25	105	66	231	0.33	3.4	7.4	<LOD	18	31	4	18	4.2	0.7	4.5	0.87	5.2	0.89	2.6	0.39	2.6	5	3.7

CVM Table

Table A.8: Compositional Variation Matrix of the 340 analyzed Ic-s. Each column i (i = 1,$\cdots$S) shows the variances after a log-ratio transformation using the component x_i as divisos. vt = total variation. τ_i = total sum of the variances in column i. vt/τ_i = percentage of variance in the log-ratio covariance matrix using the component x_i, as divisor due to the total variation. $r_{v.\tau}$ = correlation between the values $\tau_{ij}(i \neq j)$ and the corresponding values τ_i (j = 1,$\cdots$,i-1, i+1,$\cdots$,S).$\Sigma_{\tau_{.i}}$ sum of the $\tau_{.i}$ values.

	Ba	CaO	Ce	Cr	Cs	Dy	Er	Eu	Fe2O3	Gd	Hf	Ho	La	Lu	MnO	Nb	Nd	Pr	SiO2	Sm	Sr	Tb	Th	TiO2	Tm	U	V	Yb	Zr
Ba	0	0.750	0.032	0.156	0.1959	0.050	0.059	0.021	0.079	0.026	0.1976	0.056	0.027	0.062	0.320	0.110	0.034	0.035	0.146	0.021	0.382	0.045	0.145	0.076	0.052	0.130	0.070	0.061	0.127
CaO	0.750	0	0.712	0.793	1.260	0.788	0.779	0.735	0.761	0.795	0.899	0.769	0.710	0.821	0.647	0.864	0.740	0.719	0.801	0.749	0.1994	0.789	0.698	0.676	0.825	0.794	0.706	0.785	0.802
Ce	0.032	0.712	0	0.089	0.330	0.066	0.066	0.018	0.058	0.034	0.1916	0.066	0.002	0.066	0.347	0.118	0.010	0.012	0.132	0.017	0.372	0.058	0.087	0.024	0.069	0.136	0.033	0.066	0.083
Cr	0.156	0.793	0.089	0	0.475	0.175	0.160	0.132	0.116	0.157	0.1906	0.173	0.097	0.149	0.470	0.199	0.101	0.104	0.195	0.128	0.430	0.170	0.105	0.080	0.176	0.1903	0.097	0.156	0.130
Cs	0.1959	1.260	0.330	0.475	0	0.194	0.196	0.1971	0.1979	0.1903	0.531	0.195	0.320	0.1909	0.559	0.1913	0.321	0.334	0.1989	0.1945	0.785	0.193	0.467	0.437	0.190	0.1953	0.421	0.199	0.347
Dy	0.050	0.788	0.066	0.175	0.194	0	0.004	0.039	0.083	0.019	0.196	0.006	0.060	0.010	0.1989	0.039	0.049	0.053	0.065	0.025	0.449	0.003	0.134	0.119	0.006	0.046	0.138	0.005	0.086
Er	0.059	0.779	0.066	0.160	0.196	0.004	0	0.046	0.083	0.027	0.164	0.004	0.061	0.008	0.1997	0.039	0.052	0.055	0.057	0.032	0.445	0.008	0.125	0.112	0.008	0.042	0.141	0.002	0.071
Eu	0.021	0.735	0.018	0.132	0.1971	0.039	0.046	0	0.062	0.015	0.1954	0.042	0.014	0.052	0.307	0.104	0.020	0.024	0.129	0.009	0.385	0.032	0.129	0.060	0.045	0.117	0.055	0.046	0.105
Fe2O3	0.079	0.761	0.058	0.116	0.1979	0.083	0.083	0.062	0	0.052	0.1984	0.080	0.057	0.075	0.1981	0.133	0.076	0.082	0.168	0.056	0.427	0.085	0.165	0.105	0.075	0.159	0.081	0.080	0.118
Gd	0.026	0.795	0.034	0.157	0.1903	0.019	0.027	0.015	0.052	0	0.1950	0.022	0.030	0.030	0.303	0.076	0.030	0.036	0.120	0.008	0.437	0.017	0.156	0.095	0.018	0.104	0.087	0.028	0.106
Hf	0.1976	0.899	0.1916	0.1906	0.531	0.196	0.164	0.1954	0.1984	0.1950	0	0.1904	0.1920	0.140	0.525	0.124	0.174	0.171	0.103	0.1915	0.664	0.199	0.089	0.199	0.196	0.139	0.323	0.166	0.120
Ho	0.056	0.769	0.066	0.173	0.195	0.006	0.004	0.042	0.080	0.022	0.1904	0	0.062	0.018	0.1993	0.054	0.057	0.062	0.074	0.031	0.433	0.010	0.154	0.118	0.011	0.057	0.138	0.004	0.082
La	0.027	0.710	0.002	0.097	0.320	0.060	0.061	0.014	0.057	0.030	0.1920	0.062	0	0.062	0.333	0.112	0.010	0.011	0.128	0.013	0.372	0.052	0.088	0.027	0.063	0.129	0.034	0.062	0.084
Lu	0.062	0.821	0.066	0.149	0.1909	0.010	0.008	0.052	0.075	0.030	0.140	0.018	0.062	0	0.310	0.031	0.049	0.053	0.056	0.032	0.488	0.013	0.110	0.111	0.007	0.045	0.141	0.009	0.066
MnO	0.320	0.647	0.347	0.470	0.559	0.1989	0.1997	0.307	0.1981	0.303	0.525	0.1993	0.333	0.310	0	0.347	0.348	0.346	0.384	0.316	0.529	0.1998	0.440	0.399	0.304	0.343	0.404	0.1998	0.391
Nb	0.110	0.864	0.118	0.199	0.1913	0.039	0.039	0.104	0.133	0.076	0.124	0.054	0.112	0.031	0.347	0	0.086	0.086	0.054	0.075	0.522	0.043	0.122	0.162	0.039	0.041	0.197	0.042	0.121
Nd	0.034	0.740	0.010	0.101	0.321	0.049	0.052	0.020	0.076	0.030	0.174	0.057	0.010	0.049	0.348	0.086	0	0.002	0.114	0.012	0.406	0.041	0.078	0.040	0.052	0.112	0.053	0.054	0.092
Pr	0.035	0.719	0.012	0.104	0.334	0.053	0.055	0.024	0.082	0.036	0.171	0.062	0.011	0.053	0.346	0.086	0.002	0	0.113	0.015	0.392	0.045	0.071	0.039	0.057	0.110	0.053	0.058	0.096
SiO2	0.146	0.801	0.132	0.195	0.1989	0.065	0.057	0.129	0.168	0.120	0.103	0.074	0.128	0.056	0.384	0.054	0.114	0.113	0	0.110	0.496	0.070	0.095	0.142	0.077	0.035	0.1916	0.056	0.075
Sm	0.021	0.749	0.017	0.128	0.1945	0.025	0.032	0.009	0.056	0.008	0.1915	0.031	0.013	0.032	0.316	0.075	0.012	0.015	0.110	0	0.403	0.020	0.109	0.064	0.027	0.098	0.063	0.034	0.094
Sr	0.382	0.1994	0.372	0.430	0.785	0.449	0.445	0.385	0.427	0.437	0.664	0.433	0.372	0.488	0.529	0.522	0.406	0.392	0.496	0.403	0	0.442	0.415	0.377	0.486	0.457	0.348	0.450	0.502
Tb	0.045	0.789	0.058	0.170	0.193	0.003	0.008	0.032	0.085	0.017	0.199	0.010	0.052	0.013	0.1998	0.043	0.041	0.045	0.070	0.020	0.442	0	0.125	0.113	0.008	0.050	0.127	0.010	0.092
Th	0.145	0.698	0.087	0.105	0.467	0.134	0.125	0.129	0.165	0.156	0.089	0.154	0.088	0.110	0.440	0.122	0.078	0.071	0.095	0.109	0.415	0.125	0	0.072	0.145	0.109	0.135	0.128	0.095
TiO2	0.076	0.676	0.024	0.080	0.437	0.119	0.112	0.060	0.105	0.095	0.199	0.118	0.027	0.111	0.399	0.162	0.040	0.039	0.142	0.064	0.377	0.113	0.072	0	0.126	0.168	0.046	0.110	0.078
Tm	0.052	0.825	0.069	0.176	0.190	0.006	0.008	0.045	0.075	0.018	0.196	0.011	0.063	0.007	0.304	0.039	0.052	0.057	0.077	0.027	0.486	0.008	0.145	0.126	0	0.058	0.143	0.009	0.089
U	0.130	0.794	0.136	0.1903	0.1953	0.046	0.042	0.117	0.159	0.104	0.139	0.057	0.129	0.045	0.343	0.041	0.112	0.110	0.035	0.098	0.457	0.050	0.109	0.168	0.058	0	0.1914	0.043	0.111
V	0.070	0.706	0.033	0.097	0.421	0.138	0.141	0.055	0.081	0.087	0.323	0.138	0.034	0.141	0.404	0.197	0.053	0.053	0.1916	0.063	0.348	0.127	0.135	0.046	0.143	0.1914	0	0.141	0.167
Yb	0.061	0.785	0.066	0.156	0.199	0.005	0.002	0.046	0.080	0.028	0.166	0.004	0.062	0.009	0.1998	0.042	0.054	0.058	0.056	0.034	0.450	0.010	0.128	0.110	0.009	0.043	0.141	0	0.065
Zr	0.127	0.802	0.083	0.130	0.347	0.086	0.071	0.105	0.118	0.106	0.120	0.082	0.084	0.066	0.391	0.121	0.092	0.096	0.075	0.094	0.502	0.092	0.095	0.078	0.089	0.111	0.167	0.065	0
t.i	3.606	21.461	3.320	5.603	9.946	3.176	3.142	3.266	4.162	3.281	7.217	3.266	3.241	3.224	10.430	4.145	3.213	3.232	4.494	3.021	12.588	3.147	4.791	4.175	3.344	4.305	4.774	3.167	4.397
vt/t.i	0.723	0.121	0.785	0.465	0.1962	0.820	0.829	0.798	0.626	0.794	0.361	0.798	0.804	0.808	0.1950	0.629	0.811	0.806	0.580	0.863	0.1907	0.828	0.544	0.624	0.779	0.605	0.546	0.823	0.593
r v.t	0.984	−0.156	0.977	0.949	0.954	0.976	0.979	0.987	0.981	0.983	0.928	0.977	0.980	0.979	0.870	0.959	0.990	0.988	0.953	0.993	0.068	0.982	0.929	0.941	0.975	0.955	0.925	0.979	0.979
vt	2.606	0	0	0	0	0	0	0	0	0	0	0	0	0	0	0	0	0	0	0	0	0	0	0	0	0	0	0	0

RSD values obtained by ED-XRF

Table A.9: RSD (%) values of net counts for every 50 observations from ED-XRF results

N	ANID	SITE	Al	Si	K	Ca	Ti	Cr	V	Mn	Fe	Co	Zn	Ga	Sr	Zr	Pb	Y	Rb
1	ELS017	ELS	5	4	6	5	6	21	41	11	4	12	9	24	2	11	158	20	5
2	ELS018	ELS	7	7	7	8	9	23	30	18	6	13	37	32	6	14	28	33	8
3	ELS019	ELS	7	7	7	19	8	22	49	19	9	15	15	33	10	18	58	45	9
4	ELS020	ELS	4	3	9	7	7	32	67	25	7	16	23	24	3	16	113	26	4
5	ELS021	ELS	15	14	16	13	14	27	36	25	13	18	16	29	12	16	54	40	20
6	ELS022	ELS	11	10	12	22	11	26	73	80	9	19	16	25	6	34	24	47	10
7	ELS023	ELS	7	7	12	8	10	34	45	28	8	15	8	38	6	20	102	26	10
8	ELS025	ELS	7	6	9	15	9	27	37	50	14	19	30	23	5	18	29	30	9
9	ELS034	ELS	5	5	5	7	8	24	49	29	3	15	25	32	4	15	103	28	5
10	ELS036	ELS	5	6	6	8	11	24	55	35	4	17	9	21	2	16	67	36	3
11	ELS037	ELS	5	4	7	6	10	26	64	50	5	17	6	36	3	16	194	27	4
12	ELS038	ELS	8	8	10	8	12	29	50	51	7	14	9	39	7	20	30	47	11
13	ELS039	ELS	4	3	6	8	7	24	54	51	3	13	71	37	3	15	107	27	3
14	ELS040	ELS	7	6	8	13	9	21	50	51	6	16	5	26	4	14	93	36	7
15	ELS041	ELS	6	6	8	14	9	24	58	75	6	20	8	38	3	20	211	44	8
16	ELS042	ELS	4	4	7	10	9	41	53	35	3	14	7	23	5	20	122	49	4
17	ELS046	ELS	5	6	6	5	8	19	39	21	4	11	14	24	7	17	48	58	7
18	ELS048	ELS	4	4	7	10	5	25	39	44	4	12	6	23	3	11	21	31	3
19	ELS049	ELS	20	16	17	42	16	37	51	40	16	15	11	19	14	16	10	64	21
20	ELS051	ELS	7	4	10	17	10	30	37	26	9	20	29	44	9	17	71	22	16
21	DUR019	DUR	23	22	22	31	25	42	52	45	22	37	24	43	27	28	63	36	24
22	DUR020	DUR	8	4	7	22	13	27	29	33	9	16	20	28	6	18	161	57	10
23	DUR021	DUR	9	6	10	20	12	26	27	28	9	19	16	23	5	20	33	23	10
24	DUR022	DUR	15	14	14	19	17	29	38	37	15	27	35	27	16	23	97	25	17
25	DUR023	DUR	5	3	4	10	7	30	33	31	8	19	14	20	5	20	79	16	3
26	ORD006	ORD	4	3	10	8	12	49	46	38	7	17	17	37	4	17	77	31	21
27	ORD020	ORD	9	4	7	12	10	45	46	38	10	16	23	64	7	15	134	50	14
28	ORD033	ORD	3	2	5	4	3	26	44	11	9	10	6	27	2	11	4	22	6
29	ORD037	ORD	5	4	11	8	12	34	49	73	9	27	9	33	4	22	60	21	15
30	ORD046	ORD	7	8	8	10	11	39	38	19	11	20	7	31	10	23	91	29	13
31	ORD061	ORD	4	3	6	7	11	41	48	38	6	24	5	31	3	25	47	35	7
32	ORD064	ORD	6	7	6	13	11	24	51	14	5	12	14	66	10	19	91	46	18
33	ORD065	ORD	3	2	3	3	3	29	32	10	2	8	5	24	1	5	6	29	3
34	ORD070	ORD	4	4	3	12	7	27	45	22	12	17	11	27	4	10	190	17	8
35	ORD072	ORD	7	5	4	13	13	40	43	32	7	25	10	53	6	20	82	32	7
36	LOG001	LOG	3	3	4	8	3	14	15	9	2	10	5	13	6	6	70	12	3
37	LOG002	LOG	21	21	24	25	22	23	31	26	21	23	21	26	23	22	18	28	23
38	LOG003	LOG	2	3	3	7	2	13	20	5	2	10	3	16	3	5	156	15	2
39	LOG005	LOG	9	9	11	13	10	16	19	16	10	12	11	16	13	10	79	13	8
40	LOG006	LOG	16	15	18	23	18	24	23	51	15	16	14	26	11	22	34	17	14
41	LOG007	LOG	6	7	6	8	6	16	21	7	5	10	6	18	6	8	62	19	5
42	LOG019	LOG	10	10	12	17	13	29	19	61	11	11	14	19	11	18	129	16	10
43	LOG033	LOG033	5	4	5	12	7	21	45	10	5	18	5	41	6	15	96	34	6
44	LOG038	LOG038	8	6	14	14	8	36	55	33	9	20	12	23	6	24	10	24	23
45	LOG072	LOG	25	24	27	26	26	31	29	27	24	23	28	60	20	19	76	22	23
46	LOG074	LOG	16	15	17	16	17	21	21	17	16	16	16	51	13	12	32	18	13
47	LOG075	LOG	2	1	2	2	2	13	16	5	1	10	5	26	4	9	39	25	4

SEM-EDS Concentrations

Table A.10: SEM-EDS Semiquantitative concentrations of the glazes from a subsample of ceramics (n= 64) (concentrations expressed in mass %). Alk: Na_2O+ K_2O. Pb/Si*:PbO/ SiO_2

Spectrum	Color	K_2O	CaO	FeO	Na_2O	MgO	Al_2O_3	SiO_2	PbO	TiO_2	SnO_2	CuO	MnO	CoO	NiO	Sb_2O_3	ZnO	BaO	P_2O_5	Pb/Si*	Alk.
NAJ002	White	3.60	4.08	0.71	1.01	0.58	6.87	42.53	26.70	0.00	13.35	0.00	0.00	0.00	0.00	0.00	0.00	0.00	0.57	0.6	4.61
NAJ008	White	1.88	2.02	0.33	1.23	0.20	5.11	38.08	39.38	0.13	11.10	0.42	0.00	0.00	0.00	0.00	0.00	0.00	0.04	1.0	3.11
NAJ014	White	1.66	2.03	0.85	1.95	0.60	4.16	37.35	45.99	0.00	5.26	0.00	0.00	0.00	0.00	0.00	0.00	0.00	0.14	1.2	3.61
NAJ015	White	3.13	3.08	0.45	1.40	0.34	6.53	42.26	32.44	0.196	10.11	0.00	0.00	0.00	0.00	0.00	0.00	0.00	0.00	0.8	4.53
NAJ016	White	1.80	1.11	0.20	1.30	0.19	4.20	40.51	39.40	0.17	11.04	0.00	0.00	0.00	0.00	0.00	0.00	0.00	0.00	1.0	3.10
NAJ028	White	4.80	2.00	0.34	0.86	0.31	3.77	43.82	31.61	0.00	12.49	0.00	0.00	0.00	0.00	0.00	0.00	0.00	0.00	0.7	5.66
NAJ029	White	1.82	1.28	0.20	1.23	0.46	4.05	39.08	36.48	0.11	15.04	0.00	0.00	0.00	0.00	0.00	0.00	0.00	0.19	0.9	3.05
NAJ033	White	1.51	1.00	0.20	1.38	0.19	4.83	36.40	44.96	0.08	9.00	0.41	0.00	0.00	0.00	0.00	0.00	0.00	0.00	1.2	2.89
NAJ041	White	3.73	3.65	0.62	1.47	0.51	6.04	44.07	26.48	0.10	13.00	0.20	0.00	0.00	0.00	0.00	0.00	0.00	0.05	0.6	5.21
NAJ044	White	3.17	4.48	0.51	0.19	0.45	6.63	44.48	27.17	0.14	11.34	0.35	0.02	0.00	0.00	0.00	0.00	0.00	0.09	0.6	4.34
NAJ053	White	1.07	1.88	0.47	1.62	0.19	4.56	38.69	46.88	0.00	4.58	0.00	0.00	0.00	0.00	0.00	0.00	0.00	0.00	1.2	2.69
NAJ064	White	1.61	2.73	0.53	1.16	0.43	4.95	37.17	28.87	0.09	22.06	0.30	0.00	0.00	0.00	0.00	0.00	0.00	0.09	0.8	2.78
NAJ066	White	1.81	3.34	0.56	1.28	0.20	5.57	38.97	35.88	0.16	11.80	0.32	0.04	0.00	0.00	0.00	0.00	0.00	0.00	0.9	3.09
NAJ068	White	3.32	1.86	0.37	0.69	0.20	5.78	42.28	34.62	0.82	9.20	0.69	0.00	0.00	0.00	0.00	0.00	0.00	0.14	0.8	4.01
NAJ076b	Blue	3.52	2.47	0.90	0.73	0.96	3.49	63.32	20.54	0.00	3.41	0.00	0.19	0.00	0.13	0.00	0.00	0.00	0.31	0.3	4.25
NAJ076w	White	3.86	1.95	0.41	0.92	0.19	4.13	51.59	29.97	0.07	6.89	0.00	0.00	0.00	0.00	0.00	0.00	0.00	0.00	0.6	4.78
NAJ076y	Yellow	2.94	2.84	5.87	0.91	0.81	2.69	34.56	35.07	0.00	3.01	0.00	0.70	0.00	0.00	10.61	0.00	0.00	0.00	1.0	3.84
NAJ077b	Blue	2.20	1.51	0.43	1.11	0.39	4.10	37.41	36.22	0.15	16.45	0.00	0.00	0.03	0.00	0.00	0.00	0.00	0.00	1.0	3.31
NAJ077w	White	2.42	1.55	0.37	1.15	0.30	4.18	38.77	34.96	0.00	16.29	0.00	0.00	0.00	0.00	0.00	0.00	0.00	0.00	0.9	3.57
NAJ085b	Blue	2.52	2.32	0.56	1.13	0.32	4.63	38.32	37.81	0.07	12.14	0.00	0.00	0.17	0.00	0.00	0.00	0.00	0.00	1.0	3.66
NAJ085g	Greenish	2.28	3.19	0.63	0.90	0.45	5.29	38.18	43.44	0.12	4.64	0.88	0.00	0.00	0.00	0.00	0.00	0.00	0.00	1.1	3.18
NAJ087g	Green	1.27	5.74	1.47	1.21	0.68	6.53	36.78	35.30	0.19	7.56	3.23	0.00	0.00	0.00	0.00	0.00	0.00	0.00	1.0	2.48
NAJ087w	White	1.48	3.83	0.94	1.23	0.51	4.93	40.74	30.88	0.00	14.27	1.19	0.00	0.00	0.00	0.00	0.00	0.00	0.00	0.8	2.71
NAJ092g	Gold	5.08	5.36	0.99	0.97	0.19	5.00	52.04	24.74	0.11	4.52	0.00	0.00	0.00	0.00	0.00	0.00	0.00	0.00	0.5	6.05
NAJ092w	White	4.71	4.69	0.93	0.55	0.88	3.68	43.97	36.45	0.07	4.07	0.00	0.00	0.00	0.00	0.00	0.00	0.00	0.00	0.8	5.25
NAJ093g	Gold	4.55	3.50	0.50	1.01	0.56	3.95	51.21	29.12	0.00	5.08	0.45	0.00	0.00	0.00	0.00	0.00	0.00	0.06	0.6	5.56
NAJ093w	White	4.45	4.37	0.73	1.04	0.71	4.32	50.30	28.62	0.00	5.46	0.00	0.00	0.00	0.00	0.00	0.00	0.00	0.00	0.6	5.49
ORD086	White	3.02	1.90	0.20	1.10	0.20	4.09	42.18	36.52	0.00	10.68	0.00	0.00	0.00	0.00	0.00	0.00	0.00	0.00	0.9	4.12
ORD085	White	1.61	2.08	0.33	1.36	0.32	4.14	43.45	40.19	0.11	6.42	0.00	0.00	0.00	0.00	0.00	0.00	0.00	0.00	0.9	2.97
ORD080	Honey	0.33	0.15	2.29	0.20	0.37	6.22	30.65	58.63	0.16	0.00	0.95	0.00	0.00	0.00	0.00	0.00	0.00	0.00	1.9	0.59
ORD070g	Green	1.65	3.04	1.22	1.35	0.40	5.28	47.32	31.98	0.13	6.52	1.10	0.00	0.00	0.00	0.00	0.00	0.00	0.00	0.7	3.00
ORD070b	Black	1.24	2.89	1.47	1.12	0.35	3.81	46.99	33.84	0.71	4.39	0.57	2.62	0.00	0.00	0.00	0.00	0.00	0.00	0.7	2.36
ORD061w	White	2.45	4.68	1.28	1.44	0.42	6.07	45.51	32.00	0.16	3.83	2.00	0.00	0.00	0.00	0.00	0.17	0.00	0.00	0.7	3.89
ORD061g	Green	2.82	4.35	0.19	1.70	0.32	6.29	46.89	30.19	0.32	4.12	1.80	0.00	0.00	0.00	0.00	0.00	0.00	0.00	0.6	4.52

Continued

Spectrum	Color	K_2O	CaO	FeO	Na_2O	MgO	Al_2O_3	SiO_2	PbO	TiO_2	SnO_2	CuO	MnO	CoO	NiO	Sb_2O_3	ZnO	BaO	P_2O_5	Pb/Si*	Alk.
ORD047g	Greenish	0.59	1.90	1.68	0.55	0.31	7.69	38.24	46.58	0.47	0.00	0.00	0.00	0.00	0.00	0.00	0.52	1.47	0.00	1.2	1.14
ORD046	White	1.27	1.76	0.38	0.71	0.10	5.82	43.26	39.82	0.00	6.87	0.00	0.00	0.00	0.00	0.00	0.00	0.00	0.00	0.9	1.97
ORD042	Honey	0.60	0.00	1.73	0.31	0.51	7.78	28.41	58.94	0.42	0.00	0.76	0.00	0.00	0.00	0.00	0.55	0.00	0.00	2.1	0.91
ORD020	White	1.51	2.13	0.41	0.72	0.07	3.99	42.31	41.31	0.20	7.28	0.00	0.00	0.00	0.00	0.00	0.00	0.00	0.00	1.0	2.23
ORD011b	Honey	0.99	0.58	2.53	2.18	0.32	7.19	39.70	46.19	0.31	0.00	0.00	0.00	0.00	0.00	0.00	0.00	0.00	0.00	1.2	3.17
ORD006g	White	1.46	1.34	0.60	0.90	0.15	5.53	44.66	36.99	0.11	8.26	0.00	0.00	0.00	0.00	0.00	0.00	0.00	0.00	0.8	2.37
ORD011w	Greenish	2.28	4.28	0.59	0.91	0.19	5.45	43.09	32.55	0.15	9.69	0.81	0.00	0.00	0.00	0.00	0.00	0.00	0.00	0.8	3.19
ORD006w	White	2.46	3.69	0.67	0.89	0.19	5.77	44.76	33.53	0.20	7.16	0.42	0.14	0.00	0.00	0.00	0.00	0.00	0.00	0.7	3.35
ORD006b	Black	2.88	2.73	0.96	1.07	0.20	4.94	47.81	33.85	0.31	3.88	0.41	0.87	0.00	0.00	0.00	0.00	0.00	0.00	0.7	3.95
ORD003	White	2.65	2.61	0.69	0.92	0.19	4.88	48.10	34.32	0.19	4.90	0.00	0.47	0.00	0.00	0.00	0.00	0.00	0.04	0.7	3.57
DUR026w	White	1.15	3.03	0.74	1.37	0.20	3.61	40.47	36.27	0.15	12.94	0.00	0.00	0.00	0.00	0.00	0.00	0.00	0.00	0.9	2.52
DUR026g	Green	1.42	2.52	0.61	1.49	0.20	4.48	41.71	35.63	0.00	10.43	1.48	0.00	0.00	0.00	0.00	0.00	0.00	0.00	0.9	2.91
DUR024w	White	0.66	2.17	0.69	0.30	0.32	4.61	37.52	47.29	0.00	6.44	0.00	0.00	0.00	0.00	0.00	0.00	0.00	0.00	1.3	0.96
DUR024g	Green	0.72	2.09	0.60	0.19	0.19	4.67	38.01	44.79	0.32	6.83	1.51	0.00	0.00	0.00	0.00	0.00	0.00	0.00	1.2	0.94
DUR016	White	0.98	0.66	0.97	0.09	0.37	7.20	41.66	40.36	0.15	7.05	0.52	0.00	0.00	0.00	0.00	0.00	0.00	0.00	1.0	1.07
DUR008	White	0.96	0.38	0.31	0.20	0.16	4.61	41.19	44.05	0.33	7.76	0.00	0.00	0.00	0.00	0.00	0.00	0.00	0.00	1.1	1.23
DUR006	Blue	1.32	1.89	0.20	1.02	0.13	3.77	41.85	44.76	0.00	4.38	0.57	0.00	0.05	0.00	0.00	0.00	0.01	0.00	1.1	2.34
DUR001	White	1.35	0.89	0.34	0.58	0.10	4.28	44.89	42.91	0.40	4.25	0.00	0.00	0.00	0.00	0.00	0.00	0.00	0.00	1.0	1.93
ELS048	White	0.88	0.71	0.56	0.41	0.15	5.96	37.77	53.16	0.41	0.00	0.00	0.00	0.00	0.00	0.00	0.00	0.00	0.00	1.4	1.29
ELS046	White	3.26	3.51	1.27	0.73	0.19	8.64	58.23	12.05	0.19	11.20	0.00	0.00	0.00	0.00	0.00	0.00	0.00	0.71	0.2	3.99
ELS021	Green	1.15	0.88	0.69	0.48	0.08	5.80	48.82	39.67	0.19	0.00	2.20	0.00	0.00	0.00	0.00	0.00	0.00	0.00	0.8	1.63
ELS008	Black	1.89	1.73	1.04	1.10	0.20	7.84	45.94	32.47	0.62	6.77	0.00	0.00	0.00	0.00	0.00	0.00	0.00	0.32	0.7	3.00
ELS007	Green	1.30	1.73	0.62	0.58	0.39	5.79	41.68	43.90	0.47	0.00	3.46	0.07	0.00	0.00	0.00	0.00	0.00	0.00	1.1	1.87
ELS005	White	2.26	0.73	1.30	0.79	0.07	7.61	46.16	36.97	0.56	0.00	3.55	0.00	0.00	0.00	0.00	0.00	0.00	0.00	0.8	3.05
LOG003	Honey	0.74	3.23	1.87	0.50	1.11	6.93	22.29	62.53	0.19	0.00	0.59	0.00	0.00	0.00	0.00	0.00	0.00	0.00	2.8	1.24
LOG028	Honey	1.07	3.80	2.71	0.36	1.15	9.66	34.87	45.91	0.46	0.00	0.00	0.00	0.00	0.00	0.00	0.00	0.00	0.00	1.3	1.43
LOG034	Honey	1.60	6.32	4.09	0.19	0.44	6.04	30.87	50.09	0.19	0.00	0.00	0.00	0.00	0.00	0.00	0.06	0.00	0.00	1.6	1.85
LOG037	Honey	1.53	4.12	2.60	0.91	1.46	5.93	33.62	49.62	0.16	0.00	0.00	0.00	0.00	0.00	0.00	0.06	0.00	0.00	1.5	2.44
LOG038b	Blue	7.44	3.92	1.34	0.47	0.70	3.40	52.88	26.15	0.12	3.26	0.00	0.00	0.15	0.00	0.00	0.00	0.00	0.16	0.5	7.91
LOG038w	White	7.05	3.39	0.46	0.40	0.53	2.67	53.93	28.06	0.08	3.43	0.00	0.00	0.00	0.00	0.00	0.00	0.00	0.00	0.5	7.45
LOG042b	Black	3.35	6.05	2.53	0.11	0.20	7.85	46.38	16.98	0.78	6.83	0.72	3.94	0.00	0.00	0.00	0.00	0.00	4.24	0.4	3.46
LOG042g	Green	1.61	1.26	0.42	1.65	0.20	4.77	47.57	37.11	0.00	3.40	1.94	0.00	0.00	0.00	0.00	0.00	0.00	0.00	0.8	3.26
LOG042w	White	2.28	2.12	0.79	1.92	0.47	7.22	56.49	23.11	0.03	4.87	0.00	0.00	0.00	0.00	0.00	0.00	0.00	0.70	0.4	4.20
LOG044g	Green	1.61	1.26	0.42	1.65	0.20	4.77	47.57	37.11	0.00	3.40	1.94	0.00	0.00	0.00	0.00	0.00	0.00	0.00	0.8	3.26
LOG044w	White	1.60	1.45	0.60	1.55	0.19	5.17	43.87	40.55	0.00	5.02	0.00	0.00	0.00	0.00	0.00	0.00	0.00	0.00	0.9	3.15
LOG050	Greenish	1.00	3.05	2.40	0.47	1.12	8.82	27.67	55.17	0.20	0.00	0.00	0.00	0.00	0.00	0.00	0.00	0.00	0.00	2.0	1.47
LOG051	Brown	1.90	5.63	2.91	0.31	1.19	9.53	44.43	33.56	0.54	0.00	0.00	0.00	0.00	0.00	0.00	0.00	0.00	0.00	0.8	2.21
LOG054	Honey	0.95	3.49	3.96	0.49	0.78	7.30	31.05	51.33	0.19	0.01	0.00	0.00	0.00	0.00	0.00	0.45	0.00	0.00	1.7	1.44
LOG059	Honey	1.68	1.87	3.92	0.41	0.51	4.61	41.86	44.80	0.34	0.00	0.00	0.00	0.00	0.00	0.00	0.00	0.00	0.00	1.1	2.09

Continued

Spectrum	Color	K_2O	CaO	FeO	Na_2O	MgO	Al_2O_3	SiO_2	PbO	TiO_2	SnO_2	CuO	MnO	CoO	NiO	Sb_2O_3	ZnO	BaO	P_2O_5	Pb/Si*	Alk.
LOG060	Green	0.20	3.22	1.54	0.46	0.88	5.00	28.41	58.49	0.19	0.00	1.55	0.00	0.00	0.00	0.00	0.00	0.00	0.00	2.1	0.74
LOG061	Honey	1.08	4.07	3.37	0.43	0.76	5.41	28.29	56.34	0.17	0.08	0.00	0.00	0.00	0.00	0.00	0.00	0.00	0.00	2.0	1.50
LOG062	White	2.17	1.98	0.58	0.60	0.02	2.99	43.23	41.02	0.00	7.41	0.00	0.00	0.00	0.00	0.00	0.00	0.00	0.00	0.9	2.77
LOG085	Honey	0.55	3.32	5.39	0.64	0.65	3.31	30.06	55.61	0.47	0.00	0.00	0.00	0.00	0.00	0.00	0.00	0.00	0.00	1.9	1.19
LOG075	Brown	1.16	2.42	1.49	0.88	0.71	4.71	39.69	48.27	0.19	0.00	0.43	0.02	0.00	0.00	0.00	0.00	0.00	0.00	1.2	2.04

Appendix B

Inventory

Table B.1: Description of the Ceramic Sample. SU:Stratigraphic Unit.

ANID	SITE	REGION	SU	TYPOLOGY	FORM	GROUP	FABRIC
ELS001	Elosu	TBC	NA	Lead glazed with slip	Plate	ELS	F-I
ELS002	Elosu	TBC	NA	Lead glazed with slip	Plate	ELS	F-I
ELS003	Elosu	TBC	NA	Lead glazed with slip	Bowl	ELS	F-II
ELS004	Elosu	TBC	NA	Uncoated	Vase	MIC	NA
ELS005	Elosu	TBC	NA	Lead glazed with slip	Plate	ELS	F-I
ELS006	Elosu	TBC	NA	Tin lead glazed	Bowl	ELS	F-III
ELS007	Elosu	TBC	NA	Lead glazed with slip	Flowerpot	ELS	F-II
ELS008	Elosu	TBC	NA	Tin lead glazed	Flowerpot	ELS	F-I
ELS009	Elosu	TBC	NA	Tin lead glazed	Flowerpot	ELS	F-I
ELS010	Elosu	TBC	NA	Tin lead glazed	Bowl	ELS	F-I
ELS011	Elosu	TBC	NA	Tin lead glazed	Plate	ELS	F-II
ELS012	Elosu	TBC	NA	Tin lead glazed	Bowl	ELS	F-I
ELS013	Elosu	TBC	NA	Tin lead glazed	Flowerpot	ELS	F-II
ELS014	Elosu	TBC	NA	Lead glazed with slip	Flowerpot	ELS	F-II
ELS015	Elosu	TBC	NA	Tin lead glazed	Bowl	ELS	F-I
ELS016	Elosu	TBC	NA	Tin lead glazed	Flowerpot	ELS	F-II
ELS017	Elosu	TBC	NA	Tin lead glazed	Bowl	ELS	F-I
ELS018	Elosu	TBC	NA	Lead glazed with slip	Undefined	ELS	F-III
ELS019	Elosu	TBC	NA	Lead glazed with slip	Plate	ELS	F-I
ELS020	Elosu	TBC	NA	Tin lead glazed	Plate	ELS	F-II
ELS021	Elosu	TBC	NA	Tin lead glazed	Flowerpot	ELS	F-II
ELS022	Elosu	TBC	NA	Uncoated	Kiln Utensil	ELS	F-II
ELS023	Elosu	TBC	NA	Uncoated	Bowl	ELS	F-II
ELS024	Elosu	TBC	NA	Uncoated	Fired Clay Pellet	ELS	F-I
ELS025	Elosu	TBC	NA	Uncoated	Kiln Utensil	ELS	F-III
ELS026	Elosu	TBC	NA	Uncoated	Kiln Utensil	ELS	F-II
ELS027	Elosu	TBC	NA	Uncoated	Kiln Utensil	ELS	F-II
ELS028	Elosu	TBC	NA	Uncoated	Kiln Utensil	ELS	F-II
ELS029	Elosu	TBC	NA	Uncoated	Kiln Utensil	ELS	F-II
ELS030	Elosu	TBC	NA	Uncoated	Kiln Utensil	ELS	F-II
ELS031	Elosu	TBC	NA	Uncoated	Kiln Utensil	ELS	F-II
ELS032	Elosu	TBC	NA	Uncoated	Kiln Utensil	ELS	F-II
ELS033	Elosu	TBC	NA	Uncoated	Kiln Utensil	ELS	F-II
ELS034	Elosu	TBC	NA	Lead glazed with slip	Flowerpot	ELS	F-II
ELS035	Elosu	TBC	NA	Uncoated	Kiln Utensil	ELS	F-II
ELS036	Elosu	TBC	NA	Lead glazed with slip	Flowerpot	ELS	F-I
ELS037	Elosu	TBC	NA	Tin lead glazed	Undefined	ELS	F-II
ELS038	Elosu	TBC	NA	Tin lead glazed	Bowl	ELS	F-II
ELS039	Elosu	TBC	NA	Lead glazed with slip	Flowerpot	ELS	F-I
ELS040	Elosu	TBC	NA	Tin lead glazed	Bowl	ELS	F-II
ELS041	Elosu	TBC	NA	Tin lead glazed	Bowl	ELS	F-III
ELS042	Elosu	TBC	NA	Tin lead glazed	Bowl	ELS	F-III
ELS043	Elosu	TBC	NA	Lead glazed with slip	Bowl	ELS	F-I
ELS044	Elosu	TBC	NA	Tin lead glazed	Bowl	ELS	F-III
ELS045	Elosu	TBC	NA	Tin lead glazed	Bowl	ELS	F-III
ELS046	Elosu	TBC	NA	Lead glazed with slip	Bowl	ELS	F-II
ELS047	Elosu	TBC	NA	Lead glazed with slip	Bowl	ELS	F-I
ELS048	Elosu	TBC	NA	Lead glazed with slip	Plate	ELS	F-I
ELS049	Elosu	TBC	NA	Tin lead glazed	Bowl	ELS	F-I

Continued

ANID	SITE	REGION	SU	TYPOLOGY	FORM	GROUP	FABRIC
ELS050	Elosu	TBC	NA	Uncoated	Kiln Utensil	ELS	F-III
ELS051	Elosu	TBC	NA	Uncoated	Kiln Utensil	ELS	F-III
DUR001	Durango	TBC	NA	Tin lead glazed	Bowl	DUR	F-I
DUR002	Durango	TBC	NA	Tin lead glazed	Bowl	DUR	F-II
DUR003	Durango	TBC	NA	Tin lead glazed	Bowl	DUR	F-II
DUR004	Durango	TBC	NA	Tin lead glazed	Bowl	DUR	F-I
DUR005	Durango	TBC	NA	Uncoated	Bowl	UNG	NA
DUR006	Durango	TBC	NA	Tin lead glazed	Plate	UNG	NA
DUR007	Durango	TBC	NA	Lead glazed	Cooking Pot	UNG	NA
DUR008	Durango	TBC	NA	Tin lead glazed	Bowl	DUR-MIC	F-I
DUR010	Durango	TBC	NA	Tin lead glazed	Lid	UNG	NA
DUR011	Durango	TBC	NA	Tin lead glazed	Bowl	DUR-MIC	F-I
DUR013	Durango	TBC	NA	Tin lead glazed	Bowl	DUR	F-II
DUR014	Durango	TBC	NA	Tin lead glazed	Bowl	UNG	NA
DUR015	Durango	TBC	NA	Uncoated	Kiln Utensil	DUR	F-II
DUR016	Durango	TBC	NA	Tin lead glazed	Big Bowl	DUR-MIC	F-II
DUR017	Durango	TBC	NA	Uncoated	Kiln Utensil	DUR	F-II
DUR018	Durango	TBC	NA	Uncoated	Kiln Utensil	DUR	F-II
DUR019	Durango	TBC	NA	Uncoated	Kiln Utensil	UNG	F-II
DUR020	Durango	TBC	NA	Uncoated	Kiln Utensil	DUR	F-II
DUR021	Durango	TBC	NA	Uncoated	Kiln Utensil	DUR	F-II
DUR022	Durango	TBC	NA	Uncoated	Kiln Utensil	DUR	F-II
DUR023	Durango	TBC	NA	Uncoated	Kiln Utensil	DUR	F-II
DUR024	Durango	TBC	NA	Tin lead glazed	Bowl	DUR	F-II
DUR025	Durango	TBC	NA	Tin lead glazed	Flowerpot	DUR	F-I
DUR026	Durango	TBC	NA	Tin lead glazed	Bowl	UNG	NA
DUR027	Durango	TBC	NA	Uncoated	Kiln Utensil	DUR	F-II
DUR028	Durango	TBC	NA	Tin lead glazed	Bowl?	DUR	F-II
ORD001	Orduña	TBC	NA	Tin lead glazed	Plate	ORD-A	F-II
ORD002	Orduña	TBC	NA	Tin lead glazed	Plate	ORD-A	F-I
ORD003	Orduña	TBC	NA	Tin lead glazed	Bowl	ORD-A	F-II
ORD004	Orduña	TBC	NA	Tin lead glazed	Bowl	ORD-A	F-II
ORD005	Orduña	TBC	NA	Tin lead glazed	Basin	ORD-A	F-II
ORD006	Orduña	TBC	NA	Tin lead glazed	Bowl	ORD-A	F-I
ORD007	Orduña	TBC	NA	Tin lead glazed	Plate	ORD-A	F-I
ORD008	Orduña	TBC	NA	Tin lead glazed	Plate	ORD-A	F-I
ORD009	Orduña	TBC	NA	Tin lead glazed	Plate	ORD-A	F-I
ORD010	Orduña	TBC	NA	Tin lead glazed	Bowl	ORD-MEL-A	F-I
ORD011	Orduña	TBC	NA	Tin lead glazed	Jar	ORD-MEL-A	F-I
ORD012	Orduña	TBC	NA	Tin lead glazed	Bowl	ORD-MEL-A	F-I
ORD013	Orduña	TBC	NA	Tin lead glazed	Bowl	ORD-MEL-A	F-I
ORD014	Orduña	TBC	2	Tin lead glazed	Bowl	UNG	NA
ORD015	Orduña	TBC	NA	Lead glazed	Pot	ORD-D	F-II
ORD016	Orduña	TBC	NA	Lead glazed	Bowl	ORD-MEL-A	F-I
ORD017	Orduña	TBC	NA	Lead glazed	Bowl	ORD-MEL-A	F-I
ORD018	Orduña	TBC	NA	Lead glazed	Bowl	ORD-D	F-I
ORD019	Orduña	TBC	2	Tin lead glazed	Bowl	UNG	NA
ORD020	Orduña	TBC	NA	Tin lead glazed	Jar	ORD-A	F-I
ORD021	Orduña	TBC	NA	Tin lead glazed	Jar	ORD-A	F-II
ORD022	Orduña	TBC	NA	Tin lead glazed	Jar	ORD-A	F-II
ORD023	Orduña	TBC	NA	Tin lead glazed	Vessel (potter-mistake)	ORD-A	F-II
ORD024	Orduña	TBC	NA	Uncoated	Kiln-utensil	ORD-A	F-II
ORD025	Orduña	TBC	NA	Uncoated	Kiln-utensil	ORD-A	F-II
ORD026	Orduña	TBC	NA	Uncoated	Vessel (potter-mistake)	ORD-D	F-I
ORD027	Orduña	TBC	NA	Uncoated	Kiln-utensil	ORD-A	F-I
ORD028	Orduña	TBC	NA	Uncoated	Kiln-utensil	ORD-A	F-I

Continued

ANID	SITE	REGION	SU	TYPOLOGY	FORM	GROUP	FABRIC
ORD029	Orduña	TBC	2	Tin lead glazed	Bowl	ORD-C	F-III
ORD030	Orduña	TBC	NA	Lead glazed	Basin	ORD-A	F-I
ORD031	Orduña	TBC	NA	Uncoated	Potter-mistake	ORD-A	F-II
ORD032	Orduña	TBC	NA	Tin lead glazed	Basin	ORD-A	F-I
ORD033	Orduña	TBC	NA	Uncoated	Kiln-utensil	ORD-A	F-II
ORD034	Orduña	TBC	NA	Tin lead glazed	Kiln-utensil	ORD-A	F-II
ORD035	Orduña	TBC	NA	Uncoated	Kiln-utensil	ORD-A	F-II
ORD036	Orduña	TBC	NA	Uncoated	Kiln-utensil	ORD-A	F-II
ORD037	Orduña	TBC	NA	Uncoated	Kiln-utensil	ORD-A	F-II
ORD039	Orduña	TBC	NA	Uncoated	Kiln-utensil	ORD-A	F-II
ORD040	Orduña	TBC	NA	Uncoated	Kiln-utensil	ORD-D	F-II
ORD042	Orduña	TBC	14	Lead glazed	Bowl	ORD-MEL-A	F-I
ORD043	Orduña	TBC	14	Lead glazed	Bowl	ORD-MEL-A	F-I
ORD044	Orduña	TBC	14	Tin lead glazed	Plate	ORD-C	F-II
ORD045	Orduña	TBC	NA	Tin lead glazed	Bowl	ORD-A	F-I
ORD046	Orduña	TBC	NA	Tin lead glazed	Bowl	ORD-A	F-I
ORD047	Orduña	TBC	2	Lead glazed	Jar	UNG	NA
ORD048	Orduña	TBC	2	Tin lead glazed	Bowl	ORD-A	F-I
ORD049	Orduña	TBC	14	Tin lead glazed	Plate	ORD-C	F-II
ORD050	Orduña	TBC	2	Lead glazed	Bowl	ORD-MEL-A	F-I
ORD051	Orduña	TBC	2	Lead glazed	Mug	ORD-MEL-B	F-I
ORD053	Orduña	TBC	2	Lead glazed	Bowl	ORD-MEL-A	F-I
ORD055	Orduña	TBC	2	Tin lead glazed	Bowl	UNG	NA
ORD056	Orduña	TBC	2	Tin lead glazed	Pot	MIC	F-I
ORD057	Orduña	TBC	2	Uncoated	Pot	MIC	F-I
ORD058	Orduña	TBC	2	Uncoated	Inform	MIC	F-I
ORD059	Orduña	TBC	2	Tin lead glazed	Inform	UNG	F-I
ORD060	Orduña	TBC	NA	Tin lead glazed	Bowl	ORD-A	F-II
ORD061	Orduña	TBC	NA	Tin lead glazed	Bowl	ORD-A	F-II
ORD062	Orduña	TBC	NA	Tin lead glazed	Bowl	ORD-A	F-I
ORD063	Orduña	TBC	2,060	Uncoated	Kiln-utensil	UNG	NA
ORD064	Orduña	TBC	2,060	Uncoated	Kiln-utensil	ORD-A	F-II
ORD065	Orduña	TBC	2,060	Uncoated	Kiln-utensil	ORD-A	F-I
ORD066	Orduña	TBC	2,030	Uncoated	Kiln-utensil	ORD-A	F-I
ORD067	Orduña	TBC	2,030	Uncoated	Kiln-utensil	ORD-A	F-I
ORD068	Orduña	TBC	2,030	Tin lead glazed	Home stoup	ORD-C	F-II
ORD069	Orduña	TBC	2,030	Tin lead glazed	Bowl	ORD-A	F-II
ORD070	Orduña	TBC	2,030	Tin lead glazed	Plate	ORD-A	F-II
ORD071	Orduña	TBC	2,030	Tin lead glazed	Jar (potter-mistake)	UNG	NA
ORD072	Orduña	TBC	1,025	Tin lead glazed	Plate	ORD-A	F-I
ORD073	Orduña	TBC	1,025	Tin lead glazed	Bowl	UNG	NA
ORD074	Orduña	TBC	1,025	Tin lead glazed	Bowl	UNG	NA
ORD075	Orduña	TBC	2,060	Tin lead glazed	Jar	ORD-C	F-III
ORD076	Orduña	TBC	2,060	Tin lead glazed	Plate	UNG	NA
ORD077	Orduña	TBC	2,060	Tin lead glazed	Basin	UNG	NA
ORD078	Orduña	TBC	2,060	Lead glazed	Basin	ORD-MEL-B	F-I
ORD079	Orduña	TBC	2,060	Lead glazed	Basin	ORD-MEL-B	F-I
ORD080	Orduña	TBC	2,060	Lead glazed	Basin	ORD-MEL-B	F-I
ORD081	Orduña	TBC	2,060	Lead glazed	Basin	ORD-MEL-B	F-I
ORD082	Orduña	TBC	2,060	Lead glazed	Basin	ORD-MEL-B	F-I
ORD083	Orduña	TBC	80	Tin lead glazed	Bowl	ORD-B	F-III
ORD084	Orduña	TBC	80	Tin lead glazed	Bowl	ORD-B	F-II
ORD085	Orduña	TBC	80	Tin lead glazed	Plate	ORD-B	F-II
ORD086	Orduña	TBC	80	Tin lead glazed	Bowl	ORD-B	F-III
ORD087	Orduña	TBC	80	Tin lead glazed	Plate	UNG	NA
ORD088	Orduña	TBC	80	Tin lead glazed	Bowl	ORD-B	F-II

Continued

ANID	SITE	REGION	SU	TYPOLOGY	FORM	GROUP	FABRIC
ORD089	Orduña	TBC	80	Tin lead glazed	Jar	ORD-B	F-III
ORD090	Orduña	TBC	80	Tin lead glazed	Plate	ORD-B	F-II
ORD091	Orduña	TBC	80	Tin lead glazed	Plate	ORD-B	F-II
ORD092	Orduña	TBC	80	Tin lead glazed	Plate	ORD-B	F-II
ORD093	Orduña	TBC	80	Tin lead glazed	Plate	ORD-B	F-II
ORD094	Orduña	TBC	80	Tin lead glazed	Bowl	ORD-B	F-II
ORD095	Orduña	TBC	80	Tin lead glazed	Bowl	ORD-B	F-I
ORD096	Orduña	TBC	80	Tin lead glazed	Bowl	ORD-B	F-I
ORD097	Orduña	TBC	80	Tin lead glazed	Bowl	ORD-B	F-I
ORD098	Orduña	TBC	80	Tin lead glazed	Plate	ORD-B	F-II
ORD099	Orduña	TBC	80	Tin lead glazed	Plate	ORD-B	F-III
ORD100	Orduña	TBC	80	Tin lead glazed	Plate	ORD-B	F-III
ORD101	Orduña	TBC	80	Tin lead glazed	Plate	ORD-B	F-III
NAJ001	Nájera	LR	1, 244	Tin lead glazed	Porringer	NAJ-A	F-I
NAJ002	Nájera	LR	257	Tin lead glazed	Porringer	NAJ-A	F-II
NAJ003	Nájera	LR	NA	Tin lead glazed	Porringer	NAJ-A	F-III
NAJ004	Nájera	LR	NA	Tin lead glazed	Porringer	NAJ-A	F-II
NAJ005	Nájera	LR	NA	Tin lead glazed	Porringer	NAJ-A	F-III
NAJ006	Nájera	LR	NA	Tin lead glazed	Porringer	NAJ-A	F-II
NAJ007	Nájera	LR	NA	Tin lead glazed	Porringer	NAJ-A	F-III
NAJ008	Nájera	LR	NA	Tin lead glazed	Porringer	NAJ-A	F-III
NAJ009	Nájera	LR	NA	Tin lead glazed	Porringer	NAJ-A	F-II
NAJ010	Nájera	LR	NA	Tin lead glazed	Porringer	NAJ-A	F-III
NAJ011	Nájera	LR	NA	Tin lead glazed	Porringer	NAJ-B	F-I
NAJ012	Nájera	LR	NA	Tin lead glazed	Porringer	NAJ-B	F-I
NAJ013	Nájera	LR	NA	Tin lead glazed	Porringer	NAJ-A	F-I
NAJ014	Nájera	LR	NA	Tin lead glazed	Porringer	NAJ-B	F-I
NAJ015	Nájera	LR	NA	Tin lead glazed	Porringer	NAJ-A	F-III
NAJ016	Nájera	LR	NA	Tin lead glazed	Porringer	NAJ-A	F-I
NAJ017	Nájera	LR	NA	Tin lead glazed	Porringer	NAJ-A	F-II
NAJ018	Nájera	LR	NA	Tin lead glazed	Porringer	NAJ-A	F-I
NAJ019	Nájera	LR	NA	Tin lead glazed	Porringer	NAJ-A	F-II
NAJ020	Nájera	LR	NA	Tin lead glazed	Porringer	NAJ-A	F-II
NAJ021	Nájera	LR	NA	Tin lead glazed	Porringer	NAJ-A	F-II
NAJ022	Nájera	LR	NA	Tin lead glazed	Porringer	NAJ-A	F-III
NAJ023	Nájera	LR	NA	Tin lead glazed	Porringer	NAJ-A	F-I
NAJ024	Nájera	LR	NA	Tin lead glazed	Porringer	UNG	NA
NAJ025	Nájera	LR	NA	Tin lead glazed	Porringer	TAL	F-I
NAJ026	Nájera	LR	NA	Tin lead glazed	Bowl	UNG	F-II
NAJ027	Nájera	LR	NA	Tin lead glazed	Porringer	NAJ-A	F-III
NAJ028	Nájera	LR	NA	Tin lead glazed	Bowl	NAJ-A	F-II
NAJ029	Nájera	LR	NA	Tin lead glazed	Bowl	TAL	F-I
NAJ030	Nájera	LR	NA	Tin lead glazed	Bowl	NAJ-A	F-II
NAJ031	Nájera	LR	NA	Tin lead glazed	Bowl	NAJ-A	F-II
NAJ032	Nájera	LR	NA	Tin lead glazed	Cup	NAJ-A	F-II
NAJ033	Nájera	LR	NA	Tin lead glazed	Cup	TAL	F-II
NAJ034	Nájera	LR	NA	Tin lead glazed	Bowl	NAJ-A	F-II
NAJ035	Nájera	LR	NA	Tin lead glazed	bowl	UNG	NA
NAJ036	Nájera	LR	NA	Tin lead glazed	Plate	NAJ-B	F-II
NAJ037	Nájera	LR	NA	Tin lead glazed	Bowl	NAJ-B	F-I
NAJ038	Nájera	LR	NA	Tin lead glazed	Jug	NAJ-A	F-I
NAJ039	Nájera	LR	NA	Tin lead glazed	Jug	NAJ-B	F-I
NAJ040	Nájera	LR	NA	Tin lead glazed	Plate	NAJ-A	F-II
NAJ041	Nájera	LR	NA	Tin lead glazed	Plate	NAJ-A	F-II
NAJ042	Nájera	LR	NA	Tin lead glazed	Plate	UNG	F-II
NAJ043	Nájera	LR	NA	Tin lead glazed	Plate	UNG	F-III

Continued

ANID	SITE	REGION	SU	TYPOLOGY	FORM	GROUP	FABRIC
NAJ044	Nájera	LR	NA	Tin lead glazed	Plate	NAJ-A	F-III
NAJ045	Nájera	LR	NA	Tin lead glazed	Plate	NAJ-A	F-II
NAJ046	Nájera	LR	NA	Tin lead glazed	Plate	NAJ-B	F-II
NAJ047	Nájera	LR	NA	Tin lead glazed	Plate	NAJ-B	F-II
NAJ048	Nájera	LR	NA	Tin lead glazed	Plate	UNG	NA
NAJ049	Nájera	LR	NA	Tin lead glazed	Plate	NAJ-A	F-I
NAJ050	Nájera	LR	NA	Tin lead glazed	Plate	NAJ-B	F-II
NAJ051	Nájera	LR	NA	Tin lead glazed	Plate	NAJ-B	F-I
NAJ052	Nájera	LR	NA	Tin lead glazed	Plate	NAJ-A	F-II
NAJ053	Nájera	LR	NA	Tin lead glazed	Plate	UNG	NA
NAJ054	Nájera	LR	NA	Tin lead glazed	Plate	NAJ-A	F-III
NAJ055	Nájera	LR	NA	Tin lead glazed	Plate	NAJ-A	F-III
NAJ056	Nájera	LR	NA	Tin lead glazed	Plate	NAJ-A	F-IV
NAJ057	Nájera	LR	NA	Tin lead glazed	Plate	NAJ-A	F-III
NAJ058	Nájera	LR	NA	Tin lead glazed	Plate	NAJ-B	F-II
NAJ059	Nájera	LR	NA	Tin lead glazed	Plate	NAJ-A	F-I
NAJ062	Nájera	LR	NA	Tin lead glazed	Plate	NAJ-A	F-I
NAJ063	Nájera	LR	NA	Tin lead glazed	Plate	NAJ-B	F-III
NAJ064	Nájera	LR	NA	Tin lead glazed	Jar	NAJ-A	F-II
NAJ065	Nájera	LR	NA	Tin lead glazed	Jar	NAJ-A	F-III
NAJ066	Nájera	LR	NA	Tin lead glazed	Jar	NAJ-A	F-III
NAJ067	Nájera	LR	NA	Tin lead glazed	Jar	NAJ-A	F-III
NAJ068	Nájera	LR	NA	Tin lead glazed	Jar	NAJ-A	F-III
NAJ069	Nájera	LR	NA	Tin lead glazed	Jar	NAJ-A	F-II
NAJ070	Nájera	LR	NA	Tin lead glazed	Jar	NAJ-A	F-III
NAJ071	Nájera	LR	NA	Tin lead glazed	Jar	TAL	F-II
NAJ073	Nájera	LR	NA	Tin lead glazed	Jar	NAJ-A	F-III
NAJ074	Nájera	LR	NA	Tin lead glazed	Bowl	NAJ-A	F-III
NAJ075	Nájera	LR	NA	Tin lead glazed	Plate	NAJ-A	F-III
NAJ076	Nájera	LR	NA	Tin lead glazed	Plate	NAJ-B	F-III
NAJ077	Nájera	LR	NA	Tin lead glazed	Jug	NAJ-A	F-I
NAJ078	Nájera	LR	NA	Tin lead glazed	Sauceboat	NAJ-A	F-I
NAJ079	Nájera	LR	NA	Tin lead glazed	Jar	NAJ-A	F-III
NAJ080	Nájera	LR	NA	Tin lead glazed	Jar	NAJ-A	F-III
NAJ081	Nájera	LR	NA	Tin lead glazed	Jar	NAJ-A	F-III
NAJ082	Nájera	LR	NA	Tin lead glazed	Jar	NAJ-A	F-III
NAJ083	Nájera	LR	NA	Tin lead glazed	Jar	NAJ-B	F-II
NAJ085	Nájera	LR	NA	Tin lead glazed	Jar	NAJ-A	F-III
NAJ087	Nájera	LR	NA	Tin lead glazed	Porringer	NAJ-A	F-III
NAJ088	Nájera	LR	NA	Tin lead glazed	Lid	MUEL	F-I
NAJ089	Nájera	LR	211	Tin lead glazed	Porringer	MUEL	F-I
NAJ090	Nájera	LR	NA	Tin lead glazed	Porringer	MUEL	F-I
NAJ091	Nájera	LR	NA	Tin lead glazed	Canister	MUEL	F-I
NAJ092	Nájera	LR	NA	Tin lead glazed	Canister	MUEL	F-I
NAJ093	Nájera	LR	NA	Tin lead glazed	Plate	MUEL	F-II
NAJ094	Nájera	LR	NA	Tin lead glazed	Lid	MIC	F-I
NAJ095	Nájera	LR	NA	Uncoated	Lid	MIC	F-I
NAJ097	Nájera	LR	NA	Uncoated	Cooking Pot	MIC	F-I
NAJ098	Nájera	LR	NA	Uncoated	Cooking Pot	MIC	F-I
NAJ099	Nájera	LR	NA	Uncoated	Cooking Pot	MIC	F-I
NAJ100	Nájera	LR	NA	Uncoated	Big jar	MIC	F-I
NAJ101	Nájera	LR	NA	Uncoated	Big jar	MIC	F-I
LOG001	Logroño	LR	277	Uncoated	Pitcher	LOG-C	F-II
LOG002	Logroño	LR	277	Uncoated	Pitcher	LOG-C	F-II
LOG003	Logroño	LR	277	Lead glazed	Pitcher	LOG-C	F-II
LOG004	Logroño	LR	277	Uncoated	Pitcher	LOG-C	F-II

Continued

ANID	SITE	REGION	SU	TYPOLOGY	FORM	GROUP	FABRIC
LOG005	Logroño	LR	277	Uncoated	Pitcher	LOG-C	F-II
LOG006	Logroño	LR	277	Uncoated	Pitcher	LOG-C	F-II
LOG007	Logroño	LR	277	Uncoated	Mug	LOG-C	F-II
LOG008	Logroño	LR	277	Uncoated	Cooking Pot	LOG-A	F-I
LOG009	Logroño	LR	277	Painted pottery	Small Jug	LOG-B	F-I
LOG015	Logroño	LR	317	Uncoated	Cooking Pot	LOG-C	F-II
LOG016	Logroño	LR	317	Waste	Undefined	LOG-C	F-II
LOG017	Logroño	LR	317	Waste	Undefined	LOG-C	F-II
LOG018	Logroño	LR	317	Waste	Undefined	LOG-C	F-II
LOG019	Logroño	LR	317	Uncoated	Pitcher	LOG-C	F-I
LOG020	Logroño	LR	317	Uncoated	Pitcher	LOG-C	F-II
LOG021	Logroño	LR	317	Uncoated	Cooking Pot	LOG-A	F-I
LOG022	Logroño	LR	317	Uncoated	Cooking Pot	LOG-A	F-I
LOG023	Logroño	LR	317	Uncoated	Cooking Pot	LOG-A	F-I
LOG026	Logroño	LR	267	Waste	Undefined	LOG-B	F-I
LOG028	Logroño	LR	277	Lead glazed	Jar	LOG-B	F-I
LOG030	Logroño	LR	317	Uncoated	Kiln Utensil	LOG-C	F-II
LOG031	Logroño	LR	317	Uncoated	Kiln Utensil	LOG-C	F-II
LOG032	Logroño	LR	317	Uncoated	Kiln Utensil	UNG	NA
LOG033	Logroño	LR	165	Uncoated	Kiln Utensil	LOG-B	F-I
LOG034	Logroño	LR	223	Uncoated	Kiln Utensil	LOG-B	F-I
LOG035	Logroño	LR	312	Uncoated	Kiln Utensil	LOG-B	F-II
LOG036	Logroño	LR	281	Uncoated	Undefined	LOG-B	F-I
LOG037	Logroño	LR	273	Lead glazed	Bowl	UNG	NA
LOG038	Logroño	LR	221	Tin lead glazed	Bowl	LOG-E	F-I
LOG039	Logroño	LR	221	Tin lead glazed	Bowl?	LOG-E	F-I
LOG040	Logroño	LR	252	Tin lead glazed	Plate	UNG	NA
LOG041	Logroño	LR	225	Tin lead glazed	Bowl?	UNG	NA
LOG042	Logroño	LR	252	Tin lead glazed	Bowl	TER	F-I
LOG043	Logroño	LR	288	Tin lead glazed	Bowl	TER	F-I
LOG044	Logroño	LR	288	Tin lead glazed	Bowl	TER	F-I
LOG045	Logroño	LR	252	Tin lead glazed	Bowl	TER	F-I
LOG046	Logroño	LR	225	Tin lead glazed	Plate	UNG	NA
LOG047	Logroño	LR	225	Tin lead glazed	Bowl	LOG-E	F-III
LOG048	Logroño	LR	288	Tin lead glazed	Bowl	TER	F-I
LOG049	Logroño	LR	223	Lead glazed	Small Jar	UNG	NA
LOG050	Logroño	LR	255	Lead glazed	Undefined	LOG-B	F-I
LOG051	Logroño	LR	280	Lead glazed	Undefined	LOG-B	F-I
LOG052	Logroño	LR	255	Lead glazed	Undefined	LOG-B	F-I
LOG053	Logroño	LR	275	Lead glazed	Pitcher	LOG-C	F-II
LOG054	Logroño	LR	221	Lead glazed	Mortar	LOG-B	F-II
LOG055	Logroño	LR	317	Lead glazed	Porringer	LOG-E	F-II
LOG056	Logroño	LR	179	Uncoated	Jar	LOG-B	F-I
LOG059	Logroño	LR	179	Lead glazed	Jar	LOG-B	F-I
LOG060	Logroño	LR	179	Lead glazed	Cup	LOG-B	F-I
LOG061	Logroño	LR	179	Lead glazed	Bowl	LOG-B	F-I
LOG062	Logroño	LR	221	Tin lead glazed	Lid	LOG-B	F-I
LOG063	Logroño	LR	221	Lead glazed	Mortar	LOG-B	F-I
LOG066	Logroño	LR	296	Lead glazed	Jar	LOG-B	F-I
LOG067	Logroño	LR	281	Uncoated	Fired Clay Pellet	LOG-B	F-II
LOG068	Logroño	LR	281	Uncoated	Fired Clay Pellet	LOG-B	F-II
LOG069	Logroño	LR	281	Uncoated	Fired Clay Pellet	LOG-B	F-II
LOG070	Logroño	LR	281	Uncoated	Fired Clay Pellet	LOG-C	F-II
LOG071	Logroño	LR	183	Uncoated	Mug	LOG-C	F-II
LOG072	Logroño	LR	288	Lead glazed	Pitcher	LOG-C	F-II
LOG073	Logroño	LR	243	Lead glazed	Plate	LOG-C	F-II

Continued

ANID	SITE	REGION	SU	TYPOLOGY	FORM	GROUP	FABRIC
LOG074	Logroño	LR	288	Lead glazed	Bowl	LOG-C	F-II
LOG075	Logroño	LR	288	Lead glazed	Mug	LOG-C	F-II
LOG076	Logroño	LR	182	Tin lead glazed	Bowl	TER	F-I
LOG077	Logroño	LR	288	Uncoated	Lid	LOG-A	F-I
LOG078	Logroño	LR	288	Uncoated	Lid	LOG-A	F-I
LOG080	Logroño	LR	281	Uncoated	Kiln Utensil	LOG-B	F-II
LOG081	Logroño	LR	179	Uncoated	Roof Tile	LOG-D	F-I
LOG082	Logroño	LR	179	Waste	Roof Tile	LOG-B	F-II
LOG083	Logroño	LR	179	Waste	Roof Tile	LOG-D	F-I
LOG084	Logroño	LR	179	Uncoated	Roof Tile	LOG-B	F-II
LOG085	Logroño	LR	179	Lead glazed	Roof Tile	LOG-B	F-II
LOG086	Logroño	LR	286	Lead glazed	Undefined	LOG-C	F-II
LOG087	Logroño	LR	296	Lead glazed	Roof Tile	LOG-B	F-II
LOG088	Logroño	LR	296	Lead glazed	Roof Tile	LOG-B	F-II
LOG089	Logroño	LR	297	Lead glazed	Pitcher	LOG-C	F-II
LOG090	Logroño	LR	297	Uncoated	Roof Tile	UNG	NA
LOG091	Logroño	LR	297	Uncoated	Roof Tile	LOG-C	F-II

Appendix C

Photographs

All the images were obtained by the procedure described in the page 51. The following pictures shown here were kindly provided by ArqueoRioja company: LOG037, LOG038, LOG039, LOG041, LOG043, LOG044, LOG045, LOG046, LOG047, LOG048, LOG054, LOG056, LOG059, LOG060, LOG063, LOG078 and LOG080.

LOG001

LOG002

LOG003

LOG004

LOG005

LOG006

LOG007

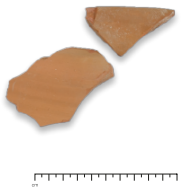

LOG008

LOG009

LOG015

LOG016

LOG017

LOG018

LOG019

LOG020

LOG021

LOG022

LOG023

LOG026

LOG028


LOG031


LOG032


LOG033


LOG033


LOG034


LOG035


LOG036


LOG037


LOG038

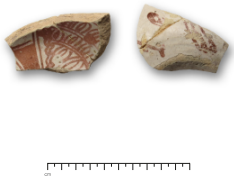
LOG039


LOG040


LOG041


LOG042


LOG043


LOG044


LOG045


LOG046


LOG047


LOG048


LOG049

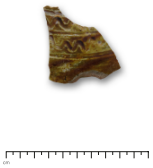

LOG050

LOG051

LOG052

LOG053

LOG054

LOG055

LOG056

LOG059

LOG060

LOG061

LOG062

LOG063

LOG066

LOG067

LOG068

LOG069

LOG070

LOG071

LOG072

LOG073

LOG074

LOG075

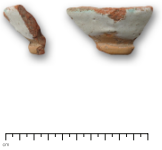

LOG076

LOG077

LOG078

LOG080

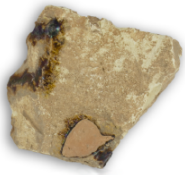

LOG081

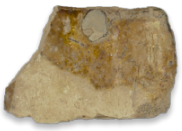

LOG082

LOG083

LOG084

LOG085

LOG086

LOG087

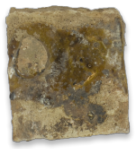

LOG088

LOG089

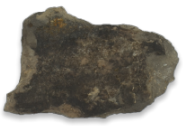

LOG090

LOG091

NAJ001

NAJ002

NAJ003

NAJ004

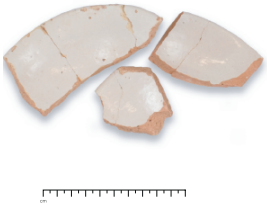

NAJ005

NAJ006

NAJ007

NAJ008

NAJ009

NAJ010

NAJ011

NAJ012

NAJ013

NAJ014

NAJ015

NAJ016

NAJ017

NAJ018

NAJ019

NAJ020


NAJ021


NAJ022


NAJ023


NAJ024

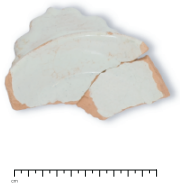
NAJ025


NAJ026


NAJ027


NAJ028


NAJ029


NAJ030


NAJ031


NAJ032


NAJ033


NAJ034


NAJ035


NAJ036


NAJ037


NAJ038


NAJ039


NAJ040

NAJ041

NAJ042

NAJ043

NAJ044

NAJ045

NAJ046

NAJ047

NAJ048

NAJ049

NAJ050

NAJ051

NAJ052

NAJ053

NAJ054

NAJ055

NAJ056

NAJ057

NAJ058

NAJ059

NAJ063

NAJ064

NAJ065

NAJ066

NAJ067

NAJ068

NAJ069

NAJ070

NAJ071

NAJ073

NAJ074

NAJ075

NAJ076

NAJ077

NAJ078

NAJ079

NAJ080

NAJ081

NAJ082

NAJ083

NAJ085

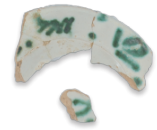

NAJ087

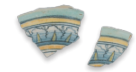

NAJ088

NAJ089

NAJ090

NAJ091

NAJ092

NAJ093

NAJ094

NAJ095

NAJ097

NAJ098

NAJ199

NAJ100

NAJ101


ORD001

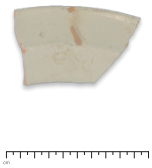
ORD002


ORD003


ORD004


ORD005

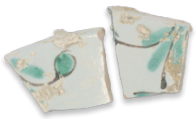
ORD006


ORD007

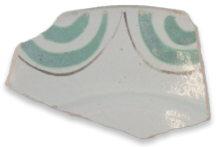
ORD008


ORD09


ORD010


ORD011


ORD012


ORD013


ORD014


ORD015


ORD016


ORD017


ORD018


ORD019


ORD020

ORD021

ORD022

ORD023

ORD024

ORD025

ORD026

ORD027

ORD028

ORD029

ORD030

ORD031

ORD032

ORD033

ORD034

ORD035

ORD036

ORD037

ORD039

ORD039

ORD042

ORD043

ORD044

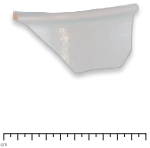

ORD045

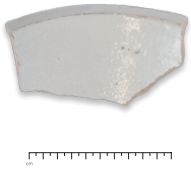

ORD046

ORD047

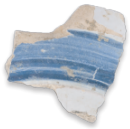

ORD048

ORD049

ORD050

ORD051

ORD053

ORD055

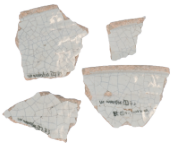

ORD056

ORD057

ORD058

ORD059

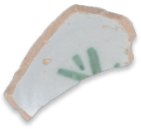

ORD060

ORD061

ORD062

ORD063

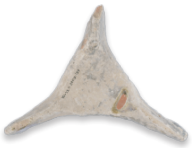

ORD064

ORD055

ORD066

ORD067

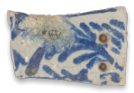

ORD068

ORD069

ORD070

ORD071

ORD072

ORD073

ORD074

ORD075

ORD076

ORD077

ORD078

ORD079

ORD080

ORD081

ORD082

ORD083

ORD084

ORD085

ORD086

ORD087

ORD088

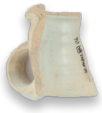

ORD089

ORD090

ORD091

ORD092

ORD093

ORD094

ORD095

ORD096

ORD097

ORD098

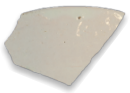

ORD099

ORD100

ORD101

DUR001

DUR002

DUR003

DUR004

DUR005

DUR006

DUR007

DUR008

DUR010

DUR011

DUR013

DUR014

DUR015

DUR016

DUR017

DUR018

DUR019

DUR020

DUR021

DUR022

DUR023

DUR024

DUR025

DUR026

DUR027

DUR028

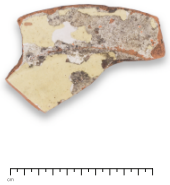

ELS001

ELS002

ELS003

ELS004

ELS005

ELS006

ELS007

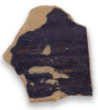

ELS008

ELS009

ELS010

ELS011

ELS012

ELS013

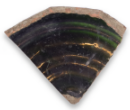

ELS014

ELS015

ELS016

ELS017

ELS018

ELS019

ELS020

ELS021

ELS022

ELS023

ELS024

ELS025

ELS026

ELS027

ELS028

ELS029

ELS030

ELS031

ELS032

ELS033

ELS034

ELS035

ELS036

ELS037

ELS038

ELS049

ELS040

Appendix D

Archaeological Profiles

All the archaeological profiles were drawn according to the procedure followed in the page 52.

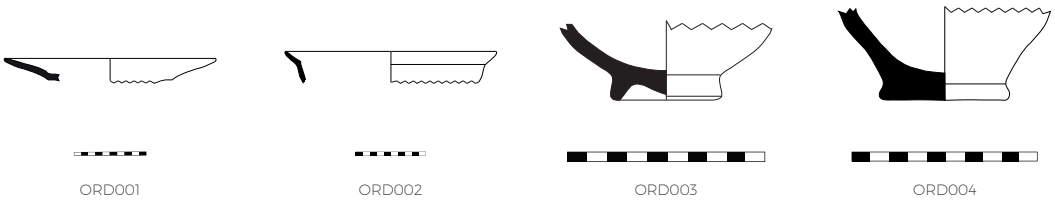

ORD001 ORD002 ORD003 ORD004

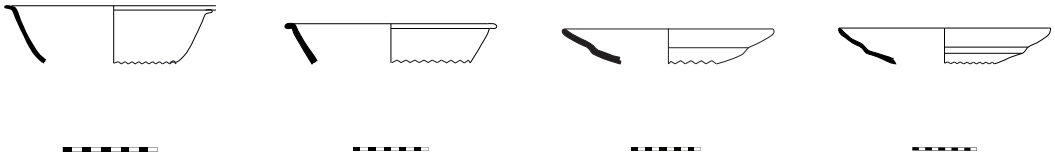

ORD005 ORD006 ORD007 ORD008

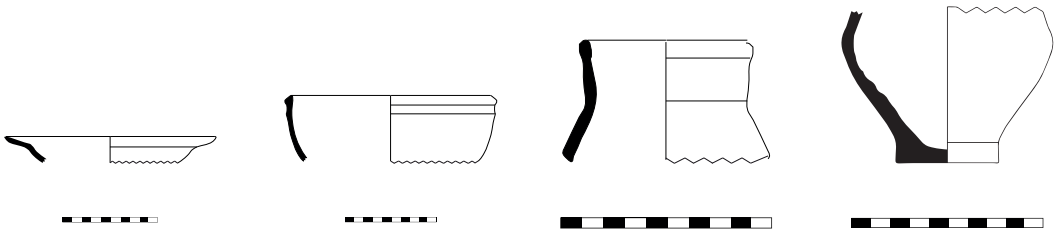

ORD09 ORD010 ORD011 ORD012

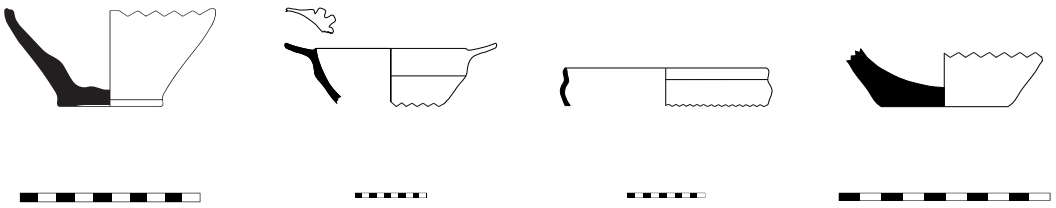

ORD013 ORD014 ORD015 ORD016

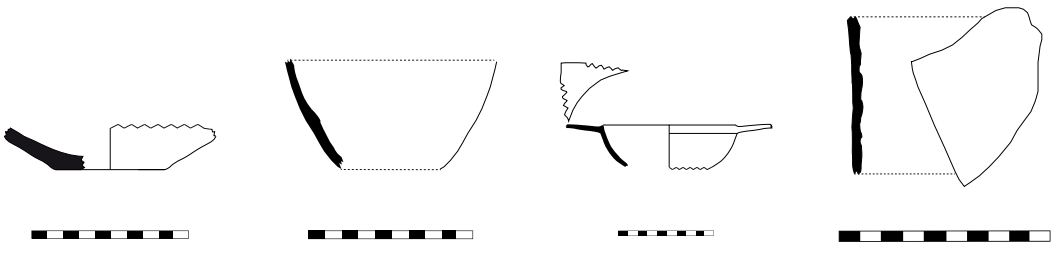

ORD017 ORD018 ORD019 ORD020

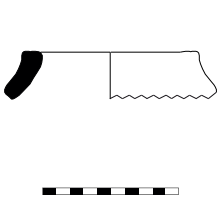
ORD021

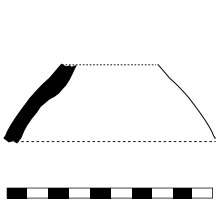
ORD022


ORD023

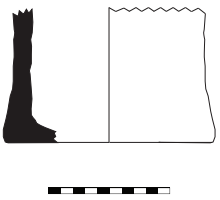
ORD024


ORD025

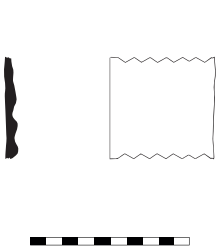
ORD026


ORD027

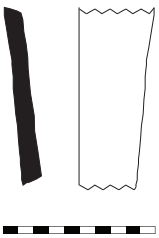
ORD028

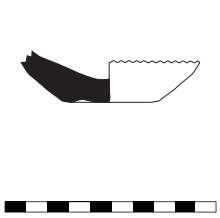
ORD029

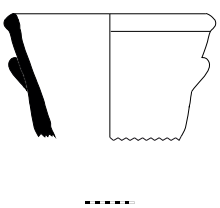
ORD030

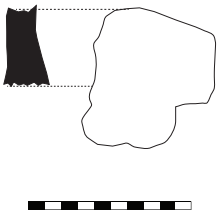
ORD031

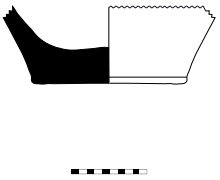
ORD032

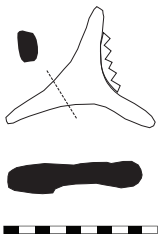
ORD033

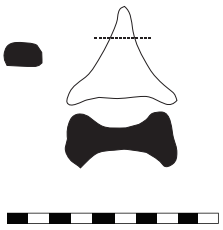
ORD034

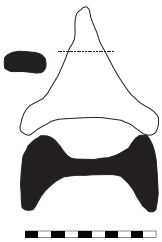
ORD035

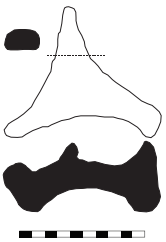
ORD036

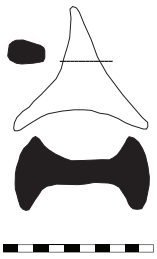
ORD037

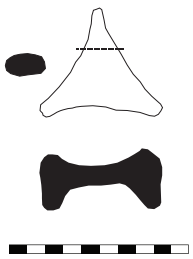
ORD039

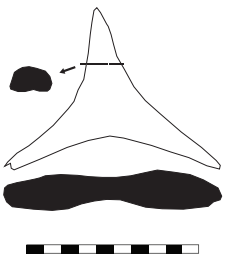
ORD040

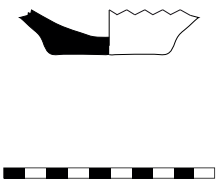
ORD042

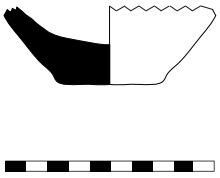

ORD043

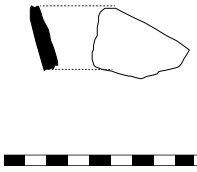

ORD044

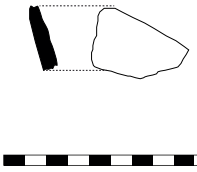

ORD045

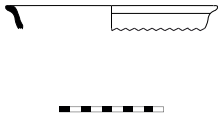

ORD046

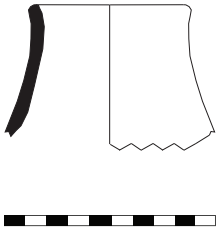

ORD047

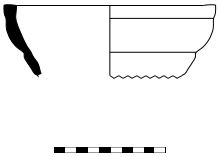

ORD048

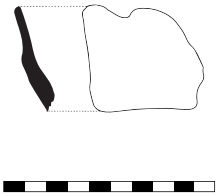

ORD049

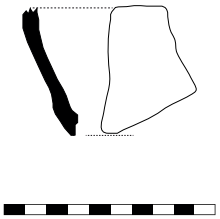

ORD050

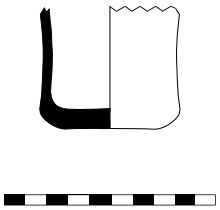

ORD051

ORD053

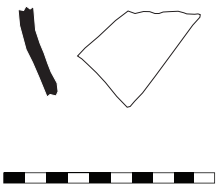

ORD055

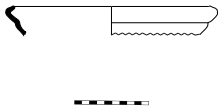

ORD056

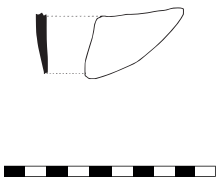

ORD057

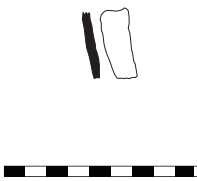

ORD058

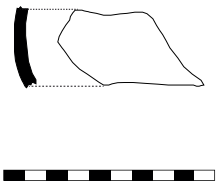

ORD059

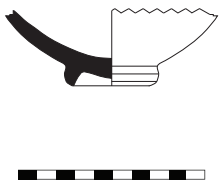

ORD060

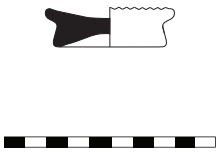

ORD061

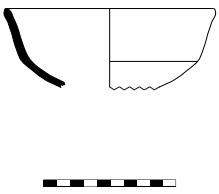

ORD062

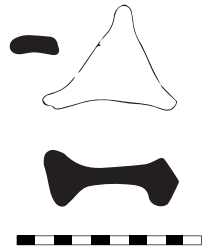

ORD063

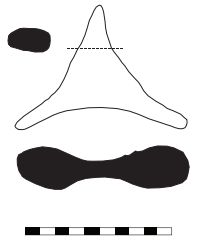

ORD064

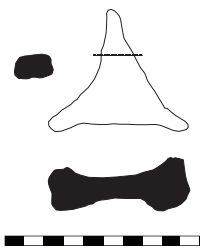
ORD055

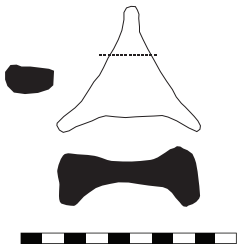
ORD066

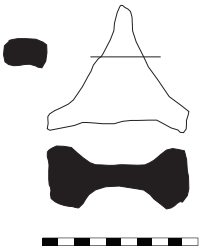
ORD067

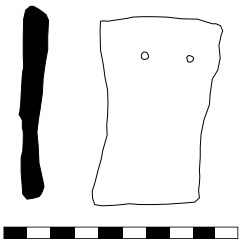
ORD068

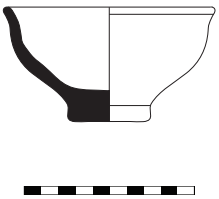
ORD069

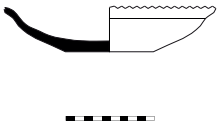
ORD070

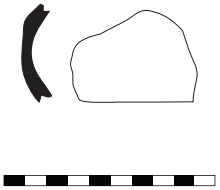
ORD071

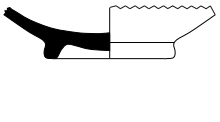
ORD072

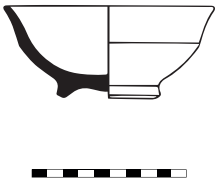
ORD073

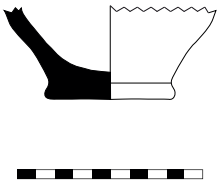
ORD074

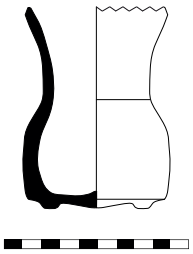
ORD075

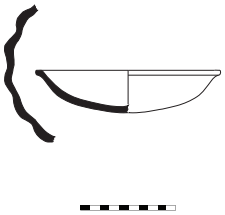
ORD076

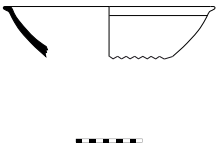
ORD077

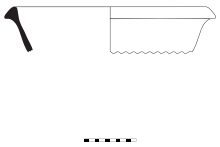
ORD079

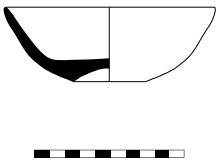
ORD083

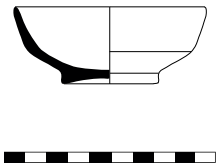
ORD084

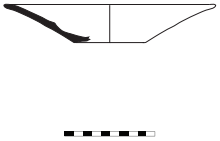
ORD085

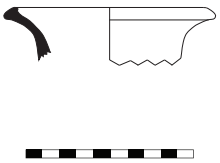
ORD086

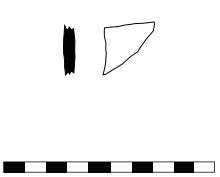
ORD087

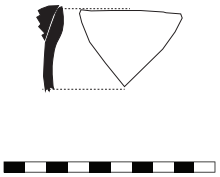
ORD088

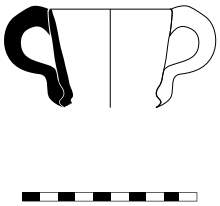

ORD089

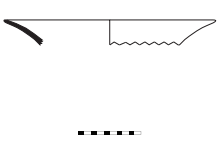

ORD090

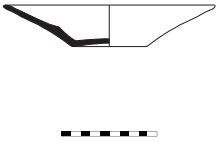

ORD091

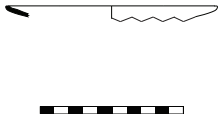

ORD092

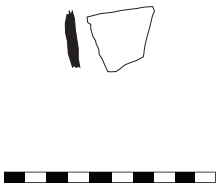

ORD093

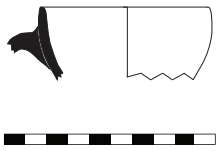

ORD094

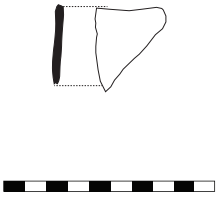

ORD095

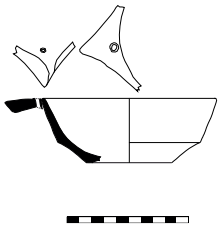

ORD096

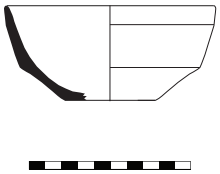

ORD097

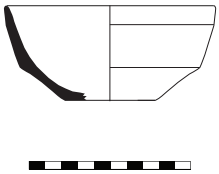

ORD098

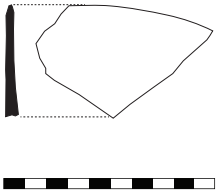

ORD099

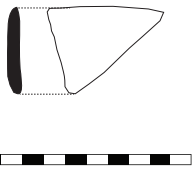

ORD100

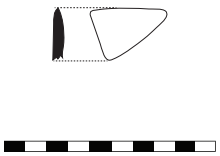

ORD101

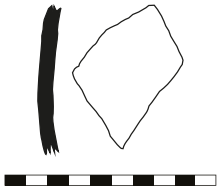
DUR001

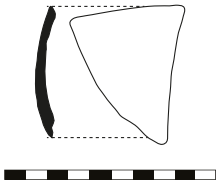
DUR002

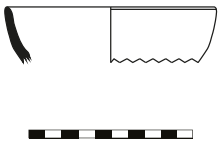
DUR003

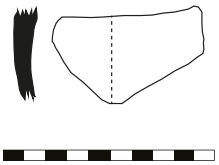
DUR004

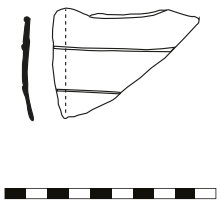
DUR005

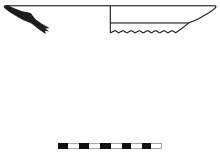
DUR006

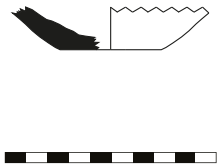
DUR007

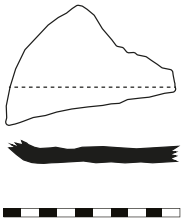
DUR008

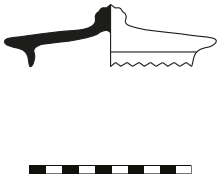
DUR010

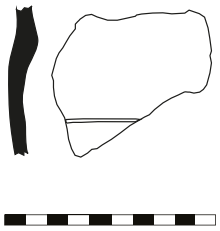
DUR011

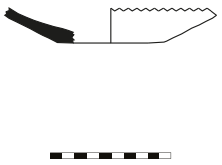
DUR013

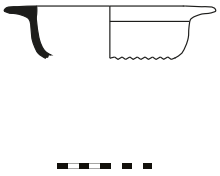
DUR014

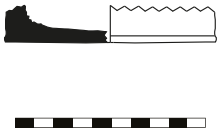
DUR015

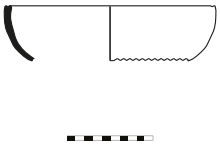
DUR016

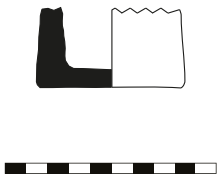
DUR017

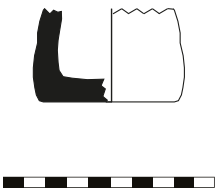
DUR018

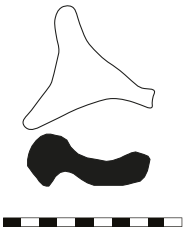
DUR019

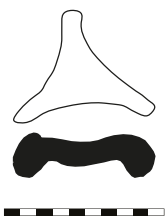
DUR020

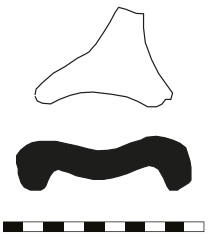
DUR021

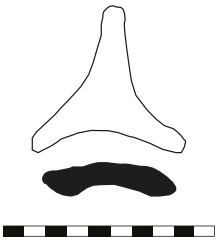
DUR022

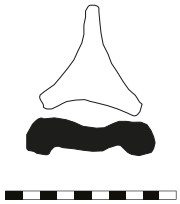

DUR023

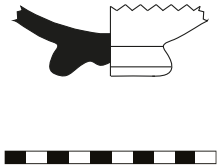

DUR024

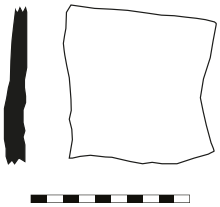

DUR025

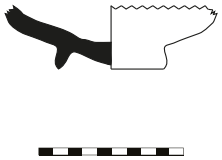

DUR026

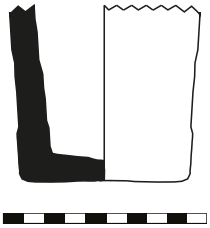

DUR027

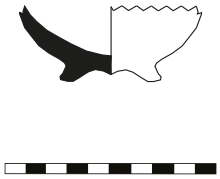

DUR028

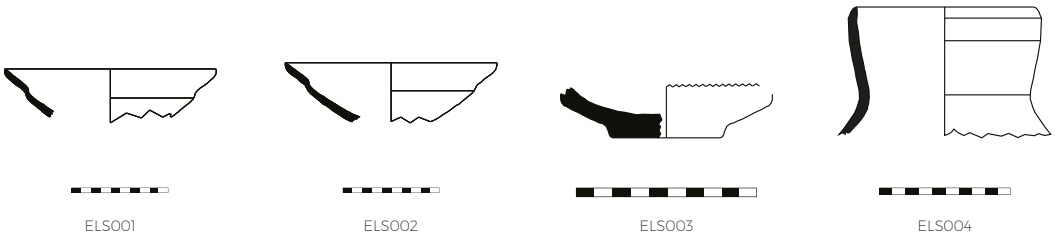

ELS001 ELS002 ELS003 ELS004

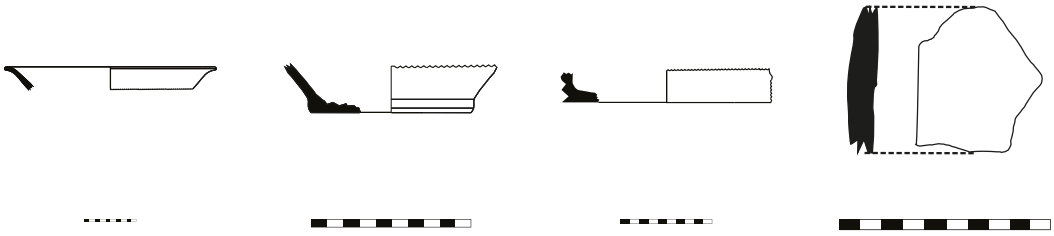

ELS005 ELS006 ELS007 ELS008

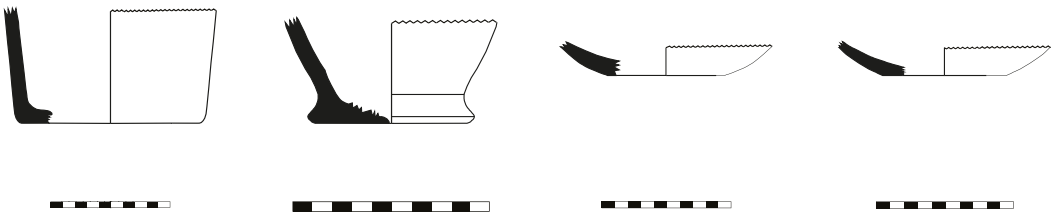

ELS009 ELS010 ELS011 ELS012

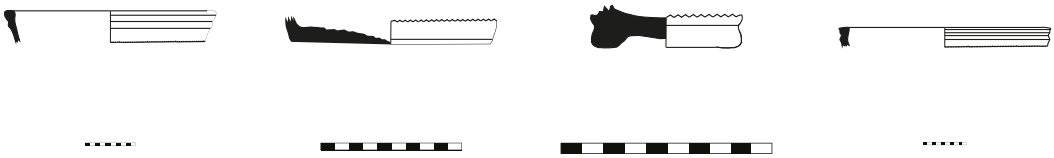

ELS013 ELS014 ELS015 ELS016

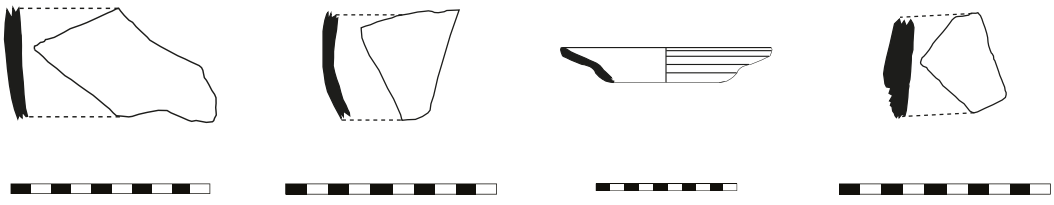

ELS017 ELS018 ELS019 ELS020

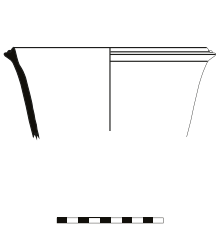
ELS021

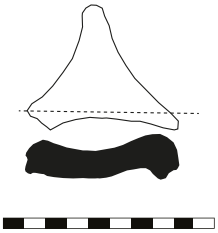
ELS022

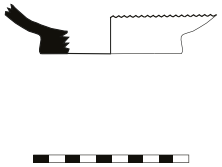
ELS023

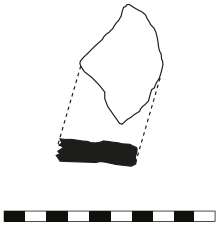
ELS024

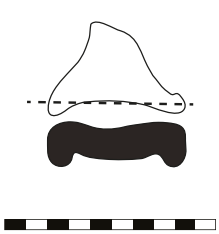
ELS025

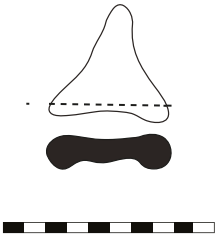
ELS026

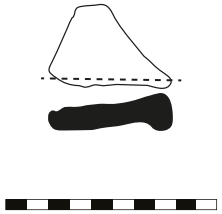
ELS027

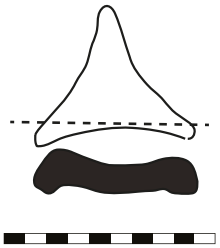
ELS028

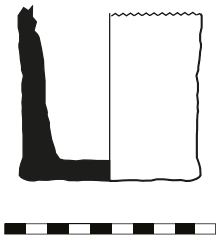
ELS029

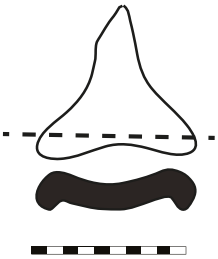
ELS030

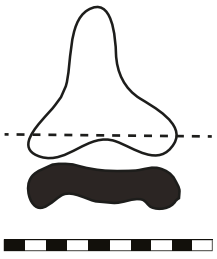
ELS031

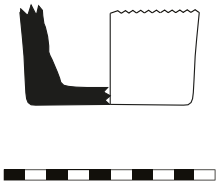
ELS032

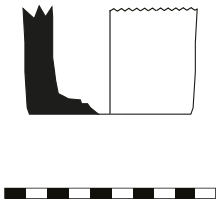
ELS033

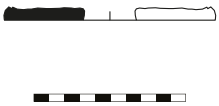
ELS034

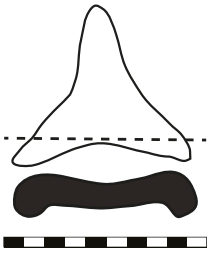
ELS035

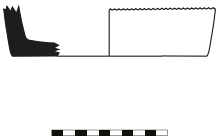
ELS036

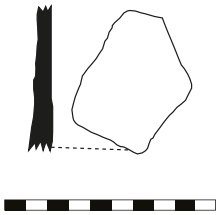
ELS037

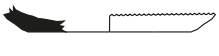
ELS038

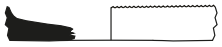
ELS049

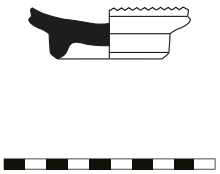
ELS040

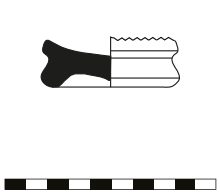

ELS041

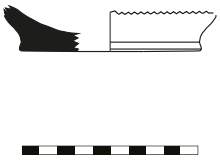

ELS042

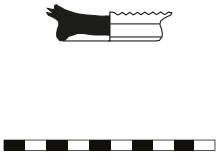

ELS043

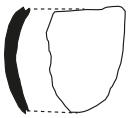

ELS044

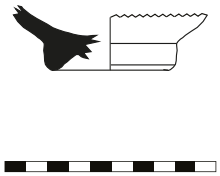

ELS045

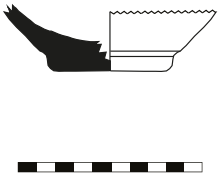

ELS046

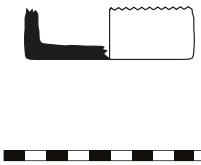

ELS047

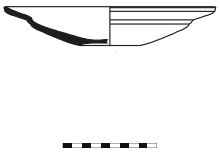

ELS048

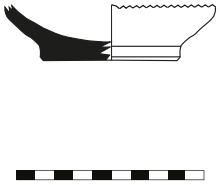

ELS049

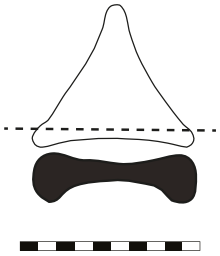

ELS050

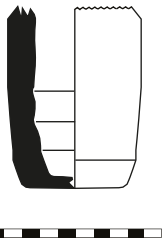

ELS051

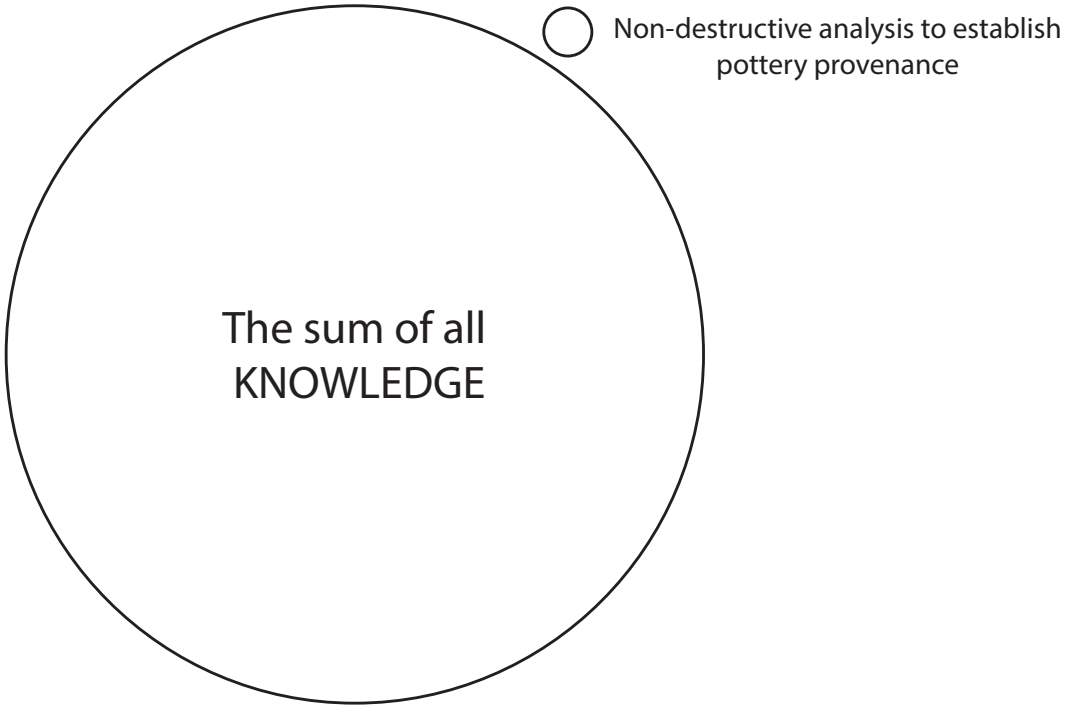
Non-destructive analysis to establish
pottery provenance
The sum of all
KNOWLEDGE